Springer Series in
OPTICAL SCIENCES 124

founded by H.K.V. Lotsch

Springer Series in

OPTICAL SCIENCES

The Springer Series in Optical Sciences, under the leadership of Editor-in-Chief *William T. Rhodes*, Georgia Institute of Technology, USA, provides an expanding selection of research monographs in all major areas of optics: lasers and quantum optics, ultrafast phenomena, optical spectroscopy techniques, optoelectronics, quantum information, information optics, applied laser technology, industrial applications, and other topics of contemporary interest.
With this broad coverage of topics, the series is of use to all research scientists and engineers who need up-to-date reference books.

The editors encourage prospective authors to correspond with them in advance of submitting a manuscript. Submission of manuscripts should be made to the Editor-in-Chief or one of the Editors. See also www.springeronline.com/series/624

A. Doicu T. Wriedt Y.A. Eremin

Light Scattering by Systems of Particles

Null-Field Method with Discrete Sources: Theory and Programs

With 123 Figures, 4 in Color and 9 Tables

Springer

Adrian Doicu
Institut für Methodik der Fernerkundung
Deutsches Institut für Luft- und Raumfahrt e.V.
D-82234 Oberpfaffenhofen, Germany
E-mail: adrian.doicu@dlr.de

Thomas Wriedt
University of Bremen, FB4, VT
Badgasteiner Str. 3, 28359 Bremen, Germany
E-mail: thw@iwt.uni-bremen.de

Yuri A. Eremin
Applied Mathematics and Computer Science Faculty
Moscow State University
119899 Moscow, Russia
E-mail: eremin@cs.msu.su

ISSN 0342-4111

ISBN-10 3-540-33696-6 Springer Berlin Heidelberg New York

ISBN-13 978-3-540-33696-9 Springer Berlin Heidelberg New York

Library of Congress Control Number: 2006929447

Typesetting by the Authors and SPi using a Springer LaTeX macro package
Cover concept by eStudio Calamar Steinen using a background picture from The Optics Project. Courtesy of John T. Foley, Professor, Department of Physics and Astronomy, Mississippi State University, USA.
Cover production: *design & production* GmbH, Heidelberg

Printed on acid-free paper SPIN: 11554325 57/3100/SPi 5 4 3 2 1 0

To our families:
Aniela and Alexandru
Ursula and Jannis
Natalia, Elena and Oleg

Preface

Since the classic paper by Mie [159] or even the papers by Clebsch [37] and Lorenz [146] there is a permanent preoccupation in light scattering theory. Mie was interested in the varied colors exhibited by colloidal suspensions of noble metal spheres, but nowadays, the theory of light scattering by particles covers a much broader and diverse field. Particles encountered in practical applications are no longer considered spherical; they are nonspherical, nonrotational symmetric, inhomogeneous, coated, chiral or anisotropic.

Light scattering simulation is needed in optical particle characterization, to understand new physical phenomena or to design new particle diagnostics systems. Other examples of applications are climatology and remote sensing of Earth and planetary atmospheres, which rely on the analysis of the parameters of radiation scattered by aerosols, clouds, and precipitation. Similar electromagnetic modeling methods are needed to investigate microwave scattering by raindrops and ice crystals, while electromagnetic scattering is also encountered in astrophysics, ocean and biological optics, optical communications engineering, and photonics technology. Specifically, in near-field- or nano-optics and the design of optical sensor, biosensors or particle surface scanners, light scattering by particles on or near infinite surfaces is of interest.

Many techniques have been developed for analyzing scattering problems. Each of the available methods generally has a range of applicability that is determined by the size of the particle relative to the wavelength of the incident radiation. Classical methods of solution like the finite-difference method, finite element method or integral equation method, owing to their universality, lead to computational algorithms that are expensive in computer resources. This significantly restricts their use in studying electromagnetic scattering by large particles. In the last years, the null-field method has become an efficient and powerful tool for rigorously computing electromagnetic scattering by single and compounded particles significantly larger than a wavelength. In many applications, it compares favorably to other techniques in terms of efficiency, accuracy, and size parameter range and is the only method that has been used in computations for thousand of particles in random orientation.

The null-field method (otherwise known as the extended boundary condition method, Schelkunoff equivalent current method, Eswald–Oseen extinction theorem and **T**-matrix method) has been developed by Waterman [253, 254] as a technique for computing electromagnetic scattering by perfectly conducting and dielectric particles. In time, the null-field method has been applied to a wide range of scattering problems. A compilation of **T**-matrix publications and a classification of various references into a set of narrower subject categories has recently been given by Mishchenko et al. [172]. Peterson and Ström [187, 189], Varadan [233], and Ström and Zheng [219] extended the null-field method to the case of an arbitrary number of particles and to multilayered and composite particles. Lakhtakia et al. [135] applied the null-field method to chiral particles, while Varadan et al. [236] treated multiple scattering in random media. A number of modifications to the null-field method have been suggested, especially to improve the numerical stability in computations for particles with extreme geometries. These techniques include formal modifications of the single spherical coordinate-based null-field method [25, 109], different choices of basis functions and the application of the spheroidal coordinate formalism [12, 89] and the use of discrete sources [49]. Mishchenko [163] developed analytical procedures for averaging scattering characteristics over particle orientations and increased the efficiency of the method. At the same time, several computer programs for computing electromagnetic scattering by axisymmetric particles in fixed and random orientations have been designed. In this context, we mention the Fortran programs included with the book by Barber and Hill [8] and the Internet available computer programs developed by Mishchenko et al. [169]. For specific applications, other computer codes have been developed by various research groups, but these programs are currently not yet publicly available.

This monograph is based on our own research activity over the last decade and is intended to provide an exhaustive analysis of the null-field method and to present appropriate computer programs for solving various scattering problems. The following outline should provide a fair idea of the main intent and content of the book.

In the first chapter, we recapitulate the fundamentals of classical electromagnetics and optics which are required to present the theory of the null-field method. This part contains explicit derivations of all important results and is mainly based on the textbooks of Kong [122] and Mishchenko et al. [169].

The next chapter provides a comprehensive analysis of the null-field method for various electromagnetic scattering problems. This includes scattering by

- Homogeneous, dielectric (isotropic, uniaxial anisotropic, chiral), and perfectly conducting particles with axisymmetric and nonaxisymmetric surfaces
- Inhomogeneous, layered and composite particles,
- Clusters of arbitrarily shaped particles, and
- Particles on or near a plane surface.

The null-field method is used to compute the **T** matrix of each individual particle and the **T**-matrix formalism is employed to analyze systems of particles. For homogeneous, composite and layered, axisymmetric particles, the null-field method with discrete sources is applied to improve the numerical stability of the conventional method. Evanescent wave scattering and scattering by a half-space with randomly distributed particles are also discussed. To extend the domain of applicability of the method, plane waves and Gaussian laser beams are considered as external excitations.

The last chapter covers the numerical analysis of the null-field method by presenting some exemplary computational results. For all scattering problems discussed in the preceding chapters we developed a Fortran software package which is provided on a CD-ROM with the book. After a description of the Fortran programs we present a number of exemplary computational results with the intension to demonstrate the broad range of applicability of the method. These should enable the readers to adapt and extend the programs to other specific applications and to gain some practical experience with the methods outlined in the book. Because it is hardly possible to comprehensively address all aspects and computational issues, we choose those topics that we think are currently the most interesting applications in the growing field of light scattering theory. As we are continuously working in this field, further extensions of the programs and more computational results will hopefully become available at our web page www.t-matrix.de. The computer programs have been extensively tested, but we cannot guarantee that the programs are free of errors. In this regard, we like to encourage the readers to communicate us any errors in the program or documentation. This software is published under German Copyright Law (Urheberrechtsgesetz, UrhG) and in this regard the readers are granted the right to apply the software but not to copy, to sell or distribute it nor to make it available to the public in any form. We provide the software without warranty of any kind. No liability is taken for any loss or damages, direct or indirect, that may result through the use of the programs.

This volume is intended for engineering and physics students as well as researchers in scattering theory, and therefore we decided to leave out rigorous mathematical details. The properties of scalar and vector spherical wave functions, addition theorems under translation and rotation of the coordinate systems and some completeness results are presented in appendices. These can be regarded as a collection of necessary formulas.

We would like to thank Elena Eremina, Jens Hellmers, Sorin Pulbere, Norbert Riefler, and Roman Schuh for many useful discussions and for performing extensive simulation and validation tests with the programs provided with the book. We also thankfully acknowledge support from DFG (Deutsche Forschungsgemeinschaft) and RFBR (Russian Foundation of Basic Research) which funded our research in light scattering theory.

Bremen,
April 2006

Adrian Doicu
Thomas Wriedt
Yuri Eremin

Researching for and writing of this book were both very personal but shared experience. My new research activity in the field of inversion methods for atmospheric remote sensing has left me little free time for writing. Fortunately, I have had assistance of my wife Aniela. She read what I had written, spent countless hours editing the manuscript and helped me in the testing and comparing of computer codes. Without the encouragement and the stimulus given by Aniela, this book might never have been completed. For her love and support, which buoyed me through the darkest time of self-doubt and fear, I sincerely thank.

München, *Adrian Doicu*
April 2006

Contents

1

Basic Theory of Electromagnetic Scattering

This chapter is devoted to present the fundamentals of the electromagnetic scattering theory which are relevant in the analysis of the null-field method. We begin with a brief discussion on the physical background of Maxwell's equations and establish vector spherical wave expansions for the incident field. We then derive new systems of vector functions for internal field approximations by analyzing wave propagation in isotropic, anisotropic and chiral media, and present the $\boldsymbol{T}$-matrix formulation for electromagnetic scattering. We decided to leave out some technical details in the presentation. Therefore, the integral and orthogonality relations, the addition theorems and the basic properties of the scalar and vector spherical wave functions are reviewed in Appendices A and B.

1.1 Maxwell's Equations and Constitutive Relations

In this section, we formulate the Maxwell equations that govern the behavior of the electromagnetic fields. We present the fundamental laws of electromagnetism, derive the boundary conditions and describe the properties of isotropic, anisotropic and chiral media by constitutive relations. Our presentation follows the treatment of Kong [122] and Mishchenko et al. [169]. Other excellent textbooks on classical electrodynamics and optics have been given by Stratton [215], Tsang et al. [228], Jackson [110], van de Hulst [105], Kerker [115], Bohren and Huffman [17], and Born and Wolf [19].

The behavior of the macroscopic field at interior points in material media is governed by Maxwell's equations:

$$\nabla \times \boldsymbol{E} = -\frac{\partial \boldsymbol{B}}{\partial t} \quad \text{(Faraday's induction law)}\,, \tag{1.1}$$

$$\nabla \times \boldsymbol{H} = \boldsymbol{J} + \frac{\partial \boldsymbol{D}}{\partial t} \quad \text{(Maxwell–Ampere law)}\,, \tag{1.2}$$

$$\nabla \cdot \boldsymbol{D} = \rho \quad \text{(Gauss' electric field law)}\,, \tag{1.3}$$

$$\nabla \cdot \boldsymbol{B} = 0 \quad \text{(Gauss' magnetic field law)}\,, \tag{1.4}$$

where t is time, $\boldsymbol{E}$ the electric field, $\boldsymbol{H}$ the magnetic field, $\boldsymbol{B}$ the magnetic induction, $\boldsymbol{D}$ the electric displacement and ρ and $\boldsymbol{J}$ the electric charge density and current density, respectively. The first three equations in Maxwell's theory are independent, because the Gauss magnetic field law can be obtained from Faraday's law by taking the divergence and by setting the integration constant with respect to time equal to zero. Analogously, taking the divergence of Maxwell–Ampere law and using the Gauss electric field law we obtain the continuity equation:

$$\nabla \cdot \boldsymbol{J} + \frac{\partial \rho}{\partial t} = 0\,, \tag{1.5}$$

which expresses the conservation of electric charge. The Gauss magnetic field law and the continuity equation should be treated as auxiliary or dependent equations in the entire system of equations (1.1)–(1.5). The charge and current densities are associated with the so-called "free" charges, and for a source-free medium, $\boldsymbol{J} = 0$ and $\rho = 0$. In this case, the Gauss electric field law can be obtained from Maxwell–Ampere law and only the first two equations in Maxwell's theory are independent.

In our analysis we will assume that all fields and sources are time harmonic. With ω being the angular frequency and $\mathrm{j} = \sqrt{-1}$, we write

$$\boldsymbol{E}(\boldsymbol{r}, t) = \mathrm{Re}\left\{\boldsymbol{E}(\boldsymbol{r})\mathrm{e}^{-\mathrm{j}\omega t}\right\}$$

and similarly for other field quantities. The vector field $\boldsymbol{E}(\boldsymbol{r})$ in the frequency domain is a complex quantity, while $\boldsymbol{E}(\boldsymbol{r}, t)$ in the time domain is real. As a result of the Fourier component Ansatz, the Maxwell equations in the frequency domain become

$$\begin{aligned}
\nabla \times \boldsymbol{E} &= \mathrm{j}\,\omega \boldsymbol{B}\,,\\
\nabla \times \boldsymbol{H} &= \boldsymbol{J} - \mathrm{j}\,\omega \boldsymbol{D}\,,\\
\nabla \cdot \boldsymbol{D} &= \rho\,,\\
\nabla \cdot \boldsymbol{B} &= 0\,.
\end{aligned}$$

Taking into account the continuity equation in the frequency domain $\nabla \cdot \boldsymbol{J} - \mathrm{j}\,\omega\rho = 0$, we may express the Maxwell–Ampere law and the Gauss electric field law as

$$\begin{aligned}
\nabla \times \boldsymbol{H} &= -\mathrm{j}\,\omega \boldsymbol{D}_{\mathrm{t}}\,,\\
\nabla \cdot \boldsymbol{D}_{\mathrm{t}} &= 0\,,
\end{aligned}$$

where

$$\boldsymbol{D}_{\mathrm{t}} = \boldsymbol{D} + \frac{\mathrm{j}}{\omega}\boldsymbol{J}$$

is the total electric displacement.

Across the interface separating two different media the fields may be discontinuous and a boundary condition is associated with each of Maxwell's equations. To derive the boundary conditions, we consider a regular domain D enclosed by a surface S with outward normal unit vector $\boldsymbol{n}$, and use the *curl* theorem

$$\int_D \nabla \times \boldsymbol{a}\,\mathrm{d}V = \int_S \boldsymbol{n} \times \boldsymbol{a}\,\mathrm{d}S\,,$$

to obtain

$$\int_S \boldsymbol{n} \times \boldsymbol{E}\,\mathrm{d}S = \mathrm{j}\,\omega \int_D \boldsymbol{B}\,\mathrm{d}V\,,$$
$$\int_S \boldsymbol{n} \times \boldsymbol{H}\,\mathrm{d}S = \int_D \boldsymbol{J}\,\mathrm{d}V - \mathrm{j}\,\omega \int_D \boldsymbol{D}\,\mathrm{d}V\,,$$

and the Gauss theorem

$$\int_D \nabla \cdot \boldsymbol{a}\,\mathrm{d}V = \int_S \boldsymbol{n} \cdot \boldsymbol{a}\,\mathrm{d}S\,,$$

to derive

$$\int_S \boldsymbol{n} \cdot \boldsymbol{D}\,\mathrm{d}S = \int_D \rho\,\mathrm{d}V\,,$$
$$\int_S \boldsymbol{n} \cdot \boldsymbol{B}\,\mathrm{d}S = 0\,.$$

Note that the *curl* theorem follows from Gauss theorem applied to the vector field $\boldsymbol{c} \times \boldsymbol{a}$, where $\boldsymbol{c}$ is a constant vector, and the identity $\nabla \cdot (\boldsymbol{c} \times \boldsymbol{a}) = -\boldsymbol{c} \cdot (\nabla \times \boldsymbol{a})$. We then consider a surface boundary joining two different media 1 and 2, denote by $\boldsymbol{n}_1$ the surface normal pointing toward medium 2, and assume that the surface of discontinuity is contained in D. We choose the domain of analysis in the form of a thin slab with thickness h and area ΔS, and let the volume approach zero by letting h go to zero and then letting ΔS go to zero (Fig. 1.1). Terms involving vector or dot product by $\boldsymbol{n}$ will be dropped except when $\boldsymbol{n}$ is in the direction of $\boldsymbol{n}_1$ or $-\boldsymbol{n}_1$. Assuming that $\boldsymbol{D}$ and $\boldsymbol{B}$ are finite in the region of integration, and that the boundary may support a surface current $\boldsymbol{J}_\mathrm{s}$ such that $\boldsymbol{J}_\mathrm{s} = \lim_{h \to 0} h\boldsymbol{J}$, and a surface charge

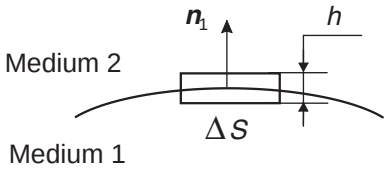

Fig. 1.1. The surface of discontinuity and a thin slab of thickness h and area ΔS

density ρ_s such that $\rho_\mathrm{s} = \lim_{h\to 0} h\rho$, we see that the tangential component of $\boldsymbol{E}$ is continuous:

$$\boldsymbol{n}_1 \times (\boldsymbol{E}_2 - \boldsymbol{E}_1) = 0\,,$$

the tangential component of $\boldsymbol{H}$ is discontinuous:

$$\boldsymbol{n}_1 \times (\boldsymbol{H}_2 - \boldsymbol{H}_1) = \boldsymbol{J}_\mathrm{s}\,,$$

the normal component of $\boldsymbol{B}$ is continuous:

$$\boldsymbol{n}_1 \cdot (\boldsymbol{B}_2 - \boldsymbol{B}_1) = 0\,,$$

and the normal component of $\boldsymbol{D}$ is discontinuous:

$$\boldsymbol{n}_1 \cdot (\boldsymbol{D}_2 - \boldsymbol{D}_1) = \rho_\mathrm{s}\,.$$

Energy conservation follows from Maxwell's equations. The vector identity

$$\nabla \cdot (\boldsymbol{a} \times \boldsymbol{b}) = \boldsymbol{b} \cdot (\nabla \times \boldsymbol{a}) - \boldsymbol{a} \cdot (\nabla \times \boldsymbol{b})$$

yields the Poynting theorem in the time domain:

$$\nabla \cdot (\boldsymbol{E} \times \boldsymbol{H}) + \boldsymbol{H} \cdot \frac{\partial \boldsymbol{B}}{\partial t} + \boldsymbol{E} \cdot \frac{\partial \boldsymbol{D}}{\partial t} = -\boldsymbol{E} \cdot \boldsymbol{J},$$

and the Poynting vector defined as

$$\boldsymbol{S} = \boldsymbol{E} \times \boldsymbol{H}$$

is interpreted as the power flow density. Integrating over a finite domain D with boundary S, and using the Gauss theorem, yields

$$-\int_D \boldsymbol{E} \cdot \boldsymbol{J}\,\mathrm{d}V = \int_S \boldsymbol{S} \cdot \boldsymbol{n}\,\mathrm{d}S + \int_D \left(\boldsymbol{H} \cdot \frac{\partial \boldsymbol{B}}{\partial t} + \boldsymbol{E} \cdot \frac{\partial \boldsymbol{D}}{\partial t}\right)\,\mathrm{d}V\,,$$

where as before, $\boldsymbol{n}$ is the outward normal unit vector to the surface S. The above equation states that the power supplied by the sources within a volume is equal to the sum of the increase in electromagnetic energy and the Poynting's power flowing out through the volume boundary. Poynting's theorem can also be derived in the frequency domain:

$$\nabla \cdot (\boldsymbol{E} \times \boldsymbol{H}^*) = \mathrm{j}\omega\,(\boldsymbol{B} \cdot \boldsymbol{H}^* - \boldsymbol{E} \cdot \boldsymbol{D}^*) - \boldsymbol{E} \cdot \boldsymbol{J}^*\,,$$

where the asterisk denotes a complex-conjugate value. The complex Poynting vector is defined as $\boldsymbol{S} = \boldsymbol{E} \times \boldsymbol{H}^*$ and the term $-\int_D \boldsymbol{E} \cdot \boldsymbol{J}^*\,\mathrm{d}V$ is interpreted as the complex power supplied by the source.

In practice, the angular frequency ω is such high that a measuring instrument is not capable of following the rapid oscillations of the power flow but

rather responds to a time average power flow. Considering the time-harmonic vector fields $\boldsymbol{a}$ and $\boldsymbol{b}$,

$$\boldsymbol{a}(\boldsymbol{r},t) = \frac{1}{2}\left[\boldsymbol{a}(\boldsymbol{r})\mathrm{e}^{-\mathrm{j}\omega t} + \boldsymbol{a}^*(\boldsymbol{r})\mathrm{e}^{\mathrm{j}\omega t}\right] ,$$

$$\boldsymbol{b}(\boldsymbol{r},t) = \frac{1}{2}\left[\boldsymbol{b}(\boldsymbol{r})\mathrm{e}^{-\mathrm{j}\omega t} + \boldsymbol{b}^*(\boldsymbol{r})\mathrm{e}^{\mathrm{j}\omega t}\right] ,$$

we express the dot product of the vectors as

$$\begin{aligned} c(\boldsymbol{r},t) &= \boldsymbol{a}(\boldsymbol{r},t)\cdot\boldsymbol{b}(\boldsymbol{r},t) \\ &= \frac{1}{2}\mathrm{Re}\left\{\boldsymbol{a}(\boldsymbol{r})\cdot\boldsymbol{b}^*(\boldsymbol{r}) + \boldsymbol{a}(\boldsymbol{r})\cdot\boldsymbol{b}(\boldsymbol{r})\mathrm{e}^{-2\mathrm{j}\omega t}\right\} . \end{aligned}$$

Defining the time average of c as

$$\langle c(\boldsymbol{r})\rangle = \lim_{T\to\infty}\frac{1}{T}\int_0^{\mathrm{T}} c(\boldsymbol{r},t)\,\mathrm{d}t\,,$$

where T is a time interval, we derive

$$\langle c(\boldsymbol{r})\rangle = \frac{1}{2}\mathrm{Re}\left\{\boldsymbol{a}(\boldsymbol{r})\cdot\boldsymbol{b}^*(\boldsymbol{r})\right\} ,$$

while for the cross product of the vectors

$$\boldsymbol{c}(\boldsymbol{r},t) = \boldsymbol{a}(\boldsymbol{r},t)\times\boldsymbol{b}(\boldsymbol{r},t)\,,$$

we similarly obtain

$$\langle \boldsymbol{c}(\boldsymbol{r})\rangle = \frac{1}{2}\mathrm{Re}\left\{\boldsymbol{a}(\boldsymbol{r})\times\boldsymbol{b}^*(\boldsymbol{r})\right\} .$$

Thus, the time average of the dot or cross product of two time-harmonic complex quantities is equal to half of the real part of the respective product of one quantity and the complex conjugate of the other. In this regard, the time-averaged Poynting vector is given by

$$\langle \boldsymbol{S}\rangle = \frac{1}{2}\mathrm{Re}\left\{\boldsymbol{E}\times\boldsymbol{H}^*\right\} .$$

The three independent vector equations (1.1)–(1.3) are equivalent to seven scalar differential equations, while the number of unknown scalar functions is 16. Obviously, the three independent equations are not sufficient to form a complete systems of equations to solve for the unknown functions, and for this reason, the equations given by (1.1)–(1.4) are known as the indefinite form of the Maxwell equations. Note that for a free-source medium, we have six scalar differential equations with 12 unknown scalar functions. To make the Maxwell equations definite we need more information and this additional

information is given by the constitutive relations. The constitutive relations provide a description of media and give functional dependence among vector fields. For isotropic media, the constitutive relations read as

$$\begin{aligned} \boldsymbol{D} &= \varepsilon \boldsymbol{E}\,, \\ \boldsymbol{B} &= \mu \boldsymbol{H}\,, \\ \boldsymbol{J} &= \sigma \boldsymbol{E} \quad \text{(Ohm's law)}\,, \end{aligned} \tag{1.6}$$

where ε is the electric permittivity, μ is the magnetic permeability and σ is the electric conductivity. The above equations provide nine scalar relations that make the number of unknowns and the number of equations compatible, while for a source-free medium, the first two constitutive relations guarantee this compatibility. When the constitutive relations between the vector fields are specified, Maxwell equations become definite. In free space $\varepsilon_0 = 8.85 \times 10^{-12}\,\mathrm{F\,m^{-1}}$ and $\mu_0 = 4\pi \times 10^{-7}\,\mathrm{H\,m^{-1}}$, while in a material medium, the permittivity and permeability are determined by the electrical and magnetic properties of the medium. A dielectric material can be characterized by a free-space part and a part depending on the polarization vector $\boldsymbol{P}$ such that

$$\boldsymbol{D} = \varepsilon_0 \boldsymbol{E} + \boldsymbol{P}\,.$$

The polarization $\boldsymbol{P}$ symbolizes the average electric dipole moment per unit volume and is given by

$$\boldsymbol{P} = \varepsilon_0 \chi_\mathrm{e} \boldsymbol{E}\,,$$

where χ_e is the electric susceptibility. A magnetic material can also be characterized by a free-space part and a part depending on the magnetization vector $\boldsymbol{M}$,

$$\boldsymbol{B} = \mu_0 \boldsymbol{H} + \mu_0 \boldsymbol{M}\,,$$

where $\boldsymbol{M}$ symbolizes the average magnetic dipole moment per unit volume,

$$\boldsymbol{M} = \chi_\mathrm{m} \boldsymbol{H}\,,$$

and χ_m is the magnetic susceptibility. A medium is diamagnetic if $\mu < \mu_0$ and paramagnetic if $\mu > \mu_0$, while for a nonmagnetic medium we have $\mu = \mu_0$. The permittivity and permeability of isotropic media can be written as

$$\begin{aligned} \varepsilon &= \varepsilon_0 \varepsilon_\mathrm{r} = \varepsilon_0 \left(1 + \chi_\mathrm{e}\right)\,, \\ \mu &= \mu_0 \mu_\mathrm{r} = \mu_0 \left(1 + \chi_\mathrm{m}\right)\,, \end{aligned}$$

where ε_r and μ_r stand for the corresponding relative quantities. The constitutive relation for the total electric displacement is

$$\boldsymbol{D}_\mathrm{t} = \varepsilon_\mathrm{t} \boldsymbol{E}\,,$$

where the complex permittivity ε_{t} is given by

$$\varepsilon_{\mathrm{t}} = \varepsilon_0 \varepsilon_{\mathrm{rt}} = \varepsilon_0 \left(1 + \chi_{\mathrm{e}} + \frac{\mathrm{j}\sigma}{\omega \varepsilon_0}\right)$$

with $\varepsilon_{\mathrm{rt}}$ being the complex relative permittivity. Both the conductivity and the susceptibility contribute to the imaginary part of the permittivity, $\mathrm{Im}\{\varepsilon_{\mathrm{t}}\} = \varepsilon_0 \mathrm{Im}\{\chi_{\mathrm{e}}\} + \mathrm{Re}\{\sigma/\omega\}$, and a complex value for ε_{t} means that the medium is absorbing. Usually, $\mathrm{Im}\{\chi_{\mathrm{e}}\}$ is associated with the "bound" charge current density and $\mathrm{Re}\{\sigma/\omega\}$ with the "free" charge current density, and absorption is determined by the sum of these two quantities. Note that for a free-source medium, $\sigma = 0$ and $\varepsilon_{\mathrm{rt}} = \varepsilon_{\mathrm{r}} = 1 + \chi_{\mathrm{e}}$. The simplest solution to Maxwell's equations in source-free media is the vector plane wave solution. The behavior of a vector plane wave in an isotropic medium is characterized by the dispersion relation

$$k = \omega \sqrt{\varepsilon \mu}\,,$$

which relates the wave number k to the properties of the medium and to the angular frequency ω of the wave. The dimensionless quantity

$$m = c \sqrt{\varepsilon \mu}$$

is the refractive index of the medium, where $c = 1/\sqrt{\varepsilon_0 \mu_0}$ is the speed of light in vacuum, and if $k_0 = \omega \sqrt{\varepsilon_0 \mu_0}$ is the wave number in free space, we see that

$$m = \frac{k}{k_0}\,.$$

The constitutive relations for anisotropic media are

$$\begin{aligned} \boldsymbol{D} &= \overline{\varepsilon} \boldsymbol{E}\,, \\ \boldsymbol{B} &= \overline{\mu} \boldsymbol{H}\,, \end{aligned} \tag{1.7}$$

where $\overline{\varepsilon}$ and $\overline{\mu}$ are the permittivity and permeability tensors, respectively. In our analysis we will consider electrically anisotropic media for which the permittivity is a tensor and the permeability is a scalar. Except for amorphous materials and crystals with cubic symmetry, the permittivity is always a tensor, and in general, the permittivity tensor of a crystal is symmetric. Since there exists a coordinate transformation that transforms a symmetric matrix into a diagonal matrix, we can take this coordinate system as reference frame and we have

$$\overline{\varepsilon} = \begin{bmatrix} \varepsilon_x & 0 & 0 \\ 0 & \varepsilon_y & 0 \\ 0 & 0 & \varepsilon_z \end{bmatrix}\,. \tag{1.8}$$

This reference frame is called the principal coordinate system and the three coordinate axes are known as the principal axes of the crystal. If $\varepsilon_x \neq \varepsilon_y \neq \varepsilon_z$,

the medium is biaxial, and if $\varepsilon = \varepsilon_x = \varepsilon_y$ and $\varepsilon \neq \varepsilon_z$, the medium is uniaxial. Orthorhombic, monoclinic and triclinic crystals are biaxial, while tetragonal, hexagonal and rhombohedral crystals are uniaxial. For uniaxial crystals, the principal axis that exhibits the anisotropy is called the optic axis. The crystal is positive uniaxial if $\varepsilon_z > \varepsilon$ and negative uniaxial if $\varepsilon_z < \varepsilon$.

In our analysis, we will investigate the electromagnetic response of isotropic, chiral media exposed to arbitrary external excitations. The lack of geometric symmetry between a particle and its mirror image is referred to as chirality or optical activity. A chiral medium is characterized by either a left- or a right-handedness in its microstructure, and as a result, left- and right-hand circularly polarized fields propagate through it with differing phase velocities. For a source-free, isotropic, chiral medium, the constitutive relations read as

$$\begin{aligned} \boldsymbol{D} &= \varepsilon \boldsymbol{E} + \beta\varepsilon \nabla \times \boldsymbol{E}\,, \\ \boldsymbol{B} &= \mu \boldsymbol{H} + \beta\mu \nabla \times \boldsymbol{H}\,, \end{aligned}$$

where the real number β is known as the chirality parameter. The Maxwell equations can be written compactly in matrix form as

$$\nabla \times \begin{bmatrix} \boldsymbol{E} \\ \boldsymbol{H} \end{bmatrix} = \boldsymbol{K} \begin{bmatrix} \boldsymbol{E} \\ \boldsymbol{H} \end{bmatrix}, \quad \nabla \cdot \begin{bmatrix} \boldsymbol{E} \\ \boldsymbol{H} \end{bmatrix} = 0\,, \tag{1.9}$$

where

$$\boldsymbol{K} = \frac{1}{1-\beta^2 k^2} \begin{bmatrix} \beta k^2 & \mathrm{j}\omega\mu \\ -\mathrm{j}\omega\varepsilon & \beta k^2 \end{bmatrix}$$

and $k = \omega\sqrt{\varepsilon\mu}$.

Without loss of generality and so as to simplify our notations we make the following transformations:

$$\begin{aligned} \boldsymbol{E} \to \frac{1}{\sqrt{\varepsilon_0}}\boldsymbol{E}, \boldsymbol{H} \to \frac{1}{\sqrt{\mu_0}}\boldsymbol{H}\,, \\ \boldsymbol{D} \to \sqrt{\varepsilon_0}\boldsymbol{D}, \boldsymbol{B} \to \sqrt{\mu_0}\boldsymbol{B}\,. \end{aligned}$$

As a result, the Maxwell equations for a free-source medium become more "symmetric":

$$\begin{aligned} \nabla \times \boldsymbol{E} &= \mathrm{j}k_0 \boldsymbol{B}\,, \\ \nabla \times \boldsymbol{H} &= -\mathrm{j}k_0 \boldsymbol{D}\,, \\ \nabla \cdot \boldsymbol{D} &= 0\,, \\ \nabla \cdot \boldsymbol{B} &= 0\,, \end{aligned} \tag{1.10}$$

the constitutive relations are given by (1.6) and (1.7) with ε and μ being the relative permittivity and permeability, respectively, the wave number is $k = k_0\sqrt{\varepsilon\mu}$, and the $\boldsymbol{K}$ matrix in (1.9) takes the form

$$\boldsymbol{K} = \frac{1}{1-\beta^2 k^2} \begin{bmatrix} \beta k^2 & \mathrm{j}k_0\mu \\ -\mathrm{j}k_0\varepsilon & \beta k^2 \end{bmatrix}. \tag{1.11}$$

1.2 Incident Field

In this section, we characterize the polarization state of vector plane waves and derive vector spherical wave expansions for the incident field. The first topic is relevant in the analysis of the scattered field, while the second one plays an important role in the derivation of the transition matrix.

1.2.1 Polarization

In addition to intensity and frequency, a monochromatic (time harmonic) electromagnetic wave is characterized by its state of polarization. This concept is useful when we discuss the polarization of the scattered field since the polarization state of a beam is changed on interaction with a particle.

We consider a right-handed Cartesian coordinate system $OXYZ$ with a fixed spatial orientation. This reference frame will be referred to as the global coordinate system or the laboratory coordinate system. The direction of propagation of the vector plane wave is specified by the unit vector $\boldsymbol{e}_k$, or equivalently, by the zenith and azimuth angles β and α, respectively (Fig. 1.2). The polarization state of the incident wave will be described in terms of the vertical polarization unit vector $\boldsymbol{e}_\alpha = \boldsymbol{e}_z \times \boldsymbol{e}_k / |\boldsymbol{e}_z \times \boldsymbol{e}_k|$ and the horizontal polarization vector $\boldsymbol{e}_\beta = \boldsymbol{e}_\alpha \times \boldsymbol{e}_k$. Note that other names for vertical polarization are TM polarization, parallel polarization and p polarization, while other names for horizontal polarization are TE polarization, perpendicular polarization and s polarization.

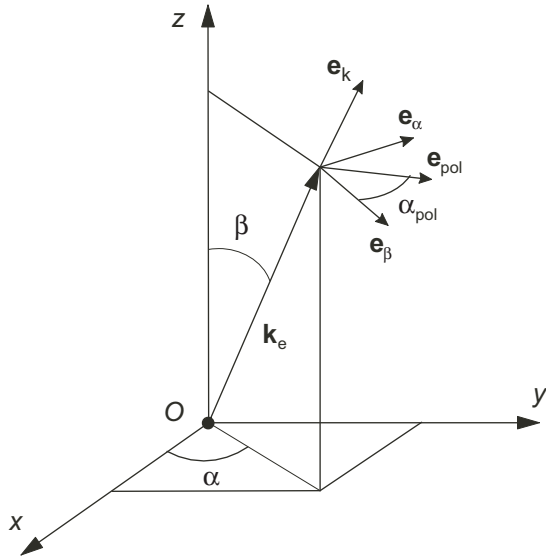

Fig. 1.2. Wave vector in the global coordinate system

In the frequency domain, a vector plane wave propagating in a medium with constant wave number $k_\mathrm{s} = k_0\sqrt{\varepsilon_\mathrm{s}\mu_\mathrm{s}}$ is given by

$$\boldsymbol{E}_\mathrm{e}(\boldsymbol{r}) = \boldsymbol{E}_\mathrm{e0}\mathrm{e}^{\mathrm{j}\boldsymbol{k}_\mathrm{e}\cdot\boldsymbol{r}}\,, \quad \boldsymbol{E}_\mathrm{e0}\cdot\boldsymbol{e}_k = 0\,, \tag{1.12}$$

where k_0 is the wave number in free space, $\boldsymbol{k}_\mathrm{e}$ is the wave vector, $\boldsymbol{k}_\mathrm{e} = k_\mathrm{s}\boldsymbol{e}_k$, $\boldsymbol{E}_\mathrm{e0}$ is the complex amplitude vector,

$$\boldsymbol{E}_\mathrm{e0} = E_{\mathrm{e0},\beta}\boldsymbol{e}_\beta + E_{\mathrm{e0},\alpha}\boldsymbol{e}_\alpha\,,$$

and $E_{\mathrm{e0},\beta}$ and $E_{\mathrm{e0},\alpha}$ are the complex amplitudes in the β- and α-direction, respectively. An equivalent representation for $\boldsymbol{E}_\mathrm{e0}$ is

$$\boldsymbol{E}_\mathrm{e0} = |\boldsymbol{E}_\mathrm{e0}|\,\boldsymbol{e}_\mathrm{pol}\,, \tag{1.13}$$

where $\boldsymbol{e}_\mathrm{pol}$ is the complex polarization unit vector, $|\boldsymbol{e}_\mathrm{pol}| = 1$, and

$$\boldsymbol{e}_\mathrm{pol} = \frac{1}{|\boldsymbol{E}_\mathrm{e0}|}\left(E_{\mathrm{e0},\beta}\boldsymbol{e}_\beta + E_{\mathrm{e0},\alpha}\boldsymbol{e}_\alpha\right)\,.$$

Inserting (1.13) into (1.12), gives the representation

$$\boldsymbol{E}_\mathrm{e}(\boldsymbol{r}) = |\boldsymbol{E}_\mathrm{e0}|\,\boldsymbol{e}_\mathrm{pol}\mathrm{e}^{\mathrm{j}\boldsymbol{k}_\mathrm{e}\cdot\boldsymbol{r}}\,, \quad \boldsymbol{e}_\mathrm{pol}\cdot\boldsymbol{e}_k = 0\,,$$

and obviously, $|\boldsymbol{E}_\mathrm{e}(\boldsymbol{r})| = |\boldsymbol{E}_\mathrm{e0}|$.

There are three ways of describing the polarization state of vector plane waves.

1. Setting

$$\begin{aligned} E_{\mathrm{e0},\beta} &= a_\beta\mathrm{e}^{\mathrm{j}\delta_\beta}\,,\\ E_{\mathrm{e0},\alpha} &= a_\alpha\mathrm{e}^{\mathrm{j}\delta_\alpha}\,, \end{aligned} \tag{1.14}$$

where a_β and a_α are the real non-negative amplitudes, and δ_β and δ_α are the real phases, we characterize the polarization state of a vector plane wave by a_β, a_α and the phase difference $\Delta\delta = \delta_\beta - \delta_\alpha$.

2. Taking into account the representation of a vector plane wave in the time domain

$$\boldsymbol{E}_\mathrm{e}(\boldsymbol{r},t) = \mathrm{Re}\left\{\boldsymbol{E}_\mathrm{e}(\boldsymbol{r})\mathrm{e}^{-\mathrm{j}\omega t}\right\} = \mathrm{Re}\left\{\boldsymbol{E}_\mathrm{e0}\mathrm{e}^{\mathrm{j}(\boldsymbol{k}_\mathrm{e}\cdot\boldsymbol{r}-\omega t)}\right\}\,,$$

where $\boldsymbol{E}_\mathrm{e}(\boldsymbol{r},t)$ is the real electric vector, we deduce that (cf. (1.14))

$$\begin{aligned} E_{\mathrm{e},\beta}(\boldsymbol{r},t) &= a_\beta\cos\left(\delta_\beta + \boldsymbol{k}_\mathrm{e}\cdot\boldsymbol{r} - \omega t\right)\,,\\ E_{\mathrm{e},\alpha}(\boldsymbol{r},t) &= a_\alpha\cos\left(\delta_\alpha + \boldsymbol{k}_\mathrm{e}\cdot\boldsymbol{r} - \omega t\right)\,, \end{aligned}$$

where

$$\boldsymbol{E}_\mathrm{e}(\boldsymbol{r},t) = E_{\mathrm{e},\beta}(\boldsymbol{r},t)\boldsymbol{e}_\beta + E_{\mathrm{e},\alpha}(\boldsymbol{r},t)\boldsymbol{e}_\alpha\,.$$

At any fixed point in space the endpoint of the real electric vector describes an ellipse which is also known as the vibration ellipse [17]. The vibration ellipse can be traced out in two opposite senses: clockwise and anticlockwise. If the real electric vector rotates clockwise, as viewed by an observer looking in the direction of propagation, the polarization of the ellipse is right-handed and the polarization is left-handed if the electric vector rotates anticlockwise. The two opposite senses of rotation lead to a classification of vibration ellipses according to their handedness. In addition to its handedness, a vibration ellipse is characterized by $E_0 = \sqrt{a^2 + b^2}$, where a and b are the semi-major and semi-minor axes of the ellipse, the orientation angle ψ and the ellipticity angle χ (Fig. 1.3). The orientation angle ψ is the angle between the α-axis and the major axis, and $\psi \in [0, \pi)$. The ellipticity angle χ is usually expressed as $\tan\chi = \pm b/a$, where the plus sign corresponds to right-handed elliptical polarization, and $\chi \in [-\pi/4, \pi/4]$.

We now proceed to relate the complex amplitudes $E_{\mathrm{e}0,\beta}$ and $E_{\mathrm{e}0,\alpha}$ to the ellipsometric parameters E_0, ψ and χ. Representing the semi-axes of the vibration ellipse as

$$\begin{aligned} b &= \pm E_0 \sin\chi\,, \\ a &= E_0 \cos\chi\,, \end{aligned} \tag{1.15}$$

where the plus sign corresponds to right-handed polarization, and taking into account the parametric representation of the ellipse in the principal coordinate system $O\alpha'\beta'$

$$\begin{aligned} E'_{\mathrm{e},\beta}(\boldsymbol{r},t) &= \pm b \sin\left(\boldsymbol{k}_{\mathrm{e}} \cdot \boldsymbol{r} - \omega t\right)\,, \\ E'_{\mathrm{e},\alpha}(\boldsymbol{r},t) &= a \cos\left(\boldsymbol{k}_{\mathrm{e}} \cdot \boldsymbol{r} - \omega t\right)\,, \end{aligned}$$

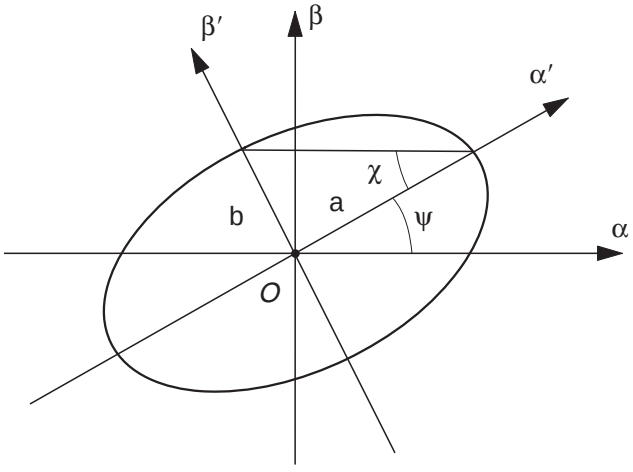

Fig. 1.3. Vibration ellipse

we obtain

$$E'_{\mathrm{e},\beta}(\boldsymbol{r},t) = E_0 \sin\chi \sin\left(\boldsymbol{k}_\mathrm{e}\cdot\boldsymbol{r}-\omega t\right) = E_0 \sin\chi \cos\left(\boldsymbol{k}_\mathrm{e}\cdot\boldsymbol{r}-\omega t-\frac{\pi}{2}\right) ,$$
$$E'_{\mathrm{e},\alpha}(\boldsymbol{r},t) = E_0 \cos\chi \cos\left(\boldsymbol{k}_\mathrm{e}\cdot\boldsymbol{r}-\omega t\right) .$$

In the frequency domain, the complex amplitude vector $\boldsymbol{E}'_{\mathrm{e}0}$ defined as

$$\boldsymbol{E}'_\mathrm{e}(\boldsymbol{r},t) = \mathrm{Re}\left\{\boldsymbol{E}'_{\mathrm{e}0}\mathrm{e}^{\mathrm{j}(\boldsymbol{k}_\mathrm{e}\cdot\boldsymbol{r}-\omega t)}\right\} ,$$

where

$$\boldsymbol{E}'_\mathrm{e}(\boldsymbol{r},t) = E'_{\mathrm{e},\beta}(\boldsymbol{r},t)\boldsymbol{e}'_\beta + E'_{\mathrm{e},\alpha}(\boldsymbol{r},t)\boldsymbol{e}'_\alpha ,$$

has the components

$$E'_{\mathrm{e}0,\beta} = -\mathrm{j}E_0 \sin\chi ,$$
$$E'_{\mathrm{e}0,\alpha} = E_0 \cos\chi .$$

Using the transformation rule for rotation of a two-dimensional coordinate system we obtain the desired relations

$$E_{\mathrm{e}0,\beta} = E_0\left(\cos\chi\sin\psi - \mathrm{j}\sin\chi\cos\psi\right) ,$$
$$E_{\mathrm{e}0,\alpha} = E_0\left(\cos\chi\cos\psi + \mathrm{j}\sin\chi\sin\psi\right) ,$$

and

$$\begin{aligned}\boldsymbol{e}_\mathrm{pol} = {} & \left(\cos\chi\sin\psi - \mathrm{j}\sin\chi\cos\psi\right)\boldsymbol{e}_\beta \\ & + \left(\cos\chi\cos\psi + \mathrm{j}\sin\chi\sin\psi\right)\boldsymbol{e}_\alpha . \end{aligned} \tag{1.16}$$

If $b = 0$, the ellipse degenerates into a straight line and the wave is linearly polarized. In this specific case $\chi = 0$ and

$$E_{\mathrm{e}0,\beta} = E_0\sin\psi = E_0\cos\left(\frac{\pi}{2}-\psi\right) = E_0\cos\alpha_\mathrm{pol} ,$$
$$E_{\mathrm{e}0,\alpha} = E_0\cos\psi = E_0\sin\left(\frac{\pi}{2}-\psi\right) = E_0\sin\alpha_\mathrm{pol} ,$$

where α_pol is the polarization angle and

$$\alpha_\mathrm{pol} = \pi/2 - \psi , \quad \alpha_\mathrm{pol} \in (-\pi/2, \pi/2] . \tag{1.17}$$

In view of (1.16) and (1.17) it is apparent that the polarization unit vector is real and is given by

$$\boldsymbol{e}_\mathrm{pol} = \cos\alpha_\mathrm{pol}\boldsymbol{e}_\beta + \sin\alpha_\mathrm{pol}\boldsymbol{e}_\alpha . \tag{1.18}$$

If $a = b$, the ellipse is a circle and the wave is circularly polarized. We have $\tan\chi = \pm 1$, which implies $\chi = \pm\pi/4$, and choosing $\psi = \pi/2$, we obtain

$$E_{\mathrm{e}0,\beta} = \frac{\sqrt{2}}{2} E_0 \,,$$

$$E_{\mathrm{e}0,\alpha} = \pm \mathrm{j} \frac{\sqrt{2}}{2} E_0 \,.$$

The polarization unit vectors of right- and left-circularly polarized waves then become

$$\boldsymbol{e}_{\mathrm{R}} = \frac{\sqrt{2}}{2} \left(\boldsymbol{e}_\beta + \mathrm{j} \boldsymbol{e}_\alpha \right) \,,$$

$$\boldsymbol{e}_{\mathrm{L}} = \frac{\sqrt{2}}{2} \left(\boldsymbol{e}_\beta - \mathrm{j} \boldsymbol{e}_\alpha \right) \,,$$

and we see that these basis vectors are orthonormal in the sense that $\boldsymbol{e}_{\mathrm{R}} \cdot \boldsymbol{e}_{\mathrm{R}}^* = 1$, $\boldsymbol{e}_{\mathrm{L}} \cdot \boldsymbol{e}_{\mathrm{L}}^* = 1$ and $\boldsymbol{e}_{\mathrm{R}} \cdot \boldsymbol{e}_{\mathrm{L}}^* = 0$.

3. The polarization characteristics of the incident field can also be described by the coherency and Stokes vectors. Although the ellipsometric parameters completely specify the polarization state of a monochromatic wave, they are difficult to measure directly (with the exception of the intensity E_0^2). In contrast, the Stokes parameters are measurable quantities and are of greater usefulness in scattering problems. The coherency vector is defined as

$$\boldsymbol{J}_{\mathrm{e}} = \frac{1}{2} \sqrt{\frac{\varepsilon_{\mathrm{s}}}{\mu_{\mathrm{s}}}} \begin{bmatrix} E_{\mathrm{e}0,\beta} E_{\mathrm{e}0,\beta}^* \\ E_{\mathrm{e}0,\beta} E_{\mathrm{e}0,\alpha}^* \\ E_{\mathrm{e}0,\alpha} E_{\mathrm{e}0,\beta}^* \\ E_{\mathrm{e}0,\alpha} E_{\mathrm{e}0,\alpha}^* \end{bmatrix} \,, \tag{1.19}$$

while the Stokes vector is given by

$$\boldsymbol{I}_{\mathrm{e}} = \begin{bmatrix} I_{\mathrm{e}} \\ Q_{\mathrm{e}} \\ U_{\mathrm{e}} \\ V_{\mathrm{e}} \end{bmatrix} = \boldsymbol{D} \boldsymbol{J}_{\mathrm{e}} = \frac{1}{2} \sqrt{\frac{\varepsilon_{\mathrm{s}}}{\mu_{\mathrm{s}}}} \begin{bmatrix} |E_{\mathrm{e}0,\beta}|^2 + |E_{\mathrm{e}0,\alpha}|^2 \\ |E_{\mathrm{e}0,\beta}|^2 - |E_{\mathrm{e}0,\alpha}|^2 \\ -E_{\mathrm{e}0,\alpha} E_{\mathrm{e}0,\beta}^* - E_{\mathrm{e}0,\beta} E_{\mathrm{e}0,\alpha}^* \\ \mathrm{j} \left(E_{\mathrm{e}0,\alpha} E_{\mathrm{e}0,\beta}^* - E_{\mathrm{e}0,\beta} E_{\mathrm{e}0,\alpha}^* \right) \end{bmatrix} \,, \tag{1.20}$$

where $\boldsymbol{D}$ is a transformation matrix and

$$\boldsymbol{D} = \begin{bmatrix} 1 & 0 & 0 & 1 \\ 1 & 0 & 0 & -1 \\ 0 & -1 & -1 & 0 \\ 0 & -\mathrm{j} & \mathrm{j} & 0 \end{bmatrix} \,. \tag{1.21}$$

The first Stokes parameter I_{e},

$$I_{\mathrm{e}} = \frac{1}{2}\sqrt{\frac{\varepsilon_{\mathrm{s}}}{\mu_{\mathrm{s}}}}\,|\boldsymbol{E}_{\mathrm{e}0}|^2$$

is the intensity of the wave, while the Stokes parameters Q_{e}, U_{e} and V_{e} describe the polarization state of the wave. The Stokes parameters are defined with respect to a reference plane containing the direction of wave propagation, and Q_{e} and U_{e} depend on the choice of the reference frame. If the unit vectors $\boldsymbol{e}_\beta$ and $\boldsymbol{e}_\alpha$ are rotated through an angle φ (Fig. 1.4), the transformation from the Stokes vector $\boldsymbol{I}_{\mathrm{e}}$ to the Stokes vector $\boldsymbol{I}'_{\mathrm{e}}$ (relative to the rotated unit vectors $\boldsymbol{e}'_\beta$ and $\boldsymbol{e}'_\alpha$) is given by

$$\boldsymbol{I}'_{\mathrm{e}} = \boldsymbol{L}\,(\varphi)\,\boldsymbol{I}_{\mathrm{e}}\,, \tag{1.22}$$

where the Stokes rotation matrix $\boldsymbol{L}$ is

$$\boldsymbol{L}\,(\varphi) = \begin{bmatrix} 1 & 0 & 0 & 0 \\ 0 & \cos 2\varphi & -\sin 2\varphi & 0 \\ 0 & \sin 2\varphi & \cos 2\varphi & 0 \\ 0 & 0 & 0 & 1 \end{bmatrix}. \tag{1.23}$$

The Stokes parameters can be expressed in terms of a_β, a_α and $\Delta\delta$ as (omitting the factor $\frac{1}{2}\sqrt{\varepsilon_{\mathrm{s}}/\mu_{\mathrm{s}}}$)

$$\begin{aligned} I_{\mathrm{e}} &= a_\beta^2 + a_\alpha^2\,, \\ Q_{\mathrm{e}} &= a_\beta^2 - a_\alpha^2\,, \\ U_{\mathrm{e}} &= -2a_\beta a_\alpha \cos\Delta\delta\,, \\ V_{\mathrm{e}} &= 2a_\beta a_\alpha \sin\Delta\delta\,, \end{aligned}$$

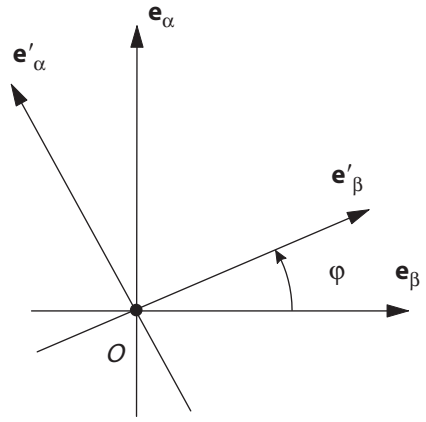

Fig. 1.4. Rotation of the polarization unit vectors through the angle φ

and in terms of E_0, ψ and χ, as

$$\begin{aligned} I_{\rm e} &= E_0^2\,, \\ Q_{\rm e} &= -E_0^2 \cos 2\chi \cos 2\psi\,, \\ U_{\rm e} &= -E_0^2 \cos 2\chi \sin 2\psi\,, \\ V_{\rm e} &= -E_0^2 \sin 2\chi\,. \end{aligned}$$

The above relations show that the Stokes parameters carry information about the amplitudes and the phase difference, and are operationally defined in terms of measurable quantities (intensities). For a linearly polarized plane wave, $\chi = 0$ and $V_{\rm e} = 0$, while for a circularly polarized plane wave, $\chi = \pm\pi/4$ and $Q_{\rm e} = U_{\rm e} = 0$. Thus, the Stokes vector of a linearly polarized wave of unit amplitude is given by $\boldsymbol{I}_{\rm e} = [1, \cos 2\alpha_{\rm pol}, -\sin 2\alpha_{\rm pol}, 0]^{\rm T}$, while the Stokes vector of a circularly polarized wave of unit amplitude is $\boldsymbol{I}_{\rm e} = [1, 0, 0, \mp 1]^{\rm T}$.

The Stokes parameters of a monochromatic plane wave are not independent since

$$I_{\rm e}^2 = Q_{\rm e}^2 + U_{\rm e}^2 + V_{\rm e}^2\,, \tag{1.24}$$

and we may conclude that only three parameters are required to characterize the state of polarization. For quasi-monochromatic light, the amplitude of the electric field fluctuate in time and the Stokes parameters are expressed in terms of the time-averaged quantities $\langle E_{{\rm e}0,p} E^*_{{\rm e}0,q}\rangle$, where p and q stand for β and α. In this case, the equality in (1.24) is replaced by the inequality

$$I_{\rm e}^2 \geq Q_{\rm e}^2 + U_{\rm e}^2 + V_{\rm e}^2\,,$$

and the quantity

$$P = \frac{\sqrt{Q_{\rm e}^2 + U_{\rm e}^2 + V_{\rm e}^2}}{I_{\rm e}}$$

is known as the degree of polarization of the quasi-monochromatic beam. For natural (unpolarized) light, $P = 0$, while for fully polarized light $P = 1$. The Stokes vector defined by (1.20) is one possible representation of polarization. Other representations are discussed by Hovenier and van der Mee [101], while a detailed discussion of the polarimetric definitions can be found in [17,169,171].

1.2.2 Vector Spherical Wave Expansion

The derivation of the transition matrix in the framework of the null-field method requires the expansion of the incident field in terms of (localized) vector spherical wave functions. This expansion must be provided in the particle coordinate system, where in general, the particle coordinate system $Oxyz$ is obtained by rotating the global coordinate system $OXYZ$ through the Euler angles $\alpha_{\rm p}$, $\beta_{\rm p}$ and $\gamma_{\rm p}$ (Fig. 1.5). In our analysis, vector plane waves and Gaussian beams are considered as external excitations.

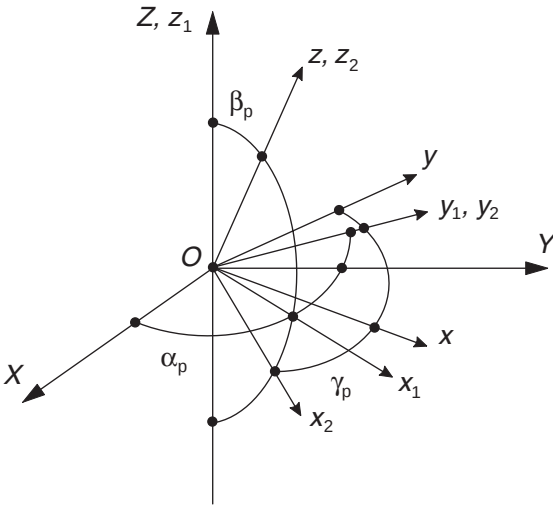

Fig. 1.5. Euler angles α_p, β_p and γ_p specifying the orientation of the particle coordinate system $Oxyz$ with respect to the global coordinate system $OXYZ$. The transformation $OXYZ \to Oxyz$ is achieved by means of three successive rotations: (1) rotation about the Z-axis through α_p, $OXYZ \to Ox_1y_1z_1$, (2) rotation about the y_1-axis through β_p, $Ox_1y_1z_1 \to Ox_2y_2z_2$ and (3) rotation about the z_2-axis through γ_p, $Ox_2y_2z_2 \to Oxyz$

Vector Plane Wave

We consider a vector plane wave of unit amplitude propagating in the direction $(\beta_\mathrm{g}, \alpha_\mathrm{g})$ with respect to the global coordinate system. Passing from spherical coordinates to Cartesian coordinates and using the transformation rules under coordinate rotations we may compute the spherical angles β and α of the wave vector in the particle coordinate system. Thus, in the particle coordinate system we have the representation

$$\boldsymbol{E}_\mathrm{e}(\boldsymbol{r}) = \boldsymbol{e}_\mathrm{pol}\mathrm{e}^{\mathrm{j}\boldsymbol{k}_\mathrm{e}\cdot\boldsymbol{r}}\,, \quad \boldsymbol{e}_\mathrm{pol}\cdot\boldsymbol{e}_k = 0\,,$$

where as before, $\boldsymbol{k}_\mathrm{e} = k_\mathrm{s}\boldsymbol{e}_k$.

The vector spherical waves expansion of the incident field reads as

$$\boldsymbol{E}_\mathrm{e}(\boldsymbol{r}) = \sum_{n=1}^{\infty}\sum_{m=-n}^{n} a_{mn}\boldsymbol{M}^1_{mn}\left(k_\mathrm{s}\boldsymbol{r}\right) + b_{mn}\boldsymbol{N}^1_{mn}\left(k_\mathrm{s}\boldsymbol{r}\right)\,, \tag{1.25}$$

where the expansion coefficients are given by [9, 228]

$$\begin{aligned} a_{mn} &= 4\mathrm{j}^n\boldsymbol{e}_\mathrm{pol}\cdot\boldsymbol{m}^*_{mn}(\beta,\alpha) \\ &= -\frac{4\mathrm{j}^n}{\sqrt{2n(n+1)}}\boldsymbol{e}_\mathrm{pol}\cdot\left[\mathrm{j}m\pi_n^{|m|}(\beta)\boldsymbol{e}_\beta + \tau_n^{|m|}(\beta)\boldsymbol{e}_\alpha\right]\mathrm{e}^{-\mathrm{j}m\alpha}\,, \end{aligned}$$

$$b_{mn} = -4\mathrm{j}^{n+1}\boldsymbol{e}_{\mathrm{pol}} \cdot \boldsymbol{n}^*_{mn}(\beta,\alpha)$$
$$= -\frac{4\mathrm{j}^{n+1}}{\sqrt{2n(n+1)}}\boldsymbol{e}_{\mathrm{pol}} \cdot \left[\tau_n^{|m|}(\beta)\boldsymbol{e}_\beta - \mathrm{j}m\pi_n^{|m|}(\beta)\boldsymbol{e}_\alpha\right] \mathrm{e}^{-\mathrm{j}m\alpha}\,. \quad (1.26)$$

To give a justification of the above expansion we consider the integral representation

$$\boldsymbol{e}_{\mathrm{pol}}(\beta,\alpha)\mathrm{e}^{\mathrm{j}\boldsymbol{k}_{\mathrm{e}}(\beta,\alpha)\cdot\boldsymbol{r}} = \int_0^{2\pi}\int_0^{\pi} \boldsymbol{e}_{\mathrm{pol}}(\beta,\alpha)\mathrm{e}^{\mathrm{j}\boldsymbol{k}(\beta',\alpha')\cdot\boldsymbol{r}}$$
$$\times\delta(\alpha'-\alpha)\delta(\cos\beta'-\cos\beta)\sin\beta'\,\mathrm{d}\beta'\,\mathrm{d}\alpha'\,, \quad (1.27)$$

and expand the tangential field

$$\boldsymbol{f}\,(\beta,\alpha,\beta',\alpha') = \boldsymbol{e}_{\mathrm{pol}}(\beta,\alpha)\delta(\alpha'-\alpha)\delta(\cos\beta'-\cos\beta) \quad (1.28)$$

in vector spherical harmonics

$$\boldsymbol{f}\,(\beta,\alpha,\beta',\alpha') = \frac{1}{4\pi\mathrm{j}^n}\sum_{n=1}^{\infty}\sum_{m=-n}^{n} a_{mn}\boldsymbol{m}_{mn}\,(\beta',\alpha') + \mathrm{j}b_{mn}\boldsymbol{n}_{mn}\,(\beta',\alpha')\,. \quad (1.29)$$

Using the orthogonality relations of vector spherical harmonics we see that the expansion coefficients a_{mn} and b_{mn} are given by

$$a_{mn} = 4\mathrm{j}^n\int_0^{2\pi}\int_0^{\pi} \boldsymbol{f}\,(\beta,\alpha,\beta',\alpha')\cdot\boldsymbol{m}^*_{mn}\,(\beta',\alpha')\sin\beta'\,\mathrm{d}\beta'\,\mathrm{d}\alpha'$$
$$= 4\mathrm{j}^n\boldsymbol{e}_{\mathrm{pol}}(\beta,\alpha)\cdot\boldsymbol{m}^*_{mn}(\beta,\alpha)\,,$$
$$b_{mn} = -4\mathrm{j}^{n+1}\int_0^{2\pi}\int_0^{\pi} \boldsymbol{f}\,(\beta,\alpha,\beta',\alpha')\cdot\boldsymbol{n}^*_{mn}\,(\beta',\alpha')\sin\beta'\,\mathrm{d}\beta'\,\mathrm{d}\alpha'$$
$$= -4\mathrm{j}^{n+1}\boldsymbol{e}_{\mathrm{pol}}(\beta,\alpha)\cdot\boldsymbol{n}^*_{mn}(\beta,\alpha)\,.$$

Substituting (1.28) and (1.29) into (1.27) and taking into account the integral representations for the regular vector spherical wave functions (cf. (B.26) and (B.27)) yields (1.25).

The polarization unit vector of a linearly polarized vector plane wave is given by (1.18). If the vector plane wave propagates along the z-axis we have $\beta = \alpha = 0$ and for $\beta = 0$, the spherical vector harmonics are zero unless $m = \pm 1$. Using the special values of the angular functions π_n^1 and τ_n^1 when $\beta = 0$,

$$\pi_n^1\,(0) = \tau_n^1\,(0) = \frac{1}{2\sqrt{2}}\sqrt{n(n+1)(2n+1)}\,,$$

we obtain

$$a_{\pm 1n} = -\mathrm{j}^n\sqrt{2n+1}\,(\pm\mathrm{j}\cos\alpha_{\mathrm{pol}} + \sin\alpha_{\mathrm{pol}})\,,$$
$$b_{\pm 1n} = -\mathrm{j}^{n+1}\sqrt{2n+1}\,(\cos\alpha_{\mathrm{pol}} \mp \mathrm{j}\sin\alpha_{\mathrm{pol}})\,.$$

Thus, for a vector plane wave polarized along the x-axis we have

$$a_{1n} = -a_{-1n} = \mathrm{j}^{n-1}\sqrt{2n+1}\,,$$
$$b_{1n} = b_{-1n} = \mathrm{j}^{n-1}\sqrt{2n+1}\,,$$

while for a vector plane wave polarized along the y-axis we have

$$a_{1n} = a_{-1n} = \mathrm{j}^{n-2}\sqrt{2n+1}\,,$$
$$b_{1n} = -b_{-1n} = \mathrm{j}^{n-2}\sqrt{2n+1}\,.$$

Gaussian Beam

Many optical particle sizing instruments and particle characterization methods are based on scattering by particles illuminated with laser beams. A laser beam has a Gaussian intensity distribution and the often used appellation Gaussian beam appears justified. A mathematical description of a Gaussian beam relies on Davis approximations [45]. An nth Davis beam corresponds to the first n terms in the series expansion of the exact solution to the Maxwell equations in power of the beam parameter s,

$$s = \frac{w_0}{l}\,,$$

where w_0 is the waist radius and l is the diffraction length, $l = k_\mathrm{s} w_0^2$. According to Barton and Alexander [9], the first-order approximation is accurate to $s < 0.07$, while the fifth-order is accurate to $s < 0.02$, if the maximum percent error of the solution is less than 1.2%. Each nth Davis beam appears under three versions which are: the mathematical conservative version, the L-version and the symmetrized version [145]. None of these beams are exact solutions to the Maxwell equations, so that each nth Davis beam can be considered as a "pseudo-electromagnetic" field.

In the $\boldsymbol{T}$-matrix method a Gaussian beam is expanded in terms of vector spherical wave functions by replacing the pseudo-electromagnetic field of an nth Davis beam by an equivalent electromagnetic field, so that both fields have the same values on a spherical surface [81, 83, 85]. As a consequence of the equivalence method, the expansion coefficients (or the beam shape coefficients) are computed by integrating the incident field over the spherical surface. Because these fields are rapidly varying, the evaluation of the coefficients by numerical integration requires dense grids in both the θ- and φ-direction and the computer run time is excessively long.

For weakly focused Gaussian beams, the generalized localized approximation to the beam shape coefficients represents a pleasing alternative (see, for instance, [84, 87]). The form of the analytical approximation was found in part by analogy to the propagation of geometrical light rays and in part by numerical experiments. This is not a rigorous method but its use simplifies and significantly speeds up the numerical computations. A justification of

the localized approximations for both on- and off-axis beams has been given by Lock and Gouesbet [145] and Gouesbet and Lock [82]. We note that the focused beam generated by the localized approximation is a good approximation to a Gaussian beam for $s \leq 0.1$.

We consider the geometry depicted in Fig. 1.6 and assume that the middle of the beam waist is located at the point O_b. The particle coordinate system $Oxyz$ and the beam coordinate system $O_\mathrm{b}x_\mathrm{b}y_\mathrm{b}z_\mathrm{b}$ have identical spatial orientation, and the position vector of the particle center O in the system $O_\mathrm{b}x_\mathrm{b}y_\mathrm{b}z_\mathrm{b}$ is denoted by $\boldsymbol{r}_0$. The Gaussian beam is of unit amplitude, propagates along the z_b-axis and is linearly polarized along the x_b-axis. In the particle coordinate system, the expansion of the Gaussian beam in vector spherical wave functions is given by

$$\boldsymbol{E}_\mathrm{e}(\boldsymbol{r}) = \sum_{n=1}^{\infty} \sum_{m=-n}^{n} \widetilde{a}_{mn} \boldsymbol{M}_{mn}^{1}\left(k_\mathrm{s}\boldsymbol{r}\right) + \widetilde{b}_{mn} \boldsymbol{N}_{mn}^{1}\left(k_\mathrm{s}\boldsymbol{r}\right) ,$$

and the generalized localized approximation to the Davis first-order beam is

$$\widetilde{a}_{mn} = K_{mn} \Psi_0 \mathrm{e}^{\mathrm{j}k_\mathrm{s}z_0} \left[\mathrm{e}^{\mathrm{j}(m-1)\varphi_0} J_{m-1}\left(u\right) - \mathrm{e}^{\mathrm{j}(m+1)\varphi_0} J_{m+1}\left(u\right)\right] ,$$

$$\widetilde{b}_{mn} = K_{mn} \Psi_0 \mathrm{e}^{\mathrm{j}k_\mathrm{s}z_0} \left[\mathrm{e}^{\mathrm{j}(m-1)\varphi_0} J_{m-1}\left(u\right) + \mathrm{e}^{\mathrm{j}(m+1)\varphi_0} J_{m+1}\left(u\right)\right] ,$$

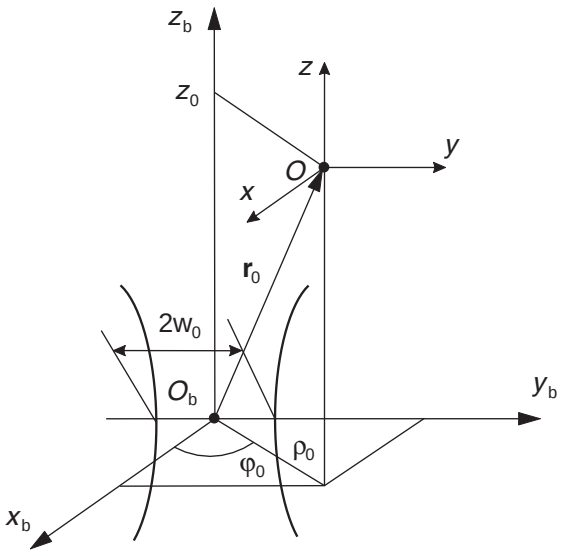

Fig. 1.6. The particle coordinate system $Oxyz$ and the beam coordinate system $Ox_\mathrm{b}y_\mathrm{b}z_\mathrm{b}$ have the same spatial orientation

where (ρ_0, φ_0, z_0) are the cylindrical coordinates of $\boldsymbol{r}_0$,

$$\Psi_0 = \mathrm{j}Q \exp\left(-\mathrm{j}Q\frac{\rho_0^2+\rho_n^2}{w_0^2}\right), \quad Q = \frac{1}{\mathrm{j}-2z_0/l}, \quad \rho_n = \frac{1}{k_s}\left(n+\frac{1}{2}\right),$$

and

$$u = 2Q\frac{\rho_0\rho_n}{w_0^2}.$$

The normalization constant K_{mn} is given by

$$K_{mn} = 2\mathrm{j}^n\sqrt{\frac{n(n+1)}{2n+1}}$$

for $m = 0$, and by

$$K_{mn} = (-1)^{|m|}\frac{\mathrm{j}^{n+|m|}}{\left(n+\frac{1}{2}\right)^{|m|-1}}\sqrt{\frac{2n+1}{n(n+1)}\cdot\frac{(n+|m|)!}{(n-|m|)!}}$$

for $m \neq 0$. If both coordinate systems coincide ($\rho_0 = 0$), all expansion coefficients are zero unless $m = \pm 1$ and

$$\widetilde{a}_{1n} = -\widetilde{a}_{-1n} = \mathrm{j}^{n-1}\sqrt{2n+1}\exp\left(-\frac{\rho_n^2}{w_0^2}\right),$$

$$\widetilde{b}_{1n} = \widetilde{b}_{-1n} = \mathrm{j}^{n-1}\sqrt{2n+1}\exp\left(-\frac{\rho_n^2}{w_0^2}\right).$$

The Gaussian beam becomes a plane wave if w_0 tends to infinity and for this specific case, the expressions of the expansion coefficients reduce to those of a vector plane wave.

We next consider the general situation depicted in Fig. 1.7 and assume that the auxiliary coordinate system $O_\mathrm{b}X_\mathrm{b}Y_\mathrm{b}Z_\mathrm{b}$ and the global coordinate system $OXYZ$ have the same spatial orientation. The Gaussian beam propagates in a direction characterized by the zenith and azimuth angles β_g and α_g, respectively, while the polarization unit vector encloses the angle α_pol with the x_b-axis of the beam coordinate system $O_\mathrm{b}x_\mathrm{b}y_\mathrm{b}z_\mathrm{b}$. As before, the particle coordinate system is obtained by rotating the global coordinate system through the Euler angles α_p, β_p and γ_p. The expansion of the Gaussian beam in the particle coordinate system is obtained by using the addition theorem for vector spherical wave functions under coordinate rotations (cf. (B.52) and (B.53)), and the result is

$$\boldsymbol{E}_\mathrm{e}(\boldsymbol{r}) = \sum_{n=1}^{\infty}\sum_{m=-n}^{n} a_{mn}\boldsymbol{M}_{mn}^1(k_\mathrm{s}\boldsymbol{r}) + b_{mn}\boldsymbol{N}_{mn}^1(k_\mathrm{s}\boldsymbol{r}),$$

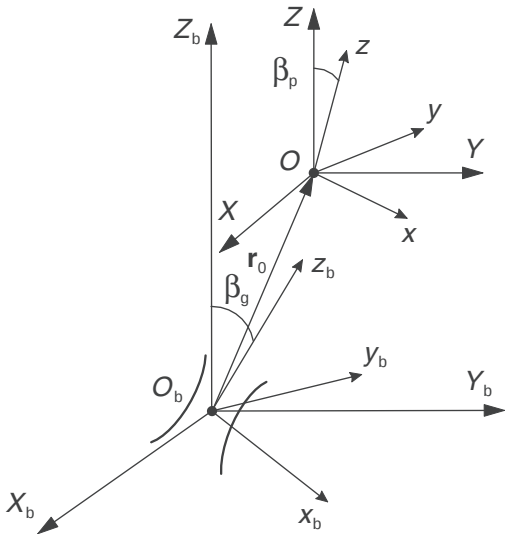

Fig. 1.7. General orientations of the particle and beam coordinate systems

where

$$a_{mn} = \sum_{m'=-n}^{n} \sum_{m''=-n}^{n} D^n_{m'm''}\left(-\alpha_{\rm pol}, -\beta_{\rm g}, -\alpha_{\rm g}\right) D^n_{m''m}\left(\alpha_p, \beta_p, \gamma_p\right) \widetilde{a}_{m'n}\,,$$

$$b_{mn} = \sum_{m'=-n}^{n} \sum_{m''=-n}^{n} D^n_{m'm''}\left(-\alpha_{\rm pol}, -\beta_{\rm g}, -\alpha_{\rm g}\right) D^n_{m''m}\left(\alpha_p, \beta_p, \gamma_p\right) \widetilde{b}_{m'n}\,,$$

and the Wigner D-functions $D^n_{m''m}$ are given by (B.34).

Remark. Another representation of a Gaussian beam is the integral representation over plane waves [48, 116]. This can be obtained by using Fourier analysis and by replacing the pseudo-vector potential of a nth Davis beam by an equivalent vector potential (satisfying the wave equation), so that both vector fields have the same values in a plane $z = \text{const}$.

1.3 Internal Field

To solve the scattering problem in the framework of the null-field method it is necessary to approximate the internal field by a suitable system of vector functions. For isotropic particles, regular vector spherical wave functions of the interior wave equation are used for internal field approximations. In this section we derive new systems of vector functions for anisotropic and chiral particles by representing the electromagnetic fields (propagating in anisotropic

and chiral media) as integrals over plane waves. For each plane wave, we solve the Maxwell equations and derive the dispersion relation following the treatment of Kong [122]. The dispersion relation which relates the amplitude of the wave vector $\boldsymbol{k}$ to the properties of the medium enable us to reduce the three-dimensional integrals to two-dimensional integrals over the unit sphere. The integral representations are then transformed into series representations by expanding appropriate tangential vector functions in vector spherical harmonics. The new basis functions are the vector quasi-spherical wave functions (for anisotropic media) and the vector spherical wave functions of left- and right-handed type (for chiral media).

1.3.1 Anisotropic Media

Maxwell equations describing electromagnetic wave propagation in a source-free, electrically anisotropic medium are given by (1.10), while the constitutive relations are given by (1.7) with the scalar permeability μ in place of the permeability tensor $\overline{\mu}$. In the principal coordinate system, the first constitutive relation can be written as

$$\boldsymbol{E} = \overline{\lambda}\boldsymbol{D}\,,$$

where the impermittivity tensor $\overline{\lambda}$ is given by

$$\overline{\lambda} = \begin{bmatrix} \lambda_x & 0 & 0 \\ 0 & \lambda_y & 0 \\ 0 & 0 & \lambda_z \end{bmatrix}\,,$$

and $\lambda_x = 1/\varepsilon_x$, $\lambda_y = 1/\varepsilon_y$ and $\lambda_z = 1/\varepsilon_z$.

The electromagnetic fields can be expressed as integrals over plane waves by considering the inverse Fourier transform (excepting the factor $1/(2\pi)^3$):

$$\boldsymbol{A}(\boldsymbol{r}) = \int \mathcal{A}\,(\boldsymbol{k})\,\mathrm{e}^{\mathrm{j}\boldsymbol{k}\cdot\boldsymbol{r}}\,\mathrm{d}V\,(\boldsymbol{k})\,,$$

where $\boldsymbol{A}$ stands for $\boldsymbol{E}$, $\boldsymbol{D}$, $\boldsymbol{H}$ and $\boldsymbol{B}$, and $\mathcal{A}$ stands for the Fourier transforms $\mathcal{E}$, $\mathcal{D}$, $\mathcal{H}$ and $\mathcal{B}$. Using the identities

$$\nabla \times \boldsymbol{A}(\boldsymbol{r}) = \mathrm{j}\int \boldsymbol{k} \times \mathcal{A}\,(\boldsymbol{k})\,\mathrm{e}^{\mathrm{j}\boldsymbol{k}\cdot\boldsymbol{r}}\,\mathrm{d}V\,(\boldsymbol{k})\,,$$

$$\nabla \cdot \boldsymbol{A}(\boldsymbol{r}) = \mathrm{j}\int \boldsymbol{k} \cdot \mathcal{A}\,(\boldsymbol{k})\,\mathrm{e}^{\mathrm{j}\boldsymbol{k}\cdot\boldsymbol{r}}\,\mathrm{d}V\,(\boldsymbol{k})\,,$$

we see that the Maxwell equations for the Fourier transforms take the forms

$$\boldsymbol{k} \times \mathcal{E} = k_0\mathcal{B}\,, \quad \boldsymbol{k} \times \mathcal{H} = -k_0\mathcal{D}\,,$$
$$\boldsymbol{k} \cdot \mathcal{D} = 0\,, \quad \boldsymbol{k} \cdot \mathcal{B} = 0\,,$$

and the plane wave solutions read as

$$\begin{aligned}
\mathcal{E}_\beta &= \frac{k_0}{k}\mathcal{B}_\alpha\,, \quad \mathcal{E}_\alpha = -\frac{k_0}{k}\mathcal{B}_\beta\,,\\
\mathcal{H}_\beta &= -\frac{k_0}{k}\mathcal{D}_\alpha\,, \quad \mathcal{H}_\alpha = \frac{k_0}{k}\mathcal{D}_\beta\,,\\
\mathcal{D}_k &= 0\,, \quad \mathcal{B}_k = 0\,,
\end{aligned} \tag{1.30}$$

where (k, β, α) and $(\boldsymbol{e}_k, \boldsymbol{e}_\beta, \boldsymbol{e}_\alpha)$ are the spherical coordinates and the spherical unit vectors of the wave vector $\boldsymbol{k}$, respectively, and in general, $(\mathcal{A}_k, \mathcal{A}_\beta, \mathcal{A}_\alpha)$ are the spherical coordinates of the vector $\mathcal{A}$. The constitutive relations for the transformed fields $\mathcal{E} = \overline{\lambda}\mathcal{D}$ and $\mathcal{H} = (1/\mu)\mathcal{B}$ can be written in spherical coordinates by using the transformation

$$\begin{bmatrix} \mathcal{A}_x \\ \mathcal{A}_y \\ \mathcal{A}_z \end{bmatrix} = \begin{bmatrix} \cos\alpha\sin\beta & \cos\alpha\cos\beta & -\sin\alpha \\ \sin\alpha\sin\beta & \sin\alpha\cos\beta & \cos\alpha \\ \cos\beta & -\sin\beta & 0 \end{bmatrix} \begin{bmatrix} \mathcal{A}_k \\ \mathcal{A}_\beta \\ \mathcal{A}_\alpha \end{bmatrix},$$

and the result is

$$\begin{aligned}
\mathcal{E}_k &= \lambda_{k\beta}\mathcal{D}_\beta + \lambda_{k\alpha}\mathcal{D}_\alpha\,,\\
\mathcal{E}_\beta &= \lambda_{\beta\beta}\mathcal{D}_\beta + \lambda_{\beta\alpha}\mathcal{D}_\alpha\,,\\
\mathcal{E}_\alpha &= \lambda_{\alpha\beta}\mathcal{D}_\beta + \lambda_{\alpha\alpha}\mathcal{D}_\alpha\,,
\end{aligned} \tag{1.31}$$

and

$$\mathcal{H}_k = 0\,, \quad \mathcal{H}_\beta = \frac{1}{\mu}\mathcal{B}_\beta\,, \quad \mathcal{H}_\alpha = \frac{1}{\mu}\mathcal{B}_\alpha\,, \tag{1.32}$$

where

$$\begin{aligned}
\lambda_{k\beta} &= \left(\lambda_x\cos^2\alpha + \lambda_y\sin^2\alpha - \lambda_z\right)\sin\beta\cos\beta\,,\\
\lambda_{k\alpha} &= (\lambda_y - \lambda_x)\sin\alpha\cos\alpha\sin\beta\,,\\
\lambda_{\beta\beta} &= \left(\lambda_x\cos^2\alpha + \lambda_y\sin^2\alpha\right)\cos^2\beta + \lambda_z\sin^2\beta\,,\\
\lambda_{\beta\alpha} &= (\lambda_y - \lambda_x)\sin\alpha\cos\alpha\cos\beta\,,
\end{aligned}$$

and

$$\begin{aligned}
\lambda_{\alpha\beta} &= \lambda_{\beta\alpha}\,,\\
\lambda_{\alpha\alpha} &= \lambda_x\sin^2\alpha + \lambda_y\cos^2\alpha\,.
\end{aligned}$$

Equations (1.30) and (1.32) are then used to express $\mathcal{E}_\beta$, $\mathcal{E}_\alpha$ and $\mathcal{H}_\beta$, $\mathcal{H}_\alpha$ in terms of $\mathcal{D}_\beta$, $\mathcal{D}_\alpha$, and we obtain

$$\begin{aligned}
\mathcal{E}_\beta &= \mu\frac{k_0^2}{k^2}\mathcal{D}_\beta\,, \quad \mathcal{E}_\alpha = \mu\frac{k_0^2}{k^2}\mathcal{D}_\alpha\,,\\
\mathcal{H}_\beta &= -\frac{k_0}{k}\mathcal{D}_\alpha\,, \quad \mathcal{H}_\alpha = \frac{k_0}{k}\mathcal{D}_\beta\,.
\end{aligned} \tag{1.33}$$

The last two equations in (1.31) and the first two equations in (1.33) yield a homogeneous system of equations for $\mathcal{D}_\beta$ and $\mathcal{D}_\alpha$

$$\begin{bmatrix} \lambda_{\beta\beta} - \mu\frac{k_0^2}{k^2} & \lambda_{\beta\alpha} \\ \lambda_{\beta\alpha} & \lambda_{\alpha\alpha} - \mu\frac{k_0^2}{k^2} \end{bmatrix} \begin{bmatrix} \mathcal{D}_\beta \\ \mathcal{D}_\alpha \end{bmatrix} = 0\,. \tag{1.34}$$

Requiring nontrivial solutions we set the determinant equal to zero and obtain two values for the wave number k^2,

$$k_{1,2}^2 = k_0^2 \frac{\mu}{\lambda_{1,2}}\,,$$

where

$$\lambda_1 = \frac{1}{2}\left[(\lambda_{\beta\beta} + \lambda_{\alpha\alpha}) - \sqrt{(\lambda_{\beta\beta} - \lambda_{\alpha\alpha})^2 + 4\lambda_{\beta\alpha}^2}\right]\,,$$

and

$$\lambda_2 = \frac{1}{2}\left[(\lambda_{\beta\beta} + \lambda_{\alpha\alpha}) + \sqrt{(\lambda_{\beta\beta} - \lambda_{\alpha\alpha})^2 + 4\lambda_{\beta\alpha}^2}\right]\,.$$

The above relations are the dispersion relations for the extraordinary waves, which are the permissible characteristic waves in anisotropic media. For an extraordinary wave, the magnitude of the wave vector depends on the direction of propagation, while for an ordinary wave, k is independent of β and α. Straightforward calculations show that for real values of λ_x, λ_y and λ_z, $\lambda_{\beta\beta}\lambda_{\alpha\alpha} > \lambda_{\beta\alpha}^2$ and as a result $\lambda_1 > 0$ and $\lambda_2 > 0$. The two characteristic waves, corresponding to the two values of k^2, have the $\mathcal{D}$ vectors orthogonal to each other, i.e., $\mathcal{D}^{(1)} \cdot \mathcal{D}^{(2)} = 0$. In view of (1.34) it is apparent that the components of the vectors $\mathcal{D}^{(1)}$ and $\mathcal{D}^{(2)}$ can be expressed in terms of two independent scalar functions $\mathcal{D}_\alpha$ and $\mathcal{D}_\beta$. For $k_1 = k_0\sqrt{\mu/\lambda_1}$ we set

$$\mathcal{D}_\beta^{(1)} = f\mathcal{D}_\alpha\,, \quad \mathcal{D}_\alpha^{(1)} = \mathcal{D}_\alpha\,,$$

while for $k_2 = k_0\sqrt{\mu/\lambda_2}$ we choose

$$\mathcal{D}_\beta^{(2)} = -\mathcal{D}_\beta\,, \quad \mathcal{D}_\alpha^{(2)} = f\mathcal{D}_\beta\,,$$

where

$$f = -\frac{\lambda_{\beta\alpha}}{\Delta\lambda}$$

and

$$\Delta\lambda = \frac{1}{2}\left[(\lambda_{\beta\beta} - \lambda_{\alpha\alpha}) + \sqrt{(\lambda_{\beta\beta} - \lambda_{\alpha\alpha})^2 + 4\lambda_{\beta\alpha}^2}\right]\,.$$

Next, we define the tangential fields

$$\boldsymbol{v}_\alpha = f\boldsymbol{e}_\beta + \boldsymbol{e}_\alpha\,,$$
$$\boldsymbol{v}_\beta = -\boldsymbol{e}_\beta + f\boldsymbol{e}_\alpha\,,$$

and note that the vectors $\boldsymbol{v}_\alpha$ and $\boldsymbol{v}_\beta$ are orthogonal to each other, $\boldsymbol{v}_\alpha \cdot \boldsymbol{v}_\beta = 0$, and $\boldsymbol{v}_\alpha = -\boldsymbol{e}_k \times \boldsymbol{v}_\beta$ and $\boldsymbol{v}_\beta = \boldsymbol{e}_k \times \boldsymbol{v}_\alpha$. Taking into account that $\boldsymbol{k}_1(\boldsymbol{e}_k) = k_1(\boldsymbol{e}_k)\,\boldsymbol{e}_k$ and $\boldsymbol{k}_2(\boldsymbol{e}_k) = k_2(\boldsymbol{e}_k)\,\boldsymbol{e}_k$, we find the following integral representation for the electric displacement:

$$\boldsymbol{D}(\boldsymbol{r}) = \int_\Omega \left[\mathcal{D}_\alpha(\boldsymbol{e}_k)\,\boldsymbol{v}_\alpha(\boldsymbol{e}_k)\,\mathrm{e}^{\mathrm{j}\boldsymbol{k}_1(\boldsymbol{e}_k)\cdot\boldsymbol{r}} + \mathcal{D}_\beta(\boldsymbol{e}_k)\,\boldsymbol{v}_\beta(\boldsymbol{e}_k)\,\mathrm{e}^{\mathrm{j}\boldsymbol{k}_2(\boldsymbol{e}_k)\cdot\boldsymbol{r}}\right]\mathrm{d}\Omega(\boldsymbol{e}_k)\ ,$$

with Ω being the unit sphere. The result, the integral representation for the electric field is

$$\boldsymbol{E}(\boldsymbol{r}) = \frac{1}{\varepsilon_{xy}} \times \int_\Omega \left[\mathcal{D}_\alpha(\boldsymbol{e}_k)\,\boldsymbol{w}^{\mathrm{e}}_\alpha(\boldsymbol{e}_k)\,\mathrm{e}^{\mathrm{j}\boldsymbol{k}_1(\boldsymbol{e}_k)\cdot\boldsymbol{r}} - \mathcal{D}_\beta(\boldsymbol{e}_k)\,\boldsymbol{w}^{\mathrm{e}}_\beta(\boldsymbol{e}_k)\,\mathrm{e}^{\mathrm{j}\boldsymbol{k}_2(\boldsymbol{e}_k)\cdot\boldsymbol{r}}\right]\mathrm{d}\Omega(\boldsymbol{e}_k)\ ,$$

where

$$\varepsilon_{xy} = \frac{1}{2}(\varepsilon_x + \varepsilon_y)\ ,$$

and

$$\boldsymbol{w}^{\mathrm{e}}_\alpha = \varepsilon_{xy}\left[(\lambda_{k\beta} f + \lambda_{k\alpha})\,\boldsymbol{e}_k + \lambda_1 \boldsymbol{v}_\alpha\right]\ ,$$
$$\boldsymbol{w}^{\mathrm{e}}_\beta = \varepsilon_{xy}\left[(\lambda_{k\beta} - \lambda_{k\alpha} f)\,\boldsymbol{e}_k - \lambda_2 \boldsymbol{v}_\beta\right]\ ,$$

while for the magnetic field, we have

$$\boldsymbol{H}(\boldsymbol{r}) = -\frac{1}{\sqrt{\varepsilon_{xy}\mu}}\int_\Omega \left[\mathcal{D}_\alpha(\boldsymbol{e}_k)\,\boldsymbol{w}^{\mathrm{h}}_\alpha(\boldsymbol{e}_k)\,\mathrm{e}^{\mathrm{j}\boldsymbol{k}_1(\boldsymbol{e}_k)\cdot\boldsymbol{r}} + \mathcal{D}_\beta(\boldsymbol{e}_k)\,\boldsymbol{w}^{\mathrm{h}}_\beta(\boldsymbol{e}_k)\,\mathrm{e}^{\mathrm{j}\boldsymbol{k}_2(\boldsymbol{e}_k)\cdot\boldsymbol{r}}\right]\mathrm{d}\Omega(\boldsymbol{e}_k)\ ,$$

where

$$\boldsymbol{w}^{\mathrm{h}}_\alpha = -\sqrt{\varepsilon_{xy}\lambda_1}\,\boldsymbol{v}_\beta\,,$$
$$\boldsymbol{w}^{\mathrm{h}}_\beta = \sqrt{\varepsilon_{xy}\lambda_2}\,\boldsymbol{v}_\alpha\,.$$

For uniaxial anisotropic media we set $\lambda = \lambda_x = \lambda_y$, derive the relations

$$\begin{aligned}
&\lambda_{k\beta} = (\lambda - \lambda_z)\sin\beta\cos\beta\,, \quad \lambda_{k\alpha} = 0\,,\\
&\lambda_{\beta\beta} = \lambda\cos^2\beta + \lambda_z\sin^2\beta\,, \quad \lambda_{\beta\alpha} = 0\,,\\
&\lambda_{\alpha\beta} = 0\,, \quad \lambda_{\alpha\alpha} = \lambda\,,
\end{aligned}$$

and use the identities $\lambda_1 = \lambda_{\alpha\alpha}$ and $\lambda_2 = \lambda_{\beta\beta}$, to obtain

$$k_1^2 = k_0^2\varepsilon\mu\,, \tag{1.35}$$
$$k_2^2 = k_0^2\frac{\varepsilon\mu}{\cos^2\beta + \frac{\varepsilon}{\varepsilon_z}\sin^2\beta}\,, \tag{1.36}$$

where $\lambda = 1/\varepsilon$ and $\lambda_z = 1/\varepsilon_z$. Equation (1.35) is the dispersion relation for ordinary waves, while (1.36) is the dispersion relation for extraordinary waves. For $f = 0$ it follows that $\mathcal{D}_\beta^{(1)} = 0$ and $\mathcal{D}_\alpha^{(2)} = 0$, and further that $\mathcal{D}_\alpha^{(1)} = \mathcal{D}_\alpha$ and $\mathcal{D}_\beta^{(2)} = -\mathcal{D}_\beta$. The electric displacement is then given by

$$\boldsymbol{D}(\boldsymbol{r}) = \int_0^{2\pi} \int_0^{\pi} \left[\mathcal{D}_\alpha(\beta,\alpha)\boldsymbol{e}_\alpha \mathrm{e}^{\mathrm{j}\boldsymbol{k}_1(\beta,\alpha)\cdot\boldsymbol{r}} - \mathcal{D}_\beta(\beta,\alpha)\boldsymbol{e}_\beta \mathrm{e}^{\mathrm{j}\boldsymbol{k}_2(\beta,\alpha)\cdot\boldsymbol{r}}\right] \sin\beta \,\mathrm{d}\beta \,\mathrm{d}\alpha \,, \tag{1.37}$$

where $\boldsymbol{k}_1(\beta,\alpha) = k_1\boldsymbol{e}_k(\beta,\alpha)$, $\boldsymbol{k}_2(\beta,\alpha) = k_2(\beta)\boldsymbol{e}_k(\beta,\alpha)$, and for notation simplification, the dependence of the spherical unit vectors $\boldsymbol{e}_\alpha$ and $\boldsymbol{e}_\beta$ on the spherical angles β and α is omitted. For $\varepsilon_{xy} = \varepsilon$, the integral representations for the electric and magnetic fields become

$$\begin{aligned}\boldsymbol{E}(\boldsymbol{r}) = \frac{1}{\varepsilon} \int_0^{2\pi} \int_0^{\pi} \Big\{ & \mathcal{D}_\alpha(\beta,\alpha)\boldsymbol{e}_\alpha \mathrm{e}^{\mathrm{j}\boldsymbol{k}_1(\beta,\alpha)\cdot\boldsymbol{r}} \\ & - \varepsilon \left[\lambda_{k\beta}(\beta)\boldsymbol{e}_k + \lambda_{\beta\beta}(\beta)\boldsymbol{e}_\beta\right] \mathcal{D}_\beta(\beta,\alpha) \mathrm{e}^{\mathrm{j}\boldsymbol{k}_2(\beta,\alpha)\cdot\boldsymbol{r}} \Big\} \sin\beta \,\mathrm{d}\beta \,\mathrm{d}\alpha \,,\end{aligned} \tag{1.38}$$

and

$$\begin{aligned}\boldsymbol{H}(\boldsymbol{r}) = -\frac{1}{\sqrt{\varepsilon\mu}} \int_0^{2\pi} \int_0^{\pi} \Big[& \mathcal{D}_\alpha(\beta,\alpha)\boldsymbol{e}_\beta \mathrm{e}^{\mathrm{j}\boldsymbol{k}_1(\beta,\alpha)\cdot\boldsymbol{r}} \\ & + \sqrt{\varepsilon\lambda_{\beta\beta}(\beta)}\mathcal{D}_\beta(\beta,\alpha)\boldsymbol{e}_\alpha \mathrm{e}^{\mathrm{j}\boldsymbol{k}_2(\beta,\alpha)\cdot\boldsymbol{r}} \Big] \sin\beta \,\mathrm{d}\beta \,\mathrm{d}\alpha \,,\end{aligned} \tag{1.39}$$

respectively. For isotropic media, the only nonzero λ functions are $\lambda_{\beta\beta}$ and $\lambda_{\alpha\alpha}$, and we have $\lambda_{\beta\beta} = \lambda_{\alpha\alpha} = \lambda$. The two waves degenerate into one (ordinary) wave, i.e., $k_1 = k_2 = k$, and the dispersion relation is

$$k^2 = k_0^2 \varepsilon\mu \,.$$

Next we proceed to derive series representations for the electric and magnetic fields propagating in uniaxial anisotropic media. On the unit sphere, the tangential vector function $\mathcal{D}_\alpha(\beta,\alpha)\boldsymbol{e}_\alpha - \mathcal{D}_\beta(\beta,\alpha)\boldsymbol{e}_\beta$ can be expanded in terms of the vector spherical harmonics $\boldsymbol{m}_{mn}$ and $\boldsymbol{n}_{mn}$ as follows:

$$\begin{aligned}\mathcal{D}_\alpha(\beta,\alpha)\boldsymbol{e}_\alpha - \mathcal{D}_\beta(\beta,\alpha)\boldsymbol{e}_\beta = -\varepsilon \sum_{n=1}^{\infty} \sum_{m=-n}^{n} \frac{1}{4\pi \mathrm{j}^{n+1}} \big[& -\mathrm{j}c_{mn}\boldsymbol{m}_{mn}(\beta,\alpha) \\ & + d_{mn}\boldsymbol{n}_{mn}(\beta,\alpha)\big] \,.\end{aligned} \tag{1.40}$$

Because the system of vector spherical harmonics is orthogonal and complete in $L^2(\Omega)$, the series representation (1.40) is valid for any tangential vector field. Taking into account the expressions of the vector spherical harmonics (cf. (B.8) and (B.9)) we deduce that the expansions of $\mathcal{D}_\beta$ and $\mathcal{D}_\alpha$ are given by

$$-\mathcal{D}_\beta(\beta,\alpha) = -\varepsilon \sum_{n=1}^{\infty}\sum_{m=-n}^{n} \frac{1}{4\pi \mathrm{j}^{n+1}} \frac{1}{\sqrt{2n(n+1)}} \Big[m\pi_n^{|m|}(\beta) c_{mn} + \tau_n^{|m|}(\beta) d_{mn} \Big] \mathrm{e}^{\mathrm{j}m\alpha}$$

and

$$\mathcal{D}_\alpha(\beta,\alpha) = -\varepsilon \sum_{n=1}^{\infty}\sum_{m=-n}^{n} \frac{1}{4\pi \mathrm{j}^{n+1}} \frac{1}{\sqrt{2n(n+1)}} \Big[\mathrm{j}\tau_n^{|m|}(\beta) c_{mn} + jm\pi_n^{|m|}(\beta) d_{mn} \Big] \mathrm{e}^{\mathrm{j}m\alpha} \,,$$

respectively. Inserting the above expansions into (1.38) and (1.39), yields the series representations

$$\boldsymbol{E}(\boldsymbol{r}) = \sum_{n=1}^{\infty}\sum_{m=-n}^{n} c_{mn} \boldsymbol{X}_{mn}^{\mathrm{e}}(\boldsymbol{r}) + d_{mn} \boldsymbol{Y}_{mn}^{\mathrm{e}}(\boldsymbol{r}) \,, \tag{1.41}$$

$$\boldsymbol{H}(\boldsymbol{r}) = -\mathrm{j}\sqrt{\frac{\varepsilon}{\mu}} \sum_{n=1}^{\infty}\sum_{m=-n}^{n} c_{mn} \boldsymbol{X}_{mn}^{\mathrm{h}}(\boldsymbol{r}) + d_{mn} \boldsymbol{Y}_{mn}^{\mathrm{h}}(\boldsymbol{r}) \,, \tag{1.42}$$

where the new vector functions are defined as

$$\boldsymbol{X}_{mn}^{\mathrm{e}}(\boldsymbol{r}) = -\frac{1}{4\pi \mathrm{j}^{n+1}} \frac{1}{\sqrt{2n(n+1)}} \int_0^{2\pi}\int_0^{\pi} \Big\{ \mathrm{j}\tau_n^{|m|}(\beta) \mathrm{e}^{\mathrm{j}\boldsymbol{k}_1(\beta,\alpha)\cdot\boldsymbol{r}} \boldsymbol{e}_\alpha + \varepsilon \left[\lambda_{k\beta}(\beta)\boldsymbol{e}_k + \lambda_{\beta\beta}(\beta)\boldsymbol{e}_\beta \right] m\pi_n^{|m|}(\beta) \mathrm{e}^{\mathrm{j}\boldsymbol{k}_2(\beta,\alpha)\cdot\boldsymbol{r}} \Big\} \times \mathrm{e}^{\mathrm{j}m\alpha} \sin\beta \,\mathrm{d}\beta \,\mathrm{d}\alpha \,, \tag{1.43}$$

$$\boldsymbol{Y}_{mn}^{\mathrm{e}}(\boldsymbol{r}) = -\frac{1}{4\pi \mathrm{j}^{n+1}} \frac{1}{\sqrt{2n(n+1)}} \int_0^{2\pi}\int_0^{\pi} \Big\{ jm\pi_n^{|m|}(\beta) \mathrm{e}^{\mathrm{j}\boldsymbol{k}_1(\beta,\alpha)\cdot\boldsymbol{r}} \boldsymbol{e}_\alpha + \varepsilon \left[\lambda_{k\beta}(\beta)\boldsymbol{e}_k + \lambda_{\beta\beta}(\beta)\boldsymbol{e}_\beta \right] \tau_n^{|m|}(\beta) \mathrm{e}^{\mathrm{j}\boldsymbol{k}_2(\beta,\alpha)\cdot\boldsymbol{r}} \Big\} \mathrm{e}^{\mathrm{j}m\alpha} \sin\beta \,\mathrm{d}\beta \,\mathrm{d}\alpha \,, \tag{1.44}$$

$$\boldsymbol{X}_{mn}^{\mathrm{h}}(\boldsymbol{r}) = -\frac{1}{4\pi \mathrm{j}^{n+1}} \frac{1}{\sqrt{2n(n+1)}} \int_0^{2\pi}\int_0^{\pi} \Big[\tau_n^{|m|}(\beta) \mathrm{e}^{\mathrm{j}\boldsymbol{k}_1(\beta,\alpha)\cdot\boldsymbol{r}} \boldsymbol{e}_\beta + \mathrm{j}\sqrt{\varepsilon\lambda_{\beta\beta}(\beta)} m\pi_n^{|m|}(\beta) \mathrm{e}^{\mathrm{j}\boldsymbol{k}_2(\beta,\alpha)\cdot\boldsymbol{r}} \boldsymbol{e}_\alpha \Big] \mathrm{e}^{\mathrm{j}m\alpha} \sin\beta \,\mathrm{d}\beta \,\mathrm{d}\alpha \,, \tag{1.45}$$

and

$$\boldsymbol{Y}_{mn}^{\mathrm{h}}(\boldsymbol{r}) = -\frac{1}{4\pi \mathrm{j}^{n+1}} \frac{1}{\sqrt{2n(n+1)}} \int_0^{2\pi}\int_0^{\pi} \Big[m\pi_n^{|m|}(\beta) \mathrm{e}^{\mathrm{j}\boldsymbol{k}_1(\beta,\alpha)\cdot\boldsymbol{r}} \boldsymbol{e}_\beta + \mathrm{j}\sqrt{\varepsilon\lambda_{\beta\beta}(\beta)} \tau_n^{|m|}(\beta) \mathrm{e}^{\mathrm{j}\boldsymbol{k}_2(\beta,\alpha)\cdot\boldsymbol{r}} \boldsymbol{e}_\alpha \Big] \mathrm{e}^{\mathrm{j}m\alpha} \sin\beta \,\mathrm{d}\beta \,\mathrm{d}\alpha \,. \tag{1.46}$$

In (1.38)–(1.39), the electromagnetic fields are expressed in terms of the unknown scalar functions $\mathcal{D}_\alpha$ and $\mathcal{D}_\beta$, while in (1.41) and (1.42), the electromagnetic fields are expressed in terms of the unknown expansion coefficients c_{mn} and d_{mn}. These unknowns will be determined from the boundary conditions for each specific scattering problem. The vector functions $\boldsymbol{X}_{mn}^{\mathrm{e,h}}$ and $\boldsymbol{Y}_{mn}^{\mathrm{e,h}}$ can be regarded as a generalization of the regular vector spherical wave functions $\boldsymbol{M}_{mn}^{1}$ and $\boldsymbol{N}_{mn}^{1}$. For isotropic media, we have $\varepsilon\lambda_{\beta\beta} = 1$, $\lambda_{k\beta} = 0$ and $k_1 = k_2 = k$, and we see that both systems of vector functions are equivalent:

$$\begin{aligned}\boldsymbol{X}_{mn}^{\mathrm{e}}(\boldsymbol{r}) &= \boldsymbol{Y}_{mn}^{\mathrm{h}}(\boldsymbol{r}) = \boldsymbol{M}_{mn}^{1}(k\boldsymbol{r})\,,\\ \boldsymbol{Y}_{mn}^{\mathrm{e}}(\boldsymbol{r}) &= \boldsymbol{X}_{mn}^{\mathrm{h}}(\boldsymbol{r}) = \boldsymbol{N}_{mn}^{1}(k\boldsymbol{r})\,.\end{aligned} \tag{1.47}$$

As a result, we obtain the familiar expansions of the electromagnetic fields in terms of vector spherical wave functions of the interior wave equation:

$$\boldsymbol{E}(\boldsymbol{r}) = \sum_{n=1}^{\infty}\sum_{m=-n}^{n} c_{mn}\boldsymbol{M}_{mn}^{1}(k\boldsymbol{r}) + d_{mn}\boldsymbol{N}_{mn}^{1}(k\boldsymbol{r})\,,$$

$$\boldsymbol{H}(\boldsymbol{r}) = -\mathrm{j}\sqrt{\frac{\varepsilon}{\mu}}\sum_{n=1}^{\infty}\sum_{m=-n}^{n} c_{mn}\boldsymbol{N}_{mn}^{1}(k\boldsymbol{r}) + d_{mn}\boldsymbol{M}_{mn}^{1}(\boldsymbol{k}r)\,.$$

Although the derivation of $\boldsymbol{X}_{mn}^{\mathrm{e,h}}$ and $\boldsymbol{Y}_{mn}^{\mathrm{e,h}}$ differs from that of Kiselev et al. [119], the resulting systems of vector functions are identical except for a multiplicative constant. Accordingly to Kiselev et al. [119], this system of vector functions will be referred to as the system of vector quasi-spherical wave functions. In (1.43)–(1.46) the integration over α can be analytically performed by using the relations

$$\begin{aligned}\boldsymbol{e}_k &= \sin\beta\cos\alpha\boldsymbol{e}_x + \sin\beta\sin\alpha\boldsymbol{e}_y + \cos\beta\boldsymbol{e}_z\,,\\ \boldsymbol{e}_\beta &= \cos\beta\cos\alpha\boldsymbol{e}_x + \cos\beta\sin\alpha\boldsymbol{e}_y - \sin\beta\boldsymbol{e}_z\,,\\ \boldsymbol{e}_\alpha &= -\sin\alpha\boldsymbol{e}_x + \cos\alpha\boldsymbol{e}_y\,,\end{aligned}$$

and the standard integrals

$$\begin{aligned}I_m(x,\varphi) &= \int_0^{2\pi} \mathrm{e}^{\mathrm{j}x\cos(\alpha-\varphi)}e^{jm\alpha}\,\mathrm{d}\alpha = 2\pi\mathrm{j}^m\mathrm{e}^{\mathrm{j}m\varphi}J_m(x)\,,\\ I_m^{\mathrm{c}}(x,\varphi) &= \int_0^{2\pi}\cos\alpha\mathrm{e}^{\mathrm{j}x\cos(\alpha-\varphi)}\mathrm{e}^{\mathrm{j}m\alpha}\,\mathrm{d}\alpha = \pi\left[\mathrm{j}^{m+1}\mathrm{e}^{\mathrm{j}(m+1)\varphi}J_{m+1}(x)\right.\\ &\quad\left.+\,\mathrm{j}^{m-1}\mathrm{e}^{\mathrm{j}(m-1)\varphi}J_{m-1}(x)\right]\,,\\ I_m^{\mathrm{s}}(x,\varphi) &= \int_0^{2\pi}\sin\alpha\mathrm{e}^{\mathrm{j}x\cos(\alpha-\varphi)}\mathrm{e}^{\mathrm{j}m\alpha}\,\mathrm{d}\alpha = -\mathrm{j}\pi\left[\mathrm{j}^{m+1}\mathrm{e}^{\mathrm{j}(m+1)\varphi}J_{m+1}(x)\right.\\ &\quad\left.-\,\mathrm{j}^{m-1}\mathrm{e}^{\mathrm{j}(m-1)\varphi}J_{m-1}(x)\right]\,,\end{aligned}$$

where $(\boldsymbol{e}_x, \boldsymbol{e}_y, \boldsymbol{e}_z)$ are the Cartesian unit vectors and J_m is the cylindrical Bessel functions of order m. The expressions of the Cartesian components of the vector function $\boldsymbol{X}^{\mathrm{e}}_{mn}$ read as

$$\begin{aligned} X^{\mathrm{e}}_{mn,x}(\boldsymbol{r}) = -\frac{1}{4\pi \mathrm{j}^{n+1}} \frac{1}{\sqrt{2n(n+1)}} \int_0^{\pi} \Big\{ & -\mathrm{j}\tau_n^{|m|}(\beta) I^{\mathrm{s}}_m(x_1, \varphi) \mathrm{e}^{\mathrm{j}y_1(r,\theta,\beta)} \\ & + \varepsilon \left[\lambda_{\beta\beta}(\beta) \cos\beta + \lambda_{k\beta}(\beta) \sin\beta \right] m\pi_n^{|m|}(\beta) \\ & \times I^{\mathrm{c}}_m(x_2, \varphi) \mathrm{e}^{\mathrm{j}y_2(r,\theta,\beta)} \Big\} \sin\beta \, \mathrm{d}\beta \end{aligned} \tag{1.48}$$

$$\begin{aligned} X^{\mathrm{e}}_{mn,y}(\boldsymbol{r}) = -\frac{1}{4\pi \mathrm{j}^{n+1}} \frac{1}{\sqrt{2n(n+1)}} \int_0^{\pi} \Big\{ & \mathrm{j}\tau_n^{|m|}(\beta) I^{\mathrm{c}}_m(x_1, \varphi) \mathrm{e}^{\mathrm{j}y_1(r,\theta,\beta)} \\ & + \varepsilon \left[\lambda_{\beta\beta}(\beta) \cos\beta + \lambda_{k\beta}(\beta) \sin\beta \right] m\pi_n^{|m|}(\beta) \\ & \times I^{\mathrm{s}}_m(x_2, \varphi) \mathrm{e}^{\mathrm{j}y_2(r,\theta,\beta)} \Big\} \sin\beta \, \mathrm{d}\beta \,, \end{aligned} \tag{1.49}$$

$$\begin{aligned} X^{\mathrm{e}}_{mn,z}(\boldsymbol{r}) = -\frac{1}{4\pi \mathrm{j}^{n+1}} \frac{1}{\sqrt{2n(n+1)}} \int_0^{\pi} & \varepsilon \left[\lambda_{k\beta}(\beta) \cos\beta - \lambda_{\beta\beta}(\beta) \sin\beta \right] \\ & \times m\pi_n^{|m|}(\beta) I_m(x_2, \varphi) \mathrm{e}^{\mathrm{j}y_2(r,\theta,\beta)} \sin\beta \, \mathrm{d}\beta \,, \end{aligned} \tag{1.50}$$

where $x_1(r,\theta,\beta) = k_1 r \sin\beta \sin\theta$, $x_2(r,\theta,\beta) = k_2(\beta) r \sin\beta \sin\theta$, $y_1(r,\theta,\beta) = k_1 r \cos\beta \cos\theta$ and $y_2(r,\theta,\beta) = k_2(\beta) r \cos\beta \cos\theta$, while the expressions of the Cartesian components of the vector functions $\boldsymbol{Y}^{\mathrm{e}}_{mn}$ are given by (1.48)–(1.50) with $m\pi_n^{|m|}$ and $\tau_n^{|m|}$ interchanged. Similarly, the Cartesian components of the vector function $\boldsymbol{X}^{\mathrm{h}}_{mn}$ are

$$\begin{aligned} X^{\mathrm{h}}_{mn,x}(\boldsymbol{r}) = -\frac{1}{4\pi \mathrm{j}^{n+1}} \frac{1}{\sqrt{2n(n+1)}} \int_0^{\pi} \Big[& \tau_n^{|m|}(\beta) \cos\beta I^{\mathrm{c}}_m(x_1, \varphi) \mathrm{e}^{\mathrm{j}y_1(r,\theta,\beta)} \\ & - \mathrm{j}\sqrt{\varepsilon\lambda_{\beta\beta}(\beta)} m\pi_n^{|m|}(\beta) I^{\mathrm{s}}_m(x_2, \varphi) \mathrm{e}^{\mathrm{j}y_2(r,\theta,\beta)} \Big] \sin\beta \, \mathrm{d}\beta \,, \end{aligned} \tag{1.51}$$

$$\begin{aligned} X^{\mathrm{h}}_{mn,y}(\boldsymbol{r}) = -\frac{1}{4\pi \mathrm{j}^{n+1}} \frac{1}{\sqrt{2n(n+1)}} \int_0^{\pi} \Big[& \tau_n^{|m|}(\beta) \cos\beta I^{\mathrm{s}}_m(x_1, \varphi) \mathrm{e}^{\mathrm{j}y_1(r,\theta,\beta)} \\ & + \mathrm{j}\sqrt{\varepsilon\lambda_{\beta\beta}(\beta)} m\pi_n^{|m|}(\beta) I^{\mathrm{c}}_m(x_2, \varphi) \mathrm{e}^{\mathrm{j}y_2(r,\theta,\beta)} \Big] \sin\beta \, \mathrm{d}\beta \,, \end{aligned} \tag{1.52}$$

$$X^{\mathrm{h}}_{mn,z}(\boldsymbol{r}) = \frac{1}{4\pi \mathrm{j}^{n+1}} \frac{1}{\sqrt{2n(n+1)}} \int_0^{\pi} \tau_n^{|m|}(\beta) I_m(x_1, \varphi) \mathrm{e}^{\mathrm{j}y_1(r,\theta,\beta)} \sin^2\beta \, \mathrm{d}\beta \,, \tag{1.53}$$

and as before, the components of the vector functions $\boldsymbol{Y}_{mn}^{\mathrm{h}}$ are given by (1.51)–(1.53) with $m\pi_n^{|m|}$ and $\tau_n^{|m|}$ interchanged.

In the above analysis, $\boldsymbol{X}_{mn}^{\mathrm{e,h}}$ and $\boldsymbol{Y}_{mn}^{\mathrm{e,h}}$ are expressed in the principal coordinate system, but in general, it is necessary to transform these vector functions from the principal coordinate system to the particle coordinate system through a rotation. The vector quasi-spherical wave functions can also be defined for biaxial media ($\varepsilon_x \neq \varepsilon_y \neq \varepsilon_z$) by considering the expansion of the tangential vector function $\mathcal{D}_\alpha(\beta,\alpha)\boldsymbol{v}_\alpha + \mathcal{D}_\beta(\beta,\alpha)\boldsymbol{v}_\beta$ in terms of vector spherical harmonics.

1.3.2 Chiral Media

For a source-free, isotropic, chiral medium, the Maxwell equations are given by (1.10), with the $\boldsymbol{K}$ matrix defined by (1.11). Following Bohren [16], the electromagnetic field is transformed to

$$\begin{bmatrix} \boldsymbol{E} \\ \boldsymbol{H} \end{bmatrix} = \boldsymbol{A} \begin{bmatrix} \boldsymbol{L} \\ \boldsymbol{R} \end{bmatrix},$$

where $\boldsymbol{A}$ is a transformation matrix and

$$\boldsymbol{A} = \begin{bmatrix} 1 & -\mathrm{j}\sqrt{\frac{\mu}{\varepsilon}} \\ -\mathrm{j}\sqrt{\frac{\varepsilon}{\mu}} & 1 \end{bmatrix}.$$

The transformed fields $\boldsymbol{L}$ and $\boldsymbol{R}$ are the left- and right-handed circularly polarized waves, or simply the waves of left- and right-handed types. Explicitly, the electromagnetic field transformation is

$$\boldsymbol{E} = \boldsymbol{L} - \mathrm{j}\sqrt{\frac{\mu}{\varepsilon}}\boldsymbol{R},$$

$$\boldsymbol{H} = -\mathrm{j}\sqrt{\frac{\varepsilon}{\mu}}\boldsymbol{L} + \boldsymbol{R}$$

and note that this linear transformation diagonalizes the matrix $\boldsymbol{K}$,

$$\Lambda = \boldsymbol{A}^{-1}\boldsymbol{K}\boldsymbol{A} = \begin{bmatrix} \frac{k}{1-\beta k} & 0 \\ 0 & -\frac{k}{1+\beta k} \end{bmatrix}.$$

Defining the wave numbers

$$k_{\mathrm{L}} = \frac{k}{1-\beta k},$$

$$k_{\mathrm{R}} = \frac{k}{1+\beta k},$$

we see that the waves of left- and right-handed types satisfy the equations

$$\nabla \times \boldsymbol{L} = k_{\mathrm{L}} \boldsymbol{L}\,, \quad \nabla \cdot \boldsymbol{L} = 0 \tag{1.54}$$

and

$$\nabla \times \boldsymbol{R} = -k_{\mathrm{R}} \boldsymbol{R}\,, \quad \nabla \cdot \boldsymbol{R} = 0, \tag{1.55}$$

respectively.

For chiral media, we use the same technique as for anisotropic media and express the left- and right-handed circularly polarized waves as integrals over plane waves. For the Fourier transform corresponding to waves of left-handed type,

$$\boldsymbol{L}(\boldsymbol{r}) = \int \mathcal{L}\left(\boldsymbol{k}\right) \mathrm{e}^{\mathrm{j}\boldsymbol{k}\cdot\boldsymbol{r}}\, \mathrm{d}V\left(\boldsymbol{k}\right)\,,$$

the differential equations (1.54) yield

$$\mathcal{L}_\beta = -\mathrm{j}\frac{k_{\mathrm{L}}}{k}\mathcal{L}_\alpha\,,$$

$$\mathcal{L}_\alpha = \mathrm{j}\frac{k_{\mathrm{L}}}{k}\mathcal{L}_\beta\,,$$

and $\mathcal{L}_k = 0$. The above set of equations form a system of homogeneous equations and setting the determinant equal to zero, gives the dispersion relation for the waves of left-handed type

$$k^2 = k_{\mathrm{L}}^2\,.$$

Choosing $\mathcal{L}_\beta$ as an independent scalar function, we express $\boldsymbol{L}$ as

$$\boldsymbol{L}(\boldsymbol{r}) = \int_0^{2\pi}\int_0^{\pi} \left(\boldsymbol{e}_\beta + \mathrm{j}\boldsymbol{e}_\alpha\right) \mathcal{L}_\beta(\beta,\alpha) \mathrm{e}^{\mathrm{j}\boldsymbol{k}_{\mathrm{L}}(\beta,\alpha)\cdot\boldsymbol{r}} \sin\beta\, \mathrm{d}\beta\, \mathrm{d}\alpha\,, \tag{1.56}$$

where $\boldsymbol{k}_{\mathrm{L}}(\beta,\alpha) = k_{\mathrm{L}}\boldsymbol{e}_k(\beta,\alpha)$. The tangential field $(\boldsymbol{e}_\beta + \mathrm{j}\boldsymbol{e}_\alpha)\mathcal{L}_\beta$ is orthogonal to the vector spherical harmonics of right-handed type with respect to the scalar product in $L^2_{\tan}(\Omega)$ (cf. (B.16) and (B.17)), and as result, $(\boldsymbol{e}_\beta + \mathrm{j}\boldsymbol{e}_\alpha)\mathcal{L}_\beta$ possesses an expansion in terms of vector spherical harmonics of left-handed type (cf. (B.14))

$$\begin{aligned}\left(\boldsymbol{e}_\beta + \mathrm{j}\boldsymbol{e}_\alpha\right) \mathcal{L}_\beta(\beta,\alpha) &= \sum_{n=1}^{\infty}\sum_{m=-n}^{n} \frac{1}{2\sqrt{2}\pi\mathrm{j}^n} c_{mn} \boldsymbol{l}_{mn}(\beta,\alpha) \\ &= \sum_{n=1}^{\infty}\sum_{m=-n}^{n} \frac{1}{4\pi\mathrm{j}^n} c_{mn} \left[\boldsymbol{m}_{mn}(\beta,\alpha) + \mathrm{j}\boldsymbol{n}_{mn}(\beta,\alpha)\right]\,.\end{aligned} \tag{1.57}$$

Inserting (1.57) into (1.56), yields

$$\boldsymbol{L}(\boldsymbol{r}) = -\sum_{n=1}^{\infty}\sum_{m=-n}^{n}\frac{1}{4\pi \mathrm{j}^{n+1}}c_{mn}\int_0^{2\pi}\int_0^{\pi}[-\mathrm{j}\boldsymbol{m}_{mn}(\beta,\alpha) + \boldsymbol{n}_{mn}(\beta,\alpha)]\,\mathrm{e}^{\mathrm{j}\boldsymbol{k}_{\mathrm{L}}(\beta,\alpha)\cdot\boldsymbol{r}}\sin\beta\,\mathrm{d}\beta\,\mathrm{d}\alpha\,,$$

whence, using the integral representation for the vector spherical wave functions (cf. (B.26) and (B.27)), gives

$$\begin{aligned}\boldsymbol{L}(\boldsymbol{r}) &= \sum_{n=1}^{\infty}\sum_{m=-n}^{n}c_{mn}\boldsymbol{L}_{mn}\left(k_{\mathrm{L}}\boldsymbol{r}\right)\\ &= \sum_{n=1}^{\infty}\sum_{m=-n}^{n}c_{mn}\left[\boldsymbol{M}^{1}_{mn}\left(k_{\mathrm{L}}\boldsymbol{r}\right)+\boldsymbol{N}^{1}_{mn}\left(k_{\mathrm{L}}\boldsymbol{r}\right)\right]\,,\end{aligned}$$

where the vector spherical wave functions of left-handed type $\boldsymbol{L}_{mn}$ are defined as

$$\boldsymbol{L}_{mn} = \boldsymbol{M}^{1}_{mn} + \boldsymbol{N}^{1}_{mn}\,. \tag{1.58}$$

For the waves of right-handed type we proceed analogously. We obtain the integral representation

$$\boldsymbol{R}(\boldsymbol{r}) = \int_0^{2\pi}\int_0^{\pi}\left(\boldsymbol{e}_{\beta}-\mathrm{j}\boldsymbol{e}_{\alpha}\right)\mathcal{R}_{\beta}(\beta,\alpha)\mathrm{e}^{\mathrm{j}\boldsymbol{k}_{\mathrm{R}}(\beta,\alpha)\cdot\boldsymbol{r}}\sin\beta\,\mathrm{d}\beta\,\mathrm{d}\alpha$$

with $\mathcal{R}_{\beta}$ being an independent scalar function, and the expansion

$$\begin{aligned}\boldsymbol{R}(\boldsymbol{r}) &= \sum_{n=1}^{\infty}\sum_{m=-n}^{n}d_{mn}\boldsymbol{R}_{mn}\left(k_{\mathrm{R}}\boldsymbol{r}\right)\\ &= \sum_{n=1}^{\infty}\sum_{m=-n}^{n}d_{mn}\left[\boldsymbol{M}^{1}_{mn}\left(k_{\mathrm{R}}\boldsymbol{r}\right)-\boldsymbol{N}^{1}_{mn}\left(k_{\mathrm{R}}\boldsymbol{r}\right)\right]\end{aligned}$$

with the vector spherical wave functions of right-handed type $\boldsymbol{R}_{mn}$ being defined as

$$\boldsymbol{R}_{mn} = \boldsymbol{M}^{1}_{mn} - \boldsymbol{N}^{1}_{mn}\,. \tag{1.59}$$

In conclusion, the electric and magnetic fields propagating in isotropic, chiral media possess the expansions [16, 17, 135]

$$\begin{aligned}\boldsymbol{E}(\boldsymbol{r}) &= \sum_{n=1}^{\infty}\sum_{m=-n}^{n}c_{mn}\boldsymbol{L}_{mn}\left(k_{\mathrm{L}}\boldsymbol{r}\right)-\mathrm{j}\sqrt{\frac{\mu}{\varepsilon}}d_{mn}\boldsymbol{R}_{mn}\left(k_{\mathrm{R}}\boldsymbol{r}\right)\,,\\ \boldsymbol{H}(\boldsymbol{r}) &= \sum_{n=1}^{\infty}\sum_{m=-n}^{n}-\mathrm{j}\sqrt{\frac{\varepsilon}{\mu}}c_{mn}\boldsymbol{L}_{mn}\left(k_{\mathrm{L}}\boldsymbol{r}\right)+d_{mn}\boldsymbol{R}_{mn}\left(k_{\mathrm{R}}\boldsymbol{r}\right)\,.\end{aligned}$$

An exhaustive treatment of electromagnetic wave propagation in isotropic, chiral media has been given by Lakhtakia et al. [136]. This analysis deals with the conservation of energy and momentum, properties of the infinite-medium Green's function and the mathematical expression of Huygens's principle.

1.4 Scattered Field

In this section we consider the basic properties of the scattered field as they are determined by energy conservation and by the propagation properties of the fields in source-free regions. The results are presented for electromagnetic scattering by dielectric particles, which is modeled by the transmission boundary-value problem. To formulate the transmission boundary-value problem we consider a bounded domain D_i (of class C^2) with boundary S and exterior D_s, and denote by $\boldsymbol{n}$ the unit normal vector to S directed into D_s (Fig. 1.8). The relative permittivity and relative permeability of the domain D_t are ε_t and μ_t, where $\mathrm{t} = \mathrm{s}, \mathrm{i}$, and the wave number in the domain D_t is $k_\mathrm{t} = k_0\sqrt{\varepsilon_\mathrm{t}\mu_\mathrm{t}}$, where k_0 is the wave number in free space. The unbounded domain D_s is assumed to be lossless, i.e., $\varepsilon_\mathrm{s} > 0$ and $\mu_\mathrm{s} > 0$, and the external excitation is considered to be a vector plane wave

$$\boldsymbol{E}_\mathrm{e}(\boldsymbol{r}) = \boldsymbol{E}_{\mathrm{e}0}\mathrm{e}^{\mathrm{j}\boldsymbol{k}_\mathrm{e}\cdot\boldsymbol{r}}\,, \quad \boldsymbol{H}_\mathrm{e}(\boldsymbol{r}) = \sqrt{\frac{\varepsilon_\mathrm{s}}{\mu_\mathrm{s}}}\boldsymbol{e}_k \times \boldsymbol{E}_{\mathrm{e}0}\mathrm{e}^{\mathrm{j}\boldsymbol{k}_\mathrm{e}\cdot\boldsymbol{r}}\,,$$

where $\boldsymbol{E}_{\mathrm{e}0}$ is the complex amplitude vector and $\boldsymbol{e}_k$ is the unit vector in the direction of the wave vector $\boldsymbol{k}_\mathrm{e}$. The transmission boundary-value problem has the following formulation.

Given $\boldsymbol{E}_\mathrm{e}, \boldsymbol{H}_\mathrm{e}$ as an entire solution to the Maxwell equations representing the external excitation, find the vector fields $\boldsymbol{E}_\mathrm{s}, \boldsymbol{H}_\mathrm{s} \in C^1(D_\mathrm{s}) \cap C(\overline{D}_\mathrm{s})$ and $\boldsymbol{E}_\mathrm{i}, \boldsymbol{H}_\mathrm{i} \in C^1(D_\mathrm{i}) \cap C(\overline{D}_\mathrm{i})$ satisfying the Maxwell equations

$$\nabla \times \boldsymbol{E}_\mathrm{t} = \mathrm{j}k_0\mu_\mathrm{t}\boldsymbol{H}_\mathrm{t}, \quad \nabla \times \boldsymbol{H}_\mathrm{t} = -\mathrm{j}k_0\varepsilon_\mathrm{t}\boldsymbol{E}_\mathrm{t}, \tag{1.60}$$

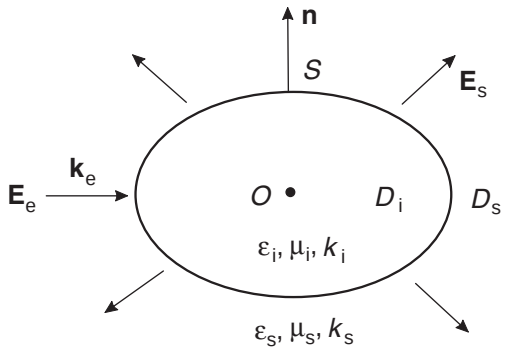

Fig. 1.8. The domain D_i with boundary S and exterior D_s

in D_{t}, $\mathrm{t}=\mathrm{s},\mathrm{i}$, *and the two transmission conditions*

$$\begin{aligned}\boldsymbol{n}\times\boldsymbol{E}_{\mathrm{i}}-\boldsymbol{n}\times\boldsymbol{E}_{\mathrm{s}}&=\boldsymbol{n}\times\boldsymbol{E}_{\mathrm{e}}\,,\\ \boldsymbol{n}\times\boldsymbol{H}_{\mathrm{i}}-\boldsymbol{n}\times\boldsymbol{H}_{\mathrm{s}}&=\boldsymbol{n}\times\boldsymbol{H}_{\mathrm{e}}\,,\end{aligned}\tag{1.61}$$

on S. *In addition, the scattered field* $\boldsymbol{E}_{\mathrm{s}},\boldsymbol{H}_{\mathrm{s}}$ *must satisfy the Silver–Müller radiation condition*

$$\frac{\boldsymbol{r}}{r}\times\sqrt{\mu_{\mathrm{s}}}\boldsymbol{H}_{\mathrm{s}}+\sqrt{\epsilon_{\mathrm{s}}}\boldsymbol{E}_{\mathrm{s}}=\mathrm{o}\left(\frac{1}{r}\right),\quad as\quad r\to\infty\,,\tag{1.62}$$

uniformly for all directions $\boldsymbol{r}/r$.

It should be emphasized that for the assumed smoothness conditions, the transmission boundary-value problem possesses an unique solution [177].

Our presentation is focused on the analysis of the scattered field in the far-field region. We begin with a basic representation theorem for electromagnetic scattering and then introduce the primary quantities which define the single-scattering law: the far-field patterns and the amplitude matrix. Because the measurement of the amplitude matrix is a complicated experimental problem, we characterize the scattering process by other measurable quantities as for instance the optical cross-sections and the phase and extinction matrices.

In our analysis, we will frequently use the Green second vector theorem

$$\begin{aligned}&\int_D\left[\boldsymbol{a}\cdot(\nabla\times\nabla\times\boldsymbol{b})-\boldsymbol{b}\cdot(\nabla\times\nabla\times\boldsymbol{a})\right]\mathrm{d}V\\ &=\int_S\boldsymbol{n}\cdot\left[\boldsymbol{b}\times(\nabla\times\boldsymbol{a})-\boldsymbol{a}\times(\nabla\times\boldsymbol{b})\right]\mathrm{d}S\,,\end{aligned}$$

where D is a bounded domain with boundary S and $\boldsymbol{n}$ is the outward unit normal vector to S.

1.4.1 Stratton–Chu Formulas

Representation theorems for electromagnetic fields have been given by Stratton and Chu [216]. If $\boldsymbol{E}_{\mathrm{s}}$, $\boldsymbol{H}_{\mathrm{s}}$ is a radiating solution to Maxwell's equations in D_{s}, then we have the Stratton–Chu formulas

$$\begin{aligned}\begin{pmatrix}\boldsymbol{E}_{\mathrm{s}}(\boldsymbol{r})\\0\end{pmatrix}&=\nabla\times\int_S\boldsymbol{e}_{\mathrm{s}}(\boldsymbol{r}')\,g(k_{\mathrm{s}},\boldsymbol{r},\boldsymbol{r}')\,\mathrm{d}S(\boldsymbol{r}')\\ &\quad+\frac{\mathrm{j}}{k_0\varepsilon_{\mathrm{s}}}\nabla\times\nabla\times\int_S\boldsymbol{h}_{\mathrm{s}}(\boldsymbol{r}')\,g(k_{\mathrm{s}},\boldsymbol{r},\boldsymbol{r}')\,\mathrm{d}S(\boldsymbol{r}')\,,\quad\begin{pmatrix}\boldsymbol{r}\in D_{\mathrm{s}}\\ \boldsymbol{r}\in D_{\mathrm{i}}\end{pmatrix}\end{aligned}\tag{1.63}$$

and

$$\begin{pmatrix} \boldsymbol{H}_{\mathrm{s}}(\boldsymbol{r}) \\ 0 \end{pmatrix} = \nabla \times \int_S \boldsymbol{h}_{\mathrm{s}}(\boldsymbol{r}')\, g(k_{\mathrm{s}}, \boldsymbol{r}, \boldsymbol{r}')\, \mathrm{d}S(\boldsymbol{r}') \\ -\frac{\mathrm{j}}{k_0 \mu_{\mathrm{s}}} \nabla \times \nabla \times \int_S \boldsymbol{e}_{\mathrm{s}}(\boldsymbol{r}')\, g(k_{\mathrm{s}}, \boldsymbol{r}, \boldsymbol{r}')\, \mathrm{d}S(\boldsymbol{r}'), \quad \begin{pmatrix} \boldsymbol{r} \in D_{\mathrm{s}} \\ \boldsymbol{r} \in D_{\mathrm{i}} \end{pmatrix},$$

where g is the Green function and the surface fields $\boldsymbol{e}_{\mathrm{s}}$ and $\boldsymbol{h}_{\mathrm{s}}$ are the tangential components of the electric and magnetic fields on the particle surface, i.e., $\boldsymbol{e}_{\mathrm{s}} = \boldsymbol{n} \times \boldsymbol{E}_{\mathrm{s}}$ and $\boldsymbol{h}_{\mathrm{s}} = \boldsymbol{n} \times \boldsymbol{H}_{\mathrm{s}}$, respectively. In the above equations we use a compact way of writing two formulas (for $\boldsymbol{r} \in D_{\mathrm{s}}$ and for $\boldsymbol{r} \in D_{\mathrm{i}}$) as a single equation.

A similar result holds for vector functions satisfying the Maxwell equations in bounded domains. With $\boldsymbol{E}_{\mathrm{i}}$, $\boldsymbol{H}_{\mathrm{i}}$ being a solution to Maxwell's equations in D_{i} we have

$$\begin{pmatrix} -\boldsymbol{E}_{\mathrm{i}}(\boldsymbol{r}) \\ 0 \end{pmatrix} = \nabla \times \int_S \boldsymbol{e}_{\mathrm{i}}(\boldsymbol{r}')\, g(k_{\mathrm{i}}, \boldsymbol{r}, \boldsymbol{r}')\, \mathrm{d}S(\boldsymbol{r}') \\ +\frac{\mathrm{j}}{k_0 \varepsilon_{\mathrm{i}}} \nabla \times \nabla \times \int_S \boldsymbol{h}_{\mathrm{i}}(\boldsymbol{r}')\, g(k_{\mathrm{i}}, \boldsymbol{r}, \boldsymbol{r}')\, \mathrm{d}S(\boldsymbol{r}'), \quad \begin{pmatrix} \boldsymbol{r} \in D_{\mathrm{i}} \\ \boldsymbol{r} \in D_{\mathrm{s}} \end{pmatrix}$$

and

$$\begin{pmatrix} -\boldsymbol{H}_{\mathrm{i}}(\boldsymbol{r}) \\ 0 \end{pmatrix} = \nabla \times \int_S \boldsymbol{h}_{\mathrm{i}}(\boldsymbol{r}')\, g(k_{\mathrm{i}}, \boldsymbol{r}, \boldsymbol{r}')\, \mathrm{d}S(\boldsymbol{r}') \\ -\frac{\mathrm{j}}{k_0 \mu_{\mathrm{i}}} \nabla \times \nabla \times \int_S \boldsymbol{e}_{\mathrm{i}}(\boldsymbol{r}')\, g(k_{\mathrm{i}}, \boldsymbol{r}, \boldsymbol{r}')\, \mathrm{d}S(\boldsymbol{r}'), \quad \begin{pmatrix} \boldsymbol{r} \in D_{\mathrm{i}} \\ \boldsymbol{r} \in D_{\mathrm{s}} \end{pmatrix},$$

where $\boldsymbol{e}_{\mathrm{i}} = \boldsymbol{n} \times \boldsymbol{E}_{\mathrm{i}}$ and $\boldsymbol{h}_{\mathrm{i}} = \boldsymbol{n} \times \boldsymbol{H}_{\mathrm{i}}$.

A rigorous proof of these representation theorems on the assumptions $\boldsymbol{E}_{\mathrm{s}}$, $\boldsymbol{H}_{\mathrm{s}} \in C^1(D_{\mathrm{s}}) \cap C(\overline{D}_{\mathrm{s}})$ and $\boldsymbol{E}_{\mathrm{i}}$, $\boldsymbol{H}_{\mathrm{i}} \in C^1(D_{\mathrm{i}}) \cap C(\overline{D}_{\mathrm{i}})$ can be found in Colton and Kress [39]. An alternative proof can be given if we accept the validity of Green's second vector theorem for generalized functions such as the three-dimensional Dirac delta function $\delta(\boldsymbol{r} - \boldsymbol{r}')$. To prove the representation theorem for vector fields satisfying the Maxwell equations in bounded domains we use the Green second vector theorem for a divergence free vector field $\boldsymbol{a}$ ($\nabla \cdot \boldsymbol{a} = 0$). Using the vector identities $\nabla \times \nabla \times \boldsymbol{b} = -\Delta \boldsymbol{b} + \nabla\nabla \cdot \boldsymbol{b}$ and $\boldsymbol{a} \cdot (\nabla\nabla \cdot \boldsymbol{b}) = \nabla \cdot (\boldsymbol{a}\nabla \cdot \boldsymbol{b})$ for $\nabla \cdot \boldsymbol{a} = 0$, and the Gauss divergence theorem we see that

$$\int_D [\boldsymbol{a} \cdot \Delta \boldsymbol{b} + \boldsymbol{b} \cdot (\nabla \times \nabla \times \boldsymbol{a})]\, \mathrm{d}V = \int_S \{\boldsymbol{n} \cdot \boldsymbol{a}\, (\nabla \cdot \boldsymbol{b}) + \boldsymbol{n} \cdot [\boldsymbol{a} \times (\nabla \times \boldsymbol{b}) \\ + (\nabla \times \boldsymbol{a}) \times \boldsymbol{b}]\}\, \mathrm{d}S. \tag{1.64}$$

In the above equations, the simplified notations $\nabla\nabla \cdot \boldsymbol{a}$ and $\boldsymbol{a}\nabla \cdot \boldsymbol{b}$ should be understood as $\nabla(\nabla \cdot \boldsymbol{a})$ and $\boldsymbol{a}(\nabla \cdot \boldsymbol{b})$, respectively. Next, we choose an

arbitrary constant unit vector $\boldsymbol{u}$ and apply Green's second vector theorem (1.64) to $\boldsymbol{a}(\boldsymbol{r}') = \boldsymbol{E}_{\rm i}(\boldsymbol{r}')$ and $\boldsymbol{b}(\boldsymbol{r}') = g(k_{\rm i}, \boldsymbol{r}', \boldsymbol{r})\boldsymbol{u}$, for $\boldsymbol{r} \in D_{\rm i}$. Recalling that

$$\Delta' g\left(k_{\rm i}, \boldsymbol{r}', \boldsymbol{r}\right) + k_{\rm i}^2 g\left(k_{\rm i}, \boldsymbol{r}', \boldsymbol{r}\right) = -\delta\left(\boldsymbol{r}' - \boldsymbol{r}\right) , \tag{1.65}$$

and $\nabla' \times \nabla' \times \mathbf{E}_{\rm i} = k_{\rm i}^2 \mathbf{E}_{\rm i}$, we see that the left-hand side of (1.64) is

$$\begin{aligned}
&\int_{D_{\rm i}} \left\{\boldsymbol{E}_{\rm i}\left(\boldsymbol{r}'\right) \cdot \Delta' g\left(k_{\rm i}, \boldsymbol{r}', \boldsymbol{r}\right) \boldsymbol{u} + g\left(k_{\rm i}, \boldsymbol{r}', \boldsymbol{r}\right) \boldsymbol{u} \cdot \left[\nabla' \times \nabla' \times \boldsymbol{E}_{\rm i}\left(\boldsymbol{r}'\right)\right]\right\} \\
&\qquad \times \mathrm{d}V\left(\boldsymbol{r}'\right) \\
&= -\int_{D_{\rm i}} \boldsymbol{u} \cdot \boldsymbol{E}_{\rm i}\left(\boldsymbol{r}'\right) \delta\left(\boldsymbol{r}' - \boldsymbol{r}\right) \mathrm{d}V\left(\boldsymbol{r}'\right) = -\boldsymbol{u} \cdot \boldsymbol{E}_{\rm i}(\boldsymbol{r}) .
\end{aligned}$$

Taking into account that for $\boldsymbol{r}' \neq \boldsymbol{r}$,

$$\nabla' \times \nabla' \times g\left(k_{\rm i}, \boldsymbol{r}', \boldsymbol{r}\right) \boldsymbol{u} = k_{\rm i}^2 g\left(k_{\rm i}, \boldsymbol{r}', \boldsymbol{r}\right) \boldsymbol{u} + \nabla' \nabla' \cdot g\left(k_{\rm i}, \boldsymbol{r}', \boldsymbol{r}\right) \boldsymbol{u} ,$$

we rewrite the right-hand side of (1.64) as

$$\begin{aligned}
&\int_S \left\{\boldsymbol{n} \cdot \boldsymbol{E}_{\rm i}\left[\nabla' \cdot g\left(k_{\rm i}, \cdot \boldsymbol{r}\right) \boldsymbol{u}\right] + \boldsymbol{n} \cdot \left[\boldsymbol{E}_{\rm i} \times \left(\nabla' \times g\left(k_{\rm i}, \cdot \boldsymbol{r}\right) \boldsymbol{u}\right)\right.\right. \\
&\qquad \left.\left. + \left(\nabla' \times \boldsymbol{E}_{\rm i}\right) \times g\left(k_{\rm i}, \cdot \boldsymbol{r}\right) \boldsymbol{u}\right]\right\} \mathrm{d}S \\
&= \int_S \left\{\boldsymbol{n} \cdot \boldsymbol{E}_{\rm i}\left[\nabla' \cdot g\left(k_{\rm i}, \cdot \boldsymbol{r}\right) \boldsymbol{u}\right] + \boldsymbol{n} \cdot \left[\boldsymbol{E}_{\rm i} \times \left(\nabla' \times g\left(k_{\rm i}, \cdot \boldsymbol{r}\right) \boldsymbol{u}\right)\right]\right. \\
&\qquad + \frac{1}{k_{\rm i}^2} \boldsymbol{n} \cdot \left[\left(\nabla' \times \boldsymbol{E}_{\rm i}\right) \times \left(\nabla' \times \nabla' \times g\left(k_{\rm i}, \cdot \boldsymbol{r}\right) \boldsymbol{u}\right)\right. \\
&\qquad \left.\left. - \left(\nabla' \times \boldsymbol{E}_{\rm i}\right) \times \nabla' \nabla' \cdot g\left(k_{\rm i}, \cdot \boldsymbol{r}\right) \boldsymbol{u}\right]\right\} \mathrm{d}S .
\end{aligned}$$

From Stokes theorem we have

$$\int_S \boldsymbol{n} \cdot \left\{\nabla' \times \left[\boldsymbol{H}_{\rm i} \nabla' \cdot g\left(k_{\rm i}, \cdot \boldsymbol{r}\right) \boldsymbol{u}\right]\right\} \mathrm{d}S = 0 ,$$

whence, using the vector identity $\nabla \times (\alpha \boldsymbol{b}) = \nabla \alpha \times \boldsymbol{b} + \alpha \nabla \times \boldsymbol{b}$ and the Maxwell equations, we obtain

$$\begin{aligned}
&\int_S \boldsymbol{n} \cdot \boldsymbol{E}_{\rm i}\left[\nabla' \cdot g\left(k_{\rm i}, \cdot, \boldsymbol{r}\right) \boldsymbol{u}\right] \mathrm{d}S \\
&= \frac{1}{k_{\rm i}^2} \int_S \boldsymbol{n} \cdot \left[\left(\nabla' \times \boldsymbol{E}_{\rm i}\right) \times \nabla' \nabla' \cdot g\left(k_{\rm i}, \cdot, \boldsymbol{r}\right) \boldsymbol{u}\right] \mathrm{d}S .
\end{aligned}$$

Finally, using the vector identity $\boldsymbol{a} \cdot (\boldsymbol{b} \times \boldsymbol{c}) = (\boldsymbol{a} \times \boldsymbol{b}) \cdot \boldsymbol{c}$, the symmetry relation $\nabla' g(k_{\rm i}, \boldsymbol{r}', \boldsymbol{r}) = -\nabla g(k_{\rm i}, \boldsymbol{r}', \boldsymbol{r})$, the Maxwell equations and the identities

$$
\begin{aligned}
&[\nabla' \times g\,(k_\mathrm{i}, \boldsymbol{r}', \boldsymbol{r})\,\boldsymbol{u}] \cdot [\boldsymbol{n}\,(\boldsymbol{r}') \times \boldsymbol{E}_\mathrm{i}\,(\boldsymbol{r}')] \\
&= \{\nabla \times g\,(k_\mathrm{i}, \boldsymbol{r}', \boldsymbol{r})\,[\boldsymbol{n}\,(\boldsymbol{r}') \times \boldsymbol{E}_\mathrm{i}\,(\boldsymbol{r}')]\} \cdot \boldsymbol{u}
\end{aligned}
$$

and

$$
\begin{aligned}
&[\nabla' \times \nabla' \times g\,(k_\mathrm{i}, \boldsymbol{r}', \boldsymbol{r})\,\boldsymbol{u}] \cdot [\boldsymbol{n}\,(\boldsymbol{r}') \times \boldsymbol{H}_\mathrm{i}\,(\boldsymbol{r}')] \\
&= \{\nabla \times \nabla \times g\,(k_\mathrm{i}, \boldsymbol{r}', \boldsymbol{r})\,[\boldsymbol{n}\,(\boldsymbol{r}') \times \boldsymbol{H}_\mathrm{i}\,(\boldsymbol{r}')]\} \cdot \boldsymbol{u}\,,
\end{aligned}
$$

we arrive at

$$
\begin{aligned}
-\boldsymbol{u} \cdot \boldsymbol{E}_\mathrm{i}(\boldsymbol{r}) = \boldsymbol{u} \cdot \Bigg\{ &\nabla \times \int_S \boldsymbol{n}\,(\boldsymbol{r}') \times \boldsymbol{E}_\mathrm{i}\,(\boldsymbol{r}')\, g\,(k_\mathrm{i}, \boldsymbol{r}, \boldsymbol{r}')\,\mathrm{d}S(\boldsymbol{r}') \\
&+ \frac{\mathrm{j}}{k_0 \varepsilon_\mathrm{i}} \nabla \times \nabla \times \int_S \boldsymbol{n}\,(\boldsymbol{r}') \times \boldsymbol{H}_\mathrm{i}\,(\boldsymbol{r}')\, g\,(k_\mathrm{i}, \boldsymbol{r}, \boldsymbol{r}')\,\mathrm{d}S(\boldsymbol{r}') \Bigg\}\,.
\end{aligned}
$$

Since $\boldsymbol{u}$ is arbitrary, we have established the Stratton–Chu formula for $\boldsymbol{r} \in D_\mathrm{i}$. If $\boldsymbol{r} \in D_\mathrm{s}$, we have

$$
\int_{D_\mathrm{i}} \boldsymbol{u} \cdot \boldsymbol{E}_\mathrm{i}\,(\boldsymbol{r}')\,\delta\,(\boldsymbol{r}' - \boldsymbol{r})\,\mathrm{d}V\,(\boldsymbol{r}') = 0\,,
$$

and the proof follows in a similar manner. For radiating solutions to the Maxwell equations, we see that the proof is established if we can show that

$$
\begin{aligned}
\int_{S_\mathrm{R}} \Big\{ &\boldsymbol{n} \cdot [\boldsymbol{E}_\mathrm{s} \times (\nabla' \times g\,(k_\mathrm{s}, \cdot, \boldsymbol{r})\,\boldsymbol{u}) \\
&+ \frac{1}{k_\mathrm{s}^2}\,(\nabla' \times \boldsymbol{E}_\mathrm{s}) \times (\nabla' \times \nabla' \times g\,(k_\mathrm{s}, \cdot, \boldsymbol{r})\,\boldsymbol{u})\Big]\Big\}\,\mathrm{d}S \to 0\,,
\end{aligned}
$$

as $R \to \infty$, where S_R is a spherical surface situated in the far-field region. To prove this assertion we use the Silver–Müller radiation condition and the general assumption $\mathrm{Im}\{k_\mathrm{s}\} \geq 0$.

Alternative representations for Stratton–Chu formulas involve the free space dyadic Green function $\overline{\boldsymbol{G}}$ instead of the fundamental solution g [228]. A dyad $\overline{\boldsymbol{D}}$ serves as a linear mapping from one vector to another vector, and in general, $\overline{\boldsymbol{D}}$ can be introduced as the dyadic product of two vectors: $\overline{\boldsymbol{D}} = \boldsymbol{a} \otimes \boldsymbol{b}$. The dot product of a dyad with a vector is another vector: $\overline{\boldsymbol{D}} \cdot \boldsymbol{c} = (\boldsymbol{a} \otimes \boldsymbol{b}) \cdot \boldsymbol{c} = \boldsymbol{a}(\boldsymbol{b} \cdot \boldsymbol{c})$ and $\boldsymbol{c} \cdot \overline{\boldsymbol{D}} = \boldsymbol{c} \cdot (\boldsymbol{a} \otimes \boldsymbol{b}) = (\boldsymbol{c} \cdot \boldsymbol{a})\boldsymbol{b}$, while the cross product of a dyad with a vector is another dyad: $\overline{\boldsymbol{D}} \times \boldsymbol{c} = (\boldsymbol{a} \otimes \boldsymbol{b}) \times \boldsymbol{c} = \boldsymbol{a} \otimes (\boldsymbol{b} \times \boldsymbol{c})$ and $\boldsymbol{c} \times \overline{\boldsymbol{D}} = \boldsymbol{c} \times (\boldsymbol{a} \otimes \boldsymbol{b}) = (\boldsymbol{c} \times \boldsymbol{a}) \otimes \boldsymbol{b}$. The free space dyadic Green function is defined as

$$
\overline{\boldsymbol{G}}\,(k, \boldsymbol{r}, \boldsymbol{r}') = \left(\overline{\boldsymbol{I}} + \frac{1}{k^2} \nabla \otimes \nabla\right) g\,(k, \boldsymbol{r}, \boldsymbol{r}')\,,
$$

where $\overline{\boldsymbol{I}}$ is the identity dyad ($\overline{\boldsymbol{D}} \cdot \overline{\boldsymbol{I}} = \overline{\boldsymbol{I}} \cdot \overline{\boldsymbol{D}} = \overline{\boldsymbol{D}}$). Multiplying the differential equation (1.65) by $\overline{\boldsymbol{I}}$ and using the identities

$$\nabla \times \nabla \times \left(\overline{\boldsymbol{I}} g\right) = \nabla \otimes \nabla g - \boldsymbol{I} \triangle g \,,$$

$$\nabla \times \nabla \times (\nabla \otimes \nabla g) = 0 \,,$$

gives the differential equation for the free space dyadic Green function

$$\nabla \times \nabla \times \overline{\boldsymbol{G}}\,(k, \boldsymbol{r}, \boldsymbol{r}') = k^2 \overline{\boldsymbol{G}}\,(k, \boldsymbol{r}, \boldsymbol{r}') + \delta\,(\boldsymbol{r} - \boldsymbol{r}')\,\overline{\boldsymbol{I}}\,. \tag{1.66}$$

The Stratton–Chu formula for vector fields satisfying the Maxwell equations in bounded domains read as

$$\begin{pmatrix} -\boldsymbol{E}_{\mathrm{i}}(\boldsymbol{r}) \\ 0 \end{pmatrix} = \int_S \boldsymbol{e}_{\mathrm{i}}\,(\boldsymbol{r}') \cdot \left[\nabla' \times \overline{\boldsymbol{G}}\,(k_{\mathrm{i}}, \boldsymbol{r}, \boldsymbol{r}')\right] \mathrm{d}S(\boldsymbol{r}')$$

$$+\mathrm{j}k_0\mu_{\mathrm{i}} \int_S \boldsymbol{h}_{\mathrm{i}}\,(\boldsymbol{r}') \cdot \overline{\boldsymbol{G}}\,(k_{\mathrm{i}}, \boldsymbol{r}, \boldsymbol{r}')\,\mathrm{d}S(\boldsymbol{r}')\,, \quad \begin{pmatrix} \boldsymbol{r} \in D_{\mathrm{i}} \\ \boldsymbol{r} \in D_{\mathrm{s}} \end{pmatrix}$$

and this integral representation follows from the second vector-dyadic Green theorem [220]:

$$\int_D \left[\boldsymbol{a} \cdot \left(\nabla \times \nabla \times \overline{\boldsymbol{D}}\right) - (\nabla \times \nabla \times \boldsymbol{a}) \cdot \overline{\boldsymbol{D}}\right] \mathrm{d}V$$

$$= -\int_S \boldsymbol{n} \cdot \left[\boldsymbol{a} \times \left(\nabla \times \overline{\boldsymbol{D}}\right) + (\nabla \times \boldsymbol{a}) \times \overline{\boldsymbol{D}}\right] \mathrm{d}S\,,$$

applied to $\boldsymbol{a}(\boldsymbol{r}') = \boldsymbol{E}_{\mathrm{i}}(\boldsymbol{r}')$ and $\overline{\boldsymbol{D}}(\boldsymbol{r}') = \overline{\boldsymbol{G}}(k_{\mathrm{i}}, \boldsymbol{r}', \boldsymbol{r})$, the differential equation for the free space dyadic Green function, and the identity $\boldsymbol{a} \cdot (\boldsymbol{b} \times \overline{\boldsymbol{D}}) = (\boldsymbol{a} \times \boldsymbol{b}) \cdot \overline{\boldsymbol{D}}$. For radiating solutions to the Maxwell equations, we use the asymptotic behavior of the free space dyadic Green function in the far-field region

$$\frac{\boldsymbol{r}}{r} \times \left[\nabla \times \overline{\boldsymbol{G}}\,(k_{\mathrm{s}}, \boldsymbol{r}, \boldsymbol{r}')\right] + \mathrm{j}k_{\mathrm{s}} \overline{\boldsymbol{G}}\,(k_{\mathrm{s}}, \boldsymbol{r}, \boldsymbol{r}') = \mathrm{o}\left(\frac{1}{r}\right), \quad \text{as} \quad r \to \infty\,,$$

to show that the integral over the spherical surface vanishes at infinity.

Remark. The Stratton–Chu formulas are surface-integral representations for the electromagnetic fields and are valid for homogeneous particles. For inhomogeneous particles, a volume-integral representation for the electric field can be derived. For this purpose, we consider the nonmagnetic domains D_{s} and D_{i} ($\mu_{\mathrm{s}} = \mu_{\mathrm{i}} = 1$), rewrite the Maxwell equations as

$$\nabla \times \boldsymbol{E}_{\mathrm{t}} = \mathrm{j}k_0 \boldsymbol{H}_{\mathrm{t}}\,, \quad \nabla \times \boldsymbol{H}_{\mathrm{t}} = -\mathrm{j}k_0 \varepsilon_{\mathrm{t}} \boldsymbol{E}_{\mathrm{t}} \quad \text{in} \quad D_{\mathrm{t}}\,, \quad \mathrm{t} = \mathrm{s}, \mathrm{i}\,,$$

and assume that the domain D_{i} is isotropic, linear and inhomogeneous, i.e., $\varepsilon_{\mathrm{i}} = \varepsilon_{\mathrm{i}}(\boldsymbol{r})$. The Maxwell *curl* equation for the magnetic field $\boldsymbol{H}_{\mathrm{i}}$ can be written as

$$\nabla \times \boldsymbol{H}_{\mathrm{i}} = -\mathrm{j}k_0\varepsilon_{\mathrm{s}}\boldsymbol{E}_{\mathrm{i}} - \mathrm{j}k_0\varepsilon_{\mathrm{s}}\left(\frac{\varepsilon_{\mathrm{i}}}{\varepsilon_{\mathrm{s}}} - 1\right)\boldsymbol{E}_{\mathrm{i}}$$

$$= -\mathrm{j}k_0\varepsilon_{\mathrm{s}}\boldsymbol{E}_{\mathrm{i}} - \frac{\mathrm{j}}{k_0}k_{\mathrm{s}}^2\left(m_{\mathrm{r}}^2 - 1\right)\boldsymbol{E}_{\mathrm{i}}\,,$$

where $m_{\mathrm{r}} = m_{\mathrm{r}}(\boldsymbol{r})$ is the relative refractive index and $k_{\mathrm{s}} = k_0\sqrt{\varepsilon_{\mathrm{s}}}$. Defining the total electric and magnetic fields everywhere in space by

$$\boldsymbol{E} = \begin{cases} \boldsymbol{E}_{\mathrm{s}} + \boldsymbol{E}_{\mathrm{e}} & \text{in} \quad D_{\mathrm{s}}\,, \\ \boldsymbol{E}_{\mathrm{i}} & \text{in} \quad D_{\mathrm{i}}\,, \end{cases}$$

and

$$\boldsymbol{H} = \begin{cases} \boldsymbol{H}_{\mathrm{s}} + \boldsymbol{H}_{\mathrm{e}} & \text{in} \quad D_{\mathrm{s}}\,, \\ \boldsymbol{H}_{\mathrm{i}} & \text{in} \quad D_{i}\,, \end{cases}$$

respectively, and the forcing function $\boldsymbol{J}$ by

$$\boldsymbol{J} = k_{\mathrm{s}}^2\left(m_{\mathrm{rt}}^2 - 1\right)\boldsymbol{E}\,,$$

where

$$m_{\mathrm{rt}} = \begin{cases} 1 & \text{in} \quad D_{\mathrm{s}}\,, \\ m_{\mathrm{r}} & \text{in} \quad D_{\mathrm{i}}\,, \end{cases}$$

we see that the total electric and magnetic fields satisfy the Maxwell *curl* equations,

$$\nabla \times \boldsymbol{E} = \mathrm{j}k_0\boldsymbol{H}\,, \quad \nabla \times \boldsymbol{H} = -\mathrm{j}k_0\varepsilon_{\mathrm{s}}\boldsymbol{E} - \frac{\mathrm{j}}{k_0}\boldsymbol{J} \quad \text{in} \quad D_{\mathrm{s}} \cup D_{\mathrm{i}}\,.$$

By taking the *curl* of the first equation we obtain an inhomogeneous differential equation for total electric field

$$\nabla \times \nabla \times \boldsymbol{E} - k_{\mathrm{s}}^2\boldsymbol{E} = \boldsymbol{J} \quad \text{in} \quad D_{\mathrm{s}} \cup D_{\mathrm{i}}\,. \tag{1.67}$$

Making use of the differential equation for the free space dyadic Green function (1.66) and the identity

$$\nabla \times \left[\overline{\boldsymbol{G}}\left(k_{\mathrm{s}}, \boldsymbol{r}, \boldsymbol{r}'\right) \cdot \boldsymbol{J}\left(\boldsymbol{r}'\right)\right] = \left[\nabla \times \overline{\boldsymbol{G}}\left(k_{\mathrm{s}}, \boldsymbol{r}, \boldsymbol{r}'\right)\right] \cdot \boldsymbol{J}\left(\boldsymbol{r}'\right)\,,$$

we derive

$$\nabla \times \nabla \times \left[\overline{\boldsymbol{G}}\left(k_{\mathrm{s}}, \boldsymbol{r}, \boldsymbol{r}'\right) \cdot \boldsymbol{J}\left(\boldsymbol{r}'\right)\right]$$
$$-k_{\mathrm{s}}^2\,\overline{\boldsymbol{G}}\left(k_{\mathrm{s}}, \boldsymbol{r}, \boldsymbol{r}'\right) \cdot \boldsymbol{J}\left(\boldsymbol{r}'\right) = \overline{\boldsymbol{I}} \cdot \boldsymbol{J}\left(\boldsymbol{r}'\right)\delta\left(\boldsymbol{r} - \boldsymbol{r}'\right)\,.$$

Integrating this equation over all $\boldsymbol{r}'$ and using the identity $\delta(\boldsymbol{r}-\boldsymbol{r}') = \delta(\boldsymbol{r}'-\boldsymbol{r})$, gives [131]

$$\left(\nabla \times \nabla \times \overline{\boldsymbol{I}} - k_{\mathrm{s}}^2\overline{\boldsymbol{I}}\right) \cdot \int_{\boldsymbol{R}^3} \overline{\boldsymbol{G}}\left(k_{\mathrm{s}}, \boldsymbol{r}, \boldsymbol{r}'\right) \cdot \boldsymbol{J}\left(\boldsymbol{r}'\right) \mathrm{d}V\left(\boldsymbol{r}'\right) = \boldsymbol{J}(\boldsymbol{r})\,. \tag{1.68}$$

Because (1.67) and (1.68) have the same right-hand side we deduce that

$$\boldsymbol{E}(\boldsymbol{r}) = \int_{\boldsymbol{R}^3} \overline{\boldsymbol{G}}\,(k_\mathrm{s}, \boldsymbol{r}, \boldsymbol{r}') \cdot \boldsymbol{J}\,(\boldsymbol{r}')\,\mathrm{d}V\,(\boldsymbol{r}')\;, \quad \boldsymbol{r} \in D_\mathrm{s} \cup D_\mathrm{i}$$

and, since $\boldsymbol{J} = 0$ in D_s, we obtain

$$\boldsymbol{E}(\boldsymbol{r}) = \int_{D_\mathrm{i}} \overline{\boldsymbol{G}}\,(k_\mathrm{s}, \boldsymbol{r}, \boldsymbol{r}') \cdot \boldsymbol{J}\,(\boldsymbol{r}')\,\mathrm{d}V\,(\boldsymbol{r}')\;, \quad \boldsymbol{r} \in D_\mathrm{s} \cup D_\mathrm{i}\,.$$

This vector field is the particular solution to the differential equation (1.67) that depends on the forcing function. For $\boldsymbol{r} \in D_\mathrm{s}$, the particular solution satisfies the Silver–Müller radiation condition and gives the scattered field. The solution to the homogeneous equation or the complementary solution satisfies the equation

$$\nabla \times \nabla \times \boldsymbol{E}_\mathrm{e} - k_\mathrm{s}^2 \boldsymbol{E}_\mathrm{e} = 0 \quad \text{in} \quad D_\mathrm{s} \cup D_\mathrm{i}\,.$$

and describes the field that would exist in the absence of the scattering object, i.e., the incident field. Thus, the complete solution to (1.67) can be written as

$$\begin{aligned}\boldsymbol{E}(\boldsymbol{r}) &= \boldsymbol{E}_\mathrm{e}(\boldsymbol{r}) + \int_{D_\mathrm{i}} \overline{\boldsymbol{G}}\,(k_\mathrm{s}, \boldsymbol{r}, \boldsymbol{r}') \cdot \boldsymbol{J}\,(\boldsymbol{r}')\,\mathrm{d}V\,(\boldsymbol{r}') \\ &= \boldsymbol{E}_\mathrm{e}(\boldsymbol{r}) + k_\mathrm{s}^2 \int_{D_\mathrm{i}} \overline{\boldsymbol{G}}\,(k_\mathrm{s}, \boldsymbol{r}, \boldsymbol{r}') \cdot \left[m_\mathrm{r}^2\,(\boldsymbol{r}') - 1\right] \boldsymbol{E}\,(\boldsymbol{r}')\,\mathrm{d}V\,(\boldsymbol{r}')\;, \\ \boldsymbol{r} &\in D_\mathrm{s} \cup D_\mathrm{i}\,.\end{aligned}$$

We note that for a nontrivial magnetic permeability of the particle, a volume-surface integral equation has been derived by Volakis [245], and a "pure" volume-integral equation has been given by Volakis et al. [246].

1.4.2 Far-Field Pattern and Amplitude Matrix

Application of Stratton–Chu representation theorem to the vector fields $\boldsymbol{E}_\mathrm{s}$ and $\boldsymbol{E}_\mathrm{e}$ in the domain D_s together with the boundary conditions $\boldsymbol{e}_\mathrm{s} + \boldsymbol{e}_\mathrm{e} = \boldsymbol{e}_\mathrm{i}$ and $\boldsymbol{h}_\mathrm{s} + \boldsymbol{h}_\mathrm{e} = \boldsymbol{h}_\mathrm{i}$, yield

$$\begin{aligned}\boldsymbol{E}_\mathrm{s}(\boldsymbol{r}) = \nabla \times \int_S \boldsymbol{e}_\mathrm{i}\,(\boldsymbol{r}')\,g\,(k_\mathrm{s}, \boldsymbol{r}, \boldsymbol{r}')\,\mathrm{d}S(\boldsymbol{r}') \\ + \frac{\mathrm{j}}{k_0 \varepsilon_\mathrm{s}} \nabla \times \nabla \times \int_S \boldsymbol{h}_\mathrm{i}\,(\boldsymbol{r}')\,g\,(k_\mathrm{s}, \boldsymbol{r}, \boldsymbol{r}')\,\mathrm{d}S(\boldsymbol{r}')\,, \quad \boldsymbol{r} \in D_\mathrm{s}\,,\end{aligned}$$

where $\boldsymbol{E}_\mathrm{s}, \boldsymbol{H}_\mathrm{s}$ and $\boldsymbol{E}_\mathrm{i}, \boldsymbol{H}_\mathrm{i}$ solve the transmission boundary-value problem. The above equation is known as the Huygens principle and it expresses the field in the domain D_s in terms of the surface fields on the surface S (see, for

example, [229]). Application of Stratton–Chu representation theorem in the domain D_i gives the (general) null-field equation or the extinction theorem:

$$\boldsymbol{E}_\mathrm{e}(\boldsymbol{r}) + \nabla \times \int_S \boldsymbol{e}_\mathrm{i}(\boldsymbol{r}')\, g(k_\mathrm{s}, \boldsymbol{r}, \boldsymbol{r}')\, \mathrm{d}S(\boldsymbol{r}') + \frac{\mathrm{j}}{k_0 \varepsilon_\mathrm{s}} \nabla \times \nabla \times \int_S \boldsymbol{h}_\mathrm{i}(\boldsymbol{r}')\, g(k_\mathrm{s}, \boldsymbol{r}, \boldsymbol{r}')\, \mathrm{d}S(\boldsymbol{r}') = 0\,, \quad \boldsymbol{r} \in D_\mathrm{i}\,,$$

which shows that the radiation of the surface fields into D_i extinguishes the incident wave [229]. In the null-field method, the extinction theorem is used to derive a set of integral equations for the surface fields, while the Huygens principle is employed to compute the scattered field.

Every radiating solution $\boldsymbol{E}_\mathrm{s}, \boldsymbol{H}_\mathrm{s}$ to the Maxwell equations has the asymptotic form

$$\boldsymbol{E}_\mathrm{s}(\boldsymbol{r}) = \frac{\mathrm{e}^{\mathrm{j}k_\mathrm{s} r}}{r} \left\{ \boldsymbol{E}_{\mathrm{s}\infty}(\boldsymbol{e}_r) + \mathrm{O}\left(\frac{1}{r}\right) \right\}, \quad r \to \infty\,,$$

$$\boldsymbol{H}_\mathrm{s}(\boldsymbol{r}) = \frac{\mathrm{e}^{\mathrm{j}k_\mathrm{s} r}}{r} \left\{ \boldsymbol{H}_{\mathrm{s}\infty}(\boldsymbol{e}_r) + \mathrm{O}\left(\frac{1}{r}\right) \right\}, \quad r \to \infty\,,$$

uniformly for all directions $\boldsymbol{e}_r = \boldsymbol{r}/r$. The vector fields $\boldsymbol{E}_{\mathrm{s}\infty}$ and $\boldsymbol{H}_{\mathrm{s}\infty}$ defined on the unit sphere are the electric and magnetic far-field patterns, respectively, and satisfy the relations:

$$\boldsymbol{H}_{\mathrm{s}\infty} = \sqrt{\frac{\varepsilon_\mathrm{s}}{\mu_\mathrm{s}}}\, \boldsymbol{e}_r \times \boldsymbol{E}_{\mathrm{s}\infty}\,,$$

$$\boldsymbol{e}_r \cdot \boldsymbol{E}_{\mathrm{s}\infty} = \boldsymbol{e}_r \cdot \boldsymbol{H}_{\mathrm{s}\infty} = 0\,.$$

Because $\boldsymbol{E}_{\mathrm{s}\infty}$ also depends on the incident direction $\boldsymbol{e}_k$, $\boldsymbol{E}_{\mathrm{s}\infty}$ is known as the scattering amplitude from the direction $\boldsymbol{e}_k$ into the direction $\boldsymbol{e}_r$ [229]. Using the Huygens principle and the asymptotic expressions

$$\nabla \times \left[\boldsymbol{a}(\boldsymbol{r}') \frac{\mathrm{e}^{\mathrm{j}k_\mathrm{s}|\boldsymbol{r}-\boldsymbol{r}'|}}{|\boldsymbol{r}-\boldsymbol{r}'|} \right] = \mathrm{j}k_\mathrm{s} \frac{\mathrm{e}^{\mathrm{j}k_\mathrm{s} r}}{r} \left\{ \mathrm{e}^{-\mathrm{j}k_\mathrm{s} \boldsymbol{e}_r \cdot \boldsymbol{r}'} \boldsymbol{e}_r \times \boldsymbol{a}(\boldsymbol{r}') + \mathrm{O}\left(\frac{a}{r}\right) \right\},$$

$$\nabla \times \nabla \times \left[\boldsymbol{a}(\boldsymbol{r}') \frac{\mathrm{e}^{\mathrm{j}k_\mathrm{s}|\boldsymbol{r}-\boldsymbol{r}'|}}{|\boldsymbol{r}-\boldsymbol{r}'|} \right] = k_\mathrm{s}^2 \frac{\mathrm{e}^{\mathrm{j}k_\mathrm{s} r}}{r} \times \left\{ \mathrm{e}^{-\mathrm{j}k_\mathrm{s} \boldsymbol{e}_r \cdot \boldsymbol{r}'} \boldsymbol{e}_r \times [\boldsymbol{a}(\boldsymbol{r}') \times \boldsymbol{e}_r] + \mathrm{O}\left(\frac{a}{r}\right) \right\},$$

as $r \to \infty$, we obtain the following integral representations for the far-field patterns [40]

$$\boldsymbol{E}_{\mathrm{s}\infty}(\boldsymbol{e}_r) = \frac{\mathrm{j}k_\mathrm{s}}{4\pi} \int_S \left\{ \boldsymbol{e}_r \times \boldsymbol{e}_\mathrm{s}(\boldsymbol{r}') + \sqrt{\frac{\mu_\mathrm{s}}{\varepsilon_\mathrm{s}}}\, \boldsymbol{e}_r \times [\boldsymbol{h}_\mathrm{s}(\boldsymbol{r}') \times \boldsymbol{e}_r] \right\} \mathrm{e}^{-\mathrm{j}k_\mathrm{s} \boldsymbol{e}_r \cdot \boldsymbol{r}'} \mathrm{d}S(\boldsymbol{r}')\,, \quad (1.69)$$

$$\boldsymbol{H}_{\mathrm{s}\infty}(\boldsymbol{e}_r) = \frac{\mathrm{j}k_{\mathrm{s}}}{4\pi}\int_S \left\{ \boldsymbol{e}_r \times \boldsymbol{h}_{\mathrm{s}}(\boldsymbol{r}') - \sqrt{\frac{\varepsilon_{\mathrm{s}}}{\mu_{\mathrm{s}}}}\boldsymbol{e}_r \times [\boldsymbol{e}_{\mathrm{s}}(\boldsymbol{r}') \times \boldsymbol{e}_r] \right\} \mathrm{e}^{-\mathrm{j}k_{\mathrm{s}}\boldsymbol{e}_r\cdot\boldsymbol{r}'}\,\mathrm{d}S(\boldsymbol{r}') \ . \quad (1.70)$$

The quantity $\sigma_{\mathrm{d}} = |\boldsymbol{E}_{\mathrm{s}\infty}|^2$ is called the differential scattering cross-section and describes the angular distribution of the scattered light. The differential scattering cross-section depends on the polarization state of the incident field and on the incident and scattering directions. The quantities $\sigma_{\mathrm{dp}} = |E_{\mathrm{s}\infty,\theta}|^2$ and $\sigma_{\mathrm{ds}} = |E_{\mathrm{s}\infty,\varphi}|^2$ are referred to as the differential scattering cross-sections for parallel and perpendicular polarizations, respectively. The differential scattering cross-section has the dimension of area, and a dimensionless quantity is the normalized differential scattering cross-section $\sigma_{\mathrm{dn}} = \sigma_{\mathrm{d}}/\pi a_{\mathrm{c}}^2$, where a_{c} is a characteristic dimension of the particle.

To introduce the concepts of tensor scattering amplitude and amplitude matrix it is necessary to choose an orthonormal unit system for polarization description. In Sect. 1.2 we chose a global coordinate system and used the vertical and horizontal polarization unit vectors $\boldsymbol{e}_\alpha$ and $\boldsymbol{e}_\beta$, to describe the polarization state of the incident wave (Fig. 1.9a). For the scattered wave we can proceed analogously by considering the vertical and horizontal polarization unit vectors $\boldsymbol{e}_\varphi$ and $\boldsymbol{e}_\theta$. Essentially, $(\boldsymbol{e}_k, \boldsymbol{e}_\beta, \boldsymbol{e}_\alpha)$ are the spherical unit vectors of $\boldsymbol{k}_{\mathrm{e}}$, while $(\boldsymbol{e}_r, \boldsymbol{e}_\theta, \boldsymbol{e}_\varphi)$ are the spherical unit vectors of $\boldsymbol{k}_{\mathrm{s}}$ in

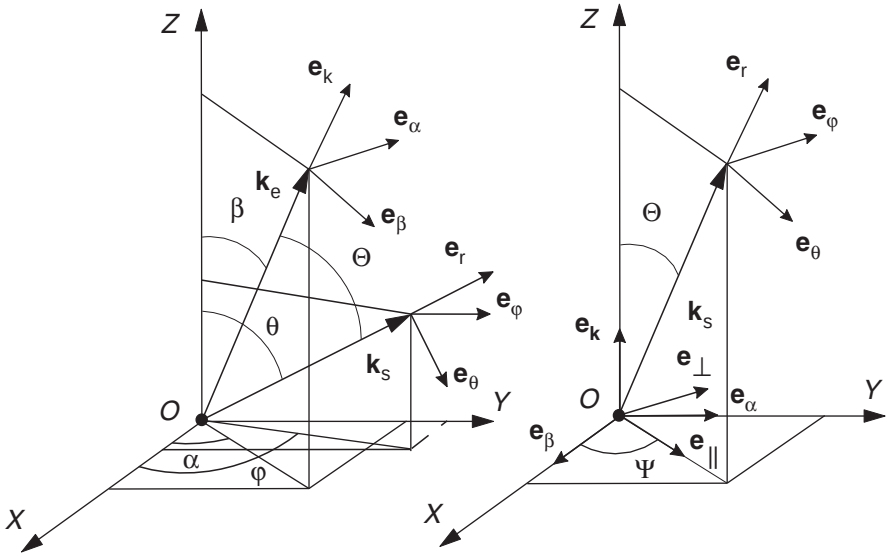

Fig. 1.9. Reference frames: (**a**) global coordinate system and (**b**) beam coordinate system

the global coordinate system. A second choice is the system based on the scattering plane. In this case we consider the beam coordinate system with the Z-axis directed along the incidence direction, and define the Stokes vectors with respect to the scattering plane, that is, the plane through the direction of incidence and scattering (Fig. 1.9b). For the scattered wave, the polarization description is in terms of the vertical and horizontal polarization unit vectors $\boldsymbol{e}_\varphi$ and $\boldsymbol{e}_\theta$, while for the incident wave, the polarization description is in terms of the unit vectors $\boldsymbol{e}_\perp = \boldsymbol{e}_\varphi$ and $\boldsymbol{e}_\parallel = \boldsymbol{e}_\perp \times \boldsymbol{e}_k$. The advantage of this system is that the scattering amplitude can take simple forms for particles with symmetry, and the disadvantage is that $\boldsymbol{e}_\perp$ and $\boldsymbol{e}_\parallel$ depend on the scattering direction. Furthermore, any change in the direction of light incidence also changes the orientation of the particle with respect to the reference frame. In our analysis we will use a fixed global coordinate system to specify both the direction of propagation and the states of polarization of the incident and scattered waves and the particle orientation (see also, [169, 228]).

The tensor scattering amplitude or the scattering dyad is given by [169]

$$\boldsymbol{E}_{\mathrm{s}\infty}(\boldsymbol{e}_r) = \overline{\boldsymbol{A}}\,(\boldsymbol{e}_r, \boldsymbol{e}_k) \cdot \boldsymbol{E}_{\mathrm{e}0}\,, \tag{1.71}$$

and since $\boldsymbol{e}_r \cdot \boldsymbol{E}_{\mathrm{s}\infty} = 0$, it follows that:

$$\boldsymbol{e}_r \cdot \overline{\boldsymbol{A}}\,(\boldsymbol{e}_r, \boldsymbol{e}_k) = 0\,. \tag{1.72}$$

Because the incident wave is a transverse wave, $\boldsymbol{e}_k \cdot \boldsymbol{E}_{\mathrm{e}0} = 0$, the dot product $\overline{\boldsymbol{A}}(\boldsymbol{e}_r, \boldsymbol{e}_k) \cdot \boldsymbol{e}_k$ is not defined by (1.71), and to complete the definition, we take

$$\overline{\boldsymbol{A}}\,(\boldsymbol{e}_r, \boldsymbol{e}_k) \cdot \boldsymbol{e}_k = 0\,. \tag{1.73}$$

Although the scattering dyad describes the scattering of a vector plane wave, it can be used to describe the scattering of any incident field, because any regular solution to the Maxwell equations can be expressed as an integral over vector plane waves. As a consequence of (1.72) and (1.73), only four components of the scattering dyad are independent and it is convenient to introduce the 2×2 amplitude matrix $\boldsymbol{S}$ to describe the transformation of the transverse components of the incident wave into the transverse components of the scattered wave in the far-field region. The amplitude matrix is given by [17, 169, 228]

$$\begin{bmatrix} E_{\mathrm{s}\infty,\theta}(\boldsymbol{e}_r) \\ E_{\mathrm{s}\infty,\varphi}(\boldsymbol{e}_r) \end{bmatrix} = \boldsymbol{S}\,(\boldsymbol{e}_r, \boldsymbol{e}_k) \begin{bmatrix} E_{\mathrm{e}0,\beta} \\ E_{\mathrm{e}0,\alpha} \end{bmatrix}\,, \tag{1.74}$$

where $E_{\mathrm{e}0,\beta}$ and $E_{\mathrm{e}0,\alpha}$ do not depend on the incident direction. Essentially, the amplitude matrix is a generalization of the scattering amplitudes including polarization effects. The amplitude matrix provides a complete description of the far-field patterns and it depends on the incident and scattering directions as well on the size, optical properties and orientation of the particle. The elements of the amplitude matrix

$$\mathbf{S} = \begin{bmatrix} S_{\theta\beta} & S_{\theta\alpha} \\ S_{\varphi\beta} & S_{\varphi\alpha} \end{bmatrix}$$

are expressed in terms of the scattering dyad as follows:

$$\begin{aligned} S_{\theta\beta} &= \boldsymbol{e}_\theta \cdot \overline{\boldsymbol{A}} \cdot \boldsymbol{e}_\beta \,, \\ S_{\theta\alpha} &= \boldsymbol{e}_\theta \cdot \overline{\boldsymbol{A}} \cdot \boldsymbol{e}_\alpha \,, \\ S_{\varphi\beta} &= \boldsymbol{e}_\varphi \cdot \overline{\boldsymbol{A}} \cdot \boldsymbol{e}_\beta \,, \\ S_{\varphi\alpha} &= \boldsymbol{e}_\varphi \cdot \overline{\boldsymbol{A}} \cdot \boldsymbol{e}_\alpha \,. \end{aligned} \tag{1.75}$$

1.4.3 Phase and Extinction Matrices

As in optics the electric and magnetics fields cannot directly be measured because of their high frequency oscillations, other measurable quantities describing the change of the polarization state upon scattering have to be defined. The transformation of the polarization characteristic of the incident light into that of the scattered light is given by the phase matrix. The coherency phase matrix $\boldsymbol{Z}_\mathrm{c}$ relates the coherency vectors of the incident and scattered fields

$$\boldsymbol{J}_\mathrm{s}\left(r\boldsymbol{e}_r\right) = \frac{1}{r^2}\boldsymbol{Z}_\mathrm{c}\left(\boldsymbol{e}_r, \boldsymbol{e}_k\right)\boldsymbol{J}_\mathrm{e}\,,$$

where the coherency vector of the incident field $\boldsymbol{J}_\mathrm{e}$ is given by (1.19) and the coherency vector of the scattered field $\boldsymbol{J}_\mathrm{s}$ is defined as

$$\boldsymbol{J}_\mathrm{s}\left(r\boldsymbol{e}_r\right) = \frac{1}{2r^2}\sqrt{\frac{\varepsilon_\mathrm{s}}{\mu_\mathrm{s}}} \begin{bmatrix} E_{\mathrm{s}\infty,\theta}\left(\boldsymbol{e}_r\right) E^*_{\mathrm{s}\infty,\theta}\left(\boldsymbol{e}_r\right) \\ E_{\mathrm{s}\infty,\theta}\left(\boldsymbol{e}_r\right) E^*_{\mathrm{s}\infty,\varphi}\left(\boldsymbol{e}_r\right) \\ E_{\mathrm{s}\infty,\varphi}\left(\boldsymbol{e}_r\right) E^*_{\mathrm{s}\infty,\theta}\left(\boldsymbol{e}_r\right) \\ E_{\mathrm{s}\infty,\varphi}\left(\boldsymbol{e}_r\right) E^*_{\mathrm{s}\infty,\varphi}\left(\boldsymbol{e}_r\right) \end{bmatrix}.$$

Explicitly, the coherency phase matrix is given by

$$\boldsymbol{Z}_\mathrm{c} = \begin{bmatrix} |S_{\theta\beta}|^2 & S_{\theta\beta}S^*_{\theta\alpha} & S_{\theta\alpha}S^*_{\theta\beta} & |S_{\theta\alpha}|^2 \\ S_{\theta\beta}S^*_{\varphi\beta} & S_{\theta\beta}S^*_{\varphi\alpha} & S_{\theta\alpha}S^*_{\varphi\beta} & S_{\theta\alpha}S^*_{\varphi\alpha} \\ S_{\varphi\beta}S^*_{\theta\beta} & S_{\varphi\beta}S^*_{\theta\alpha} & S_{\varphi\alpha}S^*_{\theta\beta} & S_{\varphi\alpha}S^*_{\theta\alpha} \\ |S_{\varphi\beta}|^2 & S_{\varphi\beta}S^*_{\varphi\alpha} & S_{\varphi\alpha}S^*_{\varphi\beta} & |S_{\varphi\alpha}|^2 \end{bmatrix}.$$

The phase matrix $\boldsymbol{Z}$ describes the transformation of the Stokes vector of the incident field into that of the scattered field

$$\boldsymbol{I}_\mathrm{s}\left(r\boldsymbol{e}_r\right) = \frac{1}{r^2}\boldsymbol{Z}\left(\boldsymbol{e}_r, \boldsymbol{e}_k\right)\boldsymbol{I}_\mathrm{e} \tag{1.76}$$

and we have

$$\boldsymbol{Z}\left(\boldsymbol{e}_r, \boldsymbol{e}_k\right) = \boldsymbol{D}\boldsymbol{Z}_\mathrm{c}\left(\boldsymbol{e}_r, \boldsymbol{e}_k\right)\boldsymbol{D}^{-1}\,,$$

where the transformation matrix $\boldsymbol{D}$ is given by (1.21), the Stokes vector of the incident field $\boldsymbol{I}_{\mathrm{e}}$ is given by (1.20) and the Stokes vector of the scattered field $\boldsymbol{I}_{\mathrm{s}}$ is defined as

$$\boldsymbol{I}_{\mathrm{s}}\left(r\boldsymbol{e}_r\right)=\frac{1}{r^2}\begin{bmatrix} I_{\mathrm{s}}\left(\boldsymbol{e}_r\right)\\ Q_{\mathrm{s}}\left(\boldsymbol{e}_r\right)\\ U_{\mathrm{s}}\left(\boldsymbol{e}_r\right)\\ V_{\mathrm{s}}\left(\boldsymbol{e}_r\right)\end{bmatrix}=\boldsymbol{D}\boldsymbol{J}_{\mathrm{s}}\left(r\boldsymbol{e}_r\right)$$

$$=\frac{1}{2r^2}\sqrt{\frac{\varepsilon_{\mathrm{s}}}{\mu_{\mathrm{s}}}}\begin{bmatrix} \left|E_{\mathrm{s}\infty,\theta}\left(\boldsymbol{e}_r\right)\right|^2+\left|E_{\mathrm{s}\infty,\varphi}\left(\boldsymbol{e}_r\right)\right|^2\\ \left|E_{\mathrm{s}\infty,\theta}\left(\boldsymbol{e}_r\right)\right|^2-\left|E_{\mathrm{s}\infty,\varphi}\left(\boldsymbol{e}_r\right)\right|^2\\ -E_{\mathrm{s}\infty,\varphi}\left(\boldsymbol{e}_r\right)E^*_{\mathrm{s}\infty,\theta}\left(\boldsymbol{e}_r\right)-E_{\mathrm{s}\infty,\theta}\left(\boldsymbol{e}_r\right)E^*_{\mathrm{s}\infty,\varphi}\left(\boldsymbol{e}_r\right)\\ \mathrm{j}\left[E_{\mathrm{s}\infty,\varphi}\left(\boldsymbol{e}_r\right)E^*_{\mathrm{s}\infty,\theta}\left(\boldsymbol{e}_r\right)-E_{\mathrm{s}\infty,\theta}\left(\boldsymbol{e}_r\right)E^*_{\mathrm{s}\infty,\varphi}\left(\boldsymbol{e}_r\right)\right]\end{bmatrix}.$$

Explicit formulas for the elements of the phase matrix are:

$$\begin{aligned}
Z_{11}&=\frac{1}{2}\left(\left|S_{\theta\beta}\right|^2+\left|S_{\theta\alpha}\right|^2+\left|S_{\varphi\beta}\right|^2+\left|S_{\varphi\alpha}\right|^2\right),\\
Z_{12}&=\frac{1}{2}\left(\left|S_{\theta\beta}\right|^2-\left|S_{\theta\alpha}\right|^2+\left|S_{\varphi\beta}\right|^2-\left|S_{\varphi\alpha}\right|^2\right),\\
Z_{13}&=-\mathrm{Re}\left\{S_{\theta\beta}S^*_{\theta\alpha}+S_{\varphi\alpha}S^*_{\varphi\beta}\right\},\\
Z_{14}&=-\mathrm{Im}\left\{S_{\theta\beta}S^*_{\theta\alpha}-S_{\varphi\alpha}S^*_{\varphi\beta}\right\},\\
Z_{21}&=\frac{1}{2}\left(\left|S_{\theta\beta}\right|^2+\left|S_{\theta\alpha}\right|^2-\left|S_{\varphi\beta}\right|^2-\left|S_{\varphi\alpha}\right|^2\right),\\
Z_{22}&=\frac{1}{2}\left(\left|S_{\theta\beta}\right|^2-\left|S_{\theta\alpha}\right|^2-\left|S_{\varphi\beta}\right|^2+\left|S_{\varphi\alpha}\right|^2\right),\\
Z_{23}&=-\mathrm{Re}\left\{S_{\theta\beta}S^*_{\theta\alpha}-S_{\varphi\alpha}S^*_{\varphi\beta}\right\},\\
Z_{24}&=-\mathrm{Im}\left\{S_{\theta\beta}S^*_{\theta\alpha}+S_{\varphi\alpha}S^*_{\varphi\beta}\right\},\\
Z_{31}&=-\mathrm{Re}\left\{S_{\theta\beta}S^*_{\varphi\beta}+S_{\varphi\alpha}S^*_{\theta\alpha}\right\},\\
Z_{32}&=-\mathrm{Re}\left\{S_{\theta\beta}S^*_{\varphi\beta}-S_{\varphi\alpha}S^*_{\theta\alpha}\right\},\\
Z_{33}&=\mathrm{Re}\left\{S_{\theta\beta}S^*_{\varphi\alpha}+S_{\theta\alpha}S^*_{\varphi\beta}\right\},\\
Z_{34}&=\mathrm{Im}\left\{S_{\theta\beta}S^*_{\varphi\alpha}+S_{\varphi\beta}S^*_{\theta\alpha}\right\},\\
Z_{41}&=-\mathrm{Im}\left\{S_{\varphi\beta}S^*_{\theta\beta}+S_{\varphi\alpha}S^*_{\theta\alpha}\right\},\\
Z_{42}&=-\mathrm{Im}\left\{S_{\varphi\beta}S^*_{\theta\beta}-S_{\varphi\alpha}S^*_{\theta\alpha}\right\},\\
Z_{43}&=\mathrm{Im}\left\{S_{\varphi\alpha}S^*_{\theta\beta}-S_{\theta\alpha}S^*_{\varphi\beta}\right\},\\
Z_{44}&=\mathrm{Re}\left\{S_{\varphi\alpha}S^*_{\theta\beta}-S_{\theta\alpha}S^*_{\varphi\beta}\right\}.
\end{aligned}\tag{1.77}$$

The above phase matrix is also known as the pure phase matrix, because its elements follow directly from the corresponding amplitude matrix that transforms the two electric field components [100]. The phase matrix of a particle in a fixed orientation may contain sixteen nonvanishing elements. Because only phase differences occur in the expressions of Z_{ij}, $i, j = 1, 2, 3, 4$, the phase matrix elements are essentially determined by no more than seven real numbers: the four moduli $|S_{pq}|$ and the three differences in phase between the S_{pq}, where $p = \theta$, φ and $q = \beta$, α. Consequently, only seven phase matrix elements are independent and there are nine linear relations among the sixteen elements. These linear dependent relations show that a pure phase matrix has a certain internal structure. Several linear and quadratic inequalities for the phase matrix elements have been reported by exploiting the internal structure of the pure phase matrix, and the most important inequalities are $Z_{11} \geq 0$ and $|Z_{ij}| \leq Z_{11}$ for $i, j = 1, 2, 3, 4$ [102–104]. In principle, all scalar and matrix properties of pure phase matrices can be used for theoretical purposes or to test whether an experimentally or numerically determined matrix can be a pure phase matrix.

Equation (1.76) shows that electromagnetic scattering produces light with polarization characteristics different from those of the incident light. If the incident beam is unpolarized, $\boldsymbol{I}_{\rm e} = [I_{\rm e}, 0, 0, 0]^T$, the Stokes vector of the scattered field has at least one nonvanishing component other than intensity, $\boldsymbol{I}_{\rm s} = [Z_{11}I_{\rm e}, Z_{21}I_{\rm e}, Z_{31}I_{\rm e}, Z_{41}I_{\rm e}]^T$. When the incident beam is linearly polarized, $\boldsymbol{I}_{\rm e} = [I_{\rm e}, Q_{\rm e}, U_{\rm e}, 0]^T$, the scattered light may become elliptically polarized since $V_{\rm s}$ may be nonzero. However, if the incident beam is fully polarized ($P_{\rm e} = 1$), then the scattered light is also fully polarized ($P_{\rm s} = 1$) [104].

As mentioned before, a scattering particle can change the state of polarization of the incident beam after it passes the particle. This phenomenon is called dichroism and is a consequence of the different values of attenuation rates for different polarization components of the incident light. A complete description of the extinction process requires the introduction of the so-called extinction matrix. In order to derive the expression of the extinction matrix we consider the case of the forward-scattering direction, $\boldsymbol{e}_r = \boldsymbol{e}_k$, and define the coherency vector of the total field $\boldsymbol{E} = \boldsymbol{E}_{\rm s} + \boldsymbol{E}_{\rm e}$ by

$$\boldsymbol{J}\left(r\boldsymbol{e}_k\right) = \frac{1}{2}\sqrt{\frac{\varepsilon_{\rm s}}{\mu_{\rm s}}} \begin{bmatrix} E_\beta\left(r\boldsymbol{e}_k\right) E_\beta^*\left(r\boldsymbol{e}_k\right) \\ E_\beta\left(r\boldsymbol{e}_k\right) E_\alpha^*\left(r\boldsymbol{e}_k\right) \\ E_\alpha\left(r\boldsymbol{e}_k\right) E_\beta^*\left(r\boldsymbol{e}_k\right) \\ E_\alpha\left(r\boldsymbol{e}_k\right) E_\alpha^*\left(r\boldsymbol{e}_k\right) \end{bmatrix} .$$

Using the decomposition

$$\begin{aligned} E_p(\boldsymbol{r})E_q^*(\boldsymbol{r}) = {} & E_{{\rm e}0,p}E_{{\rm e}0,q}^* + E_{{\rm e}0,p}{\rm e}^{{\rm j}\boldsymbol{k}_{\rm e}\cdot\boldsymbol{r}}E_{{\rm s},q}^*(\boldsymbol{r}) \\ & + E_{{\rm s},p}(\boldsymbol{r})E_{{\rm e}0,q}^*{\rm e}^{-{\rm j}\boldsymbol{k}_{\rm e}\cdot\boldsymbol{r}} + E_{{\rm s},p}(\boldsymbol{r})E_{{\rm s},q}^*(\boldsymbol{r}) \,, \end{aligned}$$

where p and q stand for β and α, we approximate the integral of the generic term $E_pE_q^*$ in the far-field region and over a small solid angle $\Delta\Omega$ around the

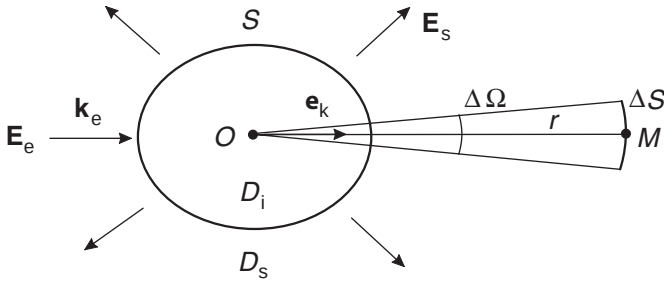

Fig. 1.10. Elementary surface ΔS in the far-field region

direction $\boldsymbol{e}_k$ by

$$\int_{\Delta\Omega} E_p(\boldsymbol{r})E_q^*(\boldsymbol{r})r^2\,\mathrm{d}\Omega\,(\boldsymbol{e}_r) \approx E_p\,(r\boldsymbol{e}_k)\,E_q^*\,(r\boldsymbol{e}_k)\,\Delta S\,,$$

where $\Delta S = r^2\Delta\Omega$ (Fig. 1.10). On the other hand, using the far-field representation for the scattered field

$$E_{\mathrm{s},p}(\boldsymbol{r}) = \frac{\mathrm{e}^{\mathrm{j}k_\mathrm{s}r}}{r}\left\{E_{\mathrm{s}\infty,p}(\boldsymbol{e}_r) + \mathrm{O}\left(\frac{1}{r}\right)\right\}$$

and the asymptotic expression of the plane wave $\exp(\mathrm{j}\boldsymbol{k}_\mathrm{e}\cdot\boldsymbol{r})$ (cf. (B.7)) we approximate the integrals of each term composing $E_pE_q^*$ as follows:

$$\int_{\Delta\Omega} E_{\mathrm{e}0,p}E_{\mathrm{e}0,q}^* r^2\,\mathrm{d}\Omega\,(\boldsymbol{e}_r) \approx E_{\mathrm{e}0,p}E_{\mathrm{e}0,q}^*\Delta S\,,$$

$$\int_{\Delta\Omega} E_{\mathrm{e}0,p}\mathrm{e}^{\mathrm{j}\boldsymbol{k}_\mathrm{e}\cdot\boldsymbol{r}}E_{\mathrm{s},q}^*(\boldsymbol{r})r^2\,\mathrm{d}\Omega\,(\boldsymbol{e}_r) \approx -\frac{2\pi\mathrm{j}}{k_\mathrm{s}}E_{\mathrm{e}0,p}E_{\mathrm{s}\infty,q}^*\,(\boldsymbol{e}_k)\;,$$

$$\int_{\Delta\Omega} E_{\mathrm{s},p}(\boldsymbol{r})E_{\mathrm{e}0,q}^*\mathrm{e}^{-\mathrm{j}\boldsymbol{k}_\mathrm{e}\cdot\boldsymbol{r}}r^2\,\mathrm{d}\Omega\,(\boldsymbol{e}_r) \approx \frac{2\pi\mathrm{j}}{k_\mathrm{s}}E_{\mathrm{s}\infty,p}\,(\boldsymbol{e}_k)\,E_{\mathrm{e}0,q}^*\,,$$

$$\int_{\Delta\Omega} E_{\mathrm{s},p}(\boldsymbol{r})E_{\mathrm{s},q}^*(\boldsymbol{r})r^2\,\mathrm{d}\Omega\,(\boldsymbol{e}_r) \approx E_{\mathrm{s}\infty,p}\,(\boldsymbol{e}_k)\,E_{\mathrm{s}\infty,q}^*\,(\boldsymbol{e}_k)\,\frac{\Delta S}{r^2}\,.$$

Neglecting the term proportional to r^{-2}, we see that

$$E_p\,(r\boldsymbol{e}_k)\,E_q^*\,(r\boldsymbol{e}_k)\,\Delta S \approx E_{\mathrm{e}0,p}E_{\mathrm{e}0,q}^*\Delta S - \frac{2\pi\mathrm{j}}{k_\mathrm{s}}\left[E_{\mathrm{e}0,p}E_{\mathrm{s}\infty,q}^*\,(\boldsymbol{e}_k) - E_{\mathrm{s}\infty,p}\,(\boldsymbol{e}_k)\,E_{\mathrm{e}0,q}^*\right]$$

and the above relation gives

$$\boldsymbol{J}\,(r\boldsymbol{e}_k)\,\Delta S \approx \boldsymbol{J}_\mathrm{e}\Delta S - \boldsymbol{K}_\mathrm{c}\,(\boldsymbol{e}_k)\,\boldsymbol{J}_\mathrm{e}\,,$$

where the coherency extinction matrix $\boldsymbol{K}_{\mathrm{c}}$ is defined as

$$\boldsymbol{K}_{\mathrm{c}} = \frac{2\pi \mathrm{j}}{k_{\mathrm{s}}} \begin{bmatrix} S^*_{\theta\beta} - S_{\theta\beta} & S^*_{\theta\alpha} & -S_{\theta\alpha} & 0 \\ S^*_{\varphi\beta} & S^*_{\varphi\alpha} - S_{\theta\beta} & 0 & -S_{\theta\alpha} \\ -S_{\varphi\beta} & 0 & S^*_{\theta\beta} - S_{\varphi\alpha} & S^*_{\theta\alpha} \\ 0 & -S_{\varphi\beta} & S^*_{\varphi\beta} & S^*_{\varphi\alpha} - S_{\varphi\alpha} \end{bmatrix} .$$

For the Stokes parameters we have

$$\boldsymbol{I}\left(r\boldsymbol{e}_k\right)\Delta S \approx \boldsymbol{I}_{\mathrm{e}}\Delta S - \boldsymbol{K}\left(\boldsymbol{e}_k\right)\boldsymbol{I}_e \tag{1.78}$$

with the extinction matrix $\boldsymbol{K}$ being defined as

$$\boldsymbol{K}\left(\boldsymbol{e}_k\right) = \boldsymbol{D}\boldsymbol{K}_{\mathrm{c}}\left(\boldsymbol{e}_k\right)\boldsymbol{D}^{-1} .$$

The explicit formulas for the elements of the extinction matrix are

$$\begin{aligned} K_{ii} &= \frac{2\pi}{k_{\mathrm{s}}}\mathrm{Im}\left\{S_{\theta\beta} + S_{\varphi\alpha}\right\} , \quad i = 1,2,3,4 , \\ K_{12} = K_{21} &= \frac{2\pi}{k_{\mathrm{s}}}\mathrm{Im}\left\{S_{\theta\beta} - S_{\varphi\alpha}\right\} , \\ K_{13} = K_{31} &= -\frac{2\pi}{k_{\mathrm{s}}}\mathrm{Im}\left\{S_{\theta\alpha} + S_{\varphi\beta}\right\} , \\ K_{14} = K_{41} &= \frac{2\pi}{k_{\mathrm{s}}}\mathrm{Re}\left\{S_{\varphi\beta} - S_{\theta\alpha}\right\} , \\ K_{23} = -K_{32} &= \frac{2\pi}{k_{\mathrm{s}}}\mathrm{Im}\left\{S_{\varphi\beta} - S_{\theta\alpha}\right\} , \\ K_{24} = -K_{42} &= -\frac{2\pi}{k_{\mathrm{s}}}\mathrm{Re}\left\{S_{\theta\alpha} + S_{\varphi\beta}\right\} , \\ K_{34} = -K_{43} &= \frac{2\pi}{k_{\mathrm{s}}}\mathrm{Re}\left\{S_{\varphi\alpha} - S_{\theta\beta}\right\} . \end{aligned} \tag{1.79}$$

The elements of the extinction matrix have the dimension of area and only seven components are independent. Equation (1.78) is an interpretation of the so-called optical theorem which will be discussed in the next section. This relation shows that the particle changes not only the total electromagnetic power received by a detector in the forward scattering direction, but also its state of polarization.

1.4.4 Extinction, Scattering and Absorption Cross-Sections

Scattering and absorption of light changes the characteristics of the incident beam after it passes the particle. Let us assume that the particle is placed in a beam of electromagnetic radiation and a detector located in the far-field region measures the radiation in the forward scattering direction ($\boldsymbol{e}_r = \boldsymbol{e}_k$). Let W

be the electromagnetic power received by the detector downstream from the particle, and W_0 the electromagnetic power received by the detector if the particle is removed. Evidently, $W_0 > W$ and we say that the presence of the particle has resulted in extinction of the incident beam. For a nonabsorbing medium, the electromagnetic power removed from the incident beam $W_0 - W$ is accounted for by absorption in the particle and scattering by the particle.

We now consider extinction from a computational point of view. In order to simplify the notations we will use the conventional expressions of the Poynting vectors and the electromagnetic powers in terms of the transformed fields introduced in Sect. 1.1 (we will omit the multiplicative factor $1/\sqrt{\varepsilon_0\mu_0}$). The time-averaged Poynting vector $\langle \boldsymbol{S} \rangle$ can be written as [17]

$$\langle \boldsymbol{S} \rangle = \frac{1}{2}\mathrm{Re}\left\{\boldsymbol{E} \times \boldsymbol{H}^*\right\} = \langle \boldsymbol{S}_{\mathrm{inc}} \rangle + \langle \boldsymbol{S}_{\mathrm{scat}} \rangle + \langle \boldsymbol{S}_{\mathrm{ext}} \rangle \ ,$$

where $\boldsymbol{E} = \boldsymbol{E}_{\mathrm{s}} + \boldsymbol{E}_{\mathrm{e}}$ and $\boldsymbol{H} = \boldsymbol{H}_{\mathrm{s}} + \boldsymbol{H}_{\mathrm{e}}$ are the total electric and magnetic fields,

$$\langle \boldsymbol{S}_{\mathrm{inc}} \rangle = \frac{1}{2}\mathrm{Re}\left\{\boldsymbol{E}_{\mathrm{e}} \times \boldsymbol{H}_{\mathrm{e}}^*\right\}$$

is the Poynting vector associated with the external excitation,

$$\langle \boldsymbol{S}_{\mathrm{scat}} \rangle = \frac{1}{2}\mathrm{Re}\left\{\boldsymbol{E}_{\mathrm{s}} \times \boldsymbol{H}_{\mathrm{s}}^*\right\}$$

is the Poynting vector corresponding to the scattered field and

$$\langle \boldsymbol{S}_{\mathrm{ext}} \rangle = \frac{1}{2}\mathrm{Re}\left\{\boldsymbol{E}_{\mathrm{e}} \times \boldsymbol{H}_{\mathrm{s}}^* + \boldsymbol{E}_{\mathrm{s}} \times \boldsymbol{H}_{\mathrm{e}}^*\right\}$$

is the Poynting vector caused by the interaction between the scattered and incident fields.

Taking into account the boundary conditions $\boldsymbol{n} \times \boldsymbol{E}_{\mathrm{i}} = \boldsymbol{n} \times \boldsymbol{E}$ and $\boldsymbol{n} \times \boldsymbol{H}_{\mathrm{i}} = \boldsymbol{n} \times \boldsymbol{H}$ on S, we express the time-averaged power absorbed by the particle as

$$\begin{aligned} W_{\mathrm{abs}} &= -\frac{1}{2}\int_S \boldsymbol{n} \cdot \mathrm{Re}\left\{\boldsymbol{E}_{\mathrm{i}} \times \boldsymbol{H}_{\mathrm{i}}^*\right\} \mathrm{d}S \\ &= -\frac{1}{2}\int_S \boldsymbol{n} \cdot \mathrm{Re}\left\{\boldsymbol{E} \times \boldsymbol{H}^*\right\} \mathrm{d}S \, . \end{aligned}$$

With S_{c} being an auxiliary surface enclosing S (Fig. 1.11), we apply the Green second vector theorem to the vector fields $\boldsymbol{E}$ and $\boldsymbol{E}^*$ in the domain D bounded by S and S_{c}. We obtain

$$\int_S \boldsymbol{n} \cdot (\boldsymbol{E} \times \boldsymbol{H}^* + \boldsymbol{E}^* \times \boldsymbol{H}) \, \mathrm{d}S = \int_{S_{\mathrm{c}}} \boldsymbol{n} \cdot (\boldsymbol{E} \times \boldsymbol{H}^* + \boldsymbol{E}^* \times \boldsymbol{H}) \, \mathrm{d}S \, ,$$

and further

$$\int_S \boldsymbol{n} \cdot \mathrm{Re}\left\{\boldsymbol{E} \times \boldsymbol{H}^*\right\} \mathrm{d}S = \int_{S_{\mathrm{c}}} \boldsymbol{n} \cdot \mathrm{Re}\left\{\boldsymbol{E} \times \boldsymbol{H}^*\right\} \mathrm{d}S \, .$$

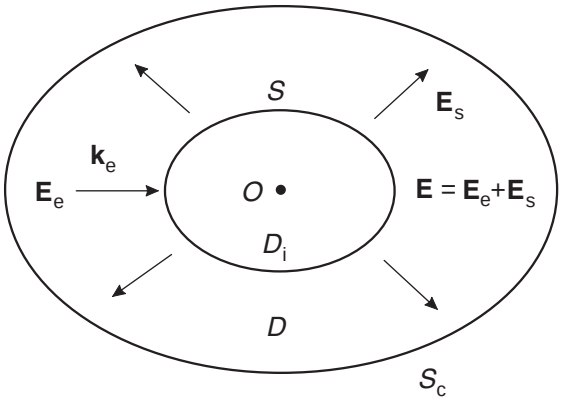

Fig. 1.11. Auxiliary surface S_c

The time-averaged power absorbed by the particle then becomes

$$\begin{aligned} W_\mathrm{abs} &= -\frac{1}{2}\int_{S_\mathrm{c}} \boldsymbol{n}\cdot\mathrm{Re}\left\{\boldsymbol{E}\times\boldsymbol{H}^*\right\}\mathrm{d}S = -\int_{S_\mathrm{c}} \boldsymbol{n}\cdot\langle\boldsymbol{S}\rangle\,\mathrm{d}S \\ &= W_\mathrm{inc} - W_\mathrm{scat} + W_\mathrm{ext}\,, \end{aligned}$$

where

$$W_\mathrm{inc} = -\int_{S_\mathrm{c}} \boldsymbol{n}\cdot\langle\boldsymbol{S}_\mathrm{inc}\rangle\,\mathrm{d}S = -\frac{1}{2}\int_{S_\mathrm{c}} \boldsymbol{n}\cdot\mathrm{Re}\left\{\boldsymbol{E}_\mathrm{e}\times\boldsymbol{H}_\mathrm{e}^*\right\}\mathrm{d}S\,, \tag{1.80}$$

$$W_\mathrm{scat} = \int_{S_\mathrm{c}} \boldsymbol{n}\cdot\langle\boldsymbol{S}_\mathrm{scat}\rangle\,\mathrm{d}S = \frac{1}{2}\int_{S_\mathrm{c}} \boldsymbol{n}\cdot\mathrm{Re}\left\{\boldsymbol{E}_\mathrm{s}\times\boldsymbol{H}_\mathrm{s}^*\right\}\mathrm{d}S\,, \tag{1.81}$$

$$W_\mathrm{ext} = -\int_{S_\mathrm{c}} \boldsymbol{n}\cdot\langle\boldsymbol{S}_\mathrm{ext}\rangle\,\mathrm{d}S = -\frac{1}{2}\int_{S_\mathrm{c}} \boldsymbol{n}\cdot\mathrm{Re}\left\{\boldsymbol{E}_\mathrm{e}\times\boldsymbol{H}_\mathrm{s}^* + \boldsymbol{E}_\mathrm{s}\times\boldsymbol{H}_\mathrm{e}^*\right\}\mathrm{d}S\,. \tag{1.82}$$

The divergence theorem applied to the excitation field in the domain D_c bounded by S_c gives

$$\int_{D_\mathrm{c}} \nabla\cdot(\boldsymbol{E}_\mathrm{e}\times\boldsymbol{H}_\mathrm{e}^*)\,\mathrm{d}V = \int_{S_\mathrm{c}} \boldsymbol{n}\cdot(\boldsymbol{E}_\mathrm{e}\times\boldsymbol{H}_\mathrm{e}^*)\,\mathrm{d}S\,,$$

whence, using

$$\nabla\cdot(\boldsymbol{E}_\mathrm{e}\times\boldsymbol{H}_\mathrm{e}^*) = jk_0\left(\mu_\mathrm{s}\left|\boldsymbol{H}_\mathrm{e}\right|^2 - \varepsilon_\mathrm{s}\left|\boldsymbol{E}_\mathrm{e}\right|^2\right)\,,$$

and

$$\mathrm{Re}\left\{\nabla\cdot(\boldsymbol{E}_\mathrm{e}\times\boldsymbol{H}_\mathrm{e}^*)\right\} = 0\,,$$

yield

$$W_\mathrm{inc} = 0\,.$$

Thus, $W_{\rm ext}$ is the sum of the electromagnetic scattering power and the electromagnetic absorption power

$$W_{\rm ext} = W_{\rm scat} + W_{\rm abs}\,.$$

For a plane wave incidence, the extinction and scattering cross-sections are given by

$$C_{\rm ext} = \frac{W_{\rm ext}}{\frac{1}{2}\sqrt{\frac{\varepsilon_{\rm s}}{\mu_{\rm s}}}\,|\boldsymbol{E}_{\rm e0}|^2}\,, \tag{1.83}$$

$$C_{\rm scat} = \frac{W_{\rm scat}}{\frac{1}{2}\sqrt{\frac{\varepsilon_{\rm s}}{\mu_{\rm s}}}\,|\boldsymbol{E}_{\rm e0}|^2}\,, \tag{1.84}$$

the absorption cross-section is

$$C_{\rm abs} = C_{\rm ext} - C_{\rm scat} \geq 0\,,$$

while the single-scattering albedo is

$$\omega = \frac{C_{\rm scat}}{C_{\rm ext}} \leq 1\,.$$

Essentially, $C_{\rm scat}$ and $C_{\rm abs}$ represent the electromagnetic powers removed from the incident wave as a result of scattering and absorption of the incident radiation, while $C_{\rm ext}$ gives the total electromagnetic power removed from the incident wave by the combined effect of scattering and absorption. The optical cross-sections have the dimension of area and depend on the direction and polarization state of the incident wave as well on the size, optical properties and orientation of the particle. The efficiencies (or efficiency factors) for extinction, scattering and absorption are defined as

$$Q_{\rm ext} = \frac{C_{\rm ext}}{G}\,, \quad Q_{\rm scat} = \frac{C_{\rm scat}}{G}\,, \quad Q_{\rm abs} = \frac{C_{\rm abs}}{G}\,,$$

where G is the particle cross-sectional area projected onto a plane perpendicular to the incident beam. In view of the definition of the normalized differential scattering cross-section, we set $G = \pi a_{\rm c}^2$, where $a_{\rm c}$ is the area-equivalent-circle radius. From the point of view of geometrical optics we expect that the extinction efficiency of all particles would be identically equal to unity. In fact, there are many particles which can scatter and absorb more light than is geometrically incident upon them [17].

The scattering cross-section is the integral of the differential scattering cross-section over the unit sphere. To prove this assertion, we express $C_{\rm scat}$ as

$$C_{\rm scat} = \frac{1}{|\boldsymbol{E}_{\rm e0}|^2}\sqrt{\frac{\mu_{\rm s}}{\varepsilon_{\rm s}}}\int_{S_{\rm c}} \boldsymbol{e}_r \cdot {\rm Re}\,\{\boldsymbol{E}_{\rm s} \times \boldsymbol{H}_{\rm s}^*\}\,{\rm d}S\,,$$

where S_c is a spherical surface situated at infinity and use the far-field representation

$$\boldsymbol{e}_r \cdot (\boldsymbol{E}_\mathrm{s} \times \boldsymbol{H}_\mathrm{s}^*) = \frac{1}{r^2}\sqrt{\frac{\varepsilon_\mathrm{s}}{\mu_\mathrm{s}}}\left[\left|\boldsymbol{E}_{\mathrm{s}\infty}\right|^2 + \mathrm{O}\left(\frac{1}{r}\right)\right], \quad r \to \infty$$

to obtain

$$C_\mathrm{scat} = \frac{1}{\left|\boldsymbol{E}_\mathrm{e0}\right|^2}\int_\Omega \left|\boldsymbol{E}_{\mathrm{s}\infty}\right|^2 \mathrm{d}\Omega\,. \tag{1.85}$$

The scattering cross-section can be expressed in terms of the elements of the phase matrix and the Stokes parameters of the incident wave. Taking into account the expressions of I_e and I_s, and using (1.76) we obtain

$$\begin{aligned} C_\mathrm{scat} &= \frac{1}{I_\mathrm{e}}\int_\Omega I_\mathrm{s}\left(\boldsymbol{e}_r\right)\mathrm{d}\Omega\left(\boldsymbol{e}_r\right) \\ &= \frac{1}{I_\mathrm{e}}\int_\Omega \left[Z_{11}\left(\boldsymbol{e}_r,\boldsymbol{e}_k\right)I_\mathrm{e} + Z_{12}\left(\boldsymbol{e}_r,\boldsymbol{e}_k\right)Q_\mathrm{e}\right. \\ &\quad \left. + Z_{13}\left(\boldsymbol{e}_r,\boldsymbol{e}_k\right)U_\mathrm{e} + Z_{14}\left(\boldsymbol{e}_r,\boldsymbol{e}_k\right)V_\mathrm{e}\right]\mathrm{d}\Omega\left(\boldsymbol{e}_r\right)\,. \end{aligned} \tag{1.86}$$

The phase function is related to the differential scattering cross-section by the relation

$$p\left(\boldsymbol{e}_r,\boldsymbol{e}_k\right) = \frac{4\pi}{C_\mathrm{scat}\left|\boldsymbol{E}_\mathrm{e0}\right|^2}\left|\boldsymbol{E}_{\mathrm{s}\infty}\left(\boldsymbol{e}_r\right)\right|^2$$

and in view of (1.85) we see that p is dimensionless and normalized, i.e.,

$$\frac{1}{4\pi}\int_\Omega p\,\mathrm{d}\Omega = 1\,.$$

The mean direction of propagation of the scattered field is defined as

$$\boldsymbol{g} = \frac{1}{C_\mathrm{scat}\left|\boldsymbol{E}_\mathrm{e0}\right|^2}\int_\Omega \left|\boldsymbol{E}_{\mathrm{s}\infty}\left(\boldsymbol{e}_r\right)\right|^2 \boldsymbol{e}_r\,\mathrm{d}\Omega\left(\boldsymbol{e}_r\right) \tag{1.87}$$

and obviously

$$\begin{aligned} \boldsymbol{g} &= \frac{1}{C_\mathrm{scat}I_\mathrm{e}}\int_\Omega I_\mathrm{s}\left(\boldsymbol{e}_r\right)\boldsymbol{e}_r\,\mathrm{d}\Omega\left(\boldsymbol{e}_r\right) \\ &= \frac{1}{C_\mathrm{scat}I_\mathrm{e}}\int_\Omega \left[Z_{11}\left(\boldsymbol{e}_r,\boldsymbol{e}_k\right)I_\mathrm{e} + Z_{12}\left(\boldsymbol{e}_r,\boldsymbol{e}_k\right)Q_\mathrm{e}\right. \\ &\quad \left. + Z_{13}\left(\boldsymbol{e}_r,\boldsymbol{e}_k\right)U_\mathrm{e} + Z_{14}\left(\boldsymbol{e}_r,\boldsymbol{e}_k\right)V_\mathrm{e}\right]\boldsymbol{e}_r\,\mathrm{d}\Omega\left(\boldsymbol{e}_r\right)\,. \end{aligned}$$

The asymmetry parameter $\langle\cos\Theta\rangle$ is the dot product between the vector $\boldsymbol{g}$ and the incident direction $\boldsymbol{e}_k$ [17, 169],

$$\langle \cos\Theta \rangle = \boldsymbol{g} \cdot \boldsymbol{e}_k = \frac{1}{C_{\mathrm{scat}} \left| \boldsymbol{E}_{\mathrm{e}0} \right|^2} \int_{\Omega} \left| \boldsymbol{E}_{\mathrm{s}\infty} \left(\boldsymbol{e}_r \right) \right|^2 \boldsymbol{e}_r \cdot \boldsymbol{e}_k \, \mathrm{d}\Omega \left(\boldsymbol{e}_r \right)$$
$$= \frac{1}{4\pi} \int_{\Omega} p \left(\boldsymbol{e}_r, \boldsymbol{e}_k \right) \cos\Theta \, \mathrm{d}\Omega \left(\boldsymbol{e}_r \right) \, ,$$

where $\cos\Theta = \boldsymbol{e}_r \cdot \boldsymbol{e}_k$, and it is apparent that the asymmetry parameter is the average cosine of the scattering angle Θ. If the particle scatters more light toward the forward direction ($\Theta = 0$), $\langle \cos\Theta \rangle$ is positive and $\langle \cos\Theta \rangle$ is negative if the scattering is directed more toward the backscattering direction ($\Theta = 180°$). If the scattering is symmetric about a scattering angle of 90°, $\langle \cos\Theta \rangle$ vanishes.

1.4.5 Optical Theorem

The expression of extinction has been derived by integrating the Poynting vector over an auxiliary surface around the particle. This derivation emphasized the conservation of energy aspect of extinction: extinction is the combined effect of absorption and scattering. A second derivation emphasizes the interference aspect of extinction: extinction is a result of the interference between the incident and forward scattered light [17]. Applying Green's second vector theorem to the vector fields $\boldsymbol{E}_{\mathrm{s}}$ and $\boldsymbol{E}_{\mathrm{e}}^*$ in the domain D bounded by S and S_{c}, we obtain

$$\int_S \boldsymbol{n} \cdot \left(\boldsymbol{E}_{\mathrm{s}} \times \boldsymbol{H}_{\mathrm{e}}^* + \boldsymbol{E}_{\mathrm{e}}^* \times \boldsymbol{H}_{\mathrm{s}} \right) \mathrm{d}S = \int_{S_{\mathrm{c}}} \boldsymbol{n} \cdot \left(\boldsymbol{E}_{\mathrm{s}} \times \boldsymbol{H}_{\mathrm{e}}^* + \boldsymbol{E}_{\mathrm{e}}^* \times \boldsymbol{H}_{\mathrm{s}} \right) \mathrm{d}S$$

and further

$$\int_S \boldsymbol{n} \cdot \mathrm{Re} \left\{ \boldsymbol{E}_{\mathrm{s}} \times \boldsymbol{H}_{\mathrm{e}}^* + \boldsymbol{E}_{\mathrm{e}}^* \times \boldsymbol{H}_{\mathrm{s}} \right\} \mathrm{d}S = \int_{S_{\mathrm{c}}} \boldsymbol{n} \cdot \mathrm{Re} \left\{ \boldsymbol{E}_{\mathrm{s}} \times \boldsymbol{H}_{\mathrm{e}}^* + \boldsymbol{E}_{\mathrm{e}}^* \times \boldsymbol{H}_{\mathrm{s}} \right\} \mathrm{d}S \, .$$

This result together with (1.82) and the identity $\mathrm{Re}\{\boldsymbol{E}_{\mathrm{e}} \times \boldsymbol{H}_{\mathrm{s}}^*\} = \mathrm{Re}\{\boldsymbol{E}_{\mathrm{e}}^* \times \boldsymbol{H}_{\mathrm{s}}\}$ give

$$W_{\mathrm{ext}} = -\frac{1}{2} \int_S \boldsymbol{n} \cdot \mathrm{Re} \left\{ \boldsymbol{E}_{\mathrm{s}} \times \boldsymbol{H}_{\mathrm{e}}^* + \boldsymbol{E}_{\mathrm{e}}^* \times \boldsymbol{H}_{\mathrm{s}} \right\} \mathrm{d}S \, ,$$

whence, using the explicit expressions for $\boldsymbol{E}_{\mathrm{e}}$ and $\boldsymbol{H}_{\mathrm{e}}$, we derive

$$W_{\mathrm{ext}} = \frac{1}{2} \mathrm{Re} \left\{ \int_S \left[\boldsymbol{E}_{\mathrm{e}0}^* \cdot \boldsymbol{h}_{\mathrm{s}} \left(\boldsymbol{r}' \right) \right.\right.$$
$$\left.\left. - \sqrt{\frac{\varepsilon_{\mathrm{s}}}{\mu_{\mathrm{s}}}} \left(\boldsymbol{e}_k \times \boldsymbol{E}_{\mathrm{e}0}^* \right) \cdot \boldsymbol{e}_{\mathrm{s}} \left(\boldsymbol{r}' \right) \right] \mathrm{e}^{-\mathrm{j}\boldsymbol{k}_{\mathrm{e}} \cdot \boldsymbol{r}'} \, \mathrm{d}S \left(\boldsymbol{r}' \right) \right\} \, .$$

In the integral representation for the electric far-field pattern (cf. (1.69)) we set $\boldsymbol{e}_r = \boldsymbol{e}_k$, take the dot product between $\boldsymbol{E}_{\mathrm{s}\infty}(\boldsymbol{e}_k)$ and $\boldsymbol{E}_{\mathrm{e}0}^*$, and obtain

$$\boldsymbol{E}_{\mathrm{e}0}^{*}\cdot\boldsymbol{E}_{\mathrm{s}\infty}\left(\boldsymbol{e}_{k}\right)=\frac{\mathrm{j}k_{\mathrm{s}}}{4\pi}\sqrt{\frac{\mu_{\mathrm{s}}}{\varepsilon_{\mathrm{s}}}}\int_{S}\left\{\boldsymbol{E}_{\mathrm{e}0}^{*}\cdot\boldsymbol{h}_{\mathrm{s}}\left(\boldsymbol{r}'\right)\right.$$
$$\left.-\sqrt{\frac{\varepsilon_{\mathrm{s}}}{\mu_{\mathrm{s}}}}\left(\boldsymbol{e}_{k}\times\boldsymbol{E}_{\mathrm{e}0}^{*}\right)\cdot\boldsymbol{e}_{\mathrm{s}}\left(\boldsymbol{r}'\right)\right\}\mathrm{e}^{-\mathrm{j}\boldsymbol{k}_{\mathrm{e}}\cdot\boldsymbol{r}'}\mathrm{d}S\left(\boldsymbol{r}'\right)\,.$$

The last two relations imply that

$$W_{\mathrm{ext}}=\frac{1}{2}\mathrm{Re}\left\{\sqrt{\frac{\varepsilon_{\mathrm{s}}}{\mu_{\mathrm{s}}}}\frac{4\pi}{jk_{\mathrm{s}}}\boldsymbol{E}_{\mathrm{e}0}^{*}\cdot\boldsymbol{E}_{\mathrm{s}\infty}\left(\boldsymbol{e}_{k}\right)\right\}$$

and further that

$$C_{\mathrm{ext}}=\frac{4\pi}{k_{\mathrm{s}}\left|\boldsymbol{E}_{\mathrm{e}0}\right|^{2}}\mathrm{Im}\left\{\boldsymbol{E}_{\mathrm{e}0}^{*}\cdot\boldsymbol{E}_{\mathrm{s}\infty}\left(\boldsymbol{e}_{k}\right)\right\}\,. \tag{1.88}$$

The above relation is a representation of the optical theorem, and since the extinction cross-section is in terms of the scattering amplitude in the forward direction, the optical theorem is also known as the extinction theorem or the forward scattering theorem. This fundamental relation can be used to compute the extinction cross-section when the imaginary part of the scattering amplitude in the forward direction is known accurately. In view of (1.88) and (1.74), and taking into account the explicit expressions of the elements of the extinction matrix we see that

$$C_{\mathrm{ext}}=\frac{1}{I_{\mathrm{e}}}\left[K_{11}\left(\boldsymbol{e}_{k}\right)I_{\mathrm{e}}+K_{12}\left(\boldsymbol{e}_{k}\right)Q_{\mathrm{e}}+K_{13}\left(\boldsymbol{e}_{k}\right)U_{\mathrm{e}}+K_{14}\left(\boldsymbol{e}_{k}\right)V_{\mathrm{e}}\right]\,. \tag{1.89}$$

1.4.6 Reciprocity

The tensor scattering amplitude satisfies a useful symmetry property which is referred to as reciprocity. As a consequence, reciprocity relations for the amplitude, phase and extinction matrices can be derived. Reciprocity is a manifestation of the symmetry of the scattering process with respect to an inversion of time and holds for particles in arbitrary orientations [169]. In order to derive this property we use the following result: if $\boldsymbol{E}_1$, $\boldsymbol{H}_1$ and $\boldsymbol{E}_2$, $\boldsymbol{H}_2$ are the total fields generated by the incident fields $\boldsymbol{E}_{\mathrm{e}1}$, $\boldsymbol{H}_{\mathrm{e}1}$ and $\boldsymbol{E}_{\mathrm{e}2}$, $\boldsymbol{H}_{\mathrm{e}2}$, respectively, we have

$$\int_{S}\boldsymbol{n}\cdot\left(\boldsymbol{E}_2\times\boldsymbol{H}_1-\boldsymbol{E}_1\times\boldsymbol{H}_2\right)\mathrm{d}S=\int_{S_{\mathrm{c}}}\boldsymbol{n}\cdot\left(\boldsymbol{E}_2\times\boldsymbol{H}_1-\boldsymbol{E}_1\times\boldsymbol{H}_2\right)\mathrm{d}S\,,$$

where as before, S_{c} is an auxiliary surface enclosing S. Since $\boldsymbol{E}_1$ and $\boldsymbol{E}_2$ are source free in the domain bounded by S and S_{c}, the above equation follows immediately from Green second vector theorem. Further, applying Green's second vector theorem to the internal fields $\boldsymbol{E}_{\mathrm{i}1}$ and $\boldsymbol{E}_{\mathrm{i}2}$ in the domain D_{i}, and taking into account the boundary conditions $\boldsymbol{n}\times\boldsymbol{E}_{\mathrm{i}1,2}=\boldsymbol{n}\times\boldsymbol{E}_{1,2}$ and $\boldsymbol{n}\times\boldsymbol{H}_{\mathrm{i}1,2}=\boldsymbol{n}\times\boldsymbol{H}_{1,2}$ on S, yields

$$\int_S \boldsymbol{n} \cdot (\boldsymbol{E}_2 \times \boldsymbol{H}_1 - \boldsymbol{E}_1 \times \boldsymbol{H}_2)\,\mathrm{d}S = 0\,,$$

whence

$$\int_{S_\mathrm{c}} \boldsymbol{n} \cdot (\boldsymbol{E}_2 \times \boldsymbol{H}_1 - \boldsymbol{E}_1 \times \boldsymbol{H}_2)\,\mathrm{d}S = 0\,, \tag{1.90}$$

follows. We take the surface S_c as a large sphere of outward unit normal vector $\boldsymbol{e}_r$, consider the limit when the radius R becomes infinite, and write the integrand in (1.90) as

$$\begin{aligned}
&\boldsymbol{E}_2 \times \boldsymbol{H}_1 - \boldsymbol{E}_1 \times \boldsymbol{H}_2 \\
&= \boldsymbol{E}_{\mathrm{e}2} \times \boldsymbol{H}_{\mathrm{e}1} - \boldsymbol{E}_{\mathrm{e}1} \times \boldsymbol{H}_{\mathrm{e}2} + \boldsymbol{E}_{\mathrm{s}2} \times \boldsymbol{H}_{\mathrm{s}1} - \boldsymbol{E}_{\mathrm{s}1} \times \boldsymbol{H}_{\mathrm{s}2} \\
&\quad + \boldsymbol{E}_{\mathrm{s}2} \times \boldsymbol{H}_{\mathrm{e}1} - \boldsymbol{E}_{\mathrm{e}1} \times \boldsymbol{H}_{\mathrm{s}2} + \boldsymbol{E}_{\mathrm{e}2} \times \boldsymbol{H}_{\mathrm{s}1} - \boldsymbol{E}_{\mathrm{s}1} \times \boldsymbol{H}_{\mathrm{e}2}\,.
\end{aligned}$$

The Green second vector theorem applied to the incident fields $\boldsymbol{E}_{\mathrm{e}1}$ and $\boldsymbol{E}_{\mathrm{e}2}$ in any bounded domain shows that the vector plane wave terms do not contribute to the integral. Furthermore, using the far-field representation

$$\begin{aligned}
&\boldsymbol{E}_{\mathrm{s}2} \times \boldsymbol{H}_{\mathrm{s}1} - \boldsymbol{E}_{\mathrm{s}1} \times \boldsymbol{H}_{\mathrm{s}2} \\
&= \frac{\mathrm{e}^{2jk_\mathrm{s}r}}{r^2} \left\{ \boldsymbol{E}_{\mathrm{s}\infty 2} \times \boldsymbol{H}_{\mathrm{s}\infty 1} - \boldsymbol{E}_{\mathrm{s}\infty 1} \times \boldsymbol{H}_{\mathrm{s}\infty 2} + \mathrm{O}\left(\frac{1}{r}\right) \right\},
\end{aligned}$$

and taking into account the transversality of the far-field patterns

$$\boldsymbol{E}_{\mathrm{s}\infty 2} \times \boldsymbol{H}_{\mathrm{s}\infty 1} - \boldsymbol{E}_{\mathrm{s}\infty 1} \times \boldsymbol{H}_{\mathrm{s}\infty 2} = 0\,,$$

we see that the integral over the scattered wave terms also vanishes. Thus, (1.90) implies that

$$\int_{S_\mathrm{c}} \boldsymbol{e}_r \cdot (\boldsymbol{E}_{\mathrm{s}2} \times \boldsymbol{H}_{\mathrm{e}1} - \boldsymbol{E}_{\mathrm{e}1} \times \boldsymbol{H}_{\mathrm{s}2})\,\mathrm{d}S = \int_{S_\mathrm{c}} \boldsymbol{e}_r \cdot (\boldsymbol{E}_{\mathrm{s}1} \times \boldsymbol{H}_{\mathrm{e}2} - \boldsymbol{E}_{\mathrm{e}2} \times \boldsymbol{H}_{\mathrm{s}1})\,\mathrm{d}S\,. \tag{1.91}$$

For plane wave incidence,

$$\boldsymbol{E}_{\mathrm{e}u}(\boldsymbol{r}) = \boldsymbol{E}_{\mathrm{e}0u} \exp\left(\mathrm{j}\boldsymbol{k}_{\mathrm{e}u} \cdot \boldsymbol{r}\right)\,, \quad \boldsymbol{k}_{\mathrm{e}u} = k_\mathrm{s}\boldsymbol{e}_{ku}\,, \quad u = 1, 2\,,$$

the integrands in (1.91) contain the term $\exp(\mathrm{j}k_\mathrm{s}R\boldsymbol{e}_{k1,2} \cdot \boldsymbol{e}_r)$. Since R is large, the stationary point method can be used to compute the integrals accordingly to the basic result

$$\frac{kR}{2\pi\mathrm{j}} \int_0^{2\pi} \int_0^{\pi} g\,(\theta, \varphi)\,\mathrm{e}^{\mathrm{j}kRf(\theta,\varphi)} \mathrm{d}\theta\,\mathrm{d}\varphi = \frac{1}{\sqrt{f_{\theta\theta} f_{\varphi\varphi} - f_{\theta\varphi}^2}} g\,(\theta_\mathrm{st}, \varphi_\mathrm{st})\,\mathrm{e}^{\mathrm{j}kRf(\theta_\mathrm{st},\varphi_\mathrm{st})}\,, \tag{1.92}$$

where $(\theta_{\rm st}, \varphi_{\rm st})$ is the stationary point of f, $f_{\theta\theta} = \partial^2 f/\partial\theta^2$, $f_{\varphi\varphi} = \partial^2 f/\partial\varphi^2$ and $f_{\theta\varphi} = \partial^2 f/\partial\theta\partial\varphi$. The integrals in (1.91) are then given by

$$\begin{aligned}
&\int_{S_{\rm c}} \boldsymbol{e}_r \cdot (\boldsymbol{E}_{\rm s2} \times \boldsymbol{H}_{\rm e1} - \boldsymbol{E}_{\rm e1} \times \boldsymbol{H}_{\rm s2})\,{\rm d}S \\
&= \quad -4\pi{\rm j}\frac{R}{k_{\rm s}}\sqrt{\frac{\varepsilon_{\rm s}}{\mu_{\rm s}}}\boldsymbol{E}_{{\rm s}\infty 2}\,(-\boldsymbol{e}_{k1}) \cdot \boldsymbol{E}_{\rm e01}{\rm e}^{-{\rm j}k_{\rm s}R}\,, \\
&\int_{S_{\rm c}} \boldsymbol{e}_r \cdot (\boldsymbol{E}_{\rm s1} \times \boldsymbol{H}_{\rm e2} - \boldsymbol{E}_{\rm e2} \times \boldsymbol{H}_{\rm s1})\,{\rm d}S \\
&= \quad -4\pi{\rm j}\frac{R}{k_{\rm s}}\sqrt{\frac{\varepsilon_{\rm s}}{\mu_{\rm s}}}\boldsymbol{E}_{{\rm s}\infty 1}\,(-\boldsymbol{e}_{k2}) \cdot \boldsymbol{E}_{\rm e02}{\rm e}^{-{\rm j}k_{\rm s}R}\,,
\end{aligned}$$

and we deduce the reciprocity relation for the far-field pattern (Fig. 1.12):

$$\boldsymbol{E}_{{\rm s}\infty 2}\,(-\boldsymbol{e}_{k1}) \cdot \boldsymbol{E}_{\rm e01} = \boldsymbol{E}_{{\rm s}\infty 1}\,(-\boldsymbol{e}_{k2}) \cdot \boldsymbol{E}_{\rm e02}\,.$$

The above relation gives

$$\boldsymbol{E}_{\rm e01} \cdot \overline{\boldsymbol{A}}\,(-\boldsymbol{e}_{k1}, \boldsymbol{e}_{k2}) \cdot \boldsymbol{E}_{\rm e02} = \boldsymbol{E}_{\rm e02} \cdot \overline{\boldsymbol{A}}\,(-\boldsymbol{e}_{k2}, \boldsymbol{e}_{k1}) \cdot \boldsymbol{E}_{\rm e01}$$

and since $\boldsymbol{a} \cdot \overline{\boldsymbol{D}} \cdot \boldsymbol{b} = \boldsymbol{b} \cdot \overline{\boldsymbol{D}}^{\rm T} \cdot \boldsymbol{a}$, and $\boldsymbol{E}_{\rm e01}$ and $\boldsymbol{E}_{\rm e02}$ are arbitrary transverse vectors, the following constraint on the tensor scattering amplitude:

$$\overline{\boldsymbol{A}}\,(-\boldsymbol{e}_{k2}, -\boldsymbol{e}_{k1}) = \overline{\boldsymbol{A}}^{\rm T}\,(\boldsymbol{e}_{k1}, \boldsymbol{e}_{k2})$$

follows. This is the reciprocity relation for the tensor scattering amplitude which relates scattering from the direction $-\boldsymbol{e}_{k1}$ into $-\boldsymbol{e}_{k2}$ to scattering from $\boldsymbol{e}_{k2}$ to $\boldsymbol{e}_{k1}$. Taking into account the representation of the amplitude matrix elements in terms of the tensor scattering amplitude and the fact that for

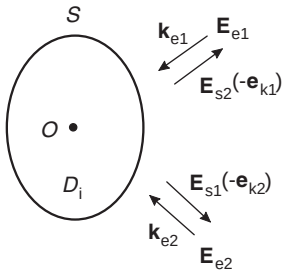

Fig. 1.12. Illustration of the reciprocity relation

$\boldsymbol{e'}_k = -\boldsymbol{e}_k$ we have $\boldsymbol{e'}_\beta = \boldsymbol{e}_\beta$ and $\boldsymbol{e'}_\alpha = -\boldsymbol{e}_\alpha$, we obtain the reciprocity relation for the amplitude matrix:

$$\boldsymbol{S}\left(-\boldsymbol{e}_{k2}, -\boldsymbol{e}_{k1}\right) = \begin{bmatrix} S_{\theta\beta}\left(\boldsymbol{e}_{k1}, \boldsymbol{e}_{k2}\right) & -S_{\varphi\beta}\left(\boldsymbol{e}_{k1}, \boldsymbol{e}_{k2}\right) \\ -S_{\theta\alpha}\left(\boldsymbol{e}_{k1}, \boldsymbol{e}_{k2}\right) & S_{\varphi\alpha}\left(\boldsymbol{e}_{k1}, \boldsymbol{e}_{k2}\right) \end{bmatrix}.$$

If we choose $\boldsymbol{e}_{k1} = -\boldsymbol{e}_{k2} = -\boldsymbol{e}_k$, we obtain

$$S_{\varphi\beta}\left(-\boldsymbol{e}_k, \boldsymbol{e}_k\right) = -S_{\theta\alpha}\left(-\boldsymbol{e}_k, \boldsymbol{e}_k\right),$$

which is a representation of the backscattering theorem [169].

From the reciprocity relation for the amplitude matrix we easily derive the reciprocity relation for the phase and extinction matrices:

$$\boldsymbol{Z}\left(-\boldsymbol{e}_k, -\boldsymbol{e}_r\right) = \boldsymbol{Q}\boldsymbol{Z}^{\mathrm{T}}\left(\boldsymbol{e}_r, \boldsymbol{e}_k\right)\boldsymbol{Q}$$

and

$$\boldsymbol{K}\left(-\boldsymbol{e}_k\right) = \boldsymbol{Q}\boldsymbol{K}^{\mathrm{T}}\left(\boldsymbol{e}_k\right)\boldsymbol{Q},$$

respectively, where $\boldsymbol{Q} = \mathrm{diag}[1, 1, -1, 1]$.

The reciprocity relations can be used in practice for testing the results of theoretical computations and laboratory measurements. It should be remarked that reciprocity relations give also rise to symmetry relations for the dyadic Green functions [229].

1.5 Transition Matrix

The transition matrix relates the expansion coefficients of the incident and scattered fields. The existence of the transition matrix is "postulated" by the $\boldsymbol{T}$-Matrix Ansatz and is a consequence of the series expansions of the incident and scattered fields and the linearity of the Maxwell equations. Historically, the transition matrix has been introduced within the null-field method formalism (see [253, 256]), and for this reason, the null-field method has often been referred to as the $\boldsymbol{T}$-matrix method. However, the null-field method is only one among many methods that can be used to compute the transition matrix. The transition matrix can also be derived in the framework of the method of moments [88], the separation of variables method [208], the discrete dipole approximation [151] and the point matching method [181]. Rother et al. [205] found a general relation between the surface Green function and the transition matrix for the exterior Maxwell problem, which in principle, allows to compute the transition matrix with the finite-difference technique.

In this section we review the general properties of the transition matrix such as unitarity and symmetry and discuss analytical procedures for averaging scattering characteristics over particle orientations. These procedures

relying on the rotation transformation rule for vector spherical wave functions are of general use because an explicit expression of the transition matrix is not required. In order to simplify our analysis we consider a vector plane wave of unit amplitude

$$\boldsymbol{E}_{\mathrm{e}}(\boldsymbol{r}) = \boldsymbol{e}_{\mathrm{pol}}\mathrm{e}^{\mathrm{j}\boldsymbol{k}_{\mathrm{e}}\cdot\boldsymbol{r}}\,, \quad \boldsymbol{H}_{\mathrm{e}}(\boldsymbol{r}) = \sqrt{\frac{\varepsilon_{\mathrm{s}}}{\mu_{\mathrm{s}}}}\boldsymbol{e}_k \times \boldsymbol{e}_{\mathrm{pol}}\mathrm{e}^{\mathrm{j}\boldsymbol{k}_{\mathrm{e}}\cdot\boldsymbol{r}}\,,$$

where $\boldsymbol{e}_{\mathrm{pol}} \cdot \boldsymbol{e}_k = 0$ and $|\boldsymbol{e}_{\mathrm{pol}}| = 1$.

1.5.1 Definition

Everywhere outside the (smallest) sphere circumscribing the particle it is appropriate to expand the scattered field in terms of radiating vector spherical wave functions

$$\boldsymbol{E}_{\mathrm{s}}(\boldsymbol{r}) = \sum_{n=1}^{\infty}\sum_{m=-n}^{n} f_{mn}\boldsymbol{M}_{mn}^{3}\left(k_{\mathrm{s}}\boldsymbol{r}\right) + g_{mn}\boldsymbol{N}_{mn}^{3}\left(k_{\mathrm{s}}\boldsymbol{r}\right) \tag{1.93}$$

and the incident field in terms of regular vector spherical wave functions

$$\boldsymbol{E}_{\mathrm{e}}(\boldsymbol{r}) = \sum_{n=1}^{\infty}\sum_{m=-n}^{n} a_{mn}\boldsymbol{M}_{mn}^{1}\left(k_{\mathrm{s}}\boldsymbol{r}\right) + b_{mn}\boldsymbol{N}_{mn}^{1}\left(k_{\mathrm{s}}\boldsymbol{r}\right)\,. \tag{1.94}$$

Within the vector spherical wave formalism, the scattering problem is solved by determining f_{mn} and g_{mn} as functions of a_{mn} and b_{mn}. Due to the linearity relations of the Maxwell equations and the constitutive relations, the relation between the scattered and incident field coefficients must be linear. This relation is given by the so-called transition matrix $\boldsymbol{T}$ as follows [256]

$$\begin{bmatrix} f_{mn} \\ g_{mn} \end{bmatrix} = \boldsymbol{T}\begin{bmatrix} a_{mn} \\ b_{mn} \end{bmatrix} = \begin{bmatrix} \boldsymbol{T}^{11} & \boldsymbol{T}^{12} \\ \boldsymbol{T}^{21} & \boldsymbol{T}^{22} \end{bmatrix}\begin{bmatrix} a_{mn} \\ b_{mn} \end{bmatrix}\,. \tag{1.95}$$

Essentially, the transition matrix depends on the physical and geometrical characteristics of the particle and is independent on the propagation direction and polarization states of the incident and scattered field.

If the transition matrix is known, the scattering characteristics (introduced in Sect. 1.4) can be readily computed. Taking into account the asymptotic behavior of the vector spherical wave functions we see that the far-field pattern can be expressed in terms of the elements of the transition matrix by the relation

$$\begin{aligned}
\boldsymbol{E}_{\mathrm{s}\infty}\left(\boldsymbol{e}_r\right) &= \frac{1}{k_{\mathrm{s}}}\sum_{n,m}\left(-\mathrm{j}\right)^{n+1}\left[f_{mn}\boldsymbol{m}_{mn}(\boldsymbol{e}_r) + \mathrm{j}g_{mn}\boldsymbol{n}_{mn}(\boldsymbol{e}_r)\right] \\
&= \frac{1}{k_{\mathrm{s}}}\sum_{n,m}\sum_{n_1,m_1}\left(-\mathrm{j}\right)^{n+1} \\
&\quad \times \left[\left(T_{mn,m_1n_1}^{11}a_{m_1n_1} + T_{mn,m_1n_1}^{12}b_{m_1n_1}\right)\boldsymbol{m}_{mn}(\boldsymbol{e}_r)\right. \\
&\quad \left. + \mathrm{j}\left(T_{mn,m_1n_1}^{21}a_{m_1n_1} + T_{mn,m_1n_1}^{22}b_{m_1n_1}\right)\boldsymbol{n}_{mn}(\boldsymbol{e}_r)\right]\,.
\end{aligned} \tag{1.96}$$

To derive the expressions of the tensor scattering amplitude and amplitude matrix, we consider the scattering and incident directions $\boldsymbol{e}_r$ and $\boldsymbol{e}_k$, and express the vector spherical harmonics as

$$\begin{aligned}\boldsymbol{x}_{mn}(\boldsymbol{e}_r) &= x_{mn,\theta}(\boldsymbol{e}_r)\,\boldsymbol{e}_\theta + x_{mn,\varphi}(\boldsymbol{e}_r)\,\boldsymbol{e}_\varphi\,,\\ \boldsymbol{x}_{mn}(\boldsymbol{e}_k) &= x_{mn,\beta}(\boldsymbol{e}_k)\,\boldsymbol{e}_\beta + x_{mn,\alpha}(\boldsymbol{e}_k)\,\boldsymbol{e}_\alpha\,,\end{aligned}$$

where $\boldsymbol{x}_{mn}$ stands for $\boldsymbol{m}_{mn}$ and $\boldsymbol{n}_{mn}$. Recalling the expressions of the incident field coefficients for a plane wave excitation (cf. (1.26))

$$\begin{aligned}a_{mn} &= 4\mathrm{j}^n \boldsymbol{e}_{\mathrm{pol}}\cdot\boldsymbol{m}^*_{mn}(\boldsymbol{e}_k)\,,\\ b_{mn} &= -4\mathrm{j}^{n+1}\boldsymbol{e}_{\mathrm{pol}}\cdot\boldsymbol{n}^*_{mn}(\boldsymbol{e}_k)\,,\end{aligned}$$

and using the definition of the tensor scattering amplitude (cf. (1.71)), we obtain

$$\begin{aligned}\overline{\boldsymbol{A}}(\boldsymbol{e}_r,\boldsymbol{e}_k) = \frac{4}{k_{\mathrm{s}}}\sum_{n,m}\sum_{n_1,m_1}(-\mathrm{j})^{n+1}\,\mathrm{j}^{n_1}\Big\{\big[&T^{11}_{mn,m_1n_1}\boldsymbol{m}_{mn}(\boldsymbol{e}_r)\\ &+ jT^{21}_{mn,m_1n_1}\boldsymbol{n}_{mn}(\boldsymbol{e}_r)\big]\otimes\boldsymbol{m}^*_{m_1n_1}(\boldsymbol{e}_k) + \big[-\mathrm{j}T^{12}_{mn,m_1n_1}\boldsymbol{m}_{mn}(\boldsymbol{e}_r)\\ &+ T^{22}_{mn,m_1n_1}\boldsymbol{n}_{mn}(\boldsymbol{e}_r)\big]\otimes\boldsymbol{n}^*_{m_1n_1}(\boldsymbol{e}_k)\Big\}\,.\end{aligned}$$

In view of (1.75), the elements of the amplitude matrix are given by

$$\begin{aligned}S_{pq}(\boldsymbol{e}_r,\boldsymbol{e}_k) = \frac{4}{k_{\mathrm{s}}}\sum_{n,m}\sum_{n_1,m_1}(-\mathrm{j})^{n+1}\,\mathrm{j}^{n_1}\Big\{\big[&T^{11}_{mn,m_1n_1}m^*_{m_1n_1,q}(\boldsymbol{e}_k)\\ &- jT^{12}_{mn,m_1n_1}n^*_{m_1n_1,q}(\boldsymbol{e}_k)\big]m_{mn,p}(\boldsymbol{e}_r)\\ &+\mathrm{j}\big[T^{21}_{mn,m_1n_1}m^*_{m_1n_1,q}(\boldsymbol{e}_k)\,,\\ &- jT^{22}_{mn,m_1n_1}n^*_{m_1n_1,q}(\boldsymbol{e}_k)\big]n_{mn,p}(\boldsymbol{e}_r)\Big\}\end{aligned}\tag{1.97}$$

for $p=\theta,\varphi$ and $q=\beta,\alpha$. For a vector plane wave linearly polarized in the β-direction, $a_{mn}=4\mathrm{j}^n m^*_{mn,\beta}$ and $b_{mn}=-4\mathrm{j}^{n+1}n^*_{mn,\beta}$, and $S_{\theta\beta}=E_{\mathrm{s}\infty,\theta}$ and $S_{\varphi\beta}=E_{\mathrm{s}\infty,\varphi}$. Analogously, for a vector plane wave linearly polarized in the α-direction, $a_{mn}=4\mathrm{j}^n m^*_{mn,\alpha}$ and $b_{mn}=-4\mathrm{j}^{n+1}n^*_{mn,\alpha}$, and $S_{\theta\alpha}=E_{\mathrm{s}\infty,\theta}$ and $S_{\varphi\alpha}=E_{\mathrm{s}\infty,\varphi}$. In practical computer calculations, this technique, relying on the computation of the far-field patterns for parallel and perpendicular polarizations, can be used to determine the elements of the amplitude matrix.

For our further analysis, it is more convenient to express the above equations in matrix form. Defining the vectors

$$\boldsymbol{s}=\begin{bmatrix}f_{mn}\\ g_{mn}\end{bmatrix}\,,\quad \boldsymbol{e}=\begin{bmatrix}a_{mn}\\ b_{mn}\end{bmatrix}$$

and the "augmented" vector of spherical harmonics

$$\boldsymbol{v}\left(\boldsymbol{e}_r\right) = \begin{bmatrix} \left(-\mathrm{j}\right)^n \boldsymbol{m}_{mn}\left(\boldsymbol{e}_r\right) \\ \mathrm{j}\left(-\mathrm{j}\right)^n \boldsymbol{n}_{mn}\left(\boldsymbol{e}_r\right) \end{bmatrix}$$

we see that

$$\boldsymbol{E}_{\mathrm{s}\infty}\left(\boldsymbol{e}_r\right) = -\frac{\mathrm{j}}{k_{\mathrm{s}}}\boldsymbol{v}^{\mathrm{T}}\left(\boldsymbol{e}_r\right)\boldsymbol{s} = -\frac{\mathrm{j}}{k_{\mathrm{s}}}\boldsymbol{v}^{\mathrm{T}}\left(\boldsymbol{e}_r\right)\boldsymbol{T}\boldsymbol{e} = -\frac{\mathrm{j}}{k_{\mathrm{s}}}\boldsymbol{e}^{\mathrm{T}}\boldsymbol{T}^{\mathrm{T}}\boldsymbol{v}\left(\boldsymbol{e}_r\right) , \qquad (1.98)$$

and, since $\boldsymbol{e} = 4\boldsymbol{e}_{\mathrm{pol}} \cdot \boldsymbol{v}^*(\boldsymbol{e}_k)$, we obtain

$$S_{pq}\left(\boldsymbol{e}_r, \boldsymbol{e}_k\right) = -\frac{4\mathrm{j}}{k_{\mathrm{s}}}\boldsymbol{v}_p^{\mathrm{T}}\left(\boldsymbol{e}_r\right)\boldsymbol{T}\boldsymbol{v}_q^*\left(\boldsymbol{e}_k\right) = -\frac{4\mathrm{j}}{k_{\mathrm{s}}}\boldsymbol{v}_q^{\dagger}\left(\boldsymbol{e}_k\right)\boldsymbol{T}^{\mathrm{T}}\boldsymbol{v}_p\left(\boldsymbol{e}_r\right) . \qquad (1.99)$$

The superscript † means complex conjugate transpose, and

$$\boldsymbol{v}_p\left(\cdot\right) = \begin{bmatrix} \left(-\mathrm{j}\right)^n m_{mn,p}\left(\cdot\right) \\ \mathrm{j}\left(-\mathrm{j}\right)^n n_{mn,p}\left(\cdot\right) \end{bmatrix} ,$$

where $p = \theta, \varphi$ for the $\boldsymbol{e}_r$-dependency and $p = \beta, \alpha$ for the $\boldsymbol{e}_k$-dependency.

The extinction and scattering cross-sections can be expressed in terms of the expansion coefficients a_{mn}, b_{mn}, f_{mn} and g_{mn}. Denoting by S_{c} the circumscribing sphere of outward unit normal vector $\boldsymbol{e}_r$ and radius R, and using the definition of the extinction cross-section (cf. (1.82) and (1.83) with $|\boldsymbol{E}_{\mathrm{e0}}| = 1$), yields

$$\begin{aligned} C_{\mathrm{ext}} &= -\sqrt{\frac{\mu_{\mathrm{s}}}{\varepsilon_{\mathrm{s}}}} \int_{S_{\mathrm{c}}} \boldsymbol{e}_r \cdot \mathrm{Re}\left\{\boldsymbol{E}_{\mathrm{e}} \times \boldsymbol{H}_{\mathrm{s}}^* + \boldsymbol{E}_{\mathrm{s}} \times \boldsymbol{H}_{\mathrm{e}}^*\right\} \mathrm{d}S \\ &= -\mathrm{Re}\left\{ \mathrm{j} \sum_{n,m} \sum_{n_1,m_1} \int_{S_{\mathrm{c}}} \left\{ \left(f_{mn} a_{m_1 n_1}^* + g_{mn} b_{m_1 n_1}^*\right) \right.\right. \\ &\quad \times \left[\left(\boldsymbol{e}_r \times \boldsymbol{M}_{mn}^3\right) \cdot \boldsymbol{N}_{m_1 n_1}^{1*} + \left(\boldsymbol{e}_r \times \boldsymbol{N}_{mn}^3\right) \cdot \boldsymbol{M}_{m_1 n_1}^{1*}\right] \\ &\quad + \left(f_{mn} b_{m_1 n_1}^* + g_{mn} a_{m_1 n_1}^*\right) \\ &\quad \left.\left. \times \left[\left(\boldsymbol{e}_r \times \boldsymbol{M}_{mn}^3\right) \cdot \boldsymbol{M}_{m_1 n_1}^{1*} + \left(\boldsymbol{e}_r \times \boldsymbol{N}_{mn}^3\right) \cdot \boldsymbol{N}_{m_1 n_1}^{1*}\right] \right\} \mathrm{d}S \right\} . \end{aligned}$$

Taking into account the orthogonality relations of the vector spherical wave functions on a spherical surface (cf. (B.18) and (B.19)) we obtain

$$\begin{aligned} C_{\mathrm{ext}} = -\mathrm{Re}\left\{ \frac{\mathrm{j}\pi R}{k_{\mathrm{s}}} \sum_{n=1}^{\infty} \sum_{m=-n}^{n} \left(f_{mn} a_{mn}^* + g_{mn} b_{mn}^*\right) \right. \\ \left. \times \left\{ h_n^{(1)}(k_{\mathrm{s}}R)\left[k_{\mathrm{s}}R\mathrm{j}_n(k_{\mathrm{s}}R)\right]' - \mathrm{j}_n(k_{\mathrm{s}}R)\left[k_{\mathrm{s}}R h_n^{(1)}(k_{\mathrm{s}}R)\right]' \right\} \right\} , \end{aligned}$$

whence, using the Wronskian relation

$$h_n^{(1)}(k_{\mathrm{s}}R)\left[k_{\mathrm{s}}R j_n(k_{\mathrm{s}}R)\right]' - \mathrm{j}_n(k_{\mathrm{s}}R)\left[k_{\mathrm{s}}R h_n^{(1)}(k_{\mathrm{s}}R)\right]' = -\frac{\mathrm{j}}{k_{\mathrm{s}}R} ,$$

we end up with

$$C_{\text{ext}} = -\frac{\pi}{k_{\text{s}}^2} \sum_{n=1}^{\infty} \sum_{m=-n}^{n} \text{Re}\left\{ f_{mn} a_{mn}^* + g_{mn} b_{mn}^* \right\} . \tag{1.100}$$

For the scattering cross-section, the expansion of the far-field pattern in terms of vector spherical harmonics (cf. (1.96)) and the orthogonality relations of the vector spherical harmonics (cf. (B.12) and (B.13)), yields

$$C_{\text{scat}} = \frac{\pi}{k_{\text{s}}^2} \sum_{n=1}^{\infty} \sum_{m=-n}^{n} |f_{mn}|^2 + |g_{mn}|^2 . \tag{1.101}$$

Thus, the extinction cross-section is given by the expansion coefficients of the incident and scattered field, while the scattering cross-section is determined by the expansion coefficients of the scattered field.

1.5.2 Unitarity and Symmetry

It is of interest to investigate general constraints of the transition matrix such as unitarity and symmetry. These properties can be established by applying the principle of conservation of energy to nonabsorbing particles ($\varepsilon_{\text{i}} > 0$ and $\mu_{\text{i}} > 0$). We begin our analysis by defining the $\mathcal{S}$ matrix in terms of the $\boldsymbol{T}$ matrix by the relation

$$\mathcal{S} = \boldsymbol{I} + 2\boldsymbol{T} ,$$

where $\boldsymbol{I}$ is the identity matrix. In the literature, the $\mathcal{S}$ matrix is also known as the scattering matrix but in our analysis we avoid this term because the scattering matrix will have another significance.

First we consider the unitarity property. Application of the divergence theorem to the total fields $\boldsymbol{E} = \boldsymbol{E}_{\text{s}} + \boldsymbol{E}_{\text{e}}$ and $\boldsymbol{H} = \boldsymbol{H}_{\text{s}} + \boldsymbol{H}_{\text{e}}$ in the domain D bounded by the surface S and a spherical surface S_{c} situated in the far-field region, yields

$$\int_D \nabla \cdot (\boldsymbol{E} \times \boldsymbol{H}^*) \, \text{d}V = -\int_S \boldsymbol{n} \cdot (\boldsymbol{E} \times \boldsymbol{H}^*) \, \text{d}S + \int_{S_{\text{c}}} \boldsymbol{e}_r \cdot (\boldsymbol{E} \times \boldsymbol{H}^*) \, \text{d}S . \tag{1.102}$$

We consider the real part of the above equation and since the bounded domain D is assumed to be lossless ($\varepsilon_{\text{s}} > 0$ and $\mu_{\text{s}} > 0$) it follows that:

$$\text{Re}\left\{ \nabla \cdot (\boldsymbol{E} \times \boldsymbol{H}^*) \right\} = \text{Re}\left\{ jk_0\mu_{\text{s}} |\boldsymbol{H}|^2 - \text{j}k_0\varepsilon_{\text{s}} |\boldsymbol{E}|^2 \right\} = 0 \quad \text{in} \quad D . \tag{1.103}$$

On the other hand, taking into account the boundary conditions $\boldsymbol{n} \times \boldsymbol{E}_{\text{i}} = \boldsymbol{n} \times \boldsymbol{E}$ and $\boldsymbol{n} \times \boldsymbol{H}_{\text{i}} = \boldsymbol{n} \times \boldsymbol{H}$ on S, we have

$$\int_S \boldsymbol{n} \cdot (\boldsymbol{E} \times \boldsymbol{H}^*) \, \text{d}S = \int_S \boldsymbol{n} \cdot (\boldsymbol{E}_{\text{i}} \times \boldsymbol{H}_{\text{i}}^*) \, \text{d}S = \int_{D_{\text{i}}} \nabla \cdot (\boldsymbol{E}_{\text{i}} \times \boldsymbol{H}_{\text{i}}^*) \, \text{d}V$$

and since for nonabsorbing particles

$$\mathrm{Re}\left\{\nabla\cdot(\boldsymbol{E}_\mathrm{i}\times\boldsymbol{H}_\mathrm{i}^*)\right\}=\mathrm{Re}\left\{\mathrm{j}k_0\mu_\mathrm{i}\left|\boldsymbol{H}_\mathrm{i}\right|^2-\mathrm{j}k_0\varepsilon_\mathrm{i}\left|\boldsymbol{E}_\mathrm{i}\right|^2\right\}=0\quad\text{in}\quad D_\mathrm{i}\,,$$

we obtain

$$\int_S\boldsymbol{n}\cdot\mathrm{Re}\left\{\boldsymbol{E}\times\boldsymbol{H}^*\right\}\mathrm{d}S=0\,. \tag{1.104}$$

Combining (1.102), (1.103) and (1.104) we deduce that

$$\int_{S_c}\boldsymbol{e}_r\cdot\mathrm{Re}\left\{\boldsymbol{E}\times\boldsymbol{H}^*\right\}\mathrm{d}S=0\,. \tag{1.105}$$

We next seek to find a series representation for the total electric field. For this purpose, we use the decomposition

$$\begin{pmatrix}\boldsymbol{M}_{mn}^1\\ \boldsymbol{N}_{mn}^1\end{pmatrix}=\frac{1}{2}\left[\begin{pmatrix}\boldsymbol{M}_{mn}^3\\ \boldsymbol{N}_{mn}^3\end{pmatrix}+\begin{pmatrix}\boldsymbol{M}_{mn}^2\\ \boldsymbol{N}_{mn}^2\end{pmatrix}\right],$$

where the vector spherical wave functions $\boldsymbol{M}_{mn}^2$ and $\boldsymbol{N}_{mn}^2$ have the same expressions as the vector spherical wave functions $\boldsymbol{M}_{mn}^3$ and $\boldsymbol{N}_{mn}^3$, but with the spherical Hankel functions of the second kind $h_n^{(2)}$ in place of the spherical Hankel functions of the first kind $h_n^{(1)}$. It should be remarked that for real arguments x, $h_n^{(2)}(x)=[h_n^{(1)}(x)]^*$. In the far-field region

$$\begin{aligned}\boldsymbol{M}_{mn}^2(k\boldsymbol{r})&=\frac{\mathrm{e}^{-\mathrm{j}kr}}{kr}\left\{\mathrm{j}^{n+1}\boldsymbol{m}_{mn}(\theta,\varphi)+\mathrm{O}\left(\frac{1}{r}\right)\right\},\\ \boldsymbol{N}_{mn}^2(k\boldsymbol{r})&=\frac{\mathrm{e}^{-\mathrm{j}kr}}{kr}\left\{\mathrm{j}^{n}\boldsymbol{n}_{mn}(\theta,\varphi)+\mathrm{O}\left(\frac{1}{r}\right)\right\},\end{aligned}$$

as $r\to\infty$, and we see that $\boldsymbol{M}_{mn}^2$ and $\boldsymbol{N}_{mn}^2$ behave as incoming transverse vector spherical waves.

The expansion of the incident field then becomes

$$\begin{aligned}\boldsymbol{E}_e&=\sum_{n,m}a_{mn}\boldsymbol{M}_{mn}^1+b_{mn}\boldsymbol{N}_{mn}^1\\ &=\frac{1}{2}\sum_{n,m}a_{mn}\boldsymbol{M}_{mn}^3+b_{mn}\boldsymbol{N}_{mn}^3+\frac{1}{2}\sum_{n,m}a_{mn}\boldsymbol{M}_{mn}^2+b_{mn}\boldsymbol{N}_{mn}^2\,,\end{aligned}$$

whence

$$\begin{aligned}\boldsymbol{E}=&\sum_{n,m}\left(f_{mn}+\frac{1}{2}a_{mn}\right)\boldsymbol{M}_{mn}^3+\left(g_{mn}+\frac{1}{2}b_{mn}\right)\boldsymbol{N}_{mn}^3\\ &+\frac{1}{2}\sum_{n,m}a_{mn}\boldsymbol{M}_{mn}^2+b_{mn}\boldsymbol{N}_{mn}^2\,,\end{aligned}$$

follows. Setting

$$c_{mn} = 2f_{mn} + a_{mn}\,,$$
$$d_{mn} = 2g_{mn} + b_{mn}\,,$$

and using the $\boldsymbol{T}$-matrix equation, yields

$$\begin{bmatrix} c_{mn} \\ d_{mn} \end{bmatrix} = \mathcal{S} \begin{bmatrix} a_{mn} \\ b_{mn} \end{bmatrix} = (\boldsymbol{I} + 2\boldsymbol{T}) \begin{bmatrix} a_{mn} \\ b_{mn} \end{bmatrix}\,.$$

The coefficients a_{mn} and b_{mn} are determined by the incoming field. Since in the far-field region $\boldsymbol{M}^2_{mn}$ and $\boldsymbol{N}^2_{mn}$ become incoming vector spherical waves, we see that the $\mathcal{S}$ matrix determines how an incoming vector spherical wave is scattered into the same one.

In the far-field region, the total electric field

$$\boldsymbol{E} = \frac{1}{2}\sum_{n,m} c_{mn}\boldsymbol{M}^3_{mn} + d_{mn}\boldsymbol{N}^3_{mn} + \frac{1}{2}\sum_{n,m} a_{mn}\boldsymbol{M}^2_{mn} + b_{mn}\boldsymbol{N}^2_{mn}$$

can be expressed as a superposition of outgoing and incoming transverse spherical waves

$$\boldsymbol{E}(\boldsymbol{r}) = \frac{\mathrm{e}^{\mathrm{j}k_\mathrm{s}r}}{r}\left\{\boldsymbol{E}^{(1)}_\infty(\boldsymbol{e}_r) + \mathrm{O}\left(\frac{1}{r}\right)\right\} + \frac{\mathrm{e}^{-\mathrm{j}k_\mathrm{s}r}}{r}\left\{\boldsymbol{E}^{(2)}_\infty(\boldsymbol{e}_r) + \mathrm{O}\left(\frac{1}{r}\right)\right\}\,,$$
$$r \to \infty \tag{1.106}$$

with

$$\boldsymbol{E}^{(1)}_\infty(\boldsymbol{e}_r) = \frac{1}{2k_\mathrm{s}}\sum_{n,m}(-\mathrm{j})^{n+1}\left[c_{mn}\boldsymbol{m}_{mn}(\boldsymbol{e}_r) + \mathrm{j}d_{mn}\boldsymbol{n}_{mn}(\boldsymbol{e}_r)\right]\,,$$

$$\boldsymbol{E}^{(2)}_\infty(\boldsymbol{e}_r) = \frac{1}{2k_\mathrm{s}}\sum_{n,m}\mathrm{j}^{n+1}\left[a_{mn}\boldsymbol{m}_{mn}(\boldsymbol{e}_r) - \mathrm{j}b_{mn}\boldsymbol{n}_{mn}(\boldsymbol{e}_r)\right]\,.$$

For the total magnetic field we proceed analogously and obtain

$$\boldsymbol{H}(\boldsymbol{r}) = \frac{\mathrm{e}^{\mathrm{j}k_\mathrm{s}r}}{r}\left\{\boldsymbol{H}^{(1)}_\infty(\boldsymbol{e}_r) + \mathrm{O}\left(\frac{1}{r}\right)\right\} + \frac{\mathrm{e}^{-\mathrm{j}k_\mathrm{s}r}}{r}\left\{\boldsymbol{H}^{(2)}_\infty(\boldsymbol{e}_r) + \mathrm{O}\left(\frac{1}{r}\right)\right\}$$
$$r \to \infty$$

with

$$\boldsymbol{H}^{(1)}_\infty = \sqrt{\frac{\varepsilon_\mathrm{s}}{\mu_\mathrm{s}}}\boldsymbol{e}_r \times \boldsymbol{E}^{(1)}_\infty\,,$$

$$\boldsymbol{H}^{(2)}_\infty = -\sqrt{\frac{\varepsilon_\mathrm{s}}{\mu_\mathrm{s}}}\boldsymbol{e}_r \times \boldsymbol{E}^{(2)}_\infty\,.$$

Thus

$$\mathrm{Re}\left\{\boldsymbol{e}_r\cdot(\boldsymbol{E}\times\boldsymbol{H}^*)\right\}=\frac{1}{r^2}\sqrt{\frac{\varepsilon_\mathrm{s}}{\mu_\mathrm{s}}}\left\{\left|\boldsymbol{E}_\infty^{(1)}\right|^2-\left|\boldsymbol{E}_\infty^{(2)}\right|^2+\mathrm{O}\left(\frac{1}{r}\right)\right\}\,,\quad r\to\infty$$

and (1.105) yields

$$\int_\Omega\left(\left|\boldsymbol{E}_\infty^{(1)}\right|^2-\left|\boldsymbol{E}_\infty^{(2)}\right|^2\right)\mathrm{d}\Omega=0\,. \tag{1.107}$$

The orthogonality relations of the vector spherical harmonics on the unit sphere give

$$\begin{aligned}\int_\Omega\left|\boldsymbol{E}_\infty^{(1)}\right|^2\mathrm{d}\Omega&=\frac{\pi}{4k_\mathrm{s}^2}\left[a_{mn}^*,b_{mn}^*\right]\mathcal{S}^\dagger\mathcal{S}\begin{bmatrix}a_{mn}\\b_{mn}\end{bmatrix},\\ \int_\Omega\left|\boldsymbol{E}_\infty^{(2)}\right|^2\mathrm{d}\Omega&=\frac{\pi}{4k_\mathrm{s}^2}\left[a_{mn}^*,b_{mn}^*\right]\begin{bmatrix}a_{mn}\\b_{mn}\end{bmatrix}\end{aligned} \tag{1.108}$$

and since the incident field is arbitrarily, (1.107) and (1.108) implies that [217, 228, 256]

$$\mathcal{S}^\dagger\mathcal{S}=\boldsymbol{I}\,. \tag{1.109}$$

The above relation is the unitary condition for nonabsorbing particles. In terms of the transition matrix, this condition is

$$\boldsymbol{T}^\dagger\boldsymbol{T}=-\frac{1}{2}\left(\boldsymbol{T}+\boldsymbol{T}^\dagger\right)\,,$$

or explicitly

$$\sum_{k=1}^{2}\sum_{n'=1}^{\infty}\sum_{m'=-n'}^{n'}T_{m'n',mn}^{ki*}T_{m'n',m_1n_1}^{kj}=-\frac{1}{2}\left(T_{m_1n_1,mn}^{ji*}+T_{mn,m_1n_1}^{ij}\right)\,. \tag{1.110}$$

For absorbing particles, the integral in (1.107) is negative. Consequently, the equality in (1.110) transforms into an inequality which is equivalent to the contractivity of the $\mathcal{S}$ matrix [169]. Taking the trace of (1.110), Mishchenko et al. [169] derived an equality (inequality) between the $\boldsymbol{T}$-matrix elements of an axisymmetric particle provided that the z-axis of the particle coordinate system is directed along the axis of symmetry.

To obtain the symmetry relation we proceed as in the derivation of the reciprocity relation for the tensor scattering amplitude, i.e., we consider the electromagnetic fields $\boldsymbol{E}_u$, $\boldsymbol{H}_u$ generated by the incident fields $\boldsymbol{E}_{eu}$, $\boldsymbol{H}_{eu}$, with $u=1,2$. The starting point is the integral (cf. (1.90))

$$\int_{S_\mathrm{c}}\boldsymbol{e}_r\cdot(\boldsymbol{E}_2\times\boldsymbol{H}_1-\boldsymbol{E}_1\times\boldsymbol{H}_2)\,\mathrm{d}S=0$$

over a spherical surface S_{c} situated in the far-field region. Then, using the asymptotic form (cf. (1.106))

$$\boldsymbol{E}_u(\boldsymbol{r}) = \frac{\mathrm{e}^{\mathrm{j}k_{\mathrm{s}}r}}{r}\left\{\boldsymbol{E}^{(1)}_{u\infty}(\boldsymbol{e}_r) + \mathrm{O}\left(\frac{1}{r}\right)\right\} + \frac{\mathrm{e}^{-\mathrm{j}k_{\mathrm{s}}r}}{r}\left\{\boldsymbol{E}^{(2)}_{u\infty}(\boldsymbol{e}_r) + \mathrm{O}\left(\frac{1}{r}\right)\right\},$$
$$r \to \infty$$

for $u = 1, 2$, we obtain

$$\int_{\Omega}\left(\boldsymbol{e}_r \times \boldsymbol{E}^{(1)}_{2\infty}\right)\cdot\left(\boldsymbol{e}_r \times \boldsymbol{E}^{(2)}_{1\infty}\right)\mathrm{d}\Omega = \int_{\Omega}\left(\boldsymbol{e}_r \times \boldsymbol{E}^{(1)}_{1\infty}\right)\cdot\left(\boldsymbol{e}_r \times \boldsymbol{E}^{(2)}_{2\infty}\right)\mathrm{d}\Omega\,. \tag{1.111}$$

Taking into account the vector spherical harmonic expansions of the far-field patterns $\boldsymbol{E}^{(1)}_{u\infty}$ and $\boldsymbol{E}^{(2)}_{u\infty}$, $u = 1, 2$, and the relations $\boldsymbol{e}_r \times \boldsymbol{m}_{mn} = \boldsymbol{n}_{mn}$ and $\boldsymbol{e}_r \times \boldsymbol{n}_{mn} = -\boldsymbol{m}_{mn}$, we see that

$$\int_{\Omega}\left(\boldsymbol{e}_r \times \boldsymbol{E}^{(1)}_{2\infty}\right)\cdot\left(\boldsymbol{e}_r \times \boldsymbol{E}^{(2)}_{1\infty}\right)\mathrm{d}\Omega = \frac{\pi}{4k_{\mathrm{s}}^2}\left[a_{1,m_1n_1}, b_{1,m_1n_1}\right]\begin{bmatrix} c_{2,-m_1n_1} \\ d_{2,-m_1n_1}\end{bmatrix},$$

$$\int_{\Omega}\left(\boldsymbol{e}_r \times \boldsymbol{E}^{(1)}_{1\infty}\right)\cdot\left(\boldsymbol{e}_r \times \boldsymbol{E}^{(2)}_{2\infty}\right)\mathrm{d}\Omega = \frac{\pi}{4k_{\mathrm{s}}^2}\left[c_{1,mn}, d_{1,mn}\right]\begin{bmatrix} a_{2,-mn} \\ b_{2,-mn}\end{bmatrix},$$

where $a_{u,mn}$, $b_{u,mn}$ are the expansion coefficients of the far-field pattern $\boldsymbol{E}^{(2)}_{u\infty}$, while $c_{u,mn}$, $d_{u,mn}$ are the expansion coefficients of the far-field pattern $\boldsymbol{E}^{(1)}_{u\infty}$. Consequently, (1.111) can be written in matrix form as

$$\left[a_{1,m_1n_1}, b_{1,m_1n_1}\right]\begin{bmatrix} \mathcal{S}^{11}_{-m_1n_1,-mn} & \mathcal{S}^{12}_{-m_1n_1,-mn} \\ \mathcal{S}^{21}_{-m_1n_1,-mn} & \mathcal{S}^{22}_{-m_1n_1,-mn}\end{bmatrix}\begin{bmatrix} a_{2,-mn} \\ b_{2,-mn}\end{bmatrix}$$
$$= \left[a_{1,m_1n_1}, b_{1,m_1n_1}\right]\begin{bmatrix} \mathcal{S}^{11}_{mn,m_1n_1} & \mathcal{S}^{21}_{mn,m_1n_1} \\ \mathcal{S}^{12}_{mn,m_1n_1} & \mathcal{S}^{22}_{mn,m_1n_1}\end{bmatrix}\begin{bmatrix} a_{2,-mn} \\ b_{2,mn}\end{bmatrix}$$

and since the above equation holds true for any incident field, we find that

$$\mathcal{S}^{ij}_{mn,m_1n_1} = \mathcal{S}^{ji}_{-m_1n_1,-mn}$$

and further that

$$T^{ij}_{mn,m_1n_1} = T^{ji}_{-m_1n_1,-mn} \tag{1.112}$$

for $i, j = 1, 2$. This relation reflects the symmetry property of the transition matrix and is of basic importance in practical computer calculations. We note that the symmetry relation (1.112) can be obtained directly from the reciprocity relation for the tensor scattering amplitude

$$\overline{\boldsymbol{A}}\,(\theta_1, \varphi_1; \theta_2, \varphi_2) = \overline{\boldsymbol{A}}^{\mathrm{T}}\,(\pi - \theta_2, \pi + \varphi_2; \pi - \theta_1, \pi + \varphi_1)$$

and the identities

$$\boldsymbol{m}_{mn}(\pi-\theta,\pi+\varphi)=(-1)^n\boldsymbol{m}_{mn}(\theta,\varphi)\ ,$$
$$\boldsymbol{n}_{mn}(\pi-\theta,\pi+\varphi)=(-1)^{n+1}\boldsymbol{n}_{mn}(\theta,\varphi)\ ,$$

and

$$\boldsymbol{m}_{-mn}(\theta,\varphi)=\boldsymbol{m}^*_{mn}(\theta,\varphi)\ ,$$
$$\boldsymbol{n}_{-mn}(\theta,\varphi)=\boldsymbol{n}^*_{mn}(\theta,\varphi)\ .$$

Additional properties of the transition matrix for particles with specific symmetries will be discussed in the next chapter. The "exact" infinite transition matrix satisfies the unitarity and symmetry conditions (1.110) and (1.112), respectively. However, in practical computer calculations, the truncated transition matrix may not satisfies these conditions and we can test the unitarity and symmetry conditions to get a rough idea regarding the convergence to be expected in the solution computation.

Remark. In the above analysis, the incident field is a vector plane wave whose source is situated at infinity. Other incident fields than vector plane waves can be considered, but we shall assume that the source of the incident field lies outside the circumscribing sphere $S_{\rm c}$. In this case, the incident field is regular everywhere inside the circumscribing sphere, and both expansions (1.93) and (1.94) are valid on $S_{\rm c}$. The $\boldsymbol{T}$-matrix equation holds true at finite distances from the particle (not only in the far-field region), and therefore, the transition matrix is also known as the "nonasymptotic vector-spherical-wave transition matrix". The properties of the transition matrix (unitarity and symmetry) can also be established by considering the energy flow through a finite sphere $S_{\rm c}$ [238]. If we now let the source of the incident field recede to infinity, we can let the surface $S_{\rm c}$ follow, i.e., we can consider the case of an arbitrary large sphere and this brings us to the precedent analysis.

1.5.3 Randomly Oriented Particles

In the following analysis we consider scattering by an ensemble of randomly oriented, identical particles. Random particle orientation means that the orientation distribution of the particles is uniform. As a consequence of random particle orientation, the scattering medium is macroscopically isotropic, i.e., the scattering characteristics are independent of the incident and scattering directions $\boldsymbol{e}_k$ and $\boldsymbol{e}_r$, and depend only on the angle between the unit vectors $\boldsymbol{e}_k$ and $\boldsymbol{e}_r$. For this type of scattering problem, it is convenient to direct the Z-axis of the global coordinate system along the incident direction and to choose the XZ-plane as the scattering plane (Fig. 1.13).

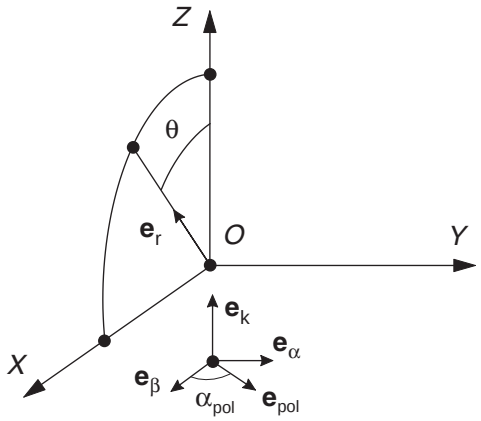

Fig. 1.13. The Z-axis of the global coordinate system is along the incident direction and the XZ-plane is the scattering plane

General Considerations

The phase matrix of a volume element containing randomly oriented particles can be written as

$$\boldsymbol{Z}\left(\boldsymbol{e}_r, \boldsymbol{e}_k\right) = \boldsymbol{Z}\left(\theta, \varphi = 0, \beta = 0, \alpha = 0\right) ,$$

where, in general, θ and φ are the polar angles of the scattering direction $\boldsymbol{e}_r$, and β and α are the polar angles of the incident direction $\boldsymbol{e}_k$. The phase matrix $\boldsymbol{Z}(\theta, 0, 0, 0)$ is known as the scattering matrix $\boldsymbol{F}$ and relates the Stokes parameters of the incident and scattered fields defined with respect to the scattering plane. Taking into account that for an incident direction (β, α), the backscattering direction is $(\pi - \beta, \alpha + \pi)$, the complete definition of the scattering matrix is [169]

$$\boldsymbol{F}(\theta) = \begin{cases} \boldsymbol{Z}(\theta, 0, 0, 0) , & \theta \in [0, \pi), \\ \boldsymbol{Z}\left(\pi, \pi, 0, 0\right) , & \theta = \pi. \end{cases}$$

The scattering matrix of a volume element containing randomly oriented particles has the following structure:

$$\boldsymbol{F}(\theta) = \begin{bmatrix} F_{11}(\theta) & F_{12}(\theta) & F_{13}(\theta) & F_{14}(\theta) \\ F_{12}(\theta) & F_{22}(\theta) & F_{23}(\theta) & F_{24}(\theta) \\ -F_{13}(\theta) & -F_{23}(\theta) & F_{33}(\theta) & F_{34}(\theta) \\ F_{14}(\theta) & F_{24}(\theta) & -F_{34}(\theta) & F_{44}(\theta) \end{bmatrix} . \tag{1.113}$$

If each particle has a plane of symmetry or, equivalently, the particles and their mirror-symmetric particles are present in equal numbers, the scattering

medium is called macroscopically isotropic and mirror-symmetric. Note that rotationally symmetric particles are obviously mirror-symmetric with respect to the plane through the axis of symmetry. Because of symmetry, the scattering matrix of a macroscopically isotropic and mirror-symmetric scattering medium has the following block-diagonal structure [103, 169]:

$$\boldsymbol{F}(\theta) = \begin{bmatrix} F_{11}(\theta) & F_{12}(\theta) & 0 & 0 \\ F_{12}(\theta) & F_{22}(\theta) & 0 & 0 \\ 0 & 0 & F_{33}(\theta) & F_{34}(\theta) \\ 0 & 0 & -F_{34}(\theta) & F_{44}(\theta) \end{bmatrix} . \tag{1.114}$$

The phase matrix can be related to the scattering matrix by using the rotation transformation rule (1.22), and this procedure involves two rotations as shown in Fig. 1.14. Taking into account that the scattering matrix relates the Stokes vectors of the incident and scattered fields specified relative to the scattering plane, $\boldsymbol{I}'_{\rm s} = (1/r^2)\boldsymbol{F}(\Theta)\boldsymbol{I}'_{\rm e}$, and using the transformation rule of the Stokes vectors under coordinate rotations $\boldsymbol{I}'_{\rm e} = \boldsymbol{L}(\sigma_1)\boldsymbol{I}_{\rm e}$ and $\boldsymbol{I}_{\rm s} = \boldsymbol{L}(-\sigma_2)\boldsymbol{I}'_{\rm s}$, we obtain

$$\boldsymbol{Z}\left(\theta,\varphi,\beta,\alpha\right) = \boldsymbol{L}\left(-\sigma_2\right)\boldsymbol{F}\left(\Theta\right)\boldsymbol{L}\left(\sigma_1\right) ,$$

where

$$\cos\Theta = \boldsymbol{e}_k \cdot \boldsymbol{e}_r = \cos\beta\cos\theta + \sin\beta\sin\theta\cos\left(\varphi-\alpha\right) ,$$

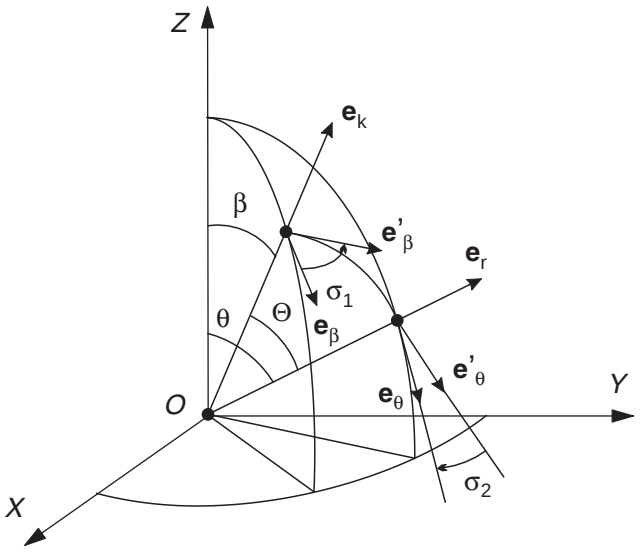

Fig. 1.14. Incident and scattering directions $\boldsymbol{e}_k$ and $\boldsymbol{e}_r$. The scattering matrix relates the Stokes vectors of the incident and scattered fields specified relative to the scattering plane

$$\cos\sigma_1 = \boldsymbol{e}'_\alpha \cdot \boldsymbol{e}_\alpha = -\frac{\sin\beta\cos\theta - \cos\beta\sin\theta\cos(\varphi-\alpha)}{\sin\Theta}\,,$$

$$\cos\sigma_2 = \boldsymbol{e}'_\varphi \cdot \boldsymbol{e}_\varphi = \frac{\cos\beta\sin\theta - \sin\beta\cos\theta\cos(\varphi-\alpha)}{\sin\Theta}\,.$$

For an ensemble of randomly positioned particles, the waves scattered by different particles are random in phase, and the Stokes parameters of these incoherent waves add up. Therefore, the scattering matrix for the ensemble is the sum of the scattering matrices of the individual particles:

$$\boldsymbol{F} = N\langle\boldsymbol{F}\rangle\,,$$

where N is number of particles and $\langle\boldsymbol{F}\rangle$ denotes the ensemble-average scattering matrix per particle. Similar relations hold for the extinction matrix and optical cross-sections. Because the particles are identical, the ensemble-average of a scattering quantity X is the orientation-averaged quantity

$$\langle X\rangle = \frac{1}{8\pi^2}\int_0^{2\pi}\int_0^{2\pi}\int_0^{\pi} X(\alpha_\mathrm{p},\beta_\mathrm{p},\gamma_\mathrm{p})\sin\beta_\mathrm{p}\,\mathrm{d}\beta_\mathrm{p}\,\mathrm{d}\alpha_\mathrm{p}\,\mathrm{d}\gamma_\mathrm{p}\,,$$

where α_p, β_p and γ_p are the particle orientation angles.

In the following analysis, the $\boldsymbol{T}$ matrix formulation is used to derive efficient analytical techniques for computing $\langle X\rangle$. These methods work much faster than the standard approaches based on the numerical averaging of results computed for many discrete orientations of the particle. We begin with the derivation of the rotation transformation rule for the transition matrix and then compute the orientation-averaged transition matrix, optical cross-sections and extinction matrix. An analytical procedure for computing the orientation-averaged scattering matrix will conclude our analysis.

Rotation Transformation of the Transition Matrix

To derive the rotation transformation rule for the transition matrix we assume that the orientation of the particle coordinate system $Oxyz$ with respect to the global coordinate system $OXYZ$ is specified by the Euler angles α_p, β_p and γ_p.

In the particle coordinate system, the expansions of the incident and scattered field are given by

$$\boldsymbol{E}_\mathrm{e}(r,\theta,\varphi) = \sum_{n=1}^{\infty}\sum_{m=-n}^{n} a_{mn}\boldsymbol{M}^1_{mn}(k_\mathrm{s}r,\theta,\varphi) + b_{mn}\boldsymbol{N}^1_{mn}(k_\mathrm{s}r,\theta,\varphi)\,,$$

$$\boldsymbol{E}_\mathrm{s}(r,\theta,\varphi) = \sum_{n=1}^{\infty}\sum_{m=-n}^{n} f_{mn}\boldsymbol{M}^3_{mn}(k_\mathrm{s}r,\theta,\varphi) + g_{mn}\boldsymbol{N}^3_{mn}(k_\mathrm{s}r,\theta,\varphi)\,,$$

while in the global coordinate system, these expansions take the form

$$\boldsymbol{E}_{\mathrm{e}}(r,\Phi,\Psi)=\sum_{n=1}^{\infty}\sum_{m=-n}^{n}\widetilde{a}_{mn}\boldsymbol{M}_{mn}^{1}(k_{\mathrm{s}}r,\Phi,\Psi)+\widetilde{b}_{mn}\boldsymbol{N}_{mn}^{1}(k_{\mathrm{s}}r,\Phi,\Psi)\,,$$

$$\boldsymbol{E}_{\mathrm{s}}(r,\Phi,\Psi)=\sum_{n=1}^{\infty}\sum_{m=-n}^{n}\widetilde{f}_{mn}\boldsymbol{M}_{mn}^{3}(r,\Phi,\Psi)+\widetilde{g}_{mn}\boldsymbol{N}_{mn}^{3}(k_{\mathrm{s}}r,\Phi,\Psi)\,.$$

Assuming the $\boldsymbol{T}$-matrix equations $\boldsymbol{s}=\boldsymbol{T}\boldsymbol{e}$ and $\widetilde{\boldsymbol{s}}=\widetilde{\boldsymbol{T}}\widetilde{\boldsymbol{e}}$, our task is to express the transition matrix in the global coordinate system $\widetilde{\boldsymbol{T}}$ in terms of the transition matrix in the particle coordinate system $\boldsymbol{T}$. Defining the "augmented" vectors of spherical wave functions in each coordinate system

$$\boldsymbol{w}_{1,3}(k_{\mathrm{s}}r,\theta,\varphi)=\begin{bmatrix}\boldsymbol{M}_{mn}^{1,3}(k_{\mathrm{s}}r,\theta,\varphi)\\ \boldsymbol{N}_{mn}^{1,3}(k_{\mathrm{s}}r,\theta,\varphi)\end{bmatrix}$$

and

$$\widetilde{\boldsymbol{w}}_{1,3}(k_{\mathrm{s}}r,\Phi,\Psi)=\begin{bmatrix}\boldsymbol{M}_{mn}^{1,3}(k_{\mathrm{s}}r,\Phi,\Psi)\\ \boldsymbol{N}_{mn}^{1,3}(k_{\mathrm{s}}r,\Phi,\Psi)\end{bmatrix}\,,$$

and using the rotation addition theorem for vector spherical wave functions, we obtain

$$\begin{aligned}\boldsymbol{E}_{\mathrm{e}}&=\boldsymbol{e}^{\mathrm{T}}\boldsymbol{w}_1=\widetilde{\boldsymbol{e}}^{\mathrm{T}}\widetilde{\boldsymbol{w}}_1=\widetilde{\boldsymbol{e}}^{\mathrm{T}}\mathcal{R}(\alpha_{\mathrm{p}},\beta_{\mathrm{p}},\gamma_{\mathrm{p}})\,\boldsymbol{w}_1\,,\\ \boldsymbol{E}_{\mathrm{s}}&=\widetilde{\boldsymbol{s}}^{\mathrm{T}}\widetilde{\boldsymbol{w}}_3=\boldsymbol{s}^{\mathrm{T}}\boldsymbol{w}_3=\boldsymbol{s}^{\mathrm{T}}\mathcal{R}(-\gamma_{\mathrm{p}},-\beta_{\mathrm{p}},-\alpha_{\mathrm{p}})\,\widetilde{\boldsymbol{w}}_3\,.\end{aligned}$$

Consequently

$$\begin{aligned}\boldsymbol{e}&=\mathcal{R}^{\mathrm{T}}(\alpha_{\mathrm{p}},\beta_{\mathrm{p}},\gamma_{\mathrm{p}})\,\widetilde{\boldsymbol{e}}\,,\\ \widetilde{\boldsymbol{s}}&=\mathcal{R}^{\mathrm{T}}(-\gamma_{\mathrm{p}},-\beta_{\mathrm{p}},-\alpha_{\mathrm{p}})\,\boldsymbol{s}\,,\end{aligned}$$

and therefore,

$$\widetilde{\boldsymbol{T}}(\alpha_{\mathrm{p}},\beta_{\mathrm{p}},\gamma_{\mathrm{p}})=\mathcal{R}^{\mathrm{T}}(-\gamma_{\mathrm{p}},-\beta_{\mathrm{p}},-\alpha_{\mathrm{p}})\,\boldsymbol{T}\mathcal{R}^{\mathrm{T}}(\alpha_{\mathrm{p}},\beta_{\mathrm{p}},\gamma_{\mathrm{p}})\,. \tag{1.115}$$

The explicit expression of the matrix elements is [169, 228, 233]

$$\begin{aligned}\widetilde{T}_{mn,m_1n_1}^{ij}(\alpha_{\mathrm{p}},\beta_{\mathrm{p}},\gamma_{\mathrm{p}})=&\sum_{m'=-n}^{n}\sum_{m_1'=-n_1}^{n_1}D_{m'm}^{n}(-\gamma_{\mathrm{p}},-\beta_{\mathrm{p}},-\alpha_{\mathrm{p}})\,T_{m'n,m_1'n_1}^{ij}\\ &\times D_{m_1m_1'}^{n_1}(\alpha_{\mathrm{p}},\beta_{\mathrm{p}},\gamma_{\mathrm{p}})\end{aligned} \tag{1.116}$$

for $i,j=1,2$.

Because the elements of the amplitude matrix can be expressed in terms of the elements of the transition matrix, the above relation can be used to express the elements of the amplitude matrix as functions of the particle orientation angles α_{p}, β_{p} and γ_{p}. The properties of the Wigner D-functions can then be used to compute the integrals over the particle orientation angles.

Orientation-Averaged Transition Matrix

The elements of the orientation-averaged transition matrix with respect to the global coordinate system are given by

$$\left\langle \widetilde{T}^{ij}_{mn,m_1n_1} \right\rangle = \frac{1}{8\pi^2} \int_0^{2\pi} \int_0^{2\pi} \int_0^{\pi} \widetilde{T}^{ij}_{mn,m_1n_1} (\alpha_\mathrm{p}, \beta_\mathrm{p}, \gamma_\mathrm{p}) \sin\beta_\mathrm{p} \, \mathrm{d}\beta_\mathrm{p} \, \mathrm{d}\alpha_\mathrm{p} \, \mathrm{d}\gamma_\mathrm{p}$$

$$= \frac{1}{8\pi^2} \sum_{m'=-n}^{n} \sum_{m'_1=-n_1}^{n_1} T^{ij}_{m'n,m'_1n_1} \int_0^{2\pi} \int_0^{2\pi} \int_0^{\pi} D^n_{m'm} (-\gamma_\mathrm{p}, -\beta_\mathrm{p}, -\alpha_\mathrm{p})$$

$$\times D^{n_1}_{m_1m'_1} (\alpha_\mathrm{p}, \beta_\mathrm{p}, \gamma_\mathrm{p}) \sin\beta_\mathrm{p} \, \mathrm{d}\beta_\mathrm{p} \, \mathrm{d}\alpha_\mathrm{p} \, \mathrm{d}\gamma_\mathrm{p} \, . \tag{1.117}$$

Using the definition of the Wigner D-functions (cf. (B.34)), the symmetry relation of the Wigner d-functions $d^n_{m'm}(-\beta_\mathrm{p}) = d^n_{mm'}(\beta_\mathrm{p})$, and integrating over α_p and γ_p, yields

$$\left\langle \widetilde{T}^{ij}_{mn,m_1n_1} \right\rangle = \frac{1}{2} \sum_{m'=-n}^{n} \sum_{m'_1=-n_1}^{n_1} \Delta_{m'm} \Delta_{m_1m'_1} \delta_{m'm'_1} \delta_{mm_1}$$

$$\times T^{ij}_{m'n,m'_1n_1} \int_0^{\pi} d^n_{mm'} (\beta_\mathrm{p}) \, d^{n_1}_{m_1m'_1} (\beta_\mathrm{p}) \sin\beta_\mathrm{p} \, \mathrm{d}\beta_\mathrm{p} \, ,$$

where $\Delta_{mm'}$ is given by (B.36). Taking into account the identities: $\Delta_{m'm} = \Delta_{mm'}$ and $(\Delta_{mm'})^2 = 1$, and using the orthogonality property of the d-functions (cf. (B.43)), we obtain [168,169]

$$\left\langle \widetilde{T}^{ij}_{mn,m_1n_1} \right\rangle = \delta_{mm_1} \delta_{nn_1} t^{ij}_n \tag{1.118}$$

with

$$t^{ij}_n = \frac{1}{2n+1} \sum_{m'=-n}^{n} T^{ij}_{m'n,m'n} \, . \tag{1.119}$$

The above relation provides a simple analytical expression for the orientation-averaged transition matrix in terms of the transition matrix in the particle coordinate system. The orientation-averaged $\langle \boldsymbol{T}^{ij} \rangle$ matrices are diagonal and their elements do not depend on the azimuthal indices m and m_1.

Orientation-Averaged Extinction and Scattering Cross-Sections

In view of the optical theorem, the orientation-averaged extinction cross-section is (cf. (1.88) with $|\boldsymbol{E}_{\mathrm{e}0}| = 1$)

$$\langle C_\mathrm{ext} \rangle = \frac{4\pi}{k_\mathrm{s}} \mathrm{Im} \left\{ \left\langle \boldsymbol{e}^*_\mathrm{pol} \cdot \boldsymbol{E}_{\mathrm{s}\infty} (\boldsymbol{e}_z) \right\rangle \right\} \, .$$

Considering the expansion of the far-field pattern in the global coordinate system (cf. (1.96)), taking the average and using the expression of the orientation-averaged transition matrix (cf. (1.118) and (1.119)), gives

$$\left\langle \boldsymbol{e}^*_{\rm pol} \cdot \boldsymbol{E}_{\rm s\infty}\left(\boldsymbol{e}_z\right)\right\rangle = \frac{1}{k_{\rm s}} \sum_{n,m} \left(-{\rm j}\right)^{n+1} \left[\left(t_n^{11} \widetilde{a}_{mn} + t_n^{12} \widetilde{b}_{mn} \right) \boldsymbol{e}^*_{\rm pol} \cdot \boldsymbol{m}_{mn}\left(\boldsymbol{e}_z\right) \right.$$
$$\left. + {\rm j} \left(t_n^{21} \widetilde{a}_{mn} + t_n^{22} \widetilde{b}_{mn} \right) \boldsymbol{e}^*_{\rm pol} \cdot \boldsymbol{n}_{mn}\left(\boldsymbol{e}_z\right) \right] ,$$

where the summation over the index m involves the values -1 and 1. In the next chapter we will show that for axisymmetric particles, $T^{ij}_{-mn,-mn} = -T^{ij}_{mn,mn}$ and $T^{ij}_{0n,0n} = 0$ for $i \neq j$, while for particles with a plane of symmetry, $T^{ij}_{mn,mn} = 0$ for $i \neq j$. Thus, for macroscopically isotropic and mirror-symmetric media, (1.119) gives $t_n^{12} = t_n^{21} = 0$. Further, using the expressions of the incident field coefficients (cf. (1.26))

$$\begin{aligned} \widetilde{a}_{mn} &= 4 j^n \boldsymbol{e}_{\rm pol} \cdot \boldsymbol{m}^*_{mn}\left(\boldsymbol{e}_z\right) , \\ \widetilde{b}_{mn} &= -4 j^{n+1} \boldsymbol{e}_{\rm pol} \cdot \boldsymbol{n}^*_{mn}\left(\boldsymbol{e}_z\right) , \end{aligned} \tag{1.120}$$

and the special values of the vector spherical harmonics in the forward direction

$$\begin{aligned} \boldsymbol{m}_{mn}\left(\boldsymbol{e}_z\right) &= \tfrac{\sqrt{2n+1}}{4} \left({\rm j} m \boldsymbol{e}_x - \boldsymbol{e}_y \right) , \\ \boldsymbol{n}_{mn}\left(\boldsymbol{e}_z\right) &= \tfrac{\sqrt{2n+1}}{4} \left(\boldsymbol{e}_x + {\rm j} m \boldsymbol{e}_y \right) , \end{aligned} \tag{1.121}$$

we obtain [163]

$$\begin{aligned} \left\langle C_{\rm ext} \right\rangle &= -\frac{2\pi}{k_{\rm s}^2} {\rm Re} \left\{ \sum_{n=1}^{\infty} (2n+1) \left(t_n^{11} + t_n^{22} \right) \right\} , \\ &= -\frac{2\pi}{k_{\rm s}^2} {\rm Re} \left\{ \sum_{n=1}^{\infty} \sum_{m=-n}^{n} T^{11}_{mn,mn} + T^{22}_{mn,mn} \right\} . \end{aligned} \tag{1.122}$$

The above relation shows that the orientation-averaged extinction cross-section for macroscopically isotropic and mirror-symmetric media is determined by the diagonal elements of the transition matrix in the particle coordinate system. The same result can be established if we consider an ensemble of randomly oriented particles (with $t_n^{12} \neq 0$ and $t_n^{21} \neq 0$) illuminated by a linearly polarized plane wave (with real polarization vector $\boldsymbol{e}_{\rm pol}$).

For an arbitrary excitation, the scattering cross-section can be expressed in the global coordinate system as

$$C_{\rm scat} = \frac{\pi}{k_{\rm s}^2} \sum_{n=1}^{\infty} \sum_{m=-n}^{n} \left| \widetilde{f}_{mn} \right|^2 + \left| \widetilde{g}_{mn} \right|^2 = \frac{\pi}{k_s^2} \widetilde{\boldsymbol{s}}^{\dagger} \widetilde{\boldsymbol{s}} ,$$

whence, using the $\boldsymbol{T}$-matrix equation $\widetilde{\boldsymbol{s}} = \widetilde{\boldsymbol{T}}\widetilde{\boldsymbol{e}}$, we obtain

$$\langle C_{\rm scat}\rangle = \frac{\pi}{k_{\rm s}^2}\widetilde{\boldsymbol{e}}^{\dagger}\left\langle \widetilde{\boldsymbol{T}}^{\dagger}\left(\alpha_{\rm p},\beta_{\rm p},\gamma_{\rm p}\right)\widetilde{\boldsymbol{T}}\left(\alpha_{\rm p},\beta_{\rm p},\gamma_{\rm p}\right)\right\rangle\widetilde{\boldsymbol{e}}\,.$$

Since

$$\widetilde{\boldsymbol{T}}\left(\alpha_{\rm p},\beta_{\rm p},\gamma_{\rm p}\right) = \mathcal{R}^{\rm T}\left(-\gamma_{\rm p},-\beta_{\rm p},-\alpha_{\rm p}\right)\boldsymbol{T}\mathcal{R}^{\rm T}\left(\alpha_{\rm p},\beta_{\rm p},\gamma_{\rm p}\right)\,,$$
$$\widetilde{\boldsymbol{T}}^{\dagger}\left(\alpha_{\rm p},\beta_{\rm p},\gamma_{\rm p}\right) = \mathcal{R}^{*}\left(\alpha_{\rm p},\beta_{\rm p},\gamma_{\rm p}\right)\boldsymbol{T}^{\dagger}\mathcal{R}^{*}\left(-\gamma_{\rm p},-\beta_{\rm p},-\alpha_{\rm p}\right)\,,$$

and in view of (B.54) and (B.55),

$$\mathcal{R}^{*}\left(-\gamma_{\rm p},-\beta_{\rm p},-\alpha_{\rm p}\right) = \left(\mathcal{R}^{\rm T}\left(-\gamma_{\rm p},-\beta_{\rm p},-\alpha_{\rm p}\right)\right)^{-1}\,,$$
$$\mathcal{R}^{*}\left(\alpha_{\rm p},\beta_{\rm p},\gamma_{\rm p}\right) = \mathcal{R}^{\rm T}\left(-\gamma_{\rm p},-\beta_{\rm p},-\alpha_{\rm p}\right)\,,$$

we see that

$$\widetilde{\boldsymbol{T}}^{\dagger}\left(\alpha_{\rm p},\beta_{\rm p},\gamma_{\rm p}\right)\widetilde{\boldsymbol{T}}\left(\alpha_{\rm p},\beta_{\rm p},\gamma_{\rm p}\right) = \mathcal{R}^{\rm T}\left(-\gamma_{\rm p},-\beta_{\rm p},-\alpha_{\rm p}\right)\boldsymbol{T}^{\dagger}\boldsymbol{T}\mathcal{R}^{\rm T}\left(\alpha_{\rm p},\beta_{\rm p},\gamma_{\rm p}\right)\,.$$

The above equation is similar to (1.115), and taking the average, we obtain

$$\left\langle\left(\boldsymbol{T}^{\dagger}\boldsymbol{T}\right)^{ij}_{mn,m_1n_1}\right\rangle = \delta_{mm_1}\delta_{nn_1}\widetilde{t}^{ij}_{n}\,,$$

where

$$\widetilde{t}^{ij}_{n} = \frac{1}{2n+1}\sum_{m'=-n}^{n}\left(\boldsymbol{T}^{\dagger}\boldsymbol{T}\right)^{ij}_{m'n,m'n}$$

or explicitly,

$$\widetilde{t}^{11}_{n} = \frac{1}{2n+1}\sum_{m'=-n}^{n}\sum_{n_1=1}^{\infty}\sum_{m_1=-n_1}^{n_1}\left|T^{11}_{m_1n_1,m'n}\right|^2+\left|T^{21}_{m_1n_1,m'n}\right|^2\,,$$

$$\widetilde{t}^{12}_{n} = \frac{1}{2n+1}\sum_{m'=-n}^{n}\sum_{n_1=1}^{\infty}\sum_{m_1=-n_1}^{n_1}T^{11*}_{m_1n_1,m'n}T^{12}_{m_1n_1,m'n}$$
$$+T^{21*}_{m_1n_1,m'n}T^{22}_{m_1n_1,m'n}\,,$$

$$\widetilde{t}^{21}_{n} = \widetilde{t}^{12*}_{n}\,,$$

$$\widetilde{t}^{22}_{n} = \frac{1}{2n+1}\sum_{m'=-n}^{n}\sum_{n_1=1}^{\infty}\sum_{m_1=-n_1}^{n_1}\left|T^{12}_{m_1n_1,m'n}\right|^2+\left|T^{22}_{m_1n_1,m'n}\right|^2\,.$$

The orientation-averaged scattering cross-section then becomes

$$\langle C_{\rm scat}\rangle = \frac{\pi}{k_{\rm s}^2}\sum_{n,m}\widetilde{t}_n^{11}\left|\widetilde{a}_{mn}\right|^2 + \widetilde{t}_n^{12}\widetilde{a}_{mn}^{*}\widetilde{b}_{mn} + \widetilde{t}_n^{21}\widetilde{a}_{mn}\widetilde{b}_{mn}^{*} + \widetilde{t}_n^{22}\left|\widetilde{b}_{mn}\right|^2 , \tag{1.123}$$

where as before, the summation over the index m involves the values -1 and 1. For macroscopically isotropic and mirror-symmetric media, $\widetilde{t}_n^{12} = \widetilde{t}_n^{21} = 0$, and using (1.120) and (1.121), we obtain [120, 162]

$$\begin{aligned}\langle C_{\rm scat}\rangle &= \frac{2\pi}{k_{\rm s}^2}\sum_{n=1}^{\infty}(2n+1)\left(\widetilde{t}_n^{11}+\widetilde{t}_n^{22}\right)\\ &= \frac{2\pi}{k_{\rm s}^2}\sum_{n=1}^{\infty}\sum_{m=-n}^{n}\sum_{n_1=1}^{\infty}\sum_{m_1=-n_1}^{n_1}\left|T_{m_1n_1,mn}^{11}\right|^2+\left|T_{m_1n_1,mn}^{12}\right|^2\\ &\quad+\left|T_{m_1n_1,mn}^{21}\right|^2+\left|T_{m_1n_1,mn}^{22}\right|^2 .\end{aligned} \tag{1.124}$$

Thus, the orientation-averaged scattering cross-section for macroscopically isotropic and mirror-symmetric media is proportional to the sum of the squares of the absolute values of the transition matrix in the particle coordinate system. The same result holds true for an ensemble of randomly oriented particles illuminated by a linearly polarized plane wave.

Despite the derivation of simple analytical formulas, the above analysis shows that the orientation-averaged extinction and scattering cross-sections for macroscopically isotropic and mirror-symmetric media do not depend on the polarization state of the incident wave. The orientation-averaged extinction and scattering cross-sections are invariant with respect to rotations and translations of the coordinate system and using these properties, Mishchenko et al. [169] have derived several invariants of the transition matrix.

Orientation-Averaged Extinction Matrix

To compute the orientation-averaged extinction matrix it is necessary to evaluate the orientation-averaged quantities $\langle S_{pq}(\boldsymbol{e}_z,\boldsymbol{e}_z)\rangle$. Taking into account the expressions of the elements of the amplitude matrix (cf. (1.97)), the equation of the orientation-averaged transition matrix (cf. (1.118) and (1.119)) and the expressions of the vector spherical harmonics in the forward direction (cf. (1.121)), we obtain

$$\langle S_{\theta\beta}\left(\boldsymbol{e}_z,\boldsymbol{e}_z\right)\rangle = \langle S_{\varphi\alpha}\left(\boldsymbol{e}_z,\boldsymbol{e}_z\right)\rangle = -\frac{\mathrm{j}}{2k_{\rm s}}\sum_{n=1}^{\infty}(2n+1)\left(t_n^{11}+t_n^{22}\right) ,$$

$$\langle S_{\theta\alpha}\left(\boldsymbol{e}_z,\boldsymbol{e}_z\right)\rangle = -\langle S_{\varphi\beta}\left(\boldsymbol{e}_z,\boldsymbol{e}_z\right)\rangle = -\frac{1}{2k_{\rm s}}\sum_{n=1}^{\infty}(2n+1)\left(t_n^{12}+t_n^{21}\right) .$$

Inserting these expansions into the equations specifying the elements of the extinction matrix (cf. (1.79)), we see that the nonzero matrix elements are

$$\langle K_{ii}\rangle = -\frac{2\pi}{k_{\rm s}^2}{\rm Re}\left\{\sum_{n=1}^{\infty}(2n+1)\left(t_n^{11}+t_n^{22}\right)\right\}, \quad i=1,2,3,4 \tag{1.125}$$

and

$$\begin{aligned}\langle K_{14}\rangle = \langle K_{41}\rangle &= \tfrac{2\pi}{k_{\rm s}^2}{\rm Re}\left\{\sum_{n=1}^{\infty}(2n+1)\left(t_n^{12}+t_n^{21}\right)\right\},\\ \langle K_{23}\rangle = -\langle K_{32}\rangle &= \tfrac{2\pi}{k_{\rm s}^2}{\rm Im}\left\{\sum_{n=1}^{\infty}(2n+1)\left(t_n^{12}+t_n^{21}\right)\right\}.\end{aligned} \tag{1.126}$$

In terms of the elements of the extinction matrix, the orientation-averaged extinction cross-section is (cf. (1.89))

$$\langle C_{\rm ext}\rangle = \frac{1}{I_{\rm e}}\left[\langle K_{11}\rangle I_{\rm e} + \langle K_{14}\rangle V_{\rm e}\right],$$

while for macroscopically isotropic and mirror-symmetric media, the identities $t_n^{12}=t_n^{21}=0$, imply

$$\langle K_{14}\rangle = \langle K_{41}\rangle = \langle K_{23}\rangle = \langle K_{32}\rangle = 0\,.$$

In this specific case, the orientation-averaged extinction matrix becomes diagonal with diagonal elements being equal to the orientation-averaged extinction cross-section per particle, $\langle \boldsymbol{K}\rangle = \langle C_{\rm ext}\rangle \boldsymbol{I}$.

Orientation-Averaged Scattering Matrix

By definition, the orientation-averaged scattering matrix is the orientation-averaged phase matrix with $\beta=0$ and $\alpha=\varphi=0$. In the present analysis we consider the calculation of the general orientation-averaged phase matrix $\langle \boldsymbol{Z}(\boldsymbol{e}_r,\boldsymbol{e}_k;\alpha_{\rm p},\beta_{\rm p},\gamma_{\rm p})\rangle$ without taking into account the specific choice of the incident and scattering directions. We give guidelines for computing the quantities of interest, but we do not derive a final formula for the average phase matrix.

According to the definition of the phase matrix we see that the orientation-averaged quantities $\langle S_{pq}(\boldsymbol{e}_r,\boldsymbol{e}_k)S^*_{p_1q_1}(\boldsymbol{e}_r,\boldsymbol{e}_k)\rangle$, with $p,p_1=\theta,\varphi$ and $q,q_1=\beta,\alpha$, need to be computed. In view of (1.99), we have

$$\begin{aligned}&\left\langle S_{pq}\left(\boldsymbol{e}_r,\boldsymbol{e}_k\right)S^*_{p_1q_1}\left(\boldsymbol{e}_r,\boldsymbol{e}_k\right)\right\rangle\\ &= \frac{16}{k_{\rm s}^2}\left\langle\left(\boldsymbol{v}^{\dagger}_{q_1}\left(\boldsymbol{e}_k\right)\widetilde{\boldsymbol{T}}^{\rm T}\left(\alpha_{\rm p},\beta_{\rm p},\gamma_{\rm p}\right)\boldsymbol{v}_{p_1}\left(\boldsymbol{e}_r\right)\right)^*\boldsymbol{v}^{\rm T}_{p}\left(\boldsymbol{e}_r\right)\widetilde{\boldsymbol{T}}\left(\alpha_{\rm p},\beta_{\rm p},\gamma_{\rm p}\right)\boldsymbol{v}^*_{q}\left(\boldsymbol{e}_k\right)\right\rangle\\ &= \frac{16}{k_{\rm s}^2}\boldsymbol{v}^{\rm T}_{q_1}\left(\boldsymbol{e}_k\right)\left\langle\widetilde{\boldsymbol{T}}^{\dagger}\left(\alpha_{\rm p},\beta_{\rm p},\gamma_{\rm p}\right)\boldsymbol{v}^*_{p_1}\left(\boldsymbol{e}_r\right)\boldsymbol{v}^{\rm T}_{p}\left(\boldsymbol{e}_r\right)\widetilde{\boldsymbol{T}}\left(\alpha_{\rm p},\beta_{\rm p},\gamma_{\rm p}\right)\right\rangle\boldsymbol{v}^*_{q}\left(\boldsymbol{e}_k\right),\end{aligned}$$

where, as before, $\widetilde{\boldsymbol{T}}$ stands for the transition matrix in the global coordinate system. Defining the matrices

$$\boldsymbol{V}_{pp_1}(\boldsymbol{e}_r) = \boldsymbol{v}_{p_1}^*(\boldsymbol{e}_r)\,\boldsymbol{v}_p^{\mathrm{T}}(\boldsymbol{e}_r)$$

and

$$\boldsymbol{A}_{pp_1}(\boldsymbol{e}_r) = \left\langle \widetilde{\boldsymbol{T}}^{\dagger}(\alpha_{\mathrm{p}},\beta_{\mathrm{p}},\gamma_{\mathrm{p}})\,\boldsymbol{V}_{pp_1}(\boldsymbol{e}_r)\widetilde{\boldsymbol{T}}(\alpha_{\mathrm{p}},\beta_{\mathrm{p}},\gamma_{\mathrm{p}})\right\rangle ,$$

we see that

$$\left\langle S_{pq}(\boldsymbol{e}_r,\boldsymbol{e}_k)\,S_{p_1q_1}^*(\boldsymbol{e}_r,\boldsymbol{e}_k)\right\rangle = \frac{16}{k_s^2}\boldsymbol{v}_{q_1}^{\mathrm{T}}(\boldsymbol{e}_k)\,\boldsymbol{A}_{pp_1}(\boldsymbol{e}_r)\,\boldsymbol{v}_q^*(\boldsymbol{e}_k)\ . \tag{1.127}$$

Using the block-matrix decomposition

$$\boldsymbol{X} = \begin{bmatrix} \boldsymbol{X}^{11} & \boldsymbol{X}^{12} \\ \boldsymbol{X}^{21} & \boldsymbol{X}^{22} \end{bmatrix} ,$$

where $\boldsymbol{X}$ stands for $\boldsymbol{V}_{pp_1}$ and $\boldsymbol{A}_{pp_1}$, we express the submatrices of $\boldsymbol{A}_{pp_1}$ as

$$\begin{aligned}
\boldsymbol{A}_{pp_1}^{11} &= \left\langle \widetilde{\boldsymbol{T}}^{11\dagger}\boldsymbol{V}_{pp_1}^{11}\widetilde{\boldsymbol{T}}^{11} + \widetilde{\boldsymbol{T}}^{11\dagger}\boldsymbol{V}_{pp_1}^{12}\widetilde{\boldsymbol{T}}^{21} + \widetilde{\boldsymbol{T}}^{21\dagger}\boldsymbol{V}_{pp_1}^{21}\widetilde{\boldsymbol{T}}^{11} + \widetilde{\boldsymbol{T}}^{21\dagger}\boldsymbol{V}_{pp_1}^{22}\widetilde{\boldsymbol{T}}^{21}\right\rangle ,\\
\boldsymbol{A}_{pp_1}^{12} &= \left\langle \widetilde{\boldsymbol{T}}^{11\dagger}\boldsymbol{V}_{pp_1}^{11}\widetilde{\boldsymbol{T}}^{12} + \widetilde{\boldsymbol{T}}^{11\dagger}\boldsymbol{V}_{pp_1}^{12}\widetilde{\boldsymbol{T}}^{22} + \widetilde{\boldsymbol{T}}^{21\dagger}\boldsymbol{V}_{pp_1}^{21}\widetilde{\boldsymbol{T}}^{12} + \widetilde{\boldsymbol{T}}^{21\dagger}\boldsymbol{V}_{pp_1}^{22}\widetilde{\boldsymbol{T}}^{22}\right\rangle ,\\
\boldsymbol{A}_{pp_1}^{21} &= \left\langle \widetilde{\boldsymbol{T}}^{12\dagger}\boldsymbol{V}_{pp_1}^{11}\widetilde{\boldsymbol{T}}^{11} + \widetilde{\boldsymbol{T}}^{12\dagger}\boldsymbol{V}_{pp_1}^{12}\widetilde{\boldsymbol{T}}^{21} + \widetilde{\boldsymbol{T}}^{22\dagger}\boldsymbol{V}_{pp_1}^{21}\widetilde{\boldsymbol{T}}^{11} + \widetilde{\boldsymbol{T}}^{22\dagger}\boldsymbol{V}_{pp_1}^{22}\widetilde{\boldsymbol{T}}^{21}\right\rangle ,\\
\boldsymbol{A}_{pp_1}^{22} &= \left\langle \widetilde{\boldsymbol{T}}^{12\dagger}\boldsymbol{V}_{pp_1}^{11}\widetilde{\boldsymbol{T}}^{12} + \widetilde{\boldsymbol{T}}^{12\dagger}\boldsymbol{V}_{pp_1}^{12}\widetilde{\boldsymbol{T}}^{22} + \widetilde{\boldsymbol{T}}^{22\dagger}\boldsymbol{V}_{pp_1}^{21}\widetilde{\boldsymbol{T}}^{12} + \widetilde{\boldsymbol{T}}^{22\dagger}\boldsymbol{V}_{pp_1}^{22}\widetilde{\boldsymbol{T}}^{22}\right\rangle .
\end{aligned} \tag{1.128}$$

It is apparent that each matrix product in the above equations is of the form

$$\boldsymbol{W}_{pp_1}(\boldsymbol{e}_r) = \left\langle \widetilde{\boldsymbol{T}}^{kl\dagger}(\alpha_{\mathrm{p}},\beta_{\mathrm{p}},\gamma_{\mathrm{p}})\,\boldsymbol{V}_{pp_1}^{uv}(\boldsymbol{e}_r)\,\widetilde{\boldsymbol{T}}^{ij}(\alpha_{\mathrm{p}},\beta_{\mathrm{p}},\gamma_{\mathrm{p}})\right\rangle , \tag{1.129}$$

where the permissive values of the index pairs (i,j), (k,l) and (u,v) follow from (1.128). The elements of the $\boldsymbol{W}_{pp_1}$ matrix are given by

$$\begin{aligned}
(W_{pp_1})_{\widetilde{m}_1\widetilde{n}_1,m_1n_1}(\boldsymbol{e}_r) = \sum_{\widetilde{n},\widetilde{m}}\sum_{n,m}&\left\langle \widetilde{T}_{mn,m_1n_1}^{ij}(\alpha_{\mathrm{p}},\beta_{\mathrm{p}},\gamma_{\mathrm{p}})\,\widetilde{T}_{\widetilde{m}\widetilde{n},\widetilde{m}_1\widetilde{n}_1}^{kl*}(\alpha_{\mathrm{p}},\beta_{\mathrm{p}},\gamma_{\mathrm{p}})\right\rangle\\
&\times\left(V_{pp_1}^{uv}\right)_{\widetilde{m}\widetilde{n},mn}(\boldsymbol{e}_r) ,
\end{aligned} \tag{1.130}$$

and the rest of our analysis concerns with the computation of the term

$$\mathcal{T} = \left\langle \widetilde{T}_{mn,m_1n_1}^{ij}(\alpha_{\mathrm{p}},\beta_{\mathrm{p}},\gamma_{\mathrm{p}})\,\widetilde{T}_{\widetilde{m}\widetilde{n},\widetilde{m}_1\widetilde{n}_1}^{kl*}(\alpha_{\mathrm{p}},\beta_{\mathrm{p}},\gamma_{\mathrm{p}})\right\rangle . \tag{1.131}$$

It should be mentioned that for notation simplification we omit to indicate the dependency of $\mathcal{T}$ on the matrix indices.

Using the rotation transformation rule for the transition matrix (cf. (1.116)), we obtain

$$\mathcal{T} = \frac{1}{8\pi^2} \sum_{m'=-n}^{n} \sum_{m'_1=-n_1}^{n_1} \sum_{\widetilde{m}'=-\widetilde{n}}^{\widetilde{n}} \sum_{\widetilde{m}'_1=-\widetilde{n}_1}^{\widetilde{n}_1} \Big[\int_0^{2\pi} \int_0^{2\pi} \int_0^{\pi} D^{n}_{m'm}(-\gamma_\mathrm{p}, -\beta_\mathrm{p}, -\alpha_\mathrm{p})$$

$$\times D^{n_1}_{m_1 m'_1}(\alpha_\mathrm{p}, \beta_\mathrm{p}, \gamma_\mathrm{p})\, D^{\widetilde{n}*}_{\widetilde{m}'\widetilde{m}}(-\gamma_\mathrm{p}, -\beta_\mathrm{p}, -\alpha_\mathrm{p})$$

$$\times\, D^{\widetilde{n}_1 *}_{\widetilde{m}_1 \widetilde{m}'_1}(\alpha_\mathrm{p}, \beta_\mathrm{p}, \gamma_\mathrm{p}) \sin\beta_\mathrm{p}\, \mathrm{d}\beta_\mathrm{p}\, \mathrm{d}\alpha_\mathrm{p}\, \mathrm{d}\gamma_\mathrm{p} \Big] T^{ij}_{m'n,m'_1 n_1} T^{kl*}_{\widetilde{m}'\widetilde{n},\widetilde{m}'_1\widetilde{n}_1} \,.$$

Taking into account the definition of the Wigner D-functions (cf. (B.34)) and integrating over α_p and γ_p, yields

$$\mathcal{T} = \frac{1}{2} \sum_{m'=-n}^{n} \sum_{m'_1=-n_1}^{n_1} \sum_{\widetilde{m}'=-\widetilde{n}}^{\widetilde{n}} \sum_{\widetilde{m}'_1=-\widetilde{n}_1}^{\widetilde{n}_1} \delta_{m_1-m,\widetilde{m}_1-\widetilde{m}} \delta_{m'_1-m',\widetilde{m}'_1-\widetilde{m}'} \Delta$$

$$\times \left[\int_0^{\pi} d^{n}_{m'm}(-\beta_\mathrm{p})\, d^{\widetilde{n}}_{\widetilde{m}'\widetilde{m}}(-\beta_\mathrm{p})\, d^{n_1}_{m_1 m'_1}(\beta_\mathrm{p})\, d^{\widetilde{n}_1}_{\widetilde{m}_1 \widetilde{m}'_1}(\beta_\mathrm{p}) \sin\beta_\mathrm{p}\, \mathrm{d}\beta_\mathrm{p} \right]$$

$$\times T^{ij}_{m'n,m'_1 n_1} T^{kl*}_{\widetilde{m}'\widetilde{n},\widetilde{m}'_1\widetilde{n}_1} \,,$$

where $d^{n}_{mm'}$ are the Wigner d-functions defined in Appendix B,

$$\Delta = \Delta_{m'm} \Delta_{\widetilde{m}'\widetilde{m}} \Delta_{m_1 m'_1} \Delta_{\widetilde{m}_1 \widetilde{m}'_1} \,,$$

and $\Delta_{mm'}$ is given by (B.36). To compute the integral

$$\mathcal{I} = \frac{1}{2} \delta_{m_1-m,\widetilde{m}_1-\widetilde{m}} \delta_{m'_1-m',\widetilde{m}'_1-\widetilde{m}'}$$

$$\times \int_0^{\pi} d^{n}_{m'm}(-\beta_\mathrm{p})\, d^{\widetilde{n}}_{\widetilde{m}'\widetilde{m}}(-\beta_\mathrm{p})\, d^{n_1}_{m_1 m'_1}(\beta_\mathrm{p})\, d^{\widetilde{n}_1}_{\widetilde{m}_1 \widetilde{m}'_1}(\beta_\mathrm{p}) \sin\beta_\mathrm{p}\, \mathrm{d}\beta_\mathrm{p} \,,$$

we use the symmetry relations (cf. (B.39) and (B.41))

$$d^{n}_{m'm}(-\beta_\mathrm{p}) = d^{n}_{mm'}(\beta_\mathrm{p}) = (-1)^{m+m'} d^{n}_{-m-m'}(\beta_\mathrm{p}) \,,$$

$$d^{\widetilde{n}}_{\widetilde{m}'\widetilde{m}}(-\beta_\mathrm{p}) = d^{\widetilde{n}}_{\widetilde{m}\widetilde{m}'}(\beta_\mathrm{p}) = (-1)^{\widetilde{m}+\widetilde{m}'} d^{\widetilde{n}}_{-\widetilde{m}-\widetilde{m}'}(\beta_\mathrm{p}) \,,$$

the expansions of the d-functions products $d^{n_1}_{m_1 m'_1} d^{n}_{-m-m'}$ and $d^{\widetilde{n}_1}_{\widetilde{m}_1 \widetilde{m}'_1} d^{\widetilde{n}}_{-\widetilde{m}-\widetilde{m}'}$ given by (B.47), and the orthogonality property of the d-functions (cf. (B.43)).

We obtain

$$\mathcal{I} = (-1)^{m+m'+\widetilde{m}+\widetilde{m}'}(-1)^{n+n_1+\widetilde{n}+\widetilde{n}_1}\delta_{m_1-m,\widetilde{m}_1-\widetilde{m}}\delta_{m_1'-m',\widetilde{m}_1'-\widetilde{m}'}$$
$$\times \sum_{u=u_{\min}}^{u_{\max}} \frac{1}{2u+1} C^{m_1-mu}_{m_1n_1,-mn} C^{m'-m_1'u}_{-m_1'n_1,m'n} C^{\widetilde{m}_1-\widetilde{m}u}_{\widetilde{m}_1\widetilde{n}_1,-\widetilde{m}\widetilde{n}} C^{\widetilde{m}'-\widetilde{m}_1'u}_{-\widetilde{m}_1'\widetilde{n}_1,\widetilde{m}'\widetilde{n}},$$

where $C^{m+m_1u}_{mn,m_1n_1}$ are the Clebsch–Gordan coefficients defined in Appendix B, and

$$u_{\min} = \max\left(|n-n_1|, |\widetilde{n}-\widetilde{n}_1|, |m_1-m|, |\widetilde{m}_1-\widetilde{m}|, |m'-m_1'|, |\widetilde{m}'-\widetilde{m}_1'|\right),$$
$$u_{\max} = \min\left(n+n_1, \widetilde{n}+\widetilde{n}_1\right).$$

Further, using the symmetry properties of the Clebsch–Gordan coefficients (cf. (B.48) and (B.51)) we arrive at

$$\mathcal{I} = (-1)^{n+n_1+\widetilde{n}+\widetilde{n}_1}\delta_{m_1-m,\widetilde{m}_1-\widetilde{m}}\delta_{m_1'-m',\widetilde{m}_1'-\widetilde{m}'}$$
$$\times \sum_{u=u_{\min}}^{u_{\max}} \frac{2u+1}{(2n_1+1)(2\widetilde{n}_1+1)} C^{m_1n_1}_{m_1-mu,mn} C^{-m_1'n_1}_{m'-m_1'u,-m'n}$$
$$\times C^{\widetilde{m}_1\widetilde{n}_1}_{\widetilde{m}_1-\widetilde{m}u,\widetilde{m}\widetilde{n}} C^{-\widetilde{m}_1'\widetilde{n}_1}_{\widetilde{m}'-\widetilde{m}_1'u,-\widetilde{m}'\widetilde{n}}$$

and

$$\mathcal{T} = \sum_{m'=-n}^{n} \sum_{m_1'=-n_1}^{n_1} \sum_{\widetilde{m}'=-\widetilde{n}}^{\widetilde{n}} \sum_{\widetilde{m}_1'=-\widetilde{n}_1}^{\widetilde{n}_1} \Delta\mathcal{I} T^{ij}_{m'n,m_1'n_1} T^{kl*}_{\widetilde{m}'\widetilde{n},\widetilde{m}_1'\widetilde{n}_1}. \quad (1.132)$$

The orientation-averaged quantities $\langle S_{pq}(\boldsymbol{e}_r, \boldsymbol{e}_k) S^*_{p_1q_1}(\boldsymbol{e}_r, \boldsymbol{e}_k)\rangle$ can be computed from the set of equations (1.127)–(1.132).

For an incident wave propagating along the Z-axis, the augmented vector of spherical harmonics $\boldsymbol{v}_q(\boldsymbol{e}_z)$ can be computed by using (1.121). Choosing the XZ-plane as the scattering plane, i.e., setting $\varphi = 0$, we see that the matrices $\boldsymbol{V}_{pp_1}(\boldsymbol{e}_r)$ involve only the normalized angular functions $\pi_n^{|m|}(\theta)$ and $\tau_n^{|m|}(\theta)$. The resulting orientation-averaged scattering matrix can be computed at a set of polar angles θ and polynomial interpolation can be used to evaluate the orientation-averaged scattering matrix at any polar angle θ.

For macroscopically isotropic media, the orientation-averaged scattering matrix has sixteen nonzero elements (cf. (1.113)) but only ten of them are independent. For macroscopically isotropic and mirror-symmetric media, the orientation-averaged scattering matrix has a block-diagonal structure (cf. (1.114)), so that only eight elements are nonzero and only six of them are independent. In this case we determine the six quantities $\langle |S_{\theta\beta}(\theta)|^2\rangle$,

$\langle|S_{\theta\alpha}(\theta)|^2\rangle$, $\langle|S_{\varphi\beta}(\theta)|^2\rangle$, $\langle|S_{\varphi\alpha}(\theta)|^2\rangle$, $\langle S_{\theta\beta}(\theta)S^*_{\varphi\alpha}(\theta)\rangle$ and $\langle S_{\theta\alpha}(\theta)S^*_{\varphi\beta}(\theta)\rangle$, and compute the eight nonzero elements by using the relations

$$\langle F_{11}(\theta)\rangle = \frac{1}{2}\left(\left\langle|S_{\theta\beta}(\theta)|^2\right\rangle + \left\langle|S_{\theta\alpha}(\theta)|^2\right\rangle + \left\langle|S_{\varphi\beta}(\theta)|^2\right\rangle + \left\langle|S_{\varphi\alpha}(\theta)|^2\right\rangle\right) ,$$

$$\langle F_{12}(\theta)\rangle = \frac{1}{2}\left(\left\langle|S_{\theta\beta}(\theta)|^2\right\rangle - \left\langle|S_{\theta\alpha}(\theta)|^2\right\rangle + \left\langle|S_{\varphi\beta}(\theta)|^2\right\rangle - \left\langle|S_{\varphi\alpha}(\theta)|^2\right\rangle\right) ,$$

$$\langle F_{21}(\theta)\rangle = \langle F_{12}(\theta)\rangle ,$$

$$\langle F_{22}(\theta)\rangle = \frac{1}{2}\left(\left\langle|S_{\theta\beta}(\theta)|^2\right\rangle - \left\langle|S_{\theta\alpha}(\theta)|^2\right\rangle - \left\langle|S_{\varphi\beta}(\theta)|^2\right\rangle + \left\langle|S_{\varphi\alpha}(\theta)|^2\right\rangle\right) ,$$

$$\langle F_{33}(\theta)\rangle = \mathrm{Re}\left\{\left\langle S_{\theta\beta}(\theta)S^*_{\varphi\alpha}(\theta)\right\rangle + \left\langle S_{\theta\alpha}(\theta)S^*_{\varphi\beta}(\theta)\right\rangle\right\} ,$$

$$\langle F_{34}(\theta)\rangle = \mathrm{Im}\left\{\left\langle S_{\theta\beta}(\theta)S^*_{\varphi\alpha}(\theta)\right\rangle + \left\langle S_{\theta\alpha}(\theta)S^*_{\varphi\beta}(\theta)\right\rangle^*\right\} ,$$

$$\langle F_{43}(\theta)\rangle = -\langle F_{34}(\theta)\rangle ,$$

$$\langle F_{44}(\theta)\rangle = \mathrm{Re}\left\{\left\langle S_{\theta\beta}(\theta)S^*_{\varphi\alpha}(\theta)\right\rangle^* - \left\langle S_{\theta\alpha}(\theta)S^*_{\varphi\beta}(\theta)\right\rangle\right\} .$$

Other scattering characteristics as for instance the orientation-averaged scattering cross-section and the orientation-averaged mean direction of propagation of the scattered field can be expressed in terms of the elements of the orientation-averaged scattering matrix. To derive these expressions we consider the scattering plane characterized by the azimuth angle φ as shown in Fig. 1.15. In the scattering plane, the Stokes vector of the scattered wave is given by $\langle \boldsymbol{I}_\mathrm{s}(r\boldsymbol{e}_r)\rangle = (1/r^2)\langle \boldsymbol{F}(\theta)\rangle \boldsymbol{I}'_\mathrm{e}$, whence, using the transformation rule of the Stokes vector under coordinate rotation $\boldsymbol{I}'_\mathrm{e} = \boldsymbol{L}(\varphi)\boldsymbol{I}_\mathrm{e}$, we obtain

$$\langle \boldsymbol{I}_\mathrm{s}(r\boldsymbol{e}_r)\rangle = \frac{1}{r^2}\langle \boldsymbol{F}(\theta)\rangle \boldsymbol{L}(\varphi)\boldsymbol{I}_\mathrm{e} .$$

Further, taking into account the expression of the Stokes rotation matrix $\boldsymbol{L}$ (cf. (1.23)) we derive

$$\begin{aligned}\langle I_\mathrm{s}(\boldsymbol{e}_r)\rangle = {} & \langle F_{11}(\theta)\rangle I_\mathrm{e} + [\langle F_{12}(\theta)\rangle \cos 2\varphi + \langle F_{13}(\theta)\rangle \sin 2\varphi] Q_\mathrm{e} \\ & - [\langle F_{12}(\theta)\rangle \sin 2\varphi - \langle F_{13}(\theta)\rangle \cos 2\varphi] U_\mathrm{e} + \langle F_{14}(\theta)\rangle V_\mathrm{e} .\end{aligned}$$

Integrating over φ, we find that the orientation-averaged scattering cross-section and the orientation-averaged mean direction of propagation of the scattered field are given by

$$\begin{aligned}\langle C_\mathrm{scat}\rangle &= \frac{1}{I_\mathrm{e}}\int_\Omega \langle I_\mathrm{s}(\boldsymbol{e}_r)\rangle \,\mathrm{d}\Omega(\boldsymbol{e}_r) \\ &= \frac{2\pi}{I_\mathrm{e}}\int_0^\pi [\langle F_{11}(\theta)\rangle I_\mathrm{e} + \langle F_{14}(\theta)\rangle V_\mathrm{e}] \sin\theta \,\mathrm{d}\theta\end{aligned}$$

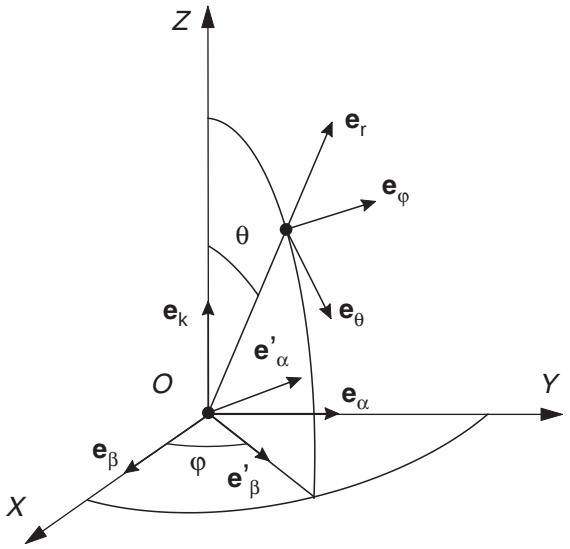

Fig. 1.15. Incident and scattering directions $\boldsymbol{e}_k$ and $\boldsymbol{e}_r$. The incident direction is along the Z-axis and the scattering matrix relates the Stokes vectors of the incident and scattered fields specified relative to the scattering plane characterized by the azimuth angle φ

and

$$\begin{aligned}\langle \boldsymbol{g} \rangle &= \frac{1}{\langle C_{\rm scat} \rangle \, I_{\rm e}} \int_{\Omega} \langle I_{\rm s}(\boldsymbol{e}_r) \rangle \, \boldsymbol{e}_r \, {\rm d}\Omega(\boldsymbol{e}_r) \\ &= \frac{2\pi}{\langle C_{\rm scat} \rangle \, I_{\rm e}} \left\{ \int_0^{\pi} \left[\langle F_{11}(\theta) \rangle \, I_{\rm e} + \langle F_{14}(\theta) \rangle \, V_{\rm e} \right] \sin\theta \cos\theta \, {\rm d}\theta \right\} \boldsymbol{e}_z \, ,\end{aligned}$$

respectively. Because the incident wave propagates along the Z-axis, the nonzero component of $\langle \boldsymbol{g} \rangle$ is the orientation-averaged asymmetry parameter $\langle \cos\Theta \rangle$. In practical computer simulations, we use the decomposition

$$\langle C_{\rm scat} \rangle = \frac{1}{I_{\rm e}} \left(\langle C_{\rm scat} \rangle_{\rm I} \, I_{\rm e} + \langle C_{\rm scat} \rangle_{\rm V} \, V_{\rm e} \right) \, ,$$

and compute the quantities $\langle C_{\rm scat} \rangle_{\rm I}$ and $\langle C_{\rm scat} \rangle_{\rm V}$ by using (1.124) and the relation

$$\langle C_{\rm scat} \rangle_{\rm V} = 2\pi \int_0^{\pi} \langle F_{14}(\theta) \rangle \sin\theta \, {\rm d}\theta \, , \tag{1.133}$$

respectively. These quantities do not depend on the polarization state of the incident wave and can be used to compute the orientation-averaged scattering cross-section for any incident polarization. For the asymmetry parameter we proceed analogously; we use the decomposition

$$\langle \cos\Theta \rangle = \frac{\langle C_{\rm scat} \rangle_{\rm I}}{\langle C_{\rm scat} \rangle} \frac{1}{I_{\rm e}} \left(\langle \cos\Theta \rangle_{\rm I} \, I_{\rm e} + \langle \cos\Theta \rangle_{\rm V} \, V_{\rm e} \right) ,$$

and compute $\langle \cos\Theta \rangle_{\rm I}$ and $\langle \cos\Theta \rangle_{\rm V}$ by using the relations

$$\langle \cos\Theta \rangle_{\rm I} = \frac{2\pi}{\langle C_{\rm scat} \rangle_{\rm I}} \int_0^\pi \langle F_{11}(\theta) \rangle \sin\theta \cos\theta \, {\rm d}\theta \tag{1.134}$$

and

$$\langle \cos\Theta \rangle_{\rm V} = \frac{2\pi}{\langle C_{\rm scat} \rangle_{\rm I}} \int_0^\pi \langle F_{14}(\theta) \rangle \sin\theta \cos\theta \, {\rm d}\theta \, , \tag{1.135}$$

respectively. For macroscopically isotropic and mirror-symmetric media,

$$\langle F_{14}(\theta) \rangle = 0$$

and consequently, $\langle C_{\rm scat} \rangle = \langle C_{\rm scat} \rangle_{\rm I}$ and $\langle \cos\Theta \rangle = \langle \cos\Theta \rangle_{\rm I}$.

Another important scattering characteristic is the angular distribution of the scattered field. For an ensemble of randomly oriented particles illuminated by a vector plane wave of unit amplitude and polarization vector $\boldsymbol{e}_{\rm pol} = e_{{\rm pol},\beta} \boldsymbol{e}_\beta + e_{{\rm pol},\alpha} \boldsymbol{e}_\alpha$, the differential scattering cross-sections in the scattering plane φ are given by

$$\begin{aligned} \langle \sigma_{\rm dp}(\theta) \rangle = {} & \left\langle \left| E_{{\rm s}\infty,\theta}(\theta) \right|^2 \right\rangle = \left\langle \left| S_{\theta\beta}(\theta) \right|^2 \right\rangle \left| E'_{{\rm e}0,\beta} \right|^2 \\ & + \left\langle \left| S_{\theta\alpha}(\theta) \right|^2 \right\rangle \left| E'_{{\rm e}0,\alpha} \right|^2 \\ & + 2{\rm Re} \left\{ \langle S_{\theta\beta}(\theta) S^*_{\theta\alpha}(\theta) \rangle \, E'_{{\rm e}0,\beta} E'^*_{{\rm e}0,\alpha} \right\} \end{aligned} \tag{1.136}$$

and

$$\begin{aligned} \langle \sigma_{\rm ds}(\theta) \rangle = {} & \left\langle \left| E_{{\rm s}\infty,\varphi}(\theta) \right|^2 \right\rangle = \left\langle \left| S_{\varphi\beta}(\theta) \right|^2 \right\rangle \left| E'_{{\rm e}0,\beta} \right|^2 \\ & + \left\langle \left| S_{\varphi\alpha}(\theta) \right|^2 \right\rangle \left| E'_{{\rm e}0,\alpha} \right|^2 \\ & + 2{\rm Re} \left\{ \left\langle S_{\varphi\beta}(\theta) S^*_{\varphi\alpha}(\theta) \right\rangle E'_{{\rm e}0,\beta} E'^*_{{\rm e}0,\alpha} \right\} , \end{aligned} \tag{1.137}$$

where

$$\begin{aligned} E'_{{\rm e}0,\beta} &= e_{{\rm pol},\beta} \cos\varphi + e_{{\rm pol},\alpha} \sin\varphi \, , \\ E'_{{\rm e}0,\alpha} &= -e_{{\rm pol},\beta} \sin\varphi + e_{{\rm pol},\alpha} \cos\varphi \, . \end{aligned}$$

It should be noted that for macroscopically isotropic and mirror-symmetric media,

$$\begin{aligned} \langle S_{\theta\beta}(\theta) S^*_{\theta\alpha}(\theta) \rangle &= 0 \, , \\ \left\langle S_{\varphi\beta}(\theta) S^*_{\varphi\alpha}(\theta) \right\rangle &= 0 \, , \end{aligned}$$

and the expressions of $\langle \sigma_{\rm dp}(\theta) \rangle$ and $\langle \sigma_{\rm ds}(\theta) \rangle$ simplify considerably.

In practice, the inequalities

$$\begin{aligned}
\langle F_{11}\rangle &\geq |\langle F_{ij}\rangle| \,, \quad i,j = 1,2,3,4 \,, \\
\left(\langle F_{11}\rangle + \langle F_{22}\rangle\right)^2 - 4\langle F_{12}\rangle^2 &\geq \left(\langle F_{33}\rangle + \langle F_{44}\rangle\right)^2 + 4\langle F_{34}\rangle^2 \,, \\
\langle F_{11}\rangle - \langle F_{22}\rangle &\geq |\langle F_{33}\rangle - \langle F_{44}\rangle| \,, \\
\langle F_{11}\rangle - \langle F_{12}\rangle &\geq |\langle F_{22}\rangle - \langle F_{12}\rangle| \,, \\
\langle F_{11}\rangle + \langle F_{12}\rangle &\geq |\langle F_{22}\rangle + \langle F_{12}\rangle| \,,
\end{aligned} \tag{1.138}$$

can be used to test the numerically obtained orientation-averaged scattering matrix [104, 169].

It should be emphasized that we do not expand the elements of the orientation-averaged scattering matrix in generalized spherical functions (or Wigner d-functions) and do not exploit the advantage of performing as much work analytically as possible. Therefore, the above averaging procedure is computationally not so fast as the scattering matrix expansion method given by Mishchenko [162]. As noted by Mishchenko et al. [169], the analyticity of the $\boldsymbol{T}$-matrix formulation can be connected with the formalism of expanding scattering matrices in generalized spherical functions to derive an efficient procedure that does not involve any angular variable.

Khlebtsov [120] and Fucile et al. [71] developed a similar formalism that exploit the rotation property of the transition matrix but avoids the expansion of the scattering matrix in generalized spherical functions. Paramonov [182] and Borghese et al. [23] extended the analytical orientation-averaging procedure to arbitrary orientation distribution functions, while the standard averaging approach employing numerical integrations over the orientation angles has been used by Wiscombe and Mugnai [263, 264] and Barber and Hill [8]. A method to compute light scattering by arbitrarily oriented rotationally symmetric particles has been given by Skaropoulos and Russchenberg [212].

2

Null-Field Method

The standard scheme for computing the transition matrix relies on the null-field method. The null-field method has been introduced by Waterman [253] as a technique for computing electromagnetic scattering by perfectly conducting particles. Later, Bates [10] studied the same problem, followed by Waterman's applications of his method to electromagnetic scattering from dielectric particles [254, 256] and to acoustic scattering [255]. The null-field method has subsequently been extended to multiple scattering problems [187, 188] and to electromagnetic scattering by multilayered and composite particles [189, 190]. Peterson and Ström [189] derived a recurrence relation for the transition matrix of a multilayered particle and analyzed particles which contains several enclosures, each with arbitrary but constant electromagnetic properties. The null-field treatment of a composite particle with two constituents uses a particular projection of the boundary conditions on the interface and treats the two constituents as separate particles by exploiting the translation addition theorem for vector spherical wave functions. However, for a large class of composite particles it is not natural to treat the two parts as separate particles. The geometric constraints which appear in the two-particles formalism (originating in the use of translations of radiating vector spherical wave functions) are eliminated, partially or completely by Ström and Zheng [219]. The case of a composite particle consisting of three or more constituents has been analyzed by Zheng [276], while the extension of the method to composite particles with concavo-convex constituents has been discussed by Zheng and Ström [279]. Applications of the null-field method to electromagnetic, acoustic and elastodynamic scattering by single and aggregated particles, to multiple scattering in random media, and to scattering by periodical and infinite surfaces can be found in [168, 169, 228, 234, 235].

Essentially, the null-field method involves the following steps:

1. Derivation of an infinite system of integral equations for the surface fields by using the general null-field equation.

2. Derivation of integral representations for the scattered field coefficients in terms of surface fields by using the Huygens principle.
3. Approximation of the surface fields by a complete and linearly independent system of (tangential) vector functions.
4. Truncation of the infinite system of null-field equations and of the scattered-field expansion.
5. Computation of the truncated transition matrix by matrix inversion.

These steps explicitly avoid invoking the Rayleigh hypothesis [11, 34] and relies on the approximation of the surface fields by a complete system of vector functions (the localized vector spherical wave functions). The completeness and linear independence of various systems of vector functions on closed surfaces, including the vector spherical wave functions, have been established by Doicu et al. [49]. For scattering problems involving inhomogeneous particles it is necessary to establish the completeness and linear independence of this system of vector functions on two enclosing surfaces and this result is given in Appendix D.

Several studies have addressed the convergence of the null-field method. Ramm [200, 201] and Kristensson et al. [126] have derived sufficiency criteria for the convergence of the null-field method, but this criteria are not satisfied for nonspherical surfaces. A major progress has been achieved by Dallas [44], who showed that for ellipsoidal surfaces, the far-field pattern converges in the least-squares sense on the unit sphere.

In this chapter, we present applications of the null-field method to electromagnetic scattering by homogeneous, isotropic, anisotropic and chiral particles, inhomogeneous, layered and composite particles and clusters of particles. Our presentation closely follows the analysis developed by Ström and his coworkers. In order to preserve the generality we assume that the particles and the infinite, exterior medium are magnetic, but in practice we always deal with nonmagnetic media ($\mu_{\rm s} = \mu_{\rm i} = 1$). In the last two sections, we treat multiple scattering in random media and scattering by a particle on or near a plane surface.

2.1 Homogeneous and Isotropic Particles

Most practical implementations of the null-field method pertain to homogenous and isotropic particles. $\boldsymbol{T}$-matrix codes for axisymmetric particles have been developed by Wiscombe and Mugnai [263], Barber and Hill [8] and Mishchenko and Travis [167]. Light scattering calculations for nonaxisymmetric particles have been reported by Barber [7], Schneider and Peden [207], Laitinen and Lumme [127], Wriedt and Comberg [269], Baran et al. [6], Havemann and Baran [98], Kahnert et al. [111, 112], and Wriedt [268]. In this section, we provide a detailed description of the null-field method in application to homogenous and isotropic particles.

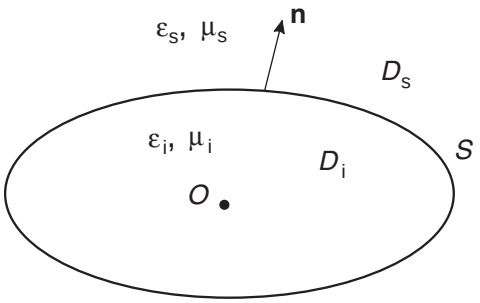

Fig. 2.1. Geometry of a homogeneous particle

2.1.1 General Formulation

The transmission boundary-value problem for homogeneous and isotropic particles has been formulated in Sect. 1.4 but we mention it in order for our analysis to be complete. We consider an homogeneous, isotropic particle occupying a domain D_i with boundary S and exterior D_s (Fig. 2.1). The unit normal vector to S directed into D_s is denoted by $\boldsymbol{n}$. The exterior domain D_s is assumed to be homogeneous, isotropic, and nonabsorbing, and if ε_t and μ_t are the relative permittivity and permeability of the domain D_t, where $\mathrm{t}=\mathrm{s}$, i, we have $\varepsilon_\mathrm{s} > 0$ and $\mu_\mathrm{s} > 0$. The wave number in the domain D_t is $k_\mathrm{t} = k_0\sqrt{\varepsilon_\mathrm{t}\mu_\mathrm{t}}$, where k_0 is the wave number in the free space. The transmission boundary-value problem for a homogeneous and isotropic particle has the following formulation.

Given $\boldsymbol{E}_\mathrm{e}, \boldsymbol{H}_\mathrm{e}$ as an entire solution to the Maxwell equations representing the external excitation, find the vector fields $\boldsymbol{E}_\mathrm{s}, \boldsymbol{H}_\mathrm{s}$ and $\boldsymbol{E}_\mathrm{i}, \boldsymbol{H}_\mathrm{i}$ satisfying the Maxwell equations

$$\nabla \times \boldsymbol{E}_\mathrm{t} = \mathrm{j}k_0\mu_\mathrm{t}\boldsymbol{H}_\mathrm{t}\,, \quad \nabla \times \boldsymbol{H}_\mathrm{t} = -\mathrm{j}k_0\varepsilon_\mathrm{t}\boldsymbol{E}_\mathrm{t}\,, \tag{2.1}$$

in D_t, $\mathrm{t}=\mathrm{s}$, i, the two transmission conditions

$$\begin{aligned} \boldsymbol{n} \times \boldsymbol{E}_\mathrm{i} - \boldsymbol{n} \times \boldsymbol{E}_\mathrm{s} &= \boldsymbol{n} \times \boldsymbol{E}_\mathrm{e}\,, \\ \boldsymbol{n} \times \boldsymbol{H}_\mathrm{i} - \boldsymbol{n} \times \boldsymbol{H}_\mathrm{s} &= \boldsymbol{n} \times \boldsymbol{H}_\mathrm{e}\,, \end{aligned} \tag{2.2}$$

on S, and the Silver–Müller radiation condition

$$\frac{\boldsymbol{r}}{r} \times \sqrt{\mu_\mathrm{s}}\boldsymbol{H}_\mathrm{s} + \sqrt{\epsilon_\mathrm{s}}\boldsymbol{E}_\mathrm{s} = \mathrm{O}\left(\frac{1}{r}\right)\,, \quad \text{as} \quad r \to \infty\,, \tag{2.3}$$

uniformly for all directions $\boldsymbol{r}/r$.

The standard scheme for computing the transition matrix in the framework of the null-field method relies on the solution of the general null-field equation

$$\boldsymbol{E}_{\mathrm{e}}(\boldsymbol{r}) + \nabla \times \int_S \boldsymbol{e}_{\mathrm{i}}(\boldsymbol{r}')\, g(k_{\mathrm{s}}, \boldsymbol{r}, \boldsymbol{r}')\, \mathrm{d}S(\boldsymbol{r}') + \frac{\mathrm{j}}{k_0 \varepsilon_{\mathrm{s}}} \nabla \times \nabla \times \int_S \boldsymbol{h}_{\mathrm{i}}(\boldsymbol{r}')\, g(k_{\mathrm{s}}, \boldsymbol{r}, \boldsymbol{r}')\, \mathrm{d}S(\boldsymbol{r}') = 0\,, \quad \boldsymbol{r} \in D_{\mathrm{i}} \tag{2.4}$$

for the surface fields $\boldsymbol{e}_{\mathrm{i}} = \boldsymbol{n} \times \boldsymbol{E}_{\mathrm{i}}$ and $\boldsymbol{h}_{\mathrm{i}} = \boldsymbol{n} \times \boldsymbol{H}_{\mathrm{i}}$, and the calculation of the scattered field from Huygens principle

$$\boldsymbol{E}_{\mathrm{s}}(\boldsymbol{r}) = \nabla \times \int_S \boldsymbol{e}_{\mathrm{i}}(\boldsymbol{r}')\, g(k_{\mathrm{s}}, \boldsymbol{r}, \boldsymbol{r}')\, \mathrm{d}S(\boldsymbol{r}') + \frac{\mathrm{j}}{k_0 \varepsilon_{\mathrm{s}}} \nabla \times \nabla \times \int_S \boldsymbol{h}_{\mathrm{i}}(\boldsymbol{r}')\, g(k_{\mathrm{s}}, \boldsymbol{r}, \boldsymbol{r}')\, \mathrm{d}S(\boldsymbol{r}')\,, \quad \boldsymbol{r} \in D_{\mathrm{s}}\,. \tag{2.5}$$

Considering the general null-field equation (2.4), we restrict $\boldsymbol{r}$ to lie on a spherical surface enclosed in D_{i}, expand the incident field and the dyad $g\overline{\boldsymbol{I}}$ in terms of regular vector spherical wave functions (cf. (1.25), (B.21) and (B.22)), and use the orthogonality of the vector spherical wave functions on spherical surfaces to obtain

$$\frac{\mathrm{j}k_{\mathrm{s}}^2}{\pi} \int_S \left[\boldsymbol{e}_{\mathrm{i}}(\boldsymbol{r}') \cdot \begin{pmatrix} \boldsymbol{N}_{\overline{\nu}}^3(k_{\mathrm{s}}\boldsymbol{r}') \\ \boldsymbol{M}_{\overline{\nu}}^3(k_{\mathrm{s}}\boldsymbol{r}') \end{pmatrix} + \mathrm{j}\sqrt{\frac{\mu_{\mathrm{s}}}{\varepsilon_{\mathrm{s}}}} \boldsymbol{h}_{\mathrm{i}}(\boldsymbol{r}') \cdot \begin{pmatrix} \boldsymbol{M}_{\overline{\nu}}^3(k_{\mathrm{s}}\boldsymbol{r}') \\ \boldsymbol{N}_{\overline{\nu}}^3(k_{\mathrm{s}}\boldsymbol{r}') \end{pmatrix} \right] \mathrm{d}S(\boldsymbol{r}') = -\begin{pmatrix} a_\nu \\ b_\nu \end{pmatrix}, \quad \nu = 1, 2, \ldots \tag{2.6}$$

For notation simplification we introduced the multi-indices $\nu = (m, n)$ and $\overline{\nu} = (-m, n)$, and used the convention $\nu = 1, 2, \ldots$, when $n = 1, 2, \ldots$, and $m = -n, \ldots, n$. The above set of integral equations will be referred to as the null-field equations.

An approximate solution to the null-field equations can be obtained by approximating the surface fields $\boldsymbol{e}_{\mathrm{i}}$ and $\boldsymbol{h}_{\mathrm{i}}$ by the complete set of regular vector spherical wave functions for the interior domain (or the interior wave equation)

$$\begin{pmatrix} \boldsymbol{e}_{\mathrm{i}}^N(\boldsymbol{r}') \\ \boldsymbol{h}_{\mathrm{i}}^N(\boldsymbol{r}') \end{pmatrix} = \sum_{\mu=1}^{N} c_\mu^N \begin{pmatrix} \boldsymbol{n}(\boldsymbol{r}') \times \boldsymbol{M}_\mu^1(k_{\mathrm{i}}\boldsymbol{r}') \\ -\mathrm{j}\sqrt{\frac{\varepsilon_{\mathrm{i}}}{\mu_{\mathrm{i}}}}\boldsymbol{n}(\boldsymbol{r}') \times \boldsymbol{N}_\mu^1(k_{\mathrm{i}}\boldsymbol{r}') \end{pmatrix} + d_\mu^N \begin{pmatrix} \boldsymbol{n}(\boldsymbol{r}') \times \boldsymbol{N}_\mu^1(k_{\mathrm{i}}\boldsymbol{r}') \\ -\mathrm{j}\sqrt{\frac{\varepsilon_{\mathrm{i}}}{\mu_{\mathrm{i}}}}\boldsymbol{n}(\boldsymbol{r}') \times \boldsymbol{M}_\mu^1(k_{\mathrm{i}}\boldsymbol{r}') \end{pmatrix}, \tag{2.7}$$

where N is a truncation multi-index and $\mu = 1, 2, \ldots, N$, when $n = 1, 2, \ldots N_{\mathrm{rank}}$, and $m = -n, \ldots, n$. In all applications of the null-field method we approximate the surface fields by finite expansions, and the coefficients c_μ^N and d_μ^N on the right-hand side of the above equation then depend on the number of

terms in the expansion. The completeness of the system $\{\boldsymbol{n}\times\boldsymbol{M}^1_\mu, \boldsymbol{n}\times\boldsymbol{N}^1_\mu\}_\mu$ implies the existence of the set of expansion coefficients $\{c^N_\mu, d^N_\mu\}^N_{\mu=1}$ and of the integer $N = N(\varepsilon)$, such that $\|\boldsymbol{e}_\mathrm{i} - \boldsymbol{e}^N_\mathrm{i}\|_{2,S} < \varepsilon$, for any $\varepsilon > 0$. In (2.7), $\boldsymbol{e}^N_\mathrm{i}$ and $\boldsymbol{h}^N_\mathrm{i}$ are expressed in terms of the same set of expansion coefficients and this choice shows that $\boldsymbol{e}_\mathrm{i}$ and $\boldsymbol{h}_\mathrm{i}$ are not independent unknowns. In fact, the surface fields $\boldsymbol{e}_\mathrm{i}$ and $\boldsymbol{h}_\mathrm{i}$ solve the general null-field equations in D_i and D_s as given by (2.4) and

$$\nabla\times\int_S \boldsymbol{e}_\mathrm{i}(\boldsymbol{r}')\,g(k_\mathrm{i},\boldsymbol{r},\boldsymbol{r}')\,\mathrm{d}S(\boldsymbol{r}') + \frac{\mathrm{j}}{k_0\varepsilon_\mathrm{i}}\nabla\times\nabla\times\int_S \boldsymbol{h}_\mathrm{i}(\boldsymbol{r}')\,g(k_\mathrm{i},\boldsymbol{r},\boldsymbol{r}')\,\mathrm{d}S(\boldsymbol{r}') = 0\,,\quad \boldsymbol{r}\in D_\mathrm{s}\,, \tag{2.8}$$

respectively, or equivalently, the infinite systems of null-field equations as given by (2.7) and

$$\int_S \left[\boldsymbol{e}_\mathrm{i}(\boldsymbol{r}')\cdot\begin{pmatrix}\boldsymbol{N}^1_\nu(k_\mathrm{i}\boldsymbol{r}')\\ \boldsymbol{M}^1_\nu(k_\mathrm{i}\boldsymbol{r}')\end{pmatrix} + \mathrm{j}\sqrt{\frac{\mu_\mathrm{i}}{\varepsilon_\mathrm{i}}}\boldsymbol{h}_\mathrm{i}(\boldsymbol{r}')\cdot\begin{pmatrix}\boldsymbol{M}^1_\nu(k_\mathrm{i}\boldsymbol{r}')\\ \boldsymbol{N}^1_\nu(k_\mathrm{i}\boldsymbol{r}')\end{pmatrix}\right]\mathrm{d}S(\boldsymbol{r}') = 0\,,\quad \nu = 1,2,\ldots, \tag{2.9}$$

respectively. Note that (2.8) is the Stratton–Chu representation theorem for the internal field in D_s, while (2.9) follows from the spherical wave expansion of the dyad $g\overline{\boldsymbol{I}}$ outside a sphere enclosing D_i. When $\boldsymbol{e}_\mathrm{i}$ and $\boldsymbol{h}_\mathrm{i}$ are treated as independent unknowns and are approximated by sub-boundary bases, the expansion coefficients are obtained by solving (2.6) and (2.9). In (2.7), the expansion of $\boldsymbol{h}^N_\mathrm{i}$ has a physical meaning: the surface fields $\boldsymbol{e}_\mathrm{i}$ and $\boldsymbol{h}_\mathrm{i}$ are the tangential components of the electric and magnetic fields $\boldsymbol{E}_\mathrm{i}$ and $\boldsymbol{H}_\mathrm{i}$, respectively. Taking into account the orthogonality relation (cf. (B.25))

$$\int_S \left[(\boldsymbol{n}\times\boldsymbol{M}^1_\mu)\cdot\begin{pmatrix}\boldsymbol{M}^1_\nu\\ \boldsymbol{N}^1_\nu\end{pmatrix} + (\boldsymbol{n}\times\boldsymbol{N}^1_\mu)\cdot\begin{pmatrix}\boldsymbol{N}^1_\nu\\ \boldsymbol{M}^1_\nu\end{pmatrix}\right]\mathrm{d}S = 0\,,$$

we see that $\boldsymbol{e}^N_\mathrm{i}$ and $\boldsymbol{h}^N_\mathrm{i}$ as given by (2.7) solve the null-field equations in D_s and therefore, the expansion coefficients c^N_μ and d^N_μ have to be determined from the null-field equations in D_i.

Inserting (2.7) into the first $2N$ null-field equations, yields

$$\boldsymbol{Q}^{31}(k_\mathrm{s},k_\mathrm{i})\,\boldsymbol{i} = -\boldsymbol{e},\,, \tag{2.10}$$

where $\boldsymbol{i} = [c^N_\mu, d^N_\mu]^\mathrm{T}$ and $\boldsymbol{e} = [a_\nu, b_\nu]^\mathrm{T}$ are vectors containing the expansion coefficients of the surface and incident fields, respectively. In general,

for nonmagnetic media with $k_1 = k_0\sqrt{\varepsilon_1}$ and $k_2 = k_0\sqrt{\varepsilon_2}$, the $\boldsymbol{Q}^{pq}(k_1, k_2)$ matrix,

$$\boldsymbol{Q}^{pq}\left(k_1, k_2\right) = \begin{bmatrix} \left(Q^{pq}\right)^{11}_{\nu\mu} & \left(Q^{pq}\right)^{12}_{\nu\mu} \\ \left(Q^{pq}\right)^{21}_{\nu\mu} & \left(Q^{pq}\right)^{22}_{\nu\mu} \end{bmatrix} ,$$

is defined as

$$\left(Q^{pq}\right)^{11}_{\nu\mu} = \frac{\mathrm{j}k_1^2}{\pi} \int_S \Big\{ \left[\boldsymbol{n}\left(\boldsymbol{r}'\right) \times \boldsymbol{M}^q_\mu\left(k_2\boldsymbol{r}'\right)\right] \cdot \boldsymbol{N}^p_\nu\left(k_1\boldsymbol{r}'\right) + \sqrt{\frac{\varepsilon_2}{\varepsilon_1}} \left[\boldsymbol{n}\left(\boldsymbol{r}'\right) \times \boldsymbol{N}^q_\mu\left(k_2\boldsymbol{r}'\right)\right] \cdot \boldsymbol{M}^p_\nu\left(k_1\boldsymbol{r}'\right) \Big\} \mathrm{d}S\left(\boldsymbol{r}'\right) , \quad (2.11)$$

$$\left(Q^{pq}\right)^{12}_{\nu\mu} = \frac{\mathrm{j}k_1^2}{\pi} \int_S \Big\{ \left[\boldsymbol{n}\left(\boldsymbol{r}'\right) \times \boldsymbol{N}^q_\mu\left(k_2\boldsymbol{r}'\right)\right] \cdot \boldsymbol{N}^p_\nu\left(k_1\boldsymbol{r}'\right) + \sqrt{\frac{\varepsilon_2}{\varepsilon_1}} \left[\boldsymbol{n}\left(\boldsymbol{r}'\right) \times \boldsymbol{M}^q_\mu\left(k_2\boldsymbol{r}'\right)\right] \cdot \boldsymbol{M}^p_\nu\left(k_1\boldsymbol{r}'\right) \Big\} \mathrm{d}S\left(\boldsymbol{r}'\right) , \quad (2.12)$$

$$\left(Q^{pq}\right)^{21}_{\nu\mu} = \frac{\mathrm{j}k_1^2}{\pi} \int_S \Big\{ \left[\boldsymbol{n}\left(\boldsymbol{r}'\right) \times \boldsymbol{M}^q_\mu\left(k_2\boldsymbol{r}'\right)\right] \cdot \boldsymbol{M}^p_\nu\left(k_1\boldsymbol{r}'\right) + \sqrt{\frac{\varepsilon_2}{\varepsilon_1}} \left[\boldsymbol{n}\left(\boldsymbol{r}'\right) \times \boldsymbol{N}^q_\mu\left(k_2\boldsymbol{r}'\right)\right] \cdot \boldsymbol{N}^p_\nu\left(k_1\boldsymbol{r}'\right) \Big\} \mathrm{d}S\left(\boldsymbol{r}'\right) , \quad (2.13)$$

and

$$\left(Q^{pq}\right)^{22}_{\nu\mu} = \frac{\mathrm{j}k_1^2}{\pi} \int_S \Big\{ \left[\boldsymbol{n}\left(\boldsymbol{r}'\right) \times \boldsymbol{N}^q_\mu\left(k_2\boldsymbol{r}'\right)\right] \cdot \boldsymbol{M}^p_\nu\left(k_1\boldsymbol{r}'\right) + \sqrt{\frac{\varepsilon_2}{\varepsilon_1}} \left[\boldsymbol{n}\left(\boldsymbol{r}'\right) \times \boldsymbol{M}^q_\mu\left(k_2\boldsymbol{r}'\right)\right] \cdot \boldsymbol{N}^p_\nu\left(k_1\boldsymbol{r}'\right) \Big\} \mathrm{d}S\left(\boldsymbol{r}'\right) . \quad (2.14)$$

Considering the scattered field representation (2.5), we replace the surface fields by their approximations and use the vector spherical wave expansion of the dyad $g\overline{\boldsymbol{I}}$ on a sphere enclosing D_i to obtain

$$\boldsymbol{E}^N_\mathrm{s}(\boldsymbol{r}) = \sum_{\nu=1}^{N} f^N_\nu \boldsymbol{M}^3_\nu\left(k_\mathrm{s}\boldsymbol{r}\right) + g^N_\nu \boldsymbol{N}^3_\nu\left(k_\mathrm{s}\boldsymbol{r}\right) , \quad (2.15)$$

where the expansion coefficients of the scattered field are given by

$$\begin{pmatrix} f^N_\nu \\ g^N_\nu \end{pmatrix} = \frac{\mathrm{j}k_\mathrm{s}^2}{\pi} \int_S \left[\boldsymbol{e}^N_\mathrm{i}\left(\boldsymbol{r}'\right) \cdot \begin{pmatrix} \boldsymbol{N}^1_\nu\left(k_\mathrm{s}\boldsymbol{r}'\right) \\ \boldsymbol{M}^1_\nu\left(k_\mathrm{s}\boldsymbol{r}'\right) \end{pmatrix} + \mathrm{j}\sqrt{\frac{\mu_\mathrm{s}}{\varepsilon_\mathrm{s}}} \boldsymbol{h}^N_\mathrm{i}\left(\boldsymbol{r}'\right) \cdot \begin{pmatrix} \boldsymbol{M}^1_\nu\left(k_\mathrm{s}\boldsymbol{r}'\right) \\ \boldsymbol{N}^1_\nu\left(k_\mathrm{s}\boldsymbol{r}'\right) \end{pmatrix} \right] \mathrm{d}S\left(\boldsymbol{r}'\right) \quad (2.16)$$

for $\nu = 1, 2, \ldots, N$. Inserting (2.7) into (2.16) yields

$$\boldsymbol{s} = \boldsymbol{Q}^{11}\left(k_{\mathrm{s}}, k_{\mathrm{i}}\right)\boldsymbol{i}\,, \tag{2.17}$$

where $\boldsymbol{s} = [f_\nu^N, g_\nu^N]^{\mathrm{T}}$ is the vector containing the expansion coefficients of the scattered field. Combining (2.10) and (2.17) we deduce that the transition matrix relating the scattered field coefficients to the incident field coefficients, $\boldsymbol{s} = \boldsymbol{T}\boldsymbol{e}$, is given by

$$\boldsymbol{T} = -\boldsymbol{Q}^{11}\left(k_{\mathrm{s}}, k_{\mathrm{i}}\right)\left[\boldsymbol{Q}^{31}\left(k_{\mathrm{s}}, k_{\mathrm{i}}\right)\right]^{-1}\,. \tag{2.18}$$

In view of (2.11)–(2.14), we see that the transition matrix computed in the particle coordinate system depends only on the physical and geometrical characteristics of the particle, such as particle shape and relative refractive index and is independent of the propagation direction and polarization states of the incident and scattered fields. In contrast to the infinite transition matrix discussed in Sect. 1.5, the transition matrix given by (2.18) is of finite dimension, and the often used appellation approximate or truncated transition matrix is justified.

2.1.2 Instability

Instability of the null-field method occurs for strongly deformed particles and large size parameters. A number of modifications to the conventional approach has been suggested, especially to improve the numerical stability in computations for particles with extreme geometries. These techniques include formal modifications of the single spherical coordinate-based null-field method by using discrete sources [49, 109], different choices of basis functions and the application of the spheroidal coordinate formalism [12, 89], and the orthogonalization method [133, 256]. For large particles, the maximum convergent size parameter can be increased by using a special form of the LU-factorization method [261] and by performing the matrix inversion using extended-precision [166]. For strongly absorbing metallic particles, Gaussian elimination with backsubstitution gives improved convergence results [174].

Formulation with Discrete Sources

The conventional derivation of the $\boldsymbol{T}$ matrix relies on the approximation of the surface fields by the system of localized vector spherical wave functions. Although these wave functions appear to provide a good approximation to the solution when the surface is not extremely aspherical, they are disadvantageous when this is not the case. The numerical instability of the $\boldsymbol{T}$-matrix calculation arises because the elements of the $\boldsymbol{Q}^{31}$ matrix differ by many orders of magnitude and the inversion process is ill-conditioned. As a result, slow convergence or divergence occur. If instead of localized vector spherical

functions we use distributed sources, it is possible to extend the applicability range of the single spherical coordinate-based null-field method. Discrete sources were used for the first time in the iterative version of the null-field method [108, 109, 132]. This iterative approach utilizes multipole spherical expansions to represent the internal fields in different overlapping regions, while the various expansions are matched in the overlapping regions to enforce the continuity of the fields throughout the entire interior volume.

In the following analysis we summarize the basic concepts of the null-field method with distributed sources. The distributed vector spherical wave functions are defined as

$$\mathcal{M}_{mn}^{1,3}(k\boldsymbol{r}) = \boldsymbol{M}_{m,|m|+l}^{1,3}\left[k(\boldsymbol{r} - z_n\boldsymbol{e}_z)\right] ,$$
$$\mathcal{N}_{mn}^{1,3}(k\boldsymbol{r}) = \boldsymbol{N}_{m,|m|+l}^{1,3}\left[k(\boldsymbol{r} - z_n\boldsymbol{e}_z)\right] ,$$

where $\{z_n\}_{n=1}^{\infty}$ is a dense set of points situated on the z-axis and in the interior of S, $\boldsymbol{e}_z$ is the unit vector in the direction of the z-axis, $n = 1, 2, \ldots, m \in \boldsymbol{Z}$, and $l = 1$ if $m = 0$ and $l = 0$ if $m \neq 0$. Taking into account the Stratton–Chu representation theorem for the incident field in D_{i} we rewrite the general null-field equation as

$$\nabla \times \int_S \left[\boldsymbol{e}_{\mathrm{i}}(\boldsymbol{r}') - \boldsymbol{e}_{\mathrm{e}}(\boldsymbol{r}')\right] g(k_{\mathrm{s}}, \boldsymbol{r}, \boldsymbol{r}')\, \mathrm{d}S(\boldsymbol{r}') \tag{2.19}$$
$$+\frac{\mathrm{j}}{k_0\varepsilon_{\mathrm{s}}}\nabla \times \nabla \times \int_S \left[\boldsymbol{h}_{\mathrm{i}}(\boldsymbol{r}') - \boldsymbol{h}_{\mathrm{e}}(\boldsymbol{r}')\right] g(k_{\mathrm{s}}, \boldsymbol{r}, \boldsymbol{r}')\, \mathrm{d}S(\boldsymbol{r}') = 0 , \quad \boldsymbol{r} \in D_{\mathrm{i}} ,$$

and derive the following set of null-field equations:

$$\frac{\mathrm{j}k_{\mathrm{s}}^2}{\pi}\int_S \left[\left[\boldsymbol{e}_{\mathrm{i}}(\boldsymbol{r}') - \boldsymbol{e}_{\mathrm{e}}(\boldsymbol{r}')\right] \cdot \begin{pmatrix} \boldsymbol{N}_{\nu}^{3}(k_{\mathrm{s}}\boldsymbol{r}') \\ \boldsymbol{M}_{\nu}^{3}(k_{\mathrm{s}}\boldsymbol{r}') \end{pmatrix}\right.$$
$$\left. + \mathrm{j}\sqrt{\frac{\mu_{\mathrm{s}}}{\varepsilon_{\mathrm{s}}}}\left[\boldsymbol{h}_{\mathrm{i}}(\boldsymbol{r}') - \boldsymbol{h}_{\mathrm{e}}(\boldsymbol{r}')\right] \cdot \begin{pmatrix} \boldsymbol{M}_{\nu}^{3}(k_{\mathrm{s}}\boldsymbol{r}') \\ \boldsymbol{N}_{\nu}^{3}(k_{\mathrm{s}}\boldsymbol{r}') \end{pmatrix}\right] \mathrm{d}S(\boldsymbol{r}') = 0 , \quad \nu = 1, 2, \ldots \tag{2.20}$$

The formulation of the null-field method with distributed vector spherical wave functions relies on two basic results. The first result states that if $\boldsymbol{e}_{\mathrm{i}}$ and $\boldsymbol{h}_{\mathrm{i}}$ solve the set of null-field equations (compare to (2.20))

$$\frac{\mathrm{j}k_{\mathrm{s}}^2}{\pi}\int_S \left[\left[\boldsymbol{e}_{\mathrm{i}}(\boldsymbol{r}') - \boldsymbol{e}_{\mathrm{e}}(\boldsymbol{r}')\right] \cdot \begin{pmatrix} \mathcal{N}_{\nu}^{3}(k_{\mathrm{s}}\boldsymbol{r}') \\ \mathcal{M}_{\nu}^{3}(k_{\mathrm{s}}\boldsymbol{r}') \end{pmatrix}\right.$$
$$\left. + \mathrm{j}\sqrt{\frac{\mu_{\mathrm{s}}}{\varepsilon_{\mathrm{s}}}}\left[\boldsymbol{h}_{\mathrm{i}}(\boldsymbol{r}') - \boldsymbol{h}_{\mathrm{e}}(\boldsymbol{r}')\right] \cdot \begin{pmatrix} \mathcal{M}_{\nu}^{3}(k_{\mathrm{s}}\boldsymbol{r}') \\ \mathcal{N}_{\nu}^{3}(k_{\mathrm{s}}\boldsymbol{r}') \end{pmatrix}\right] \mathrm{d}S(\boldsymbol{r}') = 0 ,$$
$$\nu = 1, 2, \ldots , \tag{2.21}$$

where $\nu = (m,n)$, $\overline{\nu} = (-m,n)$ and $\nu = 1,2,...$, when $n = 1,2,...$, and $m \in \boldsymbol{Z}$, then $\boldsymbol{e}_{\mathrm{i}}$ and $\boldsymbol{h}_{\mathrm{i}}$ solve the general null-field equation (2.20). The second result states the completeness and linear independence of the system of distributed vector spherical wave functions $\{\boldsymbol{n} \times \mathcal{M}_\mu^1, \boldsymbol{n} \times \mathcal{N}_\mu^1\}$ on closed surfaces. Consequently, approximating the surface fields by the finite expansions

$$\begin{pmatrix} \boldsymbol{e}_{\mathrm{i}}^N(\boldsymbol{r}') \\ \boldsymbol{h}_{\mathrm{i}}^N(\boldsymbol{r}') \end{pmatrix} = \sum_{\mu=1}^{N} c_\mu^N \begin{pmatrix} \boldsymbol{n}(\boldsymbol{r}') \times \mathcal{M}_\mu^1(k_{\mathrm{i}}\boldsymbol{r}') \\ -\mathrm{j}\sqrt{\frac{\epsilon_{\mathrm{i}}}{\mu_{\mathrm{i}}}}\boldsymbol{n}(\boldsymbol{r}') \times \mathcal{N}_\mu^1(k_{\mathrm{i}}\boldsymbol{r}') \end{pmatrix} + d_\mu^N \begin{pmatrix} \boldsymbol{n}(\boldsymbol{r}') \times \mathcal{N}_\mu^1(k_{\mathrm{i}}\boldsymbol{r}') \\ -\mathrm{j}\sqrt{\frac{\epsilon_{\mathrm{i}}}{\mu_{\mathrm{i}}}}\boldsymbol{n}(\boldsymbol{r}') \times \mathcal{M}_\mu^1(k_{\mathrm{i}}\boldsymbol{r}') \end{pmatrix}, \tag{2.22}$$

inserting (2.22) into (2.21) and using the vector spherical wave expansion of the incident field, yields

$$\widetilde{\boldsymbol{Q}}^{31}(k_{\mathrm{s}},k_{\mathrm{i}})\,\boldsymbol{i} = -\widetilde{\boldsymbol{Q}}^{31}(k_{\mathrm{s}},k_{\mathrm{s}})\,\boldsymbol{e}\,.$$

The $\widetilde{\boldsymbol{Q}}^{31}(k_{\mathrm{s}},k_{\mathrm{i}})$ matrix has the same structure as the $\boldsymbol{Q}^{31}(k_{\mathrm{s}},k_{\mathrm{i}})$ matrix, but it contains as rows and columns the vectors $\mathcal{M}_{\overline{\nu}}^3(k_{\mathrm{s}}\boldsymbol{r}')$, $\mathcal{N}_{\overline{\nu}}^3(k_{\mathrm{s}}\boldsymbol{r}')$ and $\mathcal{M}_\mu^1(k_{\mathrm{i}}\boldsymbol{r}')$, $\mathcal{N}_\mu^1(k_{\mathrm{i}}\boldsymbol{r}')$, respectively, while $\widetilde{\boldsymbol{Q}}^{31}(k_{\mathrm{s}},k_{\mathrm{s}})$ contains as rows and columns the vectors $\mathcal{M}_{\overline{\nu}}^3(k_{\mathrm{s}}\boldsymbol{r}')$, $\mathcal{N}_{\overline{\nu}}^3(k_{\mathrm{s}}\boldsymbol{r}')$ and $\boldsymbol{M}_\mu^1(k_{\mathrm{s}}\boldsymbol{r}')$, $\boldsymbol{N}_\mu^1(k_{\mathrm{s}}\boldsymbol{r}')$, respectively. To compute the scattered field we proceed as in the case of localized sources. Application of the Huygens principle yields the expansion of the scattered field in terms of localized vector spherical wave functions as in (2.15) and (2.16). Inserting (2.22) into (2.16) gives

$$\boldsymbol{s} = \widetilde{\boldsymbol{Q}}^{11}(k_{\mathrm{s}},k_{\mathrm{i}})\,\boldsymbol{i}\,,$$

and we obtain

$$\boldsymbol{T} = -\widetilde{\boldsymbol{Q}}^{11}(k_{\mathrm{s}},k_{\mathrm{i}})\left[\widetilde{\boldsymbol{Q}}^{31}(k_{\mathrm{s}},k_{\mathrm{i}})\right]^{-1}\widetilde{\boldsymbol{Q}}^{31}(k_{\mathrm{s}},k_{\mathrm{s}})\,,$$

where $\widetilde{\boldsymbol{Q}}^{11}(k_{\mathrm{s}},k_{\mathrm{i}})$ contains as rows and columns the vectors $\boldsymbol{M}_{\overline{\nu}}^1(k_{\mathrm{s}}\boldsymbol{r}')$, $\boldsymbol{N}_{\overline{\nu}}^1(k_{\mathrm{s}}\boldsymbol{r}')$ and $\mathcal{M}_\mu^1(k_{\mathrm{i}}\boldsymbol{r}')$, $\mathcal{N}_\mu^1(k_{\mathrm{i}}\boldsymbol{r}')$, respectively. Taking into account the definition of the distributed vector spherical wave functions (cf. (B.30)), we see that the $\widetilde{\boldsymbol{Q}}^{31}(k_{\mathrm{s}},k_{\mathrm{i}})$ matrix includes Hankel functions of low order which results in a better conditioned system of equations as compared to that obtained in the single spherical coordinate-based null-field method.

The use of distributed vector spherical wave functions is most effective for axisymmetric particles because, in this case, the $\boldsymbol{T}$ matrix is diagonal with respect to the azimuthal indices. For elongated particles, the sources are distributed on the axis of rotation, while for flattened particles, the sources are distributed in the complex plane (which is the dual of the symmetry plane).

The expressions of the distributed vector spherical wave functions with the origins located in the complex plane are given by (B.31) and (B.32).

Various systems of vector functions can be used instead of localized and distributed vector spherical wave functions. Formulations of the null-field method with multiple vector spherical wave functions, electric and magnetic dipoles and vector Mie potentials have been given by Doicu et al. [49]. Numerical experiments performed by Ström and Zheng [218] demonstrated that the system of tangential fields constructed from the vector spherical harmonics is suitable for analyzing particles with pronounced concavities. When the surface fields have discontinuities in their continuity or any of their derivatives, straightforward application of the global basis functions provides poor convergence of the solution. Wall [247] showed that sub-boundary bases or local basis approximations of the surface fields results in larger condition numbers of the matrix equations.

Orthogonalization Method

To ameliorate the numerical instability of the null-field method for nonabsorbing particles, Waterman [256, 257] and Lakhtakia et al. [133, 134] proposed to exploit the unitarity property of the transition matrix. To summarize this technique we consider nonabsorbing particles and use the identity $\boldsymbol{Q}^{11} = \mathrm{Re}\{\boldsymbol{Q}^{31}\}$ to rewrite the $\boldsymbol{T}$-matrix equation

$$\boldsymbol{Q}\boldsymbol{T} = -\mathrm{Re}\left\{\boldsymbol{Q}\right\}, \tag{2.23}$$

as

$$\boldsymbol{Q}\mathcal{S} = -\boldsymbol{Q}^{*},$$

where $\boldsymbol{Q} = \boldsymbol{Q}^{31}$ and $\mathcal{S} = \boldsymbol{I} + 2\boldsymbol{T}$. Applying the Gramm–Schmidt orthogonalization procedure on the row vectors of $\boldsymbol{Q}$, we construct the unitarity matrix $\widehat{\boldsymbol{Q}}$ ($\widehat{\boldsymbol{Q}}^{\dagger}\widehat{\boldsymbol{Q}} = \widehat{\boldsymbol{Q}}\widehat{\boldsymbol{Q}}^{\dagger} = \boldsymbol{I}$) such that

$$\widehat{\boldsymbol{Q}} = \boldsymbol{M}\boldsymbol{Q},$$

and derive

$$\mathcal{S} = -\widehat{\boldsymbol{Q}}^{\dagger}\left[\boldsymbol{M}\left(\boldsymbol{M}^{*}\right)^{-1}\right]\widehat{\boldsymbol{Q}}^{*} = -\widehat{\boldsymbol{Q}}^{\dagger}\widehat{\boldsymbol{M}}\widehat{\boldsymbol{Q}}^{*},$$

where $\boldsymbol{M}$ is an upper-triangular matrix with real diagonal elements and $\widehat{\boldsymbol{M}} = \boldsymbol{M}(\boldsymbol{M}^{*})^{-1}$. Taking into account the unitarity condition for the $\mathcal{S}$ matrix (cf. (1.109)),

$$\boldsymbol{I} = \mathcal{S}^{\dagger}\mathcal{S} = \widehat{\boldsymbol{Q}}^{\mathrm{T}}\widehat{\boldsymbol{M}}^{\dagger}\widehat{\boldsymbol{Q}} \cdot \widehat{\boldsymbol{Q}}^{\dagger}\widehat{\boldsymbol{M}}\widehat{\boldsymbol{Q}}^{*} = \widehat{\boldsymbol{Q}}^{\mathrm{T}}\widehat{\boldsymbol{M}}^{\dagger}\widehat{\boldsymbol{M}}\widehat{\boldsymbol{Q}}^{*},$$

and using the relation $\widehat{\boldsymbol{Q}}^{\mathrm{T}}\widehat{\boldsymbol{Q}}^{*} = \boldsymbol{I}$, we deduce that

$$\widehat{\boldsymbol{M}}^{\dagger}\widehat{\boldsymbol{M}} = \boldsymbol{I}\,. \tag{2.24}$$

Because $\boldsymbol{M}$ is upper-triangular with real diagonal elements, it follows that $\widehat{\boldsymbol{M}}$ is unit upper-triangular (all diagonal elements are equal 1). Then, (2.24) implies that $\widehat{\boldsymbol{M}} = \boldsymbol{I}$, and therefore

$$\mathcal{S} = -\widehat{\boldsymbol{Q}}^{\dagger}\widehat{\boldsymbol{Q}}^{*}\,.$$

In terms of the transition matrix, the above equation read as

$$\boldsymbol{T} = -\widehat{\boldsymbol{Q}}^{\dagger}\mathrm{Re}\left\{\widehat{\boldsymbol{Q}}\right\}$$

and this new sequence of truncated transition matrices might be expected to converge more rapidly than (2.23) because the unitarity condition is satisfied for each truncation index.

2.1.3 Symmetries of the Transition Matrix

Symmetry properties of the transition matrix can be derived for specific particle shapes. These symmetry relations can be used to test numerical codes as well as to simplify many equations of the $\boldsymbol{T}$-matrix method and develop efficient numerical procedures. In fact, the computer time for the numerical evaluation of the surface integrals (which is the most time consuming part of the $\boldsymbol{T}$-matrix calculation) can be substantially reduced. The surface integrals are usually computed in spherical coordinates and for a surface defined by

$$r = r\left(\theta,\varphi\right)\,,$$

we have

$$\boldsymbol{n}\left(\boldsymbol{r}\right)\mathrm{d}S\left(\boldsymbol{r}\right) = \boldsymbol{\sigma}\left(\boldsymbol{r}\right)r^{2}\sin\theta\,\mathrm{d}\theta\,\mathrm{d}\varphi\,,$$

where

$$\boldsymbol{\sigma}(\boldsymbol{r}) = \boldsymbol{e}_{r} - \frac{1}{r}\frac{\partial r}{\partial\theta}\boldsymbol{e}_{\theta} - \frac{1}{r\sin\theta}\frac{\partial r}{\partial\varphi}\boldsymbol{e}_{\varphi}$$

is a vector parallel to the unit normal vector $\boldsymbol{n}$. In the following analysis, we will investigate the symmetry properties of the transition matrix for axisymmetric particles and particles with azimuthal and mirror symmetries.

1. For an axisymmetric particle, the equation of the surface does not depend on φ, and therefore $\partial r/\partial\varphi = 0$. The vector $\boldsymbol{\sigma}$ has only $\boldsymbol{e}_{r}$- and $\boldsymbol{e}_{\theta}$-components and is independent of φ. The integral over the azimuthal angle can be performed analytically and we see that the result is zero unless $m = m_{1}$.

Therefore, the $\boldsymbol{T}$ matrix is diagonal with respect to the azimuthal indices m and m_1, i.e.,

$$T^{ij}_{mn,m_1n_1} = T^{ij}_{mn,mn_1}\delta_{mm_1}\,.$$

Direct calculation shows that

$$T^{ij}_{mn,mn_1} = (-1)^{i+j}T^{ij}_{-mn,-mn_1} \tag{2.25}$$

and the symmetry relation (1.112) takes the form

$$T^{ij}_{mn,mn_1} = T^{ji}_{-mn_1,-mn} = (-1)^{i+j}T^{ji}_{mn_1,mn}\,.$$

2. We consider a particle with a principal N-fold axis of rotation symmetry and assume that the axis of symmetry coincides with the z-axis of the particle coordinate system. In this case, r, $\partial r/\partial\theta$ and $\partial r/\partial\varphi$ are periodic in φ with period $2\pi/N$. Taking into account the definition of the $\boldsymbol{Q}^{pq}$ matrices, we see that the surface integrals are of the form

$$\int_0^{2\pi} f(\varphi)\,\mathrm{e}^{\mathrm{j}(m_1-m)\varphi}\mathrm{d}\varphi\,,$$

where f is a periodic function of φ,

$$f(\varphi) = f\left(\varphi + k\frac{2\pi}{N}\right)\,.$$

As a consequence of the rotation symmetry around the z-axis, the $\boldsymbol{T}$ matrix is invariant with respect to discrete rotations of angles $\alpha_k = 2\pi k/N$, $k = 1,2,\ldots,N-1$. A necessary and sufficient condition for the equation

$$\int_0^{2\pi} f(\varphi)\,\mathrm{e}^{\mathrm{j}(m_1-m)\varphi}\mathrm{d}\varphi = \mathrm{e}^{\mathrm{j}(m_1-m)k\frac{2\pi}{N}}\int_0^{2\pi} f(\varphi)\,\mathrm{e}^{\mathrm{j}(m_1-m)\varphi}\mathrm{d}\varphi$$

to hold is $|m_1-m| = lN$, $l = 0,1,\ldots$, and we conclude that

$$T^{ij}_{mn,m_1n_1} = 0$$

Further,

$$\begin{aligned}\int_0^{2\pi} f(\varphi)\,\mathrm{e}^{\mathrm{j}(m_1-m)\varphi}\mathrm{d}\varphi &= \sum_{k=1}^{N}\mathrm{e}^{\mathrm{j}(m_1-m)(k-1)\frac{2\pi}{N}}\int_0^{2\pi/N} f(\varphi)\,\mathrm{e}^{\mathrm{j}(m_1-m)\varphi}\mathrm{d}\varphi\\ &= N\int_0^{2\pi/N} f(\varphi)\,\mathrm{e}^{\mathrm{j}(m_1-m)\varphi}\mathrm{d}\varphi\,,\end{aligned}$$

for $|m_1-m| = lN$, $l = 0,1,\ldots$, and we see that

$$T^{ij}_{mn,m_1n_1} = \begin{cases} N\left(T_{\mathrm{rotsym}}\right)^{ij}_{mn,m_1n_1}\,, & |m_1-m| = lN, l = 0,1,\ldots\\ 0\,, & \text{rest}\end{cases}\,,$$

where $\left(T_{\mathrm{rotsym}}\right)^{ij}_{mn,m_1n_1}$ are the elements of the transition matrix computed by integrating φ over the interval $[0,2\pi/N]$.

3. We consider a particle with mirror symmetry and assume that the xy-plane is the horizontal plane of reflection. The surface parameterization of a particle with mirror symmetry has the property

$$r(\theta,\varphi) = r(\pi-\theta,\varphi)$$

and therefore

$$\frac{\partial r}{\partial\theta}(\theta,\varphi) = -\frac{\partial r}{\partial\theta}(\pi-\theta,\varphi)\ ,$$
$$\frac{\partial r}{\partial\varphi}(\theta,\varphi) = \frac{\partial r}{\partial\varphi}(\pi-\theta,\varphi)$$

for $0 \le \theta \le \pi/2$ and $0 \le \varphi < 2\pi$. Taking into account the symmetry relations of the normalized angular functions $\pi_n^{|m|}$ and $\tau_n^{|m|}$ (cf. (A.24) and (A.25)),

$$\pi_n^m(\pi-\theta) = (-1)^{n-m}\,\pi_n^m(\theta)\ ,$$
$$\tau_n^m(\pi-\theta) = (-1)^{n-m+1}\,\tau_n^m(\theta)\ ,$$

we find that

$$T^{ij}_{mn,m_1n_1} = \left[1+(-1)^{n+n_1+|m|+|m_1|+i+j}\right](T_{\mathrm{mirrsym}})^{ij}_{mn,m_1n_1}\ ,$$

where $(T_{\mathrm{mirrsym}})^{ij}_{mn,m_1n_1}$ are the elements of the transition matrix computed by integrating θ over the interval $[0,\pi/2]$. The above relation also shows that

$$T^{ij}_{mn,m_1n_1} = 0\,,$$

if $n+n_1+|m|+|m_1|+i+j$ is an odd number.

Exploitation of these symmetry relations leads to a reduction in CPU time by three orders of magnitude from that of a standard implementation with no geometry-specific adaptations. Additional properties of the transition matrix for particles with specific symmetries are discussed by Kahnert et al. [111] and by Havemann and Baran [98].

2.1.4 Practical Considerations

The integrals over the particle surface are usually computed by using appropriate quadrature formulas. For particles with piecewise smooth surfaces, the numerical stability and accuracy of the $\boldsymbol{T}$-matrix calculations can be improved by using separate Gaussian quadratures on each smooth section [8,170].

In practice, it is more convenient to interchange the order of summation in the surface field representations, i.e., the sum

$$\sum_{n=1}^{N_{\mathrm{rank}}}\sum_{m=-n}^{n}(\cdot)$$

is replaced by

$$\sum_{m=-M_{\rm rank}}^{M_{\rm rank}} \sum_{n=\max(1,|m|)}^{N_{\rm rank}} (\cdot) \ ,$$

where $N_{\rm rank}$ and $M_{\rm rank}$ are the maximum expansion order and the number of azimuthal modes, respectively. Consequently, the dimension of the transition matrix $\boldsymbol{T}$ is

$$\dim(\boldsymbol{T}) = 2N_{\rm max} \times 2N_{\rm max} \ ,$$

where

$$N_{\rm max} = N_{\rm rank} + M_{\rm rank}\,(2N_{\rm rank} - M_{\rm rank} + 1) \ ,$$

is the truncation multi-index appearing in (2.7). The interchange of summation orders is effective for axisymmetric particles because, in this case, the scattering problem can be reduced to a sequence of subproblems for each azimuthal mode.

An important part of the numerical analysis is the convergence procedure that checks whether the size of the transition matrix and the number of quadrature points for surface integral calculations are sufficiently large that the scattering characteristics are computed with the desired accuracy. The convergence tests presented in the literature are based on the analysis of the differential scattering cross-section [8] or the extinction and scattering cross-sections [164]. The procedure used by Barber and Hill [8] solves the scattering problem for consecutive values of $N_{\rm rank}$ and $M_{\rm rank}$, and checks the convergence of the differential scattering cross-section at a number of scattering angles. If the calculated results converge within a prescribed tolerance at 80% of the scattering angles, then convergence is achieved. The procedure developed by Mishchenko [164] is applicable to axisymmetric particles and finds reliable estimates of $N_{\rm rank}$ by checking the convergence of the quantities

$$C_{\rm e} = -\frac{2\pi}{k_{\rm s}^2} \sum_{n=1}^{N_{\rm rank}} (2n+1)\,{\rm Re}\left\{T_{0n,0n}^{11} + T_{0n,0n}^{22}\right\}$$

and

$$C_{\rm s} = \frac{2\pi}{k_{\rm s}^2} \sum_{n=1}^{N_{\rm rank}} (2n+1)\left(\left|T_{0n,0n}^{11}\right|^2 + \left|T_{0n,0n}^{22}\right|^2\right) \ .$$

The null-field method is a general technique and is applicable for arbitrarily shaped particles. However, for nonaxisymmetric particles, a semi-convergent

behavior is usually attended: the relative variations of the differential scattering cross-sections decrease with increasing the maximum expansion order, attain a relative constant level and afterwards increase. In this case, the main problem of the convergence analysis is the localization of the region of stability. The extinction and scattering cross-sections can also give information on the convergence process. Although the convergence of C_{ext} and C_{scat} does not guarantee that the differential scattering cross-section converges, the divergence of C_{ext} and C_{scat} implies the divergence of the $\boldsymbol{T}$-matrix calculation.

2.1.5 Surface Integral Equation Method

The null-field method leads to a nonsingular integral equation of the first kind. However, in the framework of the surface integral equation method, the transmission boundary-value problem can be reduced to a pair of singular integral equations of the second kind [97]. These equations are formulated in terms of two surface fields which are treated as independent unknowns. In order to elucidate the difference between the null-field method and the surface integral equation method we follow the analysis of Martin and Ola [155] and review the basic boundary integral equations for the transmission boundary-value problem. We consider the vector potential $\boldsymbol{A}_{\mathrm{a}}$ with density $\boldsymbol{a}$

$$\boldsymbol{A}_{\mathrm{a}}(\boldsymbol{r}) = \int_S \boldsymbol{a}(\boldsymbol{r}')g(k,\boldsymbol{r},\boldsymbol{r}')\,\mathrm{d}S(\boldsymbol{r}')\,, \quad r \in \boldsymbol{R}^3 - S$$

and evaluate the tangential components of the *curl* and double *curl* of the vector potential on S. For continuous tangential density, we have [39]

$$\lim_{h\to 0_+} \boldsymbol{n}(\boldsymbol{r}) \times [\nabla \times \boldsymbol{A}_{\mathrm{a}}(\boldsymbol{r} \pm h\boldsymbol{n}(\boldsymbol{r}))] = \pm\frac{1}{2}\boldsymbol{a}(\boldsymbol{r}) + (\mathcal{M}\boldsymbol{a})(\boldsymbol{r})\,, \quad \boldsymbol{r} \in S\,,$$

where $\mathcal{M}$ is the magnetic dipole operator,

$$(\mathcal{M}\boldsymbol{a})(\boldsymbol{r}) = \boldsymbol{n}(\boldsymbol{r}) \times \left[\nabla \times \int_S \boldsymbol{a}(\boldsymbol{r}')g(k,\boldsymbol{r},\boldsymbol{r}')\,\mathrm{d}S(\boldsymbol{r}')\right]\,, \quad \boldsymbol{r} \in S\,.$$

For a sufficiently smooth tangential density, we also have

$$\lim_{h\to 0_+} \boldsymbol{n}(\boldsymbol{r}) \times [\nabla \times \nabla \times \boldsymbol{A}_{\mathrm{a}}(\boldsymbol{r} \pm h\boldsymbol{n}(\boldsymbol{r}))] = (\mathcal{P}\boldsymbol{a})(\boldsymbol{r})\,, \quad \boldsymbol{r} \in S\,,$$

where the principal value singular integral operator $\mathcal{P}$, called the electric dipole operator is given by

$$(\mathcal{P}\boldsymbol{a})(\boldsymbol{r}) = \boldsymbol{n}(\boldsymbol{r}) \times \left[\nabla \times \nabla \times \int_S \boldsymbol{a}(\boldsymbol{r}')g(k,\boldsymbol{r},\boldsymbol{r}')\mathrm{d}S(\boldsymbol{r}')\right]\,, \quad \boldsymbol{r} \in S\,.$$

Considering the null-field equations for the electric and magnetic fields in D_{i} and D_{s}, and passing to the boundary along a normal direction we obtain

$$\left(\frac{1}{2}I - \mathcal{M}_{\rm s}\right)\boldsymbol{e}_{\rm i} - \frac{\rm j}{k_0\varepsilon_{\rm s}}\mathcal{P}_{\rm s}\boldsymbol{h}_{\rm i} = \boldsymbol{e}_{\rm e}\,, \tag{2.26}$$

$$\left(\frac{1}{2}I - \mathcal{M}_{\rm s}\right)\boldsymbol{h}_{\rm i} + \frac{\rm j}{k_0\mu_{\rm s}}\mathcal{P}_{\rm s}\boldsymbol{e}_{\rm i} = \boldsymbol{h}_{\rm e}\,, \tag{2.27}$$

and

$$\left(\frac{1}{2}I + \mathcal{M}_{\rm i}\right)\boldsymbol{e}_{\rm i} + \frac{\rm j}{k_0\varepsilon_{\rm i}}\mathcal{P}_{\rm i}\boldsymbol{h}_{\rm i} = 0\,, \tag{2.28}$$

$$\left(\frac{1}{2}I + \mathcal{M}_{\rm i}\right)\boldsymbol{h}_{\rm i} - \frac{\rm j}{k_0\mu_{\rm i}}\mathcal{P}_{\rm i}\boldsymbol{e}_{\rm i} = 0\,, \tag{2.29}$$

respectively. These are four boundary integral equations for the unknowns $\boldsymbol{e}_{\rm i}$ and $\boldsymbol{h}_{\rm i}$, and we consider two linear combinations of equations, i.e.,

$$\alpha_1\,(2.26) + \alpha_2\,(2.27) + \alpha_3\,(2.29) \text{ and } \beta_1\,(2.26) + \beta_2(2.27) + \beta_3(2.28)\,,$$

where α_i and $\beta_i, i = 1, 2, 3$, are constants to be chosen. Harrington [97] describes several possible choices, as shown in Table 2.1, and for all these choices we always have existence and unique solvability [155].

The above approach for deriving a pair of boundary integral equations is known as the direct method. In contrast to the null-field method, the direct method considers the null-field equations in both domains $D_{\rm i}$ and $D_{\rm s}$, and treats the surface fields as independent unknowns. The indirect method for deriving a pair of boundary integral equations relies on the representation of the electromagnetic fields in terms of four surface fields. Passing to the boundary, using the boundary conditions on the particle surface and imposing two constraints on the surface fields, yields the desired pair of boundary integral equations [97]. It should be emphasized that single integral equations for the transmission boundary-value problem have also been derived by Marx [156], Mautz [157] and Martin and Ola [155]. Another major difference to the null-field method is the discretization of the boundary integral equations, which is achieved by using the method of moments [96]. The boundary surface is discretized into a set of surface elements and on each element, the surface fields are approximated by finite expansions of basis functions. Next, a set of

Table 2.1. Choice of constants for the boundary integral equations

Formulation	α_1	α_2	α_3	β_1	β_2	β_3
E-field	1	0	0	0	0	1
H-field	0	0	1	0	1	0
Combined field	0	1	-1	1	0	-1
Mautz–Harrington	0	1	$-\beta$	1	0	$-\alpha$
Müller	0	$\mu_{\rm s}$	$\mu_{\rm i}$	$\varepsilon_{\rm s}$	0	$\varepsilon_{\rm i}$

testing functions are defined and the scalar product of each testing function is formed with both sides of the equation being solved. This results in a system of equations which is referred to as the element matrix equations. The element matrices are assembled into the global matrix of the entire "structure" and the resulting system of equations is solved for the unknown expansion coefficients.

2.1.6 Spherical Particles

An interesting feature of the null-field method is that all matrix equations become considerably simpler and reduce to the corresponding equations of the Lorenz–Mie theory when the particle is spherically. For a spherical particle of radius R, the orthogonality relations of the vector spherical harmonics show that the $\boldsymbol{Q}^{pq}$ matrices are diagonal

$$(Q^{pq})^{12}_{mn,m_1n_1} = (Q^{pq})^{21}_{mn,m_1n_1} = 0$$

for all values of m, n, m_1 and n_1, and

$$\begin{aligned}\left(Q^{31}\right)^{11}_{mn,m_1n_1} = \mathrm{j}x \Big\{ & j_n\left(m_\mathrm{r}x\right)\left[xh_n^{(1)}\left(x\right)\right]' \\ & - h_n^{(1)}\left(x\right)\left[m_\mathrm{r}xj_n\left(m_\mathrm{r}x\right)\right]' \Big\} \delta_{mm_1}\delta_{nn_1}\,, \end{aligned} \tag{2.30}$$

$$\begin{aligned}\left(Q^{31}\right)^{22}_{mn,m_1n_1} = \frac{\mathrm{j}x}{m_r} \Big\{ & -h_n^{(1)}\left(x\right)\left[m_\mathrm{r}xj_n\left(m_\mathrm{r}x\right)\right]' \\ & + m_\mathrm{r}^2 j_n\left(m_\mathrm{r}x\right)\left[xh_n^{(1)}\left(x\right)\right]' \Big\} \delta_{mm_1}\delta_{nn_1}\,, \end{aligned} \tag{2.31}$$

$$\begin{aligned}\left(Q^{33}\right)^{11}_{mn,m_1n_1} = \mathrm{j}x \Big\{ & h_n^{(1)}\left(m_\mathrm{r}x\right)\left[xh_n^{(1)}\left(x\right)\right]' \\ & - h_n^{(1)}\left(x\right)\left[m_\mathrm{r}xh_n^{(1)}\left(m_\mathrm{r}x\right)\right]' \Big\} \delta_{mm_1}\delta_{nn_1}\,, \end{aligned} \tag{2.32}$$

$$\begin{aligned}\left(Q^{33}\right)^{22}_{mn,m_1n_1} = \frac{\mathrm{j}x}{m_\mathrm{r}} \Big\{ & -h_n^{(1)}\left(x\right)\left[m_\mathrm{r}xh_n^{(1)}\left(m_\mathrm{r}x\right)\right]' \\ & + m_\mathrm{r}^2 h_n^{(1)}\left(m_\mathrm{r}x\right)\left[xh_n^{(1)}\left(x\right)\right]' \Big\} \delta_{mm_1}\delta_{nn_1}\,, \end{aligned} \tag{2.33}$$

$$\begin{aligned}\left(Q^{11}\right)^{11}_{mn,m_1n_1} = \mathrm{j}x \Big\{ & j_n\left(m_\mathrm{r}x\right)\left[xj_n\left(x\right)\right]' \\ & - j_n\left(x\right)\left[m_\mathrm{r}xj_n\left(m_\mathrm{r}x\right)\right]' \Big\} \delta_{mm_1}\delta_{nn_1}\,, \end{aligned} \tag{2.34}$$

$$\left(Q^{11}\right)^{22}_{mn,m_1n_1} = \frac{\mathrm{j}x}{m_\mathrm{r}} \left\{ -j_n\left(x\right)\left[m_\mathrm{r}xj_n\left(m_\mathrm{r}x\right)\right]' + m_\mathrm{r}^2 j_n\left(m_\mathrm{r}x\right)\left[xj_n\left(x\right)\right]' \right\} \delta_{mm_1}\delta_{nn_1}\,, \tag{2.35}$$

and

$$\left(Q^{13}\right)^{11}_{mn,m_1n_1} = \mathrm{j}x \left\{ h_n^{(1)}\left(m_\mathrm{r}x\right)\left[xj_n\left(x\right)\right]' - j_n\left(x\right)\left[m_\mathrm{r}xh_n^{(1)}\left(m_\mathrm{r}x\right)\right]' \right\} \delta_{mm_1}\delta_{nn_1}\,, \tag{2.36}$$

$$\left(Q^{13}\right)^{22}_{mn,m_1n_1} = \frac{\mathrm{j}x}{m_\mathrm{r}} \left\{ -j_n\left(x\right)\left[m_\mathrm{r}xh_n^{(1)}\left(m_\mathrm{r}x\right)\right]' + m_\mathrm{r}^2 h_n^{(1)}\left(m_\mathrm{r}x\right)\left[xj_n\left(x\right)\right]' \right\} \delta_{mm_1}\delta_{nn_1}\,, \tag{2.37}$$

where $x = k_\mathrm{s}R$ is the size parameter and

$$m_\mathrm{r} = \sqrt{\frac{\varepsilon_\mathrm{i}}{\varepsilon_\mathrm{s}}}$$

is the relative refractive index of the particle with respect to the ambient medium. The above relations are not suitable for computing the $\boldsymbol{Q}^{pq}$ matrices. Denoting by A_n and B_n the logarithmic derivatives [2, 17]

$$A_n(x) = \frac{\mathrm{d}}{\mathrm{d}x}\left\{\ln\left[xj_n\left(x\right)\right]\right\} = \frac{\left[xj_n\left(x\right)\right]'}{xj_n(x)}\,,$$

$$B_n(x) = \frac{\mathrm{d}}{\mathrm{d}x}\left\{\ln\left[xh_n^{(1)}\left(x\right)\right]\right\} = \frac{\left[xh_n^{(1)}\left(x\right)\right]'}{xh_n^{(1)}(x)}\,,$$

and using the recurrence relation (cf. (A.8))

$$\left[xz_n\left(x\right)\right]' = xz_{n-1}(x) - nz_n(x)\,,$$

where z_n stands for j_n or $h_n^{(1)}$, we rewrite (2.30)–(2.37) as

$$\left(Q^{31}\right)^{11}_{mn,m_1n_1} = -\mathrm{j}x^2 j_n\left(m_\mathrm{r}x\right)\left\{\left[m_\mathrm{r}A_n\left(m_\mathrm{r}x\right) + \frac{n}{x}\right]h_n^{(1)}\left(x\right) - h_{n-1}^{(1)}\left(x\right)\right\}\delta_{mm_1}\delta_{nn_1}\,, \tag{2.38}$$

$$\left(Q^{31}\right)^{22}_{mn,m_1n_1} = -\mathrm{j}m_\mathrm{r}x^2 j_n\left(m_\mathrm{r}x\right)\left\{\left[\frac{A_n\left(m_\mathrm{r}x\right)}{m_\mathrm{r}} + \frac{n}{x}\right]h_n^{(1)}\left(x\right) - h_{n-1}^{(1)}\left(x\right)\right\}\delta_{mm_1}\delta_{nn_1}\,, \tag{2.39}$$

$$\left(Q^{33}\right)^{11}_{mn,m_1n_1} = -\mathrm{j}x^2 h_n^{(1)}\left(m_\mathrm{r}x\right)\left\{\left[m_\mathrm{r}B_n\left(m_\mathrm{r}x\right)+\frac{n}{x}\right]h_n^{(1)}\left(x\right) - h_{n-1}^{(1)}\left(x\right)\right\}\delta_{mm_1}\delta_{nn_1}\,, \tag{2.40}$$

$$\left(Q^{33}\right)^{22}_{mn,m_1n_1} = -\mathrm{j}m_\mathrm{r}x^2 h_n^{(1)}\left(m_\mathrm{r}x\right)\left\{\left[\frac{B_n\left(m_\mathrm{r}x\right)}{m_\mathrm{r}}+\frac{n}{x}\right]h_n^{(1)}\left(x\right) - h_{n-1}^{(1)}\left(x\right)\right\}\delta_{mm_1}\delta_{nn_1}\,, \tag{2.41}$$

$$\left(Q^{11}\right)^{11}_{mn,m_1n_1} = -\mathrm{j}x^2 j_n\left(m_\mathrm{r}x\right)\left\{\left[m_\mathrm{r}A_n\left(m_\mathrm{r}x\right)+\frac{n}{x}\right]j_n\left(x\right) - j_{n-1}\left(x\right)\right\}\delta_{mm_1}\delta_{nn_1}\,, \tag{2.42}$$

$$\left(Q^{11}\right)^{22}_{mn,m_1n_1} = -\mathrm{j}m_\mathrm{r}x^2 j_n\left(m_\mathrm{r}x\right)\left\{\left[\frac{A_n\left(m_\mathrm{r}x\right)}{m_\mathrm{r}}+\frac{n}{x}\right]j_n\left(x\right) - j_{n-1}\left(x\right)\right\}\delta_{mm_1}\delta_{nn_1}\,, \tag{2.43}$$

and

$$\left(Q^{13}\right)^{11}_{mn,m_1n_1} = -\mathrm{j}x^2 h_n^{(1)}\left(m_\mathrm{r}x\right)\left\{\left[m_\mathrm{r}B_n\left(m_\mathrm{r}x\right)+\frac{n}{x}\right]j_n\left(x\right) - j_{n-1}\left(x\right)\right\}\delta_{mm_1}\delta_{nn_1}\,, \tag{2.44}$$

$$\left(Q^{13}\right)^{22}_{mn,m_1n_1} = -\mathrm{j}m_\mathrm{r}x^2 h_n^{(1)}\left(m_\mathrm{r}x\right)\left\{\left[\frac{B_n\left(m_\mathrm{r}x\right)}{m_\mathrm{r}}+\frac{n}{x}\right]j_n\left(x\right) - j_{n-1}\left(x\right)\right\}\delta_{mm_1}\delta_{nn_1}\,. \tag{2.45}$$

The functions A_n and B_n satisfy the recurrence relation

$$\Psi_n(x) = \frac{n+1}{x} - \frac{1}{\Psi_{n+1}(x)+\frac{n+1}{x}}\,,$$

where Ψ_n stands for A_n and B_n, and a stable scheme for computing Ψ_n relies on a downward recursion. Beginning with an estimate for Ψ_n, where n is larger that the number of terms required for convergence, successively lower-order logarithmic derivatives can be generated by downward recursion. It should be noted that the downward stability of Ψ_n is a consequence of the downward stability of the spherical Bessel functions j_n (see Appendix A).

The transition matrix of a spherical particle is diagonal with entries

$$T^{11}_{mn,m_1n_1} = T^1_n\delta_{mm_1}\delta_{nn_1}\,,$$
$$T^{22}_{mn,m_1n_1} = T^2_n\delta_{mm_1}\delta_{nn_1}\,,$$

where

$$T_n^1 = -\frac{\left[m_\mathrm{r} A_n\left(m_\mathrm{r} x\right) + \frac{n}{x}\right] j_n\left(x\right) - j_{n-1}\left(x\right)}{\left[m_\mathrm{r} A_n\left(m_\mathrm{r} x\right) + \frac{n}{x}\right] h_n^{(1)}\left(x\right) - h_{n-1}^{(1)}\left(x\right)} \tag{2.46}$$

and

$$T_n^2 = -\frac{\left[\frac{A_n(m_\mathrm{r} x)}{m_\mathrm{r}} + \frac{n}{x}\right] j_n\left(x\right) - j_{n-1}\left(x\right)}{\left[\frac{A_n(m_\mathrm{r} x)}{m_\mathrm{r}} + \frac{n}{x}\right] h_n^{(1)}\left(x\right) - h_{n-1}^{(1)}\left(x\right)}\,. \tag{2.47}$$

Equations (2.46) and (2.47) relating the transition matrix to the size parameter and relative refractive index are identical to the expressions of the Lorenz–Mie coefficients given by Bohren and Huffman [17].

2.2 Homogeneous and Chiral Particles

The problem of scattering by isotropic, chiral spheres has been treated by Bohren [16], and Bohren and Huffman [17] using rigorous electromagnetic field-theoretical calculations, while the analysis of nonspherical, isotropic, chiral particles has been rendered by Lakhtakia et al. [135]. To account for chirality, the surface fields have been approximated by left- and right-circularly polarized fields and the same technique is employed in our analysis. The transmission boundary-value problem for a homogeneous and isotropic, chiral particle has the following formulation.

Given $\boldsymbol{E}_\mathrm{e}, \boldsymbol{H}_\mathrm{e}$ *as an entire solution to the Maxwell equations representing the external excitation, find the vector fields* $\boldsymbol{E}_\mathrm{s}, \boldsymbol{H}_\mathrm{s}$ *and* $\boldsymbol{E}_\mathrm{i}, \boldsymbol{H}_\mathrm{i}$ *satisfying the Maxwell equations*

$$\nabla \times \boldsymbol{E}_\mathrm{s} = \mathrm{j}k_0\mu_\mathrm{s}\boldsymbol{H}_\mathrm{s}\,, \quad \nabla \times \boldsymbol{H}_\mathrm{s} = -\mathrm{j}k_0\varepsilon_\mathrm{s}\boldsymbol{E}_\mathrm{s} \tag{2.48}$$

in D_s, *and*

$$\nabla \times \begin{bmatrix} \boldsymbol{E}_\mathrm{i} \\ \boldsymbol{H}_\mathrm{i} \end{bmatrix} = \boldsymbol{K} \begin{bmatrix} \boldsymbol{E}_\mathrm{i} \\ \boldsymbol{H}_\mathrm{i} \end{bmatrix} \tag{2.49}$$

in D_i, *where*

$$\boldsymbol{K} = \frac{1}{1-\beta^2 k_\mathrm{i}^2} \begin{bmatrix} \beta k_\mathrm{i}^2 & \mathrm{j}k_0\mu_\mathrm{i} \\ -\mathrm{j}k_0\varepsilon_\mathrm{i} & \beta k_\mathrm{i}^2 \end{bmatrix}\,. \tag{2.50}$$

In addition, the vector fields must satisfy the transmission conditions (2.2) and the Silver–Müller radiation condition (2.3).

Applications of the extinction theorem and Huygens principle yield the null-field equations (2.6) and the integral representations for the scattered field coefficients (2.16). Taking into account that the electromagnetic fields propagating in an isotropic, chiral medium can be expressed as a superposition of vector spherical wave functions of left- and right-handed type (cf. Sect. 1.3), we represent the approximate surface fields as

$$\begin{pmatrix} \boldsymbol{e}_{\mathrm{i}}^{N}(\boldsymbol{r}') \\ \boldsymbol{h}_{\mathrm{i}}^{N}(\boldsymbol{r}') \end{pmatrix} = \sum_{\mu=1}^{N} c_{\mu}^{N} \begin{pmatrix} \boldsymbol{n}(\boldsymbol{r}') \times \boldsymbol{L}_{\mu}(k_{\mathrm{Li}}\boldsymbol{r}') \\ -\mathrm{j}\sqrt{\frac{\varepsilon_{\mathrm{i}}}{\mu_{\mathrm{i}}}}\boldsymbol{n}(\boldsymbol{r}') \times \boldsymbol{L}_{\mu}(k_{\mathrm{Li}}\boldsymbol{r}') \end{pmatrix} + d_{\mu}^{N} \begin{pmatrix} \boldsymbol{n}(\boldsymbol{r}') \times \boldsymbol{R}_{\mu}(k_{\mathrm{Ri}}\boldsymbol{r}') \\ \mathrm{j}\sqrt{\frac{\varepsilon_{\mathrm{i}}}{\mu_{\mathrm{i}}}}\boldsymbol{n}(\boldsymbol{r}') \times \boldsymbol{R}_{\mu}(k_{\mathrm{Ri}}\boldsymbol{r}') \end{pmatrix},$$

where $\boldsymbol{L}_{\mu}$ and $\boldsymbol{R}_{\mu}$ are given by (1.58) and (1.59), respectively, and

$$k_{\mathrm{Li}} = \frac{k_{\mathrm{i}}}{1-\beta k_{\mathrm{i}}}, \quad k_{\mathrm{Ri}} = \frac{k_{\mathrm{i}}}{1+\beta k_{\mathrm{i}}}$$

are the wave numbers of the left- and right-handed type waves. The transition matrix of a homogeneous, chiral particle then becomes

$$\boldsymbol{T} = -\boldsymbol{Q}_{\mathrm{chiral}}^{11}(k_{\mathrm{s}}, k_{\mathrm{i}}) \left[\boldsymbol{Q}_{\mathrm{chiral}}^{31}(k_{\mathrm{s}}, k_{\mathrm{i}})\right]^{-1},$$

where, for $\mu_{\mathrm{i}} = \mu_{\mathrm{s}}$, the elements of the $\boldsymbol{Q}_{\mathrm{chiral}}^{31}$ matrix are given by

$$\left(Q_{\mathrm{chiral}}^{31}\right)_{\nu\mu}^{11} = \frac{\mathrm{j}k_{\mathrm{s}}^{2}}{\pi} \int_{S} \Big\{ [\boldsymbol{n}(\boldsymbol{r}') \times \boldsymbol{L}_{\mu}(k_{\mathrm{Li}}\boldsymbol{r}')] \cdot \boldsymbol{N}_{\overline{\nu}}^{3}(k_{\mathrm{s}}\boldsymbol{r}') + \sqrt{\frac{\varepsilon_{\mathrm{i}}}{\varepsilon_{\mathrm{s}}}} [\boldsymbol{n}(\boldsymbol{r}') \times \boldsymbol{L}_{\mu}(k_{\mathrm{Li}}\boldsymbol{r}')] \cdot \boldsymbol{M}_{\overline{\nu}}^{3}(k_{\mathrm{s}}\boldsymbol{r}') \Big\} \mathrm{d}S(\boldsymbol{r}'), \quad (2.51)$$

$$\left(Q_{\mathrm{chiral}}^{31}\right)_{\nu\mu}^{12} = \frac{\mathrm{j}k_{\mathrm{s}}^{2}}{\pi} \int_{S} \Big\{ [\boldsymbol{n}(\boldsymbol{r}') \times \boldsymbol{R}_{\mu}(k_{\mathrm{Ri}}\boldsymbol{r}')] \cdot \boldsymbol{N}_{\overline{\nu}}^{3}(k_{\mathrm{s}}\boldsymbol{r}') - \sqrt{\frac{\varepsilon_{\mathrm{i}}}{\varepsilon_{\mathrm{s}}}} [\boldsymbol{n}(\boldsymbol{r}') \times \boldsymbol{R}_{\mu}(k_{\mathrm{Ri}}\boldsymbol{r}')] \cdot \boldsymbol{M}_{\overline{\nu}}^{3}(k_{\mathrm{s}}\boldsymbol{r}') \Big\} \mathrm{d}S(\boldsymbol{r}'), \quad (2.52)$$

$$\left(Q_{\mathrm{chiral}}^{31}\right)_{\nu\mu}^{21} = \frac{\mathrm{j}k_{\mathrm{s}}^{2}}{\pi} \int_{S} \Big\{ [\boldsymbol{n}(\boldsymbol{r}') \times \boldsymbol{L}_{\mu}(k_{\mathrm{Li}}\boldsymbol{r}')] \cdot \boldsymbol{M}_{\overline{\nu}}^{3}(k_{\mathrm{s}}\boldsymbol{r}') + \sqrt{\frac{\varepsilon_{\mathrm{i}}}{\varepsilon_{\mathrm{s}}}} [\boldsymbol{n}(\boldsymbol{r}') \times \boldsymbol{L}_{\mu}(k_{\mathrm{Li}}\boldsymbol{r}')] \cdot \boldsymbol{N}_{\overline{\nu}}^{3}(k_{\mathrm{s}}\boldsymbol{r}') \Big\} \mathrm{d}S(\boldsymbol{r}'), \quad (2.53)$$

and

$$\left(Q_{\mathrm{chiral}}^{31}\right)_{\nu\mu}^{22} = \frac{\mathrm{j}k_{\mathrm{s}}^{2}}{\pi} \int_{S} \Big\{ [\boldsymbol{n}(\boldsymbol{r}') \times \boldsymbol{R}_{\mu}(k_{\mathrm{Ri}}\boldsymbol{r}')] \cdot \boldsymbol{M}_{\overline{\nu}}^{3}(k_{\mathrm{s}}\boldsymbol{r}') - \sqrt{\frac{\varepsilon_{\mathrm{i}}}{\varepsilon_{\mathrm{s}}}} [\boldsymbol{n}(\boldsymbol{r}') \times \boldsymbol{R}_{\mu}(k_{\mathrm{Ri}}\boldsymbol{r}')] \cdot \boldsymbol{N}_{\overline{\nu}}^{3}(k_{\mathrm{s}}\boldsymbol{r}') \Big\} \mathrm{d}S(\boldsymbol{r}'). \quad (2.54)$$

The expressions of the elements of the $\boldsymbol{Q}_{\mathrm{chiral}}^{11}$ matrix are similar but with $\boldsymbol{M}_{\overline{\nu}}^{1}$ and $\boldsymbol{N}_{\overline{\nu}}^{1}$ in place of $\boldsymbol{M}_{\overline{\nu}}^{3}$ and $\boldsymbol{N}_{\overline{\nu}}^{3}$, respectively. It must be noted that in case the

particle is spherical, the transition matrix becomes diagonal, and the resulting solution tallies exactly with that given by Bohren [16] for chiral spheres. In addition, if $\beta = 0$, i.e., the particle becomes a nonchiral sphere, the Lorenz–Mie series solution is obtained. Finally, simply by setting $k_{\mathrm{Li}} = k_{\mathrm{Ri}} = k_{\mathrm{i}}$ and $\beta = 0$, the solution for a nonspherical, nonchiral particles is recovered. In our analysis, the ambient medium is nonchiral and a generalization of the present approach to the scattering by a chiral particle in a chiral host medium has been addressed by Lakhtakia [128].

2.3 Homogeneous and Anisotropic Particles

The scattering by anisotropic particles is mostly restricted to simple shapes such as cylinders [232] or spheres [265]. Liu et al. [143] solved the electromagnetic fields in a rotationally uniaxial medium by using the method of separation of variables, while Piller and Martin [193] analyzed three-dimensional anisotropic particles by using the generalized multipole technique. In our analysis we follow the treatment of Kiselev et al. [119] which solved the scattering problem of radially and uniformly anisotropic spheres by using the vector quasi-spherical wave functions for internal field representation. The transmission boundary-value problem for a homogeneous and uniaxial anisotropic particle has the following formulation.

Given $\boldsymbol{E}_{\mathrm{e}}, \boldsymbol{H}_{\mathrm{e}}$ as an entire solution to the Maxwell equations representing the external excitation, find the vector fields $\boldsymbol{E}_{\mathrm{s}}, \boldsymbol{H}_{\mathrm{s}}$ and $\boldsymbol{E}_{\mathrm{i}}, \boldsymbol{H}_{\mathrm{i}}$ satisfying the Maxwell equations

$$\nabla \times \boldsymbol{E}_{\mathrm{s}} = \mathrm{j}k_0\mu_{\mathrm{s}}\boldsymbol{H}_{\mathrm{s}}\,, \quad \nabla \times \boldsymbol{H}_{\mathrm{s}} = -\mathrm{j}k_0\varepsilon_{\mathrm{s}}\boldsymbol{E}_{\mathrm{s}} \tag{2.55}$$

in D_{s}, and

$$\begin{aligned} &\nabla \times \boldsymbol{E}_{\mathrm{i}} = \mathrm{j}k_0\boldsymbol{B}_{\mathrm{i}}\,, \quad \nabla \times \boldsymbol{H}_{\mathrm{i}} = -\mathrm{j}k_0\boldsymbol{D}_{\mathrm{i}}\,, \\ &\nabla \cdot \boldsymbol{B}_{\mathrm{i}} = 0\,, \quad \nabla \cdot \boldsymbol{D}_{\mathrm{i}} = 0 \end{aligned} \tag{2.56}$$

in D_{i}, where

$$\boldsymbol{D}_{\mathrm{i}} = \overline{\varepsilon}_{\mathrm{i}}\boldsymbol{E}_{\mathrm{i}}\,, \quad \boldsymbol{B}_{\mathrm{i}} = \mu_{\mathrm{i}}\boldsymbol{H}_{\mathrm{i}}\,, \tag{2.57}$$

and

$$\overline{\varepsilon}_{\mathrm{i}} = \begin{bmatrix} \varepsilon_{\mathrm{i}} & 0 & 0 \\ 0 & \varepsilon_{\mathrm{i}} & 0 \\ 0 & 0 & \varepsilon_{\mathrm{i}z} \end{bmatrix}. \tag{2.58}$$

In addition, the vector fields must satisfy the transmission conditions (2.2) and the Silver–Müller radiation condition (2.3).

Considering the null-field equations (2.6) and the integral representations for the scattered field coefficients (2.16), and taking into account the results

established in Sect. 1.3 regarding the series representations of the electromagnetic fields propagating in anisotropic media, we see that the scattering problem can be solved if we approximate the surface fields by finite expansions of vector quasi-spherical wave functions $\boldsymbol{X}_{mn}^{\mathrm{e,h}}$ and $\boldsymbol{Y}_{mn}^{\mathrm{e,h}}$ (cf. (1.48)–(1.53)),

$$\begin{pmatrix} \boldsymbol{e}_{\mathrm{i}}^{N}(\boldsymbol{r}') \\ \boldsymbol{h}_{\mathrm{i}}^{N}(\boldsymbol{r}') \end{pmatrix} = \sum_{\mu=1}^{N} c_{\mu}^{N} \begin{pmatrix} \boldsymbol{n}(\boldsymbol{r}') \times \boldsymbol{X}_{\mu}^{\mathrm{e}}(\boldsymbol{r}') \\ -\mathrm{j}\sqrt{\frac{\varepsilon_{\mathrm{i}}}{\mu_{\mathrm{i}}}}\boldsymbol{n}(\boldsymbol{r}') \times \boldsymbol{X}_{\mu}^{\mathrm{h}}(\boldsymbol{r}') \end{pmatrix} + d_{\mu}^{N} \begin{pmatrix} \boldsymbol{n}(\boldsymbol{r}') \times \boldsymbol{Y}_{\mu}^{\mathrm{e}}(\boldsymbol{r}') \\ -\mathrm{j}\sqrt{\frac{\varepsilon_{\mathrm{i}}}{\mu_{\mathrm{i}}}}\boldsymbol{n}(\boldsymbol{r}') \times \boldsymbol{Y}_{\mu}^{\mathrm{h}}(\boldsymbol{r}') \end{pmatrix}.$$

The transition matrix of an uniaxial anisotropic particle then becomes

$$\boldsymbol{T} = -\boldsymbol{Q}_{\mathrm{anis}}^{11}(k_{\mathrm{s}}, k_{\mathrm{i}}, m_{\mathrm{r}z}) \left[\boldsymbol{Q}_{\mathrm{anis}}^{31}(k_{\mathrm{s}}, k_{\mathrm{i}}, m_{\mathrm{r}z})\right]^{-1},$$

where $m_{\mathrm{r}z} = \sqrt{\varepsilon_{\mathrm{i}z}/\varepsilon_{\mathrm{s}}}$, and for $\mu_{\mathrm{i}} = \mu_{\mathrm{s}}$, the elements of the $\boldsymbol{Q}_{\mathrm{anis}}^{31}$ matrix are given by

$$\left(Q_{\mathrm{anis}}^{31}\right)_{\nu\mu}^{11} = \frac{\mathrm{j}k_{\mathrm{s}}^2}{\pi} \int_S \left[\left(\boldsymbol{n} \times \boldsymbol{X}_{\mu}^{\mathrm{e}}\right) \cdot \boldsymbol{N}_{\nu}^{3} + \sqrt{\frac{\varepsilon_{\mathrm{i}}}{\varepsilon_{\mathrm{s}}}} \left(\boldsymbol{n} \times \boldsymbol{X}_{\mu}^{\mathrm{h}}\right) \cdot \boldsymbol{M}_{\nu}^{3}\right] \mathrm{d}S, \quad (2.59)$$

$$\left(Q_{\mathrm{anis}}^{31}\right)_{\nu\mu}^{12} = \frac{\mathrm{j}k_{\mathrm{s}}^2}{\pi} \int_S \left[\left(\boldsymbol{n} \times \boldsymbol{Y}_{\mu}^{\mathrm{e}}\right) \cdot \boldsymbol{N}_{\nu}^{3} + \sqrt{\frac{\varepsilon_{\mathrm{i}}}{\varepsilon_{\mathrm{s}}}} \left(\boldsymbol{n} \times \boldsymbol{Y}_{\mu}^{\mathrm{h}}\right) \cdot \boldsymbol{M}_{\nu}^{3}\right] \mathrm{d}S, \quad (2.60)$$

$$\left(Q_{\mathrm{anis}}^{31}\right)_{\nu\mu}^{21} = \frac{\mathrm{j}k_{\mathrm{s}}^2}{\pi} \int_S \left[\left(\boldsymbol{n} \times \boldsymbol{X}_{\mu}^{\mathrm{e}}\right) \cdot \boldsymbol{M}_{\nu}^{3} + \sqrt{\frac{\varepsilon_{\mathrm{i}}}{\varepsilon_{\mathrm{s}}}} \left(\boldsymbol{n} \times \boldsymbol{X}_{\mu}^{\mathrm{h}}\right) \cdot \boldsymbol{N}_{\nu}^{3}\right] \mathrm{d}S, \quad (2.61)$$

and

$$\left(Q_{\mathrm{anis}}^{31}\right)_{\nu\mu}^{22} = \frac{\mathrm{j}k_{\mathrm{s}}^2}{\pi} \int_S \left[\left(\boldsymbol{n} \times \boldsymbol{Y}_{\mu}^{\mathrm{e}}\right) \cdot \boldsymbol{M}_{\nu}^{3} + \sqrt{\frac{\varepsilon_{\mathrm{i}}}{\varepsilon_{\mathrm{s}}}} \left(\boldsymbol{n} \times \boldsymbol{Y}_{\mu}^{\mathrm{h}}\right) \cdot \boldsymbol{N}_{\nu}^{3}\right] \mathrm{d}S. \quad (2.62)$$

The expressions of the elements of the $\boldsymbol{Q}_{\mathrm{anis}}^{11}$ matrix are similar but with $\boldsymbol{M}_{\nu}^{1}$ and $\boldsymbol{N}_{\nu}^{1}$ in place of $\boldsymbol{M}_{\nu}^{3}$ and $\boldsymbol{N}_{\nu}^{3}$, respectively. Using the properties of the vector quasi-spherical wave functions (cf. (1.47)) it is simple to show that for $\varepsilon_{\mathrm{i}z} = \varepsilon_{\mathrm{i}}$, the present approach leads to the $\boldsymbol{T}$-matrix solution of an isotropic particle.

2.4 Inhomogeneous Particles

In this section, we consider electromagnetic scattering by an arbitrarily shaped, inhomogeneous particle with an irregular inclusion. Our treatment follows the analysis of Peterson and Ström [189] for multilayered particles and is similar to the approach used by Videen et al. [243] for a sphere with an irregular inclusion. Note that an alternative derivation using the Schelkunoff's equivalence principle has been given by Wang and Barber [248].

2.4.1 Formulation with Addition Theorem

In the present analysis we will derive the expression of the transition matrix by using the translation properties of the vector spherical wave functions. The completeness property of the vector spherical wave functions on two enclosing surfaces, which is essential in our analysis, is established in Appendix D.

The scattering problem is depicted in Fig. 2.2. The surface S_1 is defined with respect to a Cartesian coordinate system $O_1x_1y_1z_1$, while the surface S_2 is defined with respect to a Cartesian coordinate system $O_2x_2y_2z_2$. By assumption, the coordinate system $O_2x_2y_2z_2$ is obtained by translating the coordinate system $O_1x_1y_1z_1$ through $\boldsymbol{r}_{12}$ and by rotating the translated coordinate system through the Euler angles α, β and γ. The boundary-value problem for the inhomogeneous particle depicted in Fig. 2.2 has the following formulation.

Given the external excitation $\boldsymbol{E}_{\rm e}, \boldsymbol{H}_{\rm e}$ *as an entire solution to the Maxwell equations, find the scattered field* $\boldsymbol{E}_{\rm s}$, $\boldsymbol{H}_{\rm s}$ *and the internal fields* $\boldsymbol{E}_{\rm i,1}$, $\boldsymbol{H}_{\rm i,1}$ *and* $\boldsymbol{E}_{\rm i,2}$, $\boldsymbol{H}_{\rm i,2}$ *satisfying the Maxwell equations*

$$\nabla \times \boldsymbol{E}_{\rm s} = {\rm j}k_0\mu_{\rm s}\boldsymbol{H}_{\rm s}\,, \quad \nabla \times \boldsymbol{H}_{\rm s} = -{\rm j}k_0\varepsilon_{\rm s}\boldsymbol{E}_{\rm s} \quad in \quad D_{\rm s}\,, \tag{2.63}$$

$$\nabla \times \boldsymbol{E}_{\rm i,1} = {\rm j}k_0\mu_{\rm i,1}\boldsymbol{H}_{\rm i,1}\,, \quad \nabla \times \boldsymbol{H}_{\rm i,1} = -{\rm j}k_0\varepsilon_{\rm i,1}\boldsymbol{E}_{\rm i,1} \quad in \quad D_{\rm i,1}\,, \tag{2.64}$$

and

$$\nabla \times \boldsymbol{E}_{\rm i,2} = {\rm j}k_0\mu_{\rm i,2}\boldsymbol{H}_{\rm i,2}\,, \quad \nabla \times \boldsymbol{H}_{\rm i,2} = -{\rm j}k_0\varepsilon_{\rm i,2}\boldsymbol{E}_{\rm i,2} \quad in \quad D_{\rm i,2}\,, \tag{2.65}$$

the boundary conditions

$$\begin{aligned} \boldsymbol{n}_1 \times \boldsymbol{E}_{\rm i,1} - \boldsymbol{n}_1 \times \boldsymbol{E}_{\rm s} &= \boldsymbol{n}_1 \times \boldsymbol{E}_{\rm e}\,, \\ \boldsymbol{n}_1 \times \boldsymbol{H}_{\rm i,1} - \boldsymbol{n}_1 \times \boldsymbol{H}_{\rm s} &= \boldsymbol{n}_1 \times \boldsymbol{H}_{\rm e}\,, \end{aligned} \tag{2.66}$$

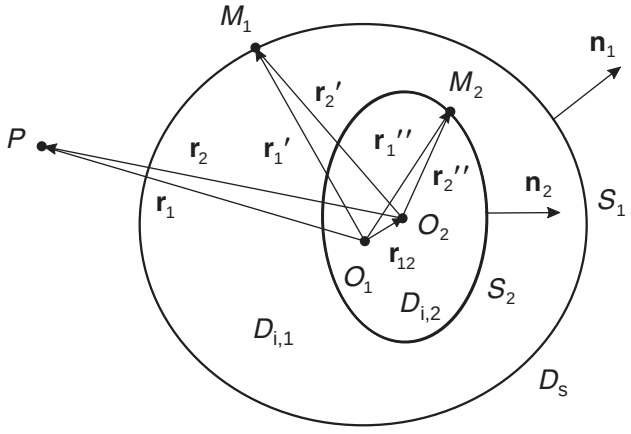

Fig. 2.2. Geometry of an inhomogeneous particle

on S_1 *and*

$$\begin{aligned} \boldsymbol{n}_2 \times \boldsymbol{E}_{\mathrm{i},1} &= \boldsymbol{n}_2 \times \boldsymbol{E}_{\mathrm{i},2}\,, \\ \boldsymbol{n}_2 \times \boldsymbol{H}_{\mathrm{i},1} &= \boldsymbol{n}_2 \times \boldsymbol{H}_{\mathrm{i},2}\,, \end{aligned} \tag{2.67}$$

onS_2, *and the Silver–Müller radiation condition for the scattered field (2.3).*

The Stratton–Chu representation theorem for the scattered field $\boldsymbol{E}_{\mathrm{s}}$ in D_{i}, where $D_{\mathrm{i}} = D_{\mathrm{i},1} \cup D_{\mathrm{i},2} \cup S_2 = D_{\mathrm{i},1} \cup \overline{D}_{\mathrm{i},2} = \boldsymbol{R}^3 - \overline{D}_{\mathrm{s}}$, together with the boundary conditions (2.66), yield the general null-field equation

$$\begin{aligned} &\boldsymbol{E}_{\mathrm{e}}(\boldsymbol{r}_1) + \nabla_1 \times \int_{S_1} \boldsymbol{e}_{\mathrm{i},1}\,(\boldsymbol{r}_1')\, g\,(k_{\mathrm{s}}, \boldsymbol{r}_1, \boldsymbol{r}_1')\, \mathrm{d}S\,(\boldsymbol{r}_1') \\ &+ \frac{\mathrm{j}}{k_0 \varepsilon_{\mathrm{s}}} \nabla_1 \times \nabla_1 \times \int_{S_1} \boldsymbol{h}_{\mathrm{i},1}\,(\boldsymbol{r}_1')\, g\,(k_{\mathrm{s}}, \boldsymbol{r}_1, \boldsymbol{r}_1')\, \mathrm{d}S\,(\boldsymbol{r}_1') = 0\,, \quad \boldsymbol{r}_1 \in D_{\mathrm{i}}\,, \end{aligned} \tag{2.68}$$

while the Stratton–Chu representation theorem for the internal field $\boldsymbol{E}_{\mathrm{i},1}$ in D_{s} and $D_{\mathrm{i},2}$ together with the boundary conditions (2.67), give the general null-field equation

$$\begin{aligned} &-\nabla_1 \times \int_{S_1} \boldsymbol{e}_{\mathrm{i},1}\,(\boldsymbol{r}_1')\, g\,(k_{\mathrm{i},1}, \boldsymbol{r}_1, \boldsymbol{r}_1')\, \mathrm{d}S\,(\boldsymbol{r}_1') \\ &- \frac{\mathrm{j}}{k_0 \varepsilon_{\mathrm{i},1}} \nabla_1 \times \nabla_1 \times \int_{S_1} \boldsymbol{h}_{\mathrm{i},1}\,(\boldsymbol{r}_1')\, g\,(k_{\mathrm{i},1}, \boldsymbol{r}_1, \boldsymbol{r}_1')\, \mathrm{d}S\,(\boldsymbol{r}_1') \\ &+ \nabla_1 \times \int_{S_2} \boldsymbol{e}_{\mathrm{i},2}\,(\boldsymbol{r}_1'')\, g\,(k_{\mathrm{i},1}, \boldsymbol{r}_1, \boldsymbol{r}_1'')\, \mathrm{d}S\,(\boldsymbol{r}_1'') \\ &+ \frac{\mathrm{j}}{k_0 \varepsilon_{\mathrm{i},2}} \nabla_1 \times \nabla_1 \times \int_{S_2} \boldsymbol{h}_{\mathrm{i},2}\,(\boldsymbol{r}_1'')\, g\,(k_{\mathrm{i},1}, \boldsymbol{r}_1, \boldsymbol{r}_1'')\, \mathrm{d}S\,(\boldsymbol{r}_1'') = 0\,, \quad \boldsymbol{r}_1 \in D_{\mathrm{s}} \cup D_{\mathrm{i},2}\,. \end{aligned} \tag{2.69}$$

In (2.68) and (2.69), the surface fields are the tangential components of the electromagnetic fields in $D_{\mathrm{i},1}$ and $D_{\mathrm{i},2}$

$$\boldsymbol{e}_{\mathrm{i},1} = \boldsymbol{n}_1 \times \boldsymbol{E}_{\mathrm{i},1}\,, \quad \boldsymbol{h}_{\mathrm{i},1} = \boldsymbol{n}_1 \times \boldsymbol{H}_{\mathrm{i},1} \quad \text{on} \quad S_1$$

and

$$\boldsymbol{e}_{\mathrm{i},2} = \boldsymbol{n}_2 \times \boldsymbol{E}_{\mathrm{i},2}, \quad \boldsymbol{h}_{\mathrm{i},2} = \boldsymbol{n}_2 \times \boldsymbol{H}_{\mathrm{i},2} \quad \text{on} \quad S_2\,,$$

respectively.

Considering the general null-field equation (2.68), we use the vector spherical wave expansions of the incident field and of the dyad $g\overline{\boldsymbol{I}}$ on a sphere enclosed in D_i, to obtain

$$\begin{aligned} &\frac{\mathrm{j}k_{\mathrm{s}}^2}{\pi} \int_{S_1} \left[\boldsymbol{e}_{\mathrm{i},1}\,(\boldsymbol{r}_1') \cdot \begin{pmatrix} \boldsymbol{N}_{\nu}^3\,(k_{\mathrm{s}}\boldsymbol{r}_1') \\ \boldsymbol{M}_{\nu}^3\,(k_{\mathrm{s}}\boldsymbol{r}_1') \end{pmatrix} \right. \\ &\left. + \mathrm{j}\sqrt{\frac{\mu_{\mathrm{s}}}{\varepsilon_{\mathrm{s}}}}\, \boldsymbol{h}_{\mathrm{i},1}\,(\boldsymbol{r}_1') \cdot \begin{pmatrix} \boldsymbol{M}_{\nu}^3\,(k_{\mathrm{s}}\boldsymbol{r}_1') \\ \boldsymbol{N}_{\nu}^3\,(k_{\mathrm{s}}\boldsymbol{r}_1') \end{pmatrix} \right] \mathrm{d}S\,(\boldsymbol{r}_1') = -\begin{pmatrix} a_\nu \\ b_\nu \end{pmatrix}, \quad \nu = 1, 2, \ldots \end{aligned} \tag{2.70}$$

For the general null-field equation (2.69) in D_{s}, we proceed analogously but restrict $\boldsymbol{r}_1$ to lie on a sphere enclosing D_{i}. We then have

$$
\begin{aligned}
&-\frac{\mathrm{j}k_{\mathrm{i},1}^2}{\pi}\int_{S_1}\left[\boldsymbol{e}_{\mathrm{i},1}\left(\boldsymbol{r}_1'\right)\cdot\begin{pmatrix}\boldsymbol{N}_{\boldsymbol{\nu}}^1(k_{\mathrm{i},1}\boldsymbol{r}_1')\\ \boldsymbol{M}_{\boldsymbol{\nu}}^1(k_{\mathrm{i},1}\boldsymbol{r}_1')\end{pmatrix}\right.\\
&\left.+\,\mathrm{j}\sqrt{\frac{\mu_{\mathrm{i},1}}{\varepsilon_{\mathrm{i},1}}}\boldsymbol{h}_{\mathrm{i},1}\left(\boldsymbol{r}_1'\right)\cdot\begin{pmatrix}\boldsymbol{M}_{\boldsymbol{\nu}}^1(k_{\mathrm{i},1}\boldsymbol{r}_1')\\ \boldsymbol{N}_{\boldsymbol{\nu}}^1(k_{\mathrm{i},1}\boldsymbol{r}_1')\end{pmatrix}\right]\mathrm{d}S\left(\boldsymbol{r}_1'\right)\\
&+\frac{\mathrm{j}k_{\mathrm{i},1}^2}{\pi}\int_{S_2}\left[\boldsymbol{e}_{\mathrm{i},2}\left(\boldsymbol{r}_2''\right)\cdot\begin{pmatrix}\boldsymbol{N}_{\boldsymbol{\nu}}^1\left(k_{\mathrm{i},1}\boldsymbol{r}_1''\right)\\ \boldsymbol{M}_{\boldsymbol{\nu}}^1(k_{\mathrm{i},1}\boldsymbol{r}_1'')\end{pmatrix}\right.\\
&\left.+\,\mathrm{j}\sqrt{\frac{\mu_{\mathrm{i},1}}{\varepsilon_{\mathrm{i},1}}}\boldsymbol{h}_{\mathrm{i},2}\left(\boldsymbol{r}_2''\right)\cdot\begin{pmatrix}\boldsymbol{M}_{\boldsymbol{\nu}}^1(k_{\mathrm{i},1}\boldsymbol{r}_1'')\\ \boldsymbol{N}_{\boldsymbol{\nu}}^1(k_{\mathrm{i},1}\boldsymbol{r}_1'')\end{pmatrix}\right]\mathrm{d}S\left(\boldsymbol{r}_2''\right)=0\,,\quad \nu=1,2,\dots\,,
\end{aligned}
\tag{2.71}
$$

where the identities $\boldsymbol{e}_{\mathrm{i},2}(\boldsymbol{r}_2'')=\boldsymbol{e}_{\mathrm{i},2}(\boldsymbol{r}_1'')$ and $\boldsymbol{h}_{\mathrm{i},2}(\boldsymbol{r}_2'')=\boldsymbol{h}_{\mathrm{i},2}(\boldsymbol{r}_1'')$ have been used. Finally, for the general null-field equation (2.69) in $D_{\mathrm{i},2}$, we pass from the origin O_1 to the origin O_2 by taking into account that the gradient is invariant to a translation of the coordinate system, use the relations

$$
\begin{aligned}
g\left(k_{\mathrm{i},1},\boldsymbol{r}_1,\boldsymbol{r}_1'\right)&=g\left(k_{\mathrm{i},1},\boldsymbol{r}_2,\boldsymbol{r}_2'\right)\,,\\
g\left(k_{\mathrm{i},1},\boldsymbol{r}_1,\boldsymbol{r}_1''\right)&=g\left(k_{\mathrm{i},1},\boldsymbol{r}_2,\boldsymbol{r}_2''\right)\,,
\end{aligned}
$$

and restrict $\boldsymbol{r}_2$ to lie on a sphere enclosed in $D_{\mathrm{i},2}$. We obtain

$$
\begin{aligned}
&-\frac{\mathrm{j}k_{\mathrm{i},1}^2}{\pi}\int_{S_1}\left[\boldsymbol{e}_{\mathrm{i},1}\left(\boldsymbol{r}_1'\right)\cdot\begin{pmatrix}\boldsymbol{N}_{\boldsymbol{\nu}}^3(k_{\mathrm{i},1}\boldsymbol{r}_2')\\ \boldsymbol{M}_{\boldsymbol{\nu}}^3(k_{\mathrm{i},1}\boldsymbol{r}_2')\end{pmatrix}\right.\\
&\left.+\,\mathrm{j}\sqrt{\frac{\mu_{\mathrm{i},1}}{\varepsilon_{\mathrm{i},1}}}\boldsymbol{h}_{\mathrm{i},1}\left(\boldsymbol{r}_1'\right)\cdot\begin{pmatrix}\boldsymbol{M}_{\boldsymbol{\nu}}^3(k_{\mathrm{i},1}\boldsymbol{r}_2')\\ \boldsymbol{N}_{\boldsymbol{\nu}}^3(k_{\mathrm{i},1}\boldsymbol{r}_2')\end{pmatrix}\right]\mathrm{d}S\left(\boldsymbol{r}_1'\right)\\
&+\frac{\mathrm{j}k_{\mathrm{i},1}^2}{\pi}\int_{S_2}\left[\boldsymbol{e}_{\mathrm{i},2}\left(\boldsymbol{r}_2''\right)\cdot\begin{pmatrix}\boldsymbol{N}_{\boldsymbol{\nu}}^3(k_{\mathrm{i},1}\boldsymbol{r}_2'')\\ \boldsymbol{M}_{\boldsymbol{\nu}}^3(k_{\mathrm{i},1}\boldsymbol{r}_2'')\end{pmatrix}\right.\\
&\left.+\,\mathrm{j}\sqrt{\frac{\mu_{\mathrm{i},1}}{\varepsilon_{\mathrm{i},1}}}\boldsymbol{h}_{\mathrm{i},2}\left(\boldsymbol{r}_2''\right)\cdot\begin{pmatrix}\boldsymbol{M}_{\boldsymbol{\nu}}^3(k_{\mathrm{i},1}\boldsymbol{r}_2'')\\ \boldsymbol{N}_{\boldsymbol{\nu}}^3(k_{\mathrm{i},1}\boldsymbol{r}_2'')\end{pmatrix}\right]\mathrm{d}S\left(\boldsymbol{r}_2''\right)=0\,,\quad \nu=1,2,\dots\,,
\end{aligned}
\tag{2.72}
$$

where, as before, the identities $\boldsymbol{e}_{\mathrm{i},1}(\boldsymbol{r}_1')=\boldsymbol{e}_{\mathrm{i},1}(\boldsymbol{r}_2')$ and $\boldsymbol{h}_{\mathrm{i},1}(\boldsymbol{r}_1')=\boldsymbol{h}_{\mathrm{i},1}(\boldsymbol{r}_2')$ have been employed. The set of integral equations (2.70)–(2.72) represent the null-field equations for the scattering problem under examination.

The surface fields $\boldsymbol{e}_{\mathrm{i},1}$ and $\boldsymbol{h}_{\mathrm{i},1}$ are the tangential components of the electric and magnetic fields in the domain $D_{\mathrm{i},1}$ bounded by the closed surfaces S_1 and S_2. Taking into account the completeness property of the system of regular and radiating vector spherical wave functions on two enclosing surfaces

(Appendix D), we approximate the surface fields $\boldsymbol{e}_{\mathrm{i},1}$ and $\boldsymbol{h}_{\mathrm{i},1}$ by the finite expansions

$$\begin{aligned}\begin{pmatrix}\boldsymbol{e}^N_{\mathrm{i},1}(\boldsymbol{r}'_1)\\ \boldsymbol{h}^N_{\mathrm{i},1}(\boldsymbol{r}'_1)\end{pmatrix} = \sum_{\mu=1}^{N} c^N_{1,\mu}&\begin{pmatrix}\boldsymbol{n}_1(\boldsymbol{r}'_1)\times\boldsymbol{M}^1_\mu(k_{\mathrm{i},1}\boldsymbol{r}'_1)\\ -\mathrm{j}\sqrt{\frac{\varepsilon_{\mathrm{i},1}}{\mu_{\mathrm{i},1}}}\boldsymbol{n}_1(\boldsymbol{r}'_1)\times\boldsymbol{N}^1_\mu(k_{\mathrm{i},1}\boldsymbol{r}'_1)\end{pmatrix}\\ +d^N_{1,\mu}&\begin{pmatrix}\boldsymbol{n}_1(\boldsymbol{r}'_1)\times\boldsymbol{N}^1_\mu(k_{\mathrm{i},1}\boldsymbol{r}'_1)\\ -\mathrm{j}\sqrt{\frac{\varepsilon_{\mathrm{i},1}}{\mu_{\mathrm{i},1}}}\boldsymbol{n}_1(\boldsymbol{r}'_1)\times\boldsymbol{M}^1_\mu(k_{\mathrm{i},1}\boldsymbol{r}'_1)\end{pmatrix}\\ +\widetilde{c}^N_{1,\mu}&\begin{pmatrix}\boldsymbol{n}_1(\boldsymbol{r}'_1)\times\boldsymbol{M}^3_\mu(k_{\mathrm{i},1}\boldsymbol{r}'_1)\\ -\mathrm{j}\sqrt{\frac{\varepsilon_{\mathrm{i},1}}{\mu_{\mathrm{i},1}}}\boldsymbol{n}_1(\boldsymbol{r}'_1)\times\boldsymbol{N}^3_\mu(k_{\mathrm{i},1}\boldsymbol{r}'_1)\end{pmatrix}\\ +\widetilde{d}^N_{1,\mu}&\begin{pmatrix}\boldsymbol{n}_1(\boldsymbol{r}'_1)\times\boldsymbol{N}^3_\mu(k_{\mathrm{i},1}\boldsymbol{r}'_1)\\ -\mathrm{j}\sqrt{\frac{\varepsilon_{\mathrm{i},1}}{\mu_{\mathrm{i},1}}}\boldsymbol{n}_1(\boldsymbol{r}'_1)\times\boldsymbol{M}^3_\mu(k_{\mathrm{i},1}\boldsymbol{r}'_1)\end{pmatrix}. \end{aligned}\tag{2.73}$$

The surface fields $\boldsymbol{e}_{\mathrm{i},2}$ and $\boldsymbol{h}_{\mathrm{i},2}$ are the tangential components of the electric and magnetic fields in the domain $D_{\mathrm{i},2}$ and the surface fields approximations can be expressed as linear combinations of regular vector spherical wave functions:

$$\begin{aligned}\begin{pmatrix}\boldsymbol{e}^N_{\mathrm{i},2}(\boldsymbol{r}''_2)\\ \boldsymbol{h}^N_{\mathrm{i},2}(\boldsymbol{r}''_2)\end{pmatrix} = \sum_{\mu=1}^{N} c^N_{2,\mu}&\begin{pmatrix}\boldsymbol{n}_2(\boldsymbol{r}''_2)\times\boldsymbol{M}^1_\mu(k_{\mathrm{i},2}\boldsymbol{r}''_2)\\ -\mathrm{j}\sqrt{\frac{\varepsilon_{\mathrm{i},2}}{\mu_{\mathrm{i},2}}}\boldsymbol{n}_2(\boldsymbol{r}''_2)\times\boldsymbol{N}^1_\mu(k_{\mathrm{i},2}\boldsymbol{r}''_2)\end{pmatrix}\\ +\mathrm{d}^N_{2,\mu}&\begin{pmatrix}\boldsymbol{n}_2(\boldsymbol{r}''_2)\times\boldsymbol{N}^1_\mu(k_{\mathrm{i},2}\boldsymbol{r}''_2)\\ -\mathrm{j}\sqrt{\frac{\varepsilon_{\mathrm{i},2}}{\mu_{\mathrm{i},2}}}\boldsymbol{n}_2(\boldsymbol{r}''_2)\times\boldsymbol{M}^1_\mu(k_{\mathrm{i},2}\boldsymbol{r}''_2)\end{pmatrix}. \end{aligned}\tag{2.74}$$

To express the resulting system of equations in matrix form we introduce the $\boldsymbol{Q}^{pq}_t(k_1,k_2)$ matrix as the $\boldsymbol{Q}^{pq}(k_1,k_2)$ matrix of the surface S_t. The elements of the $\boldsymbol{Q}^{pq}_t$ matrix are given by (2.11)–(2.14) but with S_t in place of S. For example, the elements $(Q^{pq}_t)^{11}_{\nu\mu}$ read as

$$\begin{aligned}(Q^{pq}_t)^{11}_{\nu\mu} = \frac{\mathrm{j}k_1^2}{\pi}\int_{S_t}\Big\{&\left[\boldsymbol{n}\left(\boldsymbol{r}'_t\right)\times\boldsymbol{M}^q_\mu\left(k_2\boldsymbol{r}'_t\right)\right]\cdot\boldsymbol{N}^p_{\overline{\nu}}\left(k_1\boldsymbol{r}'_t\right)\\ &+\sqrt{\frac{\varepsilon_2}{\varepsilon_1}}\left[\boldsymbol{n}\left(\boldsymbol{r}'_t\right)\times\boldsymbol{N}^q_\mu\left(k_2\boldsymbol{r}'_t\right)\right]\cdot\boldsymbol{M}^p_{\overline{\nu}}\left(k_1\boldsymbol{r}'_t\right)\Big\}\,\mathrm{d}S\left(\boldsymbol{r}'_t\right).\end{aligned}$$

Inserting (2.73) and (2.74) into (2.70), (2.71) and (2.72), using the identities (cf. (B.23), (B.24) and (B.25)),

$$\begin{aligned}&\boldsymbol{Q}^{pp}_1(k,k) = \boldsymbol{0}\,, \quad \text{for } p=1 \quad \text{or} \quad p=3\,,\\ &\boldsymbol{Q}^{13}_1(k,k) = \boldsymbol{I}\,,\\ &\boldsymbol{Q}^{31}_1(k,k) = -\boldsymbol{I}\,,\end{aligned}$$

and taking into account the transformation rules

$$\begin{bmatrix} \boldsymbol{M}^1_{\boldsymbol{\nu}}(k_{\mathrm{i},1}\boldsymbol{r}''_1) \\ \boldsymbol{N}^1_{\boldsymbol{\nu}}(k_{\mathrm{i},1}\boldsymbol{r}''_1) \end{bmatrix} = \left[\left(\mathcal{S}^{\mathrm{tr}}_{12}\right)_{\overline{\nu\mu}} \right] \begin{bmatrix} \boldsymbol{M}^1_{\mu}(k_{\mathrm{i},1}\boldsymbol{r}''_2) \\ \boldsymbol{N}^1_{\mu}(k_{\mathrm{i},1}\boldsymbol{r}''_2) \end{bmatrix}$$

and

$$\begin{bmatrix} \boldsymbol{M}^3_{\boldsymbol{\nu}}(k_{\mathrm{i},1}\boldsymbol{r}'_2) \\ \boldsymbol{N}^3_{\boldsymbol{\nu}}(k_{\mathrm{i},1}\boldsymbol{r}'_2) \end{bmatrix} = \left[\left(\mathcal{S}^{\mathrm{rt}}_{21}\right)_{\overline{\nu\mu}} \right] \begin{bmatrix} \boldsymbol{M}^3_{\mu}(k_{\mathrm{i},1}\boldsymbol{r}'_1) \\ \boldsymbol{N}^3_{\mu}(k_{\mathrm{i},1}\boldsymbol{r}'_1) \end{bmatrix} ,$$

we obtain the system of matrix equations

$$\begin{aligned} \boldsymbol{Q}^{31}_1(k_{\mathrm{s}}, k_{\mathrm{i},1})\boldsymbol{i}_1 + \boldsymbol{Q}^{33}_1(k_{\mathrm{s}}, k_{\mathrm{i},1})\widetilde{\boldsymbol{i}}_1 &= -\boldsymbol{e}\,, \\ -\widetilde{\boldsymbol{i}}_1 + \mathcal{S}^{\mathrm{tr}}_{12}\boldsymbol{Q}^{11}_2(k_{\mathrm{i},1}, k_{\mathrm{i},2})\boldsymbol{i}_2 &= 0\,, \\ \mathcal{S}^{\mathrm{rt}}_{21}\boldsymbol{i}_1 + \boldsymbol{Q}^{31}_2(k_{\mathrm{i},1}, k_{\mathrm{i},2})\boldsymbol{i}_2 &= 0\,, \end{aligned} \tag{2.75}$$

where $\boldsymbol{i}_1 = [c^N_{1,\mu}, d^N_{1,\mu}]^{\mathrm{T}}$, $\widetilde{\boldsymbol{i}}_1 = [\widetilde{c}^N_{1,\mu}, \widetilde{d}^N_{1,\mu}]^{\mathrm{T}}$, $\boldsymbol{i}_2 = [c^N_{2,\mu}, d^N_{2,\mu}]^{\mathrm{T}}$, and as before, $\boldsymbol{e} = [a_\nu, b_\nu]^{\mathrm{T}}$ is the vector containing the expansion coefficients of the incident field. The $\mathcal{S}^{\mathrm{tr}}_{12}$ matrix relates the vector spherical wave functions defined with respect to the coordinate system $O_1x_1y_1z_1$ to those defined with respect to the coordinate system $O_2x_2y_2z_2$, and can be expressed as the product of a translation and a rotation matrix:

$$\mathcal{S}^{\mathrm{tr}}_{12} = \mathcal{T}^{11}\left(k_{\mathrm{i},1}\boldsymbol{r}_{12}\right)\mathcal{R}\left(\alpha,\beta,\gamma\right)\,, \tag{2.76}$$

where $\mathcal{T}$ and $\mathcal{R}$ are defined in Appendix B. The $\mathcal{S}^{\mathrm{rt}}_{21}$ matrix describes the inverse transformation and is given by

$$\mathcal{S}^{\mathrm{rt}}_{21} = \mathcal{R}\left(-\gamma,-\beta,-\alpha\right)\mathcal{T}^{33}\left(-k_{\mathrm{i},1}\boldsymbol{r}_{12}\right) \quad \text{for} \quad r'_1 > r_{12}\,. \tag{2.77}$$

Since $\mathcal{R}$ is a block-diagonal matrix and $\mathcal{T}$ is a block-symmetric matrix it follows that $\mathcal{S}^{\mathrm{tr}}_{12}$ and $\mathcal{S}^{\mathrm{rt}}_{21}$ are also block-symmetric matrices.

Solving the system of matrix equations gives

$$\begin{aligned} \boldsymbol{i}_1 &= -\left[\boldsymbol{Q}^{31}_1(k_{\mathrm{s}}, k_{\mathrm{i},1}) + \boldsymbol{Q}^{33}_1(k_{\mathrm{s}}, k_{\mathrm{i},1})\mathcal{S}^{\mathrm{tr}}_{12}\boldsymbol{T}_2\mathcal{S}^{\mathrm{rt}}_{21}\right]^{-1}\boldsymbol{e}\,, \\ \widetilde{\boldsymbol{i}}_1 &= \mathcal{S}^{\mathrm{tr}}_{12}\boldsymbol{T}_2\mathcal{S}^{\mathrm{rt}}_{21}\boldsymbol{i}_1\,, \\ \boldsymbol{i}_2 &= -\left[\boldsymbol{Q}^{31}_2(k_{\mathrm{i},1}, k_{\mathrm{i},2})\right]^{-1}\mathcal{S}^{\mathrm{rt}}_{21}\boldsymbol{i}_1\,, \end{aligned} \tag{2.78}$$

where

$$\boldsymbol{T}_2 = -\boldsymbol{Q}^{11}_2\left(k_{\mathrm{i},1}, k_{\mathrm{i},2}\right)\left[\boldsymbol{Q}^{31}_2\left(k_{\mathrm{i},1}, k_{\mathrm{i},2}\right)\right]^{-1}$$

is the transition matrix of the inhomogeneity imbedded in a medium with relative media constants $\varepsilon_{\mathrm{i},1}$ and $\mu_{\mathrm{i},1}$.

The Stratton–Chu representation theorem for the scattered field $\boldsymbol{E}_{\mathrm{s}}$ in D_{s}, yields the expansion of the approximate scattered field $\boldsymbol{E}_{\mathrm{s}}^{N}$ in the exterior of a sphere enclosing the particle

$$\boldsymbol{E}_{\mathrm{s}}^{N}\left(\boldsymbol{r}_1\right)=\sum_{\nu=1}^{N} f_{\nu}^{N}\boldsymbol{M}_{\nu}^{3}\left(k_{\mathrm{s}}\boldsymbol{r}_1\right)+g_{\nu}^{N}\boldsymbol{N}_{\nu}^{3}\left(k_{\mathrm{s}}\boldsymbol{r}_1\right)\,,$$

where the expansion coefficients are given by

$$\begin{pmatrix} f_{\nu}^{N} \\ g_{\nu}^{N} \end{pmatrix}=\frac{\mathrm{j}k_{\mathrm{s}}^{2}}{\pi}\int_{S_1}\left[\boldsymbol{e}_{\mathrm{i},1}^{N}\left(\boldsymbol{r}'\right)\cdot\begin{pmatrix} \boldsymbol{N}_{\nu}^{1}\left(k_{\mathrm{s}}\boldsymbol{r}_1'\right) \\ \boldsymbol{M}_{\nu}^{1}\left(k_{\mathrm{s}}\boldsymbol{r}_1'\right)\end{pmatrix}\right.$$
$$\left.+\,\mathrm{j}\sqrt{\frac{\mu_{\mathrm{s}}}{\varepsilon_{\mathrm{s}}}}\boldsymbol{h}_{\mathrm{i},1}^{N}\left(\boldsymbol{r}'\right)\cdot\begin{pmatrix} \boldsymbol{M}_{\nu}^{1}\left(k_{\mathrm{s}}\boldsymbol{r}_1'\right) \\ \boldsymbol{N}_{\nu}^{1}\left(k_{\mathrm{s}}\boldsymbol{r}_1'\right)\end{pmatrix}\right]\mathrm{d}S\left(\boldsymbol{r}_1'\right)\,.$$

Taking into account the expressions of the approximate surface fields given by (2.73), we derive the matrix equation

$$\boldsymbol{s}=\boldsymbol{Q}_1^{11}\left(k_{\mathrm{s}},k_{\mathrm{i},1}\right)\boldsymbol{i}_1+\boldsymbol{Q}_1^{13}\left(k_{\mathrm{s}},k_{\mathrm{i},1}\right)\widetilde{\boldsymbol{i}}_1\,,\tag{2.79}$$

where $\boldsymbol{s}=[f_{\nu}^{N},g_{\nu}^{N}]^{\mathrm{T}}$ is the vector containing the expansion coefficients of the scattered field. Combining (2.78) and (2.79) we see that the transition matrix relating the scattered field coefficients to the incident field coefficients, $\boldsymbol{s}=\boldsymbol{T}\boldsymbol{e}$, is given by

$$\boldsymbol{T}=-\left[\boldsymbol{Q}_1^{11}\left(k_{\mathrm{s}},k_{\mathrm{i},1}\right)+\boldsymbol{Q}_1^{13}\left(k_{\mathrm{s}},k_{\mathrm{i},1}\right)\widetilde{\boldsymbol{T}}_2\right]\left[\boldsymbol{Q}_1^{31}(k_{\mathrm{s}},k_{\mathrm{i},1})+\boldsymbol{Q}_1^{33}(k_{\mathrm{s}},k_{\mathrm{i},1})\widetilde{\boldsymbol{T}}_2\right]^{-1}\,,\tag{2.80}$$

where

$$\widetilde{\boldsymbol{T}}_2=\mathcal{S}_{12}^{\mathrm{tr}}\boldsymbol{T}_2\mathcal{S}_{21}^{\mathrm{rt}}\,.\tag{2.81}$$

For a homogeneous particle $\widetilde{\boldsymbol{T}}_2=0$, and we obtain the result established in Sect. 2.1

$$\boldsymbol{T}=-\boldsymbol{Q}_1^{11}\left(k_{\mathrm{s}},k_{\mathrm{i}}\right)\left[\boldsymbol{Q}_1^{31}\left(k_{\mathrm{s}},k_{\mathrm{i}}\right)\right]^{-1}\,.$$

The expression of the transition matrix can also be written as

$$\boldsymbol{T}=\left\{\boldsymbol{T}_1-\boldsymbol{Q}_1^{13}\left(k_{\mathrm{s}},k_{\mathrm{i},1}\right)\widetilde{\boldsymbol{T}}_2\left[\boldsymbol{Q}_1^{31}(k_{\mathrm{s}},k_{\mathrm{i},1})\right]^{-1}\right\}$$
$$\times\left\{\boldsymbol{I}+\boldsymbol{Q}_1^{33}(k_{\mathrm{s}},k_{\mathrm{i},1})\widetilde{\boldsymbol{T}}_2\left[\boldsymbol{Q}_1^{31}(k_{\mathrm{s}},k_{\mathrm{i},1})\right]^{-1}\right\}^{-1}\,,\tag{2.82}$$

where

$$\boldsymbol{T}_1=-\boldsymbol{Q}_1^{11}\left(k_{\mathrm{s}},k_{\mathrm{i}}\right)\left[\boldsymbol{Q}_1^{31}\left(k_{\mathrm{s}},k_{\mathrm{i}}\right)\right]^{-1}$$

is the transition matrix of the host particle. If the coordinate systems $O_1x_1y_1z_1$ and $O_2x_2y_2z_2$ coincide, (2.82) is identical to the result given by Peterson and

Ström [189]. The various terms obtained by a formal expansion of the inverse in (2.82) can be interpreted as various multiple-scattering contributions to the total transition matrix. Indeed, using the representation

$$\begin{aligned}\boldsymbol{T} &= \left\{\boldsymbol{T}_1 - \boldsymbol{Q}_1^{13}\widetilde{\boldsymbol{T}}_2\left(\boldsymbol{Q}_1^{31}\right)^{-1}\right\}\left\{\boldsymbol{I} - \boldsymbol{Q}_1^{33}\widetilde{\boldsymbol{T}}_2\left(\boldsymbol{Q}_1^{31}\right)^{-1} + ...\right\} \\ &= \boldsymbol{T}_1 - \boldsymbol{Q}_1^{13}\widetilde{\boldsymbol{T}}_2\left(\boldsymbol{Q}_1^{31}\right)^{-1} - \boldsymbol{T}_1\boldsymbol{Q}_1^{33}\widetilde{\boldsymbol{T}}_2\left(\boldsymbol{Q}_1^{31}\right)^{-1} \\ &\quad + \boldsymbol{Q}_1^{13}\widetilde{\boldsymbol{T}}_2\left(\boldsymbol{Q}_1^{31}\right)^{-1}\boldsymbol{Q}_1^{33}\widetilde{\boldsymbol{T}}_2\left(\boldsymbol{Q}_1^{31}\right)^{-1} + \dots\end{aligned}$$

we see that the term $\boldsymbol{T}_1$ represents a reflection at S_1, $\boldsymbol{Q}_1^{13}\widetilde{\boldsymbol{T}}_2(\boldsymbol{Q}_1^{31})^{-1}$ represents a passage of a wave through S_1 and a reflection at S_2, $\boldsymbol{T}_1\boldsymbol{Q}_1^{33}\widetilde{\boldsymbol{T}}_2(\boldsymbol{Q}_1^{31})^{-1}$ represents a refraction of a wave through S_1 and two consecutive reflections at S_2 and S_1, etc.

The expressions of the total transition matrix given by (2.80) or (2.82) are important in practical applications. As it has been shown by Peterson and Ström [189], this result can be extended to the case of S_1 containing an arbitrary number of separate enclosures by simply replacing $\boldsymbol{T}_2$ with the system transition matrix of the particles. In the later sections we will derive the transition matrix for a system of particles and the present formalism will enable us to analyze scattering by an arbitrarily shaped, inhomogeneous particle with an arbitrary number of irregular inclusions. In this context it should be mentioned that the separation of variables solution for a single sphere (the Lorenz–Mie theory) can be extended to spheres with one or more eccentrically positioned spherical inclusions by using the translation addition theorem for vector spherical wave functions. Theories of scattering by eccentrically stratified spheres have been derived by Fikioris and Uzunoglu [64], Borghese et al. [22], Fuller [73], Mackowski and Jones [152] and Ngo et al. [180], while treatments for a sphere with multiple spherical inclusions have been rendered by Borghese et al. [20], Fuller [75] and Ioannidou and Chrissoulidis [107]. A detailed review of the separation of variable method for inhomogeneous spheres has been given by Fuller and Mackowski [77]. The separation of variable method has also been employed in spheroidal coordinate systems by Cooray and Ciric [41] and Li et al. [141] to analyze the scattering by inhomogeneous spheroids.

2.4.2 Formulation without Addition Theorem

In our previous analysis we assumed the geometric constraint $r_1' > r_{12}$ (cf. (2.77)), which originates in the use of the translation addition theorem for radiating vector spherical wave functions. In this section we present a formalism that avoids the use of any local origin translation. To simplify our analysis, we assume that the coordinate systems $O_1x_1y_1z_1$ and $O_2x_2y_2z_2$ have the same spatial orientation and set $\alpha = \beta = \gamma = 0$. We begin by defining the $\boldsymbol{Q}_t^{pq}(k_1, i, k_2, j)$ matrix

$$\boldsymbol{Q}_t^{pq}\left(k_1,i,k_2,j\right)=\begin{bmatrix}\left(Q_t^{pq}\right)_{\nu\mu}^{11} & \left(Q_t^{pq}\right)_{\nu\mu}^{12}\\ \left(Q_t^{pq}\right)_{\nu\mu}^{21} & \left(Q_t^{pq}\right)_{\nu\mu}^{22}\end{bmatrix}, \tag{2.83}$$

as

$$\left(Q_t^{pq}\right)_{\nu\mu}^{11}=\frac{\mathrm{j}k_1^2}{\pi}\int_{S_t}\Big\{\left[\boldsymbol{n}\left(\boldsymbol{r}'_j\right)\times\boldsymbol{M}_\mu^q\left(k_2\boldsymbol{r}'_j\right)\right]\cdot\boldsymbol{N}_{\overline{\nu}}^p\left(k_1\boldsymbol{r}'_i\right)$$
$$+\sqrt{\frac{\varepsilon_2}{\varepsilon_1}}\left[\boldsymbol{n}\left(\boldsymbol{r}'_j\right)\times\boldsymbol{N}_\mu^q\left(k_2\boldsymbol{r}'_j\right)\right]\cdot\boldsymbol{M}_{\overline{\nu}}^p\left(k_1\boldsymbol{r}'_i\right)\Big\}\,\mathrm{d}S\left(\boldsymbol{r}'\right), \tag{2.84}$$

$$\left(Q_t^{pq}\right)_{\nu\mu}^{12}=\frac{\mathrm{j}k_1^2}{\pi}\int_{S_t}\Big\{\left[\boldsymbol{n}\left(\boldsymbol{r}'_j\right)\times\boldsymbol{N}_\mu^q\left(k_2\boldsymbol{r}'_j\right)\right]\cdot\boldsymbol{N}_{\overline{\nu}}^p\left(k_1\boldsymbol{r}'_i\right)$$
$$+\sqrt{\frac{\varepsilon_2}{\varepsilon_1}}\left[\boldsymbol{n}\left(\boldsymbol{r}'_j\right)\times\boldsymbol{M}_\mu^q\left(k_2\boldsymbol{r}'_j\right)\right]\cdot\boldsymbol{M}_{\overline{\nu}}^p\left(k_1\boldsymbol{r}'_i\right)\Big\}\,\mathrm{d}S\left(\boldsymbol{r}'\right), \tag{2.85}$$

$$\left(Q_t^{pq}\right)_{\nu\mu}^{21}=\frac{\mathrm{j}k_1^2}{\pi}\int_{S_t}\Big\{\left[\boldsymbol{n}\left(\boldsymbol{r}'_j\right)\times\boldsymbol{M}_\mu^q\left(k_2\boldsymbol{r}'_j\right)\right]\cdot\boldsymbol{M}_{\overline{\nu}}^p\left(k_1\boldsymbol{r}'_i\right)$$
$$+\sqrt{\frac{\varepsilon_2}{\varepsilon_1}}\left[\boldsymbol{n}\left(\boldsymbol{r}'_j\right)\times\boldsymbol{N}_\mu^q\left(k_2\boldsymbol{r}'_j\right)\right]\cdot\boldsymbol{N}_{\overline{\nu}}^p\left(k_1\boldsymbol{r}'_i\right)\Big\}\,\mathrm{d}S\left(\boldsymbol{r}'\right), \tag{2.86}$$

and

$$\left(Q_t^{pq}\right)_{\nu\mu}^{22}=\frac{\mathrm{j}k_1^2}{\pi}\int_{S_t}\Big\{\left[\boldsymbol{n}\left(\boldsymbol{r}'_j\right)\times\boldsymbol{N}_\mu^q\left(k_2\boldsymbol{r}'_j\right)\right]\cdot\boldsymbol{M}_{\overline{\nu}}^p\left(k_1\boldsymbol{r}'_i\right)$$
$$+\sqrt{\frac{\varepsilon_2}{\varepsilon_1}}\left[\boldsymbol{n}\left(\boldsymbol{r}'_j\right)\times\boldsymbol{M}_\mu^q\left(k_2\boldsymbol{r}'_j\right)\right]\cdot\boldsymbol{N}_{\overline{\nu}}^p\left(k_1\boldsymbol{r}'_i\right)\Big\}\,\mathrm{d}S\left(\boldsymbol{r}'\right). \tag{2.87}$$

The vectors $\boldsymbol{r}'$, $\boldsymbol{r}'_i$ and $\boldsymbol{r}'_j$ are the position vectors of a point M on the surface S_t, and are defined with respect to the origins O, O_i and O_j, respectively (Fig. 2.3). In terms of the new $\boldsymbol{Q}_t^{pq}$ matrices, the system of matrix equations (2.75) can be written as

$$\begin{aligned}\boldsymbol{Q}_1^{33}(k_\mathrm{s},1,k_{\mathrm{i},1},1)\widetilde{\boldsymbol{i}}_1+\boldsymbol{Q}_1^{31}(k_\mathrm{s},1,k_{\mathrm{i},1},1)\boldsymbol{i}_1&=-\boldsymbol{e}\,,\\ -\widetilde{\boldsymbol{i}}_1+\boldsymbol{Q}_2^{11}(k_{\mathrm{i},1},1,k_{\mathrm{i},2},2)\boldsymbol{i}_2&=0\,,\\ -\boldsymbol{Q}_1^{31}(k_{\mathrm{i},1},2,k_{\mathrm{i},1},1)\boldsymbol{i}_1+\boldsymbol{Q}_2^{31}(k_{\mathrm{i},1},2,k_{\mathrm{i},2},2)\boldsymbol{i}_2&=0\,,\end{aligned} \tag{2.88}$$

while the matrix equation (2.79) reads as

$$\boldsymbol{s}=\boldsymbol{Q}_1^{13}\left(k_\mathrm{s},1,k_{\mathrm{i},1},1\right)\widetilde{\boldsymbol{i}}_1+\boldsymbol{Q}_1^{11}\left(k_\mathrm{s},1,k_{\mathrm{i},1},1\right)\boldsymbol{i}_1\,. \tag{2.89}$$

Using the substitution method we eliminate the unknown vector $\boldsymbol{i}_2$ from the last two matrix equations in (2.88) and obtain

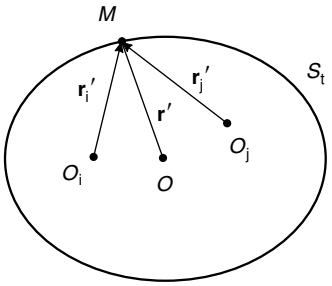

Fig. 2.3. Position vectors of a point M on the surface S_t with respect to the origins O, O_i and O_j

$$\widetilde{\boldsymbol{i}}_1 = \widetilde{\boldsymbol{T}}_2 \boldsymbol{i}_1 \tag{2.90}$$

with

$$\widetilde{\boldsymbol{T}}_2 = \boldsymbol{Q}_2^{11}(k_{\mathrm{i},1}, 1, k_{\mathrm{i},2}, 2) \left[\boldsymbol{Q}_2^{31}(k_{\mathrm{i},1}, 2, k_{\mathrm{i},2}, 2)\right]^{-1} \boldsymbol{Q}_1^{31}(k_{\mathrm{i},1}, 2, k_{\mathrm{i},1}, 1)\,. \tag{2.91}$$

Equation (2.89) and the first matrix equation in (2.88), written in compact matrix notation as

$$\begin{bmatrix} \boldsymbol{s} \\ \boldsymbol{e} \end{bmatrix} = \mathcal{Q}_1\left(k_{\mathrm{s}}, k_{\mathrm{i},1}\right) \begin{bmatrix} \widetilde{\boldsymbol{i}}_1 \\ \boldsymbol{i}_1 \end{bmatrix}, \tag{2.92}$$

where

$$\mathcal{Q}_1\left(k_{\mathrm{s}}, k_{\mathrm{i},1}\right) = \begin{bmatrix} \boldsymbol{Q}_1^{13}\left(k_{\mathrm{s}}, 1, k_{\mathrm{i},1}, 1\right) & \boldsymbol{Q}_1^{11}\left(k_{\mathrm{s}}, 1, k_{\mathrm{i},1}, 1\right) \\ -\boldsymbol{Q}_1^{33}(k_{\mathrm{s}}, 1, k_{\mathrm{i},1}, 1) & -\boldsymbol{Q}_1^{31}(k_{\mathrm{s}}, 1, k_{\mathrm{i},1}, 1) \end{bmatrix}, \tag{2.93}$$

then yield

$$\begin{aligned} \boldsymbol{T} = &- \left[\boldsymbol{Q}_1^{11}\left(k_{\mathrm{s}}, 1, k_{\mathrm{i},1}, 1\right) + \boldsymbol{Q}_1^{13}\left(k_{\mathrm{s}}, 1, k_{\mathrm{i},1}, 1\right) \widetilde{\boldsymbol{T}}_2\right] \\ &\times \left[\boldsymbol{Q}_1^{31}(k_{\mathrm{s}}, 1, k_{\mathrm{i},1}, 1) + \boldsymbol{Q}_1^{33}(k_{\mathrm{s}}, 1, k_{\mathrm{i},1}, 1)\widetilde{\boldsymbol{T}}_2\right]^{-1}. \end{aligned} \tag{2.94}$$

The expression of the transition matrix is identical to that given by (2.80), but the $\widetilde{\boldsymbol{T}}_2$ matrix is now given by (2.91) instead of (2.81). If the origins O_1 and O_2 coincide

$$\boldsymbol{Q}_1^{31}(k_{\mathrm{i},1}, 1, k_{\mathrm{i},1}, 1) = -\boldsymbol{I}$$

and we see that the $\widetilde{\boldsymbol{T}}_2$ matrix is the transition matrix of the inhomogeneity:

$$\widetilde{\boldsymbol{T}}_2 = \boldsymbol{T}_2 = -\boldsymbol{Q}_2^{11}(k_{\mathrm{i},1}, 1, k_{\mathrm{i},2}, 1) \left[\boldsymbol{Q}_2^{31}(k_{\mathrm{i},1}, 1, k_{\mathrm{i},2}, 1)\right]^{-1}.$$

This formalism will be used in Sect. 2.5 to derive a recurrence relation for the transition matrix of a multilayered particle.

2.5 Layered Particles

A layered particle is an inhomogeneous particle consisting of several consecutively enclosing surfaces S_l, $l = 1, 2, \ldots, \mathcal{N}$. Each surface S_l is defined with respect to a coordinate system $O_l x_l y_l z_l$ and we assume that the coordinate systems $O_l x_l y_l z_l$ have the same spatial orientation. The layered particle is immersed in a medium with optical constants ε_s and μ_s, while the relative media constants and the wave number in the domain between S_l and S_{l+1} are $\varepsilon_{\mathrm{i},l}$, $\mu_{\mathrm{i},l}$ and $k_{\mathrm{i},l}$, respectively. The geometry of a (multi)layered particle is shown in Fig. 2.4. The case $\mathcal{N} = 2$ has been treated in the previous section and the objective of the present analysis is to extend the results established for two-layered particles to multilayered particles.

2.5.1 General Formulation

For a particle with $\mathcal{N}$ layers, the system of matrix equations consists in the null-field equations in the interior of S_1,

$$\boldsymbol{Q}_1^{33}(k_\mathrm{s}, 1, k_{\mathrm{i},1}, 1)\widetilde{\boldsymbol{i}}_1 + \boldsymbol{Q}_1^{31}(k_\mathrm{s}, 1, k_{\mathrm{i},1}, 1)\boldsymbol{i}_1 = -\boldsymbol{e}\,, \tag{2.95}$$

the null-field equations in the exterior of S_{l-1} and the interior of S_l

$$\begin{aligned} &-\widetilde{\boldsymbol{i}}_{l-1} + \boldsymbol{Q}_l^{13}(k_{\mathrm{i},l-1}, l-1, k_{\mathrm{i},l}, l)\widetilde{\boldsymbol{i}}_l \\ &\quad + \boldsymbol{Q}_l^{11}(k_{\mathrm{i},l-1}, l-1, k_{\mathrm{i},l}, l)\boldsymbol{i}_l = 0\,, \end{aligned} \tag{2.96}$$

$$\begin{aligned} &-\boldsymbol{Q}_{l-1}^{31}(k_{\mathrm{i},l-1}, l, k_{\mathrm{i},l-1}, l-1)\boldsymbol{i}_{l-1} + \boldsymbol{Q}_l^{33}(k_{\mathrm{i},l-1}, l, k_{\mathrm{i},l}, l)\widetilde{\boldsymbol{i}}_l \\ &\qquad + \boldsymbol{Q}_l^{31}(k_{\mathrm{i},l-1}, l, k_{\mathrm{i},l}, l)\boldsymbol{i}_l = 0 \\ &\quad l = 2, 3, \ldots, \mathcal{N}-1 \end{aligned} \tag{2.97}$$

the null-field equations in the exterior of $S_{\mathcal{N}-1}$ and the interior of $S_\mathcal{N}$

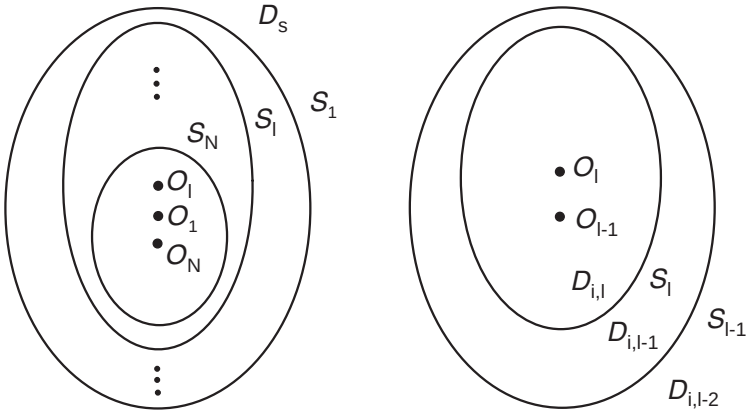

Fig. 2.4. Geometry of a multilayered particle

$$-\widetilde{\boldsymbol{i}}_{\mathcal{N}-1}+\boldsymbol{Q}_{\mathcal{N}}^{11}(k_{\mathrm{i},\mathcal{N}-1},\mathcal{N}-1,k_{\mathrm{i},\mathcal{N}},\mathcal{N})\boldsymbol{i}_{\mathcal{N}}=0\,, \tag{2.98}$$

$$-\boldsymbol{Q}_{\mathcal{N}-1}^{31}(k_{\mathrm{i},\mathcal{N}-1},\mathcal{N},k_{\mathrm{i},\mathcal{N}-1},\mathcal{N}-1)\boldsymbol{i}_{\mathcal{N}-1}+\boldsymbol{Q}_{\mathcal{N}}^{31}(k_{\mathrm{i},\mathcal{N}-1},\mathcal{N},k_{\mathrm{i},\mathcal{N}},\mathcal{N})\boldsymbol{i}_{\mathcal{N}}=0 \tag{2.99}$$

and the matrix equation corresponding to the scattered field representation

$$\boldsymbol{s}=\boldsymbol{Q}_1^{13}\left(k_{\mathrm{s}},1,k_{\mathrm{i},1},1\right)\widetilde{\boldsymbol{i}}_1+\boldsymbol{Q}_1^{11}\left(k_{\mathrm{s}},1,k_{\mathrm{i},1},1\right)\boldsymbol{i}_1\,. \tag{2.100}$$

For two consecutive layers, the surface fields $\widetilde{\boldsymbol{i}}_{l-1}$ and $\boldsymbol{i}_{l-1}$ are related to the surface fields $\widetilde{\boldsymbol{i}}_l$ and $\boldsymbol{i}_l$ by the matrix equation

$$\begin{bmatrix}\widetilde{\boldsymbol{i}}_{l-1}\\ \boldsymbol{i}_{l-1}\end{bmatrix}=\mathcal{Q}_l\left(k_{\mathrm{i},l-1},k_{\mathrm{i},l}\right)\begin{bmatrix}\widetilde{\boldsymbol{i}}_l\\ \boldsymbol{i}_l\end{bmatrix}\,, \tag{2.101}$$

where

$$\begin{aligned}\mathcal{Q}_l\left(k_{\mathrm{i},l-1},k_{\mathrm{i},l}\right)=&\begin{bmatrix}\boldsymbol{I} & \boldsymbol{0}\\ \boldsymbol{0} & \left[\boldsymbol{Q}_{l-1}^{31}(k_{\mathrm{i},l-1},l,k_{\mathrm{i},l-1},l-1)\right]^{-1}\end{bmatrix}\\ &\times\begin{bmatrix}\boldsymbol{Q}_l^{13}(k_{\mathrm{i},l-1},l-1,k_{\mathrm{i},l},l) & \boldsymbol{Q}_l^{11}(k_{\mathrm{i},l-1},l-1,k_{\mathrm{i},l},l)\\ \boldsymbol{Q}_l^{33}(k_{\mathrm{i},l-1},l,k_{\mathrm{i},l},l) & \boldsymbol{Q}_l^{31}(k_{\mathrm{i},l-1},l,k_{\mathrm{i},l},l)\end{bmatrix}\end{aligned} \tag{2.102}$$

and $l=2,3,\ldots,\mathcal{N}-1$. For the surface fields $\widetilde{\boldsymbol{i}}_{\mathcal{N}-1}$and $\boldsymbol{i}_{\mathcal{N}-1}$, that is, for $l=\mathcal{N}$, we have

$$\widetilde{\boldsymbol{i}}_{\mathcal{N}-1}=\widetilde{\boldsymbol{T}}_{\mathcal{N}}\boldsymbol{i}_{\mathcal{N}-1} \tag{2.103}$$

with

$$\begin{aligned}\widetilde{\boldsymbol{T}}_{\mathcal{N}}=&\boldsymbol{Q}_{\mathcal{N}}^{11}(k_{\mathrm{i},\mathcal{N}-1},\mathcal{N}-1,k_{\mathrm{i},\mathcal{N}},\mathcal{N})\left[\boldsymbol{Q}_{\mathcal{N}}^{31}(k_{\mathrm{i},\mathcal{N}-1},\mathcal{N},k_{\mathrm{i},\mathcal{N}},\mathcal{N})\right]^{-1}\\ &\times\boldsymbol{Q}_{\mathcal{N}-1}^{31}(k_{\mathrm{i},\mathcal{N}-1},\mathcal{N},k_{\mathrm{i},\mathcal{N}-1},\mathcal{N}-1)\,.\end{aligned} \tag{2.104}$$

Then, using the matrix equation

$$\begin{bmatrix}\boldsymbol{s}\\ \boldsymbol{e}\end{bmatrix}=\mathcal{Q}_1\left(k_{\mathrm{s}},k_{\mathrm{i},1}\right)\begin{bmatrix}\widetilde{\boldsymbol{i}}_1\\ \boldsymbol{i}_1\end{bmatrix}$$

with $\mathcal{Q}_1$ being given by (2.93), we see that

$$\begin{bmatrix}\boldsymbol{s}\\ \boldsymbol{e}\end{bmatrix}=\mathcal{Q}\begin{bmatrix}\widetilde{\boldsymbol{i}}_{\mathcal{N}-1}\\ \boldsymbol{i}_{\mathcal{N}-1}\end{bmatrix}\,,$$

where

$$\mathcal{Q}=\mathcal{Q}_1\left(k_{\mathrm{s}},k_{\mathrm{i},1}\right)\mathcal{Q}_2\left(k_{\mathrm{i},1},k_{\mathrm{i},2}\right)\ldots\mathcal{Q}_{\mathcal{N}-1}\left(k_{\mathrm{i},\mathcal{N}-2},k_{\mathrm{i},\mathcal{N}-1}\right)\,.$$

Finally, using (2.103) and denoting by $(\mathcal{Q})^{ij}$, $i,j=1,2$, the block-matrix components of $\mathcal{Q}$, we obtain the expression of the transition matrix in terms of $\mathcal{Q}$ and $\widetilde{\boldsymbol{T}}_{\mathcal{N}}$:

$$\boldsymbol{T} = \left[(\mathcal{Q})^{12} + (\mathcal{Q})^{11}\,\widetilde{\boldsymbol{T}}_{\mathcal{N}}\right]\left[(\mathcal{Q})^{22} + (\mathcal{Q})^{21}\,\widetilde{\boldsymbol{T}}_{\mathcal{N}}\right]^{-1} .$$

The structure of the above equations is such that a recurrence relation for computing the transition matrix can be established. For this purpose, we define the matrix $\widetilde{\boldsymbol{T}}_{l+1,l+2,\ldots,\mathcal{N}}$ as

$$\widetilde{\boldsymbol{i}}_l = \widetilde{\boldsymbol{T}}_{l+1,l+2,\ldots,\mathcal{N}}\boldsymbol{i}_l\,.$$

and use (2.101) to obtain

$$\widetilde{\boldsymbol{i}}_{l-1} = \left[(\mathcal{Q}_l)^{12} + (\mathcal{Q}_l)^{11}\,\widetilde{\boldsymbol{T}}_{l+1,l+2,\ldots,\mathcal{N}}\right]\boldsymbol{i}_l\,,$$
$$\boldsymbol{i}_{l-1} = \left[(\mathcal{Q}_l)^{22} + (\mathcal{Q}_l)^{21}\,\widetilde{\boldsymbol{T}}_{l+1,l+2,\ldots,\mathcal{N}}\right]\boldsymbol{i}_l\,,$$

where $(\mathcal{Q}_l)^{ij}$, $i,j = 1,2$, are the block-matrix components of $\mathcal{Q}_l(k_{\mathrm{i},l-1}, k_{\mathrm{i},l})$. Hence, the matrix $\widetilde{\boldsymbol{T}}_{l,l+1,\ldots,\mathcal{N}}$, satisfying $\widetilde{\boldsymbol{i}}_{l-1} = \widetilde{\boldsymbol{T}}_{l,l+1,\ldots,\mathcal{N}}\boldsymbol{i}_{l-1}$, can be computed by using the downward recurrence relation

$$\widetilde{\boldsymbol{T}}_{l,l+1,\ldots,\mathcal{N}} = \left[(\mathcal{Q}_l)^{12} + (\mathcal{Q}_l)^{11}\,\widetilde{\boldsymbol{T}}_{l+1,l+2,\ldots,\mathcal{N}}\right] \times \left[(\mathcal{Q}_l)^{22} + (\mathcal{Q}_l)^{21}\,\widetilde{\boldsymbol{T}}_{l+1,l+2,\ldots,\mathcal{N}}\right]^{-1} \tag{2.105}$$

for $l = \mathcal{N}-1, \mathcal{N}-2, \ldots, 1$. For $l = \mathcal{N}-1$, $\widetilde{\boldsymbol{T}}_{\mathcal{N}}$ is given by (2.104), while for $l = 1$, $\mathcal{Q}_l$ is the matrix $\mathcal{Q}_1(k_{\mathrm{s}}, k_{\mathrm{i},1})$ and $\widetilde{\boldsymbol{T}}_{l,l+1,\ldots,\mathcal{N}}$ is the transition matrix of the layered particle

$$\boldsymbol{T} = \widetilde{\boldsymbol{T}}_{1,2,\ldots,\mathcal{N}} = -\left[\boldsymbol{Q}_1^{11}\,(k_{\mathrm{s}},1,k_{\mathrm{i},1},1) + \boldsymbol{Q}_1^{13}\,(k_{\mathrm{s}},1,k_{\mathrm{i},1},1)\,\widetilde{\boldsymbol{T}}_{2,3,\ldots,\mathcal{N}}\right] \times \left[\boldsymbol{Q}_1^{31}(k_{\mathrm{s}},1,k_{\mathrm{i},1},1) + \boldsymbol{Q}_1^{33}(k_{\mathrm{s}},1,k_{\mathrm{i},1},1)\widetilde{\boldsymbol{T}}_{2,3,\ldots,\mathcal{N}}\right]^{-1} .$$

If the origins coincide, the above relations simplify considerably, since

$$\mathcal{Q}_l\,(k_{\mathrm{i},l-1}, k_{\mathrm{i},l}) = \begin{bmatrix} \boldsymbol{Q}_l^{13}(k_{\mathrm{i},l-1},1,k_{\mathrm{i},l},1) & \boldsymbol{Q}_l^{11}(k_{\mathrm{i},l-1},1,k_{\mathrm{i},l},1) \\ -\boldsymbol{Q}_l^{33}(k_{\mathrm{i},l-1},1,k_{\mathrm{i},l},1) & -\boldsymbol{Q}_l^{31}(k_{\mathrm{i},l-1},1,k_{\mathrm{i},l},1) \end{bmatrix} \tag{2.106}$$

and

$$\widetilde{\boldsymbol{T}}_{\mathcal{N}} = \boldsymbol{T}_{\mathcal{N}} = -\boldsymbol{Q}_{\mathcal{N}}^{11}(k_{\mathrm{i},\mathcal{N}-1},1,k_{\mathrm{i},\mathcal{N}},1)\left[\boldsymbol{Q}_{\mathcal{N}}^{31}(k_{\mathrm{i},\mathcal{N}-1},1,k_{\mathrm{i},\mathcal{N}},1)\right]^{-1} .$$

We obtain

$$\boldsymbol{T}_{l,l+1,\ldots,\mathcal{N}} = -\left[\boldsymbol{Q}_l^{11}(k_{\mathrm{i},l-1},1,k_{\mathrm{i},l},1) + \boldsymbol{Q}_l^{13}(k_{\mathrm{i},l-1},1,k_{\mathrm{i},l},1)\boldsymbol{T}_{l+1,l+2,\ldots,\mathcal{N}}\right] \times \left[\boldsymbol{Q}_l^{31}(k_{\mathrm{i},l-1},1,k_{\mathrm{i},l},1) + \boldsymbol{Q}_l^{33}(k_{\mathrm{i},l-1},1,k_{\mathrm{i},l},1)\boldsymbol{T}_{l+1,l+2,\ldots,\mathcal{N}}\right]^{-1} \tag{2.107}$$

and further

$$\begin{aligned}\boldsymbol{T}_{l,l+1,\ldots,\mathcal{N}} = &\left\{\boldsymbol{T}_l - \boldsymbol{Q}_l^{13}(k_{\mathrm{i},l-1},1,k_{\mathrm{i},l},1)\boldsymbol{T}_{l+1,l+2,\ldots,\mathcal{N}}\right.\\ &\left.\times\left[\boldsymbol{Q}_l^{31}(k_{\mathrm{i},l-1},1,k_{\mathrm{i},l},1)\right]^{-1}\right\}\left\{\boldsymbol{I}+\boldsymbol{Q}_l^{33}(k_{\mathrm{i},l-1},1,k_{\mathrm{i},l},1)\right.\\ &\left.\times\boldsymbol{T}_{l+1,l+2,\ldots,\mathcal{N}}\left[\boldsymbol{Q}_l^{31}(k_{\mathrm{i},l-1},1,k_{\mathrm{i},l},1)\right]^{-1}\right\}^{-1} \end{aligned} \tag{2.108}$$

of which (2.82) is the simplest special case. Note that in (2.107) and (2.108), $\boldsymbol{T}_{l,l+1,\ldots,\mathcal{N}}$ is the total transition matrix of the layered particle with outer surface S_l.

2.5.2 Practical Formulation

In practical computer calculations it is simpler to solve the system of matrix equations (2.95)–(2.99) for all unknown vectors $\widetilde{\boldsymbol{i}}_l$ and $\boldsymbol{i}_l$, $l=1,2,\ldots,\mathcal{N}-1$, and $\boldsymbol{i}_{\mathcal{N}}$. For this purpose, we consider the global matrix

$$\boldsymbol{A}=\begin{bmatrix} \boldsymbol{A}^1 & \boldsymbol{0} & \boldsymbol{0} & \ldots & \boldsymbol{0} & \boldsymbol{0}\\ \boldsymbol{A}^{12} & \boldsymbol{A}^{21} & \boldsymbol{0} & \ldots & \boldsymbol{0} & \boldsymbol{0}\\ \boldsymbol{0} & \boldsymbol{A}^{23} & \boldsymbol{A}^{32} & \ldots & \boldsymbol{0} & \boldsymbol{0}\\ \boldsymbol{0} & \boldsymbol{0} & \boldsymbol{0} & \ldots & \boldsymbol{A}^{\mathcal{N}-1,\mathcal{N}-2} & \boldsymbol{0}\\ \boldsymbol{0} & \boldsymbol{0} & \boldsymbol{0} & \ldots & \boldsymbol{A}^{\mathcal{N}-1,\mathcal{N}} & \boldsymbol{A}^{\mathcal{N}} \end{bmatrix},$$

where

$$\boldsymbol{A}^1=\left[\boldsymbol{Q}_1^{33}(k_{\mathrm{s}},1,k_{\mathrm{i},1},1)\,\boldsymbol{Q}_1^{31}(k_{\mathrm{s}},1,k_{\mathrm{i},1},1)\right], \tag{2.109}$$

$$\boldsymbol{A}^{l,l-1}=\begin{bmatrix} \boldsymbol{Q}_l^{13}(k_{\mathrm{i},l-1},l-1,k_{\mathrm{i},l},l)\;\boldsymbol{Q}_l^{11}(k_{\mathrm{i},l-1},l-1,k_{\mathrm{i},l},l)\\ \boldsymbol{Q}_l^{33}(k_{\mathrm{i},l-1},l,k_{\mathrm{i},l},l) \qquad \boldsymbol{Q}_l^{31}(k_{\mathrm{i},l-1},l,k_{\mathrm{i},l},l) \end{bmatrix}, \tag{2.110}$$

$$\boldsymbol{A}^{l-1,l}=\begin{bmatrix} -\boldsymbol{I} & \boldsymbol{0}\\ \boldsymbol{0} & -\boldsymbol{Q}_{l-1}^{31}(k_{\mathrm{i},l-1},l,k_{\mathrm{i},l-1},l-1) \end{bmatrix}, \tag{2.111}$$

and

$$\boldsymbol{A}^{\mathcal{N}}=\begin{bmatrix} \boldsymbol{Q}_{\mathcal{N}}^{11}(k_{\mathrm{i},\mathcal{N}-1},\mathcal{N}-1,k_{\mathrm{i},\mathcal{N}},\mathcal{N})\\ \boldsymbol{Q}_{\mathcal{N}}^{31}(k_{\mathrm{i},\mathcal{N}-1},\mathcal{N},k_{\mathrm{i},\mathcal{N}},\mathcal{N}) \end{bmatrix}. \tag{2.112}$$

Then, denoting by $\mathcal{A}$ the inverse of $\boldsymbol{A}$,

$$\mathcal{A}=\boldsymbol{A}^{-1}=\begin{bmatrix} \mathcal{A}^{11} & \mathcal{A}^{12} & \ldots & \mathcal{A}^{1,2\mathcal{N}-1}\\ \mathcal{A}^{21} & \mathcal{A}^{22} & \ldots & \mathcal{A}^{2,2\mathcal{N}-1}\\ \mathcal{A}^{2\mathcal{N}-1,1} & \mathcal{A}^{2\mathcal{N}-1,2} & \ldots & \mathcal{A}^{2\mathcal{N}-1,2\mathcal{N}-1} \end{bmatrix},$$

we express $\widetilde{\boldsymbol{i}}_1$ and $\boldsymbol{i}_1$ as

$$\widetilde{\boldsymbol{i}}_1 = -\mathcal{A}^{11}\boldsymbol{e}\,, \quad \boldsymbol{i}_1 = -\mathcal{A}^{21}\boldsymbol{e}\,,$$

and use (2.100) to obtain

$$\boldsymbol{T} = -\left[\boldsymbol{Q}_1^{13}\left(k_\mathrm{s}, 1, k_{\mathrm{i},1}, 1\right)\mathcal{A}^{11} + \boldsymbol{Q}_1^{11}\left(k_\mathrm{s}, 1, k_{\mathrm{i},1}, 1\right)\mathcal{A}^{21}\right]\,.$$

For axisymmetric layers and axial positions of the origins O_l (along the z-axis of rotation), the scattering problem decouples over the azimuthal modes and the transition matrix can be computed separately for each m. Specifically, for each layer l, we compute the $\boldsymbol{Q}_l$ matrices and assemble these matrices into the global matrix $\boldsymbol{A}$. The matrix $\boldsymbol{A}$ is inverted, and the blocks 11 and 21 of the inverse matrix are used for $\boldsymbol{T}$-matrix calculation. Because $\boldsymbol{A}$ is a sparse matrix, appropriate LU–factorization routines (for sparse systems of equations) can be employed.

An important feature of this solution method is that the expansion orders of the surface field approximations can be different. To derive the dimension of the global matrix $\boldsymbol{A}$, we consider an axisymmetric particle. If $N_\mathrm{rank}(l)$ is the maximum expansion order of the layer l and, for a given azimuthal mode m, $2N_\mathrm{max}(l) \times 2N_\mathrm{max}(l)$ is the dimension of the corresponding $\boldsymbol{Q}$ matrices, where

$$N_\mathrm{max}(l) = \begin{cases} N_\mathrm{rank}(l)\,, & m = 0 \\ N_\mathrm{rank}(l) - |m| + 1\,, & m \neq 0 \end{cases}\,,$$

then, the dimension of the global matrix $\boldsymbol{A}$ is given by

$$\dim\left(\boldsymbol{A}\right) = 2N_\mathrm{max} \times 2N_\mathrm{max}\,,$$

with

$$N_\mathrm{max} = N_\mathrm{max}\left(\mathcal{N}\right) + 2\sum_{l=1}^{\mathcal{N}-1} N_\mathrm{max}(l)\,.$$

The dimension and occupation of the matrix $\boldsymbol{A}$ is shown in Table 2.2 for three layers.

Since

$$\dim\left(\mathcal{A}^{11}\right) = \dim\left(\mathcal{A}^{21}\right) = \dim\left(\boldsymbol{Q}_1^{13}\right) = \dim\left(\boldsymbol{Q}_1^{11}\right) = 2N_\mathrm{max}(1) \times 2N_\mathrm{max}(1)\,,$$

it follows that

$$\dim\left(\boldsymbol{T}\right) = 2N_\mathrm{max}(1) \times 2N_\mathrm{max}(1)\,.$$

Thus, the dimension of the transition matrix is given by the maximum expansion order corresponding to the first layer, while the maximum expansion

Table 2.2. Occupation of the global matrix

	$2N_{\max}(1)$	$2N_{\max}(1)$	$2N_{\max}(2)$	$2N_{\max}(2)$	$2N_{\max}(3)$
$2N_{\max}(1)$	$\boldsymbol{Q}_1^{33}$	$\boldsymbol{Q}_1^{31}$	$\mathbf{0}$	$\mathbf{0}$	$\mathbf{0}$
$2N_{\max}(1)$	$-\boldsymbol{I}(-\boldsymbol{Q}_1^{13})$	$\mathbf{0}$	$\boldsymbol{Q}_2^{13}$	$\boldsymbol{Q}_2^{11}$	$\mathbf{0}$
$2N_{\max}(2)$	$\mathbf{0}$	$-\boldsymbol{Q}_1^{31}$	$\boldsymbol{Q}_2^{33}$	$\boldsymbol{Q}_2^{31}$	$\mathbf{0}$
$2N_{\max}(2)$	$\mathbf{0}$	$\mathbf{0}$	$-\boldsymbol{I}(-\boldsymbol{Q}_2^{13})$	$\mathbf{0}$	$\boldsymbol{Q}_3^{11}$
$2N_{\max}(3)$	$\mathbf{0}$	$\mathbf{0}$	$\mathbf{0}$	$-\boldsymbol{Q}_2^{31}$	$\boldsymbol{Q}_3^{31}$

For distributed sources, the identity matrix $\boldsymbol{I}$ is replaced by the $\boldsymbol{Q}^{13}$ matrix

orders corresponding to the subsequent layers are in descending order. In contrast to these prescriptions, the solution method using a recurrence relation for $\boldsymbol{T}$-matrix calculation requires all matrices to be of the same order, i.e.,

$$\dim(\boldsymbol{T}) = \dim\bigl(\widetilde{\boldsymbol{T}}_{l,l+1,\ldots,\mathcal{N}}\bigr) = \frac{1}{2}\dim(\mathcal{Q}_l) = 2N_{\max}(1) \times 2N_{\max}(1)\,.$$

This requirement implies that the same number of basis functions must be used to approximate the surface fields on each layer. For concentrically layered spheres, this requirement is not problematic because the basis functions are orthogonal on spherical surfaces. For nonspherical layered particles, we approximate the surface fields by a complete system of vector functions and it is natural to use fewer basis functions for smaller layer surfaces. However, for convergence tests it is simpler to consider a single truncation index [181,248].

2.5.3 Formulation with Discrete Sources

For a two-layered particle as shown in Fig. 2.2, the null-field equations formulated in terms of distributed vector spherical wave functions (compare to (2.70), (2.71) and (2.72))

$$\begin{aligned}\frac{\mathrm{j}k_{\mathrm{s}}^2}{\pi}\int_{S_1}\Biggl\{&[\boldsymbol{e}_{\mathrm{i},1}(\boldsymbol{r}_1') - \boldsymbol{e}_{\mathrm{e}}(\boldsymbol{r}_1')]\cdot\begin{pmatrix}\mathcal{N}_{\nu}^{3}(k_{\mathrm{s}}\boldsymbol{r}_1')\\ \mathcal{M}_{\nu}^{3}(k_{\mathrm{s}}\boldsymbol{r}_1')\end{pmatrix}\\ &+\mathrm{j}\sqrt{\frac{\mu_{\mathrm{s}}}{\varepsilon_{\mathrm{s}}}}\,[\boldsymbol{h}_{\mathrm{i},1}(\boldsymbol{r}_1') - \boldsymbol{h}_{\mathrm{e}}(\boldsymbol{r}_1')]\cdot\begin{pmatrix}\mathcal{M}_{\nu}^{3}(k_{\mathrm{s}}\boldsymbol{r}_1')\\ \mathcal{N}_{\nu}^{3}(k_{\mathrm{s}}\boldsymbol{r}_1')\end{pmatrix}\Biggr\}\mathrm{d}S(\boldsymbol{r}_1') = 0\,,\quad \nu = 1,2,\ldots\,,\end{aligned} \tag{2.113}$$

$$\begin{aligned}-\frac{\mathrm{j}k_{\mathrm{i},1}^2}{\pi}\int_{S_1}\Biggl[&\boldsymbol{e}_{\mathrm{i},1}(\boldsymbol{r}_1')\cdot\begin{pmatrix}\mathcal{N}_{\boldsymbol{\nu}}^{1}(k_{\mathrm{i},1}\boldsymbol{r}_1')\\ \mathcal{M}_{\boldsymbol{\nu}}^{1}(k_{\mathrm{i},1}\boldsymbol{r}_1')\end{pmatrix}\\ &+\mathrm{j}\sqrt{\frac{\mu_{\mathrm{i},1}}{\varepsilon_{\mathrm{i},1}}}\boldsymbol{h}_{\mathrm{i},1}(\boldsymbol{r}_1')\cdot\begin{pmatrix}\mathcal{M}_{\boldsymbol{\nu}}^{1}(k_{\mathrm{i},1}\boldsymbol{r}_1')\\ \mathcal{N}_{\boldsymbol{\nu}}^{1}(k_{\mathrm{i},1}\boldsymbol{r}_1')\end{pmatrix}\Biggr]\mathrm{d}S(\boldsymbol{r}_1')\end{aligned}$$

$$+\frac{\mathrm{j}k_{\mathrm{i},1}^2}{\pi}\int_{S_2}\left[\boldsymbol{e}_{\mathrm{i},2}\left(\boldsymbol{r}_2''\right)\cdot\begin{pmatrix}\mathcal{N}_{\boldsymbol{\nu}}^1\left(k_{\mathrm{i},1}\boldsymbol{r}_1''\right)\\ \mathcal{M}_{\boldsymbol{\nu}}^1(k_{\mathrm{i},1}\boldsymbol{r}_1'')\end{pmatrix}\right. \tag{2.114}$$

$$\left.+\,\mathrm{j}\sqrt{\frac{\mu_{\mathrm{i},1}}{\varepsilon_{\mathrm{i},1}}}\boldsymbol{h}_{\mathrm{i},2}\left(\boldsymbol{r}_2''\right)\cdot\begin{pmatrix}\mathcal{M}_{\boldsymbol{\nu}}^1(k_{\mathrm{i},1}\boldsymbol{r}_1'')\\ \mathcal{N}_{\boldsymbol{\nu}}^1(k_{\mathrm{i},1}\boldsymbol{r}_1'')\end{pmatrix}\right]\mathrm{d}S\left(\boldsymbol{r}_2''\right)=0\,,\quad \nu=1,2,\ldots\,,$$

and

$$-\frac{\mathrm{j}k_{\mathrm{i},1}^2}{\pi}\int_{S_1}\left[\boldsymbol{e}_{\mathrm{i},1}\left(\boldsymbol{r}_1'\right)\cdot\begin{pmatrix}\mathcal{N}_{\boldsymbol{\nu}}^3(k_{\mathrm{i},1}\boldsymbol{r}_2')\\ \mathcal{M}_{\boldsymbol{\nu}}^3(k_{\mathrm{i},1}\boldsymbol{r}_2')\end{pmatrix}\right.$$

$$\left.+\,\mathrm{j}\sqrt{\frac{\mu_{\mathrm{i},1}}{\varepsilon_{\mathrm{i},1}}}\boldsymbol{h}_{\mathrm{i},1}\left(\boldsymbol{r}_1'\right)\cdot\begin{pmatrix}\mathcal{M}_{\boldsymbol{\nu}}^3(k_{\mathrm{i},1}\boldsymbol{r}_2')\\ \mathcal{N}_{\boldsymbol{\nu}}^3(k_{\mathrm{i},1}\boldsymbol{r}_2')\end{pmatrix}\right]\mathrm{d}S\left(\boldsymbol{r}_1'\right)$$

$$+\frac{\mathrm{j}k_{\mathrm{i},1}^2}{\pi}\int_{S_2}\left[\boldsymbol{e}_{\mathrm{i},2}\left(\boldsymbol{r}_2''\right)\cdot\begin{pmatrix}\mathcal{N}_{\boldsymbol{\nu}}^3(k_{\mathrm{i},1}\boldsymbol{r}_2'')\\ \mathcal{M}_{\boldsymbol{\nu}}^3(k_{\mathrm{i},1}\boldsymbol{r}_2'')\end{pmatrix}\right. \tag{2.115}$$

$$\left.+\,\mathrm{j}\sqrt{\frac{\mu_{\mathrm{i},1}}{\varepsilon_{\mathrm{i},1}}}\boldsymbol{h}_{\mathrm{i},2}\left(\boldsymbol{r}_2''\right)\cdot\begin{pmatrix}\mathcal{M}_{\boldsymbol{\nu}}^3(k_{\mathrm{i},1}\boldsymbol{r}_2'')\\ \mathcal{N}_{\boldsymbol{\nu}}^3(k_{\mathrm{i},1}\boldsymbol{r}_2'')\end{pmatrix}\right]\mathrm{d}S\left(\boldsymbol{r}_2''\right)=0\,,\quad \nu=1,2,\ldots$$

are equivalent to the general null-field equations (2.68) and (2.69). The distributed vector spherical wave functions in (2.113)–(2.115) are defined as

$$\mathcal{M}_{mn}^{1,3}(k\boldsymbol{r}_1)=\boldsymbol{M}_{m,|m|+l}^{1,3}\left[k(\boldsymbol{r}_1-z_{1,n}\boldsymbol{e}_z)\right]\,,$$
$$\mathcal{N}_{mn}^{1,3}(k\boldsymbol{r}_1)=\boldsymbol{N}_{m,|m|+l}^{1,3}\left[k(\boldsymbol{r}_1-z_{1,n}\boldsymbol{e}_z)\right]\,,$$

and

$$\mathcal{M}_{mn}^{1,3}(k\boldsymbol{r}_2)=\boldsymbol{M}_{m,|m|+l}^{1,3}\left[k(\boldsymbol{r}_2-z_{2,n}\boldsymbol{e}_z)\right]\,,$$
$$\mathcal{N}_{mn}^{1,3}(k\boldsymbol{r}_2)=\boldsymbol{N}_{m,|m|+l}^{1,3}\left[k(\boldsymbol{r}_2-z_{2,n}\boldsymbol{e}_z)\right]\,,$$

where $\{z_{1,n}\}_{n=1}^{\infty}$ is a dense set of points situated on the z-axis and in the interior of S_1, while $\{z_{2,n}\}_{n=1}^{\infty}$ is a dense set of points situated on the z-axis and in the interior of S_2. Due to their completeness property, the distributed vector spherical wave functions can be used to approximate the surface fields as in (2.73) and (2.74) but with $\mathcal{M}_{\mu}^{1,3}(k_{\mathrm{i},1}\boldsymbol{r}_1')$, $\mathcal{N}_{\mu}^{1,3}(k_{\mathrm{i},1}\boldsymbol{r}_1')$ in place of $\boldsymbol{M}_{\mu}^{1,3}(k_{\mathrm{i},1}\boldsymbol{r}_1')$, $\boldsymbol{N}_{\mu}^{1,3}(k_{\mathrm{i},1}\boldsymbol{r}_1')$ and $\mathcal{M}_{\mu}^{1}(k_{\mathrm{i},2}\boldsymbol{r}_2'')$, $\mathcal{N}_{\mu}^{1}(k_{\mathrm{i},2}\boldsymbol{r}_2'')$ in place of $\boldsymbol{M}_{\mu}^{1}(k_{\mathrm{i},2}\boldsymbol{r}_2'')$, $\boldsymbol{N}_{\mu}^{1}(k_{\mathrm{i},2}\boldsymbol{r}_2'')$, respectively.

For a multilayered particle, it is apparent that the solution methods with distributed sources use essentially the same matrix equations as the solution methods with localized sources. The matrices $\boldsymbol{A}^1$, $\boldsymbol{A}^{l,l-1}$ and $\boldsymbol{A}^{\mathcal{N}}$ are given by (2.109), (2.110) and (2.112), respectively, with $\tilde{\boldsymbol{Q}}_l^{pq}$ in place of $\boldsymbol{Q}_l^{pq}$, while the matrix $\boldsymbol{A}^{l-1,l}$ is

$$\boldsymbol{A}^{l-1,l} = \begin{bmatrix} -\widetilde{\boldsymbol{Q}}_{l-1}^{13}(k_{\mathrm{i},l-1}, l-1, k_{\mathrm{i},l-1}, l-1) & \boldsymbol{0} \\ \boldsymbol{0} & -\widetilde{\boldsymbol{Q}}_{l-1}^{31}(k_{\mathrm{i},l-1}, l, k_{\mathrm{i},l-1}, l-1) \end{bmatrix} .$$

The expressions of the elements of the $\widetilde{\boldsymbol{Q}}_l^{pq}$ matrix are given by (2.84)–(2.87) with the localized vector spherical wave functions replaced by the distributed vector spherical wave functions. The transition matrix is

$$\begin{aligned} \boldsymbol{T} = & \left[\widetilde{\boldsymbol{Q}}_1^{13}(k_\mathrm{s}, 1, k_{\mathrm{i},1}, 1)\,\mathcal{A}^{11} + \widetilde{\boldsymbol{Q}}_1^{11}(k_\mathrm{s}, 1, k_{\mathrm{i},1}, 1)\,\mathcal{A}^{21}\right] \\ & \times \widetilde{\boldsymbol{Q}}_1^{31}(k_\mathrm{s}, 1, k_\mathrm{s}, 1) , \end{aligned}$$

where the $\widetilde{\boldsymbol{Q}}_1^{11}(k_\mathrm{s}, 1, k_{\mathrm{i},1}, 1)$ and $\widetilde{\boldsymbol{Q}}_1^{13}(k_\mathrm{s}, 1, k_{\mathrm{i},1}, 1)$ matrices contain as rows the vectors $\boldsymbol{M}_{\overline{\nu}}^1(k_\mathrm{s}\boldsymbol{r}_1')$, $\boldsymbol{N}_{\overline{\nu}}^1(k_\mathrm{s}\boldsymbol{r}_1')$ and as columns the vectors $\mathcal{M}_\mu^1(k_{\mathrm{i},1}\boldsymbol{r}_1')$, $\mathcal{N}_\mu^1(k_{\mathrm{i},1}\boldsymbol{r}_1')$ and $\mathcal{M}_\mu^3(k_{\mathrm{i},1}\boldsymbol{r}_1')$, $\mathcal{N}_\mu^3(k_{\mathrm{i},1}\boldsymbol{r}_1')$, respectively, while the $\widetilde{\boldsymbol{Q}}^{31}(k_\mathrm{s}, 1, k_\mathrm{s}, 1)$ matrix contains as rows and columns the vectors $\mathcal{M}_{\overline{\nu}}^3(k_\mathrm{s}\boldsymbol{r}_1')$, $\mathcal{N}_{\overline{\nu}}^3(k_\mathrm{s}\boldsymbol{r}_1')$ and $\boldsymbol{M}_\mu^1(k_\mathrm{s}\boldsymbol{r}_1')$, $\boldsymbol{N}_\mu^1(k_\mathrm{s}\boldsymbol{r}_1')$, respectively.

The use of distributed vector spherical wave functions improves the numerical stability of the null-field method for highly elongated and flattened layered particles. Although the above formalism is valid for nonaxisymmetric particles, the method is most effective for axisymmetric particles, in which case the z-axis of the particle coordinate system is the axis of rotation. Applications of the null-field method with distributed sources to axisymmetric layered spheroids with large aspect ratios have been given by Doicu and Wriedt [50].

2.5.4 Concentrically Layered Spheres

For a concentrically layered sphere, the precedent relations simplify to those obtained in the framework of the Lorenz–Mie theory. In this specific case, we use the recurrence relation (2.107) with $\mathcal{Q}_l$ given by (2.106). All matrices are diagonal and denoting by $(T_{l,l+1,\ldots,\mathcal{N}})_n^1$ and $(T_{l,l+1,\ldots,\mathcal{N}})_n^2$ the elements of the matrix $\boldsymbol{T}_{l,l+1,\ldots,\mathcal{N}}$, we rewrite the recurrence relation as

$$\begin{aligned} & (T_{l,l+1,\ldots,\mathcal{N}})_n^1 \\ & = -\frac{j_n(x_l)\left[m_{\mathrm{r},l}x_l j_n(m_{\mathrm{r},l}x_l)\right]' r_n - j_n(m_{\mathrm{r},l}x_l)\left[x_l j_n(x_l)\right]' p_n}{h_n^{(1)}(x_l)\left[m_{\mathrm{r},l}x_l j_n(m_{\mathrm{r},l}x_l)\right]' r_n - j_n(m_{\mathrm{r},l}x_l)\left[x_l h_n^{(1)}(x_l)\right]' p_n} , \end{aligned} \tag{2.116}$$

$$\begin{aligned} & (T_{l,l+1,\ldots,\mathcal{N}})_n^2 \\ & = -\frac{j_n(x_l)\left[m_{\mathrm{r},l}x_l j_n(m_{\mathrm{r},l}x_l)\right]' q_n - m_{\mathrm{r},l}^2 j_n(m_{\mathrm{r},l}x_l)\left[x_l j_n(x_l)\right]' s_n}{h_n^{(1)}(x_l)\left[m_{\mathrm{r},l}x_l j_n(m_{\mathrm{r},l}x_l)\right]' q_n - m_{\mathrm{r},l}^2 j_n(m_{\mathrm{r},l}x_l)\left[x_l h_n^{(1)}(x_l)\right]' s_n} , \end{aligned} \tag{2.117}$$

where

$$p_n = 1 + \left(T_{l+1,l+2,\ldots,\mathcal{N}}\right)_n^1 \frac{h_n^{(1)}\left(m_{\mathrm{r},l}x_l\right)}{j_n\left(m_{\mathrm{r},l}x_l\right)}\,, \tag{2.118}$$

$$s_n = 1 + \left(T_{l+1,l+2,\ldots,\mathcal{N}}\right)_n^2 \frac{h_n^{(1)}\left(m_{\mathrm{r},l}x_l\right)}{j_n\left(m_{\mathrm{r},l}x_l\right)}\,, \tag{2.119}$$

$$r_n = 1 + \left(T_{l+1,l+2,\ldots,\mathcal{N}}\right)_n^1 \frac{\left[m_{\mathrm{r},l}x_l h_n^{(1)}\left(m_{\mathrm{r},l}x_l\right)\right]'}{\left[m_{\mathrm{r},l}x_l j_n\left(m_{\mathrm{r},l}x_l\right)\right]'}\,, \tag{2.120}$$

$$q_n = 1 + \left(T_{l+1,l+2,\ldots,\mathcal{N}}\right)_n^2 \frac{\left[m_{\mathrm{r},l}x_l h_n^{(1)}\left(m_{\mathrm{r},l}x_l\right)\right]'}{\left[m_{\mathrm{r},l}x_l j_n\left(m_{\mathrm{r},l}x_l\right)\right]'}\,, \tag{2.121}$$

$x_l = k_{\mathrm{i},l}R_l = k_0 m_l R_l$ is the size parameter of the layer l and

$$m_{\mathrm{r},l} = \frac{m_l}{m_{l-1}}$$

is the relative refractive index of the layer l with respect to the layer $l-1$. To obtain a stable scheme for computing the $\boldsymbol{T}$ matrix, we express the above recurrence relation in terms of the logarithmic derivatives A_n and B_n:

$$\left(T_{l,l+1,\ldots,\mathcal{N}}\right)_n^1 = -\frac{\left[m_{\mathrm{r},l}A_n\left(m_{\mathrm{r},l}x_l\right)r_n + \frac{n}{x_l}p_n\right]j_n\left(x_l\right) - j_{n-1}\left(x_l\right)p_n}{\left[m_{\mathrm{r},l}A_n\left(m_{\mathrm{r},l}x_l\right)r_n + \frac{n}{x_l}p_n\right]h_n^{(1)}\left(x_l\right) - h_{n-1}^{(1)}\left(x_l\right)p_n}\,, \tag{2.122}$$

$$\left(T_{l,l+1,\ldots,\mathcal{N}}\right)_n^2 = -\frac{\left[\frac{A_n\left(m_{\mathrm{r},l}x_l\right)}{m_{\mathrm{r},l}}q_n + \frac{n}{x_l}s_n\right]j_n\left(x_l\right) - j_{n-1}\left(x_l\right)s_n}{\left[\frac{A_n\left(m_{\mathrm{r},l}x_l\right)}{m_{\mathrm{r},l}}q_n + \frac{n}{x_l}s_n\right]h_n^{(1)}\left(x_l\right) - h_{n-1}^{(1)}\left(x_l\right)s_n}\,, \tag{2.123}$$

where p_n and s_n are given by (2.118) and (2.119), respectively, and r_n and q_n are now given by

$$r_n = 1 + \left(T_{l+1,l+2,\ldots,\mathcal{N}}\right)_n^1 \frac{B_n\left(m_{\mathrm{r},l}x_l\right)}{A_n\left(m_{\mathrm{r},l}x_l\right)}\frac{h_n^{(1)}\left(m_{\mathrm{r},l}x_l\right)}{j_n\left(m_{\mathrm{r},l}x_l\right)}$$

and

$$q_n = 1 + \left(T_{l+1,l+2,\ldots,\mathcal{N}}\right)_n^2 \frac{B_n\left(m_{\mathrm{r},l}x_l\right)}{A_n\left(m_{\mathrm{r},l}x_l\right)}\frac{h_n^{(1)}\left(m_{\mathrm{r},l}x_l\right)}{j_n\left(m_{\mathrm{r},l}x_l\right)}\,,$$

respectively.

The computation of Lorenz–Mie coefficients for concentrically layered spheres has been considered by Kerker [115], Toon and Ackerman [222], and Fuller [76], while recursive algorithms for multilayered spheres have been developed by Bhandari [13] and Mackowski et al. [154].

2.6 Multiple Particles

In this section we extend the null-field method to the case of an arbitrary number of particles by using the translation properties of the vector spherical wave functions. Taking into account the geometric restriction that the particles do not overlap in space, we derive the expression of the transition matrix for restricted values of translations. Our treatment closely follows the original derivation given by Peterson and Ström [187, 188].

2.6.1 General Formulation

For reasons of clarity of the presentation we first consider the generic case of two homogeneous particles immersed in a homogeneous medium with a relative permittivity $\varepsilon_{\rm s}$ and a relative permeability $\mu_{\rm s}$. The scattering geometry is depicted in Fig. 2.5. The surfaces S_1 and S_2 are defined with respect to the particle coordinate systems $O_1x_1y_1z_1$ and $O_2x_2y_2z_2$, respectively, while the coordinate system of the ensemble or the global coordinate system is denoted by $Oxyz$. The coordinate system $O_1x_1y_1z_1$ is obtained by translating the coordinate system $Oxyz$ through $\boldsymbol{r}_{01}$ and by rotating the translated coordinate system through the Euler angles α_1, β_1 and γ_1. Similarly, the coordinate system $O_2x_2y_2z_2$ is obtained by translating the coordinate system $Oxyz$ through $\boldsymbol{r}_{02}$ and by rotating the translated coordinate system through the Euler angles α_2, β_2 and γ_2. The main assumption of our analysis is that the smallest circumscribing spheres of the particles centered at O_1 and O_2, respectively, do not overlap. The boundary-value problem for the two scattering particles depicted in Fig. 2.5 has the following formulation.

Given the external excitation $\boldsymbol{E}_{\rm e}, \boldsymbol{H}_{\rm e}$ *as an entire solution to the Maxwell equations, find the scattered field* $\boldsymbol{E}_{\rm s}$, $\boldsymbol{H}_{\rm s}$ *and the internal fields* $\boldsymbol{E}_{\rm i,1}$, $\boldsymbol{H}_{\rm i,1}$

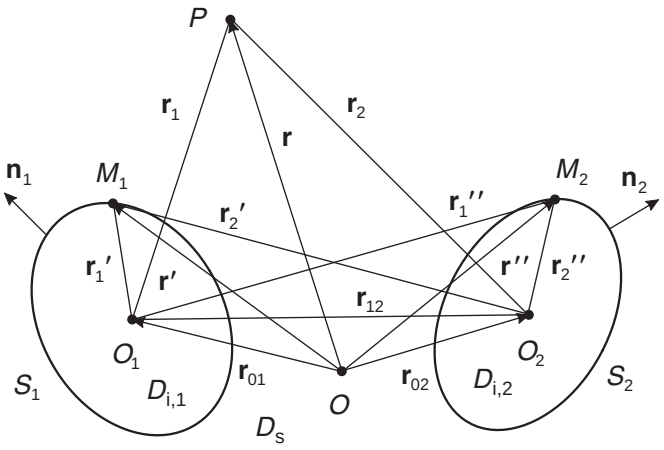

Fig. 2.5. Geometry of two scattering particles

and $\boldsymbol{E}_{\mathrm{i},2}$, $\boldsymbol{H}_{\mathrm{i},2}$ *satisfying the Maxwell equations*

$$\nabla \times \boldsymbol{E}_{\mathrm{s}} = \mathrm{j}k_0\mu_{\mathrm{s}}\boldsymbol{H}_{\mathrm{s}}\,, \quad \nabla \times \boldsymbol{H}_{\mathrm{s}} = -\mathrm{j}k_0\varepsilon_{\mathrm{s}}\boldsymbol{E}_{\mathrm{s}} \quad \textit{in} \quad D_{\mathrm{s}}\,, \tag{2.124}$$

$$\nabla \times \boldsymbol{E}_{\mathrm{i},1} = \mathrm{j}k_0\mu_{\mathrm{i},1}\boldsymbol{H}_{\mathrm{i},1}\,, \quad \nabla \times \boldsymbol{H}_{\mathrm{i},1} = -\mathrm{j}k_0\varepsilon_{\mathrm{i},1}\boldsymbol{E}_{\mathrm{i},1} \quad \textit{in} \quad D_{\mathrm{i},1}\,, \tag{2.125}$$

and

$$\nabla \times \boldsymbol{E}_{\mathrm{i},2} = \mathrm{j}k_0\mu_{\mathrm{i},2}\boldsymbol{H}_{\mathrm{i},2}\,, quad\nabla \times \boldsymbol{H}_{\mathrm{i},2} = -\mathrm{j}k_0\varepsilon_{\mathrm{i},2}\boldsymbol{E}_{\mathrm{i},2} \quad \textit{in} \quad D_{\mathrm{i},2}\,, \tag{2.126}$$

the boundary conditions

$$\begin{aligned} \boldsymbol{n}_1 \times \boldsymbol{E}_{\mathrm{i},1} - \boldsymbol{n}_1 \times \boldsymbol{E}_{\mathrm{s}} &= \boldsymbol{n}_1 \times \boldsymbol{E}_{\mathrm{e}}\,, \\ \boldsymbol{n}_1 \times \boldsymbol{H}_{\mathrm{i},1} - \boldsymbol{n}_1 \times \boldsymbol{H}_{\mathrm{s}} &= \boldsymbol{n}_1 \times \boldsymbol{H}_{\mathrm{e}} \end{aligned} \tag{2.127}$$

on S_1 *and*

$$\begin{aligned} \boldsymbol{n}_2 \times \boldsymbol{E}_{\mathrm{i},2} - \boldsymbol{n}_2 \times \boldsymbol{E}_{\mathrm{s}} &= \boldsymbol{n}_2 \times \boldsymbol{E}_{\mathrm{e}}\,, \\ \boldsymbol{n}_2 \times \boldsymbol{H}_{\mathrm{i},2} - \boldsymbol{n}_2 \times \boldsymbol{H}_{\mathrm{s}} &= \boldsymbol{n}_2 \times \boldsymbol{H}_{\mathrm{e}} \end{aligned} \tag{2.128}$$

on S_2, *and the Silver–Müller radiation condition for the scattered field (2.3).*

The Stratton–Chu representation theorem for the scattered field $\boldsymbol{E}_{\mathrm{s}}$ in $D_{\mathrm{i},1}$ and $D_{\mathrm{i},2}$ together with the boundary conditions (2.127) and (2.128) yield the general null-field equation

$$\begin{aligned} &\boldsymbol{E}_{\mathrm{e}}(\boldsymbol{r}) + \nabla \times \int_{S_1} \boldsymbol{e}_{\mathrm{i},1}\left(\boldsymbol{r}'\right) g\left(k_{\mathrm{s}}, \boldsymbol{r}, \boldsymbol{r}'\right) \mathrm{d}S\left(\boldsymbol{r}'\right) \\ &+\frac{\mathrm{j}}{k_0\varepsilon_{\mathrm{s}}} \nabla \times \nabla \times \int_{S_1} \boldsymbol{h}_{\mathrm{i},1}\left(\boldsymbol{r}'\right) g\left(k_{\mathrm{s}}, \boldsymbol{r}, \boldsymbol{r}'\right) \mathrm{d}S\left(\boldsymbol{r}'\right) \\ &+\nabla \times \int_{S_2} \boldsymbol{e}_{\mathrm{i},2}\left(\boldsymbol{r}''\right) g\left(k_{\mathrm{s}}, \boldsymbol{r}, \boldsymbol{r}''\right) \mathrm{d}S\left(\boldsymbol{r}''\right) \\ &+\frac{\mathrm{j}}{k_0\varepsilon_{\mathrm{s}}} \nabla \times \nabla \times \int_{S_2} \boldsymbol{h}_{\mathrm{i},2}\left(\boldsymbol{r}''\right) g\left(k_{\mathrm{s}}, \boldsymbol{r}, \boldsymbol{r}''\right) \mathrm{d}S\left(\boldsymbol{r}''\right) = 0\,, \quad \boldsymbol{r} \in D_{\mathrm{i},1} \cup D_{\mathrm{i},2}\,. \end{aligned}$$

Before we derive the null-field equations, we seek to find a relation between the expansion coefficients of the incident field in the global coordinate system $Oxyz$,

$$\boldsymbol{E}_{\mathrm{e}}(\boldsymbol{r}) = \sum_{\nu} a_\nu \boldsymbol{M}_\nu^1\left(k_{\mathrm{s}}\boldsymbol{r}\right) + b_\nu \boldsymbol{N}_\nu^1\left(k_{\mathrm{s}}\boldsymbol{r}\right)$$

and the expansion coefficients of the incident field in the particle coordinate system $O_1x_1y_1z_1$,

$$\boldsymbol{E}_{\mathrm{e}}\left(\boldsymbol{r}_1\right) = \sum_{\nu} a_{1,\nu} \boldsymbol{M}_\nu^1\left(k_{\mathrm{s}}\boldsymbol{r}_1\right) + b_{1,\nu} \boldsymbol{N}_\nu^1\left(k_{\mathrm{s}}\boldsymbol{r}_1\right)\,.$$

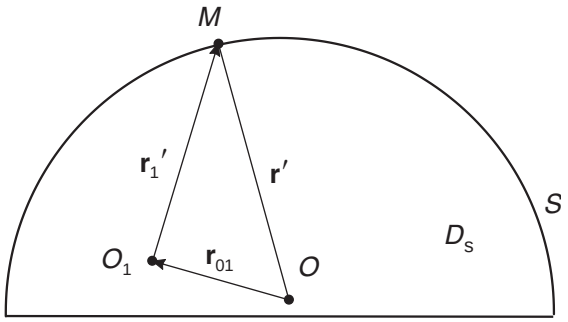

Fig. 2.6. Auxiliary surface S

For this purpose we choose a sufficiently large auxiliary surface S enclosing O and O_1 (Fig. 2.6) and in each coordinate system we use the Stratton–Chu representation theorem for the incident field in the interior of S. We obtain

$$\begin{pmatrix} a_\nu \\ b_\nu \end{pmatrix} = -\frac{\mathrm{j}k_\mathrm{s}^2}{\pi} \int_S \left[\boldsymbol{e}_\mathrm{e}(\boldsymbol{r}') \begin{pmatrix} \boldsymbol{N}_{\overline{\nu}}^3(k_\mathrm{s}\boldsymbol{r}') \\ \boldsymbol{M}_{\overline{\nu}}^3(k_\mathrm{s}\boldsymbol{r}') \end{pmatrix} + \mathrm{j}\sqrt{\frac{\mu_\mathrm{s}}{\varepsilon_\mathrm{s}}} \boldsymbol{h}_\mathrm{e}(\boldsymbol{r}') \begin{pmatrix} \boldsymbol{M}_{\overline{\nu}}^3(k_\mathrm{s}\boldsymbol{r}') \\ \boldsymbol{N}_{\overline{\nu}}^3(k_\mathrm{s}\boldsymbol{r}') \end{pmatrix} \right] \mathrm{d}S(\boldsymbol{r}') \ ,$$

and

$$\begin{pmatrix} a_{1,\nu} \\ b_{1,\nu} \end{pmatrix} = -\frac{\mathrm{j}k_\mathrm{s}^2}{\pi} \int_S \left[\boldsymbol{e}_\mathrm{e}(\boldsymbol{r}_1') \begin{pmatrix} \boldsymbol{N}_{\overline{\nu}}^3(k_\mathrm{s}\boldsymbol{r}_1') \\ \boldsymbol{M}_{\overline{\nu}}^3(k_\mathrm{s}\boldsymbol{r}_1') \end{pmatrix} + \mathrm{j}\sqrt{\frac{\mu_\mathrm{s}}{\varepsilon_\mathrm{s}}} \boldsymbol{h}_\mathrm{e}(\boldsymbol{r}_1') \begin{pmatrix} \boldsymbol{M}_{\overline{\nu}}^3(k_\mathrm{s}\boldsymbol{r}_1') \\ \boldsymbol{N}_{\overline{\nu}}^3(k_\mathrm{s}\boldsymbol{r}_1') \end{pmatrix} \right] \mathrm{d}S(\boldsymbol{r}_1') \ ,$$

respectively. Using the addition theorem for radiating vector spherical wave functions

$$\begin{bmatrix} \boldsymbol{M}_{\overline{\boldsymbol{\nu}}}^3(k_\mathrm{s}\boldsymbol{r}_1') \\ \boldsymbol{N}_{\overline{\boldsymbol{\nu}}}^3(k_\mathrm{s}\boldsymbol{r}_1') \end{bmatrix} = \left[\left(\mathcal{S}_{10}^\mathrm{rt}\right)_{\overline{\boldsymbol{\nu}\mu}} \right] \begin{bmatrix} \boldsymbol{M}_{\overline{\mu}}^3(k_\mathrm{s}\boldsymbol{r}') \\ \boldsymbol{N}_{\overline{\mu}}^3(k_\mathrm{s}\boldsymbol{r}') \end{bmatrix} ,$$

where

$$\mathcal{S}_{10}^\mathrm{rt} = \mathcal{R}(-\gamma_1, -\beta_1, -\alpha_1)\, \mathcal{T}^{33}(-k_\mathrm{s}\boldsymbol{r}_{01}) \ , \quad \text{for} \quad r' > r_{01}$$

and taking into account that $\mathcal{S}_{10}^\mathrm{rt}$ is a block-symmetric matrix, yields

$$\begin{bmatrix} a_{1,\nu} \\ b_{1,\nu} \end{bmatrix} = \left[\left(\mathcal{S}_{10}^\mathrm{rt}\right)_{\overline{\nu\mu}} \right] \begin{bmatrix} a_\mu \\ b_\mu \end{bmatrix} . \tag{2.129}$$

The condition $r' > r_{01}$ can always be satisfied in practice by an appropriate choice of the auxiliary surface S, whence, using the identity $\mathcal{T}^{33}(-k_{\mathrm{s}}\boldsymbol{r}_{01}) = \mathcal{T}^{11}(-k_{\mathrm{s}}\boldsymbol{r}_{01})$, we see that

$$\mathcal{S}_{10}^{\mathrm{rt}} = \mathcal{R}\left(-\gamma_1, -\beta_1, -\alpha_1\right)\mathcal{T}^{11}\left(-k_{\mathrm{s}}\boldsymbol{r}_{01}\right) .$$

We proceed now to derive the set of null-field equations. Passing from the origin O to the origin O_1, using the relations

$$g\left(k_{\mathrm{s}}, \boldsymbol{r}, \boldsymbol{r}'\right) = g\left(k_{\mathrm{s}}, \boldsymbol{r}_1, \boldsymbol{r}_1'\right) ,$$
$$g\left(k_{\mathrm{s}}, \boldsymbol{r}, \boldsymbol{r}''\right) = g\left(k_{\mathrm{s}}, \boldsymbol{r}_1, \boldsymbol{r}_1''\right) ,$$

and restricting $\boldsymbol{r}_1$ to lie on a sphere enclosed in $D_{\mathrm{i},1}$, gives

$$\begin{aligned}
&\frac{\mathrm{j}k_{\mathrm{s}}^2}{\pi}\int_{S_1}\left[\boldsymbol{e}_{\mathrm{i},1}\left(\boldsymbol{r}_1'\right)\cdot\begin{pmatrix}\boldsymbol{N}_{\boldsymbol{\nu}}^3(k_{\mathrm{s}}\boldsymbol{r}_1')\\ \boldsymbol{M}_{\boldsymbol{\nu}}^3(k_{\mathrm{s}}\boldsymbol{r}_1')\end{pmatrix}\right.\\
&\left.+\,\mathrm{j}\sqrt{\frac{\mu_{\mathrm{s}}}{\varepsilon_{\mathrm{s}}}}\boldsymbol{h}_{\mathrm{i},1}\left(\boldsymbol{r}_1'\right)\cdot\begin{pmatrix}\boldsymbol{M}_{\boldsymbol{\nu}}^3(k_{\mathrm{s}}\boldsymbol{r}_1')\\ \boldsymbol{N}_{\boldsymbol{\nu}}^3(k_{\mathrm{s}}\boldsymbol{r}_1')\end{pmatrix}\right]\mathrm{d}S\left(\boldsymbol{r}_1'\right)\\
&+\frac{\mathrm{j}k_{\mathrm{s}}^2}{\pi}\int_{S_2}\left[\boldsymbol{e}_{\mathrm{i},2}\left(\boldsymbol{r}_2''\right)\cdot\begin{pmatrix}\boldsymbol{N}_{\boldsymbol{\nu}}^3(k_{\mathrm{s}}\boldsymbol{r}_1'')\\ \boldsymbol{M}_{\boldsymbol{\nu}}^3(k_{\mathrm{s}}\boldsymbol{r}_1'')\end{pmatrix}\right.\\
&\left.+\,\mathrm{j}\sqrt{\frac{\mu_{\mathrm{s}}}{\varepsilon_{\mathrm{s}}}}\boldsymbol{h}_{\mathrm{i},2}\left(\boldsymbol{r}_2''\right)\cdot\begin{pmatrix}\boldsymbol{M}_{\boldsymbol{\nu}}^3(k_{\mathrm{s}}\boldsymbol{r}_1'')\\ \boldsymbol{N}_{\boldsymbol{\nu}}^3(k_{\mathrm{s}}\boldsymbol{r}_1'')\end{pmatrix}\right]\mathrm{d}S\left(\boldsymbol{r}_2''\right) = -\begin{pmatrix}a_{1,\nu}\\ b_{1,\nu}\end{pmatrix}, \quad \nu = 1, 2, \ldots ,
\end{aligned} \tag{2.130}$$

where the identities $\boldsymbol{e}_{\mathrm{i},2}(\boldsymbol{r}_2'') = \boldsymbol{e}_{\mathrm{i},2}(\boldsymbol{r}_1'')$ and $\boldsymbol{h}_{\mathrm{i},2}(\boldsymbol{r}_2'') = \boldsymbol{h}_{\mathrm{i},2}(\boldsymbol{r}_1'')$ have been used. For the general null-field equation in $D_{\mathrm{i},2}$ we proceed analogously but restrict $\boldsymbol{r}_2$ to lie on a sphere enclosed in $D_{\mathrm{i},2}$. We obtain

$$\begin{aligned}
&\frac{\mathrm{j}k_{\mathrm{s}}^2}{\pi}\int_{S_1}\left[\boldsymbol{e}_{\mathrm{i},1}\left(\boldsymbol{r}_1'\right)\cdot\begin{pmatrix}\boldsymbol{N}_{\boldsymbol{\nu}}^3(k_{\mathrm{s}}\boldsymbol{r}_2')\\ \boldsymbol{M}_{\boldsymbol{\nu}}^3(k_{\mathrm{s}}\boldsymbol{r}_2')\end{pmatrix}\right.\\
&\left.+\,\mathrm{j}\sqrt{\frac{\mu_{\mathrm{s}}}{\varepsilon_{\mathrm{s}}}}\boldsymbol{h}_{\mathrm{i},1}\left(\boldsymbol{r}_1'\right)\cdot\begin{pmatrix}\boldsymbol{M}_{\boldsymbol{\nu}}^3(k_{\mathrm{s}}\boldsymbol{r}_2')\\ \boldsymbol{N}_{\boldsymbol{\nu}}^3(k_{\mathrm{s}}\boldsymbol{r}_2')\end{pmatrix}\right]\mathrm{d}S\left(\boldsymbol{r}_1'\right)\\
&+\frac{\mathrm{j}k_{\mathrm{s}}^2}{\pi}\int_{S_2}\left[\boldsymbol{e}_{\mathrm{i},2}\left(\boldsymbol{r}_2''\right)\cdot\begin{pmatrix}\boldsymbol{N}_{\boldsymbol{\nu}}^3(k_{\mathrm{s}}\boldsymbol{r}_2'')\\ \boldsymbol{M}_{\boldsymbol{\nu}}^3(k_{\mathrm{s}}\boldsymbol{r}_2'')\end{pmatrix}\right.\\
&\left.+\,\mathrm{j}\sqrt{\frac{\mu_{\mathrm{s}}}{\varepsilon_{\mathrm{s}}}}\boldsymbol{h}_{\mathrm{i},2}\left(\boldsymbol{r}_2''\right)\cdot\begin{pmatrix}\boldsymbol{M}_{\boldsymbol{\nu}}^3(k_{\mathrm{s}}\boldsymbol{r}_2'')\\ \boldsymbol{N}_{\boldsymbol{\nu}}^3(k_{\mathrm{s}}\boldsymbol{r}_2'')\end{pmatrix}\right]\mathrm{d}S\left(\boldsymbol{r}_2''\right) = -\begin{pmatrix}a_{2,\nu}\\ b_{2,\nu}\end{pmatrix}, \quad \nu = 1, 2, \ldots ,
\end{aligned} \tag{2.131}$$

where, as before, we have taken into account that $\boldsymbol{e}_{\mathrm{i},1}(\boldsymbol{r}_1') = \boldsymbol{e}_{\mathrm{i},1}(\boldsymbol{r}_2')$ and $\boldsymbol{h}_{\mathrm{i},1}(\boldsymbol{r}_1') = \boldsymbol{h}_{\mathrm{i},1}(\boldsymbol{r}_2')$.

The surface fields $\boldsymbol{e}_{\mathrm{i},1}$, $\boldsymbol{h}_{\mathrm{i},1}$ and $\boldsymbol{e}_{\mathrm{i},2}$, $\boldsymbol{h}_{\mathrm{i},2}$ are the tangential components of the electric and magnetic fields in the domains $D_{\mathrm{i},1}$ and $D_{\mathrm{i},2}$, respectively, and the surface fields approximations can be expressed as linear combinations of regular vector spherical wave functions,

$$\begin{aligned}\begin{pmatrix}\boldsymbol{e}^N_{\mathrm{i},1}(\boldsymbol{r}'_1)\\ \boldsymbol{h}^N_{\mathrm{i},1}(\boldsymbol{r}'_1)\end{pmatrix} &= \sum_{\mu=1}^{N} c^N_{1,\mu}\begin{pmatrix}\boldsymbol{n}_1(\boldsymbol{r}'_1)\times\boldsymbol{M}^1_\mu(k_{\mathrm{i},1}\boldsymbol{r}'_1)\\ -\mathrm{j}\sqrt{\frac{\varepsilon_{\mathrm{i},1}}{\mu_{\mathrm{i},1}}}\boldsymbol{n}_1(\boldsymbol{r}'_1)\times\boldsymbol{N}^1_\mu(k_{\mathrm{i},1}\boldsymbol{r}'_1)\end{pmatrix}\\ &\quad + d^N_{1,\mu}\begin{pmatrix}\boldsymbol{n}_1(\boldsymbol{r}'_1)\times\boldsymbol{N}^1_\mu(k_{\mathrm{i},1}\boldsymbol{r}'_1)\\ -\mathrm{j}\sqrt{\frac{\varepsilon_{\mathrm{i},1}}{\mu_{\mathrm{i},1}}}\boldsymbol{n}_1(\boldsymbol{r}'_1)\times\boldsymbol{M}^1_\mu(k_{\mathrm{i},1}\boldsymbol{r}'_1)\end{pmatrix}\end{aligned} \tag{2.132}$$

and

$$\begin{aligned}\begin{pmatrix}\boldsymbol{e}^N_{\mathrm{i},2}(\boldsymbol{r}''_2)\\ \boldsymbol{h}^N_{\mathrm{i},2}(\boldsymbol{r}''_2)\end{pmatrix} &= \sum_{\mu=1}^{N} c^N_{2,\mu}\begin{pmatrix}\boldsymbol{n}_2(\boldsymbol{r}''_2)\times\boldsymbol{M}^1_\mu(k_{\mathrm{i},2}\boldsymbol{r}''_2)\\ -\mathrm{j}\sqrt{\frac{\varepsilon_{\mathrm{i},2}}{\mu_{\mathrm{i},2}}}\boldsymbol{n}_2(\boldsymbol{r}''_2)\times\boldsymbol{N}^1_\mu(k_{\mathrm{i},2}\boldsymbol{r}''_2)\end{pmatrix}\\ &\quad + d^N_{2,\mu}\begin{pmatrix}\boldsymbol{n}_2(\boldsymbol{r}''_2)\times\boldsymbol{N}^1_\mu(k_{\mathrm{i},2}\boldsymbol{r}''_2)\\ -\mathrm{j}\sqrt{\frac{\varepsilon_{\mathrm{i},2}}{\mu_{\mathrm{i},2}}}\boldsymbol{n}_2(\boldsymbol{r}''_2)\times\boldsymbol{M}^1_\mu(k_{\mathrm{i},2}\boldsymbol{r}''_2)\end{pmatrix}.\end{aligned} \tag{2.133}$$

Inserting (2.132) and (2.133) into (2.130) and (2.131), using the addition theorem for vector spherical wave functions

$$\begin{bmatrix}\boldsymbol{M}^3_{\boldsymbol{\nu}}(k_{\mathrm{s}}\boldsymbol{r}''_1)\\ \boldsymbol{N}^3_{\boldsymbol{\nu}}(k_{\mathrm{s}}\boldsymbol{r}''_1)\end{bmatrix} = \begin{bmatrix}\left(\widetilde{\mathcal{S}}^{\mathrm{rtr}}_{12}\right)_{\overline{\nu\mu}}\end{bmatrix}\begin{bmatrix}\boldsymbol{M}^1_{\overline{\mu}}(k_{\mathrm{s}}\boldsymbol{r}''_2)\\ \boldsymbol{N}^1_{\overline{\mu}}(k_{\mathrm{s}}\boldsymbol{r}''_2)\end{bmatrix}$$

with

$$\widetilde{\mathcal{S}}^{\mathrm{rtr}}_{12} = \mathcal{R}\left(-\gamma_1,-\beta_1,-\alpha_1\right)\mathcal{T}^{31}\left(k_{\mathrm{s}}\boldsymbol{r}_{12}\right)\mathcal{R}\left(\alpha_2,\beta_2,\gamma_2\right), \quad \text{for} \quad r''_2 < r_{12},$$

and

$$\begin{bmatrix}\boldsymbol{M}^3_{\boldsymbol{\nu}}(k_{\mathrm{s}}\boldsymbol{r}'_2)\\ \boldsymbol{N}^3_{\boldsymbol{\nu}}(k_{\mathrm{s}}\boldsymbol{r}'_2)\end{bmatrix} = \begin{bmatrix}\left(\widetilde{\mathcal{S}}^{\mathrm{rtr}}_{21}\right)_{\overline{\nu\mu}}\end{bmatrix}\begin{bmatrix}\boldsymbol{M}^1_{\overline{\mu}}(k_{\mathrm{s}}\boldsymbol{r}'_1)\\ \boldsymbol{N}^1_{\overline{\mu}}(k_{\mathrm{s}}\boldsymbol{r}'_1)\end{bmatrix},$$

with

$$\widetilde{\mathcal{S}}^{\mathrm{rtr}}_{21} = \mathcal{R}\left(-\gamma_2,-\beta_2,-\alpha_2\right)\mathcal{T}^{31}\left(-k_{\mathrm{s}}\boldsymbol{r}_{12}\right)\mathcal{R}\left(\alpha_1,\beta_1,\gamma_1\right) \quad \text{for} \quad r'_1 < r_{12},$$

and taking into account the transformation rule for the incident field coefficients (2.129), yields the system of matrix equations

$$\begin{aligned}\boldsymbol{Q}^{31}_1(k_{\mathrm{s}},k_{\mathrm{i},1})\boldsymbol{i}_1 + \widetilde{\mathcal{S}}^{\mathrm{rtr}}_{12}\boldsymbol{Q}^{11}_2(k_{\mathrm{s}},k_{\mathrm{i},2})\boldsymbol{i}_2 &= -\mathcal{S}^{\mathrm{rt}}_{10}\boldsymbol{e},\\ \widetilde{\mathcal{S}}^{\mathrm{rtr}}_{21}\boldsymbol{Q}^{11}_1(k_{\mathrm{s}},k_{\mathrm{i},1})\boldsymbol{i}_1 + \boldsymbol{Q}^{31}_2(k_{\mathrm{s}},k_{\mathrm{i},2})\boldsymbol{i}_2 &= -\mathcal{S}^{\mathrm{rt}}_{20}\boldsymbol{e},\end{aligned} \tag{2.134}$$

where $\boldsymbol{i}_1 = [c^N_{1,\mu}, d^N_{1,\mu}]^{\mathrm{T}}$, $\boldsymbol{i}_2 = [c^N_{2,\mu}, d^N_{2,\mu}]^{\mathrm{T}}$, and as usually, $\boldsymbol{e} = [a_\nu, b_\nu]^{\mathrm{T}}$ is the vector containing the expansion coefficients of the incident field in the global coordinate system. Further, defining the scattered field coefficients

$$\begin{aligned}\boldsymbol{s}_1 &= \boldsymbol{Q}_1^{11}(k_{\mathrm{s}}, k_{\mathrm{i},1})\boldsymbol{i}_1\,,\\ \boldsymbol{s}_2 &= \boldsymbol{Q}_2^{11}(k_{\mathrm{s}}, k_{\mathrm{i},2})\boldsymbol{i}_2\,,\end{aligned}$$

and introducing the individual transition matrices,

$$\begin{aligned}\boldsymbol{T}_1 &= -\boldsymbol{Q}_1^{11}\left(k_{\mathrm{s}}, k_{\mathrm{i},1}\right)\left[\boldsymbol{Q}_1^{31}\left(k_{\mathrm{s}}, k_{\mathrm{i},1}\right)\right]^{-1}\,,\\ \boldsymbol{T}_2 &= -\boldsymbol{Q}_2^{11}\left(k_{\mathrm{s}}, k_{\mathrm{i},2}\right)\left[\boldsymbol{Q}_2^{31}\left(k_{\mathrm{s}}, k_{\mathrm{i},2}\right)\right]^{-1}\,,\end{aligned}$$

we rewrite the matrix system (2.134) as

$$\begin{aligned}\boldsymbol{s}_1 - \boldsymbol{T}_1\widetilde{\mathcal{S}}_{12}^{\mathrm{rtr}}\boldsymbol{s}_2 &= \boldsymbol{T}_1\mathcal{S}_{10}^{\mathrm{rt}}\boldsymbol{e}\,,\\ \boldsymbol{s}_2 - \boldsymbol{T}_2\widetilde{\mathcal{S}}_{21}^{\mathrm{rtr}}\boldsymbol{s}_1 &= \boldsymbol{T}_2\mathcal{S}_{20}^{\mathrm{rt}}\boldsymbol{e}\,,\end{aligned}$$

and find the solutions

$$\begin{aligned}\boldsymbol{s}_1 &= \boldsymbol{T}_1\left(\boldsymbol{I} - \widetilde{\mathcal{S}}_{12}^{\mathrm{rtr}}\boldsymbol{T}_2\widetilde{\mathcal{S}}_{21}^{\mathrm{rtr}}\boldsymbol{T}_1\right)^{-1}\left(\mathcal{S}_{10}^{\mathrm{rt}} + \widetilde{\mathcal{S}}_{12}^{\mathrm{rtr}}\boldsymbol{T}_2\mathcal{S}_{20}^{\mathrm{rt}}\right)\,,\\ \boldsymbol{s}_2 &= \boldsymbol{T}_2\left(\boldsymbol{I} - \widetilde{\mathcal{S}}_{21}^{\mathrm{rtr}}\boldsymbol{T}_1\widetilde{\mathcal{S}}_{12}^{\mathrm{rtr}}\boldsymbol{T}_2\right)^{-1}\left(\mathcal{S}_{20}^{\mathrm{rt}} + \widetilde{\mathcal{S}}_{21}^{\mathrm{rtr}}\boldsymbol{T}_1\mathcal{S}_{10}^{\mathrm{rt}}\right)\,.\end{aligned}\tag{2.135}$$

To compute the $\boldsymbol{T}$ matrix of the two-particles system and to derive a scattered-field expansion centered at the origin O of the global coordinate system we use the Stratton–Chu representation theorem for the scattered field $\boldsymbol{E}_{\mathrm{s}}$ in D_{s}. In the exterior of a sphere enclosing the particles, the expansion of the approximate scattered field $\boldsymbol{E}_{\mathrm{s}}^N$ in terms of radiating vector spherical wave functions reads as

$$\boldsymbol{E}_{\mathrm{s}}^N(\boldsymbol{r}) = \sum_{\nu=1}^{N} f_\nu^N\boldsymbol{M}_\nu^3\left(k_{\mathrm{s}}\boldsymbol{r}\right) + g_\nu^N\boldsymbol{N}_\nu^3\left(k_{\mathrm{s}}\boldsymbol{r}\right)\,,$$

where the expansion coefficients are given by

$$\begin{aligned}\begin{pmatrix} f_\nu^N \\ g_\nu^N \end{pmatrix} = \frac{\mathrm{j}k_{\mathrm{s}}^2}{\pi}\int_{S_1}&\left[\boldsymbol{e}_{\mathrm{i},1}^N\left(\boldsymbol{r}_1'\right)\begin{pmatrix}\boldsymbol{N}_{\overline{\nu}}^1(k_{\mathrm{s}}\boldsymbol{r}') \\ \boldsymbol{M}_{\overline{\nu}}^1(k_{\mathrm{s}}\boldsymbol{r}')\end{pmatrix}\right.\\ &\left.+\,\mathrm{j}\sqrt{\frac{\mu_{\mathrm{s}}}{\varepsilon_{\mathrm{s}}}}\boldsymbol{h}_{\mathrm{i},1}^N\left(\boldsymbol{r}_1'\right)\begin{pmatrix}\boldsymbol{M}_{\overline{\nu}}^1(k_{\mathrm{s}}\boldsymbol{r}') \\ \boldsymbol{N}_{\overline{\nu}}^1(k_{\mathrm{s}}\boldsymbol{r}')\end{pmatrix}\right]\mathrm{d}S\left(\boldsymbol{r}_1'\right)\\ +\frac{\mathrm{j}k_{\mathrm{s}}^2}{\pi}\int_{S_2}&\left[\boldsymbol{e}_{\mathrm{i},2}^N\left(\boldsymbol{r}_2''\right)\begin{pmatrix}\boldsymbol{N}_{\overline{\nu}}^1(k_{\mathrm{s}}\boldsymbol{r}'') \\ \boldsymbol{M}_{\overline{\nu}}^1(k_{\mathrm{s}}\boldsymbol{r}'')\end{pmatrix}\right.\\ &\left.+\,\mathrm{j}\sqrt{\frac{\mu_{\mathrm{s}}}{\varepsilon_{\mathrm{s}}}}\boldsymbol{h}_{\mathrm{i},2}^N\left(\boldsymbol{r}_2''\right)\begin{pmatrix}\boldsymbol{M}_{\overline{\nu}}^1(k_{\mathrm{s}}\boldsymbol{r}'') \\ \boldsymbol{N}_{\overline{\nu}}^1(k_{\mathrm{s}}\boldsymbol{r}'')\end{pmatrix}\right]\mathrm{d}S\left(\boldsymbol{r}_2''\right)\,.\end{aligned}\tag{2.136}$$

Finally, using the addition theorem for the regular vector spherical wave functions

$$\begin{bmatrix} \boldsymbol{M}_{\overline{\nu}}^{1}(k_{\mathrm{s}}\boldsymbol{r}') \\ \boldsymbol{N}_{\overline{\nu}}^{1}(k_{\mathrm{s}}\boldsymbol{r}') \end{bmatrix} = \left[\left(\mathcal{S}_{01}^{\mathrm{tr}}\right)_{\overline{\nu}\overline{\mu}} \right] \begin{bmatrix} \boldsymbol{M}_{\overline{\mu}}^{1}(k_{\mathrm{s}}\boldsymbol{r}_1') \\ \boldsymbol{N}_{\overline{\mu}}^{1}(k_{\mathrm{s}}\boldsymbol{r}_1') \end{bmatrix}$$

with

$$\mathcal{S}_{01}^{\mathrm{tr}} = \mathcal{T}^{11}\left(k_{\mathrm{s}}\boldsymbol{r}_{01}\right)\mathcal{R}\left(\alpha_1,\beta_1,\gamma_1\right) ,$$

and

$$\begin{bmatrix} \boldsymbol{M}_{\overline{\nu}}^{1}(k_{\mathrm{s}}\boldsymbol{r}'') \\ \boldsymbol{N}_{\overline{\nu}}^{1}(k_{\mathrm{s}}\boldsymbol{r}'') \end{bmatrix} = \left[\left(\mathcal{S}_{02}^{\mathrm{tr}}\right)_{\overline{\nu}\overline{\mu}} \right] \begin{bmatrix} \boldsymbol{M}_{\overline{\mu}}^{1}(k_{\mathrm{s}}\boldsymbol{r}_2'') \\ \boldsymbol{N}_{\overline{\mu}}^{1}(k_{\mathrm{s}}\boldsymbol{r}_2'') \end{bmatrix}$$

with

$$\mathcal{S}_{02}^{\mathrm{tr}} = \mathcal{T}^{11}\left(k_{\mathrm{s}}\boldsymbol{r}_{02}\right)\mathcal{R}\left(\alpha_2,\beta_2,\gamma_2\right) ,$$

we obtain

$$\begin{aligned} \boldsymbol{s} &= \mathcal{S}_{01}^{\mathrm{tr}}\boldsymbol{Q}_1^{11}(k_{\mathrm{s}},k_{\mathrm{i},1})\boldsymbol{i}_1 + \mathcal{S}_{02}^{\mathrm{tr}}\boldsymbol{Q}_2^{11}(k_{\mathrm{s}},k_{\mathrm{i},2})\boldsymbol{i}_2 \\ &= \mathcal{S}_{01}^{\mathrm{tr}}\boldsymbol{s}_1 + \mathcal{S}_{02}^{\mathrm{tr}}\boldsymbol{s}_2 , \end{aligned} \tag{2.137}$$

where $\boldsymbol{s} = [f_\nu^N, g_\nu^N]^{\mathrm{T}}$ is the vector containing the expansion coefficients of the scattered field in the global coordinate system. Combining (2.135) and (2.137), and using the identities $\mathcal{S}_{20}^{\mathrm{rt}}(\mathcal{S}_{10}^{\mathrm{rt}})^{-1} = \mathcal{S}_{21}^{\mathrm{rtr}}$ and $\mathcal{S}_{10}^{\mathrm{rt}}(\mathcal{S}_{20}^{\mathrm{rt}})^{-1} = \mathcal{S}_{12}^{\mathrm{rtr}}$, yields [187]

$$\begin{aligned} \boldsymbol{T} = {} & \mathcal{S}_{01}^{\mathrm{tr}}\boldsymbol{T}_1\left(\boldsymbol{I} - \widetilde{\mathcal{S}}_{12}^{\mathrm{rtr}}\boldsymbol{T}_2\widetilde{\mathcal{S}}_{21}^{\mathrm{rtr}}\boldsymbol{T}_1\right)^{-1}\left(\boldsymbol{I} + \widetilde{\mathcal{S}}_{12}^{\mathrm{rtr}}\boldsymbol{T}_2\mathcal{S}_{21}^{\mathrm{rtr}}\right)\mathcal{S}_{10}^{\mathrm{rt}} \\ & + \mathcal{S}_{02}^{\mathrm{tr}}\boldsymbol{T}_2\left(\boldsymbol{I} - \widetilde{\mathcal{S}}_{21}^{\mathrm{rtr}}\boldsymbol{T}_1\widetilde{\mathcal{S}}_{12}^{\mathrm{rtr}}\boldsymbol{T}_2\right)^{-1}\left(\boldsymbol{I} + \widetilde{\mathcal{S}}_{21}^{\mathrm{rtr}}\boldsymbol{T}_1\mathcal{S}_{12}^{\mathrm{rtr}}\right)\mathcal{S}_{20}^{\mathrm{rt}} , \end{aligned} \tag{2.138}$$

where the explicit expressions of the transformation matrices $\mathcal{S}_{21}^{\mathrm{rtr}}$ and $\mathcal{S}_{12}^{\mathrm{rtr}}$ are given by

$$\mathcal{S}_{12}^{\mathrm{rtr}} = \mathcal{R}\left(-\gamma_1,-\beta_1,-\alpha_1\right)\mathcal{T}^{11}\left(k_{\mathrm{s}}\boldsymbol{r}_{12}\right)\mathcal{R}\left(\alpha_2,\beta_2,\gamma_2\right) ,$$

and

$$\mathcal{S}_{21}^{\mathrm{rtr}} = \mathcal{R}\left(-\gamma_2,-\beta_2,-\alpha_2\right)\mathcal{T}^{11}\left(-k_{\mathrm{s}}\boldsymbol{r}_{12}\right)\mathcal{R}\left(\alpha_1,\beta_1,\gamma_1\right) ,$$

respectively. Equation (2.138) gives the system transition matrix $\boldsymbol{T}$ in terms of the individual transition matrices $\boldsymbol{T}_1$ and $\boldsymbol{T}_2$, and the transformation matrices $\mathcal{S}$ and $\widetilde{\mathcal{S}}$. $\mathcal{S}$ and $\widetilde{\mathcal{S}}$ involve translations of the regular and radiating vector spherical wave functions, respectively, and geometric constraints are introduced by the $\widetilde{\mathcal{S}}$ matrices. Obviously, the geometric restrictions $r_{12} > r_2''$

and $r_{12} > r_1'$ introduced by the $\widetilde{\mathcal{S}}$ matrices are fulfilled if the smallest circumscribing spheres of the particles do not overlap. The following feature of equation (2.138) is apparent: if $\boldsymbol{T}_2 = 0$, then $\boldsymbol{T} = \mathcal{S}_{01}^{\rm tr}\boldsymbol{T}_1\mathcal{S}_{10}^{\rm rt}$, and if $\boldsymbol{T}_1 = 0$, then $\boldsymbol{T} = \mathcal{S}_{02}^{\rm tr}\boldsymbol{T}_2\mathcal{S}_{20}^{\rm rt}$, as it should. In general, $\boldsymbol{T}$ is a sum of two terms, each of which is a modification of these limiting values. The various terms in a formal expansion of the inverses occurring in (2.138) can be considered as multiple-scattering contributions. The terms involving only $\boldsymbol{T}_1$ and $\boldsymbol{T}_2$ represent reflections at S_1 and S_2, respectively, the terms involving only $\boldsymbol{T}_1\widetilde{\mathcal{S}}_{12}^{\rm rtr}\boldsymbol{T}_2$ and $\boldsymbol{T}_2\widetilde{\mathcal{S}}_{21}^{\rm rtr}\boldsymbol{T}_1$ represent consecutive reflections at S_2 and S_1, and S_1 and S_2, respectively, etc.

2.6.2 Formulation for a System with $\mathcal{N}$ Particles

The generalization of the $\boldsymbol{T}$-matrix relation to a system with more than two constituents is straightforward. The system of matrix equations consists in the null-field equations in the interior of S_l

$$\boldsymbol{s}_l - \boldsymbol{T}_l \sum_{p\neq l}^{\mathcal{N}} \widetilde{\mathcal{S}}_{lp}^{\rm rtr}\boldsymbol{s}_p = \boldsymbol{T}_l\mathcal{S}_{l0}^{\rm rt}\boldsymbol{e} \quad \text{for} \quad l = 1,2,\ldots,\mathcal{N} \tag{2.139}$$

and the matrix equation corresponding to the scattered field representation

$$\boldsymbol{s} = \sum_{l=1}^{\mathcal{N}} \mathcal{S}_{0l}^{\rm tr}\boldsymbol{s}_l\,. \tag{2.140}$$

In practical computer calculations it is convenient to consider the global matrix $\boldsymbol{A}$ with block-matrix components

$$\begin{aligned}
&\boldsymbol{A}^{ll} = \boldsymbol{I}\,, l = 1,2,\ldots,\mathcal{N}\,,\\
&\boldsymbol{A}^{lp} = -\boldsymbol{T}_l\widetilde{\mathcal{S}}_{lp}^{\rm rtr}\,, \quad l \neq p\,, \quad l,p = 1,2,\ldots,\mathcal{N}\,,
\end{aligned}$$

and to express the solution to the system of matrix equations (2.139) as

$$\boldsymbol{s}_l = \left(\sum_{p=1}^{\mathcal{N}} \mathcal{A}^{lp}\boldsymbol{T}_p\mathcal{S}_{p0}^{\rm rt}\right)\boldsymbol{e}\,, \quad l = 1,2,\ldots,\mathcal{N}\,, \tag{2.141}$$

where $\mathcal{A}$ stay for $\boldsymbol{A}^{-1}$, and $\mathcal{A}^{lp}$, $l,p = 1,2,\ldots,\mathcal{N}$, are the block-matrix components of $\mathcal{A}$. In view of (2.140), the system $\boldsymbol{T}$-matrix becomes

$$\boldsymbol{T} = \sum_{l=1}^{\mathcal{N}}\sum_{p=1}^{\mathcal{N}} \mathcal{S}_{0l}^{\rm tr}\mathcal{A}^{lp}\boldsymbol{T}_p\mathcal{S}_{p0}^{\rm rt}$$

and this transition matrix can be used to compute the scattering characteristics for fixed or random orientations of the ensemble [153, 165].

In order to estimate the computer memory requirement it is important to know the dimensions of the matrices involved in the calculation. If $N_{\rm rank}(l)$ and $M_{\rm rank}(l)$ are the maximum expansion order and the number of azimuthal modes for the lth particle, then the dimension of the transition matrix $\boldsymbol{T}_l$ is $\dim(\boldsymbol{T}_l) = 2N_{\rm max}(l) \times 2N_{\rm max}(l)$, where

$$N_{\rm max}(l) = N_{\rm rank}\,(l) + M_{\rm rank}\,(l)\,[2N_{\rm rank}(l) - M_{\rm rank}(l) + 1]\ .$$

The dimension of the global matrix $\boldsymbol{A}$ is

$$\dim\,(\boldsymbol{A}) = 2\sum_{l=1}^{\mathcal{N}} N_{\rm max}(l) \times 2\sum_{l=1}^{\mathcal{N}} N_{\rm max}(l)\,,$$

since

$$\dim\left(\boldsymbol{A}^{lp}\right) = \dim\left(\mathcal{A}^{lp}\right) = 2N_{\rm max}(l) \times 2N_{\rm max}(p)\,.$$

If $N_{\rm max}$ gives the dimension of the system $\boldsymbol{T}$-matrix

$$\dim\,(\boldsymbol{T}) = 2N_{\rm max} \times 2N_{\rm max}\,,$$

we have

$$\dim\left(\mathcal{S}_{p0}^{\rm rt}\right) = 2N_{\rm max}(p) \times 2N_{\rm max}\,,$$
$$\dim\left(\mathcal{S}_{0l}^{\rm tr}\right) = 2N_{\rm max} \times 2N_{\rm max}(l)\,.$$

In our computer code, the parameters $N_{\rm max}$ and $N_{\rm max}(l)$, $l = 1, 2, \ldots, \mathcal{N}$, are independent. $N_{\rm max}(l)$ is given by the size parameter of the lth particle, while $N_{\rm max}$ is given by the size parameter of a sphere centered at O and enclosing the particles.

2.6.3 Superposition $\boldsymbol{T}$-matrix Method

For a system of $\mathcal{N}$ particles with $\alpha_l = \beta_l = \gamma_l = 0$, $l = 1, 2, \ldots, \mathcal{N}$, the transformations of the vector spherical vector wave functions involve only the addition theorem under coordinate translations, i.e.,

$$\mathcal{S}_{0l}^{\rm tr} = \mathcal{T}^{11}\,(k_{\rm s}\boldsymbol{r}_{0l})\ ,$$
$$\mathcal{S}_{p0}^{\rm rt} = \mathcal{T}^{11}\,(-k_{\rm s}\boldsymbol{r}_{0p})\ ,$$

and

$$\widetilde{\mathcal{S}}_{lp}^{\rm rtr} = \mathcal{T}^{31}\,(k_{\rm s}\boldsymbol{r}_{lp})$$

for $l, p = 1, 2, \ldots, \mathcal{N}$. Consequently, the matrix equation (2.139) takes the form

$$\boldsymbol{s}_l = \boldsymbol{T}_l \left[\mathcal{T}^{11}\left(-k_{\mathrm{s}}\boldsymbol{r}_{0l}\right)\boldsymbol{e} + \sum_{p\neq l}^{\mathcal{N}} \mathcal{T}^{31}\left(k_{\mathrm{s}}\boldsymbol{r}_{lp}\right)\boldsymbol{s}_p \right] , \tag{2.142}$$

while (2.140) becomes

$$\boldsymbol{s} = \sum_{l=1}^{\mathcal{N}} \mathcal{T}^{11}\left(k_{\mathrm{s}}\boldsymbol{r}_{0l}\right)\boldsymbol{s}_l \, . \tag{2.143}$$

The precedent equations can be written in explicit form by indicating the vector and matrix indices

$$\left[\left(s_l\right)_\nu\right] = \left[\left(T_l\right)_{\nu\nu'}\right] \left\{ \left[\mathcal{T}^{11}_{\nu'\overline{\mu}}\left(-k_{\mathrm{s}}\boldsymbol{r}_{0l}\right)\right]\left[e_\mu\right] \sum_{p\neq l}^{\mathcal{N}} \left[\mathcal{T}^{31}_{\nu'\overline{\mu}}\left(k_{\mathrm{s}}\boldsymbol{r}_{lp}\right)\right]\left[\left(s_p\right)_\mu\right] \right\} , \tag{2.144}$$

$$\left[s_\nu\right] = \sum_{l=1}^{\mathcal{N}} \left[\mathcal{T}^{11}_{\nu\overline{\mu}}\left(k_{\mathrm{s}}\boldsymbol{r}_{0l}\right)\right]\left[\left(s_l\right)_\mu\right] , \tag{2.145}$$

and can also be derived by using the so-called superposition $\boldsymbol{T}$-matrix method [169]. The superposition $\boldsymbol{T}$-matrix method reproduces the two cooperative effects characterizing aggregate scattering: interaction between particles and far-field interference [273]. The interaction effect take into account that each particle is excited by the initial incident field and the fields scattered by all other particles, while the far-field interference is a result of the incident and scattered phase differences from different particles. The superposition $\boldsymbol{T}$-matrix method involves the following general steps:

1. The expansions of the incident and scattered fields in each particle coordinate system.
2. The representation of the field exciting a particle by a single-field expansion (which includes the incident field and the scattered fields from all other particles).
3. The solution of the transmission boundary-value problem for each particle.
4. The derivation of the scattered-field expansion in the global coordinate system.

The interaction effect is taken into account in steps 2 and 3, where the scattered fields from other particles are transformed and included in the incident field on each particle, while the interference effect is taken into account in steps 1 and 4 that address the incident and scattered path differences, respectively. For a system of $\mathcal{N}$ spheres, the individual component $\boldsymbol{T}$ matrices are diagonal with the standard Lorenz–Mie coefficients along their main diagonal, and in this case, the superposition $\boldsymbol{T}$-matrix method is also known as the multisphere separation of variables technique or the multisphere superposition method [21, 24, 29, 72, 150]. Solution of (2.144) have been obtained using direct matrix inversion, method of successive orders of scattering, conjugate

gradient methods and iterative approaches [74, 95, 198, 244, 271]. Originally all methods were implemented for spherical particles, but Xu [274] recently extended his computer code for axisymmetric particles.

In the following analysis, we derive (2.144) and (2.145) by using the superposition $\boldsymbol{T}$-matrix method. The field exciting the lth particle can be expressed as

$$\boldsymbol{E}_{\mathrm{exc},l}\left(\boldsymbol{r}_l\right) = \boldsymbol{E}_{\mathrm{e}}\left(\boldsymbol{r}_l\right) + \sum_{p\neq l}^{\mathcal{N}} \boldsymbol{E}_{\mathrm{s},p}\left(\boldsymbol{r}_l\right) \ ,$$

where $\boldsymbol{E}_{\mathrm{e}}$ is the incident field and $\boldsymbol{E}_{\mathrm{s},p}$ is the field scattered by the pth particle. In the null-field method, transformation rules between the expansion coefficients of the incident and scattered fields in different coordinate systems have been derived by using the integral representations for the expansion coefficients. In the superposition $\boldsymbol{T}$-matrix method, these transformations are obtained by using the series representations for the electromagnetic fields in different coordinate systems. For the external excitation, we consider the vector spherical wave expansion

$$\boldsymbol{E}_{\mathrm{e}}(\boldsymbol{r}) = \sum_{\mu} a_\mu \boldsymbol{M}_\mu^1\left(k_{\mathrm{s}}\boldsymbol{r}\right) + b_\mu \boldsymbol{N}_\mu^1\left(k_{\mathrm{s}}\boldsymbol{r}\right)$$

and use the addition theorem

$$\begin{bmatrix} \boldsymbol{M}_\mu^1\left(k_{\mathrm{s}}\boldsymbol{r}\right) \\ \boldsymbol{N}_\mu^1\left(k_{\mathrm{s}}\boldsymbol{r}\right) \end{bmatrix} = \left[\mathcal{T}_{\mu\nu}^{11}\left(k_{\mathrm{s}}\boldsymbol{r}_{0l}\right)\right] \begin{bmatrix} \boldsymbol{M}_\nu^1\left(k_{\mathrm{s}}\boldsymbol{r}_l\right) \\ \boldsymbol{N}_\nu^1\left(k_{\mathrm{s}}\boldsymbol{r}_l\right) \end{bmatrix} \ ,$$

to obtain

$$\boldsymbol{E}_{\mathrm{e}}\left(\boldsymbol{r}_l\right) = \sum_{\nu} a_{l,\nu} \boldsymbol{M}_\nu^1\left(k_{\mathrm{s}}\boldsymbol{r}_l\right) + b_{l,\nu} \boldsymbol{N}_\nu^1\left(k_{\mathrm{s}}\boldsymbol{r}_l\right)$$

with

$$\begin{bmatrix} a_{l,\nu} \\ b_{l,\nu} \end{bmatrix} = \left[\mathcal{T}_{\mu\nu}^{11}\left(k_{\mathrm{s}}\boldsymbol{r}_{0l}\right)\right] \begin{bmatrix} a_\mu \\ b_\mu \end{bmatrix} \ .$$

Similarly, for the field scattered by the pth particle, we consider the series representation

$$\boldsymbol{E}_{\mathrm{s},p}\left(\boldsymbol{r}_p\right) = \sum_{\mu} f_{p,\mu} \boldsymbol{M}_\mu^3\left(k_{\mathrm{s}}\boldsymbol{r}_p\right) + g_{p,\mu} \boldsymbol{N}_\mu^3\left(k_{\mathrm{s}}\boldsymbol{r}_p\right)$$

and use the addition theorem

$$\begin{bmatrix} \boldsymbol{M}_{\boldsymbol{\mu}}^3\left(k_{\mathrm{s}}\boldsymbol{r}_p\right) \\ \boldsymbol{N}_\mu^3\left(k_{\mathrm{s}}\boldsymbol{r}_p\right) \end{bmatrix} = \left[\mathcal{T}_{\mu\nu}^{31}\left(k_{\mathrm{s}}\boldsymbol{r}_{pl}\right)\right] \begin{bmatrix} \boldsymbol{M}_\nu^1\left(k_{\mathrm{s}}\boldsymbol{r}_l\right) \\ \boldsymbol{N}_\nu^1\left(k_{\mathrm{s}}\boldsymbol{r}_l\right) \end{bmatrix} \quad \text{for} \quad r_l < r_{pl} \ ,$$

to derive

$$\boldsymbol{E}_{\mathrm{s},p}\left(\boldsymbol{r}_l\right) = \sum_{\nu} f_{lp,\nu}\boldsymbol{M}^1_{\nu}\left(k_{\mathrm{s}}\boldsymbol{r}_l\right) + g_{lp,\nu}\boldsymbol{N}^1_{\nu}\left(k_{\mathrm{s}}\boldsymbol{r}_l\right)$$

with

$$\begin{bmatrix} f_{lp,\nu} \\ g_{lp,\nu} \end{bmatrix} = \left[\mathcal{T}^{31}_{\mu\nu}\left(k_{\mathrm{s}}\boldsymbol{r}_{pl}\right)\right] \begin{bmatrix} f_{p,\mu} \\ g_{p,\mu} \end{bmatrix} .$$

Thus, the field exciting the lth particle can be expressed in terms of regular vector spherical wave functions centered at the origin O_l

$$\boldsymbol{E}_{\mathrm{exc},l}\left(\boldsymbol{r}_l\right) = \sum_{\nu} \widetilde{a}_{l,\nu}\boldsymbol{M}^1_{\nu}\left(k_{\mathrm{s}}\boldsymbol{r}_l\right) + \widetilde{b}_{l,\nu}\boldsymbol{N}^1_{\nu}\left(k_{\mathrm{s}}\boldsymbol{r}_l\right) ,$$

where the expansion coefficients are given by

$$\left[\left(\widetilde{e}_l\right)_{\nu}\right] = \left[\mathcal{T}^{11}_{\mu\nu}\left(k_{\mathrm{s}}\boldsymbol{r}_{0l}\right)\right]\left[e_{\mu}\right] + \sum_{p\neq l}^{\mathcal{N}}\left[\mathcal{T}^{31}_{\mu\nu}\left(k_{\mathrm{s}}\boldsymbol{r}_{pl}\right)\right]\left[\left(s_p\right)_{\mu}\right]$$

and as usually, $\widetilde{\boldsymbol{e}}_l = [\widetilde{a}_{l,\nu}, \widetilde{b}_{l,\nu}]^{\mathrm{T}}$. Further, using the $\boldsymbol{T}$-matrix equation $\boldsymbol{s}_l = \boldsymbol{T}_l\widetilde{\boldsymbol{e}}_l$, we obtain

$$\left[\left(s_l\right)_{\nu}\right] = \left[\left(T_l\right)_{\nu\nu'}\right]\left[\left[\mathcal{T}^{11}_{\mu\nu'}\left(k_{\mathrm{s}}\boldsymbol{r}_{0l}\right)\right]\left[e_{\mu}\right] + \sum_{p\neq l}^{\mathcal{N}}\left[\mathcal{T}^{31}_{\mu\nu'}\left(k_{\mathrm{s}}\boldsymbol{r}_{pl}\right)\right]\left[\left(s_p\right)_{\mu}\right]\right] , \quad (2.146)$$

and since (cf. (B.74) and (B.75))

$$\left[\mathcal{T}^{31}_{\overline{\nu'}\overline{\mu}}\left(k_{\mathrm{s}}\boldsymbol{r}_{lp}\right)\right] = \left[\mathcal{T}^{31}_{\mu\nu'}\left(k_{\mathrm{s}}\boldsymbol{r}_{pl}\right)\right]$$

and

$$\left[\mathcal{T}^{11}_{\overline{\nu'}\overline{\mu}}\left(-k_{\mathrm{s}}\boldsymbol{r}_{0l}\right)\right] = \left[\mathcal{T}^{11}_{\overline{\nu'}\overline{\mu}}\left(k_{\mathrm{s}}\boldsymbol{r}_{l0}\right)\right] = \left[\mathcal{T}^{11}_{\mu\nu'}\left(k_{\mathrm{s}}\boldsymbol{r}_{0l}\right)\right] ,$$

we see that (2.144) and (2.146) coincide.

The scattered field is a superposition of fields that are scattered from the individual particles,

$$\begin{aligned}\boldsymbol{E}_{\mathrm{s}}(\boldsymbol{r}) &= \sum_{l=1}^{\mathcal{N}} \boldsymbol{E}_{\mathrm{s},l}\left(\boldsymbol{r}_l\right) \\ &= \sum_{l=1}^{\mathcal{N}}\sum_{\mu} f_{l,\mu}\boldsymbol{M}^3_{\mu}\left(k_{\mathrm{s}}\boldsymbol{r}_l\right) + g_{l,\mu}\boldsymbol{N}^3_{\mu}\left(k_{\mathrm{s}}\boldsymbol{r}_l\right) , \end{aligned} \quad (2.147)$$

whence, using the addition theorem

$$\begin{bmatrix} \boldsymbol{M}_{\boldsymbol{\mu}}^{3}\left(k_{\mathrm{s}}\boldsymbol{r}_{l}\right) \\ \boldsymbol{N}_{\mu}^{3}\left(k_{\mathrm{s}}\boldsymbol{r}_{l}\right) \end{bmatrix} = \left[\mathcal{T}_{\mu\nu}^{33}\left(-k_{\mathrm{s}}\boldsymbol{r}_{0l}\right)\right] \begin{bmatrix} \boldsymbol{M}_{\nu}^{3}\left(k_{\mathrm{s}}\boldsymbol{r}\right) \\ \boldsymbol{N}_{\nu}^{3}\left(k_{\mathrm{s}}\boldsymbol{r}\right) \end{bmatrix} \quad \text{for} \quad r > r_{0l}\,,$$

we derive the scattered-field expansion centered at O

$$\boldsymbol{E}_{\mathrm{s}}(\boldsymbol{r}) = \sum_{\nu} f_{\nu}\boldsymbol{M}_{\nu}^{3}\left(k_{\mathrm{s}}\boldsymbol{r}\right) + g_{\nu}\boldsymbol{N}_{\nu}^{3}\left(k_{\mathrm{s}}\boldsymbol{r}\right)$$

with

$$[s_{\nu}] = \sum_{l=1}^{\mathcal{N}} \left[\mathcal{T}_{\mu\nu}^{33}\left(-k_{\mathrm{s}}\boldsymbol{r}_{0l}\right)\right] \left[\left(s_{l}\right)_{\mu}\right]. \tag{2.148}$$

Since,

$$\left[\mathcal{T}_{\overline{\nu}\overline{\mu}}^{11}\left(k_{\mathrm{s}}\boldsymbol{r}_{0l}\right)\right] = \left[\mathcal{T}_{\mu\nu}^{11}\left(-k_{\mathrm{s}}\boldsymbol{r}_{0l}\right)\right] = \left[\mathcal{T}_{\mu\nu}^{33}\left(-k_{\mathrm{s}}\boldsymbol{r}_{0l}\right)\right],$$

we see that (2.145) and (2.148) are identical.

2.6.4 Formulation with Phase Shift Terms

For an ensemble of $\mathcal{N}$ particles with $\alpha_l = \beta_l = \gamma_l = 0$, $l = 1, 2, \ldots, \mathcal{N}$, the system $\boldsymbol{T}$-matrix is given by

$$\boldsymbol{T} = \sum_{l=1}^{\mathcal{N}} \sum_{p=1}^{\mathcal{N}} \mathcal{T}^{11}\left(k_{\mathrm{s}}\boldsymbol{r}_{0l}\right) \mathcal{A}^{lp} \boldsymbol{T}_{p} \mathcal{T}^{11}\left(-k_{\mathrm{s}}\boldsymbol{r}_{0p}\right). \tag{2.149}$$

In (2.149), the translation matrices $\mathcal{T}^{11}(-k_{\mathrm{s}}\boldsymbol{r}_{0p})$ and $\mathcal{T}^{11}(k_{\mathrm{s}}\boldsymbol{r}_{0l})$ give the relations between the expansion coefficients of the incident and scattered fields in different coordinate systems. In the present analysis, these relations are derived by using the direct phase differences between the electromagnetic fields in different coordinate systems.

For a vector plane wave of unit amplitude and wave vector $\boldsymbol{k}_{\mathrm{e}}$, $\boldsymbol{k}_{\mathrm{e}} = k_{\mathrm{s}}\boldsymbol{e}_{k}$, we have

$$\begin{aligned} \boldsymbol{E}_{\mathrm{e}}\left(\boldsymbol{r}_{l}\right) &= \boldsymbol{e}_{\mathrm{pol}} \mathrm{e}^{\mathrm{j}k_{\mathrm{s}}\boldsymbol{e}_{k}\cdot\boldsymbol{r}_{0l}} \mathrm{e}^{\mathrm{j}k_{\mathrm{s}}\boldsymbol{e}_{k}\cdot\left(\boldsymbol{r}-\boldsymbol{r}_{0l}\right)} \\ &= \mathrm{e}^{\mathrm{j}k_{\mathrm{s}}\boldsymbol{e}_{k}\cdot\boldsymbol{r}_{0l}} \sum_{\nu} a_{\nu}\boldsymbol{M}_{\nu}^{1}\left(k_{\mathrm{s}}\boldsymbol{r}_{l}\right) + b_{\nu}\boldsymbol{N}_{\nu}^{1}\left(k_{\mathrm{s}}\boldsymbol{r}_{l}\right) \\ &= \sum_{\nu} a_{l,\nu}\boldsymbol{M}_{\nu}^{1}\left(k_{\mathrm{s}}\boldsymbol{r}_{l}\right) + b_{l,\nu}\boldsymbol{N}_{\nu}^{1}\left(k_{\mathrm{s}}\boldsymbol{r}_{l}\right) \end{aligned}$$

and therefore

$$\begin{bmatrix} a_{l,\nu} \\ b_{l,\nu} \end{bmatrix} = \mathrm{e}^{\mathrm{j}k_{\mathrm{s}}\boldsymbol{e}_{k}\cdot\boldsymbol{r}_{0l}} \begin{bmatrix} a_{\nu} \\ b_{\nu} \end{bmatrix}.$$

Further, using the far-field representation of the field scattered by the lth particle,

$$\boldsymbol{E}_{\mathrm{s},l}(\boldsymbol{r}_l) = \frac{\mathrm{e}^{\mathrm{j}k_\mathrm{s}r_l}}{r_l}\left\{\boldsymbol{E}_{\mathrm{s}\infty,l}(\boldsymbol{e}_r) + O\left(\frac{1}{r_l}\right)\right\}$$

and the approximation

$$\frac{\mathrm{e}^{\mathrm{j}k_\mathrm{s}r_l}}{r_l} = \frac{\mathrm{e}^{\mathrm{j}k_\mathrm{s}r}\mathrm{e}^{-\mathrm{j}k_\mathrm{s}\boldsymbol{e}_r\cdot\boldsymbol{r}_{0l}}}{r}\left[1+\mathrm{O}\left(\frac{1}{r}\right)\right],$$

we see that the angular-dependent vector of scattering coefficients

$$\boldsymbol{s}\left(\boldsymbol{e}_r\right) = \sum_{l=1}^{\mathcal{N}} \mathrm{e}^{-\mathrm{j}k_\mathrm{s}\boldsymbol{e}_r\cdot\boldsymbol{r}_{0l}}\boldsymbol{s}_l$$

approximates the $\boldsymbol{s}$ vector in the far-field region, and that the angular-dependent transition matrix

$$\boldsymbol{T}\left(\boldsymbol{e}_r\right) = \sum_{l=1}^{\mathcal{N}}\sum_{p=1}^{\mathcal{N}} \mathrm{e}^{\mathrm{j}k_\mathrm{s}(\boldsymbol{e}_k\cdot\boldsymbol{r}_{0p}-\boldsymbol{e}_r\cdot\boldsymbol{r}_{0l})}\mathcal{A}^{lp}\boldsymbol{T}_p \tag{2.150}$$

approximates the $\boldsymbol{T}$ matrix in the far-field region. For spherical particles, this method is known as the generalized multiparticle Mie-solution [272, 273].

Equation (2.150) shows that we have to impose

$$\dim\left(\boldsymbol{T}\right) = \dim\left(\mathcal{A}^{lp}\boldsymbol{T}_p\right) = \dim\left(\boldsymbol{T}_{lp}\right),$$

where $\boldsymbol{T}_{lp} = \mathcal{A}^{lp}\boldsymbol{T}_p$. Assuming $\dim(\boldsymbol{T}) = 2N_\mathrm{max}\times 2N_\mathrm{max}$, we can set $N_\mathrm{max}(p) = N_\mathrm{max}$ for all $p = 1, 2, \ldots, \mathcal{N}$, and in this case, $\dim(\boldsymbol{T}) = \dim(\boldsymbol{T}_p)$. Alternatively, we can set $N_\mathrm{max} = \max_p N_\mathrm{max}(p)$ and use the convention $(T_{lp})_{\nu\mu} \equiv 0$ whenever $\nu > 2N_\mathrm{max}(l)$ and $\mu > 2N_\mathrm{max}(p)$. This formulation avoids the computation of the translation matrices $\mathcal{T}^{11}$ and involves only the inversion of the global matrix $\boldsymbol{A}$. The dimensions of $\mathcal{T}^{11}$ depend on translation distances and are proportional to the overall dimension of the cluster, while the dimension of $\boldsymbol{A}$ is determined by the size parameters of the individual particles. Therefore, the generalized multiparticle Mie-solution is limited by the largest possible individual particle size in a cluster and not by the overall cluster size. However, the angular-dependent transition matrix can not be used in the analytical orientation-averaging procedure described in Sect. 1.5 and in view of our computer implementation, this method is not effective for $\boldsymbol{T}$-matrix calculations.

2.6.5 Recursive Aggregate T-matrix Algorithm

If the number of particles increases, the dimension of the global matrix $\boldsymbol{A}$ becomes excessively large. Wang and Chew [250, 251] proposed a recursive $\boldsymbol{T}$-matrix algorithm, which computes the $\boldsymbol{T}$ matrix of a system of n components by using the transition matrices of the newly added q components and the

$\boldsymbol{T}$ matrix of the previous system of $n-q$ components. In this section we use the recursive $\boldsymbol{T}$-matrix algorithm to analyze electromagnetic scattering by a system of identical particles randomly distributed inside an "imaginary" spherical surface.

Let us consider $N_{\rm cs}$ circumscribing spheres with radii $R_{\rm cs}(k)$, $k=1,2,\ldots,N_{\rm cs}$, in increasing order. Inside the sphere of radius $R_{\rm cs}(1)$ there are $\mathcal{N}(1)$ particles having their centers located at $\boldsymbol{r}_{0l}^{(1)}$, $l=1,2,\ldots,\mathcal{N}(1)$, and in each spherical shell bounded by the radii $R_{\rm cs}(k-1)$ and $R_{\rm cs}(k)$ there are $\mathcal{N}(k)$ particles having their centers located at $\boldsymbol{r}_{0l}^{(k)}$, $l=1,2,\ldots,\mathcal{N}(k)$. Obviously, $\mathcal{N}=\sum_{p=1}^{N_{\rm cs}}\mathcal{N}(p)$ is the total number of particles and $R_{\rm cs}(N_{\rm cs})$ is the radius of the circumscribing sphere containing the particles. For simplicity, we assume that the particles are identical and have the same spatial orientation. The scattering geometry for the problem under examination is depicted in Fig. 2.7.

At the first iteration step, we compute the system $\boldsymbol{T}$-matrix $\boldsymbol{T}^{(1)}$ of all particles situated inside the sphere of radius $R_{\rm cs}(1)$. At the iteration step k, we compute the system $\boldsymbol{T}$-matrix $\boldsymbol{T}^{(k)}$ of all particles situated inside the sphere of radius $R_{\rm cs}(k)$ by considering a $[\mathcal{N}(k)+1]$-scatterer problem. In fact, the transition matrix $\boldsymbol{T}^{(k)}$ is computed by using the system $\boldsymbol{T}$-matrix $\boldsymbol{T}^{(k-1)}$ of the previous $\sum_{p=1}^{k-1}\mathcal{N}(p)$ particles situated inside the sphere of radius $R_{\rm cs}(k-1)$ and the individual transition matrix $\boldsymbol{T}_{\rm p}$ of all $\mathcal{N}(k)$ particles situated in the spherical shell between $R_{\rm cs}(k-1)$ and $R_{\rm cs}(k)$. In this specific case, the block-matrix components of the global matrix $\boldsymbol{A}$ are given by

$$\boldsymbol{A}^{ll}=\boldsymbol{I}\,,\quad l=1,2,\ldots,\mathcal{N}(k)+1\,,$$

$$\boldsymbol{A}^{lp}=-\boldsymbol{T}_{\rm p}\mathcal{T}^{31}\left(k_{\rm s}\boldsymbol{r}_{lp}^{(k)}\right)\,,\quad l\neq p\,,\quad l,p=1,2,\ldots,\mathcal{N}(k)\,,$$

$$\boldsymbol{A}^{l,\mathcal{N}(k)+1}=-\boldsymbol{T}_{\rm p}\mathcal{T}^{31}\left(k_{\rm s}\boldsymbol{r}_{l0}^{(k)}\right)=-\boldsymbol{T}_{\rm p}\mathcal{T}^{31}\left(-k_{\rm s}\boldsymbol{r}_{0l}^{(k)}\right)\,,\quad l=1,2,\ldots,\mathcal{N}(k)\,,$$

$$\boldsymbol{A}^{\mathcal{N}(k)+1,l}=-\boldsymbol{T}^{(k-1)}\mathcal{T}^{31}\left(k_{\rm s}\boldsymbol{r}_{0l}^{(k)}\right)\,,\quad l=1,2,\ldots,\mathcal{N}(k)\,.$$

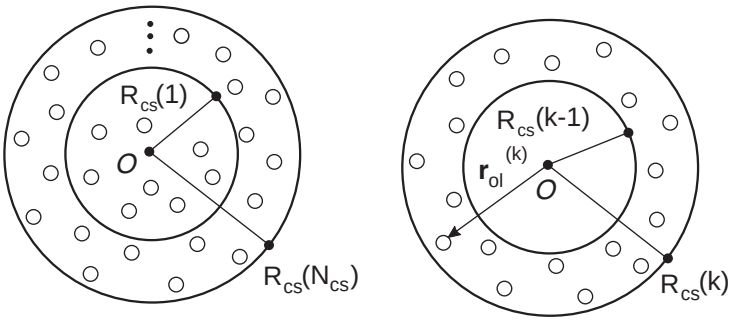

Fig. 2.7. Illustration of the recursive T-matrix algorithm for many spheres

If $\mathcal{A} = \boldsymbol{A}^{-1}$, and $\mathcal{A}^{lp}$, $l, p = 1, 2, \ldots, \mathcal{N}(k) + 1$, are the block-matrix components of $\mathcal{A}$, the recurrence relation for $\boldsymbol{T}$-matrix calculation read as

$$\boldsymbol{T}^{(k)} = \mathcal{A}^{\mathcal{N}(k)+1,\mathcal{N}(k)+1}\boldsymbol{T}^{(k-1)} + \sum_{l=1}^{\mathcal{N}(k)} \mathcal{A}^{\mathcal{N}(k)+1,l}\boldsymbol{T}_{\mathrm{p}}\mathcal{T}^{11}\left(-k_{\mathrm{s}}\boldsymbol{r}_{0l}^{(k)}\right)$$
$$+ \sum_{l=1}^{\mathcal{N}(k)} \mathcal{T}^{11}\left(k_{\mathrm{s}}\boldsymbol{r}_{0l}^{(k)}\right)\left[\mathcal{A}^{l,\mathcal{N}(k)+1}\boldsymbol{T}^{(k-1)} + \sum_{p=1}^{\mathcal{N}(k)} \mathcal{A}^{lp}\boldsymbol{T}_{\mathrm{p}}\mathcal{T}^{11}\left(-k_{\mathrm{s}}\boldsymbol{r}_{0p}^{(k)}\right)\right].$$

The procedure is repeated until all $\mathcal{N}$ particles are exhausted. At each iteration step, only a $[\mathcal{N}(k)+1]$-scatterer problem needs to be solved, where $\mathcal{N}(k)$ usually is much smaller than $\mathcal{N}$. Thus, we can keep the dimension of the problem manageable even when $\mathcal{N}$ is very large. The geometric constraint of the $\boldsymbol{T}$-matrix method requires that the $\mathcal{N}(k)$ particles completely reside inside the spherical shell between $R_{\mathrm{cs}}(k-1)$ and $R_{\mathrm{cs}}(k)$. However, for a large number of particles and small size parameters, numerical simulations certify the accuracy of the recursive scheme even if this geometric constraint is violated.

As mentioned before, the $\mathcal{T}^{11}(-k_{\mathrm{s}}\boldsymbol{r}_{0l})$ matrices are used to translate the incident field from the global coordinate system to the lth particle coordinate system, while the $\mathcal{T}^{11}(k_{\mathrm{s}}\boldsymbol{r}_{0l})$ matrices are used to translate the scattered fields from the basis of the lth particle to the global coordinate system. A recursive $\boldsymbol{T}$-matrix algorithm using phase shift terms instead of translation matrices has been proposed by Auger and Stout [4].

2.7 Composite Particles

A composite particle consists of several nonenclosing parts, each characterized by arbitrary but constant values of electric permittivity and magnetic permeability. The null-field analysis of composite particles using the addition theorem for regular and radiating vector spherical wave functions is equivalent to the multiple scattering formalism [189]. The translation addition theorem for radiating vector spherical wave functions introduces geometric constraints which are not fulfilled for composite particles. Several alternative expressions for the transition matrix have been derived by Ström and Zheng [219] using the $\boldsymbol{Q}$ matrices for open surfaces (the interfaces between the different parts of a composite particle). In the present analysis we avoid the use of any local origin translation and consider a formalism based on closed-surface $\boldsymbol{Q}$ matrices.

2.7.1 General Formulation

To simplify our presentation we first consider a composite particle with two homogeneous parts as shown in Fig. 2.8. We assume that the surfaces $S_{1\mathrm{c}} = S_1 \cup S_{12}$ and $S_{2\mathrm{c}} = S_2 \cup S_{12}$ are star-shaped with respect to O_1 and O_2,

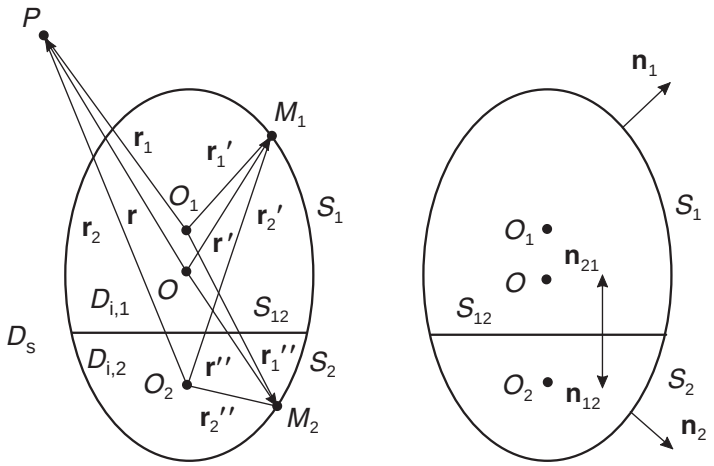

Fig. 2.8. Geometry of a composite particle

respectively. The main reason for introducing the star-shapedness restriction is that we want to keep the individual constituents reasonably simple. A novel feature is the appearance of edges, which are allowed by the basic regularity assumptions of the $\boldsymbol{T}$-matrix formalism [256]. A composite particle can be treated by the multiple scattering formalism under appropriate geometrical conditions. The boundary-value problem for the composite particle depicted in Fig. 2.8 has the following formulation.

Given the external excitation $\boldsymbol{E}_{\rm e}, \boldsymbol{H}_{\rm e}$ *as an entire solution to the Maxwell equations, find the scattered field* $\boldsymbol{E}_{\rm s}$, $\boldsymbol{H}_{\rm s}$ *and the internal fields* $\boldsymbol{E}_{\rm i,1}$, $\boldsymbol{H}_{\rm i,1}$ *and* $\boldsymbol{E}_{\rm i,2}$, $\boldsymbol{H}_{\rm i,2}$ *satisfying the Maxwell equations*

$$\nabla \times \boldsymbol{E}_{\rm s} = {\rm j}k_0\mu_{\rm s}\boldsymbol{H}_{\rm s}\,, \quad \nabla \times \boldsymbol{H}_{\rm s} = -{\rm j}k_0\varepsilon_{\rm s}\boldsymbol{E}_{\rm s} \quad in \quad D_{\rm s}\,, \tag{2.151}$$

$$\nabla \times \boldsymbol{E}_{\rm i,1} = {\rm j}k_0\mu_{\rm i,1}\boldsymbol{H}_{\rm i,1}\,, \quad \nabla \times \boldsymbol{H}_{\rm i,1} = -{\rm j}k_0\varepsilon_{\rm i,1}\boldsymbol{E}_{\rm i,1} \quad in \quad D_{\rm i,1}\,, \tag{2.152}$$

and

$$\nabla \times \boldsymbol{E}_{\rm i,2} = {\rm j}k_0\mu_{\rm i,2}\boldsymbol{H}_{\rm i,2}\,, \quad \nabla \times \boldsymbol{H}_{\rm i,2} = -{\rm j}k_0\varepsilon_{\rm i,2}\boldsymbol{E}_{\rm i,2} \quad in \quad D_{\rm i,2}\,, \tag{2.153}$$

the boundary conditions

$$\begin{aligned} \boldsymbol{n}_1 \times \boldsymbol{E}_{\rm i,1} - \boldsymbol{n}_1 \times \boldsymbol{E}_{\rm s} &= \boldsymbol{n}_1 \times \boldsymbol{E}_{\rm e}\,, \\ \boldsymbol{n}_1 \times \boldsymbol{H}_{\rm i,1} - \boldsymbol{n}_1 \times \boldsymbol{H}_{\rm s} &= \boldsymbol{n}_1 \times \boldsymbol{H}_{\rm e} \end{aligned} \tag{2.154}$$

on S_1,

$$\begin{aligned} \boldsymbol{n}_2 \times \boldsymbol{E}_{\rm i,2} - \boldsymbol{n}_2 \times \boldsymbol{E}_{\rm s} &= \boldsymbol{n}_2 \times \boldsymbol{E}_{\rm e}\,, \\ \boldsymbol{n}_2 \times \boldsymbol{H}_{\rm i,2} - \boldsymbol{n}_2 \times \boldsymbol{H}_{\rm s} &= \boldsymbol{n}_2 \times \boldsymbol{H}_{\rm e} \end{aligned} \tag{2.155}$$

on S_2, *and*

$$\begin{aligned} \boldsymbol{n}_{12} \times \boldsymbol{E}_{\mathrm{i},1} + \boldsymbol{n}_{21} \times \boldsymbol{E}_{\mathrm{i},2} = 0\,, \\ \boldsymbol{n}_{12} \times \boldsymbol{H}_{\mathrm{i},1} + \boldsymbol{n}_{21} \times \boldsymbol{H}_{\mathrm{i},2} = 0 \end{aligned} \tag{2.156}$$

on S_{12}, *and the Silver–Müller radiation condition for the scattered field (2.3).*

The Stratton–Chu representation theorem for the incident and scattered fields in D_i, where $D_\mathrm{i} = D_{\mathrm{i},1} \cup D_{\mathrm{i},2} \cup S_{12} = \boldsymbol{R}^3 - \overline{D}_\mathrm{s}$, together with the boundary conditions (2.154) and (2.155), lead to the general null-field equation

$$\begin{aligned} &\nabla \times \int_{S_1} \left[\boldsymbol{e}_{\mathrm{i},1}\left(\boldsymbol{r}'\right) - \boldsymbol{e}_\mathrm{e}\left(\boldsymbol{r}'\right)\right] g\left(k_\mathrm{s}, \boldsymbol{r}, \boldsymbol{r}'\right) \mathrm{d}S\left(\boldsymbol{r}'\right) \\ &\quad + \frac{\mathrm{j}}{k_0 \varepsilon_\mathrm{s}} \nabla \times \nabla \times \int_{S_1} \left[\boldsymbol{h}_{\mathrm{i},1}\left(\boldsymbol{r}'\right) - \boldsymbol{h}_\mathrm{e}\left(\boldsymbol{r}'\right)\right] g\left(k_\mathrm{s}, \boldsymbol{r}, \boldsymbol{r}'\right) \mathrm{d}S\left(\boldsymbol{r}'\right) \\ &\quad + \nabla \times \int_{S_2} \left[\boldsymbol{e}_{\mathrm{i},2}\left(\boldsymbol{r}''\right) - \boldsymbol{e}_\mathrm{e}\left(\boldsymbol{r}''\right)\right] g\left(k_\mathrm{s}, \boldsymbol{r}, \boldsymbol{r}''\right) \mathrm{d}S\left(\boldsymbol{r}''\right) \\ &\quad + \frac{\mathrm{j}}{k_0 \varepsilon_\mathrm{s}} \nabla \times \nabla \times \int_{S_2} \left[\boldsymbol{h}_{\mathrm{i},2}\left(\boldsymbol{r}''\right) - \boldsymbol{h}_\mathrm{e}\left(\boldsymbol{r}''\right)\right] g\left(k_\mathrm{s}, \boldsymbol{r}, \boldsymbol{r}''\right) \mathrm{d}S\left(\boldsymbol{r}''\right) = 0\,, \quad \boldsymbol{r} \in D_\mathrm{i}\,. \end{aligned} \tag{2.157}$$

Passing from the origin O to the origin O_1, using the identities

$$\begin{aligned} g\left(k_\mathrm{s}, \boldsymbol{r}, \boldsymbol{r}'\right) = g\left(k_\mathrm{s}, \boldsymbol{r}_1, \boldsymbol{r}_1'\right)\,, \\ g\left(k_\mathrm{s}, \boldsymbol{r}, \boldsymbol{r}''\right) = g\left(k_\mathrm{s}, \boldsymbol{r}_1, \boldsymbol{r}_1''\right)\,, \end{aligned}$$

restricting $\boldsymbol{r}_1$ to lie on a sphere enclosed in $D_{\mathrm{i},1}$ and taking into account the integral form of the boundary conditions (2.156)

$$\begin{aligned} \int_{S_{12}} \boldsymbol{e}_{\mathrm{i},1} \cdot \begin{pmatrix} \boldsymbol{N}_{\boldsymbol{\nu}}^3 \\ \boldsymbol{M}_{\boldsymbol{\nu}}^3 \end{pmatrix} \mathrm{d}S + \int_{S_{12}} \boldsymbol{e}_{\mathrm{i},2} \cdot \begin{pmatrix} \boldsymbol{N}_{\boldsymbol{\nu}}^3 \\ \boldsymbol{M}_{\boldsymbol{\nu}}^3 \end{pmatrix} \mathrm{d}S = 0\,, \\ \int_{S_{12}} \boldsymbol{h}_{\mathrm{i},1} \cdot \begin{pmatrix} \boldsymbol{M}_{\boldsymbol{\nu}}^3 \\ \boldsymbol{N}_{\boldsymbol{\nu}}^3 \end{pmatrix} \mathrm{d}S + \int_{S_{12}} \boldsymbol{h}_{\mathrm{i},2} \cdot \begin{pmatrix} \boldsymbol{M}_{\boldsymbol{\nu}}^3 \\ \boldsymbol{N}_{\boldsymbol{\nu}}^3 \end{pmatrix} \mathrm{d}S = 0\,, \end{aligned}$$

yields

$$\begin{aligned} &\frac{\mathrm{j}k_\mathrm{s}^2}{\pi} \int_{S_{1\mathrm{c}}} \left\{ \left[\boldsymbol{e}_{\mathrm{i},1}\left(\boldsymbol{r}_1'\right) - \boldsymbol{e}_\mathrm{e}\left(\boldsymbol{r}_1'\right)\right] \cdot \begin{pmatrix} \boldsymbol{N}_{\boldsymbol{\nu}}^3(k_\mathrm{s}\boldsymbol{r}_1') \\ \boldsymbol{M}_{\boldsymbol{\nu}}^3(k_\mathrm{s}\boldsymbol{r}_1') \end{pmatrix} \right. \\ &\quad \left. + \mathrm{j}\sqrt{\frac{\mu_\mathrm{s}}{\varepsilon_\mathrm{s}}} \left[\boldsymbol{h}_{\mathrm{i},1}\left(\boldsymbol{r}_1'\right) - \boldsymbol{h}_\mathrm{e}\left(\boldsymbol{r}_1'\right)\right] \cdot \begin{pmatrix} \boldsymbol{M}_{\boldsymbol{\nu}}^3(k_\mathrm{s}\boldsymbol{r}_1') \\ \boldsymbol{N}_{\boldsymbol{\nu}}^3(k_\mathrm{s}\boldsymbol{r}_1') \end{pmatrix} \right\} \mathrm{d}S\left(\boldsymbol{r}_1'\right) \\ &\quad + \frac{\mathrm{j}k_\mathrm{s}^2}{\pi} \int_{S_{2\mathrm{c}}} \left\{ \left[\boldsymbol{e}_{\mathrm{i},2}\left(\boldsymbol{r}_2''\right) - \boldsymbol{e}_\mathrm{e}\left(\boldsymbol{r}_1''\right)\right] \cdot \begin{pmatrix} \boldsymbol{N}_{\boldsymbol{\nu}}^3\left(k_\mathrm{s}\boldsymbol{r}_1''\right) \\ \boldsymbol{M}_{\boldsymbol{\nu}}^3(k_\mathrm{s}\boldsymbol{r}_1'') \end{pmatrix} \right. \\ &\quad \left. + \mathrm{j}\sqrt{\frac{\mu_\mathrm{s}}{\varepsilon_\mathrm{s}}} \left[\boldsymbol{h}_{\mathrm{i},2}\left(\boldsymbol{r}_2''\right) - \boldsymbol{h}_\mathrm{e}\left(\boldsymbol{r}_1''\right)\right] \cdot \begin{pmatrix} \boldsymbol{M}_{\boldsymbol{\nu}}^3(k_\mathrm{s}\boldsymbol{r}_1'') \\ \boldsymbol{N}_{\boldsymbol{\nu}}^3(k_\mathrm{s}\boldsymbol{r}_1'') \end{pmatrix} \right\} \mathrm{d}S\left(\boldsymbol{r}_2''\right) = 0\,, \quad \nu = 1, 2, \ldots \end{aligned} \tag{2.158}$$

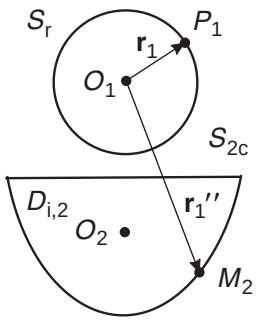

Fig. 2.9. Illustration of the auxiliary sphere in the exterior of S_{2c}

The physical fact that the tangential fields are continuous across the intersecting surface is the key to the structure of the null-field equations, and it is not used explicitly latter on. To simplify the null-field equations (2.158) we use the Stratton–Chu representation theorem for the incident field in the interior and exterior of the closed surface S_{2c}

$$\begin{pmatrix} -\boldsymbol{E}_e(\boldsymbol{r}_1) \\ 0 \end{pmatrix} = \nabla \times \int_{S_{2c}} \boldsymbol{e}_e\left(\boldsymbol{r}_1''\right) g\left(k_s, \boldsymbol{r}_1, \boldsymbol{r}_1''\right) \mathrm{d}S(\boldsymbol{r}_1'') + \frac{\mathrm{j}}{k_0 \varepsilon_s} \nabla \times \nabla \times \int_{S_{2c}} \boldsymbol{h}_e\left(\boldsymbol{r}_1''\right) g\left(k_s, \boldsymbol{r}_1, \boldsymbol{r}_1''\right) \mathrm{d}S(\boldsymbol{r}_1''), \quad \begin{pmatrix} \boldsymbol{r}_1 \in D_{i,2} \\ \boldsymbol{r}_1 \in \boldsymbol{R}^3 - \overline{D}_{i,2} \end{pmatrix}.$$

Choosing an auxiliary sphere in the exterior of S_{2c} as in Fig. 2.9, and restricting $\boldsymbol{r}_1$ to lie on this sphere, we derive

$$\frac{\mathrm{j}k_s^2}{\pi} \int_{S_{2c}} \left[\boldsymbol{e}_e\left(\boldsymbol{r}_1''\right) \cdot \begin{pmatrix} \boldsymbol{N}_\nu^3\left(k_s \boldsymbol{r}_1''\right) \\ \boldsymbol{M}_\nu^3\left(k_s \boldsymbol{r}_1''\right) \end{pmatrix} + \mathrm{j}\sqrt{\frac{\mu_s}{\varepsilon_s}} \boldsymbol{h}_e\left(\boldsymbol{r}_1''\right) \cdot \begin{pmatrix} \boldsymbol{M}_\nu^3\left(k_s \boldsymbol{r}_1''\right) \\ \boldsymbol{N}_\nu^3\left(k_s \boldsymbol{r}_1''\right) \end{pmatrix} \right] \mathrm{d}S\left(\boldsymbol{r}_1''\right) = 0, \quad \nu = 1, 2, \ldots,$$

whence, using the identities $\boldsymbol{e}_e(\boldsymbol{r}') = \boldsymbol{e}_e(\boldsymbol{r}_1')$ and $\boldsymbol{h}_e(\boldsymbol{r}') = \boldsymbol{h}_e(\boldsymbol{r}_1')$, we obtain

$$\begin{aligned} &\frac{\mathrm{j}k_s^2}{\pi} \int_{S_{1c}} \left\{ \left[\boldsymbol{e}_{i,1}\left(\boldsymbol{r}_1'\right) - \boldsymbol{e}_e\left(\boldsymbol{r}'\right) \right] \cdot \begin{pmatrix} \boldsymbol{N}_{\boldsymbol{\nu}}^3(k_s \boldsymbol{r}_1') \\ \boldsymbol{M}_{\boldsymbol{\nu}}^3(k_s \boldsymbol{r}_1') \end{pmatrix} \right. \\ &\left. + \mathrm{j}\sqrt{\frac{\mu_s}{\varepsilon_s}} \left[\boldsymbol{h}_{i,1}\left(\boldsymbol{r}_1'\right) - \boldsymbol{h}_e\left(\boldsymbol{r}'\right) \right] \cdot \begin{pmatrix} \boldsymbol{M}_{\boldsymbol{\nu}}^3(k_s \boldsymbol{r}_1') \\ \boldsymbol{N}_{\boldsymbol{\nu}}^3(k_s \boldsymbol{r}_1') \end{pmatrix} \right\} \mathrm{d}S\left(\boldsymbol{r}_1'\right) \\ &+ \frac{\mathrm{j}k_s^2}{\pi} \int_{S_{2c}} \left[\boldsymbol{e}_{i,2}\left(\boldsymbol{r}_2''\right) \cdot \begin{pmatrix} \boldsymbol{N}_{\boldsymbol{\nu}}^3\left(k_s \boldsymbol{r}_1''\right) \\ \boldsymbol{M}_{\boldsymbol{\nu}}^3(k_s \boldsymbol{r}_1'') \end{pmatrix} \right. \\ &\left. + \mathrm{j}\sqrt{\frac{\mu_s}{\varepsilon_s}} \boldsymbol{h}_{i,2}\left(\boldsymbol{r}_2''\right) \cdot \begin{pmatrix} \boldsymbol{M}_{\boldsymbol{\nu}}^3(k_s \boldsymbol{r}_1'') \\ \boldsymbol{N}_{\boldsymbol{\nu}}^3(k_s \boldsymbol{r}_1'') \end{pmatrix} \right] \mathrm{d}S\left(\boldsymbol{r}_2''\right) = 0, \quad \nu = 1, 2, \ldots \end{aligned} \tag{2.159}$$

Similarly, passing from origin O to origin O_2 and restricting $\boldsymbol{r}_2$ to lie on a sphere enclosed in $D_{\mathrm{i},2}$, gives

$$\begin{aligned}
&\frac{\mathrm{j}k_{\mathrm{s}}^2}{\pi}\int_{S_{1\mathrm{c}}}\left[\boldsymbol{e}_{\mathrm{i},1}\left(\boldsymbol{r}_1'\right)\cdot\begin{pmatrix}\boldsymbol{N}_{\boldsymbol{\nu}}^3(k_{\mathrm{s}}\boldsymbol{r}_2')\\ \boldsymbol{M}_{\boldsymbol{\nu}}^3(k_{\mathrm{s}}\boldsymbol{r}_2')\end{pmatrix}\right.\\
&\left.+\,\mathrm{j}\sqrt{\frac{\mu_{\mathrm{s}}}{\varepsilon_{\mathrm{s}}}}\boldsymbol{h}_{\mathrm{i},1}\left(\boldsymbol{r}_1'\right)\cdot\begin{pmatrix}\boldsymbol{M}_{\boldsymbol{\nu}}^3(k_{\mathrm{s}}\boldsymbol{r}_2')\\ \boldsymbol{N}_{\boldsymbol{\nu}}^3(k_{\mathrm{s}}\boldsymbol{r}_2')\end{pmatrix}\right]\mathrm{d}S\left(\boldsymbol{r}_1'\right)\\
&+\frac{\mathrm{j}k_{\mathrm{s}}^2}{2}\int_{S_{2\mathrm{c}}}\left\{\left[\boldsymbol{e}_{\mathrm{i},2}\left(\boldsymbol{r}_2''\right)-\boldsymbol{e}_{\mathrm{e}}\left(\boldsymbol{r}''\right)\right]\cdot\begin{pmatrix}\boldsymbol{N}_{\boldsymbol{\nu}}^3\left(k_{\mathrm{s}}\boldsymbol{r}_2''\right)\\ \boldsymbol{M}_{\boldsymbol{\nu}}^3(k_{\mathrm{s}}\boldsymbol{r}_2'')\end{pmatrix}\right.\\
&\left.+\,\mathrm{j}\sqrt{\frac{\mu_{\mathrm{s}}}{\varepsilon_{\mathrm{s}}}}\left[\boldsymbol{h}_{\mathrm{i},2}\left(\boldsymbol{r}_2''\right)-\boldsymbol{h}_{\mathrm{e}}\left(\boldsymbol{r}''\right)\right]\cdot\begin{pmatrix}\boldsymbol{M}_{\boldsymbol{\nu}}^3(k_{\mathrm{s}}\boldsymbol{r}_2'')\\ \boldsymbol{N}_{\boldsymbol{\nu}}^3(k_{\mathrm{s}}\boldsymbol{r}_2'')\end{pmatrix}\right\}\mathrm{d}S\left(\boldsymbol{r}_2''\right)=0\,,\quad \nu=1,2,\ldots
\end{aligned}\tag{2.160}$$

The surface fields $\boldsymbol{e}_{\mathrm{i},1}$, $\boldsymbol{h}_{\mathrm{i},1}$ and $\boldsymbol{e}_{\mathrm{i},2}$, $\boldsymbol{h}_{\mathrm{i},2}$ are approximated by finite expansions in terms of regular vector spherical wave functions as in (2.132) and (2.133) respectively. Inserting these expansions into the null-field equations (2.159) and (2.160), yields the system of matrix equations

$$\begin{aligned}
\boldsymbol{Q}_1^{31}(k_{\mathrm{s}},1,k_{\mathrm{i},1},1)\boldsymbol{i}_1+\boldsymbol{Q}_2^{31}(k_{\mathrm{s}},1,k_{\mathrm{i},2},2)\boldsymbol{i}_2&=\boldsymbol{Q}_1^{31}(k_{\mathrm{s}},1,k_{\mathrm{s}},0)\boldsymbol{e}\,,\\
\boldsymbol{Q}_1^{31}(k_{\mathrm{s}},2,k_{\mathrm{i},1},1)\boldsymbol{i}_1+\boldsymbol{Q}_2^{31}(k_{\mathrm{s}},2,k_{\mathrm{i},2},2)\boldsymbol{i}_2&=\boldsymbol{Q}_2^{31}(k_{\mathrm{s}},2,k_{\mathrm{s}},0)\boldsymbol{e}\,,
\end{aligned}\tag{2.161}$$

where the significance of the vectors $\boldsymbol{i}_1$, $\boldsymbol{i}_2$ and $\boldsymbol{e}$ is as in Sect. 2.6. The $\boldsymbol{Q}$ matrices involving vector spherical wave functions with arguments referring to different origins are given by (2.84)–(2.87).

To compute the scattered-field expansion centered at the origin O we use the Stratton–Chu representation theorem for the scattered field $\boldsymbol{E}_{\mathrm{s}}$ in D_{s}. The expressions of the scattered field coefficients are given by (2.136) with $S_{1\mathrm{c}}$ and $S_{2\mathrm{c}}$ in place of S_1 and S_2, respectively, and in matrix form, we have

$$\boldsymbol{s}=\boldsymbol{Q}_1^{11}(k_{\mathrm{s}},0,k_{\mathrm{i},1},1)\boldsymbol{i}_1+\boldsymbol{Q}_2^{11}(k_{\mathrm{s}},0,k_{\mathrm{i},2},2)\boldsymbol{i}_2\,.\tag{2.162}$$

The null-field equations (2.161) and the scattered field equation (2.162) completely describe the $\boldsymbol{T}$-matrix calculation and correspond to equations (2.134) and (2.137) of Sect. 2.6.

2.7.2 Formulation for a Particle with $\mathcal{N}$ Constituents

For a composite particle with $\mathcal{N}$ constituents, the system of matrix equations consists in the null-field equations in the interior of $S_{l\mathrm{c}}$

$$\sum_{p=1}^{\mathcal{N}}\boldsymbol{Q}_p^{31}(k_{\mathrm{s}},l,k_{\mathrm{i},p},p)\boldsymbol{i}_p=\boldsymbol{Q}_l^{31}(k_{\mathrm{s}},l,k_{\mathrm{s}},0)\boldsymbol{e}\,,\quad\text{for}\quad l=1,2,\ldots,\mathcal{N}\tag{2.163}$$

and the matrix equation corresponding to the scattered field representation

$$\boldsymbol{s}=\sum_{l=1}^{\mathcal{N}}\boldsymbol{Q}_l^{11}(k_{\mathrm{s}},0,k_{\mathrm{i},l},l)\boldsymbol{i}_l\,.\tag{2.164}$$

Considering the global matrix $\boldsymbol{A}$ with block-matrix components

$$\boldsymbol{A}^{lp} = \boldsymbol{Q}_p^{31}(k_{\rm s}, l, k_{{\rm i},p}, p)\,, \quad l,p = 1,2,\ldots,\mathcal{N}\,, \tag{2.165}$$

we express the solution to the system of matrix equations (2.163) as

$$\boldsymbol{i}_l = \left(\sum_{p=1}^{\mathcal{N}} \mathcal{A}^{lp}\boldsymbol{Q}_p^{31}(k_{\rm s}, p, k_{\rm s}, 0)\right)\boldsymbol{e}\,, \quad l = 1,2,\ldots,\mathcal{N}\,,$$

where $\mathcal{A}$ stay for $\boldsymbol{A}^{-1}$, and $\mathcal{A}^{lp},\ l,p = 1,2,\ldots,\mathcal{N}$, are the block-matrix components of $\mathcal{A}$. In view of (2.164), the transition matrix of the composite particle becomes

$$\boldsymbol{T} = \sum_{l=1}^{\mathcal{N}}\sum_{p=1}^{\mathcal{N}} \boldsymbol{Q}_l^{11}(k_{\rm s}, 0, k_{{\rm i},l}, l)\mathcal{A}^{lp}\boldsymbol{Q}_p^{31}(k_{\rm s}, p, k_{\rm s}, 0)\,.$$

For an axisymmetric composite particle, the transition matrix is block-diagonal with each block matrix corresponding to a different azimuthal mode m. Since there is no coupling between the different m indices, each block matrix can be computed separately. To derive the dimension of the transition matrix, we consider an axisymmetric particle and set

$$N_{\rm max}(l) = \begin{cases} N_{\rm rank}(l)\,, & m = 0 \\ N_{\rm rank}(l) - |m| + 1\,, & m \neq 0 \end{cases},$$

where $N_{\rm rank}(l)$ is the maximum expansion order of the region l and m is the azimuthal mode. Then, we have

$$\begin{aligned} \dim\left(\boldsymbol{Q}_p^{31}\right) &= 2N_{\rm max}(p) \times 2N_{\rm max}\,, \\ \dim\left(\boldsymbol{A}^{lp}\right) &= 2N_{\rm max}(l) \times 2N_{\rm max}(p)\,, \\ \dim\left(\boldsymbol{Q}_l^{11}\right) &= 2N_{\rm max} \times 2N_{\rm max}(l), \end{aligned}$$

and therefore

$$\dim\left(\boldsymbol{T}\right) = 2N_{\rm max} \times 2N_{\rm max}\,.$$

Thus, $N_{\rm max}$ gives the dimension of the transition matrix and

$$N_{\rm max} = \begin{cases} N_{\rm rank}\,, & m = 0, \\ N_{\rm rank} - |m| + 1\,, & m \neq 0, \end{cases}$$

where $N_{\rm rank}$ is determined by the size parameter of the composite particle. It should be mentioned that in our computer code, $N_{\rm rank}$ and $N_{\rm rank}(l),\ l = 1,2,\ldots,\mathcal{N}$, are independent parameters controlling the $\boldsymbol{T}$-matrix calculations.

The contributions of Zheng [276, 277], Zheng and Ström [279], and Zheng and Shao [278] demonstrated the applicability of the null-field method to particles with complex geometries and optical properties. The above formalism can be extended to nonaxisymmetric particles in which case, the domain of analysis can be discretized into many volume elements with different shapes and optical constants.

2.7.3 Formulation with Discrete Sources

For a composite particle with two constituents, the null-field equations formulated in terms of distributed vector spherical wave functions

$$\begin{aligned}
&\frac{\mathrm{j}k_\mathrm{s}^2}{\pi}\int_{S_{1\mathrm{c}}}\left\{[\boldsymbol{e}_{\mathrm{i},1}(\boldsymbol{r}_1')-\boldsymbol{e}_\mathrm{e}(\boldsymbol{r}')]\cdot\begin{pmatrix}\mathcal{N}_{\boldsymbol{\nu}}^3(k_\mathrm{s}\boldsymbol{r}_1')\\ \mathcal{M}_{\boldsymbol{\nu}}^3(k_\mathrm{s}\boldsymbol{r}_1')\end{pmatrix}\right.\\
&\left.+[\boldsymbol{e}_{\mathrm{i},1}(\boldsymbol{r}_1')-\boldsymbol{e}_\mathrm{e}(\boldsymbol{r}')]\cdot\begin{pmatrix}\mathcal{N}_{\boldsymbol{\nu}}^3(k_\mathrm{s}\boldsymbol{r}_1')\\ \mathcal{M}_{\boldsymbol{\nu}}^3(k_\mathrm{s}\boldsymbol{r}_1')\end{pmatrix}\right\}\mathrm{d}S(\boldsymbol{r}_1')\\
&+\frac{\mathrm{j}k_\mathrm{s}^2}{\pi}\int_{S_{2\mathrm{c}}}\left[\boldsymbol{e}_{\mathrm{i},2}(\boldsymbol{r}_2'')\cdot\begin{pmatrix}\mathcal{N}_{\boldsymbol{\nu}}^3(k_\mathrm{s}\boldsymbol{r}_1'')\\ \mathcal{M}_{\boldsymbol{\nu}}^3(k_\mathrm{s}\boldsymbol{r}_1'')\end{pmatrix}\right.\\
&\left.+\mathrm{j}\sqrt{\frac{\mu_\mathrm{s}}{\varepsilon_\mathrm{s}}}\boldsymbol{h}_{\mathrm{i},2}(\boldsymbol{r}_2'')\cdot\begin{pmatrix}\mathcal{M}_{\boldsymbol{\nu}}^3(k_\mathrm{s}\boldsymbol{r}_1'')\\ \mathcal{N}_{\boldsymbol{\nu}}^3(k_\mathrm{s}\boldsymbol{r}_1'')\end{pmatrix}\right]\mathrm{d}S(\boldsymbol{r}_2'')=0\,,\quad \nu=1,2,\ldots
\end{aligned}\tag{2.166}$$

and

$$\begin{aligned}
&\frac{\mathrm{j}k_\mathrm{s}^2}{\pi}\int_{S_{1\mathrm{c}}}\left[\boldsymbol{e}_{\mathrm{i},1}(\boldsymbol{r}_1')\cdot\begin{pmatrix}\mathcal{N}_{\boldsymbol{\nu}}^3(k_\mathrm{s}\boldsymbol{r}_2')\\ \mathcal{M}_{\boldsymbol{\nu}}^3(k_\mathrm{s}\boldsymbol{r}_2')\end{pmatrix}\right.\\
&\left.+\mathrm{j}\sqrt{\frac{\mu_\mathrm{s}}{\varepsilon_\mathrm{s}}}\boldsymbol{h}_{\mathrm{i},1}(\boldsymbol{r}_1')\cdot\begin{pmatrix}\mathcal{M}_{\boldsymbol{\nu}}^3(k_\mathrm{s}\boldsymbol{r}_2')\\ \mathcal{N}_{\boldsymbol{\nu}}^3(k_\mathrm{s}\boldsymbol{r}_2')\end{pmatrix}\right]\mathrm{d}S(\boldsymbol{r}_1')\\
&+\frac{\mathrm{j}k_\mathrm{s}^2}{2}\int_{S_{2\mathrm{c}}}\left\{[\boldsymbol{e}_{\mathrm{i},2}(\boldsymbol{r}_2'')-\boldsymbol{e}_\mathrm{e}(\boldsymbol{r}'')]\cdot\begin{pmatrix}\mathcal{N}_{\boldsymbol{\nu}}^3(k_\mathrm{s}\boldsymbol{r}_2'')\\ \mathcal{M}_{\boldsymbol{\nu}}^3(k_\mathrm{s}\boldsymbol{r}_2'')\end{pmatrix}\right.\\
&\left.+\mathrm{j}\sqrt{\frac{\mu_\mathrm{s}}{\varepsilon_\mathrm{s}}}[\boldsymbol{h}_{\mathrm{i},2}(\boldsymbol{r}_2'')-\boldsymbol{h}_\mathrm{e}(\boldsymbol{r}'')]\cdot\begin{pmatrix}\mathcal{M}_{\boldsymbol{\nu}}^3(k_\mathrm{s}\boldsymbol{r}_2'')\\ \mathcal{N}_{\boldsymbol{\nu}}^3(k_\mathrm{s}\boldsymbol{r}_2'')\end{pmatrix}\right\}\mathrm{d}S(\boldsymbol{r}_2'')=0\,,\quad \nu=1,2,\ldots
\end{aligned}\tag{2.167}$$

are equivalent to the general null-field equation (2.157). The distributed vector spherical wave functions in (2.166)–(2.167) are defined as

$$\begin{aligned}
\mathcal{M}_{mn}^{1,3}(k\boldsymbol{r}_1)&=\boldsymbol{M}_{m,|m|+l}^{1,3}[k(\boldsymbol{r}_1-z_{1,n}\boldsymbol{e}_z)]\,,\\
\mathcal{N}_{mn}^{1,3}(k\boldsymbol{r}_1)&=\boldsymbol{N}_{m,|m|+l}^{1,3}[k(\boldsymbol{r}_1-z_{1,n}\boldsymbol{e}_z)]\,,
\end{aligned}$$

and

$$\begin{aligned}
\mathcal{M}_{mn}^{1,3}(k\boldsymbol{r}_2)&=\boldsymbol{M}_{m,|m|+l}^{1,3}[k(\boldsymbol{r}_2-z_{2,n}\boldsymbol{e}_z)]\,,\\
\mathcal{N}_{mn}^{1,3}(k\boldsymbol{r}_2)&=\boldsymbol{N}_{m,|m|+l}^{1,3}[k(\boldsymbol{r}_2-z_{2,n}\boldsymbol{e}_z)]\,,
\end{aligned}$$

where $\{z_{1,n}\}_{n=1}^{\infty}$ is a dense set of points situated on the z-axis and in the interior of $S_{1\mathrm{c}}$, while $\{z_{2,n}\}_{n=1}^{\infty}$ is a dense set of points situated on the z-axis and in the interior of $S_{2\mathrm{c}}$. In the null-field method with discrete sources,

the approximate surface fields $\boldsymbol{e}^N_{\mathrm{i},1}$, $\boldsymbol{h}^N_{\mathrm{i},1}$ and $\boldsymbol{e}^N_{\mathrm{i},2}$, $\boldsymbol{h}^N_{\mathrm{i},2}$ are expressed as linear combinations of distributed vector spherical wave functions as in (2.132) and (2.133) but with $\mathcal{M}^1_\mu(k_{\mathrm{i},1}\boldsymbol{r}'_1)$, $\mathcal{N}^1_\mu(k_{\mathrm{i},1}\boldsymbol{r}'_1)$ in place of $\boldsymbol{M}^1_\mu(k_{\mathrm{i},1}\boldsymbol{r}'_1)$, $\boldsymbol{N}^1_\mu(k_{\mathrm{i},1}\boldsymbol{r}'_1)$ and $\mathcal{M}^1_\mu(k_{\mathrm{i},2}\boldsymbol{r}''_2)$, $\mathcal{N}^1_\mu(k_{\mathrm{i},2}\boldsymbol{r}''_2)$ in place of $\boldsymbol{M}^1_\mu(k_{\mathrm{i},2}\boldsymbol{r}''_2)$, $\boldsymbol{N}^1_\mu(k_{\mathrm{i},2}\boldsymbol{r}''_2)$, respectively.

For a composite particle with $\mathcal{N}$ constituents, the block-matrix elements $\boldsymbol{A}^{lp}$ are given by (2.165) with $\widetilde{\boldsymbol{Q}}^{31}_p$ in place of $\boldsymbol{Q}^{31}_p$, and the expressions of the elements of the $\widetilde{\boldsymbol{Q}}^{31}_p$ matrix are given by (2.84)–(2.87) with the localized vector spherical wave functions replaced by the distributed vector spherical wave functions. The transition matrix is

$$\boldsymbol{T} = \sum_{l=1}^{\mathcal{N}} \sum_{p=1}^{\mathcal{N}} \widetilde{\boldsymbol{Q}}^{11}_l(k_{\mathrm{s}}, 0, k_{\mathrm{i},l}, l)\mathcal{A}^{lp}\widetilde{\boldsymbol{Q}}^{31}_p(k_{\mathrm{s}}, p, k_{\mathrm{s}}, 0)\,,$$

where the $\widetilde{\boldsymbol{Q}}^{11}_l$ matrices contains as rows the vectors $\boldsymbol{M}^1_{\overline{\nu}}$, $\boldsymbol{N}^1_{\overline{\nu}}$ and as columns the vectors $\mathcal{M}^1_\mu$, $\mathcal{N}^1_\mu$, while the $\widetilde{\boldsymbol{Q}}^{31}_p$ matrices contains as rows and columns the vectors $\mathcal{M}^3_{\overline{\nu}}$, $\mathcal{N}^3_{\overline{\nu}}$ and $\boldsymbol{M}^1_\mu$, $\boldsymbol{N}^1_\mu$, respectively.

For axisymmetric particles, the z-axis of the particle coordinate system is the axis of rotation and the use of distributed vector spherical wave functions improves the numerical stability of the $\boldsymbol{T}$-matrix calculations, especially for highly elongated and flattened composite particles [51].

2.8 Complex Particles

The transition matrix for complex particles consisting of a number of arbitrary constituents can be derived by combining the results established in the previous sections. As an example, we consider the particle geometry depicted in Fig. 2.10. The scatterer is a composite particle with two inhomogeneous constituents and each inhomogeneous part is a layered particle. We denote by $\widetilde{\boldsymbol{i}}_1$ and $\boldsymbol{i}_1$ the vectors containing the expansion coefficients of the internal fields in $D_{i,1}$, by $\widetilde{\boldsymbol{i}}_2$ and $\boldsymbol{i}_2$ the vectors containing the expansion coefficients of the internal fields in $D_{i,2}$ and by $\boldsymbol{i}_3$ and $\boldsymbol{i}_4$ the vectors containing the expansion coefficients of the internal fields in $D_{i,3}$ and $D_{i,4}$, respectively. $\widetilde{\boldsymbol{i}}_1$ and $\widetilde{\boldsymbol{i}}_2$ refer to the expansion coefficients corresponding to radiating vector spherical wave functions, while $\boldsymbol{i}_1$, $\boldsymbol{i}_2$, $\boldsymbol{i}_3$ and $\boldsymbol{i}_4$ refer to the expansion coefficients corresponding to regular vector spherical wave functions.

Taking into account the results established for composite particles, we see that the null-field equations in the interior of $S_{1\mathrm{c}} = S_1 \cup S_{12}$ and $S_{2\mathrm{c}} = S_2 \cup S_{12}$ are

$$\begin{aligned}&\boldsymbol{Q}^{33}_1(k_s, 1, k_{i,1}, 1)\widetilde{\boldsymbol{i}}_1 + \boldsymbol{Q}^{31}_1(k_s, 1, k_{i,1}, 1)\boldsymbol{i}_1\\ &+\boldsymbol{Q}^{33}_2(k_s, 1, k_{i,2}, 2)\widetilde{\boldsymbol{i}}_2 + \boldsymbol{Q}^{31}_2(k_s, 1, k_{i,2}, 2)\boldsymbol{i}_2 = \boldsymbol{Q}^{31}_1(k_s, 1, k_s, 0)\boldsymbol{e}\,,\end{aligned}$$

and

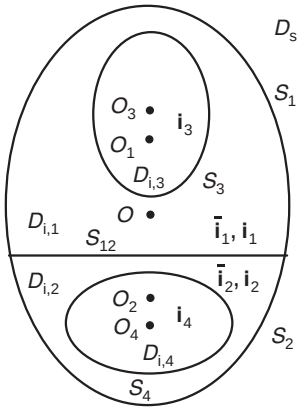

Fig. 2.10. Geometry of a complex particle

$$\boldsymbol{Q}_1^{33}(k_s,2,k_{i,1},1)\widetilde{\boldsymbol{i}}_1+\boldsymbol{Q}_1^{31}(k_s,2,k_{i,1},1)\boldsymbol{i}_1$$
$$+\boldsymbol{Q}_2^{33}(k_s,2,k_{i,2},2)\widetilde{\boldsymbol{i}}_2+\boldsymbol{Q}_2^{31}(k_s,2,k_{i,2},2)\boldsymbol{i}_2=\boldsymbol{Q}_2^{31}(k_s,2,k_s,0)\boldsymbol{e}\,,$$

respectively. Using the results established for inhomogeneous particles, we deduce that the null-field equations in the exterior of S_{1c} and the interior of S_3 are

$$-\widetilde{\boldsymbol{i}}_1+\boldsymbol{Q}_3^{11}(k_{i,1},1,k_{i,3},3)\boldsymbol{i}_3=0\,,$$
$$-\boldsymbol{Q}_1^{31}(k_{i,1},3,k_{i,1},1)\boldsymbol{i}_1+\boldsymbol{Q}_3^{31}(k_{i,1},3,k_{i,3},3)\boldsymbol{i}_3=0\,,$$

while the null-field equations in the exterior of S_{2c} and the interior of S_4 take the forms

$$-\widetilde{\boldsymbol{i}}_2+\boldsymbol{Q}_4^{11}(k_{i,2},2,k_{i,4},4)\boldsymbol{i}_4=0\,,$$
$$-\boldsymbol{Q}_2^{31}(k_{i,2},4,k_{i,2},2)\boldsymbol{i}_2+\boldsymbol{Q}_4^{31}(k_{i,2},4,k_{i,4},4)\boldsymbol{i}_4=0\,.$$

To derive the coefficients of the scattered-field expansion centered at O we proceed as in the case of composite particles and obtain

$$\boldsymbol{s}=\boldsymbol{Q}_1^{13}(k_s,0,k_{i,1},1)\widetilde{\boldsymbol{i}}_1+\boldsymbol{Q}_1^{11}(k_s,0,k_{i,1},1)\boldsymbol{i}_1$$
$$+\boldsymbol{Q}_2^{13}(k_s,0,k_{i,2},2)\widetilde{\boldsymbol{i}}_2+\boldsymbol{Q}_2^{11}(k_s,0,k_{i,2},2)\boldsymbol{i}_2\,.$$

The above equations form a system of seven equations with seven unknowns. Eliminating the vectors corresponding to the internal fields it is possible to obtain a relation between the scattered and incident field coefficients and thus, to derive the expression of the transition matrix.

The $\boldsymbol{T}$-matrix description is also suitable for scattering configurations with several layered particles, Fig. 2.11, or inhomogeneous particles with several enclosures, Fig. 2.12. In the first case, we compute the transition matrices

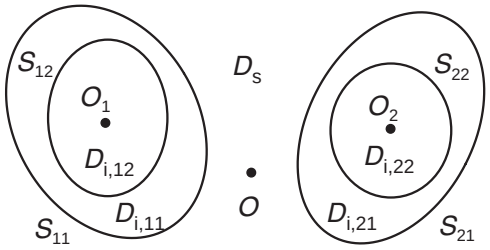

Fig. 2.11. Geometry of two layered particles

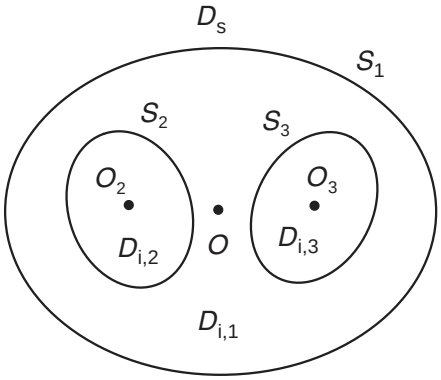

Fig. 2.12. Geometry of an inhomogeneous particle with two enclosures

of each layered particle with the formalism presented in Sect. 2.5, and then use the multiple scattering formalism to derive the transition matrix of the ensemble. In the second case, we compute the transition matrix of the two-particle system, and then calculate the transition matrix of the inhomogeneous particle using the formalism presented in Sect. 2.4. In fact, we can consider any combination of separate and consecutively enclosing surfaces and for each case immediately write down the expression of the transition matrix according to the prescriptions given in the earlier sections.

2.9 Effective Medium Model

The optical properties of heterogeneous materials are of considerable interest in atmospheric science, astronomy and optical particle sizing. Random dispersions of inclusions in a homogeneous host medium can be equivalently considered as effectively homogeneous after using various homogenization formalisms [36,210]. The effective permittivity of a heterogeneous material relates

the average electric displacement to the average electric field [137],

$$\langle \boldsymbol{D} \rangle = \varepsilon_{\text{eff}} \langle \boldsymbol{E} \rangle \ ,$$

where $\langle \boldsymbol{D} \rangle = \int_D \boldsymbol{D} \mathrm{d}V$, $\langle \boldsymbol{E} \rangle = \int_D \boldsymbol{E} \ \mathrm{d}V$ and D is the domain occupied by the heterogeneous material. The effective-medium theories operate with various assumptions which determine their domain of applicability. The usual derivations of the effective-medium approximations are based on electrostatic considerations and assume that the inclusions are much smaller than the wavelength and that the interactions between the inclusions can be neglected. The average electric displacement is expressed in terms of the average electric and polarization fields

$$\langle \boldsymbol{D} \rangle = \varepsilon_{\text{s}} \langle \boldsymbol{E} \rangle + \langle \boldsymbol{P} \rangle \ ,$$

while the average polarization field $\langle \boldsymbol{P} \rangle$ is related to the dipole moment of a single inclusion $\boldsymbol{p}$ by the relation

$$\langle \boldsymbol{P} \rangle = n_0 \boldsymbol{p} \, ,$$

where ε_{s} is the relative permittivity of the host medium and n_0 is the number of particles per unit volume. Defining the exciting field $\boldsymbol{E}_{\text{exc}}$ as the local field which exists within a fictitious cavity that has the shape of an inclusion

$$\boldsymbol{E}_{\text{exc}} = \langle \boldsymbol{E} \rangle + \frac{1}{3\varepsilon_{\text{s}}} \langle \boldsymbol{P} \rangle$$

and assuming that the dipole moment can be expressed in terms of the exciting field as

$$\boldsymbol{p} = \alpha \boldsymbol{E}_{\text{exc}}$$

with α being the polarizability scalar, yields

$$\varepsilon_{\text{eff}} = \varepsilon_{\text{s}} \frac{3\varepsilon_{\text{s}} + 2n_0\alpha}{3\varepsilon_{\text{s}} - n_0\alpha} \, . \tag{2.168}$$

The main issue in the effective-medium approximations is to relate the polarizability α to the relative permittivity ε_{r}, where $\varepsilon_{\text{r}} = \varepsilon_{\text{i}}/\varepsilon_{\text{s}}$, and ε_{i} is the relative permittivity of the inclusion. For spherical particles and at frequencies for which the inclusions can be considered very small, the Maxwell–Garnett formula uses the relation

$$\alpha = \frac{4}{3}\pi R^3 \varepsilon_{\text{s}} \frac{3\left(\varepsilon_{\text{r}} - 1\right)}{\varepsilon_{\text{r}} + 2} \, , \tag{2.169}$$

which yields

$$\varepsilon_{\text{eff}} = \varepsilon_{\text{s}} \frac{1 + 2c\frac{\varepsilon_{\text{r}}-1}{\varepsilon_{\text{r}}+2}}{1 - c\frac{\varepsilon_{\text{r}}-1}{\varepsilon_{\text{r}}+2}} \, , \tag{2.170}$$

where R is the radius of the spherical particles and c is the fractional volume (or the fractional concentration) of the particles, $c = (4/3)\pi R^3 n_0$. Note that size-dependent Maxwell–Garnett formulas incorporating finite-size effects have been derived by using the Lorenz–Mie theory [52, 57], the volume integral equation method [129] and variational approaches [211]. However, in microscopic view, waves propagating in the composite do undergo multiple correlated scattering between the particles. When the concentration of the inclusions is high and the size of the inclusion becomes comparable to the wavelength, more complete models which takes into account the inclusion size, statistical correlations, and multiple-scattering effects, are needed.

In this section, we consider the scattering of a vector plane wave incident on a half-space with randomly distributed particles. Our treatment follows the procedure described by Varadan et al. [236], Varadan and Varadan [235], and Bringi et al. [28] and concerns with the analysis of the coherent scattered field and in particular, of the effective propagation constants in the case of normal incidence. This approach is based on the $\boldsymbol{T}$-matrix method and on spherical statistics, even though the particles may be nonspherical. Lax's quasi-crystalline approximation [138] is employed to truncate the hierarchy of equations relating the different orders of correlations between the particles, and the hole correction and the Percus–Yevick [186] approximation are used to model the pair distribution function. The integral equation of the quasi-crystalline approximation gives rise to the generalized Lorentz–Lorenz law and the generalized Ewald–Oseen extinction theorem. The generalized Lorentz–Lorenz law consists of a homogeneous system of equations and the resulting dispersion relation gives the effective propagation constant for the coherent wave. The generalized Ewald–Oseen extinction theorem is an inhomogeneous equation that relates the transmitted coherent field to the amplitude, polarization, and direction of propagation of the incident field.

Other contributions which are related to the present analysis includes the work of Foldy [69], Waterman and Truell [258], Fikioris and Waterman [65], Twerski [230, 231], Tsang and Kong [223, 224] and Tsang et al. [227]. The case of a plane electromagnetic wave obliquely incident on a half-space with densely distributed particles and the computation of the incoherent field with the distorted Born approximation have been considered Tsang and Kong [225, 226].

2.9.1 $\boldsymbol{T}$-matrix Formulation

The scattering geometry is shown in Fig. 2.13. A linearly polarized plane wave is incident on a half-space with $\mathcal{N}$ identical particles centered at $\boldsymbol{r}_{0l}$, $l = 1, 2, \ldots, \mathcal{N}$, and each particle is assumed to have an imaginary circumscribing spherical shell of radius R. The particles have the same orientation and we choose $\alpha_l = \beta_l = \gamma_l = 0$ for $l = 1, 2, \ldots, \mathcal{N}$. The relative permittivity and relative permeability of the homogeneous particles are $\varepsilon_{\rm i}$ and $\mu_{\rm i}$, and $\varepsilon_{\rm s}$ and $\mu_{\rm s}$ are the material constants of the background medium (which also occupies

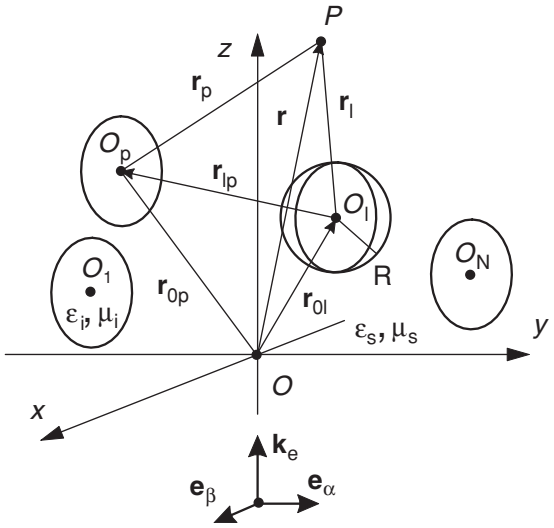

Fig. 2.13. Geometry of identical, homogeneous particles distributed in the half-space $z \geq 0$

the domain $z < 0$). The vector plane wave is of unit amplitude:

$$\boldsymbol{E}_{\mathrm{e}}(\boldsymbol{r}) = \boldsymbol{e}_{\mathrm{pol}} \mathrm{e}^{\mathrm{j}\boldsymbol{k}_{\mathrm{e}} \cdot \boldsymbol{r}} ,$$

and propagates along the z-axis of the global coordinate system, $\boldsymbol{k}_{\mathrm{e}} = k_{\mathrm{s}} \boldsymbol{e}_z$.

Our analysis is entirely based on the superposition $\boldsymbol{T}$-matrix method which expresses the scattered field $\boldsymbol{E}_{\mathrm{s}}$ in terms of the fields $\boldsymbol{E}_{\mathrm{s},l}$ scattered from each individual particle l (cf. (2.147)),

$$\begin{aligned} \boldsymbol{E}_{\mathrm{s}}(\boldsymbol{r}) &= \sum_{l=1}^{\mathcal{N}} \boldsymbol{E}_{\mathrm{s},l}\left(\boldsymbol{r}_l\right) \\ &= \sum_{l=1}^{\mathcal{N}} \sum_{\mu} f_{l,\mu} \boldsymbol{M}_{\mu}^{3}\left(k_{\mathrm{s}} \boldsymbol{r}_l\right) + g_{l,\mu} \boldsymbol{N}_{\mu}^{3}\left(k_{\mathrm{s}} \boldsymbol{r}_l\right) . \end{aligned} \tag{2.171}$$

Taking into account that the particle coordinate systems have the same spatial orientation (no rotations are involved), we rewrite the expression of the scattered field coefficients $\boldsymbol{s}_l$, $\boldsymbol{s}_l = [f_{l,\mu}, g_{l,\mu}]^{\mathrm{T}}$, given by (2.142) as

$$\boldsymbol{s}_l = \boldsymbol{T} \left[\mathrm{e}^{\mathrm{j}k_{\mathrm{s}} z_{0l}} \boldsymbol{e} + \sum_{p \neq l}^{\mathcal{N}} \mathcal{T}^{31}\left(k_{\mathrm{s}} \boldsymbol{r}_{lp}\right) \boldsymbol{s}_p \right] , \tag{2.172}$$

where $\boldsymbol{e}$ is the vector of the incident field coefficients in the global coordinate system and $\boldsymbol{T}$ is the transition matrix of a particle.

Before going any further we make some remarks on statistically averaged wave fields. We define the probability density function of finding the first particle at $\boldsymbol{r}_{01}$, the second particle at $\boldsymbol{r}_{02}$, and so forth by $p(\boldsymbol{r}_{01}, \boldsymbol{r}_{02}, \ldots, \boldsymbol{r}_{0\mathcal{N}})$. The probability density function can be written as [236]

$$\begin{aligned} p\left(\boldsymbol{r}_{01}, \boldsymbol{r}_{02}, \ldots, \boldsymbol{r}_{0\mathcal{N}}\right) &= p\left(\boldsymbol{r}_{0l}\right) p\left(\boldsymbol{r}_{01}, \boldsymbol{r}_{02}, \ldots, {}', \ldots, \boldsymbol{r}_{0\mathcal{N}} \mid \boldsymbol{r}_{0l}\right) \\ &= p\left(\boldsymbol{r}_{0l}, \boldsymbol{r}_{0p}\right) p\left(\boldsymbol{r}_{01}, \boldsymbol{r}_{02}, \ldots, {}', \ldots, {}', \ldots, \boldsymbol{r}_{0\mathcal{N}} \mid \boldsymbol{r}_{0l}, \boldsymbol{r}_{0p}\right) , \end{aligned}$$

where $p(\boldsymbol{r}_{0l})$ is the probability density of finding the particle l at $\boldsymbol{r}_{0l}$, $p(\boldsymbol{r}_{0l}, \boldsymbol{r}_{0p})$ is the joint density function of the particles l and p and the $'$ superscript indicates that the term is absent. From Bayes' rule we have

$$p\left(\boldsymbol{r}_{0l}, \boldsymbol{r}_{0p}\right) = p\left(\boldsymbol{r}_{0l}\right) p\left(\boldsymbol{r}_{0p} \mid \boldsymbol{r}_{0l}\right) ,$$

where $p(\boldsymbol{r}_{0p} \mid \boldsymbol{r}_{0l})$ is the conditional probability of finding the particle p at $\boldsymbol{r}_{0p}$ if the particle l is known to be at $\boldsymbol{r}_{0l}$. The conditional densities with one and two particles held fixed are related by the relation

$$\begin{aligned} p\left(\boldsymbol{r}_{01}, \boldsymbol{r}_{02}, \ldots, {}', \ldots, \boldsymbol{r}_{0\mathcal{N}} \mid \boldsymbol{r}_{0l}\right) &= p\left(\boldsymbol{r}_{0p} \mid \boldsymbol{r}_{0l}\right) \\ &\quad \times p\left(\boldsymbol{r}_{01}, \boldsymbol{r}_{02}, \ldots, {}', \ldots, {}', \ldots, \boldsymbol{r}_{0\mathcal{N}} \mid \boldsymbol{r}_{0l}, \boldsymbol{r}_{0p}\right) . \end{aligned}$$

The configurational average of a statistical quantity f is defined as

$$\begin{aligned} \mathcal{E}\{f\} = \int_D \cdots \int_D & f p\left(\boldsymbol{r}_{01}, \boldsymbol{r}_{02}, \ldots, \boldsymbol{r}_{0\mathcal{N}}\right) \\ & \times \mathrm{d}V\left(\boldsymbol{r}_{01}\right) \mathrm{d}V\left(\boldsymbol{r}_{02}\right), \ldots, \mathrm{d}V\left(\boldsymbol{r}_{0\mathcal{N}}\right) , \end{aligned}$$

while the conditional averages with one and two particles held fixed are

$$\begin{aligned} \mathcal{E}_l\{f\} = \int_D \cdots \int_D & f p\left(\boldsymbol{r}_{01}, \boldsymbol{r}_{02}, \ldots, {}', \ldots, \boldsymbol{r}_{0\mathcal{N}} \mid \boldsymbol{r}_{0l}\right) \\ & \times \mathrm{d}V\left(\boldsymbol{r}_{01}\right) \mathrm{d}V\left(\boldsymbol{r}_{02}\right), \ldots, {}', \ldots, \mathrm{d}V\left(\boldsymbol{r}_{0\mathcal{N}}\right) \end{aligned}$$

and

$$\begin{aligned} \mathcal{E}_{lp}\{f\} = \int_D \cdots \int_D & f p\left(\boldsymbol{r}_{01}, \boldsymbol{r}_{02}, \ldots, {}', \ldots, {}', \ldots, \boldsymbol{r}_{0\mathcal{N}} \mid \boldsymbol{r}_{0l}, \boldsymbol{r}_{0p}\right) \\ & \times \mathrm{d}V\left(\boldsymbol{r}_{01}\right) \mathrm{d}V\left(\boldsymbol{r}_{02}\right), \ldots, {}', \ldots, {}', \ldots, \mathrm{d}V\left(\boldsymbol{r}_{0\mathcal{N}}\right) , \end{aligned}$$

respectively.

Averaging (2.172) over the positions of all particles excepting the lth, we obtain the conditional configurational average of the scattered field coefficients

$$\mathcal{E}_l\left\{\boldsymbol{s}_l\right\} = \boldsymbol{T}\left[\mathrm{e}^{\mathrm{j}k_{\mathrm{s}}z_{0l}}\boldsymbol{e} + \sum_{p\neq l}^{\mathcal{N}} \frac{1}{V} \int_{D_p} \mathcal{T}^{31}\left(k_{\mathrm{s}}\boldsymbol{r}_{lp}\right) \mathcal{E}_{lp}\left\{\boldsymbol{s}_p\right\} g\left(\boldsymbol{r}_{lp}\right) \mathrm{d}V\left(\boldsymbol{r}_{0p}\right)\right] , \tag{2.173}$$

where g is the pair distribution function of a statistically homogeneous medium,

$$p\left(\boldsymbol{r}_{0p} \mid \boldsymbol{r}_{0l}\right) = \frac{1}{V} g\left(\boldsymbol{r}_{0p} - \boldsymbol{r}_{0l}\right) = \frac{1}{V} g\left(\boldsymbol{r}_{lp}\right)$$

and V is the volume accessible to the particles. In our analysis we assume that both $\mathcal{N}$ and V are very large, but the number of particles per unit volume n_0,

$$n_0 = \mathcal{N}/V,$$

is finite. The integration domain D_p is the half-space $z_{0p} \geq 0$, excluding a spherical volume of radius $2R$ centered at $\boldsymbol{r}_{0l}$, i.e., $|\boldsymbol{r}_{0p} - \boldsymbol{r}_{0l}| \geq 2R$. The above equation indicates that the conditional average with one particle fixed $\mathcal{E}_l\{\boldsymbol{s}_l\}$ is given in terms of the conditional average with two particles fixed $\mathcal{E}_{lp}\{\boldsymbol{s}_p\}$. In order to close the system we use the quasi-crystalline approximation

$$\mathcal{E}_{lp}\left\{\boldsymbol{s}_p\right\} = \mathcal{E}_p\left\{\boldsymbol{s}_p\right\} \quad \text{for} \quad l \neq p\,, \tag{2.174}$$

which implies that there is no correlation between the lth and pth particles other than there should be no interpenetration of any two particles.

To solve (2.173) we seek the plane wave solution

$$\mathcal{E}_l\left\{\boldsymbol{s}_l\right\} = \boldsymbol{s}\mathrm{e}^{\mathrm{j}K_{\mathrm{s}} z_{0l}}\,, \tag{2.175}$$

where $\boldsymbol{s}$ is the unknown vector of the scattered field coefficients and the effective wave vector $\boldsymbol{K}_{\mathrm{e}}$ is assumed to be parallel to the wave vector of the incident field, i.e., $\boldsymbol{K}_{\mathrm{e}} = K_{\mathrm{s}}\boldsymbol{e}_z$. Substituting (2.174) and (2.175) into (2.173), and taking into account that for identical particles the sum $\sum_{p\neq l}^{\mathcal{N}}$ can be replaced by $\mathcal{N}-1$ and for a sufficiently large $\mathcal{N}$, $n_0 \approx (\mathcal{N}-1)/V$, we obtain

$$\boldsymbol{s}\mathrm{e}^{\mathrm{j}K_{\mathrm{s}} z_{0l}} = \boldsymbol{T}\left[\mathrm{e}^{\mathrm{j}k_{\mathrm{s}} z_{0l}}\boldsymbol{e} + n_0 \int_{D_p} \mathcal{T}^{31}\left(k_{\mathrm{s}}\boldsymbol{r}_{lp}\right) g\left(\boldsymbol{r}_{lp}\right) \boldsymbol{s}\mathrm{e}^{\mathrm{j}K_{\mathrm{s}} z_{0p}} \mathrm{d}V\left(\boldsymbol{r}_{0p}\right)\right]. \tag{2.176}$$

The integral in (2.176) can be written as (excepting the unknown vector $\boldsymbol{s}$)

$$\mathcal{J}_l = \mathcal{J}_{1,l} + \mathcal{J}_{2,l}$$

where

$$\mathcal{J}_{1,l} = \int_{D_p} \mathcal{T}^{31}\left(k_{\mathrm{s}}\boldsymbol{r}_{lp}\right) \mathrm{e}^{\mathrm{j}K_{\mathrm{s}} z_{0p}} \mathrm{d}V\left(\boldsymbol{r}_{0p}\right)\,,$$

$$\mathcal{J}_{2,l} = \int_{D_p} \mathcal{T}^{31}\left(k_{\mathrm{s}}\boldsymbol{r}_{lp}\right) \left[g\left(\boldsymbol{r}_{lp}\right) - 1\right] \mathrm{e}^{\mathrm{j}K_{\mathrm{s}} z_{0p}} \mathrm{d}V\left(\boldsymbol{r}_{0p}\right)\,,$$

and the rest of our analysis concerns with the computation of the matrix terms $\mathcal{J}_{1,l}$ and $\mathcal{J}_{2,l}$.

In view of (2.144), $\mathcal{J}_{1,l}$ can be expressed as

$$\mathcal{J}_{1,l} = \int_{D_p} \begin{bmatrix} A^3_{-mn,-m'n'}\left(k_{\rm s}\boldsymbol{r}_{lp}\right) B^3_{-mn,-m'n'}\left(k_{\rm s}\boldsymbol{r}_{lp}\right) \\ B^3_{-mn,-m'n'}\left(k_{\rm s}\boldsymbol{r}_{lp}\right) A^3_{-mn,-m'n'}\left(k_{\rm s}\boldsymbol{r}_{lp}\right) \end{bmatrix} {\rm e}^{{\rm j}K_{\rm s}z_{0p}} {\rm d}V\left(\boldsymbol{r}_{0p}\right) ,$$

whence, taking into account the series representations for the translation coefficients (cf. (B.72) and (B.73))

$$A^3_{-mn,-m'n'}(k_{\rm s}\boldsymbol{r}_{lp}) = \frac{2{\rm j}^{n'-n}}{\sqrt{nn'(n+1)\left(n'+1\right)}} \times \sum_{n''} {\rm j}^{n''} a_1\left(-m,-m' \mid n'',n,n'\right) u^3_{m'-mn''}\left(k_{\rm s}\boldsymbol{r}_{lp}\right) ,$$

$$B^3_{-mn,-m'n'}(k_{\rm s}\boldsymbol{r}_{lp}) = \frac{2{\rm j}^{n'-n}}{\sqrt{nn'(n+1)\left(n'+1\right)}} \times \sum_{n''} {\rm j}^{n''} b_1\left(-m,-m' \mid n'',n,n'\right) u^3_{m'-mn''}\left(k_{\rm s}\boldsymbol{r}_{lp}\right)$$

with (cf. (B.68) and (B.69))

$$a_1\left(-m,-m' \mid n'',n,n'\right) = \int_0^\pi \left[mm'\pi_n^{|m|}\left(\beta\right)\pi_{n'}^{|m'|}\left(\beta\right) + \tau_n^{|m|}\left(\beta\right)\tau_{n'}^{|m'|}\left(\beta\right)\right] \times P_{n''}^{|m'-m|}\left(\cos\beta\right)\sin\beta{\rm d}\beta ,$$

$$b_1\left(-m,-m' \mid n'',n,n'\right) = -\int_0^\pi \left[m\pi_n^{|m|}\left(\beta\right)\tau_{n'}^{|m'|}\left(\beta\right) + m'\tau_n^{|m|}\left(\beta\right)\pi_{n'}^{|m'|}\left(\beta\right)\right] \times P_{n''}^{|m'-m|}\left(\cos\beta\right)\sin\beta{\rm d}\beta ,$$

we see that the calculation of $\mathcal{J}_{1,l}$ requires the computation of the integral

$$\mathcal{I}^1_{mm'n''} = \int_{D_p} {\rm e}^{{\rm j}K_{\rm s}z_{0p}} u^3_{m'-mn''}\left(k_{\rm s}\boldsymbol{r}_{lp}\right) {\rm d}V\left(\boldsymbol{r}_{0p}\right) .$$

The procedure to calculate the integral $\mathcal{I}^1_{mm'n''}$ is described in Appendix C and we have (cf. (C.2)),

$$\mathcal{I}^1_{mm'n''} = \frac{16\pi R^3}{\left(k_{\rm s}R\right)^2 - \left(K_{\rm s}R\right)^2} {\rm j}^{n''} \sqrt{\frac{2n''+1}{2}} {\rm e}^{{\rm j}K_{\rm s}z_{0l}} \delta_{mm'} F_{n''}\left(K_{\rm s},k_{\rm s},R\right) + \frac{2\pi}{k_{\rm s}^2\left(K_{\rm s}-k_{\rm s}\right)} {\rm j}^{n''+1} \sqrt{\frac{2n''+1}{2}} {\rm e}^{{\rm j}k_{\rm s}z_{0l}} \delta_{mm'}$$

with

$$F_{n''}\left(K_{\mathrm{s}},k_{\mathrm{s}},R\right)=\left(k_{\mathrm{s}}R\right)\left(h_{n''}^{(1)}\left(2k_{\mathrm{s}}R\right)\right)'j_{n''}\left(2K_{\mathrm{s}}R\right)$$
$$-\left(K_{\mathrm{s}}R\right)h_{n''}^{(1)}\left(2k_{\mathrm{s}}R\right)\left(j_{n''}\left(2K_{\mathrm{s}}R\right)\right)'.$$

Relying on this result we find that the matrix $\mathcal{J}_{1,l}$ can be decomposed into the following manner:

$$\mathcal{J}_{1,l}=\mathcal{J}_{1,R}\mathrm{e}^{\mathrm{j}K_{\mathrm{s}}z_{0l}}+\mathcal{J}_{1,z}\mathrm{e}^{\mathrm{j}k_{\mathrm{s}}z_{0l}}. \tag{2.177}$$

The elements of the matrix $\mathcal{J}_{1,R}$,

$$\mathcal{J}_{1,R}=\begin{bmatrix}\left(\mathcal{J}_{1,R}\right)_{-mn,-m'n'}^{11} & \left(\mathcal{J}_{1,R}\right)_{-mn,-m'n'}^{12}\\ \left(\mathcal{J}_{1,R}\right)_{-mn,-m'n'}^{21} & \left(\mathcal{J}_{1,R}\right)_{-mn,-m'n'}^{22}\end{bmatrix},$$

are given by

$$\left(\mathcal{J}_{1,R}\right)_{-mn,-m'n'}^{11}=\left(\mathcal{J}_{1,R}\right)_{-mn,-m'n'}^{22}$$
$$=\frac{32\pi R^3}{\left(k_{\mathrm{s}}R\right)^2-\left(K_{\mathrm{s}}R\right)^2}\frac{\mathrm{j}^{n'-n}}{\sqrt{nn'(n+1)\left(n'+1\right)}}\mathcal{R}_{mnn'}^{11}\delta_{mm'},$$

$$\left(\mathcal{J}_{1,R}\right)_{-mn,-m'n'}^{12}=\left(\mathcal{J}_{1,R}\right)_{-mn,-m'n'}^{21}$$
$$=-\frac{32\pi R^3}{\left(k_{\mathrm{s}}R\right)^2-\left(K_{\mathrm{s}}R\right)^2}\frac{\mathrm{j}^{n'-n}}{\sqrt{nn'(n+1)\left(n'+1\right)}}\mathcal{R}_{mnn'}^{12}\delta_{mm'},$$

where $\mathcal{R}_{mnn'}^{11}$ and $\mathcal{R}_{mnn'}^{12}$ are defined as

$$\mathcal{R}_{mnn'}^{11,12}=\sum_{n''=0}^{\infty}\left(-1\right)^{n''}\sqrt{\frac{2n''+1}{2}}F_{n''}\left(K_{\mathrm{s}},k_{\mathrm{s}},R\right)I_{mnn'n''}^{1,2},$$

and

$$I_{mnn'n''}^{1}=\int_0^{\pi}\left[m^2\pi_n^{|m|}\left(\beta\right)\pi_{n'}^{|m|}\left(\beta\right)+\tau_n^{|m|}\left(\beta\right)\tau_{n'}^{|m|}\left(\beta\right)\right]P_{n''}\left(\cos\beta\right)\sin\beta\mathrm{d}\beta,$$
$$I_{mnn'n''}^{2}=m\int_0^{\pi}\left[\pi_n^{|m|}\left(\beta\right)\tau_{n'}^{|m|}\left(\beta\right)+\tau_n^{|m|}\left(\beta\right)\pi_{n'}^{|m|}\left(\beta\right)\right]P_{n''}\left(\cos\beta\right)\sin\beta\mathrm{d}\beta. \tag{2.178}$$

The matrix $\mathcal{J}_{1,z}$ is of the form:

$$\mathcal{J}_{1,z}=\begin{bmatrix}\left(\mathcal{J}_{1,z}\right)_{-mn,-m'n'}^{11} & \left(\mathcal{J}_{1,z}\right)_{-mn,-m'n'}^{12}\\ \left(\mathcal{J}_{1,z}\right)_{-mn,-m'n'}^{21} & \left(\mathcal{J}_{1,z}\right)_{-mn,-m'n'}^{22}\end{bmatrix},$$

and the matrix elements are given by

$$(\mathcal{J}_{1,z})^{11}_{-mn,-m'n'} = (\mathcal{J}_{1,z})^{22}_{-mn,-m'n'} = \frac{4\pi}{k_{\rm s}^2\left(K_{\rm s}-k_{\rm s}\right)}\frac{{\rm j}^{n'-n+1}}{\sqrt{nn'(n+1)\left(n'+1\right)}}\mathcal{S}^1_{mnn'}\delta_{mm'}\,,$$

$$(\mathcal{J}_{1,z})^{12}_{-mn,-m'n'} = (\mathcal{J}_{1,z})^{21}_{-mn,-m'n'} = -\frac{4\pi}{k_{\rm s}^2\left(K_{\rm s}-k_{\rm s}\right)}\frac{{\rm j}^{n'-n+1}}{\sqrt{nn'(n+1)\left(n'+1\right)}}\mathcal{S}^2_{mnn'}\delta_{mm'}\,,$$

where the expressions of $\mathcal{S}^1_{mnn'}$ and $\mathcal{S}^2_{mnn'}$ are similar to those of $\mathcal{R}^{11}_{mnn'}$ and $\mathcal{R}^{12}_{mnn'}$ excepting the factor $F_{n''}$,

$$\mathcal{S}^{1,2}_{mnn'} = \sum_{n''=0}^{\infty}(-1)^{n''}\sqrt{\frac{2n''+1}{2}}I^{1,2}_{mnn'n''}\,.$$

For $m=1$ we have

$$\mathcal{S}^1_{1nn'} = \mathcal{S}^1_{-1nn'} = s_{nn'}\,, \tag{2.179}$$

$$\mathcal{S}^2_{1nn'} = -\mathcal{S}^2_{-1nn'} = -s_{nn'}\,, \tag{2.180}$$

where the coefficient $s_{nn'}$ is given by (cf. (C.6))

$$s_{nn'} = \frac{(-1)^{n+n'}}{4}\sqrt{n(n+1)\left(2n+1\right)}\sqrt{n'(n'+1)\left(2n'+1\right)}\,. \tag{2.181}$$

To derive the expression of $\mathcal{J}_{2,l}$, we need to compute the integral

$$\mathcal{I}^2_{mm'n''} = \int_{D_p}\left[g\left(\boldsymbol{r}_{lp}\right)-1\right]{\rm e}^{{\rm j}K_{\rm s}z_{0p}}u^3_{m'-mn''}\left(k_{\rm s}\boldsymbol{r}_{lp}\right){\rm d}V\left(\boldsymbol{r}_{0p}\right)$$

and the result is (cf. (C.3))

$$\mathcal{I}^2_{mm'n''} = 32\pi R^3 j^{n''}\sqrt{\frac{2n''+1}{2}}{\rm e}^{{\rm j}K_{\rm s}z_{0l}}\delta_{mm'}G_{n''}\left(K_s,k_s,R\right)\,,$$

where

$$G_{n''}\left(K_{\rm s},k_{\rm s},R\right) = \int_1^{\infty}\left[g\left(2Rx\right)-1\right]h^{(1)}_{n''}\left(2k_{\rm s}Rx\right)j_{n''}\left(2K_{\rm s}Rx\right)x^2{\rm d}x\,.$$

The matrix term $\mathcal{J}_{2,l}$ then becomes

$$\mathcal{J}_{2,l} = \mathcal{J}_{2,R}{\rm e}^{{\rm j}K_{\rm s}z_{0l}} \tag{2.182}$$

and the elements of the matrix $\mathcal{J}_{2,R}$,

$$\mathcal{J}_{2,R} = \begin{bmatrix} (\mathcal{J}_{2,R})^{11}_{-mn,-m'n'} & (\mathcal{J}_{2,R})^{12}_{-mn,-m'n'} \\ (\mathcal{J}_{2,R})^{21}_{-mn,-m'n'} & (\mathcal{J}_{2,R})^{22}_{-mn,-m'n'} \end{bmatrix}$$

are given by

$$\begin{aligned}(\mathcal{J}_{2,R})^{11}_{-mn,-m'n'} &= (\mathcal{J}_{2,R})^{22}_{-mn,-m'n'} \\ &= 64\pi R^3 \frac{\mathrm{j}^{n'-n}}{\sqrt{nn'(n+1)\,(n'+1)}} \mathcal{R}^{21}_{mnn'} \delta_{mm'}\,,\end{aligned}$$

$$\begin{aligned}(\mathcal{J}_{2,R})^{12}_{-mn,-m'n'} &= (\mathcal{J}_{2,R})^{21}_{-mn,-m'n'} \\ &= -64\pi R^3 \frac{\mathrm{j}^{n'-n}}{\sqrt{nn'(n+1)\,(n'+1)}} \mathcal{R}^{22}_{mnn'} \delta_{mm'}\,,\end{aligned}$$

where $\mathcal{R}^{21}_{mnn'}$ and $\mathcal{R}^{22}_{mnn'}$ are defined as

$$\mathcal{R}^{21,22}_{mnn'} = \sum_{n''=0}^{\infty} (-1)^{n''} \sqrt{\frac{2n''+1}{2}} G_{n''}\,(K_\mathrm{s}, k_\mathrm{s}, R)\, I^{1,2}_{mnn'n''}\,.$$

Taking into account the expressions of the integral terms $I^{1,2}_{mnn'n''}$ (cf. (2.178)) it is apparent that

$$\mathcal{R}^{11}_{mnn'} = \mathcal{R}^{11}_{-mnn'}\,, \quad \mathcal{R}^{12}_{mnn'} = -\mathcal{R}^{12}_{-mnn'} \tag{2.183}$$

and

$$\mathcal{R}^{21}_{mnn'} = \mathcal{R}^{21}_{-mnn'}\,, \quad \mathcal{R}^{22}_{mnn'} = -\mathcal{R}^{22}_{-mnn'}\,. \tag{2.184}$$

Substituting (2.177) and (2.182) into (2.176) gives two types of terms. One type of terms has a $\exp(\mathrm{j}k_\mathrm{s}z_{0l})$ dependence and corresponds to waves traveling with the wave number of the incident wave, while the other type of terms has a $\exp(\mathrm{j}K_\mathrm{s}z_{0l})$ dependence and corresponds to waves traveling with the wave number of the effective medium. The terms with wave number k_s should balance each other giving the generalized Ewald–Oseen extinction theorem,

$$n_0 \mathcal{J}_{1,z} \boldsymbol{s} + \boldsymbol{e} = 0\,, \tag{2.185}$$

while balancing the terms with wave number K_s gives the generalized Lorentz–Lorenz law

$$[\boldsymbol{I} - n_0 \boldsymbol{T}\,(\mathcal{J}_{1,R} + \mathcal{J}_{2,R})]\,\boldsymbol{s} = 0\,. \tag{2.186}$$

For an ensemble of particles with different orientations we proceed analogously. If the configurational distribution and the orientation distribution are assumed to be statistically independent, the total probability density

function can be expressed as a product of two functions, one of which $p(\boldsymbol{r}_{01}, \boldsymbol{r}_{02}, \ldots, \boldsymbol{r}_{0\mathcal{N}})$ describes the configurational distribution and the other of which $p(\Omega_1, \Omega_2, \ldots, \Omega_{\mathcal{N}})$ describes the distribution of particles orientations, i.e.,

$$\begin{aligned} &p\left(\boldsymbol{r}_{01}, \boldsymbol{r}_{02}, \ldots, \boldsymbol{r}_{0\mathcal{N}}; \Omega_1, \Omega_2, \ldots, \Omega_{\mathcal{N}}\right) \\ &\quad = p\left(\boldsymbol{r}_{01}, \boldsymbol{r}_{02}, \ldots, \boldsymbol{r}_{0\mathcal{N}}\right) p\left(\Omega_1, \Omega_2, \ldots, \Omega_{\mathcal{N}}\right) , \end{aligned}$$

where Ω_l is the set of Euler angles specifying the orientation of the lth particle and $\Omega_l = (\alpha_l, \beta_l, \gamma_l)$. Each of these probability density functions is normalized to unity and the problem of computing the configurational and orientation averages are separated. Assuming that the particle orientations are statistically independent

$$p\left(\Omega_1, \Omega_2, \ldots, \Omega_{\mathcal{N}}\right) = p\left(\Omega_1\right) p\left(\Omega_2\right) ... p\left(\Omega_{\mathcal{N}}\right) ,$$

and that the individual orientation distribution is uniform

$$p\left(\Omega_l\right) = \frac{1}{8\pi^2}, l = 1, 2, \ldots, \mathcal{N} ,$$

we average (2.172) over all configurations for which the lth particle is held fixed and over all orientations. We obtain

$$\left\langle \mathcal{E}_l\left\{\boldsymbol{s}_l\right\}\right\rangle = \mathrm{e}^{\mathrm{j}k_{\mathrm{s}} z_{0l}} \left\langle \widetilde{\boldsymbol{T}} \right\rangle \boldsymbol{e} + \sum_{p \neq l}^{\mathcal{N}} \frac{1}{V} \int_{D_p} \left\langle \widetilde{\boldsymbol{T}} \mathcal{T}^{31}\left(k_{\mathrm{s}} \boldsymbol{r}_{lp}\right) \mathcal{E}_p\left(\boldsymbol{s}_p\right) \right\rangle g\left(\boldsymbol{r}_{lp}\right) \mathrm{d}V\left(\boldsymbol{r}_{0p}\right) ,$$

where $\langle . \rangle$ denotes the orientation average

$$\begin{aligned} \left\langle \mathcal{E}_l\left\{\boldsymbol{s}_l\right\}\right\rangle = \frac{1}{\left(8\pi^2\right)^{\mathcal{N}}} \int_{\Omega} \cdots \int_{\Omega} \Bigg[\int_{D} \cdots \int_{D} \boldsymbol{s}_l p\left(\boldsymbol{r}_{01}, \boldsymbol{r}_{02}, \ldots, ', \ldots, \boldsymbol{r}_{0\mathcal{N}} \mid \boldsymbol{r}_{0l}\right) \\ \times \mathrm{d}V\left(\boldsymbol{r}_{01}\right) \mathrm{d}V\left(\boldsymbol{r}_{02}\right), \ldots, ', \ldots, \mathrm{d}V\left(\boldsymbol{r}_{0\mathcal{N}}\right) \Bigg] \mathrm{d}\Omega_1 \mathrm{d}\Omega_2, \ldots, \mathrm{d}\Omega_{\mathcal{N}} , \end{aligned}$$

$\boldsymbol{s}_l = \boldsymbol{s}_l(\Omega_1, \Omega_2, \ldots, \Omega_{\mathcal{N}})$, Ω is the unit sphere, $\mathrm{d}\Omega_l = \sin\beta_l \mathrm{d}\beta_l \mathrm{d}\alpha_l \mathrm{d}\gamma_l$ and

$$\left\langle \widetilde{\boldsymbol{T}} \right\rangle = \frac{1}{8\pi^2} \int_{\Omega} \widetilde{\boldsymbol{T}}\left(\alpha_l, \beta_l, \gamma_l\right) \mathrm{d}\Omega_l$$

is the orientation-averaged transition matrix. Making the assumption

$$\left\langle \widetilde{\boldsymbol{T}} \mathcal{T}^{31}\left(k_{\mathrm{s}} \boldsymbol{r}_{lp}\right) \mathcal{E}_p\left(\boldsymbol{s}_p\right) \right\rangle = \left\langle \widetilde{\boldsymbol{T}} \right\rangle \mathcal{T}^{31}\left(k_{\mathrm{s}} \boldsymbol{r}_{lp}\right) \left\langle \mathcal{E}_p\left(\boldsymbol{s}_p\right) \right\rangle ,$$

which implies that $\mathcal{E}_p\{\boldsymbol{s}_p\}$ depends only on Ω_p [227], we obtain the generalized Lorentz–Lorenz law in terms of the orientation-averaged transition matrix $\langle \widetilde{\boldsymbol{T}} \rangle$ instead of the transition matrix $\boldsymbol{T}$ of a particle in a fixed orientation. We note that the submatrices of the orientation-averaged transition matrix are diagonal and their elements do not depend on the azimuthal indices (see Sect. 1.5).

2.9.2 Generalized Lorentz–Lorenz Law

The generalized Lorentz–Lorenz law is a system of homogeneous equations for the unknown vector $\boldsymbol{s}$. For a nontrivial solution, the determinant must vanish giving an equation for the effective wave number K_s. For spherical particles or axisymmetric particles with the axis of symmetry directed along the z-axis, the transition matrix is diagonal with respect to the azimuthal indices m and m'. Because the nonvanishing incident field coefficients corresponds to $m = -1$ and $m = 1$, the above matrix equations involve only these azimuthal modes. Taking into account the symmetry relations (2.25), (2.183) and (2.184), we obtain the following equation for the effective wave number K_s

$$\det\left\{\boldsymbol{I}-\begin{bmatrix} T^{11}_{1n'',1n} & 0 & T^{12}_{1n'',1n} & 0 \\ 0 & T^{11}_{1n'',1n} & 0 & -T^{12}_{1n'',1n} \\ T^{21}_{1n'',1n} & 0 & T^{22}_{1n'',1n} & 0 \\ 0 & -T^{21}_{1n'',1n} & 0 & T^{22}_{1n'',1n} \end{bmatrix} \times \begin{bmatrix} A_{nn'} & 0 & B_{nn'} & 0 \\ 0 & A_{nn'} & 0 & -B_{nn'} \\ B_{nn'} & 0 & A_{nn'} & 0 \\ 0 & -B_{nn'} & 0 & A_{nn'} \end{bmatrix}\right\} = 0\,,$$

where

$$\begin{aligned} A_{nn'} &= n_0\left[(\mathcal{J}_{1,R})^{11}_{-1n,-1n'} + (\mathcal{J}_{2,R})^{11}_{-1n,-1n'}\right]\,, \\ B_{nn'} &= n_0\left[(\mathcal{J}_{1,R})^{12}_{-1n,-1n'} + (\mathcal{J}_{2,R})^{12}_{-1n,-1n'}\right]\,. \end{aligned} \tag{2.187}$$

The dimension of the problem can be reduced by using the properties of determinants and the final result is

$$\det\left\{\boldsymbol{I}-\begin{bmatrix} T^{11}_{1n'',1n} & T^{12}_{1n'',1n} \\ T^{21}_{1n'',1n} & T^{22}_{1n'',1n} \end{bmatrix}\begin{bmatrix} A_{nn'} & B_{nn'} \\ B_{nn'} & A_{nn'} \end{bmatrix}\right\} = 0\,. \tag{2.188}$$

In the low frequency limit, the size of the particle is considered to be very small compared to the incident wavelength. It is then sufficient to take only the lowest-order coefficients in the fields expansions, and in this limit, the elements of the $\boldsymbol{T}$ matrix can be obtained in closed form for simple shapes. For spherical particles, we have

$$\begin{aligned} T^{11}_{11,11} = T^1_1 &= \frac{\mathrm{j}}{45}\left(\varepsilon_\mathrm{r}-1\right)x^5 + \mathrm{O}\left(x^7\right)\,, \\ T^{22}_{11,11} = T^2_1 &= \frac{2\mathrm{j}}{3}\frac{\varepsilon_\mathrm{r}-1}{\varepsilon_\mathrm{r}+2}x^3 + \frac{2\mathrm{j}}{5}\frac{\left(\varepsilon_\mathrm{r}-1\right)\left(\varepsilon_\mathrm{r}-2\right)}{\left(\varepsilon_\mathrm{r}+2\right)^2}x^5 + \mathrm{O}\left(x^6\right)\,, \end{aligned}$$

where $x = k_s R$ is the size parameter. In (2.187) we proceed analogously and considering the leading terms in the expansions of the spherical Bessel and Hankel functions, we obtain

$$A_{11} = a_0 + \frac{1}{2} a_2 \,,$$
$$B_{11} = \frac{3}{2} a_1,$$

where

$$a_0 = \frac{3\mathrm{j}c}{(k_\mathrm{s}R)\left[(k_\mathrm{s}R)^2 - (K_\mathrm{s}R)^2\right]} + \frac{(1-c)^4}{(1+2c)^2} \,,$$
$$a_1 = \frac{3\mathrm{j}c\,(K_\mathrm{s}R)}{(k_\mathrm{s}R)^2\left[(k_\mathrm{s}R)^2 - (K_\mathrm{s}R)^2\right]} \,,$$
$$a_2 = \frac{3\mathrm{j}c\,(K_\mathrm{s}R)^2}{(k_\mathrm{s}R)^3\left[(k_\mathrm{s}R)^2 - (K_\mathrm{s}R)^2\right]} \,.$$

As a result, the long-wavelength equation for the effective wave number takes the form

$$\left(1 - T^{11}_{11,11} A_{11}\right)\left(1 - T^{22}_{11,11} A_{11}\right) - T^{11}_{11,11} T^{22}_{11,11} B^2_{11} = 0 \,.$$

Further, neglecting $T^{11}_{11,11}$, yields

$$1 - T^{22}_{11,11} A_{11} = 0 \,,$$

and consequently,

$$\left(\frac{K_\mathrm{s}}{k_\mathrm{s}}\right)^2 = \frac{2\chi + 6\mathrm{j}c}{2\chi - 3\mathrm{j}c} \tag{2.189}$$

with

$$\chi = (k_\mathrm{s}R)^3 \left[\frac{(1-c)^4}{(1+2c)^2} - \frac{1}{T^{22}_{11,11}}\right] \,.$$

For an ensemble of spheres of radius R and small fractional concentrations c,

$$\chi \approx \mathrm{j}\frac{3}{2}\frac{\varepsilon_\mathrm{r} + 2}{\varepsilon_\mathrm{r} - 1} \,,$$

and we obtain the dispersion relation of the Maxwell–Garnett form (2.170). At higher frequencies, the root of the equation (2.188) is searched in the complex plane using Müller's method. The initial guess is provided by (2.189) at low values of $k_\mathrm{s}R$ and these are used systematically to obtain convergence of roots at increasingly higher values of $k_\mathrm{s}R$.

2.9.3 Generalized Ewald–Oseen Extinction Theorem

After computing the singular solution K_{s}, the elements of the $\boldsymbol{s}$ vector can be expressed in terms of an arbitrary constant, and this constant will be determined from the Ewald-Oseen extinction theorem. Certainly, this strategy tacitly assumes that the system of equations (2.185) reduces to a single scalar equation and to prove this assertion we introduce the notations

$$\boldsymbol{s} = \begin{bmatrix} f_{1n'} \\ f_{-1n'} \\ g_{1n'} \\ g_{-1n'} \end{bmatrix}, \quad \boldsymbol{e} = \begin{bmatrix} a_{1n} \\ a_{-1n} \\ b_{1n} \\ b_{-1n} \end{bmatrix},$$

and (cf. (2.179) and (2.180))

$$\mathcal{J}_{1,z} = \begin{bmatrix} t_{nn'} & 0 & t_{nn'} & 0 \\ 0 & t_{nn'} & 0 & -t_{nn'} \\ t_{nn'} & 0 & t_{nn'} & 0 \\ 0 & -t_{nn'} & 0 & t_{nn'} \end{bmatrix},$$

where

$$t_{nn'} = \frac{4\pi}{k_{\mathrm{s}}^2 \left(K_{\mathrm{s}} - k_{\mathrm{s}}\right)} \frac{\mathrm{j}^{n'-n+1}}{\sqrt{nn'(n+1)\left(n'+1\right)}} s_{nn'} .$$

Using the fact that for a vector plane wave polarized along the x-axis, the incident field coefficients are given by

$$a_{1n} = -a_{-1n} = \mathrm{j}^{n-1}\sqrt{2n+1}\,,$$
$$b_{1n} = b_{-1n} = \mathrm{j}^{n-1}\sqrt{2n+1}\,,$$

we see that the matrix equation (2.185) is solved by

$$f_{1n'} = -f_{-1n'}\,,$$
$$g_{1n'} = g_{-1n'}\,,$$

and the coefficients $f_{1n'}$ and $g_{1n'}$ are the solutions of the inhomogeneous system of equations

$$n_0 \sum_{n'=0}^{\infty} t_{nn'} \left(f_{1n'} + g_{1n'}\right) = -\mathrm{j}^{n-1}\sqrt{2n+1}\,, \quad n = 1, 2, \ldots$$

Taking into account the expression of $s_{nn'}$ given by (2.181), we deduce that the above set of inhomogeneous equations reduces to a single scalar equation

$$\frac{\pi n_0}{k_{\mathrm{s}}^2 \left(K_{\mathrm{s}} - k_{\mathrm{s}}\right)} \sum_{n'=0}^{\infty} \left(-\mathrm{j}\right)^{n'} \sqrt{2n'+1} \left(f_{1n'} + g_{1n'}\right) = 1 \tag{2.190}$$

and the assertion is proved. If the incident wave is polarized along the y-axis, we have

$$f_{1n} = f_{-1n}\,,$$
$$g_{1n} = -g_{-1n}\,,$$

while the scalar equation takes the form

$$\frac{\pi \mathrm{j} n_0}{k_\mathrm{s}^2\,(K_\mathrm{s} - k_\mathrm{s})} \sum_{n'=0}^{\infty} (-\mathrm{j})^{n'}\,\sqrt{2n'+1}\,(f_{1n'} + g_{1n'}) = 1\,. \tag{2.191}$$

Thus, the procedure is to first find the singular solution of the Lorentz–Lorenz law together with the dispersion relation for the effective wave number K_s, and then to determine the arbitrary constant from the scalar equations (2.190) or (2.191). After the conditional average of the scattered field coefficients has been evaluated, the coherent reflected field can be computed by taking the configurational average of (2.171), i.e.,

$$\begin{aligned}
\mathcal{E}\left\{\boldsymbol{E}_\mathrm{s}(\boldsymbol{r})\right\} &= \int \ldots \int \boldsymbol{E}_\mathrm{s}(\boldsymbol{r}) p\left(\boldsymbol{r}_{01}, \boldsymbol{r}_{02}, \ldots, \boldsymbol{r}_{0\mathcal{N}}\right) \\
&\quad \times \mathrm{d}V\left(\boldsymbol{r}_{01}\right) \mathrm{d}V\left(\boldsymbol{r}_{02}\right), \ldots, \mathrm{d}V\left(\boldsymbol{r}_{0\mathcal{N}}\right) \\
&= \sum_{l=1}^{\mathcal{N}} \int_{D_l} \mathcal{E}_l\left\{\boldsymbol{E}_{\mathrm{s},l}\left(\boldsymbol{r}_l\right)\right\} p\left(\boldsymbol{r}_{0l}\right) \mathrm{d}V\left(\boldsymbol{r}_{0l}\right) \\
&= n_0 \int_{D_l} \mathcal{E}_l\left\{\boldsymbol{E}_{\mathrm{s},l}\left(\boldsymbol{r}_l\right)\right\} \mathrm{d}V\left(\boldsymbol{r}_{0l}\right)\,,
\end{aligned}$$

where the integration domain D_l is the half-space $z_{0l} \geq 0$ and $p(\boldsymbol{r}_{0l}) = 1/V$. We obtain

$$\mathcal{E}\left\{\boldsymbol{E}_\mathrm{s}(\boldsymbol{r})\right\} = -\frac{\pi n_0}{k_\mathrm{s}^2\,(K_\mathrm{s} + k_\mathrm{s})} \mathrm{e}^{-\mathrm{j}k_\mathrm{s}\boldsymbol{e}_z\cdot\boldsymbol{r}} \sum_{n=1}^{\infty} \mathrm{j}^n \sqrt{2n+1}\,(f_{1n} - g_{1n})\,\boldsymbol{e}_x$$

for an incident vector plane wave polarized along the x-axis, and

$$\mathcal{E}\left\{\boldsymbol{E}_\mathrm{s}(\boldsymbol{r})\right\} = -\frac{\pi \mathrm{j} n_0}{k_\mathrm{s}^2\,(K_\mathrm{s} + k_\mathrm{s})} \mathrm{e}^{-\mathrm{j}k_\mathrm{s}\boldsymbol{e}_z\cdot\boldsymbol{r}} \sum_{n=1}^{\infty} \mathrm{j}^n \sqrt{2n+1}\,(f_{1n} - g_{1n})\,\boldsymbol{e}_y$$

for an incident vector plane wave polarized along the y-axis. The above relations show that the coherent reflected field is in the backward direction and contains no depolarization.

2.9.4 Pair Distribution Functions

We conclude this section with some remarks on pair distribution functions that have been used in multiple scattering problems. For the hole-correction

approximation, the pair distribution function is given by $g(r) = 0$, for $r < 2R$, and $g(r) = 1$, for $r \geq 2R$. The hole-correction approximation assumes that the particles do not interpenetrate each other and considers uniform distribution outside the hole. When the fractional volume of the particles c is appreciable, the hole-correction approximation is not correct and the Percus–Yevick pair function is frequently employed. This pair distribution function is the solution of the Ornstein–Zernike equation for the total and direct correlation functions of two particles $h(\boldsymbol{r})$ and $d(\boldsymbol{r})$, respectively, [228]. In general, the total correlation function

$$h(\boldsymbol{r}) = g(\boldsymbol{r}) - 1\,,$$

can be expressed in terms of its Fourier transform H as

$$h(\boldsymbol{r}) = \frac{1}{(2\pi)^3}\int_{-\infty}^{\infty} H\left(\boldsymbol{p}\right)\mathrm{e}^{\mathrm{j}\boldsymbol{p}\cdot\boldsymbol{r}}\mathrm{d}V\left(\boldsymbol{p}\right)\,.$$

Passing to spherical coordinates, using the spherical wave expansion of the "plane waves" $\exp\left(\mathrm{j}\boldsymbol{p}\cdot\boldsymbol{r}\right)$ and assuming spherical symmetry for H, i.e., $H(\boldsymbol{p}) = H(p)$, we obtain

$$h\left(r\right) = \frac{1}{2\pi^2}\int_0^{\infty} H(p)\frac{\sin\left(pr\right)}{pr}p^2\mathrm{d}p$$

and further

$$h\left(2Rx\right) = \frac{1}{16\pi R^3}\int_0^{\infty} H\left(\frac{u}{2R}\right)\frac{\sin\left(ux\right)}{ux}u^2du\,, \tag{2.192}$$

where

$$x = \frac{r}{2R}\,,\quad u = 2Rp\,.$$

The Ornstein–Zernike equation with Percus–Yevick approximation has a closed-form solution for the case of a hard-sphere potential. In the Fourier transform domain, the solution to the Ornstein–Zernike equation is

$$H(p) = \frac{D(p)}{1 - n_0 D(p)}\,,$$

where the Fourier transform D of the direct correlation function is given by

$$D(p) = \frac{24c}{n_0}\left[\frac{\alpha+\beta+\delta}{u^2}\cos u - \frac{\alpha+2\beta+4\delta}{u^3}\sin u \right.$$
$$\left. - \frac{2\left(\beta+6\delta\right)}{u^4}\cos u + \frac{2\beta}{u^4} + \frac{24\delta}{u^5}\sin u + \frac{24\delta}{u^6}\left(\cos u - 1\right)\right]$$

with

$$\alpha = \frac{(1+2c)^2}{(1-c)^4},\quad \beta = -6c\frac{(1+c/2)^2}{(1-c)^4},\quad \delta = \frac{1}{2}\alpha c\,.$$

Thus, the Fourier transform $H(p)$ can be calculated readily while the total correlation function is obtained from (2.192).

2.10 Particle on or near an Infinite Surface

Computation of light scattering from particles deposited upon a surface is of great interest in the simulation, development and calibration of surface scanners for wafer inspection [214]. More recent applications include laser cleaning [149], scanning near-field optical microscopy (SNOM) [114] and plasmon resonances effects in surface-enhanced Raman spectroscopy (SERS) [30]. Several studies have addressed this scattering problem using different methods. Simplified theoretical models have been developed on the basis of Lorenz-Mie theory and Fresnel surface reflection [15,240–242]. A coupled-dipole algorithm has been employed by Taubenblatt and Tran [221] and Nebeker et al. [178] using a three dimensional array of dipoles to model a feature shape and the Sommerfeld integrals to describe the interaction between a dipole and a surface. The theoretical aspects of the coupled-dipole model has been fully outlined by Schmehl [206]. A model based on the discrete source method has been given by Eremin and Orlov [59,60], whereas the transmission conditions at the interface are satisfied analytically and the fields of discrete sources are derived by using the Green tensor for a plane surface. More details on computational methods and experimental results can be found in a book edited by Moreno and Gonzales [173].

Similar scattering problems have been solved by Kristensson and Ström [125], and Hackmann and Sammelmann [90] in the framework of the null-field method. Acoustic scattering from a buried inhomogeneity has been considered by Kristensson and Ström on the assumption that the free-field $\boldsymbol{T}$-matrix of the particle modifies the free-field $\boldsymbol{T}$-operator of the arbitrary surface. By projecting the free-field $\boldsymbol{T}$-operator of the surface onto a spherical basis, an infinite system of linear equations for the free-field $\boldsymbol{T}$-matrix of the particle has been derived. In contrast, Hackmann and Sammelmann assumed that the free-field $\boldsymbol{T}$-operator of the surface modifies the free-field $\boldsymbol{T}$-matrix of the particle, and in this case, the free-field $\boldsymbol{T}$-matrix of the particle has been projected onto a rectangular basis and an integral equation for the spectral amplitudes of the fields has been obtained.

2.10.1 Particle on or near a Plane Surface

In this section we extend the results of Bobbert and Vlieger [15] to the case of axisymmetric particles situated on or near a plane surface. The scattering problem is a multiple particles problem and the solution method is the separation of variables technique. To model the scattering problem in the framework of the separation of variables technique one must address how the radiation interacts with the particle. The incident field strikes the particle either directly or after interacting with the surface, while the fields emanating from the particle may also reflect off the surface and interact with the particle again. The transition matrix relating the incident and scattered field coefficients is computed in the framework of the null-field method and the reflection matrix

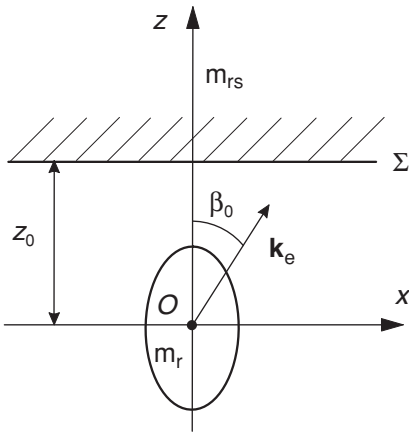

Fig. 2.14. Geometry of an axisymmetric particle situated near a plane surface. The external excitation is a vector plane wave propagating in the ambient medium

characterizing the reflection of the scattered field by the surface is computed by using the integral representation for the vector spherical wave functions.

The geometry of the scattering problem is shown in Fig. 2.14. An axisymmetric particle is situated in the neighborhood of a plane surface Σ, so that its axis of symmetry is normal to the plane surface. The z-axis of the particle coordinate system $Oxyz$ is directed along the axis of symmetry and the origin O is situated at the distance z_0 below the plane surface. The incident radiation is a linearly polarized vector plane wave propagating in the ambient medium (the medium below the surface Σ)

$$\boldsymbol{E}_{\rm e}(\boldsymbol{r}) = (E_{{\rm e}0,\beta}\boldsymbol{e}_\beta + E_{{\rm e}0,\alpha}\boldsymbol{e}_\alpha)\,{\rm e}^{{\rm j}\boldsymbol{k}_{\rm e}\cdot\boldsymbol{r}}\,, \tag{2.193}$$

and the wave vector $\boldsymbol{k}_{\rm e}$, $\boldsymbol{k}_{\rm e} = k_{\rm s}\boldsymbol{e}_k$, is assumed to be in the xz-plane and to enclose the angle β_0 with the z-axis.

The incident wave strikes the particle either directly or after interacting with the surface. The direct and the reflected incident fields are expanded in terms of regular vector spherical wave functions

$$\boldsymbol{E}_{\rm e}(\boldsymbol{r}) = \sum_{n_1=1}^{\infty}\sum_{m=-n_1}^{n_1} a^0_{mn_1}\boldsymbol{M}^1_{mn_1}(k_{\rm s}\boldsymbol{r}) + b^0_{mn_1}\boldsymbol{N}^1_{mn_1}(k_{\rm s}\boldsymbol{r}) \tag{2.194}$$

and

$$\boldsymbol{E}^{\rm R}_{\rm e}(\boldsymbol{r}) = \sum_{n_1=1}^{\infty}\sum_{m=-n_1}^{n_1} a^{\rm R}_{mn_1}\boldsymbol{M}^1_{mn_1}(k_{\rm s}\boldsymbol{r}) + b^{\rm R}_{mn_1}\boldsymbol{N}^1_{mn_1}(k_{\rm s}\boldsymbol{r})\,, \tag{2.195}$$

respectively, and we define the total expansion coefficients a_{mn_1} and b_{mn_1} by the relations

$$a_{mn_1} = a^0_{mn_1} + a^{\mathrm{R}}_{mn_1}\,,$$
$$b_{mn_1} = b^0_{mn_1} + b^{\mathrm{R}}_{mn_1}\,.$$

The coefficients $a^0_{mn_1}$ and $b^0_{mn_1}$ are the expansion coefficients of a vector plane wave traveling in the $(\beta_0, 0)$ direction,

$$a^0_{mn_1} = -\frac{4\mathrm{j}^{n_1}}{\sqrt{2n_1\,(n_1+1)}}\left[\mathrm{j}m\pi^{|m|}_{n_1}(\beta_0)\,E_{\mathrm{e}0,\beta} + \tau^{|m|}_{n_1}(\beta_0)\,E_{\mathrm{e}0,\alpha}\right]\,,$$
$$b^0_{mn_1} = -\frac{4\mathrm{j}^{n_1+1}}{\sqrt{2n_1\,(n_1+1)}}\left[\tau^{|m|}_{n_1}(\beta_0)\,E_{\mathrm{e}0,\beta} - \mathrm{j}m\pi^{|m|}_{n_1}(\beta_0)\,E_{\mathrm{e}0,\alpha}\right]\,,$$

while the coefficients $a^{\mathrm{R}}_{mn_1}$ and $b^{\mathrm{R}}_{mn_1}$ are the expansion coefficients of a vector plane wave traveling in the $(\pi-\beta_0, 0)$ direction. The part of the incident field that reflects off the surface will undergo a Fresnel reflection and it will be out of phase by an amount of $\exp(2\mathrm{j}k_{\mathrm{s}}z_0\cos\beta_0)$. This phase factor arises from the phase difference between the plane wave and its reflected wave in O. The resulting expressions for $a^{\mathrm{R}}_{mn_1}$ and $b^{\mathrm{R}}_{mn_1}$ are

$$a^{\mathrm{R}}_{mn_1} = -\frac{4\mathrm{j}^{n_1}}{\sqrt{2n_1\,(n_1+1)}}\left[\mathrm{j}m\pi^{|m|}_{n_1}(\pi-\beta_0)\,E^{\mathrm{R}}_{\mathrm{e}0,\beta} + \tau^{|m|}_{n_1}(\pi-\beta_0)\,E^{\mathrm{R}}_{\mathrm{e}0,\alpha}\right]\,,$$
$$b^{\mathrm{R}}_{mn_1} = -\frac{4\mathrm{j}^{n_1+1}}{\sqrt{2n_1\,(n_1+1)}}\left[\tau^{|m|}_{n_1}(\pi-\beta_0)\,E^{\mathrm{R}}_{\mathrm{e}0,\beta} - \mathrm{j}m\pi^{|m|}_{n_1}(\pi-\beta_0)\,E^{\mathrm{R}}_{\mathrm{e}0,\alpha}\right]\,,$$

where

$$E^{\mathrm{R}}_{\mathrm{e}0,\beta} = r_{\parallel}(\beta_0)\mathrm{e}^{2\mathrm{j}k_{\mathrm{s}}z_0\cos\beta_0}E_{\mathrm{e}0,\beta}\,,$$
$$E^{\mathrm{R}}_{\mathrm{e}0,\alpha} = r_{\perp}(\beta_0)\mathrm{e}^{2\mathrm{j}k_{\mathrm{s}}z_0\cos\beta_0}E_{\mathrm{e}0,\alpha}\,,$$

with $r_{\parallel}(\beta_0)$ and $r_{\perp}(\beta_0)$ being the Fresnel reflection coefficients for parallel and perpendicular polarizations, respectively. The Fresnel reflection coefficients are given by

$$r_{\parallel}(\beta_0) = \frac{m_{\mathrm{rs}}\cos\beta_0 - \cos\beta}{m_{\mathrm{rs}}\cos\beta_0 + \cos\beta}\,,$$
$$r_{\perp}(\beta_0) = \frac{\cos\beta_0 - m_{\mathrm{rs}}\cos\beta}{\cos\beta_0 + m_{\mathrm{rs}}\cos\beta}\,,$$

where m_{rs} is the relative refractive index of the substrate with respect to the ambient medium and β is the angle of refraction (Fig. 2.15). The angles of incidence and refraction are related to each other by Snell's law

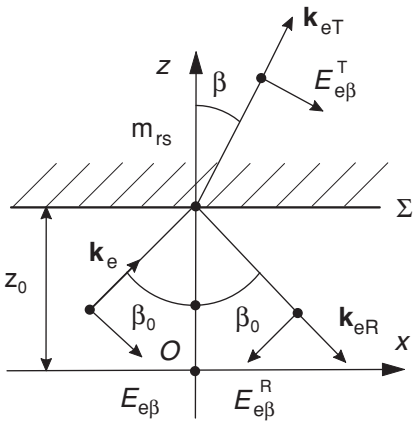

Fig. 2.15. Reflection and refraction of a vector plane wave (propagating in the ambient medium) at the interface Σ

$$\sin\beta = \frac{1}{m_{\rm rs}}\sin\beta_0\,,$$
$$\cos\beta = \pm\sqrt{1-\sin^2\beta}$$

and for real values of $m_{\rm rs}$, the sign of the square root is plus, while for complex values of $m_{\rm rs}$, the sign of the square root is chosen such that $\mathrm{Im}\{m_{\rm rs}\cos\beta\} > 0$. This choice guarantees that the amplitude of the refracted wave propagating in the positive direction of the z-axis would tend to zero with increasing the distance z.

The scattered field is expanded in terms of radiating vector spherical wave functions

$$\boldsymbol{E}_{\rm s}(\boldsymbol{r}) = \sum_{n=1}^{\infty}\sum_{m=-n}^{n} f_{mn}\boldsymbol{M}^{3}_{mn}(k_{\rm s}\boldsymbol{r}) + g_{mn}\boldsymbol{N}^{3}_{mn}(k_{\rm s}\boldsymbol{r}) \tag{2.196}$$

and the rest of our analysis concerns with the calculation of the expansion coefficients f_{mn} and g_{mn}. In addition to the fields described by (2.194)–(2.196), a fourth field exists in the ambient medium. This field is a result of the scattered field reflecting off the surface and striking the particle. It can be expressed as

$$\boldsymbol{E}^{\rm R}_{\rm s}(\boldsymbol{r}) = \sum_{n=1}^{\infty}\sum_{m=-n}^{n} f_{mn}\boldsymbol{M}^{3,{\rm R}}_{mn}(k_{\rm s}\boldsymbol{r}) + g_{mn}\boldsymbol{N}^{3,{\rm R}}_{mn}(k_{\rm s}\boldsymbol{r})\,, \tag{2.197}$$

where $\boldsymbol{M}^{3,{\rm R}}_{mn}(k_{\rm s}\boldsymbol{r})$ and $\boldsymbol{N}^{3,{\rm R}}_{mn}(k_{\rm s}\boldsymbol{r})$ are the radiating vector spherical wave functions reflected by the surface. Accordingly to Videen [240–242], the field $\boldsymbol{E}^{\rm R}_{\rm s}$ will be designated as the interacting field. For $\boldsymbol{r}$ inside a sphere enclosed in the particle and a given azimuthal mode m, we anticipate an expansion of the reflected vector spherical wave functions of the form

$$\begin{pmatrix} \boldsymbol{M}_{mn}^{3,\mathrm{R}}(k_\mathrm{s}\boldsymbol{r}) \\ \boldsymbol{N}_{mn}^{3,\mathrm{R}}(k_\mathrm{s}\boldsymbol{r}) \end{pmatrix} = \sum_{n_1=1}^{\infty} \begin{pmatrix} \alpha_{mnn_1} \\ \gamma_{mnn_1} \end{pmatrix} \boldsymbol{M}_{mn_1}^{1}(k_\mathrm{s}\boldsymbol{r}) + \begin{pmatrix} \beta_{mnn_1} \\ \delta_{mnn_1} \end{pmatrix} \boldsymbol{N}_{mn_1}^{1}(k_\mathrm{s}\boldsymbol{r}) \,. \tag{2.198}$$

Inserting (2.198) into (2.197), we derive a series representation for the interacting field in terms of regular vector spherical wave functions

$$\boldsymbol{E}_\mathrm{s}^{\mathrm{R}}(\boldsymbol{r}) = \sum_{n_1=1}^{\infty} \sum_{m=-n_1}^{n_1} f_{mn_1}^{\mathrm{R}} \boldsymbol{M}_{mn_1}^{1}(k_\mathrm{s}\boldsymbol{r}) + g_{mn_1}^{\mathrm{R}} \boldsymbol{N}_{mn_1}^{1}(k_\mathrm{s}\boldsymbol{r})] \,, \tag{2.199}$$

where

$$\begin{pmatrix} f_{mn_1}^{\mathrm{R}} \\ g_{mn_1}^{\mathrm{R}} \end{pmatrix} = \sum_{n=1}^{\infty} \begin{pmatrix} \alpha_{mnn_1} \\ \beta_{mnn_1} \end{pmatrix} f_{mn} + \begin{pmatrix} \gamma_{mnn_1} \\ \delta_{mnn_1} \end{pmatrix} g_{mn} \,. \tag{2.200}$$

In the null-field method, the scattered field coefficients are related to the expansion coefficients of the fields striking the particle by the transition matrix $\boldsymbol{T}$. For an axisymmetric particle, the equations become uncoupled, permitting a separate solution for each azimuthal mode. Thus, for a fixed azimuthal mode m, we truncate the expansions given by (2.194)–(2.196) and (2.199), and derive the following matrix equation:

$$\begin{bmatrix} f_{mn} \\ g_{mn} \end{bmatrix} = [T_{mn,mn_1}] \left(\begin{bmatrix} a_{mn_1} \\ b_{mn_1} \end{bmatrix} + \begin{bmatrix} f_{mn_1}^{\mathrm{R}} \\ g_{mn_1}^{\mathrm{R}} \end{bmatrix} \right) , \tag{2.201}$$

where n and n_1 range from 1 to N_rank, and m ranges from $-M_\mathrm{rank}$ to M_rank, with N_rank and M_rank being the maximum expansion and azimuthal orders, respectively. The expansion coefficients of the interacting field are related to the scattered field coefficients by a so called reflection matrix:

$$\begin{bmatrix} f_{mn_1}^{\mathrm{R}} \\ g_{mn_1}^{\mathrm{R}} \end{bmatrix} = [A_{mn_1 n}] \begin{bmatrix} f_{mn} \\ g_{mn} \end{bmatrix} , \tag{2.202}$$

where, in view of (2.200),

$$[A_{mn_1 n}] = \begin{bmatrix} \alpha_{mnn_1} & \gamma_{mnn_1} \\ \beta_{mnn_1} & \delta_{mnn_1} \end{bmatrix} .$$

Now it is apparent that the scattered field coefficients f_{mn} and g_{mn} can be obtained by combining the matrix equations (2.201) and (2.202), and the result is [270]

$$(\boldsymbol{I} - [T_{mn,mn_1}]\,[A_{mn_1 n}]) \begin{bmatrix} f_{mn} \\ g_{mn} \end{bmatrix} = [T_{mn,mn_1}] \begin{bmatrix} a_{mn_1} \\ b_{mn_1} \end{bmatrix} . \tag{2.203}$$

To derive the expression of the reflection matrix we use the integral representations for the radiating vector spherical wave functions

$$\begin{pmatrix} \boldsymbol{M}^3_{mn}(k_\mathrm{s}\boldsymbol{r}) \\ \boldsymbol{N}^3_{mn}(k_\mathrm{s}\boldsymbol{r}) \end{pmatrix} = -\frac{1}{2\pi \mathrm{j}^{n+1}} \frac{1}{\sqrt{2n(n+1)}} \int_0^{2\pi} \int_0^{\pi/2-\mathrm{j}\infty} \left[\begin{pmatrix} m\pi_n^{|m|}(\beta) \\ \tau_n^{|m|}(\beta) \end{pmatrix} \boldsymbol{e}_\beta + \mathrm{j} \begin{pmatrix} \tau_n^{|m|}(\beta) \\ m\pi_n^{|m|}(\beta) \end{pmatrix} \boldsymbol{e}_\alpha \right] \mathrm{e}^{\mathrm{j}m\alpha} \mathrm{e}^{\mathrm{j}\boldsymbol{k}(\beta,\alpha)\cdot\boldsymbol{r}} \sin\beta \mathrm{d}\beta \, \mathrm{d}\alpha \,, \quad (2.204)$$

where $(k_\mathrm{s}, \beta, \alpha)$ are the spherical coordinates of the wave vector $\boldsymbol{k}$, and $(\boldsymbol{e}_k, \boldsymbol{e}_\beta, \boldsymbol{e}_\alpha)$ are the spherical unit vectors of $\boldsymbol{k}$. Each reflected plane wave in (2.204) will contain a Fresnel reflection term and a phase term equivalent to $\exp(2\mathrm{j}k_\mathrm{s} z_0 \cos\beta)$. The reflected vector spherical wave functions can be expressed as

$$\begin{aligned} \begin{pmatrix} \boldsymbol{M}^{3,\mathrm{R}}_{mn}(k_\mathrm{s}\boldsymbol{r}) \\ \boldsymbol{N}^{3,\mathrm{R}}_{mn}(k_\mathrm{s}\boldsymbol{r}) \end{pmatrix} = & -\frac{1}{2\pi \mathrm{j}^{n+1}} \frac{1}{\sqrt{2n(n+1)}} \int_0^{2\pi} \int_0^{\pi/2-\mathrm{j}\infty} \left[\begin{pmatrix} m\pi_n^{|m|}(\beta) \\ \tau_n^{|m|}(\beta) \end{pmatrix} r_\parallel(\beta) \boldsymbol{e}_{\beta\mathrm{R}} \right. \\ & \left. + \mathrm{j} \begin{pmatrix} \tau_n^{|m|}(\beta) \\ m\pi_n^{|m|}(\beta) \end{pmatrix} r_\perp(\beta) \boldsymbol{e}_{\alpha_\mathrm{R}} \right] \mathrm{e}^{\mathrm{j}m\alpha} \mathrm{e}^{2\mathrm{j}k_\mathrm{s} z_0 \cos\beta} \mathrm{e}^{\mathrm{j}\boldsymbol{k}_\mathrm{R}(\beta_\mathrm{R},\alpha_\mathrm{R})\cdot\boldsymbol{r}} \\ & \times \sin\beta \, \mathrm{d}\beta \, \mathrm{d}\alpha \,, \end{aligned}$$

where $\beta_\mathrm{R} = \pi - \beta$, $\alpha_\mathrm{R} = \alpha$, $(k_\mathrm{s}, \beta_\mathrm{R}, \alpha_\mathrm{R})$ are the spherical coordinates of the reflected wave vector $\boldsymbol{k}_\mathrm{R}$, and $(\boldsymbol{e}_{k\mathrm{R}}, \boldsymbol{e}_{\beta\mathrm{R}}, \boldsymbol{e}_{\alpha\mathrm{R}})$ are the spherical unit vectors of $\boldsymbol{k}_\mathrm{R}$. For $\boldsymbol{r}$ inside a sphere enclosed in the particle, we expand each plane wave in terms of regular vector spherical wave functions

$$\begin{aligned} \begin{pmatrix} \boldsymbol{e}_{\beta_\mathrm{R}} \\ \boldsymbol{e}_{\alpha_\mathrm{R}} \end{pmatrix} e^{j\boldsymbol{k}_\mathrm{R}\cdot\boldsymbol{r}} = & -\sum_{n_1=1}^{\infty} \sum_{m_1=-n_1}^{n_1} \frac{4\mathrm{j}^{n_1}}{\sqrt{2n_1\,(n_1+1)}} \left[\begin{pmatrix} \mathrm{j}m_1\pi_{n_1}^{|m_1|}(\pi-\beta) \\ \tau_{n_1}^{|m_1|}(\pi-\beta) \end{pmatrix} \right. \\ & \left. \times \boldsymbol{M}^1_{m_1 n_1}(k_\mathrm{s}\boldsymbol{r}) + \begin{pmatrix} \mathrm{j}\tau_{n_1}^{|m_1|}(\pi-\beta) \\ m_1\pi_{n_1}^{|m_1|}(\pi-\beta) \end{pmatrix} \boldsymbol{N}^1_{m_1 n_1}(k_\mathrm{s}\boldsymbol{r}) \right] \mathrm{e}^{-\mathrm{j}m_1\alpha} \end{aligned}$$

and obtain the following expressions for the elements of the reflection matrix:

$$\begin{aligned} \alpha_{mnn_1} = & \frac{2\mathrm{j}^{n_1-n}}{\sqrt{nn_1(n+1)(n_1+1)}} \int_0^{\pi/2-\mathrm{j}\infty} \left[m^2 \pi_n^{|m|}(\beta)\pi_{n_1}^{|m|}(\pi-\beta) r_\parallel(\beta) \right. \\ & \left. + \tau_n^{|m|}(\beta)\tau_{n_1}^{|m|}(\pi-\beta) r_\perp(\beta) \right] \mathrm{e}^{2\mathrm{j}k_\mathrm{s} z_0 \cos\beta} \sin\beta \, \mathrm{d}\beta \,, \end{aligned} \quad (2.205)$$

$$\begin{aligned} \beta_{mnn_1} = & \frac{2\mathrm{j}^{n_1-n}}{\sqrt{nn_1(n+1)(n_1+1)}} \int_0^{\pi/2-\mathrm{j}\infty} m \left[\pi_n^{|m|}(\beta)\tau_{n_1}^{|m|}(\pi-\beta) r_\parallel(\beta) \right. \\ & \left. + \tau_n^{|m|}(\beta)\pi_{n_1}^{|m|}(\pi-\beta) r_\perp(\beta) \right] \mathrm{e}^{2\mathrm{j}k_\mathrm{s} z_0 \cos\beta} \sin\beta \, \mathrm{d}\beta \,, \end{aligned} \quad (2.206)$$

$$\gamma_{mnn_1} = \frac{2\mathrm{j}^{n_1-n}}{\sqrt{nn_1(n+1)(n_1+1)}} \int_0^{\pi/2-\mathrm{j}\infty} m \left[\tau_n^{|m|}(\beta)\pi_{n_1}^{|m|}(\pi-\beta)r_{\parallel}(\beta) + \pi_n^{|m|}(\beta)\tau_{n_1}^{|m|}(\pi-\beta)r_{\perp}(\beta)\right] \mathrm{e}^{2\mathrm{j}k_{\mathrm{s}}z_0\cos\beta}\sin\beta\,\mathrm{d}\beta\,, \tag{2.207}$$

$$\delta_{mnn_1} = \frac{2\mathrm{j}^{n_1-n}}{\sqrt{nn_1(n+1)(n_1+1)}} \int_0^{\pi/2-\mathrm{j}\infty} \left[\tau_n^{|m|}(\beta)\tau_{n_1}^{|m|}(\pi-\beta)r_{\parallel}(\beta) + m^2\pi_n^{|m|}(\beta)\pi_{n_1}^{|m|}(\pi-\beta)r_{\perp}(\beta)\right] \mathrm{e}^{2\mathrm{j}k_{\mathrm{s}}z_0\cos\beta}\sin\beta\,\mathrm{d}\beta\,, \tag{2.208}$$

An approximate expression for the reflection matrix can be derived if we assume that the interacting radiation strikes the surface at normal incidence. Assuming $r(0) = r_{\perp}(\beta) = -r_{\parallel}(\beta)$, changing the variable from β to $\beta_{\mathrm{R}} = \pi - \beta$, and using the relations

$$\pi_n^{|m|}(\pi-\beta_{\mathrm{R}}) = (-1)^{n-|m|}\pi_n^{|m|}(\beta_{\mathrm{R}})\,,$$
$$\tau_n^{|m|}(\pi-\beta_{\mathrm{R}}) = (-1)^{n-|m|+1}\tau_n^{|m|}(\beta_{\mathrm{R}})\,,$$

yields the following simplified integral representations for the reflected vector spherical wave functions:

$$\begin{pmatrix} \boldsymbol{M}_{mn}^{3,\mathrm{R}}(k_{\mathrm{s}}\boldsymbol{r}) \\ \boldsymbol{N}_{mn}^{3,\mathrm{R}}(k_{\mathrm{s}}\boldsymbol{r}) \end{pmatrix} = -\frac{(-1)^{n-|m|}r(0)}{2\pi j^{n+1}} \frac{1}{\sqrt{2n(n+1)}} \times \int_0^{2\pi}\int_{\pi/2+\mathrm{j}\infty}^{\pi} \left[\begin{pmatrix} -m\pi_n^{|m|}(\beta_{\mathrm{R}}) \\ \tau_n^{|m|}(\beta_{\mathrm{R}}) \end{pmatrix} \boldsymbol{e}_{\beta_R} + \mathrm{j}\begin{pmatrix} -\tau_n^{|m|}(\beta_{\mathrm{R}}) \\ m\pi_n^{|m|}(\beta_{\mathrm{R}}) \end{pmatrix} \boldsymbol{e}_{\alpha_{\mathrm{R}}}\right] \times \mathrm{e}^{\mathrm{j}m\alpha_{\mathrm{R}}}\mathrm{e}^{-2\mathrm{j}k_{\mathrm{s}}z_0\cos\beta_{\mathrm{R}}}\mathrm{e}^{\mathrm{j}\boldsymbol{k}_{\mathrm{R}}(\beta_{\mathrm{R}},\alpha_{\mathrm{R}})\cdot\boldsymbol{r}}\sin\beta_{\mathrm{R}}\,\mathrm{d}\beta_{\mathrm{R}}\,\mathrm{d}\alpha_{\mathrm{R}}\,.$$

To compute $\boldsymbol{M}_{mn}^{3,\mathrm{R}}$ and $\boldsymbol{N}_{mn}^{3,\mathrm{R}}$ we introduce the image coordinate system $O'x'y'z'$ by shifting the original coordinate system a distance $2z_0$ along the positive z-axis. The geometry of the image coordinate system is shown in Fig. 2.16. Taking into account that $\boldsymbol{k}_{\mathrm{R}}\cdot\boldsymbol{r}' = \boldsymbol{k}_{\mathrm{R}}\cdot\boldsymbol{r} - 2k_{\mathrm{s}}z_0\cos\beta_{\mathrm{R}}$, where $\boldsymbol{r}' = (x', y', z')$, we identify in the resulting equation the integral representations for the radiating vector spherical wave functions in the half-space $z < 0$:

$$\begin{pmatrix} \boldsymbol{M}_{mn}^{3,\mathrm{R}}(k_{\mathrm{s}}\boldsymbol{r}) \\ \boldsymbol{N}_{mn}^{3,\mathrm{R}}(k_{\mathrm{s}}\boldsymbol{r}) \end{pmatrix} = (-1)^{n-|m|}r(0)\begin{pmatrix} -\boldsymbol{M}_{mn}^{3}(k_{\mathrm{s}}\boldsymbol{r}') \\ \boldsymbol{N}_{mn}^{3}(k_{\mathrm{s}}\boldsymbol{r}') \end{pmatrix}\,.$$

In this case the interacting field is the image of the scattered field and the expansion (2.198) can be derived by using the addition theorem for vector spherical wave functions. The elements of the reflection matrix are the translation coefficients, and as a result, the amount of computer time required to solve the scattering problem is significantly reduced. In this regard it should

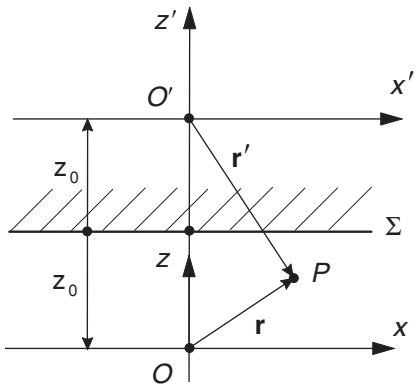

Fig. 2.16. Image coordinate system

be mentioned that the formalism using the approximate expression for the reflection matrix has been employed by Videen [240–242].

In most practical situations we are interested in the analysis of the scattered field in the far-field region and below the plane surface, i.e., for $\theta > \pi/2$. In this region we have two contributions to the scattered field: the direct electric far-field pattern $\boldsymbol{E}_{\mathrm{s}\infty}(\theta,\varphi)$,

$$\boldsymbol{E}_{\mathrm{s}\infty}(\theta,\varphi) = \frac{1}{k_{\mathrm{s}}}\sum_{n=1}^{\infty}\sum_{m=-n}^{n}(-\mathrm{j})^{n+1}\left[f_{mn}\boldsymbol{m}_{mn}(\theta,\varphi) + \mathrm{j}g_{mn}\boldsymbol{n}_{mn}(\theta,\varphi)\right] \quad (2.209)$$

and the interacting electric far-field pattern $\boldsymbol{E}^{\mathrm{R}}_{\mathrm{s}\infty}(\theta,\varphi)$,

$$\boldsymbol{E}^{\mathrm{R}}_{\mathrm{s}\infty}(\theta,\varphi) = \frac{1}{k_{\mathrm{s}}}\sum_{n=1}^{\infty}\sum_{m=-n}^{n}(-\mathrm{j})^{n+1}\left[f_{mn}\boldsymbol{m}^{\mathrm{R}}_{mn}(\theta,\varphi) + \mathrm{j}g_{mn}\boldsymbol{n}^{\mathrm{R}}_{mn}(\theta,\varphi)\right], \quad (2.210)$$

where $\boldsymbol{m}_{mn}$ and $\boldsymbol{n}_{mn}$ are the vector spherical harmonics, and $\boldsymbol{m}^{\mathrm{R}}_{mn}$ and $\boldsymbol{n}^{\mathrm{R}}_{mn}$ are the reflected vector spherical harmonics,

$$\begin{aligned}\boldsymbol{m}^{\mathrm{R}}_{mn}(\theta,\varphi) = {} & \frac{1}{\sqrt{2n(n+1)}}\mathrm{e}^{-2\mathrm{j}k_{\mathrm{s}}z_0\cos\theta} \\ & \times\left[\mathrm{j}m\pi^{|m|}_n(\pi-\theta)r_{\parallel}(\pi-\theta)\boldsymbol{e}_\theta - \tau^{|m|}_n(\pi-\theta)r_{\perp}(\pi-\theta)\boldsymbol{e}_\varphi\right]\mathrm{e}^{\mathrm{j}m\varphi},\end{aligned}$$

$$\begin{aligned}\boldsymbol{n}^{\mathrm{R}}_{mn}(\theta,\varphi) = {} & \frac{1}{\sqrt{2n(n+1)}}\mathrm{e}^{-2\mathrm{j}k_{\mathrm{s}}z_0\cos\theta} \\ & \times\left[\tau^{|m|}_n(\pi-\theta)r_{\parallel}(\pi-\theta)\boldsymbol{e}_\theta + \mathrm{j}m\pi^{|m|}_n(\pi-\theta)\,r_{\perp}(\pi-\theta)\boldsymbol{e}_\varphi\right]\mathrm{e}^{\mathrm{j}m\varphi}.\end{aligned}$$

Thus, the solution of the scattering problem in the framework of the separation of variables method involves the following steps:

1. Calculation of the $\boldsymbol{T}$ matrix relating the expansion coefficients of the fields striking the particle to the scattered field coefficients.
2. Calculation of the reflection matrix $\boldsymbol{A}$ characterizing the reflection of vector spherical wave functions by the surface.
3. Computation of an approximate solution by solving the matrix equation (2.203).
4. Computation of the far-field pattern by using (2.209) and (2.210).

In practice, we must compute the integrals in (2.205)–(2.208), which are of the form

$$I = \int_0^{\pi/2-\mathrm{j}\infty} f(\cos\beta)\,\mathrm{e}^{2\mathrm{j}q\cos\beta}\sin\beta\mathrm{d}\beta\,.$$

Changing variables from β to $x = -2\mathrm{j}q(\cos\beta - 1)$, we have

$$I = \frac{e^{2\mathrm{j}q}}{2\mathrm{j}q}\int_0^{\infty} f\left(1-\frac{x}{2\mathrm{j}q}\right)\mathrm{e}^{-x}\mathrm{d}x$$

and integrals of this type can be computed efficiently by using the Laguerre polynomials [15].

Scanning near-field optical microscopy [202,203] requires a rigorous analysis of the evanescent scattering by small particles near the surface of a dielectric prism [31, 142, 199, 252]. Scattering of evanescent waves can be analyzed by extending our formalism to the case of an incident plane wave propagating in the substrate (Fig. 2.17).

For the incident vector plane wave given by (2.193), the transmitted (or the refracted) vector plane wave is

$$\boldsymbol{E}_{\mathrm{eT}}(\boldsymbol{r}) = \left(E^{\mathrm{T}}_{\mathrm{e0},\beta}\boldsymbol{e}_{\beta T} + E^{\mathrm{T}}_{\mathrm{e0},\alpha}\boldsymbol{e}_{\alpha T}\right)\mathrm{e}^{\mathrm{j}\boldsymbol{k}_{eT}\cdot\boldsymbol{r}}\,,$$

where

$$E^{\mathrm{T}}_{\mathrm{e0},\beta} = t_{\parallel}(\beta_0)\mathrm{e}^{\mathrm{j}k_{\mathrm{s}}z_0(\cos\beta - m_{\mathrm{rs}}\cos\beta_0)}E_{\mathrm{e0},\beta}\,,$$
$$E^{\mathrm{T}}_{\mathrm{e0},\alpha} = t_{\perp}(\beta_0)\mathrm{e}^{\mathrm{j}k_{\mathrm{s}}z_0(\cos\beta - m_{\mathrm{rs}}\cos\beta_0)}E_{\mathrm{e0},\alpha}\,,$$

β_0 is the incident angle and $(\boldsymbol{e}_{k\mathrm{T}}, \boldsymbol{e}_{\beta\mathrm{T}}, \boldsymbol{e}_{\alpha\mathrm{T}})$ are the spherical unit vectors of the transmitted wave vector $\boldsymbol{k}_{\mathrm{eT}}$. The Fresnel transmission coefficients are given by

$$t_{\parallel}(\beta_0) = \frac{2m_{\mathrm{rs}}\cos\beta_0}{\cos\beta_0 + m_{\mathrm{rs}}\cos\beta}\,,$$
$$t_{\perp}(\beta_0) = \frac{2m_{\mathrm{rs}}\cos\beta_0}{m_{\mathrm{rs}}\cos\beta_0 + \cos\beta}\,,$$

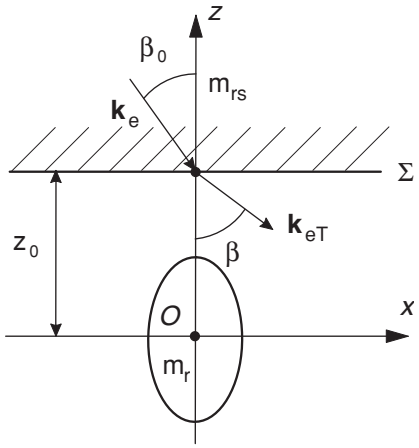

Fig. 2.17. Geometry of an axisymmetric particle situated near a plane surface. The external excitation is a vector plane wave propagating in the substrate

while the angle of refraction is computed by using Snell's law:

$$\sin\beta = m_{\rm rs}\sin\beta_0\,,$$
$$\cos\beta = \pm\sqrt{1-\sin^2\beta}\,.$$

Evanescent waves appear for real $m_{\rm rs}$ and incident angles $\beta_0 > \beta_{0\rm c}$, where $\beta_{0\rm c} = \arcsin(1/m_{\rm rs})$. In this case, $\sin\beta > 1$ and $\cos\beta$ is purely imaginary. For negative values of z, we have

$$\exp\left(\mathrm{j}\boldsymbol{k}_{\rm eT}\cdot\boldsymbol{r}\right) = \exp\left(-\mathrm{j}k_{\rm s}z\cos\beta + \mathrm{j}k_{\rm s}x\sin\beta\right) = \exp\left(\mathrm{j}k_{\rm s}\left|z\right|\cos\beta + \mathrm{j}k_{\rm s}x\sin\beta\right),$$

and we choose the sign of the square root such that $\mathrm{Im}\{\cos\beta\} > 0$. This choice guarantees that the amplitude of the refracted wave propagating in the negative direction of the z-axis decreases with increasing the distance $|z|$. The expansion coefficients of the transmitted wave are

$$a^{\rm T}_{mn_1} = -\frac{4\mathrm{j}^{n_1}}{\sqrt{2n_1\left(n_1+1\right)}}\left[\mathrm{j}m\pi^{|m|}_{n_1}(\pi-\beta)\,E^{\rm T}_{{\rm e}0,\beta} + \tau^{|m|}_{n_1}(\pi-\beta)\,E^{\rm T}_{{\rm e}0,\alpha}\right],$$

$$b^{\rm T}_{mn_1} = -\frac{4\mathrm{j}^{n_1+1}}{\sqrt{2n_1\left(n_1+1\right)}}\left[\tau^{|m|}_{n_1}(\pi-\beta)\,E^{\rm T}_{{\rm e}0,\beta} - \mathrm{j}m\pi^{|m|}_{n_1}(\pi-\beta)\,E^{\rm T}_{{\rm e}0,\alpha}\right],$$

and we see that our previous analysis remains unchanged if we replace the total expansion coefficients a_{mn_1} and b_{mn_1}, by the expansion coefficients of the transmitted wave $a^{\rm T}_{mn_1}$ and $b^{\rm T}_{mn_1}$.

2.10.2 Particle on or near an Arbitrary Surface

In the precedent analysis, we considered scattering by a particle situated near a plane surface. The scattering problem of a particle situated in the

neighborhood of an arbitrary infinite surface can be solved by using the $\boldsymbol{T}$-operator formalism. Specifically, we are interested to compute the vector spherical wave expansions of the reflected fields $\boldsymbol{E}_{\mathrm{e}}^{\mathrm{R}}$, $\boldsymbol{M}_{mn}^{3,\mathrm{R}}$ and $\boldsymbol{N}_{mn}^{3,\mathrm{R}}$ in the case of an infinite surface. For this purpose, we consider the scattering problem of an infinite surface illuminated by an arbitrary incident field and follow the analysis of Kristensson [124].

We briefly recall the definitions and the basic properties of scalar and vector plane waves [14]. The scalar plane wave is defined by

$$\chi(\boldsymbol{r}, \boldsymbol{K}_{\pm}) = \exp(\mathrm{j}\boldsymbol{K}_{\pm} \cdot \boldsymbol{r}) = \exp[\mathrm{j}\,(K_x x + K_y y \pm K_z z)]\,,$$

where

$$\boldsymbol{K}_{\pm} = K_x \boldsymbol{e}_x + K_y \boldsymbol{e}_y \pm K_z \boldsymbol{e}_z\,.$$

Using the notation $k_{\mathrm{T}} = \sqrt{K_x^2 + K_y^2}$, K_z can be expressed as $K_z = \sqrt{k^2 - k_{\mathrm{T}}^2}$, where the square root is always chosen to have a positive imaginary part. For real k, K_z is given by $K_z = \sqrt{k^2 - k_{\mathrm{T}}^2}$, if $k_{\mathrm{T}} \leq k$, and by $K_z = \mathrm{j}\sqrt{k_{\mathrm{T}}^2 - k^2}$ if $k_{\mathrm{T}} > k$. The case $k_{\mathrm{T}} \leq k$ corresponds to harmonic propagating waves, while the case $k_{\mathrm{T}} > k$ corresponds to evanescent waves. The vector plane waves $\boldsymbol{M}(\boldsymbol{r}, \boldsymbol{K}_{\pm})$ and $\boldsymbol{N}(\boldsymbol{r}, \boldsymbol{K}_{\pm})$ are defined in terms of scalar plane wave as

$$\begin{aligned}
\boldsymbol{M}\,(\boldsymbol{r}, \boldsymbol{K}_{\pm}) &= \frac{1}{k_{\mathrm{T}}} \nabla \times [\boldsymbol{e}_z \chi\,(\boldsymbol{r}, \boldsymbol{K}_{\pm})] = \mathrm{j}\frac{\boldsymbol{K}_{\mathrm{T}}}{k_{\mathrm{T}}} \chi\,(\boldsymbol{r}, \boldsymbol{K}_{\pm})\,, \\
\boldsymbol{N}\,(\boldsymbol{r}, \boldsymbol{K}_{\pm}) &= \frac{1}{k} \nabla \times \boldsymbol{M}\,(\boldsymbol{r}, \boldsymbol{K}_{\pm}) = -\left(\frac{\boldsymbol{K}_{\pm}}{k} \times \frac{\boldsymbol{K}_{\mathrm{T}}}{k_{\mathrm{T}}}\right) \chi\,(\boldsymbol{r}, \boldsymbol{K}_{\pm})\,,
\end{aligned}$$

where $\boldsymbol{K}_{\mathrm{T}}$ is the transverse component of the wave vector $\boldsymbol{K}_{\pm}$ and is given by

$$\boldsymbol{K}_{\mathrm{T}} = \boldsymbol{K}_{\pm} \times \boldsymbol{e}_z = K_y \boldsymbol{e}_x - K_x \boldsymbol{e}_y\,.$$

The orthogonality relations

$$\begin{aligned}
\int_{\Sigma} \boldsymbol{M}\,(\boldsymbol{r}, \boldsymbol{K}_{\pm}) \cdot \boldsymbol{M}\left(-\boldsymbol{r}, \boldsymbol{K}'_{\pm}\right) \mathrm{d}x\,\mathrm{d}y &= 4\pi^2 \mathrm{e}^{\pm\mathrm{j}\left(K_z - K'_z\right)z} \delta\left(K_x - K'_x, K_y - K'_y\right) \\
\int_{\Sigma} \boldsymbol{N}\,(\boldsymbol{r}, \boldsymbol{K}_{\pm}) \cdot \boldsymbol{N}\left(-\boldsymbol{r}, \boldsymbol{K}'_{\pm}\right) \mathrm{d}x\,\mathrm{d}y &= 4\pi^2 \frac{\boldsymbol{K}_{\pm} \cdot \boldsymbol{K}'_{\pm}}{kk'} \mathrm{e}^{\pm\mathrm{j}\left(K_z - K'_z\right)z} \\
&\quad \times \delta\left(K_x - K'_x, K_y - K'_y\right)\,, \\
\int_{\Sigma} \boldsymbol{M}\,(\boldsymbol{r}, \boldsymbol{K}_{\pm}) \cdot \boldsymbol{N}\left(-\boldsymbol{r}, \boldsymbol{K}'_{\pm}\right) \mathrm{d}x\,\mathrm{d}y &= \int_{\Sigma} \boldsymbol{N}\,(\boldsymbol{r}, \boldsymbol{K}_{\pm}) \cdot \boldsymbol{M}\left(-\boldsymbol{r}, \boldsymbol{K}'_{\pm}\right) \mathrm{d}x\,\mathrm{d}y = 0,
\end{aligned}$$

hold on a plane $z = \mathrm{const}$, where

$$\begin{aligned}
\boldsymbol{M}\,(-\boldsymbol{r}, \boldsymbol{K}_{\pm}) &= \frac{1}{k_{\mathrm{T}}} \nabla \times [\boldsymbol{e}_z \chi\,(-\boldsymbol{r}, \boldsymbol{K}_{\pm})] = -\mathrm{j}\frac{\boldsymbol{K}_{\mathrm{T}}}{k_{\mathrm{T}}} \chi\,(-\boldsymbol{r}, \boldsymbol{K}_{\pm})\,, \\
\boldsymbol{N}\,(-\boldsymbol{r}, \boldsymbol{K}_{\pm}) &= \frac{1}{k} \nabla \times \boldsymbol{M}\,(-\boldsymbol{r}, \boldsymbol{K}_{\pm}) = -\left(\frac{\boldsymbol{K}_{\pm}}{k} \times \frac{\boldsymbol{K}_{\mathrm{T}}}{k_{\mathrm{T}}}\right) \chi\,(-\boldsymbol{r}, \boldsymbol{K}_{\pm})\,.
\end{aligned}$$

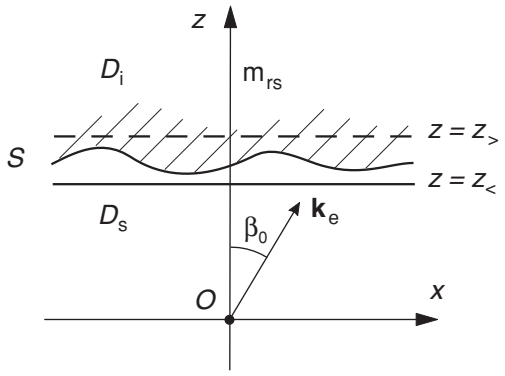

Fig. 2.18. Geometry of an infinite surface

Alternative expressions for the vector plane waves are

$$\begin{aligned} \boldsymbol{M}\left(\boldsymbol{r},\boldsymbol{K}_{\pm}\right) &= -\mathrm{j}\boldsymbol{e}_{\alpha}\chi\left(\boldsymbol{r},\boldsymbol{K}_{\pm}\right) , \\ \boldsymbol{N}\left(\boldsymbol{r},\boldsymbol{K}_{\pm}\right) &= -\boldsymbol{e}_{\beta}\chi\left(\boldsymbol{r},\boldsymbol{K}_{\pm}\right) , \end{aligned} \tag{2.211}$$

and

$$\begin{aligned} \boldsymbol{M}\left(-\boldsymbol{r},\boldsymbol{K}_{\pm}\right) &= \mathrm{j}\boldsymbol{e}_{\alpha}\chi\left(-\boldsymbol{r},\boldsymbol{K}_{\pm}\right) , \\ \boldsymbol{N}\left(-\boldsymbol{r},\boldsymbol{K}_{\pm}\right) &= -\boldsymbol{e}_{\beta}\chi\left(-\boldsymbol{r},\boldsymbol{K}_{\pm}\right) , \end{aligned} \tag{2.212}$$

where $(\boldsymbol{e}_k, \boldsymbol{e}_{\beta}, \boldsymbol{e}_{\alpha})$ are the spherical unit vectors of the wave vector $\boldsymbol{K}_{\pm}$.

We consider now the scattering geometry depicted in Fig. 2.18. The incident field $\boldsymbol{E}_{\mathrm{e}}$ is a vector plane wave or any radiating vector spherical wave functions. To solve the scattering problem in the framework of the $\boldsymbol{T}$-operator method we apply the Huygens principle to a surface consisting of a finite part of S and a lower half-sphere. Letting the radius of the sphere tend to infinity and assuming that the integrals over S exist and the integrals over the lower half-sphere vanish (radiation conditions), we obtain

$$\begin{aligned} \left.\begin{matrix} \boldsymbol{E}(\boldsymbol{r}) \\ 0 \end{matrix}\right\} = \boldsymbol{E}_{\mathrm{e}}(\boldsymbol{r}) + \int_S \Big\{ \left[\boldsymbol{n}\left(\boldsymbol{r}'\right) \times E_{\mathrm{i}}\left(\boldsymbol{r}'\right)\right] \cdot \left[\nabla' \times \overline{\boldsymbol{G}}\left(k_{\mathrm{s}}, \boldsymbol{r}', \boldsymbol{r}\right)\right] \\ + \left[\boldsymbol{n}\left(\boldsymbol{r}'\right) \times \left(\nabla' \times \boldsymbol{E}_{\mathrm{i}}\left(\boldsymbol{r}'\right)\right)\right] \cdot \overline{\boldsymbol{G}}\left(k_{\mathrm{s}}, \boldsymbol{r}', \boldsymbol{r}\right) \Big\} \mathrm{d}S\left(\boldsymbol{r}'\right) , \quad \begin{cases} \boldsymbol{r} \in D_{\mathrm{s}} \\ \boldsymbol{r} \in D_{\mathrm{i}} \end{cases} , \end{aligned} \tag{2.213}$$

where $\boldsymbol{E}(\boldsymbol{r}) = \boldsymbol{E}_{\mathrm{e}}(\boldsymbol{r}) + \boldsymbol{E}_{\mathrm{s}}(\boldsymbol{r})$ is the total field in the domain D_{s} and $\overline{\boldsymbol{G}}(k_{\mathrm{s}}, \boldsymbol{r}', \boldsymbol{r})$ is the free space dyadic Green function of wave number k_{s}. The dyadic Green function can be expanded in terms of vector plane waves, [14, 124]

$$\overline{\boldsymbol{G}}(k_\mathrm{s},\boldsymbol{r}',\boldsymbol{r}) = \frac{\mathrm{j}k_\mathrm{s}}{8\pi^2}\int_{\boldsymbol{R}^2}\left[\boldsymbol{M}\left(-\boldsymbol{r}',\boldsymbol{K}_+^\mathrm{s}\right)\,\boldsymbol{M}\left(\boldsymbol{r},\boldsymbol{K}_+^\mathrm{s}\right)\right.$$
$$\left.+\,\boldsymbol{N}\left(-\boldsymbol{r}',\boldsymbol{K}_+^\mathrm{s}\right)\,\boldsymbol{N}\left(\boldsymbol{r},\boldsymbol{K}_+^\mathrm{s}\right)\right]\frac{\mathrm{d}K_x^\mathrm{s}\,\mathrm{d}K_y^\mathrm{s}}{k_\mathrm{s}K_z^\mathrm{s}}$$

for $z > z'$, and

$$\overline{\boldsymbol{G}}(k_\mathrm{s},\boldsymbol{r}',\boldsymbol{r}) = \frac{\mathrm{j}k_\mathrm{s}}{8\pi^2}\int_{\boldsymbol{R}^2}\left[\boldsymbol{M}\left(-\boldsymbol{r}',\boldsymbol{K}_-^\mathrm{s}\right)\,\boldsymbol{M}\left(\boldsymbol{r},\boldsymbol{K}_-^\mathrm{s}\right)\right.$$
$$\left.+\,\boldsymbol{N}\left(-\boldsymbol{r}',\boldsymbol{K}_-^\mathrm{s}\right)\,\boldsymbol{N}\left(\boldsymbol{r},\boldsymbol{K}_-^\mathrm{s}\right)\right]\frac{\mathrm{d}K_x^\mathrm{s}\,\mathrm{d}K_y^\mathrm{s}}{k_\mathrm{s}K_z^\mathrm{s}}$$

for $z < z'$, where the superscript s indicates that the vector plane waves correspond to the domain D_s.

The incident field is a prescribed field, whose sources are assumed to be situated in D_s. This means that in any case, the sources are below the fictitious plane $z = z_>$ and we can represent the external excitation as an integral over up-going vector plane waves

$$\boldsymbol{E}_\mathrm{e}(\boldsymbol{r}) = \int_{\boldsymbol{R}^2}\left[A(\boldsymbol{K}_+^\mathrm{s})\,\boldsymbol{M}(\boldsymbol{r},\boldsymbol{K}_+^\mathrm{s}) + B(\boldsymbol{K}_+^\mathrm{s})\,\boldsymbol{N}(\boldsymbol{r},\boldsymbol{K}_+^\mathrm{s})\right]\frac{\mathrm{d}K_x^\mathrm{s}\,\mathrm{d}K_y^\mathrm{s}}{k_\mathrm{s}K_z^\mathrm{s}}\,.$$

For $\boldsymbol{r} \in D_\mathrm{i}$ and $z > z_>$, we use the plane wave expansion of the Green dyad and the orthogonality properties of the vector plane waves to obtain

$$A\left(\boldsymbol{K}_+^\mathrm{s}\right) = -\frac{\mathrm{j}k_\mathrm{s}^2}{8\pi^2}\int_S\left\{\left[\boldsymbol{n}(\boldsymbol{r}')\times\boldsymbol{E}_\mathrm{i}(\boldsymbol{r}')\right]\cdot\boldsymbol{N}\left(-\boldsymbol{r}',\boldsymbol{K}_+^\mathrm{s}\right)\right. \tag{2.214}$$
$$\left.+\frac{1}{k_\mathrm{s}}\left[\boldsymbol{n}\left(\boldsymbol{r}'\right)\times\left(\nabla'\times\boldsymbol{E}_\mathrm{i}\left(\boldsymbol{r}'\right)\right)\right]\cdot\boldsymbol{M}\left(-\boldsymbol{r}',\boldsymbol{K}_+^\mathrm{s}\right)\right\}\mathrm{d}S\left(\boldsymbol{r}'\right)\,,$$

$$B\left(\boldsymbol{K}_+^\mathrm{s}\right) = -\frac{\mathrm{j}k_\mathrm{s}^2}{8\pi^2}\int_S\left\{\left[\boldsymbol{n}(\boldsymbol{r}')\times\boldsymbol{E}_\mathrm{i}(\boldsymbol{r}')\right]\cdot\boldsymbol{M}\left(-\boldsymbol{r}',\boldsymbol{K}_+^\mathrm{s}\right)\right. \tag{2.215}$$
$$\left.+\frac{1}{k_\mathrm{s}}\left[\boldsymbol{n}\left(\boldsymbol{r}'\right)\times\left(\nabla'\times\boldsymbol{E}_\mathrm{i}\left(\boldsymbol{r}'\right)\right)\right]\cdot\boldsymbol{N}\left(-\boldsymbol{r}',\boldsymbol{K}_+^\mathrm{s}\right)\right\}\mathrm{d}S\left(\boldsymbol{r}'\right)\,.$$

Taking into account that the tangential vector plane waves $\boldsymbol{n}\times\boldsymbol{M}(\cdot,\boldsymbol{K}_+^\mathrm{i})$ and $\boldsymbol{n}\times\boldsymbol{N}(\cdot,\boldsymbol{K}_+^\mathrm{i})$, form a complete system of vector function on S, we represent the surface fields $\boldsymbol{n}\times\boldsymbol{E}_\mathrm{i}$ and $\boldsymbol{n}\times(\nabla\times\boldsymbol{E}_\mathrm{i})$ as integrals over up-going vector plane waves, i.e.,

$$\boldsymbol{n}\left(\boldsymbol{r}'\right)\times\boldsymbol{E}_\mathrm{i}\left(\boldsymbol{r}'\right) = \int_{\boldsymbol{R}^2}\left[C\left(\boldsymbol{K}_+^\mathrm{i}\right)c\left(\boldsymbol{K}_+^\mathrm{i}\right)\boldsymbol{n}\left(\boldsymbol{r}'\right)\times\boldsymbol{M}\left(\boldsymbol{r}',\boldsymbol{K}_+^\mathrm{i}\right)\right. \tag{2.216}$$
$$\left.+\,D\left(\boldsymbol{K}_+^\mathrm{i}\right)d\left(\boldsymbol{K}_+^\mathrm{i}\right)\boldsymbol{n}\left(\boldsymbol{r}'\right)\times\boldsymbol{N}\left(\boldsymbol{r}',\boldsymbol{K}_+^\mathrm{i}\right)\right]\mathrm{d}K_x^\mathrm{i}\,\mathrm{d}K_y^\mathrm{i}$$

and

$$\boldsymbol{n}\left(\boldsymbol{r}'\right)\times\left[\nabla'\times\boldsymbol{E}_{\mathrm{i}}\left(\boldsymbol{r}'\right)\right]=k_{\mathrm{i}}\int_{\boldsymbol{R}^2}\left[C\left(\boldsymbol{K}_{+}^{\mathrm{i}}\right)c\left(\boldsymbol{K}_{+}^{\mathrm{i}}\right)\,\boldsymbol{n}\left(\boldsymbol{r}'\right)\times\boldsymbol{N}\left(\boldsymbol{r}',\boldsymbol{K}_{+}^{\mathrm{i}}\right)\right.$$
$$\left.+\,D\left(\boldsymbol{K}_{+}^{\mathrm{i}}\right)d\left(\boldsymbol{K}_{+}^{\mathrm{i}}\right)\boldsymbol{n}\left(\boldsymbol{r}'\right)\times\boldsymbol{M}\left(\boldsymbol{r}',\boldsymbol{K}_{+}^{\mathrm{i}}\right)\right]\mathrm{d}K_x^{\mathrm{i}}\,\mathrm{d}K_y^{\mathrm{i}}\,, \tag{2.217}$$

respectively. The plane wave transmission coefficients in (2.216) and (2.217) are given by

$$c\left(\boldsymbol{K}_{+}^{\mathrm{i}}\right)=\frac{2K_z^{\mathrm{s}}}{K_z^{\mathrm{s}}+K_z^{\mathrm{i}}}\mathrm{e}^{-\mathrm{j}(K_z^{\mathrm{i}}-K_z^{\mathrm{s}})z'}\,,$$
$$d\left(\boldsymbol{K}_{+}^{i}\right)=\frac{2m_{\mathrm{rs}}K_z^{\mathrm{s}}}{m_{\mathrm{rs}}^2K_z^{\mathrm{s}}+K_z^{\mathrm{i}}}\mathrm{e}^{-\mathrm{j}(K_z^{\mathrm{i}}-K_z^{\mathrm{s}})z'}\,, \tag{2.218}$$

where $m_{\mathrm{rs}}=k_{\mathrm{i}}/k_{\mathrm{s}}$ is the relative refractive index of the domain D_{i} with respect to the ambient medium, and the wave vectors $\boldsymbol{K}_{+}^{\mathrm{s}}$ and $\boldsymbol{K}_{+}^{\mathrm{i}}$ (in (2.218)) are related to each other by Snell's law

$$k_{\mathrm{T}}=k_{\mathrm{Ts}}=k_{\mathrm{Ti}}=\sqrt{(K_x^{\mathrm{s}})^2+(K_y^{\mathrm{s}})^2}=\sqrt{(K_x^{\mathrm{i}})^2+(K_y^{\mathrm{i}})^2}\,.$$

Inserting (2.216) and (2.217) into (2.214) and (2.215) yields

$$\begin{bmatrix}A\left(\boldsymbol{K}_{+}^{\mathrm{s}}\right)\\B\left(\boldsymbol{K}_{+}^{\mathrm{s}}\right)\end{bmatrix}=\int_{\boldsymbol{R}^2}\boldsymbol{Q}^{31}\left(\boldsymbol{K}_{+}^{\mathrm{s}},\boldsymbol{K}_{+}^{\mathrm{i}}\right)\begin{bmatrix}C\left(\boldsymbol{K}_{+}^{\mathrm{i}}\right)\\D\left(\boldsymbol{K}_{+}^{\mathrm{i}}\right)\end{bmatrix}\mathrm{d}K_x^{\mathrm{i}}\,\mathrm{d}K_y^{\mathrm{i}}\,, \tag{2.219}$$

where

$$\boldsymbol{Q}^{31}\left(\boldsymbol{K}_{+}^{\mathrm{s}},\boldsymbol{K}_{+}^{\mathrm{i}}\right)=\begin{bmatrix}\left(Q^{31}\left(\boldsymbol{K}_{+}^{\mathrm{s}},\boldsymbol{K}_{+}^{\mathrm{i}}\right)\right)^{11}&\left(Q^{31}\left(\boldsymbol{K}_{+}^{\mathrm{s}},\boldsymbol{K}_{+}^{\mathrm{i}}\right)\right)^{12}\\\left(Q^{31}\left(\boldsymbol{K}_{+}^{\mathrm{s}},\boldsymbol{K}_{+}^{\mathrm{i}}\right)\right)^{21}&\left(Q^{31}\left(\boldsymbol{K}_{+}^{\mathrm{s}},\boldsymbol{K}_{+}^{\mathrm{i}}\right)\right)^{22}\end{bmatrix}$$

and

$$\left(Q^{31}\left(\boldsymbol{K}_{+}^{\mathrm{s}},\boldsymbol{K}_{+}^{\mathrm{i}}\right)\right)^{11}=-\frac{jk_{\mathrm{s}}^2}{8\pi^2}\int_S c(\boldsymbol{K}_{+}^{\mathrm{i}})\left\{\left[\boldsymbol{n}\left(\boldsymbol{r}'\right)\times\boldsymbol{M}\left(\boldsymbol{r}',\boldsymbol{K}_{+}^{\mathrm{i}}\right)\right]\cdot\boldsymbol{N}(-\boldsymbol{r}',\boldsymbol{K}_{+}^{\mathrm{s}})\right.$$
$$\left.+\,m_{\mathrm{rs}}\left[\boldsymbol{n}\left(\boldsymbol{r}'\right)\times\boldsymbol{N}\left(\boldsymbol{r}',\boldsymbol{K}_{+}^{\mathrm{i}}\right)\right]\cdot\boldsymbol{M}(-\boldsymbol{r}',\boldsymbol{K}_{+}^{\mathrm{s}})\right\}\mathrm{d}S\left(\boldsymbol{r}'\right)\,,$$

$$\left(Q^{31}\left(\boldsymbol{K}_{+}^{\mathrm{s}},\boldsymbol{K}_{+}^{\mathrm{i}}\right)\right)^{12}=-\frac{jk_{\mathrm{s}}^2}{8\pi^2}\int_S d(\boldsymbol{K}_{+}^{\mathrm{i}})\left\{\left[\boldsymbol{n}\left(\boldsymbol{r}'\right)\times\boldsymbol{N}\left(\boldsymbol{r}',\boldsymbol{K}_{+}^{\mathrm{i}}\right)\right]\cdot\boldsymbol{N}(-\boldsymbol{r}',\boldsymbol{K}_{+}^{\mathrm{s}})\right.$$
$$\left.+\,m_{\mathrm{rs}}\left[\boldsymbol{n}\left(\boldsymbol{r}'\right)\times\boldsymbol{M}\left(\boldsymbol{r}',\boldsymbol{K}_{+}^{\mathrm{i}}\right)\right]\cdot\boldsymbol{M}(-\boldsymbol{r}',\boldsymbol{K}_{+}^{\mathrm{s}})\right\}\mathrm{d}S\left(\boldsymbol{r}'\right)\,,$$

$$\left(Q^{31}\left(\boldsymbol{K}_{+}^{\mathrm{s}},\boldsymbol{K}_{+}^{\mathrm{i}}\right)\right)^{21}=-\frac{jk_{\mathrm{s}}^2}{8\pi^2}\int_S c(\boldsymbol{K}_{+}^{\mathrm{i}})\left\{\left[\boldsymbol{n}\left(\boldsymbol{r}'\right)\times\boldsymbol{M}\left(\boldsymbol{r}',\boldsymbol{K}_{+}^{\mathrm{i}}\right)\right]\cdot\boldsymbol{M}(-\boldsymbol{r}',\boldsymbol{K}_{+}^{\mathrm{s}})\right.$$
$$\left.+\,m_{\mathrm{rs}}\left[\boldsymbol{n}\left(\boldsymbol{r}'\right)\times\boldsymbol{N}\left(\boldsymbol{r}',\boldsymbol{K}_{+}^{\mathrm{i}}\right)\right]\cdot\boldsymbol{N}(-\boldsymbol{r}',\boldsymbol{K}_{+}^{\mathrm{s}})\right\}\mathrm{d}S\left(\boldsymbol{r}'\right)\,,$$

$$\left(Q^{31}\left(\boldsymbol{K}_{+}^{\mathrm{s}},\boldsymbol{K}_{+}^{\mathrm{i}}\right)\right)^{22}=-\frac{jk_{\mathrm{s}}^{2}}{8\pi^{2}}\int_{S}d(\boldsymbol{K}_{+}^{\mathrm{i}})\left\{\left[\boldsymbol{n}\left(\boldsymbol{r}'\right)\times\boldsymbol{N}\left(\boldsymbol{r}',\boldsymbol{K}_{+}^{\mathrm{i}}\right)\right]\cdot\boldsymbol{M}(-\boldsymbol{r}',\boldsymbol{K}_{+}^{\mathrm{s}})\right.$$
$$\left.+\,m_{\mathrm{rs}}\left[\boldsymbol{n}\left(\boldsymbol{r}'\right)\times\boldsymbol{M}\left(\boldsymbol{r}',\boldsymbol{K}_{+}^{\mathrm{i}}\right)\right]\cdot\boldsymbol{N}(-\boldsymbol{r}',\boldsymbol{K}_{+}^{\mathrm{s}})\right\}\mathrm{d}S\left(\boldsymbol{r}'\right)\,.$$

We note that $(Q^{31})^{\alpha\beta}$, $\alpha,\beta=1,2$, are not functions in the usual sense and relations involving $\boldsymbol{Q}^{31}$ should be understood in a distributional sense. For a plane surface we have

$$\begin{aligned}\left(Q^{31}\left(\boldsymbol{K}_{+}^{\mathrm{s}},\boldsymbol{K}_{+}^{\mathrm{i}}\right)\right)_{\mathrm{plane}}^{11}&=\left(Q^{31}\left(\boldsymbol{K}_{+}^{\mathrm{s}},\boldsymbol{K}_{+}^{\mathrm{i}}\right)\right)_{\mathrm{plane}}^{22}\\&=k_{\mathrm{s}}K_{z}^{\mathrm{s}}\delta\left(K_{x}^{\mathrm{i}}-K_{x}^{\mathrm{s}},K_{y}^{\mathrm{i}}-K_{y}^{\mathrm{s}}\right)\,,\\\left(Q^{31}\left(\boldsymbol{K}_{+}^{\mathrm{s}},\boldsymbol{K}_{+}^{\mathrm{i}}\right)\right)_{\mathrm{plane}}^{11}&=\left(Q^{31}\left(\boldsymbol{K}_{+}^{\mathrm{s}},\boldsymbol{K}_{+}^{i}\right)\right)_{\mathrm{plane}}^{22}=0\end{aligned}$$

and the system of integral equations (2.219) simplifies to a system of algebraic equations

$$\begin{aligned}A\left(\boldsymbol{K}_{+}^{\mathrm{s}}\right)&=k_{\mathrm{s}}K_{z}^{\mathrm{s}}C\left(\boldsymbol{K}_{+}^{\mathrm{i}}\right)\,,\\B\left(\boldsymbol{K}_{+}^{\mathrm{s}}\right)&=k_{\mathrm{s}}K_{z}^{\mathrm{s}}D\left(\boldsymbol{K}_{+}^{\mathrm{i}}\right)\,.\end{aligned}$$

For solving the general case of an arbitrary surface, one has to invert a system of two-dimensional integral transforms and this is a formidable analytic and numerical problem. We can formally assume that the inverse transform exists and represent the solution as

$$\begin{bmatrix}C\left(\boldsymbol{K}_{+}^{\mathrm{i}}\right)\\D\left(\boldsymbol{K}_{+}^{\mathrm{i}}\right)\end{bmatrix}=\int_{\boldsymbol{R}^{2}}\left[\boldsymbol{Q}^{31}\left(\boldsymbol{K}_{+}^{\mathrm{s}},\boldsymbol{K}_{+}^{\mathrm{i}}\right)\right]^{-1}\begin{bmatrix}A\left(\boldsymbol{K}_{+}^{\mathrm{s}}\right)\\B\left(\boldsymbol{K}_{+}^{\mathrm{s}}\right)\end{bmatrix}\mathrm{d}K_{x}^{\mathrm{s}}\,\mathrm{d}K_{y}^{\mathrm{s}}\,.\qquad(2.220)$$

To compute the scattered field we consider (2.213) for $\boldsymbol{r}\in D_{\mathrm{s}}$, expand the free space dyadic Green function in terms of vector plane waves by assuming $z<z_{<}$, and obtain

$$\boldsymbol{E}_{\mathrm{s}}(\boldsymbol{r})=\int_{\boldsymbol{R}^{2}}\left[F(\boldsymbol{K}_{-}^{\mathrm{s}})\boldsymbol{M}(\boldsymbol{r},\boldsymbol{K}_{-}^{\mathrm{s}})+G(\boldsymbol{K}_{-}^{\mathrm{s}})\boldsymbol{N}(\boldsymbol{r},\boldsymbol{K}_{-}^{\mathrm{s}})\right]\frac{\mathrm{d}K_{x}^{\mathrm{s}}\,\mathrm{d}K_{y}^{\mathrm{s}}}{k_{\mathrm{s}}K_{z}^{\mathrm{s}}}\,,\quad(2.221)$$

where the amplitudes $F(\boldsymbol{K}_{-}^{\mathrm{s}})$ and $G(\boldsymbol{K}_{-}^{\mathrm{s}})$ are given by

$$\begin{aligned}F\left(\boldsymbol{K}_{-}^{\mathrm{s}}\right)&=\frac{\mathrm{j}k_{\mathrm{s}}^{2}}{8\pi^{2}}\int_{S}\left\{\left[\boldsymbol{n}(\boldsymbol{r}')\times\boldsymbol{E}_{\mathrm{i}}(\boldsymbol{r}')\right]\cdot\boldsymbol{N}\left(-\boldsymbol{r}',\boldsymbol{K}_{-}^{\mathrm{s}}\right)\right.\\&\left.+\frac{1}{k_{\mathrm{s}}}\left[\boldsymbol{n}\left(\boldsymbol{r}'\right)\times\left(\nabla'\times\boldsymbol{E}_{\mathrm{i}}\left(\boldsymbol{r}'\right)\right)\right]\cdot\boldsymbol{M}\left(-\boldsymbol{r}',\boldsymbol{K}_{-}^{\mathrm{s}}\right)\right\}\mathrm{d}S\left(\boldsymbol{r}'\right)\,,\\G\left(\boldsymbol{K}_{-}^{\mathrm{s}}\right)&=\frac{\mathrm{j}k_{\mathrm{s}}^{2}}{8\pi^{2}}\int_{S}\left\{\left[\boldsymbol{n}(\boldsymbol{r}')\times\boldsymbol{E}_{\mathrm{i}}(\boldsymbol{r}')\right]\cdot\boldsymbol{M}\left(-\boldsymbol{r}',\boldsymbol{K}_{-}^{\mathrm{s}}\right)\right.\\&\left.+\frac{1}{k_{\mathrm{s}}}\left[\boldsymbol{n}\left(\boldsymbol{r}'\right)\times\left(\nabla'\times\boldsymbol{E}_{\mathrm{i}}\left(\boldsymbol{r}'\right)\right)\right]\cdot\boldsymbol{N}\left(-\boldsymbol{r}',\boldsymbol{K}_{-}^{\mathrm{s}}\right)\right\}\mathrm{d}S\left(\boldsymbol{r}'\right)\,.\end{aligned}$$

Inserting the integral representations for $\boldsymbol{n} \times \boldsymbol{E}_{\mathrm{i}}$ and $\boldsymbol{n} \times (\nabla \times \boldsymbol{E}_{\mathrm{i}})$ into the above equations yields a relation between the amplitudes of the field in the domain D_{s}, $F(\boldsymbol{K}^{\mathrm{s}}_{-})$ and $G(\boldsymbol{K}^{\mathrm{s}}_{-})$, and the amplitudes of the field in the domain D_{i}, $C(\boldsymbol{K}^{\mathrm{i}}_{+})$ and $D(\boldsymbol{K}^{\mathrm{i}}_{+})$:

$$\begin{bmatrix} F\left(\boldsymbol{K}^{\mathrm{s}}_{-}\right) \\ G\left(\boldsymbol{K}^{\mathrm{s}}_{-}\right) \end{bmatrix} = \int_{\boldsymbol{R}^2} \boldsymbol{Q}^{11}\left(\boldsymbol{K}^{\mathrm{s}}_{-}, \boldsymbol{K}^{\mathrm{i}}_{+}\right) \begin{bmatrix} C\left(\boldsymbol{K}^{\mathrm{i}}_{+}\right) \\ D\left(\boldsymbol{K}^{\mathrm{i}}_{+}\right) \end{bmatrix} \mathrm{d}K^{\mathrm{i}}_{x}\, \mathrm{d}K^{\mathrm{i}}_{y}\,, \tag{2.222}$$

where

$$\boldsymbol{Q}^{11}\left(\boldsymbol{K}^{\mathrm{s}}_{-}, \boldsymbol{K}^{\mathrm{i}}_{+}\right) = \begin{bmatrix} \left(Q^{11}\left(\boldsymbol{K}^{\mathrm{s}}_{-}, \boldsymbol{K}^{\mathrm{i}}_{+}\right)\right)^{11} & \left(Q^{11}\left(\boldsymbol{K}^{\mathrm{s}}_{-}, \boldsymbol{K}^{\mathrm{i}}_{+}\right)\right)^{12} \\ \left(Q^{11}\left(\boldsymbol{K}^{\mathrm{s}}_{-}, \boldsymbol{K}^{\mathrm{i}}_{+}\right)\right)^{21} & \left(Q^{11}\left(\boldsymbol{K}^{\mathrm{s}}_{-}, \boldsymbol{K}^{\mathrm{i}}_{+}\right)\right)^{22} \end{bmatrix}$$

and

$$\begin{aligned}
\left(Q^{11}\left(\boldsymbol{K}^{\mathrm{s}}_{-}, \boldsymbol{K}^{\mathrm{i}}_{+}\right)\right)^{11} &= \frac{jk_{\mathrm{s}}^2}{8\pi^2} \int_S c(\boldsymbol{K}^{\mathrm{i}}_{+}) \left\{ \left[\boldsymbol{n}\left(\boldsymbol{r}'\right) \times \boldsymbol{M}\left(\boldsymbol{r}', \boldsymbol{K}^{\mathrm{i}}_{+}\right)\right] \cdot \boldsymbol{N}(-\boldsymbol{r}', \boldsymbol{K}^{\mathrm{s}}_{-}) \right. \\
&\quad \left. + m_{\mathrm{rs}} \left[\boldsymbol{n}\left(\boldsymbol{r}'\right) \times \boldsymbol{N}\left(\boldsymbol{r}', \boldsymbol{K}^{\mathrm{i}}_{+}\right)\right] \cdot \boldsymbol{M}(-\boldsymbol{r}', \boldsymbol{K}^{\mathrm{s}}_{-}) \right\} \mathrm{d}S\left(\boldsymbol{r}'\right)\,, \\
\left(Q^{11}\left(\boldsymbol{K}^{\mathrm{s}}_{-}, \boldsymbol{K}^{\mathrm{i}}_{+}\right)\right)^{12} &= \frac{jk_{\mathrm{s}}^2}{8\pi^2} \int_S d(\boldsymbol{K}^{\mathrm{i}}_{+}) \left\{ \left[\boldsymbol{n}\left(\boldsymbol{r}'\right) \times \boldsymbol{N}\left(\boldsymbol{r}', \boldsymbol{K}^{\mathrm{i}}_{+}\right)\right] \cdot \boldsymbol{N}(-\boldsymbol{r}', \boldsymbol{K}^{\mathrm{s}}_{-}) \right. \\
&\quad \left. + m_{\mathrm{rs}} \left[\boldsymbol{n}\left(\boldsymbol{r}'\right) \times \boldsymbol{M}\left(\boldsymbol{r}', \boldsymbol{K}^{\mathrm{i}}_{+}\right)\right] \cdot \boldsymbol{M}(-\boldsymbol{r}', \boldsymbol{K}^{\mathrm{s}}_{-}) \right\} \mathrm{d}S\left(\boldsymbol{r}'\right)\,, \\
\left(Q^{11}\left(\boldsymbol{K}^{\mathrm{s}}_{-}, \boldsymbol{K}^{\mathrm{i}}_{+}\right)\right)^{21} &= \frac{jk_{\mathrm{s}}^2}{8\pi^2} \int_S c(\boldsymbol{K}^{\mathrm{i}}_{+}) \left\{ \left[\boldsymbol{n}\left(\boldsymbol{r}'\right) \times \boldsymbol{M}\left(\boldsymbol{r}', \boldsymbol{K}^{\mathrm{i}}_{+}\right)\right] \cdot \boldsymbol{M}(-\boldsymbol{r}', \boldsymbol{K}^{\mathrm{s}}_{-}) \right. \\
&\quad \left. + m_{\mathrm{rs}} \left[\boldsymbol{n}\left(\boldsymbol{r}'\right) \times \boldsymbol{N}\left(\boldsymbol{r}', \boldsymbol{K}^{\mathrm{i}}_{+}\right)\right] \cdot \boldsymbol{N}(-\boldsymbol{r}', \boldsymbol{K}^{\mathrm{s}}_{-}) \right\} \mathrm{d}S\left(\boldsymbol{r}'\right)\,, \\
\left(Q^{11}\left(\boldsymbol{K}^{\mathrm{s}}_{-}, \boldsymbol{K}^{\mathrm{i}}_{+}\right)\right)^{22} &= \frac{jk_{\mathrm{s}}^2}{8\pi^2} \int_S d(\boldsymbol{K}^{\mathrm{i}}_{+}) \left\{ \left[\boldsymbol{n}\left(\boldsymbol{r}'\right) \times \boldsymbol{N}\left(\boldsymbol{r}', \boldsymbol{K}^{\mathrm{i}}_{+}\right)\right] \cdot \boldsymbol{M}(-\boldsymbol{r}', \boldsymbol{K}^{\mathrm{s}}_{-}) \right. \\
&\quad \left. + m_{\mathrm{rs}} \left[\boldsymbol{n}\left(\boldsymbol{r}'\right) \times \boldsymbol{M}\left(\boldsymbol{r}', \boldsymbol{K}^{\mathrm{i}}_{+}\right)\right] \cdot \boldsymbol{N}(-\boldsymbol{r}', \boldsymbol{K}^{\mathrm{s}}_{-}) \right\} \mathrm{d}S\left(\boldsymbol{r}'\right)\,.
\end{aligned}$$

Combining (2.220) and (2.222) we are led to

$$\begin{aligned}
\begin{bmatrix} F\left(\boldsymbol{K}^{\mathrm{s}}_{-}\right) \\ G\left(\boldsymbol{K}^{\mathrm{s}}_{-}\right) \end{bmatrix} &= \int_{\boldsymbol{R}^2} \int_{\boldsymbol{R}^2} \boldsymbol{Q}^{11}\left(\boldsymbol{K}^{\mathrm{s}}_{-}, \boldsymbol{K}^{\mathrm{i}}_{+}\right) \left[\boldsymbol{Q}^{31}\left(\widetilde{\boldsymbol{K}}^{\mathrm{s}}_{+}, \boldsymbol{K}^{\mathrm{i}}_{+}\right)\right]^{-1} \\
&\qquad \times \begin{bmatrix} A\left(\widetilde{\boldsymbol{K}}^{\mathrm{s}}_{+}\right) \\ B\left(\widetilde{\boldsymbol{K}}^{\mathrm{s}}_{+}\right) \end{bmatrix} \mathrm{d}\widetilde{K}^{\mathrm{s}}_{x}\, \mathrm{d}\widetilde{K}^{\mathrm{s}}_{y}\, \mathrm{d}K^{\mathrm{i}}_{x}\, \mathrm{d}K^{\mathrm{i}}_{y} \\
&= \int_{\boldsymbol{R}^2} \boldsymbol{T}\left(\boldsymbol{K}^{\mathrm{s}}_{-}, \widetilde{\boldsymbol{K}}^{\mathrm{s}}_{+}\right) \begin{bmatrix} A\left(\widetilde{\boldsymbol{K}}^{\mathrm{s}}_{+}\right) \\ B\left(\widetilde{\boldsymbol{K}}^{\mathrm{s}}_{+}\right) \end{bmatrix} \mathrm{d}\widetilde{K}^{\mathrm{s}}_{x}\, \mathrm{d}\widetilde{K}^{\mathrm{s}}_{y}\,,
\end{aligned}$$

where $\boldsymbol{T}(\boldsymbol{K}^{\mathrm{s}}_{-}, \widetilde{\boldsymbol{K}}^{\mathrm{s}}_{+})$ is the $\boldsymbol{T}$-operator of the infinite surface and

$$\boldsymbol{T}\left(\boldsymbol{K}_{-}^{\mathrm{s}}, \widetilde{\boldsymbol{K}}_{+}^{\mathrm{s}}\right)=\int_{\boldsymbol{R}^2} \boldsymbol{Q}^{11}\left(\boldsymbol{K}_{-}^{\mathrm{s}}, \boldsymbol{K}_{+}^{\mathrm{i}}\right)\left[\boldsymbol{Q}^{31}\left(\widetilde{\boldsymbol{K}}_{+}^{\mathrm{s}}, \boldsymbol{K}_{+}^{\mathrm{i}}\right)\right]^{-1} \mathrm{d}K_x^{\mathrm{i}}\,\mathrm{d}K_y^{\mathrm{i}}\,. \tag{2.223}$$

For a plane surface, the above relations simplify considerably and we have

$$\begin{aligned}\left(Q^{11}\left(\boldsymbol{K}_{-}^{\mathrm{s}}, \boldsymbol{K}_{+}^{\mathrm{i}}\right)\right)_{\mathrm{plane}}^{11} &= k_{\mathrm{s}} K_z^{\mathrm{s}} a\left(\boldsymbol{K}_{-}^{\mathrm{s}}\right) \delta\left(K_x^{\mathrm{i}}-K_x^{\mathrm{s}}, K_y^{\mathrm{i}}-K_y^{\mathrm{s}}\right)\,,\\ \left(Q^{11}\left(\boldsymbol{K}_{-}^{\mathrm{s}}, \boldsymbol{K}_{+}^{\mathrm{i}}\right)\right)_{\mathrm{plane}}^{22} &= k_{\mathrm{s}} K_z^{\mathrm{s}} b\left(\boldsymbol{K}_{-}^{\mathrm{s}}\right) \delta\left(K_x^{\mathrm{i}}-K_x^{\mathrm{s}}, K_y^{\mathrm{i}}-K_y^{\mathrm{s}}\right)\,,\end{aligned}$$

and

$$\left(Q^{11}\left(\boldsymbol{K}_{-}^{\mathrm{s}}, \boldsymbol{K}_{+}^{\mathrm{i}}\right)\right)_{\mathrm{plane}}^{11}=\left(Q^{11}\left(\boldsymbol{K}_{-}^{\mathrm{s}}, \boldsymbol{K}_{+}^{\mathrm{i}}\right)\right)_{\mathrm{plane}}^{22}=0\,,$$

where $a(\boldsymbol{K}_{-}^{\mathrm{s}})$ and $b(\boldsymbol{K}_{-}^{\mathrm{s}})$ are the reflection coefficients for a plane interface,

$$\begin{aligned}a\left(\boldsymbol{K}_{-}^{\mathrm{s}}\right) &= \frac{K_z^{\mathrm{s}}-K_z^{\mathrm{i}}}{K_z^{s}+K_z^{i}} \mathrm{e}^{2\mathrm{j}K_z^{\mathrm{s}} z'}\,,\\ b\left(\boldsymbol{K}_{-}^{\mathrm{s}}\right) &= \frac{m_{\mathrm{rs}}^2 K_z^{\mathrm{s}}-K_z^{\mathrm{i}}}{m_{\mathrm{rs}}^2 K_z^{\mathrm{s}}+K_z^{\mathrm{i}}} \mathrm{e}^{2\mathrm{j}K_z^{\mathrm{s}} z'}\,.\end{aligned} \tag{2.224}$$

Thus

$$\begin{aligned}F\left(\boldsymbol{K}_{-}^{\mathrm{s}}\right) &= a\left(\boldsymbol{K}_{-}^{\mathrm{s}}\right) A\left(\boldsymbol{K}_{+}^{\mathrm{s}}\right)\,,\\ G\left(\boldsymbol{K}_{-}^{\mathrm{s}}\right) &= b\left(\boldsymbol{K}_{-}^{\mathrm{s}}\right) B\left(\boldsymbol{K}_{+}^{\mathrm{s}}\right)\,,\end{aligned}$$

and

$$\begin{aligned}\left(\boldsymbol{T}\left(\boldsymbol{K}_{-}^{\mathrm{s}}, \widetilde{\boldsymbol{K}}_{+}^{\mathrm{s}}\right)\right)_{\mathrm{plane}}^{11} &= a\left(\boldsymbol{K}_{-}^{\mathrm{s}}\right) \delta\left(\widetilde{K}_x^{\mathrm{s}}-K_x^{\mathrm{s}}, \widetilde{K}_y^{\mathrm{s}}-K_y^{\mathrm{s}}\right)\,,\\ \left(\boldsymbol{T}\left(\boldsymbol{K}_{-}^{\mathrm{s}}, \widetilde{\boldsymbol{K}}_{+}^{\mathrm{s}}\right)\right)_{\mathrm{plane}}^{22} &= b\left(\boldsymbol{K}_{-}^{\mathrm{s}}\right) \delta\left(\widetilde{K}_x^{\mathrm{s}}-K_x^{\mathrm{s}}, \widetilde{K}_y^{\mathrm{s}}-K_y^{\mathrm{s}}\right)\,,\end{aligned}$$

where the wave vectors $\widetilde{\boldsymbol{K}}_{+}^{\mathrm{s}}$, $\boldsymbol{K}_{-}^{\mathrm{s}}$ and $\boldsymbol{K}_{+}^{\mathrm{i}}$ are related to each other by Snell's law. Actually, if $\widetilde{\boldsymbol{K}}_{+}^{\mathrm{s}}$ is an arbitrary incident wave vector, then $\boldsymbol{K}_{-}^{\mathrm{s}}$ and $\boldsymbol{K}_{+}^{\mathrm{i}}$ represents the reflected and the transmitted wave vectors, respectively. Setting $K_z^{\mathrm{s}}=k_{\mathrm{s}}\cos\beta_0$ and $K_z^{\mathrm{i}}=k_{\mathrm{i}}\cos\beta$, we see that the coefficients $a(\boldsymbol{K}_{-}^{\mathrm{s}})$ and $b(\boldsymbol{K}_{-}^{\mathrm{s}})$ given by (2.224) are the Fresnel reflection coefficients for perpendicular and parallel polarizations, respectively.

The final step of our analysis is the expansion of the scattered field given by (2.221) in terms of regular vector spherical wave functions. Transforming the integration over the rectangular components of the wave vector into an integration over polar angles and using (2.211), gives

$$\boldsymbol{E}_{\mathrm{s}}(\boldsymbol{r})=-\int_0^{2\pi}\int_{\pi/2+\mathrm{j}\infty}^{\pi}\left[G\left(\beta,\alpha\right)\boldsymbol{e}_\beta+\mathrm{j}F\left(\beta,\alpha\right)\boldsymbol{e}_\alpha\right]\mathrm{e}^{\mathrm{j}\boldsymbol{K}_{-}^{\mathrm{s}}\cdot\boldsymbol{r}}\sin\beta\,\mathrm{d}\beta\,\mathrm{d}\alpha\,,$$

where $(k_\mathrm{s}, \beta, \alpha)$ are the spherical coordinates of the wave vector $\boldsymbol{K}_-^\mathrm{s}$. Further, expanding the vector plane waves $\boldsymbol{e}_\beta \exp\left(\mathrm{j}\boldsymbol{K}_-^\mathrm{s} \cdot \boldsymbol{r}\right)$ and $\boldsymbol{e}_\alpha \exp\left(\mathrm{j}\boldsymbol{K}_-^s \cdot \boldsymbol{r}\right)$ in terms of vector spherical wave functions yields

$$\boldsymbol{E}_\mathrm{s}(\boldsymbol{r}) = \sum_{n=1}^{\infty} \sum_{m=-n}^{n} f_{mn}^\mathrm{R} \boldsymbol{M}_{mn}^1 \left(k_\mathrm{s}\boldsymbol{r}\right) + g_{mn}^\mathrm{R} \boldsymbol{N}_{mn}^1 \left(k_\mathrm{s}\boldsymbol{r}\right) , \tag{2.225}$$

where

$$f_{mn}^\mathrm{R} = \frac{4\mathrm{j}^{n+1}}{\sqrt{2n\left(n+1\right)}} \int_0^{2\pi} \int_{\pi/2+\mathrm{j}\infty}^{\pi} \left[G\left(\beta,\alpha\right) m\pi_n^{|m|}(\beta) + F\left(\beta,\alpha\right) \tau_n^{|m|}(\beta)\right] \times \mathrm{e}^{-\mathrm{j}m\alpha} \sin\beta \mathrm{d}\beta \, \mathrm{d}\alpha \,,$$

$$g_{mn}^\mathrm{R} = \frac{4\mathrm{j}^{n+1}}{\sqrt{2n\left(n+1\right)}} \int_0^{2\pi} \int_{\pi/2+\mathrm{j}\infty}^{\pi} \left[G\left(\beta,\alpha\right) \tau_n^{|m|}(\beta) + F\left(\beta,\alpha\right) m\pi_n^{|m|}(\beta)\right] \times \mathrm{e}^{-\mathrm{j}m\alpha} \sin\beta \mathrm{d}\beta \, \mathrm{d}\alpha \,.$$

Thus, the derivation of the vector spherical wave expansion of the electromagnetic field scattered by an arbitrary infinite surface involves the following steps:

1. Representation of the incident field as an integral over vector plane waves.
2. Calculation of the spectral amplitudes of the scattered field by using the $\boldsymbol{T}$-operator equation (2.223).
3. Computation of the vector spherical wave expansion of the scattered field by using (2.225).

Returning to the scattering problem of a particle near an arbitrary infinite surface, we see that our analysis is complete if, according to Step 1, we are able to represent the plane electromagnetic wave $\boldsymbol{E}_\mathrm{e}$ and the radiating vector spherical wave functions $\boldsymbol{M}_{mn}^3$ and $\boldsymbol{N}_{mn}^3$ as integrals over vector plane waves. For $\boldsymbol{E}_\mathrm{e}$, we have

$$\boldsymbol{E}_\mathrm{e}(\boldsymbol{r}) = \int_{\boldsymbol{R}^2} \left[A_\mathrm{e}(\boldsymbol{K}_+^\mathrm{s})\, \boldsymbol{M}(\boldsymbol{r}, \boldsymbol{K}_+^\mathrm{s}) + B_\mathrm{e}(\boldsymbol{K}_+^\mathrm{s})\, \boldsymbol{N}(\boldsymbol{r}, \boldsymbol{K}_+^\mathrm{s})\right] \frac{\mathrm{d}K_x^\mathrm{s}\, \mathrm{d}K_y^\mathrm{s}}{k_\mathrm{s} K_z^\mathrm{s}}$$

with

$$A_\mathrm{e}(\boldsymbol{K}_+^\mathrm{s}) = \mathrm{j}E_{\mathrm{e}0,\alpha} k_\mathrm{s} K_z^\mathrm{s}\, \delta(K_x^\mathrm{s} - K_x^\mathrm{e}, K_y^\mathrm{s} - K_y^\mathrm{e}) \,,$$
$$B_\mathrm{e}(\boldsymbol{K}_+^\mathrm{s}) = -E_{\mathrm{e}0,\beta} k_\mathrm{s} K_z^\mathrm{s}\, \delta(K_x^\mathrm{s} - K_x^\mathrm{e}, K_y^\mathrm{s} - K_y^\mathrm{e}) \,,$$

and $\boldsymbol{K}_+^\mathrm{e} = \boldsymbol{k}_\mathrm{e}$, while for $\boldsymbol{M}_{mn}^3$ and $\boldsymbol{N}_{mn}^3$, we obtain

$$\begin{pmatrix} \boldsymbol{M}_{mn}^3\left(k_\mathrm{s}\boldsymbol{r}\right) \\ \boldsymbol{N}_{mn}^3\left(k_\mathrm{s}\boldsymbol{r}\right) \end{pmatrix} = \int_{\boldsymbol{R}^2} \left[\begin{pmatrix} A_\mathrm{s}(\boldsymbol{K}_+^\mathrm{s}) \\ B_\mathrm{s}(\boldsymbol{K}_+^\mathrm{s}) \end{pmatrix} \boldsymbol{M}(\boldsymbol{r}, \boldsymbol{K}_+^\mathrm{s}) + \begin{pmatrix} B_\mathrm{s}(\boldsymbol{K}_+^\mathrm{s}) \\ A_\mathrm{s}(\boldsymbol{K}_+^\mathrm{s}) \end{pmatrix} \boldsymbol{N}(\boldsymbol{r}, \boldsymbol{K}_+^\mathrm{s}) \right] \times \frac{\mathrm{d}K_x^\mathrm{s}\, \mathrm{d}K_y^\mathrm{s}}{k_\mathrm{s} K_z^\mathrm{s}}$$

with

$$A_{\mathrm{s}}(\boldsymbol{K}_{+}^{\mathrm{s}}) = \frac{1}{2\pi \mathrm{j}^{n+1}} \frac{1}{\sqrt{2n(n+1)}} \tau_n^{|m|}(\beta) \mathrm{e}^{\mathrm{j}m\alpha} \,,$$

$$B_{\mathrm{s}}(\boldsymbol{K}_{+}^{\mathrm{s}}) = \frac{1}{2\pi \mathrm{j}^{n+1}} \frac{1}{\sqrt{2n(n+1)}} m\pi_n^{|m|}(\beta) \mathrm{e}^{\mathrm{j}m\alpha} \,.$$

The $\boldsymbol{T}$-operator solution is a formal solution since we assumed the invertibility of the integral equation (2.219). The usefulness of the formalism in numerical applications depends upon the possibility of discretizing (2.219) in a suitable way. This can be done for a class of simple infinite surfaces as for example plane surfaces or surfaces with periodic roughness and small amplitude roughness. It should be noted that for plane surfaces we obtain exactly the results derived in our earlier analysis.

3

Simulation Results

In this chapter we present computer simulation results for the scattering problems considered in Chap. 2. For the numerical analysis, we use our own software package and some existing electromagnetic scattering programs. After a concise description of the $\boldsymbol{T}$-matrix code, we present the theoretical bases of the electromagnetics programs which we used to verify the accuracy of the new implementation. We then present simulation results for homogeneous, axisymmetric and nonaxisymmetric particles, inhomogeneous, layered and composite particles, and clusters of particles. The last sections deal with scattering by a particle on or near a plane surface and the computation of the effective wave number of a half-space with randomly distributed particles.

3.1 $\boldsymbol{T}$-matrix Program

A Fortran computer program has been written to solve various scattering problems in the framework of the null-field method. This section gives a short description of the code, while more details concerning the significance of the input and output parameters are given in the documentation on CD-ROM.

The main program TMATRIX.f90 calls a $\boldsymbol{T}$-matrix routine for solving a specific scattering problem. These routines computes the $\boldsymbol{T}$-matrix of:

- Homogeneous, dielectric (isotropic, chiral) and perfectly conducting, axisymmetric particles (TAXSYM.f90),
- Homogeneous, dielectric (isotropic, uniaxial anisotropic, chiral) and perfectly conducting, nonaxisymmetric particles (TNONAXSYM.f90)
- Axisymmetric, composite particles (TCOMP.f90)
- Axisymmetric, layered particles (TLAY.f90)
- An inhomogeneous, dielectric, axisymmetric particle with an arbitrarily shaped inclusion (TINHOM.f90)
- An inhomogeneous, dielectric sphere with a spherical inclusion (TINHOM2SPH.f90)

- An inhomogeneous, dielectric sphere with an arbitrarily shaped inclusion (TINHOMSPH.f90)
- An inhomogeneous, dielectric sphere with multiple spherical inclusions (TINHOMSPHREC.f90)
- Clusters of arbitrarily shaped particles (TMULT.f90)
- Two homogeneous, dielectric spheres (TMULT2SPH.f90)
- Clusters of homogeneous, dielectric spheres (TMULTSPH.f90 and TMULTSPHREC.f90)
- Concentrically layered sphere (TSPHERE.f90)
- A homogeneous, dielectric or perfectly conducting, axisymmetric particle on or near a plane surface (TPARTSUB.f90)

Three other routine are invoked by the main program

- SCT.f90 computes the scattering characteristics of a particle using the previously calculated $\boldsymbol{T}$ matrix
- SCTAVRGSPH.f90 computes the scattering characteristics of an ensemble of polydisperse, homogeneous spherical particles
- EFMED.f90 computes the effective wave number of a half-space with randomly distributed particles

Essentially, the code performs a convergence test and computes the $\boldsymbol{T}$-matrix and the scattering characteristics of particles with uniform orientation distribution functions.

An important part of the $\boldsymbol{T}$-matrix calculation is the convergence procedure over the maximum expansion order N_{rank}, maximum azimuthal order M_{rank} and the number of integration points N_{int}. In fact, N_{rank}, M_{rank} and N_{int} are input parameters and their optimal values must be found by the user. This is accomplished by repeated convergence tests based on the analysis of the differential scattering cross-section as discussed in Sect. 2.1.

The scattering characteristics depend on the type of the orientation distribution function. By convention, the uniform distribution function is called complete if the Euler angles α_{p}, β_{p} and γ_{p} are uniformly distributed in the intervals $(0, 360^\circ)$, $(0, 180^\circ)$ and $(0, 360^\circ)$, respectively. The normalization constant is 4π for axisymmetric particles and $8\pi^2$ for nonaxisymmetric particles. The uniform distribution function is called incomplete if the Euler angles α_{p}, β_{p} and γ_{p} are uniformly distributed in the intervals $(\alpha_{\mathrm{p\,min}}, \alpha_{\mathrm{p\,max}})$, $(\beta_{\mathrm{p\,min}}, \beta_{\mathrm{p\,max}})$, and $(\gamma_{\mathrm{p\,min}}, \gamma_{\mathrm{p\,max}})$, respectively. For axisymmetric particles, the orientational average is performed over α_{p} and β_{p}, and the normalization constant is

$$(\alpha_{\mathrm{p\,max}} - \alpha_{\mathrm{p\,min}}) (\cos\beta_{\mathrm{p\,min}} - \cos\beta_{\mathrm{p\,max}}) \ ,$$

while for nonaxisymmetric particles, the orientational average is performed over α_{p}, β_{p} and γ_{p}, and the normalization constant is

$$(\alpha_{\mathrm{p\,max}} - \alpha_{\mathrm{p\,min}}) (\cos\beta_{\mathrm{p\,min}} - \cos\beta_{\mathrm{p\,max}}) (\gamma_{\mathrm{p\,max}} - \gamma_{\mathrm{p\,min}}) \ .$$

The scattering characteristics computed by the code are summarized later.

3.1.1 Complete Uniform Distribution Function

For the complete uniform distribution function, the external excitation is a vector plane wave propagating along the Z-axis of the global coordinate system and the scattering plane is the XZ-plane. The code computes the following orientation-averaged quantities:

- The scattering matrix $\langle \boldsymbol{F} \rangle$ at a set of $N_{\theta,\mathrm{RND}}$ scattering angles
- The extinction matrix $\langle \boldsymbol{K} \rangle$
- The scattering and extinction cross-sections $\langle C_{\mathrm{scat}} \rangle$ and $\langle C_{\mathrm{ext}} \rangle$ and
- The asymmetry parameter $\langle \cos \Theta \rangle$.

The scattering angles, at which the scattering matrix is evaluated, are uniformly spaced in the interval $(\theta_{\mathrm{min,RND}}, \theta_{\mathrm{max,RND}})$. The elements of the scattering matrix are expressed in terms of the ten average quantities

$$\left\langle |S_{\theta\beta}|^2 \right\rangle , \quad \left\langle |S_{\theta\alpha}|^2 \right\rangle , \quad \left\langle |S_{\varphi\beta}|^2 \right\rangle , \quad \left\langle |S_{\varphi\alpha}|^2 \right\rangle , \quad \left\langle S_{\theta\beta} S^*_{\varphi\alpha} \right\rangle ,$$
$$\left\langle S_{\theta\alpha} S^*_{\varphi\beta} \right\rangle , \quad \left\langle S_{\theta\beta} S^*_{\theta\alpha} \right\rangle , \quad \left\langle S_{\theta\beta} S^*_{\varphi\beta} \right\rangle , \quad \left\langle S_{\theta\alpha} S^*_{\varphi\alpha} \right\rangle , \quad \left\langle S_{\varphi\beta} S^*_{\varphi\alpha} \right\rangle$$

for macroscopically isotropic media, and the six average quantities

$$\left\langle |S_{\theta\beta}|^2 \right\rangle , \quad \left\langle |S_{\theta\alpha}|^2 \right\rangle , \quad \left\langle |S_{\varphi\beta}|^2 \right\rangle , \quad \left\langle |S_{\varphi\alpha}|^2 \right\rangle , \quad \left\langle S_{\theta\beta} S^*_{\varphi\alpha} \right\rangle , \quad \left\langle S_{\theta\alpha} S^*_{\varphi\beta} \right\rangle$$

for macroscopically isotropic and mirror-symmetric media. $\langle S_{pq} S^*_{p_1 q_1} \rangle$ are computed at $N_{\theta,\mathrm{GS}}$ scattering angles, which are uniformly spaced in the interval $(0, 180^\circ)$. The scattering matrix is calculated at the same sample angles and polynomial interpolation is used to evaluate the scattering matrix at any polar angle θ in the range $(\theta_{\mathrm{min,RND}}, \theta_{\mathrm{max\,RND}})$. The average quantities $\langle S_{pq} S^*_{p_1 q_1} \rangle$ can be computed by using a numerical procedure or the analytical orientation-averaging approach described in Sect. 1.5. The numerical orientation-averaging procedure chooses the angles α_{p}, β_{p} and γ_{p} to sample the intervals $(0^\circ, 360^\circ)$, $(0^\circ, 180^\circ)$ and $(0^\circ, 360^\circ)$, respectively. The prescription for choosing the angles is to

- Uniformly sample in α_{p}
- Uniformly sample in $\cos\beta_{\mathrm{p}}$ or nonuniformly sample in β_{p}
- Uniformly sample in γ_{p}

The integration over α_{p} and γ_{p} are performed with Simpson's rule, and the number of integration points N_α and N_γ must be odd numbers. The integration over β_{p} can also be performed with Simpson's rule, and in this specific case, the algorithm samples uniformly in $\cos\beta_{\mathrm{p}}$, and the number of integration points N_β is an odd number. Alternatively, Gauss–Legendre quadrature method can be used for averaging over β_{p}, and N_β can be any integer number. For the analytical orientation-averaging approach, the maximum expansion and azimuthal orders N_{rank} and M_{rank} (specifying the dimensions of the $\boldsymbol{T}$

matrix) can be reduced. In this case, a convergence test over the extinction and scattering cross-sections gives the effective values $N_{\text{rank}}^{\text{eff}}$ and $M_{\text{rank}}^{\text{eff}}$.

The orientation-averaged extinction matrix $\langle \boldsymbol{K} \rangle$ is computed by using (1.125) and (1.126), and note that for macroscopically isotropic and mirror-symmetric media the off-diagonal elements are zero and the diagonal elements are equal to the orientation-averaged extinction cross-section per particle.

For macroscopically isotropic and mirror-symmetric media, the orientation-averaged scattering and extinction cross-sections $\langle C_{\text{scat}} \rangle = \langle C_{\text{scat}} \rangle_{\text{I}}$ and $\langle C_{\text{ext}} \rangle = \langle C_{\text{ext}} \rangle_{\text{I}}$ are calculated by using (1.124) and (1.122), respectively, while for macroscopically isotropic media, the code additionally computes $\langle C_{\text{scat}} \rangle_{\text{V}}$ accordingly to (1.133), and $\langle C_{\text{ext}} \rangle_{\text{V}}$ as $\langle C_{\text{ext}} \rangle_{\text{V}} = \langle K_{14} \rangle$.

The asymmetry parameter $\langle \cos \Theta \rangle$ is determined by angular integration over the scattering angle θ. The number of integration points is $N_{\theta,\text{GS}}$ and Simpson's rule is used for calculation. For macroscopically isotropic and mirror-symmetric media, the asymmetry parameter $\langle \cos \Theta \rangle = \langle \cos \Theta \rangle_{\text{I}}$ is calculated by using (1.134), while for macroscopically isotropic media, the code supplementarily computes $\langle \cos \Theta \rangle_{\text{V}}$ accordingly to (1.135).

The physical correctness of the computed results is tested by using the inequalities (1.138) given by Hovenier and van der Mee [103]. The message that the test is not satisfied means that the computed results may be wrong.

The code also computes the average differential scattering cross-sections $\langle \sigma_{\text{dp}} \rangle$ and $\langle \sigma_{\text{ds}} \rangle$ for a specific incident polarization state and at a set of $N_{\theta,\text{GS}}$ scattering angles (cf. (1.136) and (1.137)). These scattering angles are uniformly spaced in the interval $(0°, 180°)$ and coincide with the sample angles at which the average quantities $\langle S_{pq} S_{p_1 q_1}^{*} \rangle$ are computed. The polarization state of the incident vector plane wave is specified by the complex amplitudes $E_{\text{e0},\beta}$ and $E_{\text{e0},\alpha}$, and the differential scattering cross-sections are calculated for the complex polarization unit vector

$$\boldsymbol{e}_{\text{pol}} = \frac{1}{\sqrt{|E_{\text{e0},\beta}|^2 + |E_{\text{e0},\alpha}|^2}} \left(E_{\text{e0},\beta} \boldsymbol{e}_{\beta} + E_{\text{e0},\alpha} \boldsymbol{e}_{\alpha} \right) . \tag{3.1}$$

Note that $N_{\theta,\text{GS}}$ is the number of scattering angles at which $\langle S_{pq} S_{p_1 q_1}^{*} \rangle$, $\langle \sigma_{\text{dp}} \rangle$ and $\langle \sigma_{\text{ds}} \rangle$ are computed, and also gives the number of integration points for calculating $\langle C_{\text{scat}} \rangle_{\text{V}}$, $\langle \cos \Theta \rangle_{\text{I}}$ and $\langle \cos \Theta \rangle_{\text{V}}$. Because the integrals are computed with Simpson's rule, $N_{\theta,\text{GS}}$ must be an odd number.

3.1.2 Incomplete Uniform Distribution Function

For the incomplete uniform distribution function, we use a global coordinate system to specify both the direction of propagation and the states of polarization of the incident and scattered waves, and the particle orientation. A special orientation with a constant orientation angle can be specified by setting $N_{\delta} = 1$ and $\delta_{\min} = \delta_{\max}$, where δ stands for α_{p}, β_{p} and γ_{p}. For example,

uniform particle orientation distributions around the Z-axis can be specified by setting $N_\beta = 1$ and $\beta_{\mathrm{p}\,\min} = \beta_{\mathrm{p}\,\max}$.

The scattering characteristics are averaged over the particle orientation by using a numerical procedure. The prescriptions for choosing the sample angles and the significance of the parameters are as in Sect. 3.1.1. For each particle orientation we compute the following quantities:

- The phase matrix $\boldsymbol{Z}$ at N_φ scattering planes
- The extinction matrix $\boldsymbol{K}$ for a plane wave incidence
- The scattering and extinction cross-sections C_{scat} and C_{ext} for incident parallel and perpendicular linear polarizations
- The mean direction of propagation of the scattered field $\boldsymbol{g}$ for incident parallel and perpendicular linear polarizations

The azimuthal angles describing the positions of the scattering planes at which the phase matrix is computed are $\varphi(1)$, $\varphi(2), \ldots, \varphi(N_\varphi)$. In each scattering plane i, $i = 1, 2, \ldots, N_\varphi$, the number of zenith angles is $N_\theta(i)$, while the zenith angle varies between $\theta_{\min}(i)$ and $\theta_{\max}(i)$. For each particle orientation, the phase and extinction matrices $\boldsymbol{Z}$ and $\boldsymbol{K}$ are computed by using (1.77) and (1.79), respectively, while the scattering and extinction cross-sections C_{scat} and C_{ext} are calculated accordingly to (1.101) and (1.100), respectively.

The mean direction of propagation of the scattered field $\boldsymbol{g}$ is evaluated by angular integration over the scattering angles θ and φ (cf. (1.87)), and the numbers of integration points are $N_{\theta,\mathrm{asym}}$ and $N_{\varphi,\mathrm{asym}}$. The integration over φ is performed with Simpson's rule, while the integration over θ can be performed with Simpson's rule or Gauss–Legendre quadrature method. We note that the optical cross-sections and the mean direction of propagation of the scattered field are computed for linearly polarized incident waves (vector plane waves and Gaussian beams) by choosing $\alpha_{\mathrm{pol}} = 0^\circ$ and $\alpha_{\mathrm{pol}} = 90^\circ$ (cf. (1.18)).

The code also calculates the average differential scattering cross-sections σ_{dp} and σ_{ds} in the azimuthal plane φ_{GS} and at a set of $N_{\theta,\mathrm{GS}}$ scattering angles. The average differential scattering cross-sections can be computed for scattering angles ranging from 0° to 180° in the azimuthal plane φ_{GS} and from 180° to 0° in the azimuthal plane $\varphi_{\mathrm{GS}} + 180^\circ$, or for scattering angles ranging from 0° to 180° in the azimuthal plane φ_{GS}. The calculations are performed for elliptically polarized vector plane waves (characterized by the complex polarization unit vector $\boldsymbol{e}_{\mathrm{pol}}$ as in (3.1)) and linearly polarized Gaussian beams (characterized by the polarization angle α_{pol}).

For spherical particles, the code chooses a single orientation $\alpha_{\mathrm{p}\,\min} = \alpha_{\mathrm{p}\,\max} = 0^\circ$, $\beta_{\mathrm{p}\,\min} = \beta_{\mathrm{p}\,\max} = 0^\circ$ and $\gamma_{\mathrm{p}\,\min} = \gamma_{\mathrm{p}\,\max} = 0^\circ$, and sets $M_{\mathrm{rank}} = N_{\mathrm{rank}}$.

The codes perform calculations with double- or extended-precision floating point variables. The extended-precision code is slower than the double-precision version by a factor of 5–6, but allow scattering computations for substantially larger particles. It should also be mentioned that the

CPU time consumption rapidly increases with increasing particle size and asphericity.

The program is written in a modular form, so that modifications, if required, should be fairly straightforward. In this context, the integration routines, the routines for computing spherical and associated Legendre functions or the routines for solving linear systems of equations can be replaced by more efficient routines.

The main "drawback" of the code is that the computer time requirements might by higher in comparison to other more optimized $\boldsymbol{T}$-matrix programs. Our intention was to cover a large class of electromagnetic scattering problem and therefore we sacrifice the speed in favor of the flexibility and code modularization. The code shares several modules which are of general use and are not devoted to a specific application.

3.2 Electromagnetics Programs

The on-line directories created by Wriedt [266] and Flatau [67] provide links to several electromagnetics programs. In order to validate our software package we consider several computer programs relying on different methods. This section briefly reviews these methods without entering into deep details. More information can be found in the literature cited.

3.2.1 $\boldsymbol{T}$-matrix Programs

Computer programs using the null-field method to calculate the electromagnetic scattering by homogeneous, axisymmetric particles have been given by Barber and Hill [8]. These programs compute:

- The angular scattering over a designated scattering plane or in all directions for a particle in a fixed orientation
- The angular scattering and the optical cross-sections for an ensemble of particles randomly oriented in a 2D plane or in 3D
- The scattering matrix elements for an ensemble of particles randomly oriented in 3D
- The normalized scattering cross-sections versus size parameter for a particle in fixed or random orientation
- The internal intensity distribution in the equatorial plane of a spheroidal particle

We would like to mention that the general program structure and some programming solutions given by Barber and Hill have been adopted in our computer code.

The $\boldsymbol{T}$-matrix codes developed by Mishchenko and Travis [167] and Mishchenko et al. [168, 169] are efficient numerical tools for computing electromagnetic scattering by homogeneous, axisymmetric particles with size

significantly larger than a wavelength. The following computer programs are available on the World Wide Web at www.giss.nasa.gov/~crimim:

- A Fortran code for computing the amplitude and phase matrices for a homogeneous, axisymmetric particle in an arbitrary orientation
- A Fortran code for computing the far-field scattering and absorption characteristics of a polydisperse ensemble of randomly oriented, homogeneous, axisymmetric particles

The last code is suitable for practical applications requiring the knowledge of size-, shape-, and orientation-averaged quantities such as the optical cross-sections and phase and scattering matrix elements. The implementation of the analytical orientation-averaging procedure makes this code the fastest computer program for randomly oriented, axisymmetric particles. The following computer programs are also provided at the w site www.giss.nasa.gov/~crimim:

- A Lorenz–Mie code for computing the scattering characteristics of an ensemble of polydisperse, homogeneous, spherical particles and
- The Fortran code SCSMTM for computing the $\boldsymbol{T}$-matrix of a sphere cluster and the orientation-averaged scattering matrix and optical cross-sections [153]

3.2.2 MMP Program

MMP is a Fortran code developed by Hafner and Bomholt [94] which uses the multiple multipole method for solving arbitrary 3D electromagnetic problems. In the multiple multipole method, the electromagnetic fields are expressed as linear combinations of spherical wave fields corresponding to multipole sources. By locating these sources away from the boundary, the multipole expansions are smooth on the surface and the boundary singularities are avoided. The multipoles describing the internal field are located outside the particle, while the multipoles describing the scattered field are positioned inside the particle. Not only spherical multipoles can be used for field expansions; other discrete sources as for instance distributed vector spherical wave functions, vector Mie potentials or magnetic and electric dipoles can be employed. Therefore, other names for similar concepts have been given, e.g., method of auxiliary sources [275], discrete sources method [49, 62], fictitious sources method [140, 158], or Yasuura method [113]. An overview of the discrete sources method has been given by Wriedt [267] and a review of the latest literature in this field has been published by Fairweather et al. [63]. By convention, we categorize the multiple multipole method as a discrete sources method with multiple vector spherical wave functions. Below we summarize the basic concepts of the discrete sources method for the transmission boundary-value problem.

Let $\{\boldsymbol{\Psi}_\mu^3, \boldsymbol{\Phi}_\mu^3\}$ be a system of radiating solutions to the Maxwell equations in D_s with the properties $\nabla \times \boldsymbol{\Psi}_\mu^3 = k_\mathrm{s}\boldsymbol{\Phi}_\mu^3$ and $\nabla \times \boldsymbol{\Phi}_\mu^3 = k_\mathrm{s}\boldsymbol{\Psi}_\mu^3$. Analogously,

let $\{\boldsymbol{\Psi}_\mu^1, \boldsymbol{\Phi}_\mu^1\}$ be a system of regular solutions to the Maxwell equations in D_i satisfying $\nabla \times \boldsymbol{\Psi}_\mu^1 = k_\mathrm{i}\boldsymbol{\Phi}_\mu^1$ and $\nabla \times \boldsymbol{\Phi}_\mu^1 = k_\mathrm{i}\boldsymbol{\Psi}_\mu^1$. For the transmission boundary-value problem, the system of vector functions

$$\left\{ \begin{pmatrix} \boldsymbol{n} \times \boldsymbol{\Psi}_\mu^{3,1} \\ -\mathrm{j}\sqrt{\frac{\epsilon_{\mathrm{s,i}}}{\mu_{\mathrm{s,i}}}}\boldsymbol{n} \times \boldsymbol{\Phi}_\mu^{3,1} \end{pmatrix}, \quad \begin{pmatrix} \boldsymbol{n} \times \boldsymbol{\Phi}_\mu^{3,1} \\ -\mathrm{j}\sqrt{\frac{\epsilon_{\mathrm{s,i}}}{\mu_{\mathrm{s,i}}}}\boldsymbol{n} \times \boldsymbol{\Psi}_\mu^{3,1} \end{pmatrix}, \quad \mu = 1, 2, \ldots \right\} \tag{3.2}$$

is assumed to be complete and linearly independent in $\mathfrak{L}^2_{\tan}(S)$, where $\mathfrak{L}^2_{\tan}(S)$ is the product space $\mathfrak{L}^2_{\tan}(S) = \mathcal{L}^2_{\tan}(S) \times \mathcal{L}^2_{\tan}(S)$ endowed with the scalar product

$$\left\langle \begin{pmatrix} \boldsymbol{x}^1 \\ \boldsymbol{x}^2 \end{pmatrix}, \quad \begin{pmatrix} \boldsymbol{y}^1 \\ \boldsymbol{y}^2 \end{pmatrix} \right\rangle_{2,S} = \left\langle \boldsymbol{x}^1, \boldsymbol{y}^1 \right\rangle_{2,S} + \left\langle \boldsymbol{x}^1, \boldsymbol{y}^1 \right\rangle_{2,S}$$

and $\mathcal{L}^2_{\tan}(S)$ is the space of square integrable tangential fields on the surface S. Approximate solutions to the scattered and internal fields are sought as linear combinations of basis functions (3.2),

$$\begin{pmatrix} \boldsymbol{E}^N_{\mathrm{s,i}}(\boldsymbol{r}) \\ \boldsymbol{H}^N_{\mathrm{s,i}}(\boldsymbol{r}) \end{pmatrix} = \sum_{\mu=1}^{N} a_\mu^{\mathrm{s,i}N} \begin{pmatrix} \boldsymbol{\Psi}_\mu^{3,1}(\boldsymbol{r}) \\ -\mathrm{j}\sqrt{\frac{\epsilon_{\mathrm{s,i}}}{\mu_{\mathrm{s,i}}}}\boldsymbol{\Phi}_\mu^{3,1}(\boldsymbol{r}) \end{pmatrix} + b_\mu^{\mathrm{s,i}N} \begin{pmatrix} \boldsymbol{\Phi}_\mu^{3,1}(\boldsymbol{r}) \\ -\mathrm{j}\sqrt{\frac{\epsilon_{\mathrm{s,i}}}{\mu_{\mathrm{s,i}}}}\boldsymbol{\Psi}_\mu^{3,1}(\boldsymbol{r}) \end{pmatrix}, \quad \boldsymbol{r} \in \overline{D}_{\mathrm{s,i}} .$$

The approximate electric and magnetic fields $\boldsymbol{E}^N_\mathrm{s}$ and $\boldsymbol{H}^N_\mathrm{s}$ are expressed in terms of discrete sources fields with singularities distributed in D_i, and therefore $\boldsymbol{E}^N_\mathrm{s}$ and $\boldsymbol{H}^N_\mathrm{s}$ are analytic in $\overline{D}_\mathrm{s}$. Analogously, the approximate electric and magnetic fields $\boldsymbol{E}^N_\mathrm{i}$ and $\boldsymbol{H}^N_\mathrm{i}$ are expressed in terms of discrete sources fields distributed in D_s, and $\boldsymbol{E}^N_\mathrm{i}$and $\boldsymbol{H}^N_\mathrm{i}$ are analytic in $\overline{D}_\mathrm{i}$. Then, using the Stratton–Chu representation theorem and the continuity conditions on the particle surface, we obtain the estimate

$$\begin{aligned} &\left\|\boldsymbol{E}_\mathrm{s} - \boldsymbol{E}^N_\mathrm{s}\right\|_{\infty,G_\mathrm{s}} + \left\|\boldsymbol{H}_\mathrm{s} - \boldsymbol{H}^N_\mathrm{s}\right\|_{\infty,G_\mathrm{s}} \\ &\quad + \left\|\boldsymbol{E}_\mathrm{i} - \boldsymbol{E}^N_\mathrm{i}\right\|_{\infty,G_\mathrm{i}} + \left\|\boldsymbol{H}_\mathrm{i} - \boldsymbol{H}^N_\mathrm{i}\right\|_{\infty,G_\mathrm{i}} \\ &\leq C \Big(\left\|\boldsymbol{n} \times \boldsymbol{E}^N_\mathrm{s} + \boldsymbol{n} \times \boldsymbol{E}_\mathrm{e} - \boldsymbol{n} \times \boldsymbol{E}^N_\mathrm{i}\right\|_{2,S} \\ &\quad + \left\|\boldsymbol{n} \times \boldsymbol{H}^N_\mathrm{s} + \boldsymbol{n} \times \boldsymbol{H}_\mathrm{e} - \boldsymbol{n} \times \boldsymbol{H}^N_\mathrm{i}\right\|_{2,S} \Big) \end{aligned} \tag{3.3}$$

in any closed sets $G_\mathrm{s} \subset D_\mathrm{s}$ and $G_\mathrm{i} \subset D_\mathrm{i}$, where $\|.\|_{\infty,G}$ stands for the supremum norm, $\|\boldsymbol{a}\|_{\infty,G} = \max_{\boldsymbol{r}\in G} |\boldsymbol{a}(\boldsymbol{r})|$. The estimate (3.3) reflects the basic principle of the discrete sources method: an approximate solution to the transmission boundary-value problem minimizes the residual electric and magnetic fields on the particle surface. Due to the completeness property of the

system of vector functions (3.2), the expansion coefficients $a_\mu^{\mathrm{s,i}N}$ and $b_\mu^{\mathrm{s,i}N}$, $\mu = 1, 2, \ldots, N$, can be determined by solving the minimization problem,

$$\begin{bmatrix} a_\mu^{\mathrm{s,i}N} \\ b_\mu^{\mathrm{s,i}N} \end{bmatrix} = \arg\min \Big\{ \big\| \boldsymbol{n} \times \boldsymbol{E}_{\mathrm{s}}^N + \boldsymbol{n} \times \boldsymbol{E}_{\mathrm{e}} - \boldsymbol{n} \times \boldsymbol{E}_{\mathrm{i}}^N \big\|_{2,S}^2 + \big\| \boldsymbol{n} \times \boldsymbol{H}_{\mathrm{s}}^N + \boldsymbol{n} \times \boldsymbol{H}_{\mathrm{e}} - \boldsymbol{n} \times \boldsymbol{H}_{\mathrm{i}}^N \big\|_{2,S}^2 \Big\} .$$

This minimization problem leads to a system of normal equations for the expansion coefficients. Experience has shown that this technique often gives inaccurate and numerically unstable results with highly oscillating error distributions along the boundary surface. Accurate and stable results can be obtained by using the point matching method with an overdetermined system of equations, that is, the boundary conditions are fulfilled at a set of surface points, while the number of surface points exceeds the number of unknowns (more than twice). The resulting system of equations is solved in the least-squares sense by using, for example, the QR-factorization.

The main problem in the multiple multipole method is the choice of the number, position and the order of multipoles, and the distribution of matching points. Some useful criteria can be summarized as follows. Firstly, the matching points on the boundary should be set with enough density, and the intervals between adjacent pairs of matching points must be far less than the wavelength, for suppressing errors of expansion on the boundary. Secondly, the poles should be neither too near nor too far from the boundary, since the former requirement may avoid alternative errors corresponding to nonphysical rough solution on that interval; and a well-conditioned matrix will be formulated with the latter requirement. In view of the quasi-local behavior of a multipole expansion, only a restricted area around its origin is influenced by this pole, so that a reasonable scheme is to let the area of influence of each pole fit a portion of the boundary, but the whole boundary must be covered by the areas of influence of all the poles. Finally, the highest order of a pole is limited by the density of matching points covered by its area of influence. It should be noted that the MMP code contains routines for automatically optimizing the number, location and order of multipoles. More detailed overviews on methodology, code and simulation technique can be found in the works of Ludwig [147, 148], Hafner [91] and Bomholt [18]. The attractiveness and simplicity of the physical idea of the MMP and the public availability of the code by Hafner [92, 93] have resulted in widespread applications of this technique.

In addition to the MMP code, the DSM (discrete sources method) code developed by Eremin and Orlov [61] will be used for computer simulations. This DSM code is devoted to the analysis of homogeneous, axisymmetric particles using distributed vector spherical wave functions. For highly elongated particles, the sources are distributed along the axis of symmetry of the particle, while for highly flattened particles, the sources are distributed in the complex plane (see Appendix B).

3.2.3 DDSCAT Program

DDSCAT is a freely available software package which applies the discrete dipole approximation (DDA) to calculate scattering and absorption of electromagnetic waves by particles with arbitrary geometries and complex refractive indices [55]. The discrete dipole approximation model the particle as an array of polarizable points and DDSCAT allows accurate calculations for particles with size parameter $k_{\mathrm{s}}a < 15$, provided the refractive index m_{r} is not large compared to unity, $|m_{\mathrm{r}} - 1| < 1$. The discrete dipole approximation (sometimes referred to as the coupled dipole method (CDM)) was apparently first proposed by Purcell and Pennypacker [197]. The theory was reviewed and developed further by Draine [53], Draine and Goodman [56] and Draine and Flatau [54]. An improvement of this method was given by Piller and Martin [194] applying concepts from sampling theory, while Varadan et al. [237], Lakhtakia [130] and Piller [192] extended the discrete dipole approximation to anisotropic, bi-anisotropic and high-permittivity materials, respectively. Since the discrete dipole approximation can be derived from the volume integral equation we follow the analysis of Lakhtakia and Mulholland [131] and review the basic concepts of the volume integral equation method and the discrete dipole approximation.

The volume integral equation method relies on the integral representation for the electric field

$$\boldsymbol{E}(\boldsymbol{r}) = \boldsymbol{E}_{\mathrm{e}}(\boldsymbol{r}) + k_{\mathrm{s}}^2 \int_{D_{\mathrm{i}}} \overline{\boldsymbol{G}}(k_{\mathrm{s}}, \boldsymbol{r}, \boldsymbol{r}') \cdot \left[m_{\mathrm{r}}^2(\boldsymbol{r}') - 1\right] \boldsymbol{E}(\boldsymbol{r}') \, \mathrm{d}V(\boldsymbol{r}') \,, \quad \boldsymbol{r} \in D_{\mathrm{s}} \cup D_{\mathrm{i}} \,.$$

The domain D_{i} is discretized into simply connected elements (cells) $D_{\mathrm{i},m}$, $m = 1, 2, \ldots, N_{\mathrm{cells}}$, and $D_{\mathrm{i}} = \cup_{m=1}^{N_{\mathrm{cells}}} D_{\mathrm{i},m}$. Each element $D_{\mathrm{i},m}$ is modeled as being homogeneous such that $m_{\mathrm{r}}(\boldsymbol{r}) = m_{\mathrm{r},m}$ for $\boldsymbol{r} \in D_{\mathrm{i},m}$, even though this assumption can lead to an artificial material discontinuity across the interface of two adjacent elements. As a consequence of the discretization process, the element equation reads as

$$\boldsymbol{E}(\boldsymbol{r}) = \boldsymbol{E}_{\mathrm{e}}(\boldsymbol{r}) + k_{\mathrm{s}}^2 \left(m_{\mathrm{r},m}^2 - 1\right) \int_{D_{\mathrm{i},m}} \overline{\boldsymbol{G}}(k_{\mathrm{s}}, \boldsymbol{r}, \boldsymbol{r}') \cdot \boldsymbol{E}(\boldsymbol{r}') \, \mathrm{d}V(\boldsymbol{r}')$$
$$+ k_{\mathrm{s}}^2 \sum_{n=1, n\neq m}^{N_{\mathrm{cells}}} \left(m_{\mathrm{r},n}^2 - 1\right) \int_{D_{\mathrm{i},n}} \overline{\boldsymbol{G}}(k_{\mathrm{s}}, \boldsymbol{r}, \boldsymbol{r}') \cdot \boldsymbol{E}(\boldsymbol{r}') \, \mathrm{d}V(\boldsymbol{r}') \,, \quad \boldsymbol{r} \in D_{\mathrm{i},m} \,.$$

Due to the singularity at $\boldsymbol{r}' = \boldsymbol{r}$ it is necessary to approximate the integral

$$\mathcal{E}_m(\boldsymbol{r}) = \int_{D_{\mathrm{i},m}} \overline{\boldsymbol{G}}(k_{\mathrm{s}}, \boldsymbol{r}, \boldsymbol{r}') \cdot \boldsymbol{E}(\boldsymbol{r}') \, \mathrm{d}V(\boldsymbol{r}') \,, \quad \boldsymbol{r} \in D_{\mathrm{i},m}$$

analytically in a small volume around the singularity. With D_{r} being a sphere of radius r around the singularity, we transform the integral as follows:

$$\begin{aligned}\mathcal{E}_m(\boldsymbol{r}) = &\int_{D_{\mathrm{i},m}-D_\mathrm{r}} \overline{\boldsymbol{G}}(k_\mathrm{s},\boldsymbol{r},\boldsymbol{r}')\cdot\boldsymbol{E}(\boldsymbol{r}')\,\mathrm{d}V(\boldsymbol{r}')\\ &+\int_{D_\mathrm{r}} \overline{\boldsymbol{G}}(k_\mathrm{s},\boldsymbol{r},\boldsymbol{r}')\cdot[\boldsymbol{E}(\boldsymbol{r}')-\boldsymbol{E}(\boldsymbol{r})]\,\mathrm{d}V(\boldsymbol{r}')\\ &+\int_{D_\mathrm{r}} \left[\overline{\boldsymbol{G}}(k_\mathrm{s},\boldsymbol{r},\boldsymbol{r}')-\overline{\boldsymbol{G}}_\mathrm{s}(k_\mathrm{s},\boldsymbol{r},\boldsymbol{r}')\right]\cdot\boldsymbol{E}(\boldsymbol{r})\,\mathrm{d}V(\boldsymbol{r}')\\ &+\int_{D_\mathrm{r}} \overline{\boldsymbol{G}}_\mathrm{s}(k_\mathrm{s},\boldsymbol{r},\boldsymbol{r}')\cdot\boldsymbol{E}(\boldsymbol{r})\,\mathrm{d}V(\boldsymbol{r}')\,, \end{aligned}\tag{3.4}$$

where $\overline{\boldsymbol{G}}_\mathrm{s}$ is an auxiliary dyad, and

$$\overline{\boldsymbol{G}}_\mathrm{s}(k_\mathrm{s},\boldsymbol{r},\boldsymbol{r}') = \frac{1}{k_\mathrm{s}^2}\nabla'\otimes\nabla'\left(\frac{1}{4\pi\,|\boldsymbol{r}'-\boldsymbol{r}|}\right).$$

The first term in (3.4) is a nonsingular integral that can be computed numerically. When the integration volume $D_{\mathrm{i},m}$ is spherical and sufficiently small, we can set $D_{\mathrm{i},m} = D_\mathrm{r}$ and the first term is zero. For the third term, we use the coordinate-free representations

$$\begin{aligned}\overline{\boldsymbol{G}}(k_\mathrm{s},\boldsymbol{r},\boldsymbol{r}') = \Bigg\{&\left[1+\frac{\mathrm{j}}{k_\mathrm{s}R}-\frac{1}{(k_\mathrm{s}R)^2}\right]\overline{\boldsymbol{I}}\\ &-\left[1+\frac{3\mathrm{j}}{k_\mathrm{s}R}-\frac{3}{(k_\mathrm{s}R)^2}\right]\boldsymbol{e}_R\otimes\boldsymbol{e}_R\Bigg\}\,g(R)\end{aligned}$$

and

$$\overline{\boldsymbol{G}}_\mathrm{s}(k_\mathrm{s},\boldsymbol{r},\boldsymbol{r}') = \frac{1}{(k_\mathrm{s}R)^2}\left(\overline{\boldsymbol{I}}-3\boldsymbol{e}_R\otimes\boldsymbol{e}_R\right)\frac{1}{4\pi R},$$

where $\boldsymbol{R}=\boldsymbol{r}-\boldsymbol{r}'$, $R=|\boldsymbol{R}|$, $\boldsymbol{e}_R=\boldsymbol{R}/R$ and $g(R)=\exp(\mathrm{j}k_\mathrm{s}R)/(4\pi R)$, and obtain

$$\int_{D_\mathrm{r}}\left[\overline{\boldsymbol{G}}(k_\mathrm{s},\boldsymbol{r},\boldsymbol{r}')-\overline{\boldsymbol{G}}_\mathrm{s}(k_\mathrm{s},\boldsymbol{r},\boldsymbol{r}')\right]\cdot\boldsymbol{E}(\boldsymbol{r})\,\mathrm{d}V(\boldsymbol{r}') = M\boldsymbol{E}(\boldsymbol{r})$$

with

$$M = \frac{2}{3k_\mathrm{s}^2}\left[(1-\mathrm{j}k_\mathrm{s}r)\,\mathrm{e}^{\mathrm{j}k_\mathrm{s}r}-1\right].$$

For the last term, the dyadic identity

$$\int_D \nabla'\otimes\boldsymbol{a}\,\mathrm{d}V = \int_S \boldsymbol{n}\otimes\boldsymbol{a}\,\mathrm{d}S$$

with $\boldsymbol{a}=(1/k_\mathrm{s}^2)\nabla'(1/(4\pi|\boldsymbol{r}'-\boldsymbol{r}|))$, yields

$$\int_{D_\mathrm{r}} \overline{\boldsymbol{G}}_\mathrm{s}\left(k_\mathrm{s},\boldsymbol{r},\boldsymbol{r}'\right)\cdot\boldsymbol{E}\left(\boldsymbol{r}\right)\mathrm{d}V\left(\boldsymbol{r}'\right) = -\frac{1}{k_\mathrm{s}^2}\int_{S_\mathrm{r}} \boldsymbol{n}\left(\boldsymbol{r}'\right)\left(\frac{\boldsymbol{r}'-\boldsymbol{r}}{4\pi\left|\boldsymbol{r}'-\boldsymbol{r}\right|^3}\right)\cdot\boldsymbol{E}\left(\boldsymbol{r}\right)\mathrm{d}S\left(\boldsymbol{r}'\right)$$
$$= -\frac{1}{k_\mathrm{s}^2}L\boldsymbol{E}\left(\boldsymbol{r}\right)\,,$$

where

$$L = \frac{1}{3}\,.$$

The usual tradition is to neglect the second term assuming that the field is constant or claiming that as the integration volume becomes small the integrand vanishes. As pointed out by Draine and Goodman [56], vanishing of the second term is of the same order as with the third term and cannot be omitted. Using the second-order Taylor expansion for each Cartesian component $\boldsymbol{E}_k$ of $\boldsymbol{E}$,

$$\boldsymbol{E}_k\left(\boldsymbol{r}'\right) = \boldsymbol{E}_k\left(\boldsymbol{r}\right) + \left(\boldsymbol{r}'-\boldsymbol{r}\right)\cdot\nabla\boldsymbol{E}_k\left(\boldsymbol{r}\right) + \frac{1}{2}\left(\boldsymbol{r}'-\boldsymbol{r}\right)\cdot\left[\left(\boldsymbol{r}'-\boldsymbol{r}\right)\cdot\nabla\right]\nabla\boldsymbol{E}_k\left(\boldsymbol{r}\right)\,,$$

and the vector Helmholtz equation

$$\triangle\boldsymbol{E} + m_{\mathrm{r},m}^2 k_\mathrm{s}^2\boldsymbol{E} = 0\,,\quad \text{in}\quad D_{\mathrm{i},m}$$

we obtain [185]

$$\int_{D_\mathrm{r}} \overline{\boldsymbol{G}}\left(k_\mathrm{s},\boldsymbol{r},\boldsymbol{r}'\right)\cdot\left[\boldsymbol{E}\left(\boldsymbol{r}'\right)-\boldsymbol{E}\left(\boldsymbol{r}\right)\right]\mathrm{d}V\left(\boldsymbol{r}'\right) = M_1\boldsymbol{E}\left(\boldsymbol{r}\right)$$

with

$$M_1 = \frac{m_{\mathrm{r},m}^2}{k_\mathrm{s}^2}\left\{\left[1-\mathrm{j}k_\mathrm{s}r-\frac{7}{15}\left(k_\mathrm{s}r\right)^2+\frac{2}{15}\mathrm{j}\left(k_\mathrm{s}r\right)^3\right]\mathrm{e}^{\mathrm{j}k_\mathrm{s}r}-1\right\}\,.$$

The final result is

$$\mathcal{E}_m\left(\boldsymbol{r}\right) = \left(M+M_1-\frac{1}{k_\mathrm{s}^2}L\right)\boldsymbol{E}\left(\boldsymbol{r}\right) + \int_{D_{\mathrm{i},m}-D_\mathrm{r}} \overline{\boldsymbol{G}}\left(k_\mathrm{s},\boldsymbol{r},\boldsymbol{r}'\right)\cdot\boldsymbol{E}\left(\boldsymbol{r}'\right)\mathrm{d}V\left(\boldsymbol{r}'\right)$$

and the element equation read as

$$\left[1-k_\mathrm{s}^2\left(m_{\mathrm{r},m}^2-1\right)\left(M+M_1-\frac{1}{k_\mathrm{s}^2}L\right)\right]\boldsymbol{E}\left(\boldsymbol{r}\right)$$
$$-k_\mathrm{s}^2\left(m_{\mathrm{r},m}^2-1\right)\int_{D_{\mathrm{i},m}-D_\mathrm{r}} \overline{\boldsymbol{G}}\left(k_\mathrm{s},\boldsymbol{r},\boldsymbol{r}'\right)\cdot\boldsymbol{E}\left(\boldsymbol{r}'\right)\mathrm{d}V\left(\boldsymbol{r}'\right)$$
$$= \boldsymbol{E}_\mathrm{e}\left(\boldsymbol{r}\right) + k_\mathrm{s}^2\sum_{n=1,n\neq m}^{N_\mathrm{cells}}\left(m_{\mathrm{r},n}^2-1\right)\int_{D_{\mathrm{i},n}} \overline{\boldsymbol{G}}\left(k_\mathrm{s},\boldsymbol{r},\boldsymbol{r}'\right)\cdot\boldsymbol{E}\left(\boldsymbol{r}'\right)\mathrm{d}V\left(\boldsymbol{r}'\right)\,,$$
$$\boldsymbol{r}\in D_{\mathrm{i},m}\,. \tag{3.5}$$

Within each volume element, the total field can be approximated by

$$\boldsymbol{E}(\boldsymbol{r}) \approx \sum_{k=1}^{N_{\text{basis}}} E_{km} \boldsymbol{W}_k(\boldsymbol{r}) , \quad \boldsymbol{r} \in D_{\text{i},m} ,$$

where $\boldsymbol{W}_k$ are referred to as the shape or basis functions. Frequently, node-based shape functions are used as basis functions, but edge-based shape functions, using an expansion of a vector field in terms of values associated with element faces, are better suited for simulating electromagnetic fields at corners and edges. A detailed mathematical analysis of edge-based shape functions for various two- and three-dimensional elements has been given by Graglia et al. [86]. Linear as well as higher order curvilinear elements have been discussed by Mur and deHoop [176], Lee et al. [139], Wang and Ida [249], Crowley et al. [42] and Sertel and Volakis [209]. In general, the edge-based shape functions can be categorized as either interpolatory or hierarchical. An element is referred to as hierarchical if the vector basis functions forming the nth order element are a subset of the vector basis functions forming the $(n+1)$th order element. This property allows to use lowest order elements in regions where the field is expected to vary slowly and higher order elements in regions where rapid field variation is anticipated. For a tetrahedral element, a hierarchical edge-based element up to and including second order has been introduced by Webb and Forghani [259]. Additional to node- and edge-based shape functions, low order vector spherical wave functions have been employed by Peltoniemi [185]. In our analysis we assume that the electromagnetic field is constant over each element and consider the simplest type of basis functions, the constant pulse functions: $\boldsymbol{W}_k(\boldsymbol{r}) = \boldsymbol{e}_k$ for $\boldsymbol{r} \in D_{\text{i},m}$, and $\boldsymbol{W}_k(\boldsymbol{r}) = 0$ for $\boldsymbol{r} \notin D_{\text{i},m}$, where $k = x, y, z$ and $(\boldsymbol{e}_x, \boldsymbol{e}_y, \boldsymbol{e}_z)$ are the Cartesian unit vectors. This approach is called collocation method, since a certain value of the electromagnetic field is assigned to the centroid $\boldsymbol{r}_m$ of each element, i.e., $\boldsymbol{E}(\boldsymbol{r}) \approx \boldsymbol{E}(\boldsymbol{r}_m)$ for $\boldsymbol{r} \in D_{\text{i},m}$. Substituting this expansion into (3.5) and setting $D_{\text{i},m} = D_{\text{r}}$ (which gives $\int_{D_{\text{i},m} - D_{\text{r}}} \overline{\boldsymbol{G}} \cdot \boldsymbol{E} \, \mathrm{d}V = 0$), yields the system of linear equations

$$\boldsymbol{E}_{\text{e}}(\boldsymbol{r}_m) = \sum_{n=1}^{N_{\text{cells}}} \overline{\boldsymbol{A}}_{mn} \cdot \boldsymbol{E}(\boldsymbol{r}_n) , \quad m = 1, 2, \ldots, N_{\text{cells}} , \tag{3.6}$$

where the dyadic kernel is given by

$$\begin{aligned} \overline{\boldsymbol{A}}_{mn} = & \left[1 - k_{\text{s}}^2 \left(m_{\text{r},m}^2 - 1 \right) \left(M + M_1 - \frac{1}{k_{\text{s}}^2} L \right) \right] \overline{\boldsymbol{I}} \delta_{mn} \\ & - k_{\text{s}}^2 \left(m_{\text{r},n}^2 - 1 \right) (1 - \delta_{mn}) \, V_n \overline{\boldsymbol{G}}(k_{\text{s}}, \boldsymbol{r}_m, \boldsymbol{r}_n) , \end{aligned}$$

and V_n is the volume of the n element.

In computing the self-term $\mathcal{E}_m$ we extracted from the original integrand a singular function which approximates the integrand in the neighborhood of the singularity. However, there are other efficient schemes to accurately compute

singular integrals [3]. For example, in the framework of the volume integral equation method, Sertel and Volakis [209] transferred one of the derivative of the scalar Green function to the testing function using the divergence theorem. The resulting integrals are evaluated by the annihilation method, which converts first-order singular integrals into nonsingular integrals by using an appropriate parametric transformation (change of variables).

Whereas the volume integral equation method deals with the total field, the discrete dipole approximation exploits the concept of the exciting field, each volume element being explicitly modeled as an electric dipole moment. In this regard, we consider the field that excites the volume element $D_{\mathrm{i},m}$

$$\boldsymbol{E}_{\mathrm{exc}}\left(\boldsymbol{r}_m\right) = \boldsymbol{E}_{\mathrm{e}}\left(\boldsymbol{r}_m\right) + k_{\mathrm{s}}^2 \sum_{n=1, n\neq m}^{N_{\mathrm{cells}}} \left(m_{\mathrm{r},n}^2 - 1\right) V_n \overline{\boldsymbol{G}}\left(k_{\mathrm{s}}, \boldsymbol{r}_m, \boldsymbol{r}_n\right) \cdot \boldsymbol{E}\left(\boldsymbol{r}_n\right) \quad (3.7)$$

and rewrite (3.5) as

$$\left[1 - k_{\mathrm{s}}^2 \left(m_{\mathrm{r},m}^2 - 1\right) \left(M + M_1 - \frac{1}{k_{\mathrm{s}}^2} L\right)\right] \boldsymbol{E}\left(\boldsymbol{r}_m\right) = \boldsymbol{E}_{\mathrm{exc}}\left(\boldsymbol{r}_m\right) . \quad (3.8)$$

It is clear from (3.7) that the exciting field consists of the incident field and the field contributions of all other volume elements $D_{\mathrm{i},n}$ with $n \neq m$. The heart of the discrete dipole approximation is (3.7), while (3.8) is used to express the total field in terms of the exciting field. In dyadic notations, (3.8) read as

$$\overline{\boldsymbol{A}}_{mm} \cdot \boldsymbol{E}\left(\boldsymbol{r}_m\right) = \boldsymbol{E}_{\mathrm{exc}}\left(\boldsymbol{r}_m\right) ,$$

and the desired relation is

$$\boldsymbol{E}\left(\boldsymbol{r}_m\right) = \overline{\boldsymbol{A}}_{mm}^{-1} \cdot \boldsymbol{E}_{\mathrm{exc}}\left(\boldsymbol{r}_m\right) . \quad (3.9)$$

Inserting (3.9) into (3.7), we obtain the expression of the field that excites the volume element $D_{\mathrm{i},m}$ in terms of the exciting fields of all other volume elements $D_{\mathrm{i},n}$

$$\begin{aligned} \boldsymbol{E}_{\mathrm{exc}}\left(\boldsymbol{r}_m\right) = \boldsymbol{E}_{\mathrm{e}}\left(\boldsymbol{r}_m\right) + k_{\mathrm{s}}^2 \sum_{n=1, n\neq m}^{N_{\mathrm{cells}}} \left(m_{\mathrm{r},n}^2 - 1\right) V_n \\ \times \left[\overline{\boldsymbol{G}}\left(k_{\mathrm{s}}, \boldsymbol{r}_m, \boldsymbol{r}_n\right) \cdot \overline{\boldsymbol{A}}_{nn}^{-1}\right] \cdot \boldsymbol{E}_{\mathrm{exc}}\left(\boldsymbol{r}_n\right) . \end{aligned}$$

Defining the polarizability dyad by

$$\overline{\boldsymbol{t}}_n = \varepsilon_{\mathrm{s}} \left(m_{\mathrm{r},n}^2 - 1\right) V_n \overline{\boldsymbol{A}}_{nn}^{-1}$$

and taking into account that $k_{\mathrm{s}} = k_0 \sqrt{\varepsilon_{\mathrm{s}}}$, yields

$$\boldsymbol{E}_{\mathrm{e}}\left(\boldsymbol{r}_m\right) = \sum_{n=1}^{N_{\mathrm{cells}}} \overline{\boldsymbol{B}}_{mn} \cdot \boldsymbol{E}_{\mathrm{exc}}\left(\boldsymbol{r}_n\right) , \quad m = 1, 2, \ldots, N_{\mathrm{cells}} , \quad (3.10)$$

where the dyadic kernel is

$$\overline{\boldsymbol{B}}_{mn} = \overline{\boldsymbol{I}}\delta_{mn} - k_0^2\left(1-\delta_{mn}\right)\overline{\boldsymbol{G}}\left(k_{\rm s},\boldsymbol{r}_m,\boldsymbol{r}_n\right)\cdot\bar{\boldsymbol{t}}_n\,.$$

In terms of the dipole moment $\boldsymbol{p}_m$

$$\boldsymbol{p}_m = \varepsilon_{\rm s}\left(m_{{\rm r},m}^2-1\right)V_m\boldsymbol{E}\left(\boldsymbol{r}_m\right)\,,$$

(3.9) can be written as

$$\boldsymbol{p}_m = \bar{\boldsymbol{t}}_m\cdot\boldsymbol{E}_{\rm exc}\left(\boldsymbol{r}_m\right)$$

and the effect of the exciting field can be interpreted as inducing a dipole moment $\boldsymbol{p}_m$ in each volume element $D_{{\rm i},m}$. This is the origin of the term "discrete dipole approximation."

Parenthetically we note that the discrete dipole approximation can be used to derive the size-dependent Maxwell–Garnett formula. For a collection of identical spheres of volume V and relative refractive index $m_{\rm r}$, the polarizability dyad is

$$\bar{\boldsymbol{t}}_m = \alpha\overline{\boldsymbol{I}}\,,$$

and the dipole moment satisfies the equation

$$\boldsymbol{p}_m = \alpha\boldsymbol{E}_{\rm exc}\left(\boldsymbol{r}_m\right)\,,$$

where the polarizability scalar α is given by

$$\alpha = \varepsilon_{\rm s}\left(m_{\rm r}^2-1\right)V\left[1-k_{\rm s}^2\left(m_{\rm r}^2-1\right)\left(M+M_1-\frac{1}{k_{\rm s}^2}L\right)\right]^{-1}\,. \tag{3.11}$$

The size-dependent Maxwell–Garnett formula can now be obtained by combining (3.11) and (2.168) [129].

The maximum linear cross-sectional extent $2r_m$ of $D_{{\rm i},m}$ is such that

$$\frac{r_m m_{{\rm r},m}}{\lambda} < 0.1\,,$$

that is, the dimension r_m is no more than a tenth of the wavelength in the volume element $D_{{\rm i},m}$. This condition ensures that the spatial variations of the electromagnetic field inside each volume element are small enough, so that each volume element can be thought of as a dipole scatterer. Consequently, for large scale simulations, the systems of equations (3.6) and (3.10) are excessively large and iterative solvers as the conjugate or bi-conjugate gradient method are employed. The coupling submatrices in (3.6) and (3.10) depend on the absolute distance among elements, and the overall matrices are block Töplitz. Thus, (3.6) and (3.10) can be cast in circulant form, and the fast Fourier transform can be employed to carry out the matrix–vector products [68, 80].

3.2.4 CST Microwave Studio Program

CST Microwave Studio is a commercial software package which can be used for analyzing the electromagnetic scattering by particles with complex geometries and optical properties. Essentially, the electromagnetic simulator is based on the finite integration technique (FIT) developed by Weiland [260]. The finite integration technique is simple in concept and provides a discrete reformulation of Maxwell's equations in their integral from. Following the analysis of Clemens and Weiland [38] we recall the basic properties of the discrete representation of Maxwell's equation by the finite integration technique.

The first discretization step of the finite integration method consists in the restriction of the electromagnetic field problem, which represent an open boundary problem, to a simply connected and bounded space domain Ω containing the region of interest. The next step consists in the decomposition of the computational domain into a finite number of volume elements (cells). This decomposition yields the volume element complex G, which serves as computational grid. Assuming that Ω is brick-shaped, we have the volume element complex

$$\begin{aligned} G = \{ & D_{ijk} / D_{ijk} = [x_i, x_{i+1}] \times [y_j, y_{j+1}] \times [z_k, z_{k+1}] \\ & i = 1, 2, \ldots, N_x - 1,\ j = 1, 2, \ldots, N_y - 1,\ k = 1, 2, \ldots, N_z - 1 \} \ , \end{aligned}$$

and note that each edge and facet of the volume elements are associated with a direction.

Next, we consider the integral form of the Maxwell equations, i.e., for Faraday's induction law and Maxwell–Ampere law we integrate the differential equations on an open surface and apply the Stokes theorem, while for Gauss' electric and magnetic field laws we integrate the differential equations on a bounded domain and use the Gauss theorem.

The Faraday law in integral form

$$\oint\limits_{\partial S} \boldsymbol{E} \cdot \mathrm{d}\boldsymbol{s} = - \int_S \frac{\partial \boldsymbol{B}}{\partial t} \cdot \mathrm{d}\boldsymbol{S}$$

with S being an arbitrary open surface contained in Ω, can be rewritten for the facet $S_{z,ijk}$ of the volume element D_{ijk} as the ordinary differential equation

$$e_{x,ijk} + e_{y,i+1jk} - e_{x,ij+1k} - e_{y,ijk} = -\frac{\mathrm{d}}{\mathrm{d}t} b_{z,ijk} \, ,$$

where

$$e_{x,ijk} = \int_{(x_i, y_j, z_k)}^{(x_{i+1}, y_j, z_k)} \boldsymbol{E} \cdot \mathrm{d}\boldsymbol{s}$$

is the electric voltage along the edge $L_{x,ijk}$ of the facet $S_{z,ijk}$, and

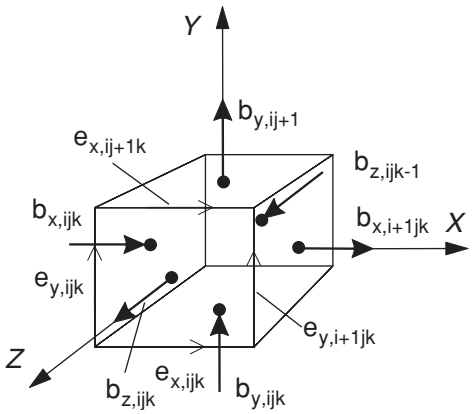

Fig. 3.1. Electric voltages and magnetic fluxes on a volume element

$$b_{z,ijk} = \int_{S_{z,ijk}} \boldsymbol{B} \cdot \mathrm{d}\boldsymbol{S}$$

represents the magnetic flux through the facet $S_{z,ijk}$. Note that the orientation of the element edges influences the signs in the differential equation (Fig. 3.1). The Gauss magnetic field law in integral form

$$\int_S \boldsymbol{B} \cdot \mathrm{d}\boldsymbol{S} = 0$$

with S being an arbitrary closed surface contained in Ω, yields for the boundary surface of the volume element D_{ijk},

$$-b_{x,ijk} + b_{x,i+1jk} - b_{y,ijk} + b_{y,ij+1k} - b_{z,ijk} + b_{z,ijk+1} = 0\,.$$

The discretization of the remaining two Maxwell equations requires the introduction of a second volume element complex $\widetilde{G}$, which is the dual of the primary volume element complex G. For the Cartesian tensor product grid G, the dual grid $\widetilde{G}$ is defined by taking the foci of the volume elements of G as gridpoints for the volume elements of $\widetilde{G}$. With this definition there is a one-to-one relation between the element edges of G cutting through the element surfaces of $\widetilde{G}$ and conversely. For the dual volume elements, the Maxwell–Ampere law

$$\oint_{\partial S} \boldsymbol{H} \cdot \mathrm{d}\boldsymbol{s} = \int_S \left(\frac{\partial \boldsymbol{D}}{\partial t} + \boldsymbol{J} \right) \cdot \mathrm{d}\boldsymbol{S}\,,$$

and the Gauss electric field law

$$\int_S \boldsymbol{D} \cdot \mathrm{d}\boldsymbol{S} = \int_D \rho \, \mathrm{d}V\,, \quad S = \partial D$$

are discretized in an analogous manner. The differential equations are formulated in terms of the magnetic grid voltages $h_{\alpha,ijk}$ along the dual edges $\widetilde{L}_{\alpha,ijk}$, the dielectric fluxes $d_{\alpha,ijk}$ and the conductive currents $j_{\alpha,ijk}$ through the dual facets $\widetilde{S}_{\alpha,ijk}$, $\alpha = x, y, z$, and the electric charge q_{ijk} in the dual volume element $\widetilde{D}_{ijk}$ ($q_{ijk} = \int_{\widetilde{D}_{ijk}} \rho \mathrm{d}V$).

Collecting the equations of all element surfaces of the complex pair $\{G, \widetilde{G}\}$ and introducing the integral voltage-vectors $\boldsymbol{e}$ and $\boldsymbol{h}$, the flux state-vectors $\boldsymbol{b}$ and $\boldsymbol{d}$, the conductive current-vector $\boldsymbol{j}$, and the electric charge-vector $\boldsymbol{q}$, we derive a set of discrete matrix equations, the so-called Maxwell grid equations

$$\boldsymbol{C}\boldsymbol{e} = -\frac{\mathrm{d}}{\mathrm{d}t}\boldsymbol{b}\,, \quad \widetilde{\boldsymbol{C}}\boldsymbol{h} = \frac{\mathrm{d}}{\mathrm{d}t}\boldsymbol{d} + \boldsymbol{j}$$

and

$$\boldsymbol{S}\boldsymbol{b} = 0\,, \quad \widetilde{\boldsymbol{S}}\boldsymbol{d} = \boldsymbol{q}\,.$$

The transformation into frequency domain for the Maxwell grid equations with $\boldsymbol{e}(t) = \mathrm{Re}\{\boldsymbol{e}\mathrm{e}^{-\mathrm{j}\omega t}\}$, yields

$$\boldsymbol{C}\boldsymbol{e} = \mathrm{j}\omega\boldsymbol{b}\,, \quad \widetilde{\boldsymbol{C}}\boldsymbol{h} = -\mathrm{j}\omega\boldsymbol{d} + \boldsymbol{j}\,.$$

The discrete curl-matrices $\boldsymbol{C}$ and $\widetilde{\boldsymbol{C}}$, and the discrete divergence matrices $\boldsymbol{S}$ and $\widetilde{\boldsymbol{S}}$ are defined on the grids G and $\widetilde{G}$, respectively, and depend only on the grid topology. The integral voltage- and flux state-variables allocated on the two different volume element complexes are related to each other by the discrete material matrix relations

$$\boldsymbol{d} = \boldsymbol{M}_{\varepsilon}\boldsymbol{e} + \boldsymbol{p}\,, \quad \boldsymbol{j} = \boldsymbol{M}_{\kappa}\boldsymbol{e}\,, \quad \boldsymbol{h} = \boldsymbol{M}_{\nu}\boldsymbol{b} - \boldsymbol{m}\,,$$

where $\boldsymbol{M}_{\varepsilon}$ is the permittivity matrix, $\boldsymbol{M}_{\kappa}$ is the matrix of conductivities, $\boldsymbol{M}_{\nu}$ is the matrix of reluctivities, and $\boldsymbol{p}$ and $\boldsymbol{m}$ are the electric and magnetic polarization vectors, respectively. The discrete grid topology matrices have the same effect as the vector operators curl and div. For instance, the discrete analog of the equation $\nabla \cdot \nabla \times = 0$ (div curl = 0) is $\boldsymbol{S}\boldsymbol{C} = 0$ and $\widetilde{\boldsymbol{S}}\widetilde{\boldsymbol{C}} = 0$. Transposition of these equations together with the relation between the discrete curl-matrices $\boldsymbol{C} = \widetilde{\boldsymbol{C}}^{\mathrm{T}}$, yields the discrete equations $\widetilde{\boldsymbol{C}}\boldsymbol{S}^{\mathrm{T}} = 0$ and $\boldsymbol{C}\widetilde{\boldsymbol{S}}^{\mathrm{T}} = 0$, both corresponding to the equation $\nabla \times \nabla = 0$ (curl grad = 0). Basic algebraic properties of the Maxwell grid equations also allow to prove conservation properties with respect to energy and charges.

The finite integration technique suffers somewhat from a deficiency in being able to model very complicated cavities including curved boundaries with high precision, but the usage of the perfect boundary approximation eliminate this deficiency [123].

3.3 Homogeneous, Axisymmetric and Nonaxisymmetric Particles

In the following analysis we show results computed with the TAXSYM and TNONAXSYM routines. The flow diagram of these routines is shown in Fig. 3.2. The input data file provides the variables specifying the optical properties, geometry, type of discrete sources and error tolerances for the convergence tests over N_{rank}, M_{rank} and N_{int}. The model parameters control the interpolation and integration processes, and the solution of the linear system of equations. The current version of the TAXSYM code is directly applicable to spheroids, cylinders and rounded oblate cylinders. Nonaxisymmetric geometries currently supported include ellipsoids, quadratic prisms and regular polyhedral prisms. The user should be able to write new routines to generate particles with other shapes. The codes can also read particle geometry information from files instead of automatically generating one of the geometries listed above.

3.3.1 Axisymmetric Particles

The scattering characteristics of axisymmetric particles can be computed with localized or distributed sources. Specifically, localized sources are used to analyze the electromagnetic scattering by particles which are not too extreme in terms of size parameter and aspect ratio, while distributed sources are employed to compute the $\boldsymbol{T}$ matrix of large particles with extreme geometries. For highly elongated particles, the sources are distributed along the axis of symmetry, while for flattened particles, the sources are distributed in the complex plane.

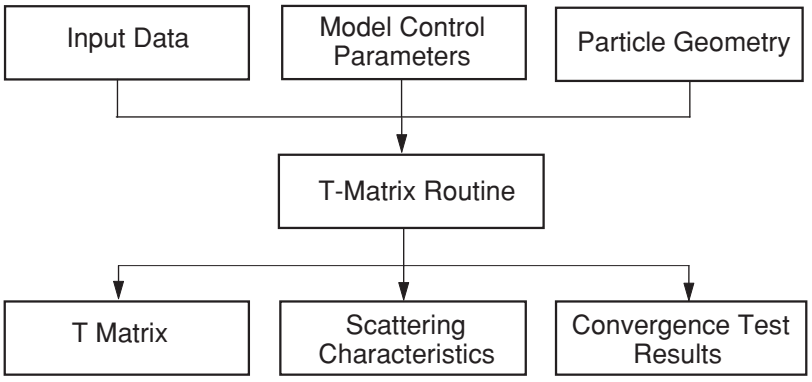

Fig. 3.2. Flow diagram of TAXSYM and TNONAXSYM routines

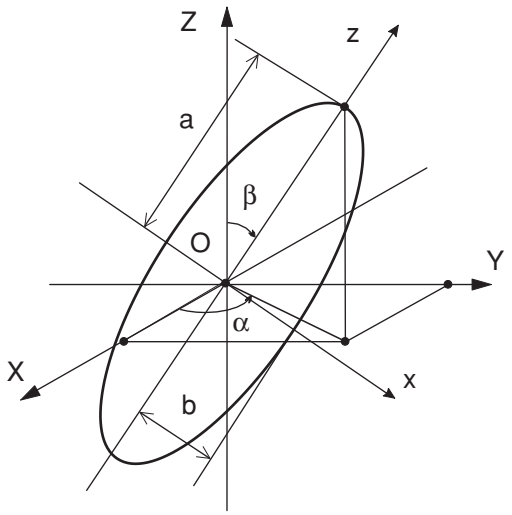

Fig. 3.3. Geometry of a prolate spheroid

Localized Sources

In our first example, we consider prolate spheroids in random and fixed orientation, and compare the results obtained with the TAXSYM code to the solutions computed with the codes developed by Mishchenko [167–169]. The orientation of the axisymmetric particle with respect to the global coordinate system is specified by the Euler angles of rotation $\alpha_{\rm p}$ and $\beta_{\rm p}$, and the incident field is a linearly polarized plane wave propagating along the Z-axis (Fig. 3.3). The rotational semi-axis (along the axis of symmetry) is $k_{\rm s}a = 10$, the horizontal semi-axis is $k_{\rm s}b = 5$, and the relative refractive index of the spheroid is $m_{\rm r} = 1.5$. The maximum expansion order and the number of integration points are $N_{\rm rank} = 17$ and $N_{\rm int} = 100$, respectively. In Figs. 3.4 and 3.5 we plot some elements of the scattering matrix for a randomly oriented spheroid. The agreement between the curves is acceptable. For a fixed orientation of the prolate spheroid, we list in Tables 3.1 and 3.2 the phase matrix elements Z_{11} and Z_{44}, and Z_{21} and Z_{42}, respectively. The Euler angles of rotation are $\alpha_{\rm p} = \beta_{\rm p} = 45^\circ$, and the matrix elements are computed in the azimuthal planes $\varphi = 45^\circ$ and $\varphi = 225^\circ$ at three zenith angles: 30°, 90°, and 150°. The relative error is around 10% for the lowest matrix element and remains below 1% for other elements.

In the next example, we show results computed for a perfectly conducting spheroid of size parameter $k_{\rm s}a = 10$, aspect ratio $a/b = 2$, and Euler angles of rotation $\alpha_{\rm p} = \beta_{\rm p} = 45^\circ$. The perfectly conducting spheroid is simulated from the dielectric spheroid by using a very high value of the relative refractive index ($m_{\rm r} = 1.{\rm e}{+}30$), and the version of the code devoted to the analysis of perfectly conducting particles is taken as reference. For this application, the

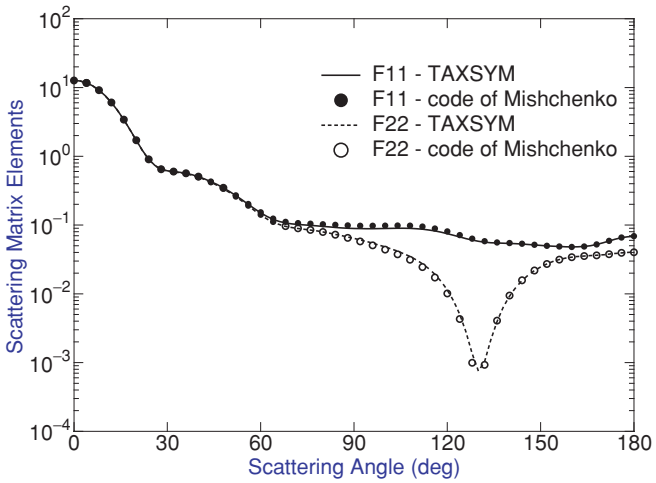

Fig. 3.4. Scattering matrix elements F_{11} and F_{22} of a dielectric prolate spheroid

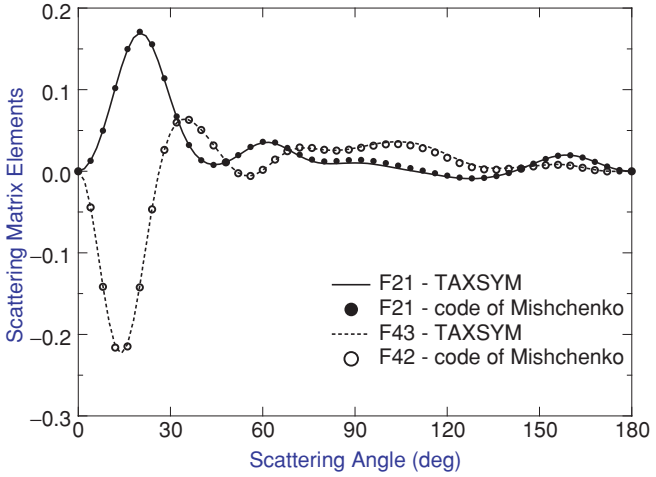

Fig. 3.5. Scattering matrix elements F_{21} and F_{43} of a dielectric prolate spheroid

maximum expansion order is $N_{\rm rank} = 18$, while the number of integration points is $N_{\rm int} = 200$. The normalized differential scattering cross-sections presented in Fig. 3.6 are similar for both methods.

To verify the accuracy of the code for isotropic, chiral particles, we consider a spherical particle of size parameter $k_{\rm s}a = 10$. The refractive index of the particle is $m_{\rm r} = 1.5$ and the chirality parameter is $\beta k_{\rm i} = 0.1$, where $k_{\rm i} = m_{\rm r}k_{\rm s}$. Calculations are performed for $N_{\rm rank} = 18$ and $N_{\rm int} = 200$. Figure 3.7 compares the normalized differential scattering cross-sections computed with the

Table 3.1. Phase matrix elements 11 and 44 computed with (a) the TAXSYM routine and (b) the code of Mishchenko

φ	θ	Z_{11} (a)	Z_{11} (b)	Z_{44} (a)	Z_{44} (b)
45°	30°	4.154e−01	4.152e−01	3.962e−01	3.961e−01
45°	90°	9.136e−01	9.142e−01	5.453e−01	5.459e−01
45°	150°	5.491e−02	5.489e−02	2.414e−03	2.420e−03
225°	30°	8.442e−01	8.439e−01	8.406e−01	8.402e−01
225°	90°	5.331e−02	5.329e−02	1.493e−04	1.360e−04
225°	150°	3.807e−02	3.805e−02	−1.400e−02	−1.402e−02

Table 3.2. Phase matrix elements 21 and 42 computed with (a) the TAXSYM routine and (b) the code of Mishchenko

φ	θ	Z_{21} (a)	Z_{21} (b)	Z_{42} (a)	Z_{42} (b)
45°	30°	2.134e−02	2.134e−02	1.229e−01	1.229e−01
45°	90°	3.016e−01	3.015e−01	6.681e−01	6.685e−01
45°	150°	−2.655e−03	−2.699e−03	−5.479e−02	−5.477e−02
225°	30°	6.677e−02	6.689e−02	−4.190e−02	−4.161e−02
225°	90°	−2.910e−02	−2.908e−02	−4.466e−02	−4.466e−02
225°	150°	−3.042e−02	−3.039e−02	1.810e−02	1.810e−02

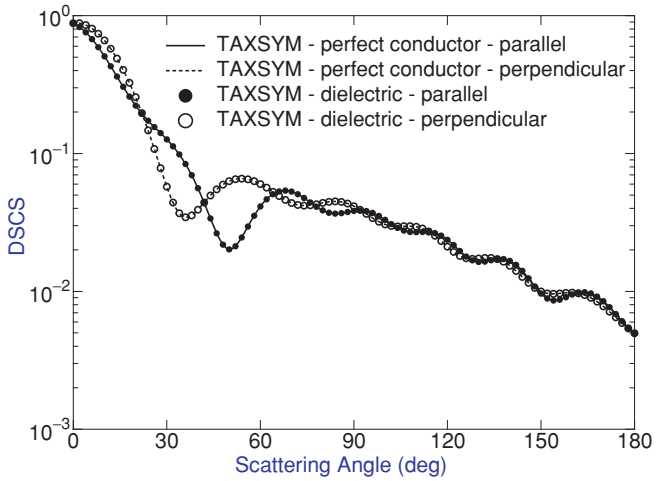

Fig. 3.6. Normalized differential scattering cross-sections of a perfectly conducting prolate spheroid

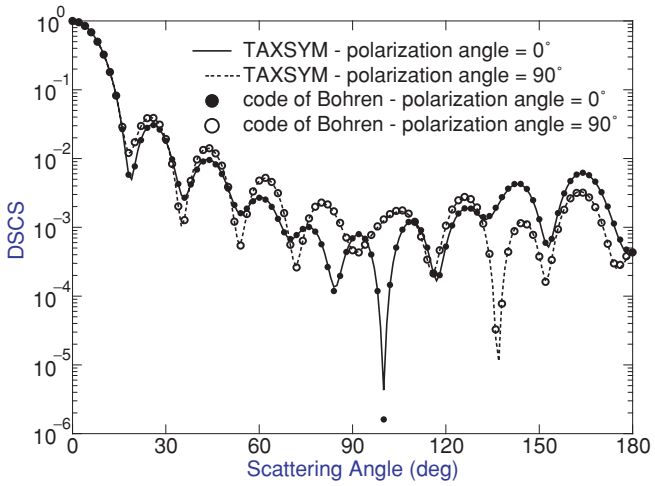

Fig. 3.7. Normalized differential scattering cross-sections of an isotropic chiral sphere

TAXSYM routine and the program developed by Bohren [16]. This program was coded by Ute Comberg and is available from www.T-matrix.de. The scattering characteristics are computed in the azimuthal plane $\varphi = 0°$ and for two polarizations of the incident wave.

In the next example, we present computer simulations for Gaussian beam scattering. The particle is a prolate spheroid with semi-axes $a = 2.0\,\mu\text{m}$ and $b = 1.0\,\mu\text{m}$, and relative refractive index $m_\text{r} = 1.5$. The wavelength of the incident radiation is $\lambda = 0.628\,\mu\text{m}$, and the orientation of the spheroid is specified by the Euler angles $\alpha_\text{p} = 0°$ and $\beta_\text{p} = 90°$. The maximum expansion and azimuthal orders are $N_\text{rank} = 30$ and $M_\text{rank} = 12$, respectively, while the number of integration points is $N_\text{int} = 300$. The variation of the differential scattering cross-sections with the axial position z_0 of the particle is shown in Fig. 3.8. The waist radius of the Gaussian beam is $w_0 = 10\,\mu\text{m}$, and the off-axis coordinates are $x_0 = y_0 = 0$. The beam parameter is $s = 1/(k_\text{s} w_0) = 0.01$, and for this value of s, the localized beam model gives accurate results. The scattering cross-section decreases from $C_\text{scat} = 16.788$ to $C_\text{scat} = 14.520$ when z_0 increases from 0 to $200\,\mu\text{m}$. Figure 3.9 illustrates the influence of the off-axis coordinate x_0 on the angular scattering for $w_0 = 10\,\mu\text{m}$ and $y_0 = z_0 = 0$. In this case, the scattering cross-section decreases more rapidly and attains the value $C_\text{scat} = 2.326$ for $x_0 = 10\,\mu\text{m}$. The results of the differential scattering cross-sections for different values of the beam waist radius are shown in Fig. 3.10. For $w_0 = 5\,\mu\text{m}$, the scattering cross-section is $C_\text{scat} = 15.654$, while for $w_0 = 2.5\,\mu\text{m}$, $C_\text{scat} = 12.280$.

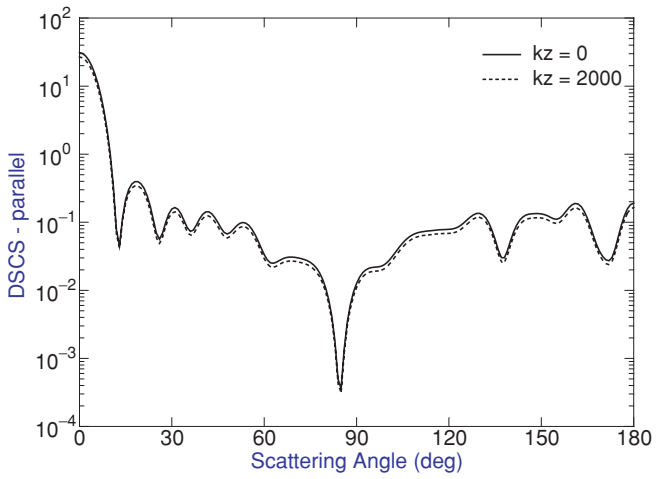

Fig. 3.8. Variation of the normalized differential scattering cross-sections with the axial position of a prolate spheroid illuminated by a Gaussian beam

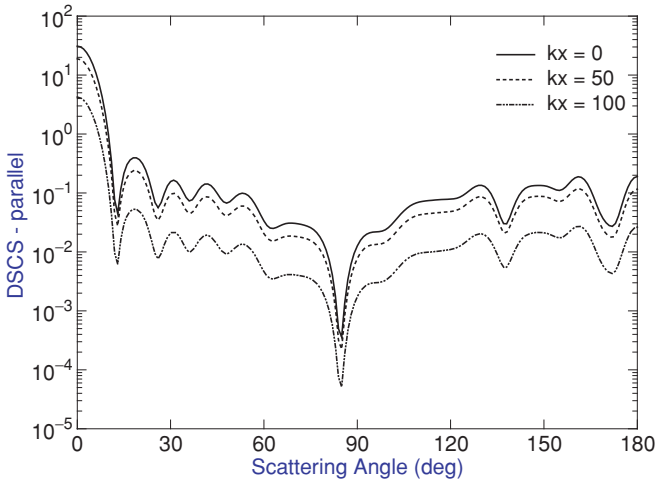

Fig. 3.9. Variation of the normalized differential scattering cross-sections with the off-axis coordinate of a prolate spheroid illuminated by a Gaussian beam

Distributed Sources

While localized sources are used for not extremely aspherical particles, distributed sources are suitable for analyzing particles with extreme geometries, i.e., particles whose shape differs significantly from a sphere. Extremely deformed particles are encountered in various scientific disciplines as for instance

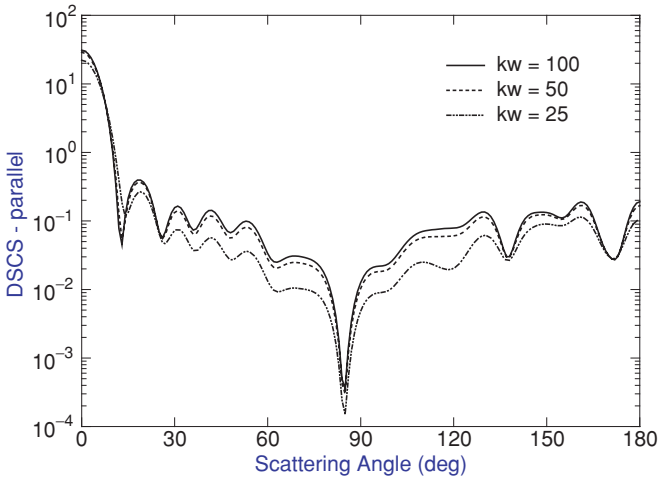

Fig. 3.10. Variation of the normalized differential scattering cross-sections with the beam waist radius

Fig. 3.11. Particles with extreme geometries: prolate spheroid, fibre, oblate cylinder and Cassini particle

astrophysics, atmospheric science and optical particle sizing. For example, light scattering by finite fibres is needed in optical characterization of asbestos or other mineral fibres, while flat particles are encountered as aluminium or mica flakes in coatings.

Figure 3.11 summarizes the particle shapes considered in our exemplary simulation results. The spheroid is a relatively simple shape but convergence problems occur for large size parameters and high aspect ratios. The finite fibre is a more extreme shape because the flank is even and without convexities. This shape is modeled by a rounded prolate cylinder, i.e., by a cylinder with two half-spheres at the ends. In polar coordinates, a rounded prolate cylinder as shown in Fig. 3.12 is described by

$$r(\theta) = \begin{cases} (a-b)\cos\theta + \sqrt{b^2 - (a-b)^2 \sin^2\theta}\,, & \theta < \theta_0, \\ b/\sin\theta\,, & \theta_0 \le \theta \le \pi - \theta_0, \\ -(a-b)\cos\theta + \sqrt{b^2 - (a-b)^2 \sin^2\theta}\,, & \pi - \theta_0 < \theta < \pi, \end{cases}$$

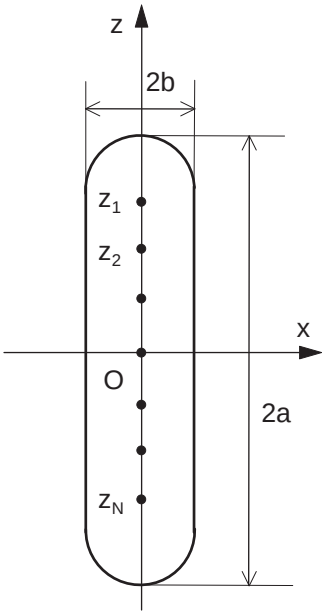

Fig. 3.12. Geometry of a prolate cylinder and the distribution of the discrete sources on the axis of symmetry

where $\theta_0 = \arctan[b/(a-b)]$. The rounded oblate cylinder is constructed quite similar, i.e., the flank is rounded and top and bottom are flat. An oblate cylinder as shown in Fig. 3.13 is described in polar coordinates by

$$r(\theta) = \begin{cases} a/\cos\theta\,, & \theta < \theta_0 \\ (b-a)\sin\theta + \sqrt{a^2 - (b-a)^2\cos^2\theta}\,, & \theta_0 \le \theta \le \pi - \theta_0 \\ -a/\cos\theta\,, & \pi - \theta_0 < \theta < \pi \end{cases},$$

where $\theta_0 = \arctan[(b-a)/a]$. Cassini particles are a real challenge for light scattering simulations because the generatrix contains concavities on its top and bottom. The Cassini ovals can be described in polar coordinates by the equation

$$r(\theta) = \sqrt{a^2 - 2a^2\sin^2\theta + \sqrt{b^4 - 4a^4\sin^2\theta + 4a^4\sin^4\theta}}$$

and the shape depends on the ratio b/a. If $a < b$ the curve is an oval loop, for $a = b$ the result is a lemniscate, and for $a > b$ the curve consists of two separate loops. If a is chosen slightly smaller than b we obtain a concave, bone-like shape, and this concavity becomes deeper as a approaches to b.

For the prolate particles considered in our simulations, the sources are distributed on the axis of symmetry as in Fig. 3.12, while for the oblate particles, the sources are distributed in the complex plane as in Fig. 3.13. The wavelength of the incident radiation is $\lambda = 0.6328\,\mu$m, the relative refractive index

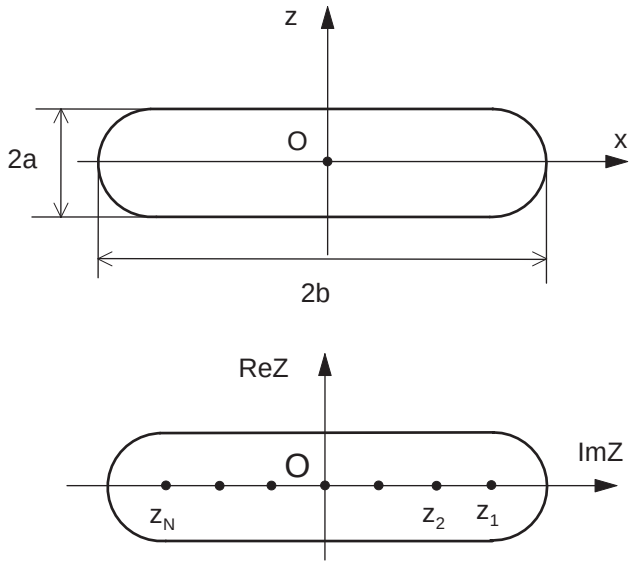

Fig. 3.13. Geometry of an oblate cylinder and the distribution of the discrete sources in the complex plane

Table 3.3. Surface parameters of particles with extreme geometries

Particle type	a (µm)	b (µm)	α_p (°)	β_p (°)
Prolate spheroid	8.5	0.85	0	0
Fibre	3	0.06	0	0
Oblate cylinder	0.03	3	0	0
Cassini particle	1.1	1.125	0	45

Table 3.4. Maximum expansion and azimuthal orders for particles with extreme geometries

Particle type	N_{rank}	N_{int}
Prolate spheroid	100	1000
Fibre	50	3000
Oblate cylinder	36	5000
Cassini particle	28	1000

is $m_r = 1.5$ and the scattering characteristics are computed in the azimuthal plane $\varphi = 0°$. The parameters describing the geometry and orientation of the particles are given in Table 3.3, while the parameters controlling the convergence process are listed in Table 3.4. Note that the Cassini particle has a diameter of about 3.15 µm and an aspect ratio of about 1/4.

In Figs. 3.14–3.17 we plot the normalized differential scattering cross-sections together with the results computed with the discrete sources method for parallel and perpendicular polarizations, and for the case of normal incidence. It is apparent that the agreement between the curves is acceptable.

We conclude this section with an extensive validation test for an oblate cylinder of radius $k_s b = 15$, length $2k_s a = 7.5$ and relative refractive index

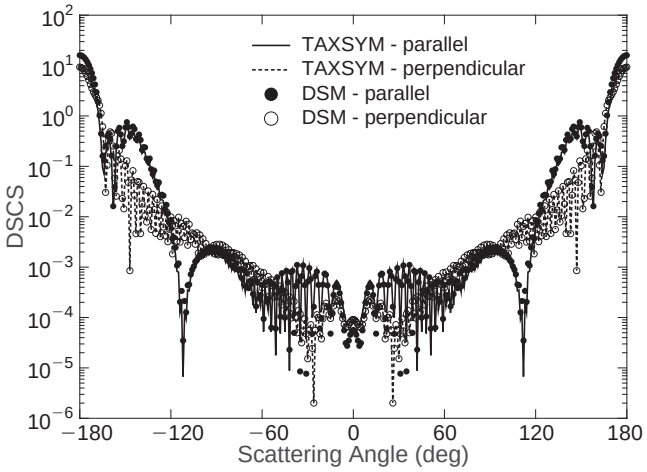

Fig. 3.14. Normalized differential scattering cross-sections of a prolate spheroid with $a = 8.5\,\mu\text{m}$ and $b = 0.85\,\mu\text{m}$. The curves are computed with the TAXSYM routine and the discrete sources method (DSM)

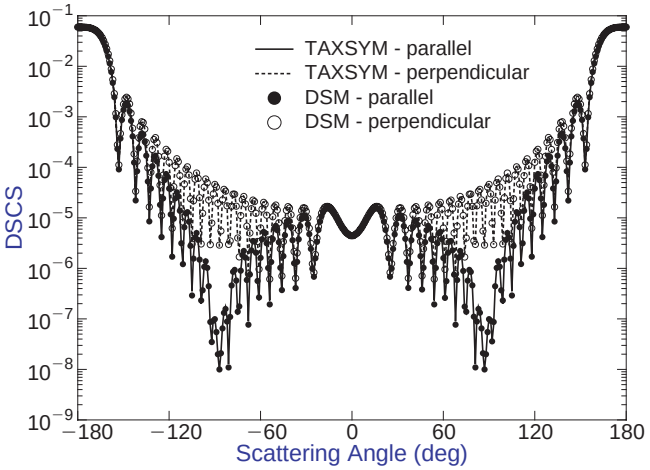

Fig. 3.15. Normalized differential scattering cross-sections of a fibre particle with $a = 3.0\,\mu\text{m}$ and $b = 0.06\,\mu\text{m}$. The curves are computed with the TAXSYM routine and the discrete sources method (DSM)

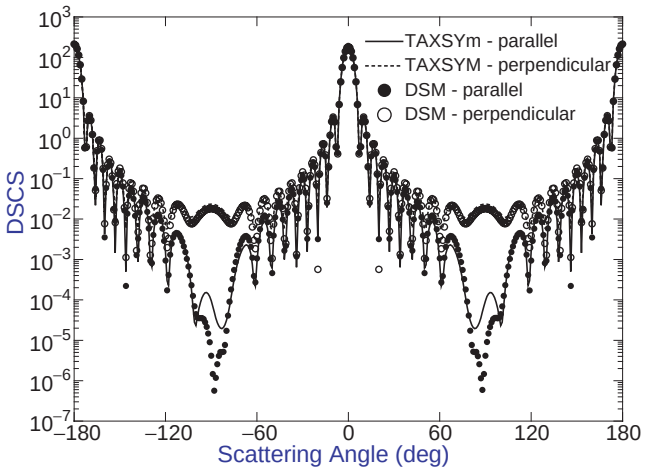

Fig. 3.16. Normalized differential scattering cross-sections of an oblate cylinder with $a = 0.03\,\mu\text{m}$ and $b = 3.0\,\mu\text{m}$. The curves are computed with the TAXSYM routine and the discrete sources method (DSM)

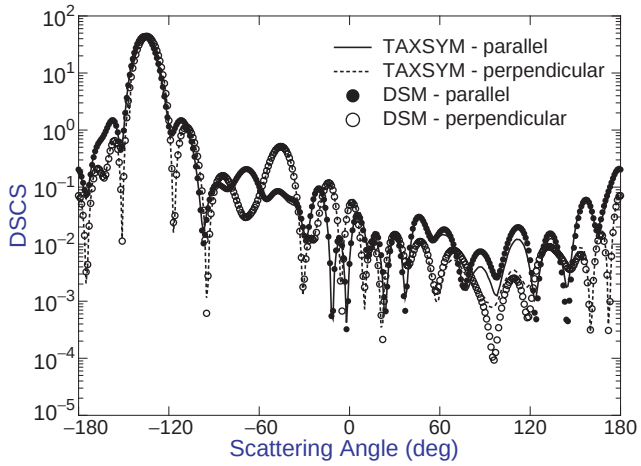

Fig. 3.17. Normalized differential scattering cross-sections of a Cassini particle with $a = 1.1$ and $b = 1.125$. The curves are computed with the TAXSYM routine and the discrete sources method (DSM)

$m_\text{r} = 1.5$. The $\boldsymbol{T}$-matrix calculations are performed with $N_\text{rank} = 30$ sources distributed in the complex plane and by using $N_\text{int} = 300$ integration points on the generatrix curve. The scattering characteristics plotted in Fig. 3.18 are calculated for the Euler angles of rotation $\alpha_\text{p} = \beta_\text{p} = 0^\circ$ and for the case of normal incidence. Also shown are the results computed with the discrete

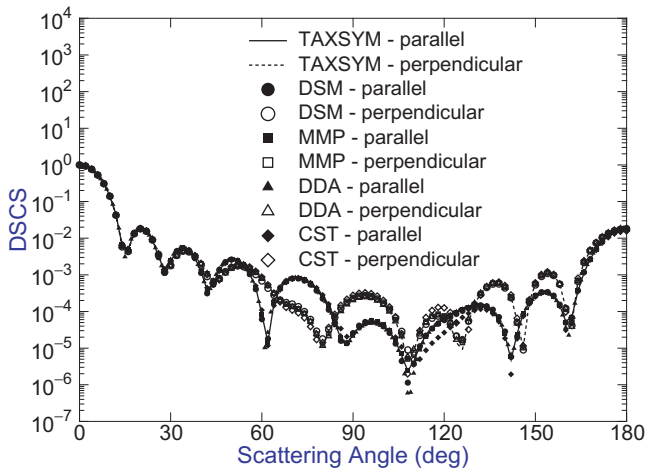

Fig. 3.18. Normalized differential scattering cross-sections of an oblate cylinder with $k_s b = 15$ and $2k_s a = 7.5$. The curves are computed with the TAXSYM routine, discrete sources method (DSM), multiple multipole method (MMP), discrete dipole approximation (DDA) and finite integration technique (CST)

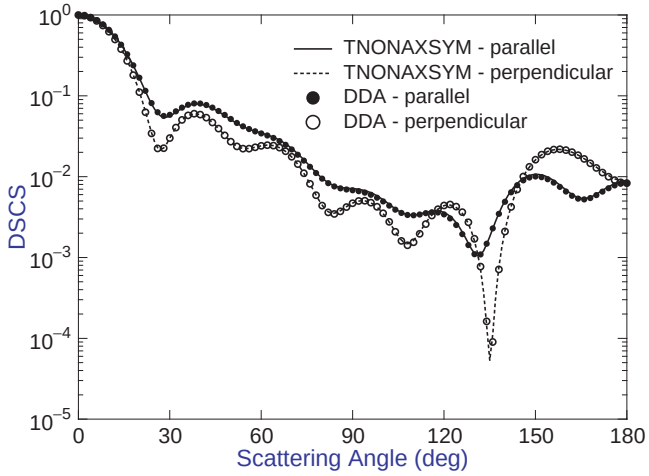

Fig. 3.19. Normalized differential scattering cross-sections of a dielectric cube computed with the TNONAXSYM routine and the discrete dipole approximation (DDA)

sources method, multiple multipole method, discrete dipole approximation and finite integration technique. No substantial differences between the curves are noted. Further scattering patterns for finite fibres having a large aspect ratio have been published by Pulbere and Wriedt [196].

3.3.2 Nonaxisymmetric Particles

In Fig. 3.19, we compare the results obtained with the TNONAXSYM routine to the discrete dipole approximation solutions. Calculations are performed for

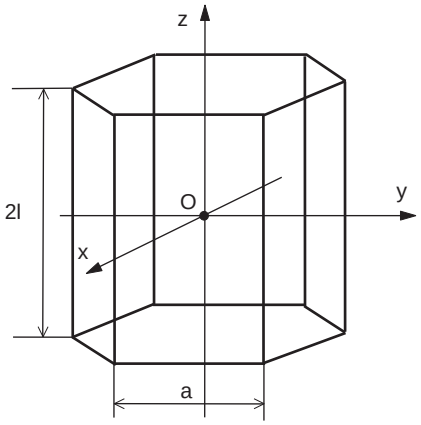

Fig. 3.20. Geometry of a hexagonal prism

a dielectric cube of length $2k_{\mathrm{s}}a = 10$ and relative refractive index $m_{\mathrm{r}} = 1.5$. The incident wave propagates along the Z-axis of the global coordinate system and the Euler orientation angles are $\alpha_{\mathrm{p}} = \beta_{\mathrm{p}} = \gamma_{\mathrm{p}} = 0°$. Convergence is achieved for $N_{\mathrm{rank}} = 14$ and $M_{\mathrm{rank}} = 12$, while the numbers of integration points on each square surface are $N_{\mathrm{int1}} = N_{\mathrm{int2}} = 24$.

As a second example, we consider a hexagonal prism (Fig. 3.20) of length $2l = 1.154\,\mu\mathrm{m}$, hexagon side $a = 1.154\,\mu\mathrm{m}$ and relative refractive index $m_{\mathrm{r}} = 1.5$. The wavelength of the incident radiation is taken to be $\lambda = 0.628\,\mu\mathrm{m}$, and the orientation of the hexagonal prism is specified by the Euler angles $\alpha_{\mathrm{p}} = \beta_{\mathrm{p}} = 0°$ and $\gamma_{\mathrm{p}} = 90°$. For this application, the maximum expansion and azimuthal orders are $N_{\mathrm{rank}} = 22$ and $M_{\mathrm{rank}} = 20$, respectively. Figure 3.21 compares results obtained with the TNONAXSYM routine and the finite integration technique. The agreement between the curves is acceptable.

Figure 3.22 illustrates the normalized differential scattering cross-sections for a positive uniaxial anisotropic cube of length $2a = 0.3\,\mu\mathrm{m}$, and relative refractive indices $m_{\mathrm{r}x} = m_{\mathrm{r}y} = 1.5$ and $m_{\mathrm{r}z} = 1.7$. The principal coordinate system coincides with the particle coordinate system, i.e., $\alpha_{\mathrm{pr}} = \beta_{\mathrm{pr}} = 0°$. Calculations are performed at a wavelength of $\lambda = 0.3\,\mu\mathrm{m}$ and for the case of normal incidence. The parameters controlling the $\boldsymbol{T}$-matrix calculations are $N_{\mathrm{rank}} = 18$ and $M_{\mathrm{rank}} = 18$, while the numbers of integration points on each cube face are $N_{\mathrm{int1}} = N_{\mathrm{int2}} = 50$. The behavior of the far-field patterns obtained with the TNONAXSYM routine, discrete dipole approximation and finite integration technique is quite similar.

Figure 3.23 shows plots of the differential scattering cross-sections versus the scattering angle for a negative uniaxial anisotropic ellipsoid of semi-axis lengths $a = 0.3\,\mu\mathrm{m}$, $b = 0.2\,\mu\mathrm{m}$ and $c = 0.1\,\mu\mathrm{m}$, and relative refractive indices $m_{\mathrm{r}x} = m_{\mathrm{r}y} = 1.5$ and $m_{\mathrm{r}z} = 1.3$. The orientation of the principal coordinate system is given by the Euler angles $\alpha_{\mathrm{pr}} = \beta_{\mathrm{pr}} = 0°$ and the wavelength of

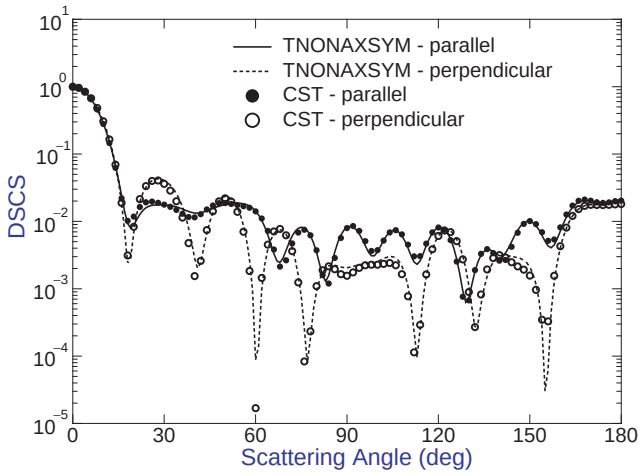

Fig. 3.21. Normalized differential scattering cross-sections of a dielectric hexagonal prism computed with the TNONAXSYM routine and the finite integration technique (CST)

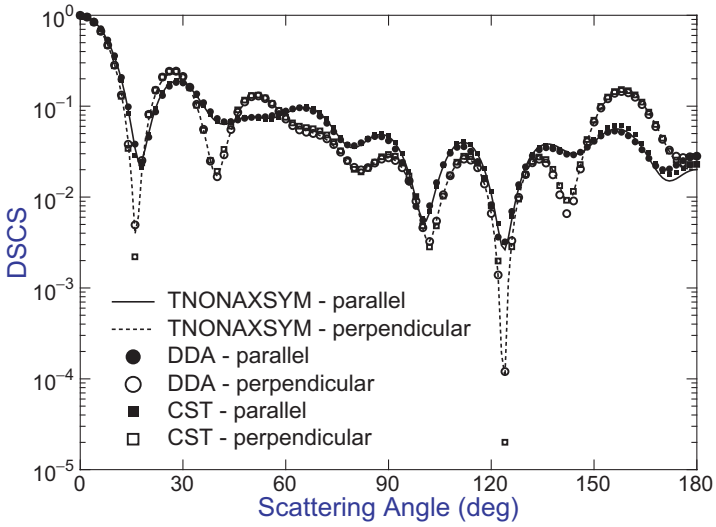

Fig. 3.22. Normalized differential scattering cross-sections of a uniaxial anisotropic cube computed with the TNONAXSYM routine, discrete dipole approximation (DDA) and finite integration technique (CST)

the incident radiation is $\lambda = 0.3\,\mu\text{m}$. The maximum expansion and azimuthal orders are $N_{\text{rank}} = 11$ and $M_{\text{rank}} = 11$, respectively, and the numbers of integration points in the zenith and azimuthal directions are $N_{\text{int1}} = 100$ and

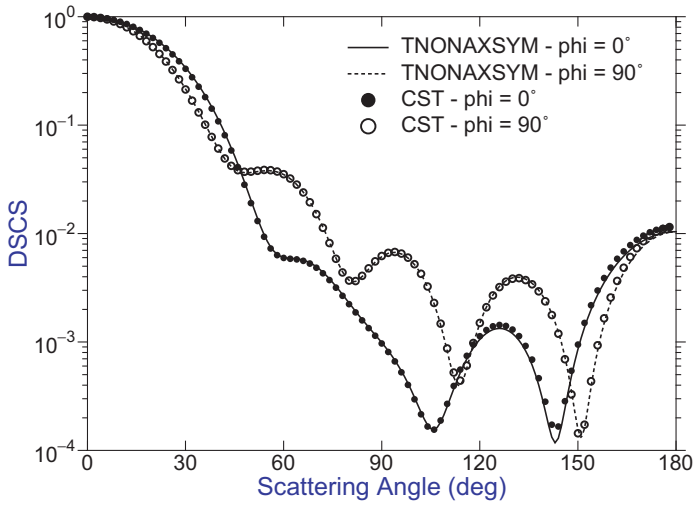

Fig. 3.23. Normalized differential scattering cross-sections of a uniaxial anisotropic ellipsoid computed with the TNONAXSYM routine and the finite integration technique (CST)

$N_{\mathrm{int2}} = 100$, respectively. The curves show that the differential scattering cross-sections are reasonably well reproduced by the TNONAXSYM routine.

Next we present calculations for a dielectric, a perfectly conducting and a chiral cube of length $2k_{\mathrm{s}}a = 10$. The refractive index of the dielectric cube is $m_{\mathrm{r}} = 1.5$ and the chirality parameter is $\beta k_{\mathrm{i}} = 0.1$. The scattering characteristics are computed by using the symmetry properties of the transition matrix. For particles with a plane of symmetry perpendicular to the axis of rotation (mirror symmetric particles with the surface parameterization $r(\theta, \varphi) = r(\pi - \theta, \varphi)$) the $\boldsymbol{T}$ matrix can be computed by integrating θ over the interval $[0, \pi/2]$, while for particles with azimuthal symmetry (particles with the surface parameterization $r(\theta, \varphi) = r(\theta, \varphi + 2\pi/N)$, where $N \geq 2$) the $\boldsymbol{T}$ matrix can be computed by integrating φ over the interval $[0, 2\pi/N]$. For $\boldsymbol{T}$-matrix calculations without mirror and azimuthal symmetries, the numbers of integration points on each square surface are $N_{\mathrm{int1}} = N_{\mathrm{int2}} = 30$. For calculations using azimuthal symmetry, the numbers of integration points on the top and bottom quarter-square surfaces are $N_{\mathrm{int1}} = N_{\mathrm{int2}} = 20$, while for calculations using mirror symmetry, the numbers of integration points on the lateral half-square surface are $N_{\mathrm{int1}} = N_{\mathrm{int2}} = 20$. The integration surfaces are shown in Fig. 3.24, and the differential scattering cross-sections are plotted in Figs. 3.25–3.27. The results obtained using different techniques are generally close to each other.

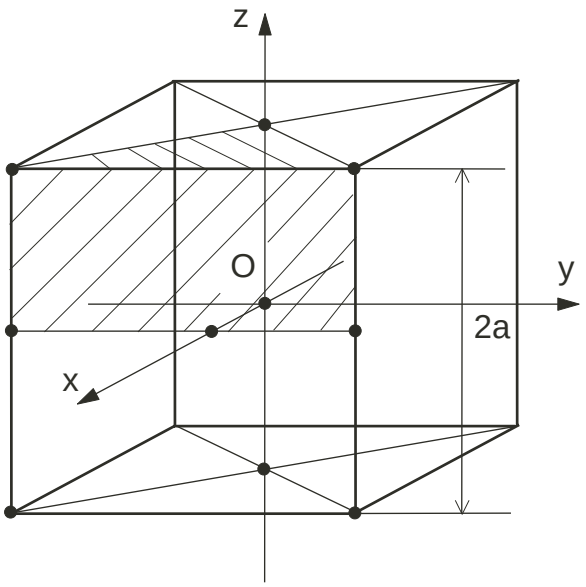

Fig. 3.24. Integration surfaces for a cube

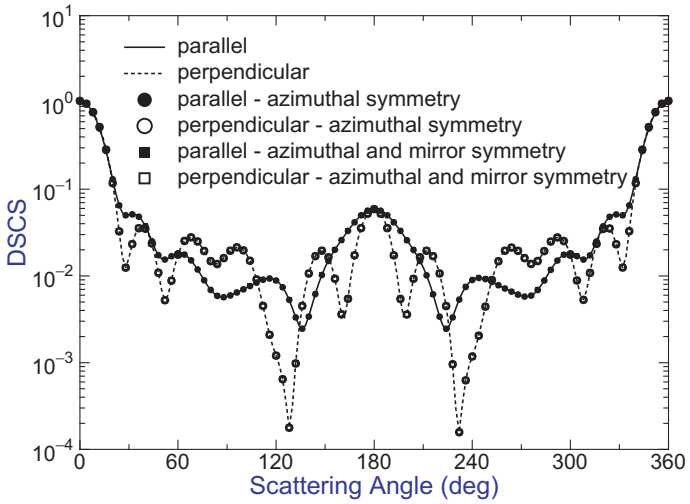

Fig. 3.25. Normalized differential scattering cross-sections of a dielectric cube using the symmetry properties of the transition matrix

3.3.3 Triangular Surface Patch Model

Some nonaxisymmetric particle shapes such as ellipsoids, quadratic prisms and regular polyhedral prisms are directly included in the Fortran program

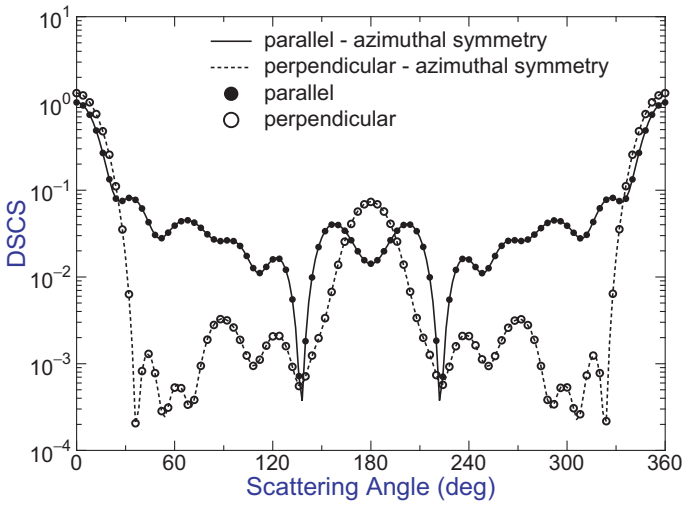

Fig. 3.26. Normalized differential scattering cross-sections of a chiral cube using the symmetry properties of the transition matrix

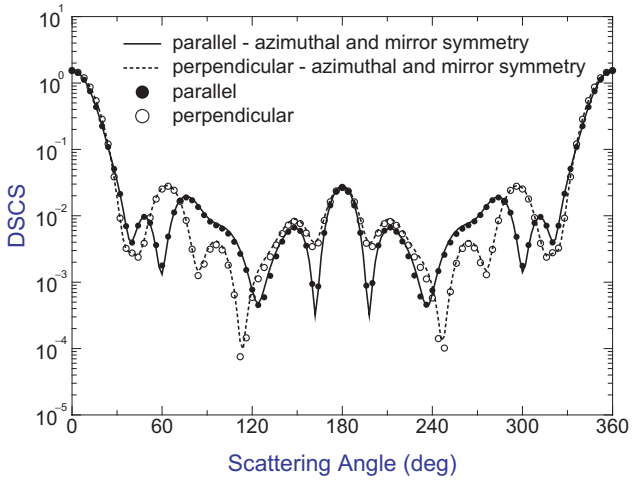

Fig. 3.27. Normalized differential scattering cross-sections of a perfectly conducting cube using the symmetry properties of the transition matrix

as it is provided on the CD-ROM with the book. To handle arbitrary particle geometries, the program can also read particle shape data from an input file.

The particle shape data is based on a surface description using a triangular surface patch model. There are various 3D object file formats suitable for a meshed particle shape. We decided for the Wavefront `.obj` file format but the

program will only support the polygonal format subset and not the free-form geometry (also included in the `.obj` file format). In this case, a triangular surface patch model of the particle surface has to be generated by an adequate software. For shapes given by an implicit equation, the HyperFun polygonizer [106, 183] supporting high-level language functional representations is a possible candidate for surface mesh generation. Function representation is a generalization of traditional implicit surfaces and constructive solid geometry, which allows the construction of complex shapes such as isosurfaces of real-valued functions [184]. The HyperFun polygonizer generates a VRML output of a sufficiently regular triangular patch model, which is then converted to the .obj file format by using the 3D Exploration program.

To compute the $\boldsymbol{T}$-matrix elements by surface integrals we employ a modified midpoint or centroid quadrature. The integral over each surface patch is approximated by multiplying the value of the integrand at the centroid by the patch area [79]

$$\int_S f \mathrm{d}S \approx \sum_i f(v_{i,\mathrm{c}}) \mathrm{area}[v_{i,1}, v_{i,2}, v_{i,3}] \,, \tag{3.12}$$

where, $v_{i,1}, v_{i,2}, v_{i,3}$ are the vertices spanning a triangle and $v_{i,\mathrm{c}}$ denotes the mass center of the triangle $[v_{i,1}, v_{i,2}, v_{i,3}]$

$$v_{i,\mathrm{c}} = \frac{1}{3} \sum_{j=1}^{3} v_{i,j} \,. \tag{3.13}$$

For a sufficiently large number of surface patches, the use of this centroid integration is satisfactorily accurate. In convergence checks versus the number of triangular faces, we found that this centroid quadrature is quite stable and the computational results are not much influenced by the number of integration elements.

As an example, we consider a sphere which has been cut at a quarter of its diameter on the z-axis as shown in Fig. 3.28. The cut sphere has been meshed

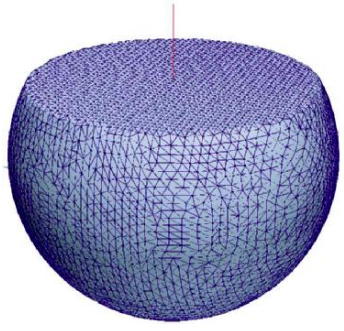

Fig. 3.28. Geometry of a cut sphere with 10,132 faces

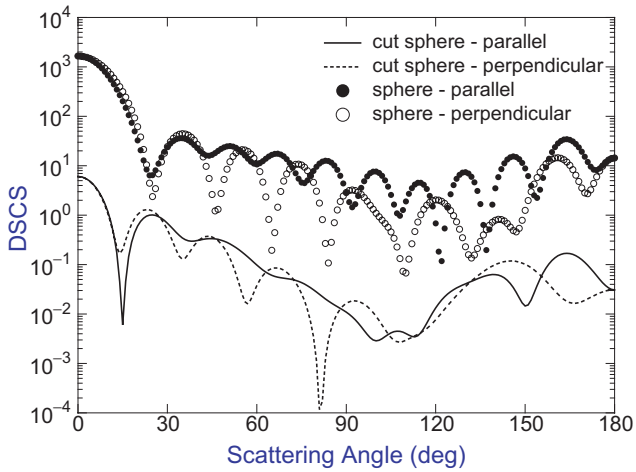

Fig. 3.29. Normalized differential scattering cross-sections of a sphere and a cut sphere

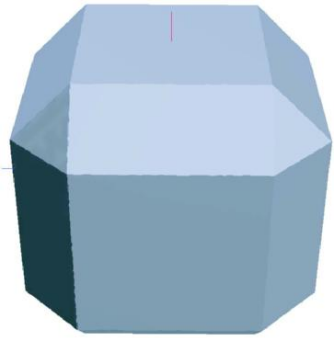

Fig. 3.30. Geometry of a cube shaped particle with 31,284 faces

with 10132 faces, the Mie parameter computed from the radius is 10, the refractive index is 1.5 and the direction of the incident plane wave is along the z-axis. In Fig. 3.29 the scattering pattern is plotted together with the scattering pattern of a sphere with the same parameters. For better visibility the curves are shifted and it is apparent that there are pronounced differences in the scattering diagrams of a sphere and a cut sphere.

There are different ways to compute scattering by arbitrary particle shapes reconstructed from a number of measured data points. Next we present an example using compactly supported radial basis functions (CS-RBF) for scattered data points processing. For this application we used the software toolkit by Kojekine et al. [121] available from www.karlson.ru. The data points represent a cube shaped particle as depicted in Fig. 3.30 and a number of 378

Fig. 3.31. Geometry of a cube shaped particle with 17,680 faces approximated by CS-RBF

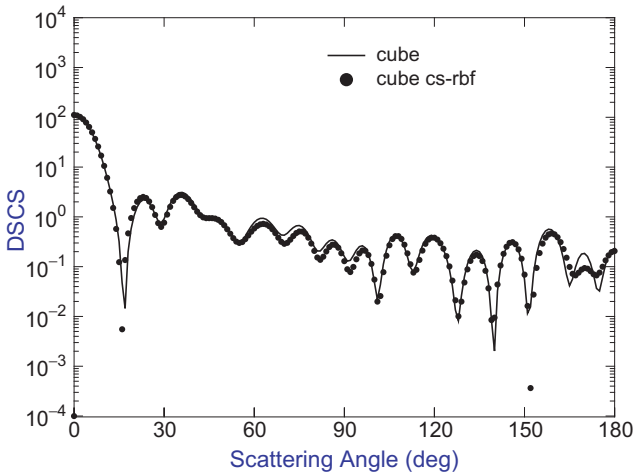

Fig. 3.32. Normalized differential scattering cross-sections for parallel polarization of a cube and a reconstructed cube

surface points were used in shape reconstruction. The result of the shape reconstruction can be seen in Fig. 3.31, while in Figs. 3.32 and 3.33 the scattering diagrams of the original and the reconstructed cubes are plotted. There are only minor differences in the backscattering region. The particle shapes have been discretized to a large number of surface patches by using a divide by four scheme and the Rational Reducer Professional software for grid reduction, so that there are finally 17,680 triangular faces with the reconstructed cube.

Scattering results for nonaxisymmetric particles using the superellipsoid as a model particle shape have been given by Wriedt [268]. The program SScaTT (Superellipsoid Scattering Tool) includes a small graphical user interface to generate various superellipsoid particle shape modes and is available

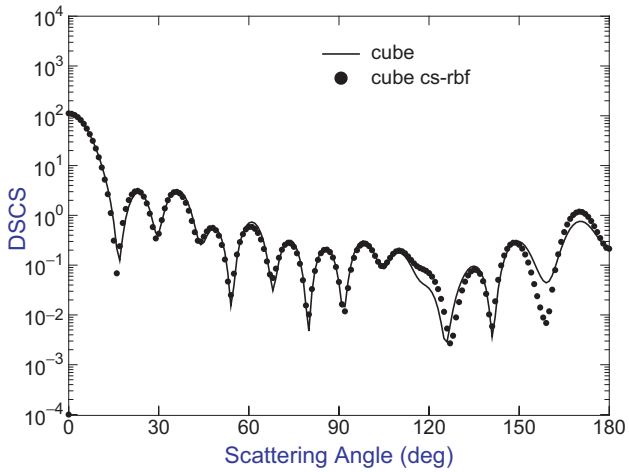

Fig. 3.33. Normalized differential scattering cross-sections for perpendicular polarization of a cube and a reconstructed cube

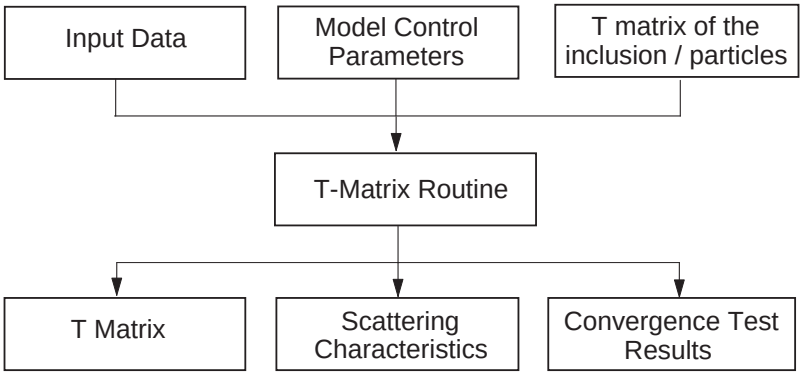

Fig. 3.34. Flow diagram of the TINHOM routine

on CD-ROM with this book. The effect of particle surface discretization on the computed scattering patterns has been analyzed by Hellmers and Wriedt [99].

3.4 Inhomogeneous Particles

This section discusses numerical and practical aspects of $\boldsymbol{T}$-matrix calculations for inhomogeneous particles. The flow diagram of the TINHOM routine is shown in Fig. 3.34. The program supports scattering computation for axisymmetric and dielectric host particles with real refractive index. The main feature of this routine is that the $\boldsymbol{T}$-matrix of the inclusion is provided as input parameter. The inclusion can be a homogeneous, axisymmetric or

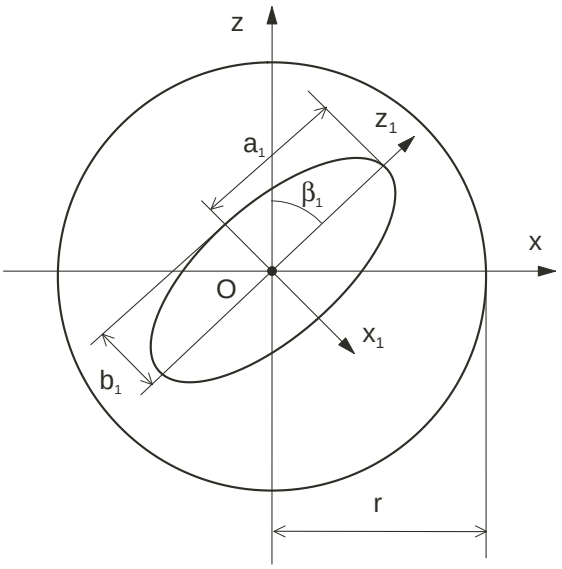

Fig. 3.35. Geometry of an inhomogeneous sphere with a spheroidal inclusion

nonaxisymmetric particle, a composite or a layered scatterer and an aggregate. This choice enables the analysis of particles with complex structure and enhances the flexibility of the program. For computing the $\boldsymbol{T}$-matrix of the inclusion, the refractive index of the ambient medium must be identical with the relative refractive index of host particle.

We consider an inhomogeneous sphere of radius $k_{\mathrm{s}}r = 10$ as shown in Fig. 3.35. The inhomogeneity is a prolate spheroid of semi-axes $k_{\mathrm{s}}a_1 = 5$ and $k_{\mathrm{s}}b_1 = 5$. The relative refractive indices of the sphere and the spheroid with respect to the ambient medium are $m_{\mathrm{r}} = 1.2$ and $m_{\mathrm{r1}} = 1.5$, respectively, and the Euler angles specifying the orientation of the prolate spheroid with respect to the particle coordinate system are $\alpha_{\mathrm{p1}} = \beta_{\mathrm{p1}} = 45°$. The differential scattering cross-sections are calculated for the case of normal incidence, and the maximum expansion and azimuthal orders for computing the inclusion $\boldsymbol{T}$ matrix are $N_{\mathrm{rank}} = 10$ and $M_{\mathrm{rank}} = 5$, respectively. In Fig. 3.36, we compare the $\boldsymbol{T}$-matrix results to those obtained with the multiple multipole method. The agreement between the scattering curves is acceptable.

In Fig. 3.37, we show an inhomogeneous sphere with a spherical inclusion. The radii of the host sphere and the inclusion are $R = 1.0\,\mu\mathrm{m}$ and $r = 0.5\,\mu\mathrm{m}$, respectively, while the relative refractive indices with respect to the ambient medium are $m_{\mathrm{r}} = 1.33$ and $m_{\mathrm{r1}} = 1.5$, respectively. The inhomogeneity is placed at the distance $z_1 = 0.25\,\mu\mathrm{m}$ with respect to the particle coordinate system and the wavelength of the incident radiation is chosen as $\lambda = 0.6328\,\mu\mathrm{m}$.

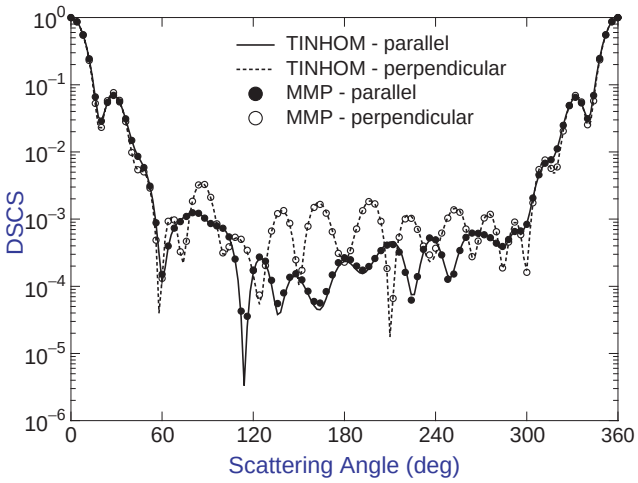

Fig. 3.36. Normalized differential scattering cross-sections of an inhomogeneous sphere with a spheroidal inclusion. The results are computed with the TINHOM routine and the multiple multipole method (MMP)

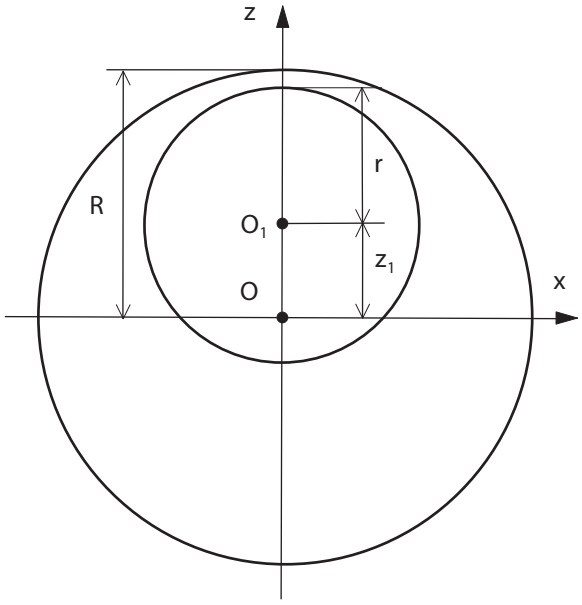

Fig. 3.37. Geometry of an inhomogeneous sphere with a spherical inclusion

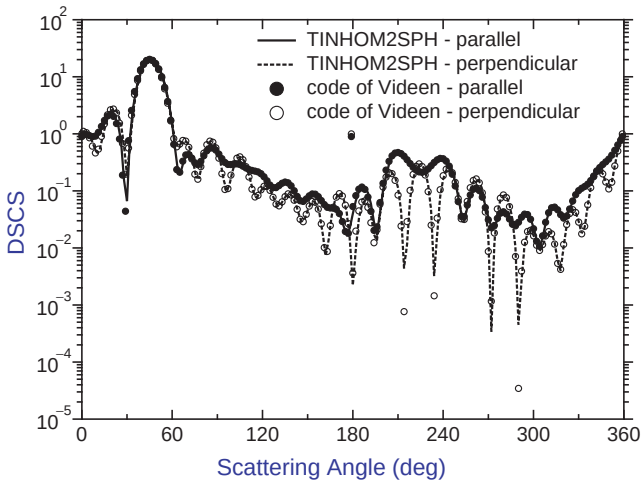

Fig. 3.38. Normalized differential scattering cross-sections of an inhomogeneous sphere with a spherical inclusion

The results of the differential scattering cross-sections computed with the TINHOM2SPH routine and the code developed by Videen et al. [243] are shown in Fig. 3.38. The plots demonstrate a complete agreement between the scattering curves. We note that the FORTRAN code developed by Videen et al. [243] (see also, [180]), uses the Lorenz–Mie theory to represent the electromagnetic fields. To exploit the orthogonality of the vector spherical wave functions, the translation addition theorem is used to re-expand the field scattered by the inhomogeneity about the origin of the host sphere.

In order to provide a numerical test of the accuracy of the recursive $\boldsymbol{T}$-matrix algorithm described in Sect. 2.6, we consider an inhomogeneous sphere with multiple spherical inclusions. The radius of the spherical inclusions is $k_{\mathrm{s}}r = 0.3$, and the maximum expansion and azimuthal orders for computing the inclusion $\boldsymbol{T}$-matrix are $N_{\mathrm{rank}} = M_{\mathrm{rank}} = 3$. The radius of the host sphere is $k_{\mathrm{s}}R = k_{\mathrm{s}}R_{\mathrm{cs}}(1) = 3.5$ and 200 inhomogeneities are generated by using the sequential addition method [47]. The relative refractive indices with respect to the ambient medium are $m_{\mathrm{r}} = 1.2$ and $m_{\mathrm{r1}} = 1.5$. According to the guidelines of the recursive $\boldsymbol{T}$-matrix algorithm, two auxiliary surfaces of radii $k_{\mathrm{s}}R_{\mathrm{cs}}(2) = 2.7$ and $k_{\mathrm{s}}R_{\mathrm{cs}}(3) = 2.2$ are considered in the interior of the host particle. The values of the maximum expansion and azimuthal orders for each auxiliary surface are given in Table 3.5. The matrix inversion is performed with the bi-conjugate gradient method instead of the LU-factorization method. The results presented in Fig. 3.39 correspond to the direct method and the recursive algorithm with one and two auxiliary surfaces. The agreement between the scattering curves is satisfactory, and note that the recursive algorithm with two auxiliary surfaces is faster by a factor of 2 than the direct method.

Table 3.5. Maximum expansion and azimuthal orders for the auxiliary surfaces

Auxiliary surface	N_{rank}	M_{rank}
1	8	5
2	6	4
3	6	4

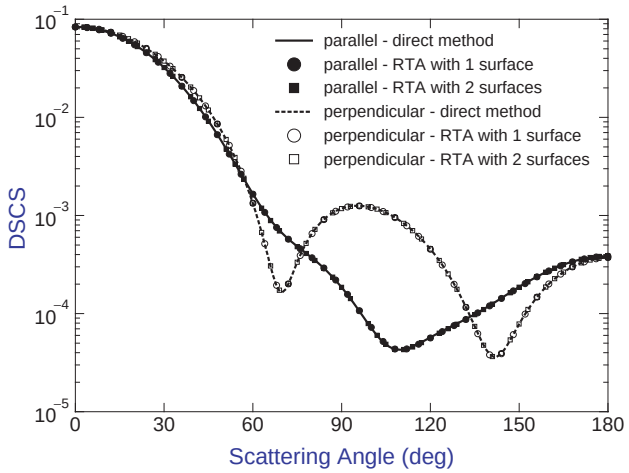

Fig. 3.39. Normalized differential scattering cross-sections of an inhomogeneous sphere with multiple spherical inclusions

3.5 Layered Particles

In the following examples we consider electromagnetic scattering by axisymmetric, layered particles. An axisymmetric, layered particle is an inhomogeneous particle consisting of several consecutively enclosing and rotationally symmetric surfaces with a common axis of symmetry. The scattering computations are performed with the TLAY routine and the set of routines devoted to the analysis of inhomogeneous particles. Particle geometries currently supported by the TLAY routine include layered spheroids and cylinders. We note that localized and distributed sources can be used for $\boldsymbol{T}$-matrix calculations, and in contrast to the TINHOM routine, the relative refractive index of the host particle can be a complex quantity (absorbing dielectric medium).

Figure 3.40 shows a layered spheroid with $k_{\mathrm{s}}a = 10$, $k_{\mathrm{s}}b = 8$, $k_{\mathrm{s}}a_1 = 8$, $k_{\mathrm{s}}b_1 = 3$ and $k_{\mathrm{s}}z_1 = 3$. The relative refractive indices of the host spheroid and the inhomogeneity with respect to the ambient medium are $m_{\mathrm{r}} = 1.2$ and $m_{\mathrm{r1}} = 1.5$, respectively. Numerical results are presented as plots of the differential scattering cross-sections for the inhomogeneous spheroid in fixed or random orientation. The scattering characteristics are computed with localized and distributed sources, whereas the distributed sources are placed

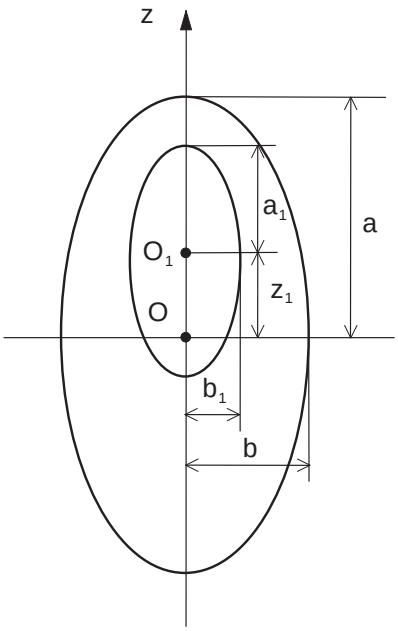

Fig. 3.40. Geometry of a layered spheroid

Table 3.6. Parameters of calculation for an oblate layered spheroid

Type of sources	$N_{\rm rank}$-host particle	$N_{\rm rank}$-inclusion	$N_{\rm int}$
Localized	17	12	500
Distributed	14	8	2,000

along the symmetry axis of the prolate spheroids. The maximum expansion orders are $N_{\rm rank} = 20$ for the host spheroid and $N_{\rm rank} = 13$ for the inclusion. The global number of integration points is $N_{\rm int} = 200$ for localized sources, and $N_{\rm int} = 1000$ for distributed sources. The TINHOM routine uses as input parameter the inclusion $\boldsymbol{T}$-matrix, which is characterized by $N_{\rm rank} = 13$ and $M_{\rm rank} = 5$. The results presented in Figs. 3.41 and 3.42 show a complete agreement between the different methods.

Scattering by oblate spheroids can be computed with localized and discrete sources distributed in the complex plane. Figure 3.43 compares results obtained with localized and distributed sources for an oblate layered spheroid with $k_{\rm s}a = 5$, $k_{\rm s}b = 10$, $k_{\rm s}a_1 = 3$ and $k_{\rm s}b_1 = 5$. The relative refractive indices are $m_{\rm r} = 1.2$ and $m_{\rm r1} = 1.5$, and the parameters of calculation are given in Table 3.6.

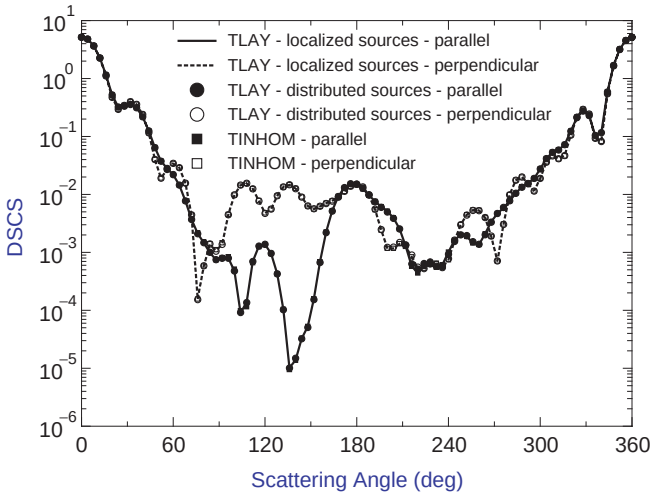

Fig. 3.41. Normalized differential scattering cross-sections of a layered spheroid

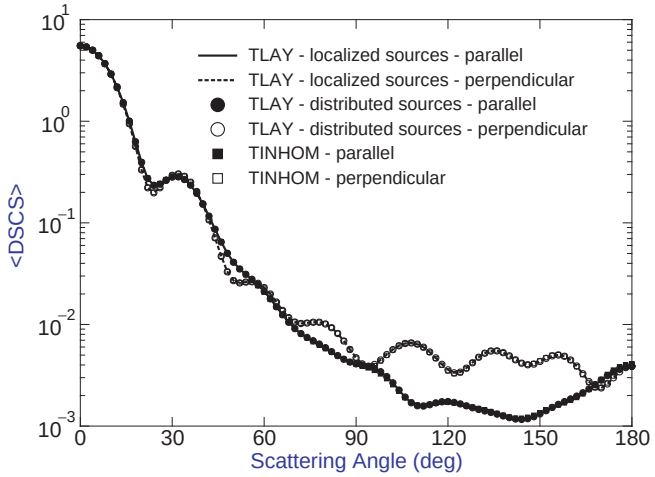

Fig. 3.42. Averaged differential scattering cross-sections of a layered spheroid

For highly elongated particles, distributed sources are required to achieve convergence. The results plotted in Fig. 3.44 correspond to a layered cylinder with $k_{\mathrm{s}}L = 10$, $k_{\mathrm{s}}r = 2$, $k_{\mathrm{s}}L_1 = 5$ and $k_{\mathrm{s}}r_1 = 1$ (Fig. 3.45). The relative refractive indices of the host particle and the inclusions are $m_{\mathrm{r}} = 1.2$ and $m_{\mathrm{r1}} = 1.4$, respectively. The maximum expansion orders are $N_{\mathrm{rank}} = 14$ for

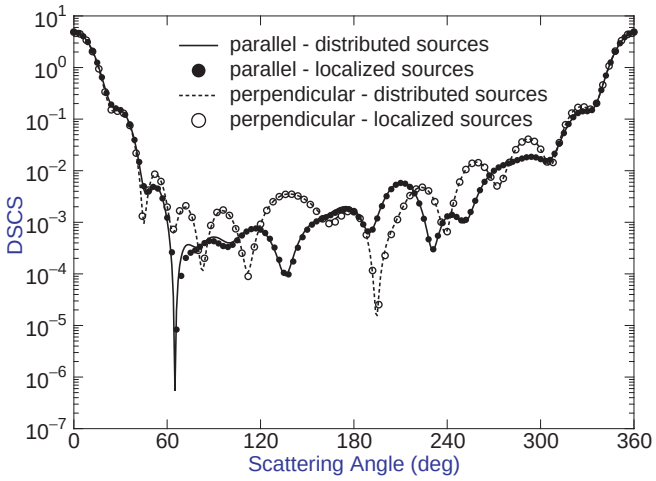

Fig. 3.43. Normalized differential scattering cross-sections of an oblate layered spheroid

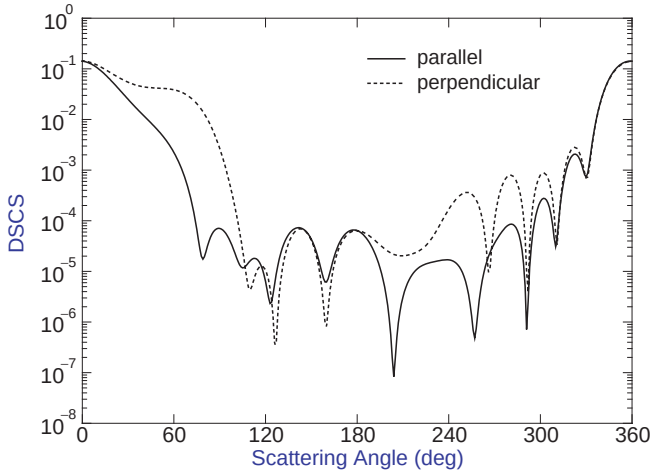

Fig. 3.44. Normalized differential scattering cross-sections of a layered cylinder

the host particle and $N_{\mathrm{rank}} = 8$ for the inclusion, while the global number of integration points is $N_{\mathrm{int}} = 1{,}000$.

In the next example, the host particle is a sphere of radius $k_{\mathrm{s}}R = 10$, the inclusion is a prolate spheroid with $k_{\mathrm{s}}a_1 = 8$ and $k_{\mathrm{s}}b_1 = 3$, and the relative refractive indices are $m_{\mathrm{r}} = 1.2$ and $m_{\mathrm{r1}} = 1.5$. Figures 3.46 and 3.47 compare results obtained with the routines TLAY, TINHOMSPH and TINHOM. The agreement between the scattering curves is very good.

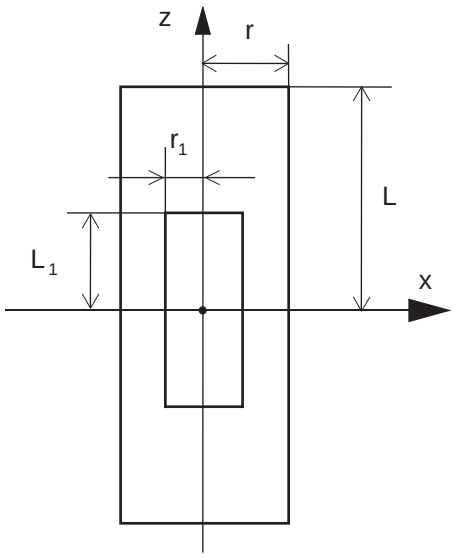

Fig. 3.45. Geometry of a layered cylinder

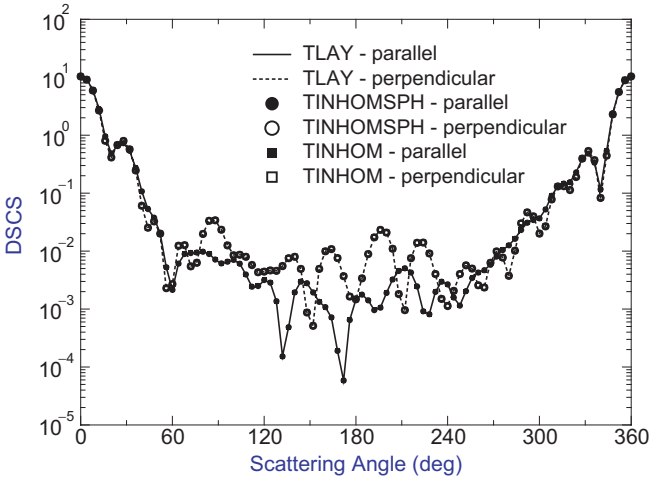

Fig. 3.46. Normalized differential scattering cross-sections of a layered particle consisting of a host sphere and a spheroidal inclusion

In Fig. 3.48, we show results for a concentrically layered sphere consisting of three layers of radii $k_s r_1 = 10$, $k_s r_2 = 7$ and $k_s r_3 = 4$. The relative refractive indices with respect to the ambient medium are $m_{r1} = 1.2 + 0.2j$, $m_{r2} = 1.5 + 0.1j$ and $m_{r3} = 1.8 + 0.3j$. The scattering curves obtained with the TSPHERE and TLAY routines are close to each other.

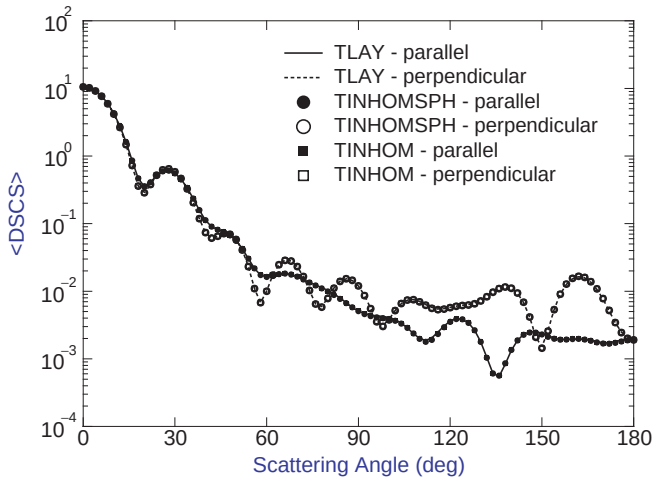

Fig. 3.47. Averaged differential scattering cross-sections of a layered particle consisting of a host sphere and a spheroidal inclusion

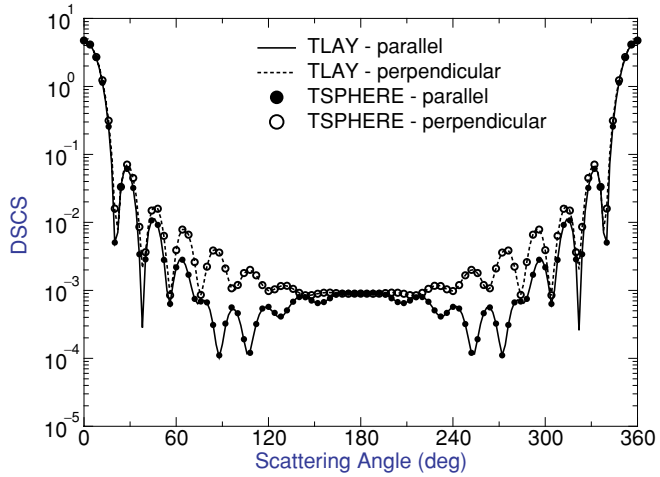

Fig. 3.48. Normalized differential scattering cross-sections of a layered sphere

3.6 Multiple Particles

In the following analysis we investigate electromagnetic scattering by a system of particles. The basic routine for analyzing this type of scattering problem is the TMULT routine. As for inhomogeneous scatterers, the individual $\boldsymbol{T}$-matrices of the particles are input parameters of the code and they may correspond to homogeneous, axisymmetric or nonaxisymmetric particles

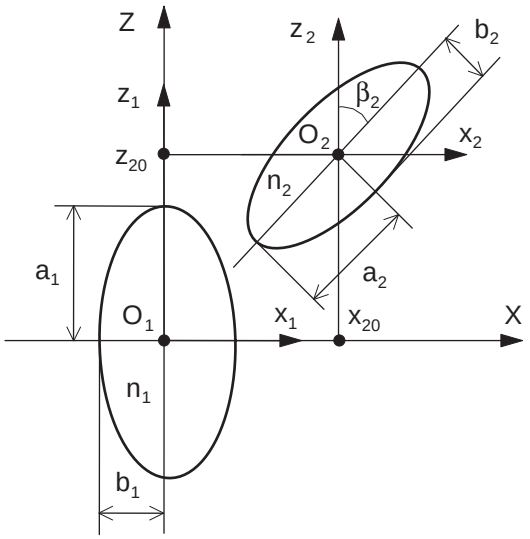

Fig. 3.49. Geometry of a system of two prolate spheroids

and inhomogeneous, composite or layered particles. The flow diagram of the TMULT routine is as in Fig. 3.34.

Figure 3.49 illustrates a system of two spheroids of semi-axes $k_s a_1 = k_s a_2 = 4$ and $k_s b_1 = k_s b_2 = 2$, and relative refractive indices $m_{r1} = m_{r2} = 1.5$. The Cartesian coordinates of the center of the second spheroid are $k_s x_{20} = k_s z_{20} = 4\sqrt{2}$ and $y_{20} = 0$, while the Euler angles specifying the orientation of the spheroids are chosen as $\alpha_{p1} = \beta_{p1} = 0°$ and $\alpha_{p2} = \beta_{p2} = 45°$. The first computational step involves the calculation of the individual $\boldsymbol{T}$-matrix of a spheroid by using the TAXSYM code, and for this calculation, the maximum expansion and azimuthal orders are $N_{rank} = 10$ and $M_{rank} = 4$, respectively. The individual $\boldsymbol{T}$-matrices are then used to compute the $\boldsymbol{T}$-matrix of the spheroids with respect to the origin O_1, and the dimension of the system $\boldsymbol{T}$-matrix is given by $N_{rank} = 20$ and $M_{rank} = 18$. In Fig. 3.50, we show the differential scattering cross-sections computed with the TMULT routine and the multiple multipole method. The scattering curves are in good agreement.

As a second example, we consider a system of five spherical particles illuminated by a plane wave propagating along the Z-axis of the global coordinate system. The spheres are identical and have a radius of $k_s r = 2$ and a relative refractive index of $m_r = 1.5$, while the length specifying the position of the spheres is $k_s l = 6$ (Fig. 3.51). The system $\boldsymbol{T}$-matrix is computed with respect to the origin O and is characterized by $N_{rank} = 18$ and $M_{rank} = 16$. The scattering characteristics are computed with the TMULTSPH routine, and numerical results are again presented in the form of the differential scattering cross-sections. The curves plotted in Fig. 3.52 correspond to a fixed orientation

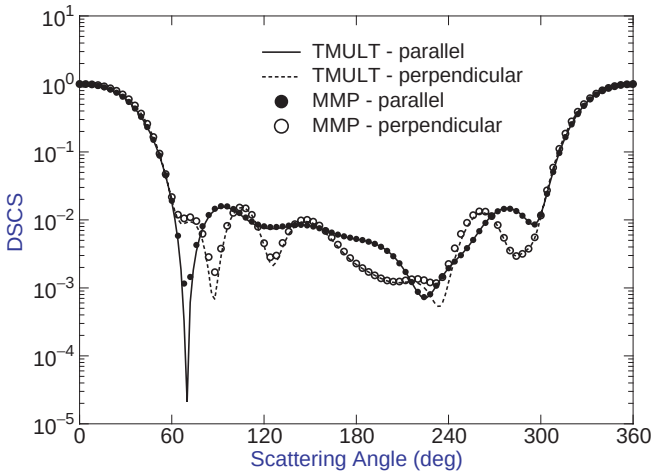

Fig. 3.50. Normalized differential scattering cross-sections of a system of two prolate spheroids computed with the TMULT routine and the multiple multipole method (MMP)

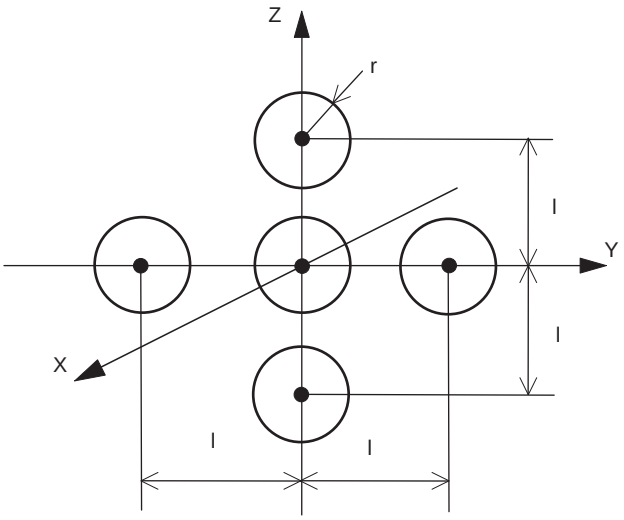

Fig. 3.51. Geometry of a system of five spheres

of the system of spheres ($\alpha_\mathrm{p} = \beta_\mathrm{p} = \gamma_\mathrm{p} = 0°$) and are similar for the $\boldsymbol{T}$-matrix and the multiple multipole solutions. For a random orientation, we compute the elements of the scattering matrix, and the results are shown in Figs. 3.53 and 3.54 together with the results computed with the SCSMTM code devel-

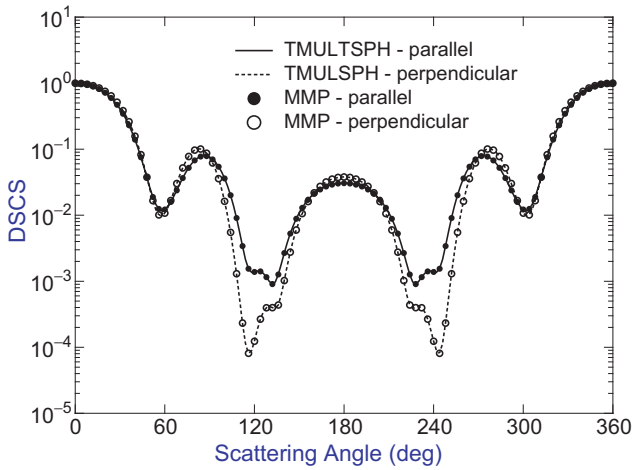

Fig. 3.52. Normalized differential scattering cross-sections of a system of five spheres computed with the TMULT routine and the multiple multipole method (MMP)

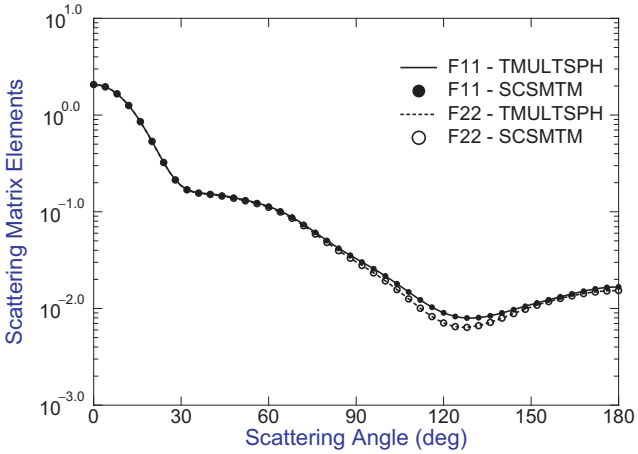

Fig. 3.53. Scattering matrix elements F_{11} and F_{22} of a system of five spheres computed with the TMULT routine and the code SCSMTM of Mackowski and Mishchenko [153]

oped by Mackowski and Mishchenko [153]. The curves are generally close to each other.

Figure 3.55 illustrates a system of four identical spheres that can be used to compare different routines. The radius of each spherical particle is $k_s r = 3$ and the relative refractive index is $m_r = 1.5$. In the global coordinate system

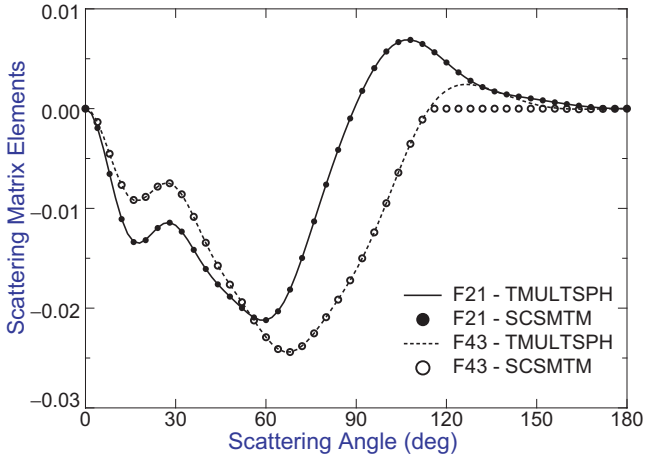

Fig. 3.54. Scattering matrix elements F_{21} and F_{43} of a system of five spheres computed with the TMULT routine and the code SCSMTM of Mackowski and Mishchenko [153]

$OXYZ$, two local coordinate systems $O_1x_1y_1z_1$ and $O_2x_2y_2z_2$ are defined, and the positions of the origins O_1 and O_2 are characterized by $x_{01} = y_{01} = z_{01} = L$ and $x_{02} = y_{02} = z_{02} = -L$, respectively, where $k_sL = 6.5$. In each local coordinate system, a system of two spheres is considered, and the distance between the sphere centers is $2k_sl = 3.5$, while the Euler angles specifying the orientation of the two-spheres system are $\alpha_{p1} = \beta_{p1} = 45°$ and $\alpha_{p2} = \beta_{p2} = 30°$. The Cartesian coordinates of the spheres are computed with respect to the global coordinate system and the TMULTSPH routine is used to compute the scattering characteristics. The dimension of the $\boldsymbol{T}$-matrix of the four-sphere system is given by $N_{rank} = 21$ and $M_{rank} = 19$. A second technique for analyzing this scattering geometry involves the computation of the $\boldsymbol{T}$-matrix of the two-sphere system by using the TMULT2SPH routine. In this case, $N_{rank} = 16$ and $M_{rank} = 5$, and the $\boldsymbol{T}$-matrix of the two-sphere system serves as input parameter for the TMULT routine. Figures 3.56 and 3.57 illustrate the differential scattering cross-sections for a fixed ($\alpha_p = \beta_p = \gamma_p = 0°$) and a random orientation of the system of spheres. The far-field patterns are reproduced very accurately by both methods.

To demonstrate the capabilities of the TMULTSPH routine we present some exemplary results for polydisperse aggregates. Monodisperse aggregates of small spherical particles are characterized by the number of primary spherule N, the fractal dimension D_f, the fractal pre-factor k_f, the radius of gyration R_g, and the radius of the primary spherules r_p. These morphological parameters are related in the form of a scaling law

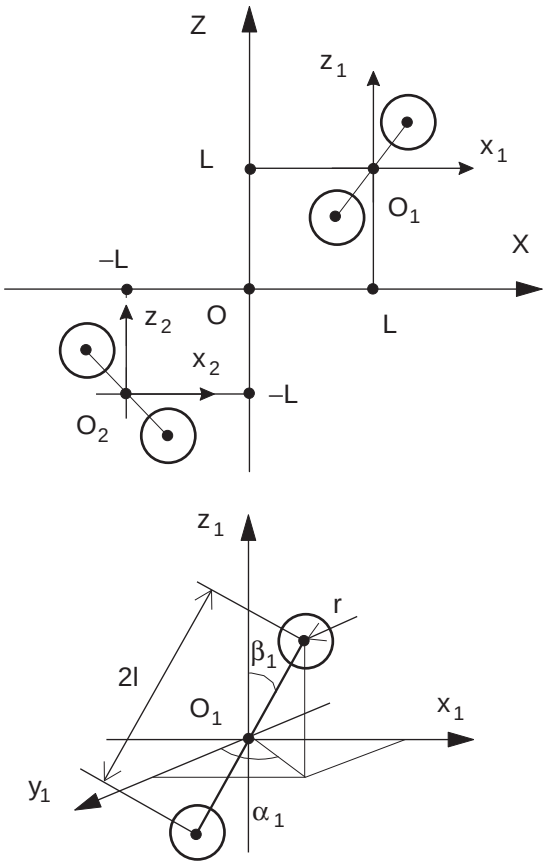

Fig. 3.55. Geometry of a system of four spheres

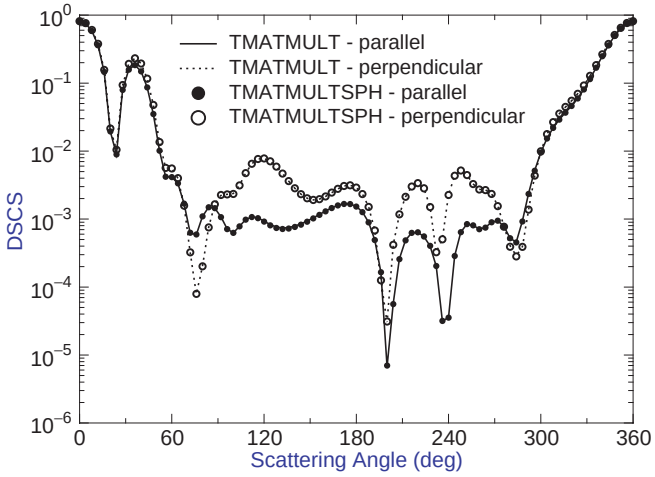

Fig. 3.56. Normalized differential scattering cross-sections of a system of four spheres

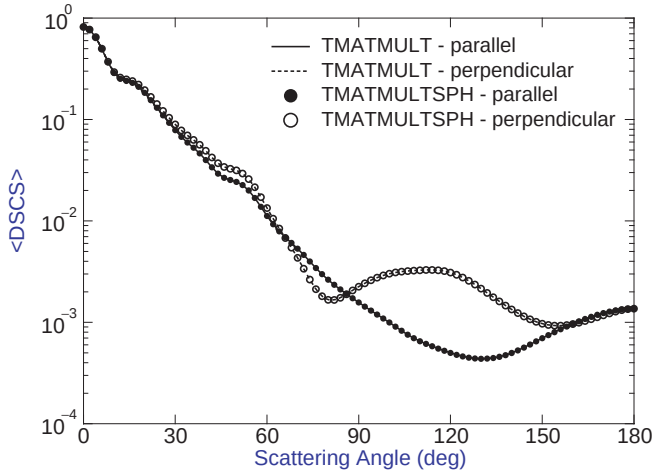

Fig. 3.57. Averaged differential scattering cross-sections of a system of four spheres

$$N = k_{\mathrm{f}} \left(\frac{R_{\mathrm{g}}}{r_{\mathrm{p}}} \right)^{D_{\mathrm{f}}} , \tag{3.14}$$

where the radius of gyration is determined from the position of each primary spherule $\boldsymbol{r}_i$ to the geometrical center of the cluster $\boldsymbol{r}_0$,

$$R_{\mathrm{g}}^2 = \frac{1}{N} \sum_{i=1}^{N} |\boldsymbol{r}_i - \boldsymbol{r}_0|^2$$

and $\boldsymbol{r}_0 = (1/N) \sum_{i=1}^{N} \boldsymbol{r}_i$. Equation (3.14) is important because the values of parameters are linked to real physical processes. If $D_f \approx 1.8$ the process belongs to a diffusion limited aggregation and if $D_f \approx 2.1$ it belongs to a reaction limited aggregation. For simulating diffusion limited aggregation, we developed a Fortran program and used the Cartesian coordinates of the spherule as input parameters for the TMULTSPH routine. This program is based on the fast algorithm described by Filippov et al. [66] and generates aggregates by using two different methods. In the first method, each new primary spherule will be stuck on the mother aggregate after touching one of the existing spherules. This method is known as the diffusion limited algorithm (DLA) and is used for aggregates not larger than about $N = 150$ spherules. With the second method, complete small aggregates are stuck on the mother aggregate. The small aggregates are generated with the DLA algorithm and consists of about 20 or more primary spherules. This method is called diffusion limited cluster cluster aggregation (DLCCA) and gives more realistic aggregates. An example of a monodisperse aggregate representing

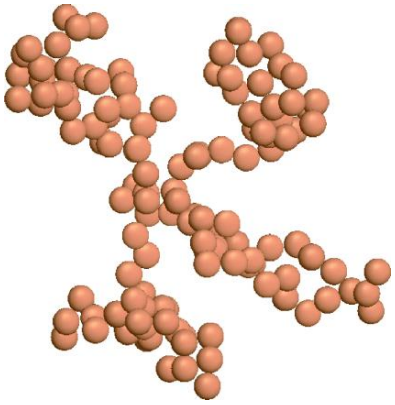

Fig. 3.58. Monodisperse aggregate with $D_\mathrm{f} = 1.8, N = 130$ and $r_\mathrm{p} = 10\,\mathrm{nm}$

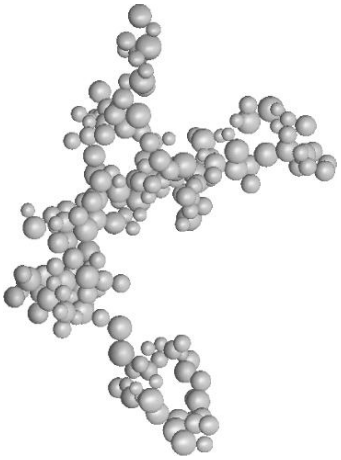

Fig. 3.59. Polydisperse aggregate with $D_\mathrm{f} = 1.8, N = 203$ and r_p between 10 and 20 nm

a soot particle from a combustion processes is shown in Fig. 3.58, while a polydisperse aggregate is shown in Fig. 3.59. For the monodisperse aggregate, the scattering characteristics are shown in Fig. 3.60, and the essential parameters controlling the convergence process are $N_\mathrm{rank} = 8$ and $M_\mathrm{rank} = 6$ for the system $\boldsymbol{T}$-matrix, and $N_\mathrm{rank} = 4$ and $M_\mathrm{rank} = 3$ for the primary spherules. The differential scattering cross-sections of the polydisperse aggregate are plotted in Fig. 3.61, and the parameters of calculation for the system $\boldsymbol{T}$-matrix increase to $N_\mathrm{rank} = 12$ and $M_\mathrm{rank} = 10$. The program described above has been used by Riefler et al. [204] to characterize soot from a flame by analyzing the measured scattering patterns.

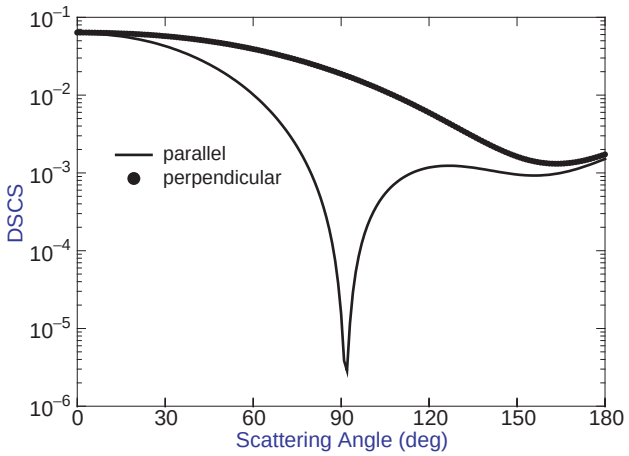

Fig. 3.60. Normalized differential scattering cross-sections of a monodisperse aggregate

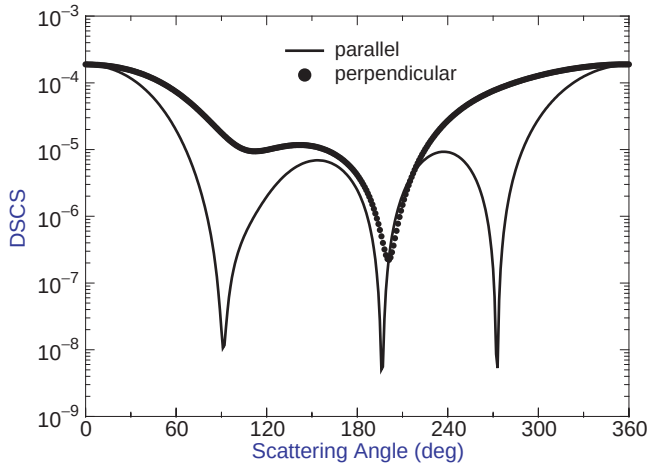

Fig. 3.61. Normalized differential scattering cross-sections of a polydisperse aggregate

3.7 Composite Particles

Electromagnetic scattering by axisymmetric, composite particles can be computed with the TCOMP routine. An axisymmetric, composite particle consists of several nonenclosing, rotationally symmetric regions with a common axis of symmetry. In contrast to the TMULT routine, TCOMP is based on a formalism which avoid the use of any local origin translation. The scattering

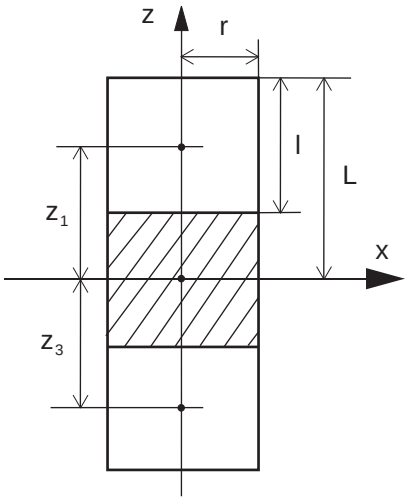

Fig. 3.62. Geometry of a composite particle consisting of three identical cylinders

characteristics can be computed with localized or distributed sources, and the program supports calculations for dielectric particles. Particle geometries included in the library are half-spheroids with offset origins and three cylinders.

In Fig. 3.62, we show a composite particle consisting of three identical cylinders of radius $k_{\mathrm{s}}r = 2$ and length $k_{\mathrm{s}}l = 4$. The axial positions of the first and third cylinder are given by $k_{\mathrm{s}}z_1 = 4$ and $k_{\mathrm{s}}z_3 = -4$, and the relative refractive indices are chosen as $m_{\mathrm{r}1} = m_{\mathrm{r}3} = 1.5$ and $m_{\mathrm{r}2} = 1.0$. Because $m_{\mathrm{r}2} = 1.0$, the scattering problem is equivalent to the multiple scattering problem of two identical cylinders. On the other hand, the composite particle can be regarded as an inhomogeneous cylinder with a cylindrical inclusion. Therefore, the scattering characteristics are computed with three independent routines: TCOMP, TMULT, and TLAY. Localized and distributed sources are used for $\boldsymbol{T}$-matrix calculations with the TCOMP routine, while distributed sources are used for calculations with the TLAY routine. Figure 3.63 shows the differential scattering cross-sections for a fixed orientation of the composite particle ($\alpha_{\mathrm{p}} = \beta_{\mathrm{p}} = 45^{\circ}$), while Fig. 3.64 illustrates the numerical results for a random orientation. The behavior of the far-field patterns are quite similar.

In order to demonstrate the capability of the code to compute the electromagnetic scattering by composite particles with elongated and flattened regions, we consider the geometry depicted in Fig. 3.65. For this application, the sources are distributed on the real and imaginary axes. The parameters specifying the particle shape are: $k_{\mathrm{s}}r = 1$, $k_{\mathrm{s}}R = 3$, $k_{\mathrm{s}}l = 6$ and $k_{\mathrm{s}}L = 7$, while the relative refractive indices are identical $m_{\mathrm{r}1} = m_{\mathrm{r}2} = m_{\mathrm{r}3} = 1.5$. For the prolate cylinders, $N_{\mathrm{rank}} = 10$ sources are distributed along the axis of symmetry, and for the oblate cylinder, $N_{\mathrm{rank}} = 10$ sources are distributed

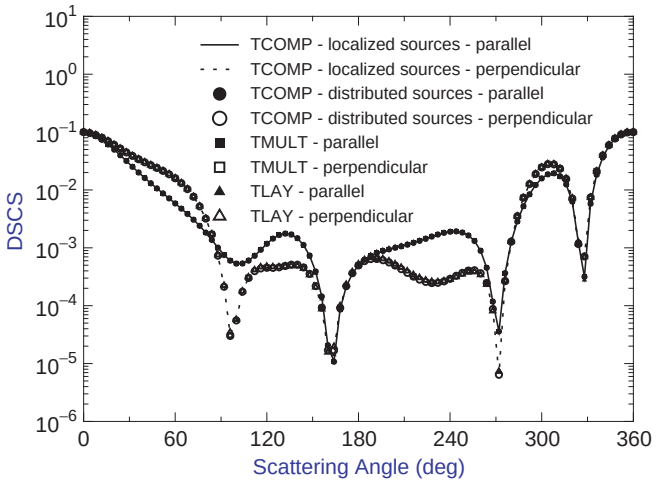

Fig. 3.63. Normalized differential scattering cross-sections of a composite particle consisting of three identical cylinders

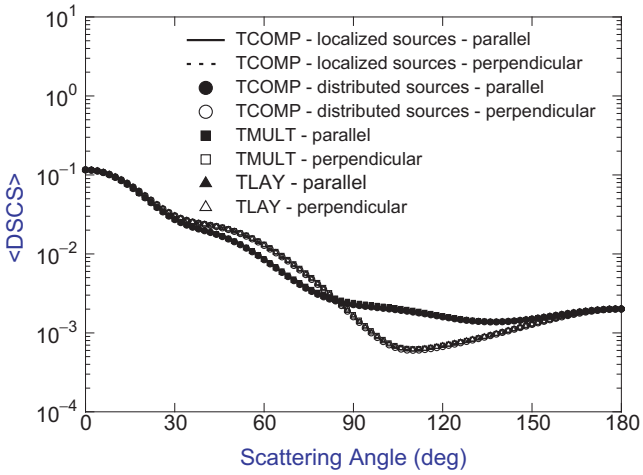

Fig. 3.64. Averaged differential scattering cross-sections of a composite particle consisting of three identical cylinders

on the imaginary axis. The global number of integration points is $N_{\text{int}} = 100$. The differential scattering cross-sections are plotted in Fig. 3.66 for the case of normal incidence.

Scattering by composite spheroids as shown in Fig. 3.67 can be computed with localized and distributed sources. The results plotted in Fig. 3.68 correspond to a composite spheroid with $k_{\text{s}}a = 20$, $k_{\text{s}}b = 5$, $k_{\text{s}}z_1 = k_{\text{s}}z_2 = 10$ and

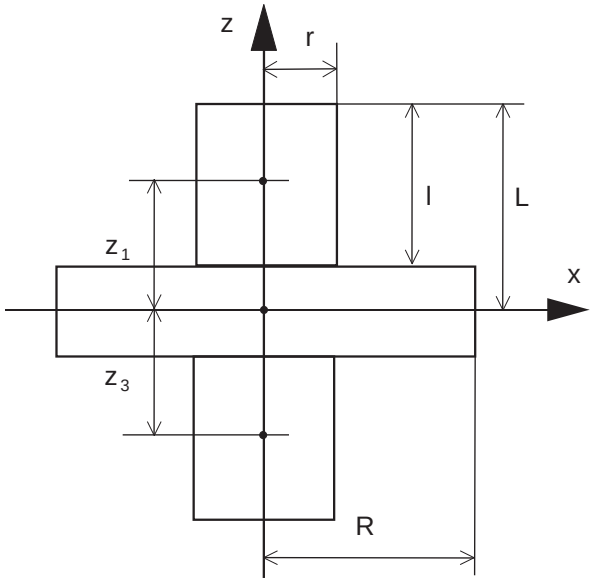

Fig. 3.65. Geometry of a composite particle consisting of three cylinders

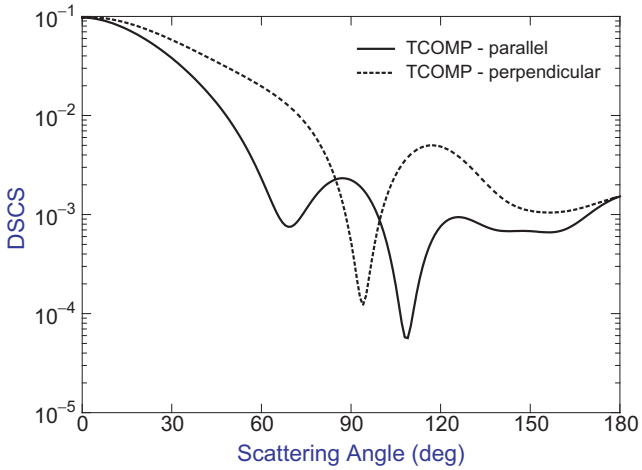

Fig. 3.66. Normalized differential scattering cross-sections of a composite particle consisting of three cylinders

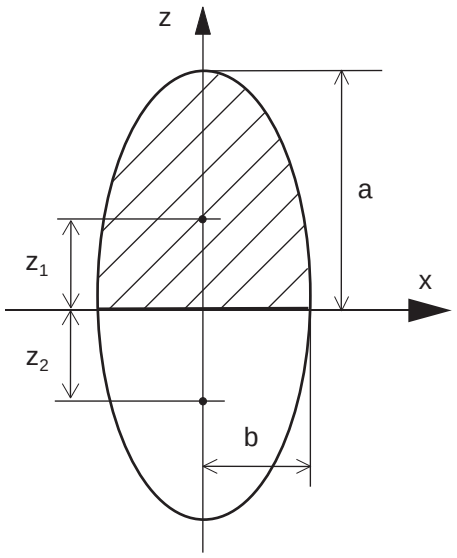

Fig. 3.67. Geometry of a composite spheroid

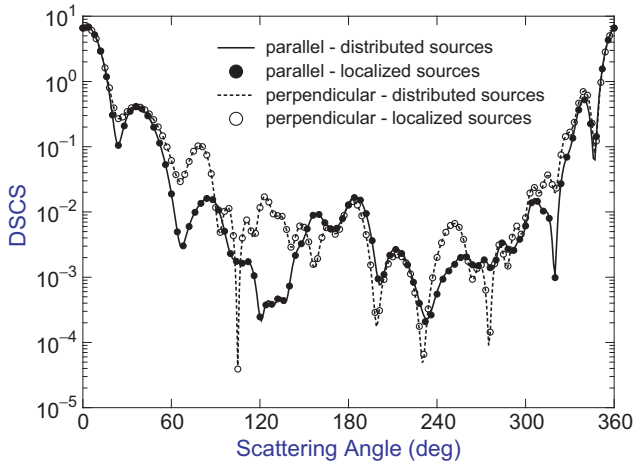

Fig. 3.68. Normalized differential scattering cross-sections of a composite spheroid

$m_{\mathrm{r}1} = m_{\mathrm{r}2} = 1.2$, while the parameters controlling the $\boldsymbol{T}$-matrix calculation are given in Table 3.7.

3.8 Complex Particles

In the following analysis we consider the inhomogeneous particle depicted in Fig. 3.69. The host particle is a sphere with radius $R = 1.0\,\mu\mathrm{m}$ and relative

Table 3.7. Parameters of calculation for a composite spheroid

Type of sources	N_{rank}-half-spheroid	N_{rank}-composite particle	N_{int}
Localized	22	34	1000
Distributed	18	32	1000

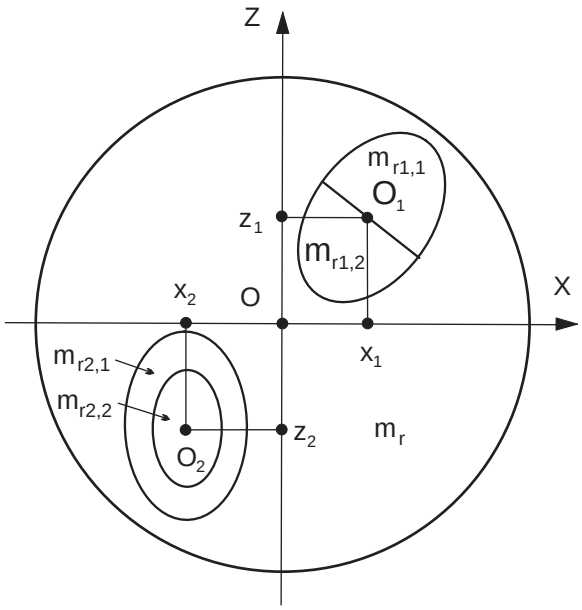

Fig. 3.69. Geometry of an inhomogeneous sphere containing a composite and a layered spheroid as separate inclusions

refractive index $m_{\text{r}} = 1.2$, while the wavelength of the incident radiation is $\lambda = 0.628\,\mu\text{m}$. The inhomogeneities are a composite and a layered prolate spheroid. The composite particle consists of two identical half-spheroids with semi-axes $a_1 = 0.3\,\mu\text{m}$ and $b_1 = 0.2\,\mu\text{m}$, and relative refractive indices (with respect to the ambient medium) $m_{\text{r1,1}} = 1.5$ and $m_{\text{r1,2}} = 1.33$. The layered particle consists of two concentric prolate spheroids with semi-axes $a_{2,1} = 0.3\,\mu\text{m}$, $b_{2,1} = 0.2\,\mu\text{m}$, and $a_{2,2} = 0.15\,\mu\text{m}$, $b_{2,2} = 0.1\,\mu\text{m}$, and relative refractive indices $m_{\text{r2,1}} = 1.5$ and $m_{\text{r2,2}} = 1.8$. The position of the composite particle with respect to the global coordinate system of the host particle is specified by the Cartesian coordinates $x_1 = y_1 = z_1 = 0.3\,\mu\text{m}$, while the Euler orientation angles are $\alpha_{\text{p1}} = \beta_{\text{p1}} = 45°$. For the layered particle, we choose $x_2 = y_2 = z_2 = -0.3\,\mu\text{m}$ and $\alpha_{\text{p2}} = \beta_{\text{p2}} = 0°$.

The results plotted in Fig. 3.70 are computed with the TMULT routine and show the differential scattering cross-sections for the two-spheroid system. The particles are placed in a medium with a refractive index of 1.2, and the

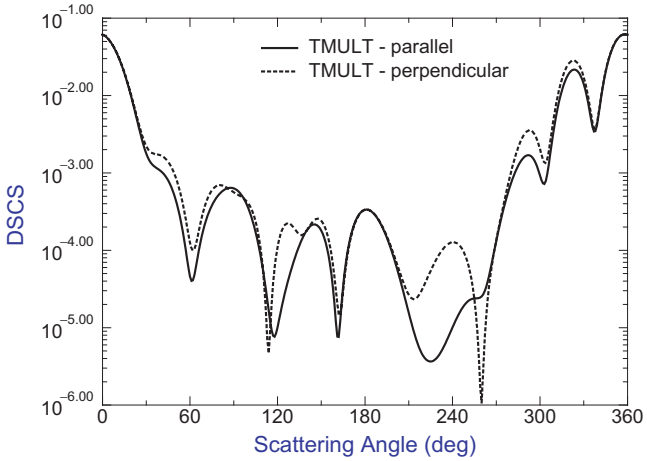

Fig. 3.70. Normalized differential scattering cross-sections of a composite and a layered particle

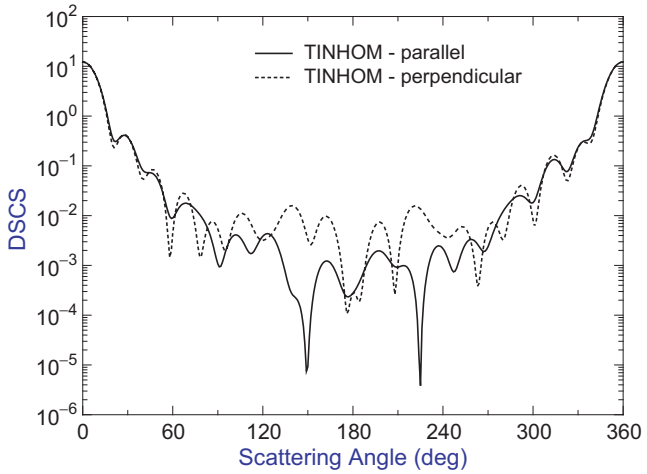

Fig. 3.71. Normalized differential scattering cross-sections of an inhomogeneous sphere. The inclusion consists of a composite and a layered particle

dimension of the system $\boldsymbol{T}$-matrix is given by $N_{\text{rank}} = 14$ and $M_{\text{rank}} = 12$. The incident wave travel along the Z-axis of the global coordinate system and the angular scattering is computed in the azimuthal plane $\varphi = 0°$. The system $\boldsymbol{T}$-matrix serves as input parameter for the TINHOM routine. The resulting $\boldsymbol{T}$-matrix is characterized by $N_{\text{rank}} = 16$ and $M_{\text{rank}} = 14$, and corresponds to a sphere containing a composite and a layered spheroid as separate inclusions. Figure 3.71 illustrates the differential scattering cross-sections for the inhomogeneous sphere in the case of normal incidence.

3.9 Particle on or Near a Plane Surface

In this section, we present scattering results for an axisymmetric particle situated on or near a plane surface. For this purpose we use the TPARTSUB routine and a computer program based on the discrete sources method [59,60].

Figures 3.72–3.74 show the differential scattering cross-sections for Fe-, Si- and SiO-spheroids with semi-axes $a = 0.05\,\mu\text{m}$ and $b = 0.025\,\mu\text{m}$. The relative refractive indices are: $m_\text{r} = 1.35 + 1.97\text{j}$ for Fe, $m_\text{r} = 4.37 + 0.08\text{j}$ for

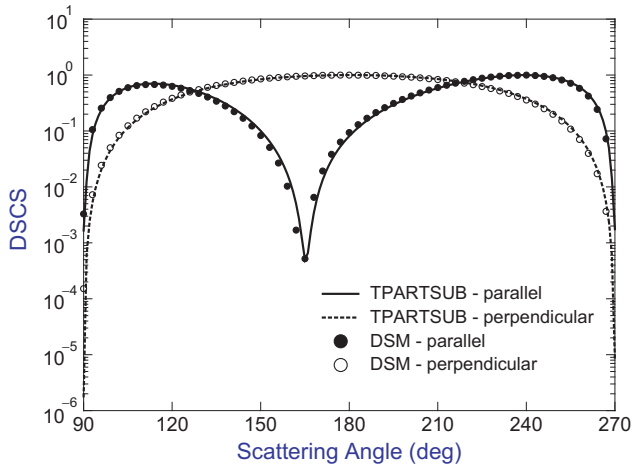

Fig. 3.72. Normalized differential scattering cross-sections of a Fe-spheroid computed with the TPARTSUB routine and the discrete sources method (DSM)

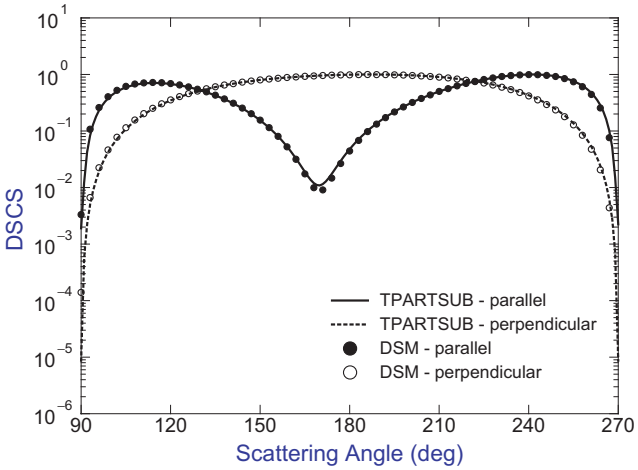

Fig. 3.73. Normalized differential scattering cross-sections of a Si-spheroid computed with the TPARTSUB routine and the discrete sources method (DSM)

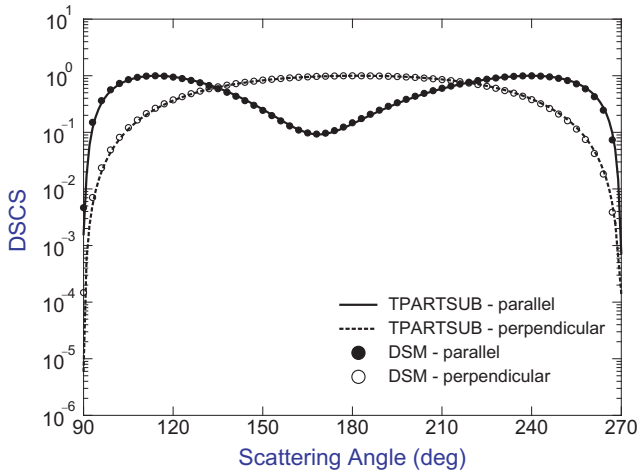

Fig. 3.74. Normalized differential scattering cross-sections of a SiO-spheroid computed with the TPARTSUB routine and the discrete sources method (DSM)

Si, and $m_r = 1.67$ for SiO. The particles are situated on a silicon substrate, the wavelength of the incident radiation is $\lambda = 0.488\,\mu$m, and the incident angle is $\beta_0 = 45°$. The plotted data show that the $\boldsymbol{T}$-matrix method leads to accurate results.

In the next example, we investigate scattering of evanescent waves by particles situated on a glass prism. We note that evanescent wave scattering is important in various sensor applications such as the total internal reflection microscopy TIRM [195]. Choosing the wavelength of the external excitation as $\lambda = 0.488\,\mu$m and taking into account that the glass prism has a refractive index of $m_{rs} = 1.5$, we deduce that the evanescent waves appear for incident angles exceeding 41.8°. In Figs. 3.75–3.77, we plot the differential scattering cross-section for Ag-, diamond-, and Si-spheres with a diameter of $d = 0.2\,\mu$m. The relative refractive indices of Ag- and diamond particles are $m_r = 0.25 + 3.14$j and $m_r = 2.43$, respectively. The scattering plane coincides with the incident plane and the angle of incidence is $\beta_0 = 60°$. The plotted data show a good agreement between the discrete sources and the $\boldsymbol{T}$-matrix solutions.

3.10 Effective Medium Model

The effective wave number of a half-space with randomly distributed spheroidal particles can be computed with the EFMED routine.

First we consider spherical particles and compare our results to the solutions obtained with the Matlab program QCAMIE included in the Electro-

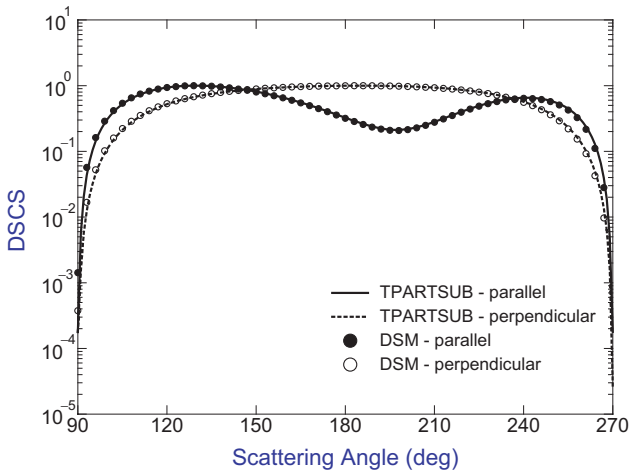

Fig. 3.75. Normalized differential scattering cross-sections of a metallic Ag-sphere computed with the TPARTSUB routine and the discrete sources method (DSM)

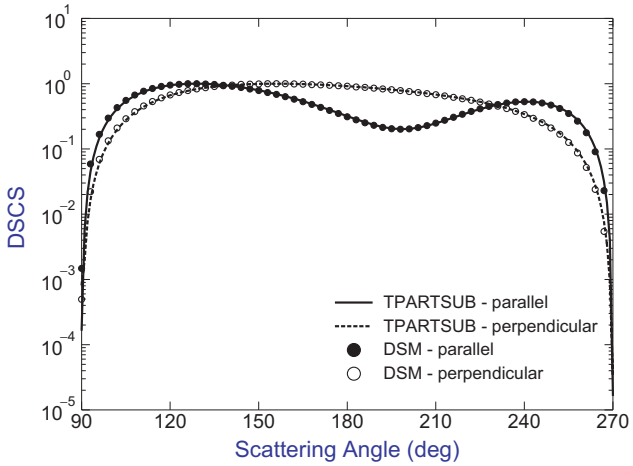

Fig. 3.76. Normalized differential scattering cross-sections of a Diamond-sphere computed with the TPARTSUB routine and the discrete sources method (DSM)

magnetic Wave Matlab Library and available from www.emwave.com. This library contains several Matlab programs which are based on the theory given in the book of Tsang et al. [229]. Figures 3.78 and 3.79 show the normalized phase velocity $k_s/\mathrm{Re}\{K_s\}$ and the effective loss tangent $2\mathrm{Im}\{K_s\}/\mathrm{Re}\{K_s\}$ as functions of the size parameter $x = k_s R$, and it is apparent that no substantial differences between the curves exist.

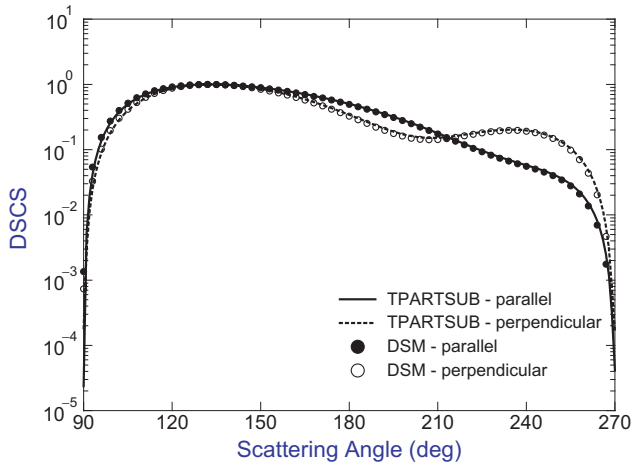

Fig. 3.77. Normalized differential scattering cross-sections of a Si-sphere computed with the TPARTSUB routine and the discrete sources method (DSM)

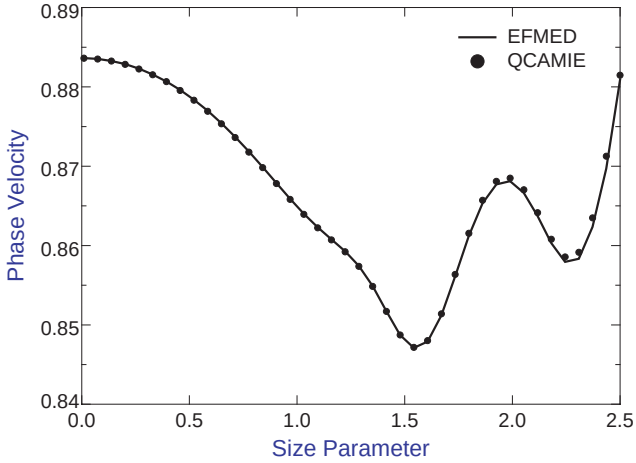

Fig. 3.78. Normalized phase velocity versus size parameter computed with the EFMED routine and the Matlab program QCAMIE

Next we consider the test examples given by Neo et al. [179] and compare the $\boldsymbol{T}$-matrix results to the solutions obtained with the long-wavelength quasi-crystalline approximation

$$K_{\mathrm{s}}^2 = k_{\mathrm{s}}^2 \left\{ 1 + \frac{3c\frac{\varepsilon_{\mathrm{r}}-1}{\varepsilon_{\mathrm{r}}+2}}{1 - c\frac{\varepsilon_{\mathrm{r}}-1}{\varepsilon_{\mathrm{r}}+2}} \left[1 + \mathrm{j}\frac{2x^3}{3} \frac{\frac{\varepsilon_{\mathrm{r}}-1}{\varepsilon_{\mathrm{r}}+2}}{1 - c\frac{\varepsilon_{\mathrm{r}}-1}{\varepsilon_{\mathrm{r}}+2}} \frac{(1-c)^4}{(1+2c)^2} \right] \right\}$$

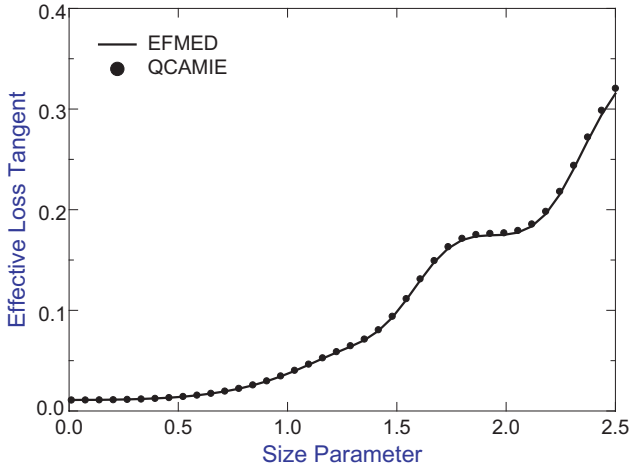

Fig. 3.79. Effective loss tangent versus size parameter computed with the EFMED routine and the Matlab program QCAMIE

and the quasi-crystalline approximation with coherent potential [118],

$$K_{\mathrm{s}}^2 = k_{\mathrm{s}}^2 \left\{ 1 + \frac{c\,(\varepsilon_{\mathrm{r}} - 1)}{1 + \frac{k_{\mathrm{s}}^2(\varepsilon_{\mathrm{r}}-1)}{3K_{\mathrm{s}}^2}\,(1-c)} \times \left[1 + \mathrm{j}\frac{2K_{\mathrm{s}}k_{\mathrm{s}}^2R^3}{9} \frac{\varepsilon_{\mathrm{r}} - 1}{1 + \frac{k_{\mathrm{s}}^2(\varepsilon_{\mathrm{r}}-1)}{3K_{\mathrm{s}}^2}\,(1-c)} \frac{(1-c)^4}{(1+2c)^2} \right] \right\} .$$

Figure 3.80 shows plots of $\mathrm{Im}\{K_{\mathrm{s}}/k_0\}$ versus concentration for spherical particles of radius $a = 3.977 \cdot 10^{-3}\,\mu\mathrm{m}$ and relative refractive index (with respect to the ambient medium) $m_{\mathrm{r}} = 1.194$. The wave number in free space is $k_0 = 10$, while the refractive index of the ambient medium is $m = 1.33$.

In Fig. 3.81 we plot $\mathrm{Im}\{K_{\mathrm{s}}/k_0\}$ versus concentration for $a = 1.047 \cdot 10^{-2}\,\mu\mathrm{m}$, $m_{\mathrm{r}} = 1.789$ and $m = 1.0$. Computed results using the $\boldsymbol{T}$-matrix method agree with the quasi-crystalline approximation. It should be observed that both the quasi-crystalline approximation and the quasi-crystalline approximation with coherent potential do predict maximum wave attenuation at a certain concentration.

In Figs. 3.82 and 3.83, we show calculations of $\mathrm{Re}\{K_{\mathrm{s}}\}$ and $\mathrm{Im}\{K_{\mathrm{s}}\}$ as functions of the size parameter $x = k_{\mathrm{s}} \max\{a, b\}$ for oblate and prolate spheroids. The spheroids are assumed to be oriented with their axis of symmetry along the Z-axis or to be randomly oriented. Since the incident wave is also assumed to propagate along the Z-axis, the medium is not anisotropic and is characterized by a single wave number K_{s}. The axial ratios are $a/b = 0.66$ for oblate spheroids and $a/b = 1.5$ for prolate spheroids. As before, the fractional

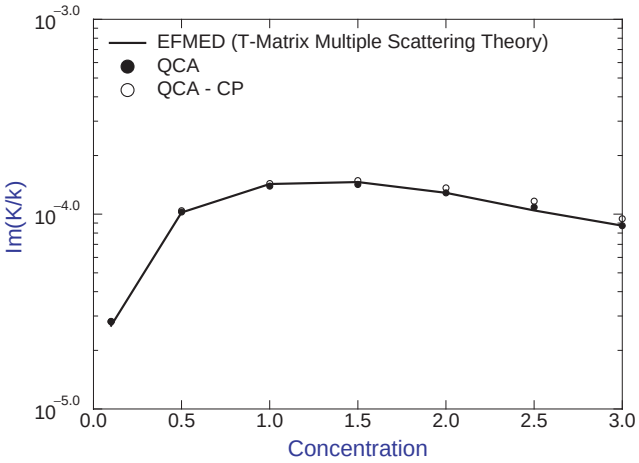

Fig. 3.80. $\mathrm{Im}\{K_\mathrm{s}/k_0\}$ for $a = 3.977 \cdot 10^{-3}\,\mu\mathrm{m}$, $m_\mathrm{r} = 1.194$ and $m = 1.33$. The results are computed with the $\boldsymbol{T}$-matrix method, quasicrystalline approximation (QCA) and quasicrystalline approximation with coherent potential (QCA-CP)

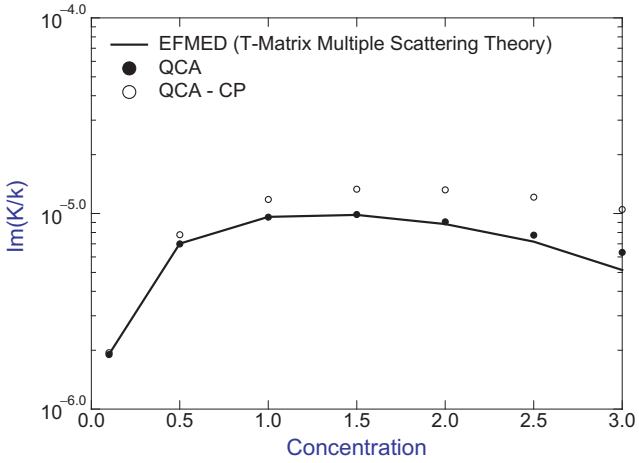

Fig. 3.81. $\mathrm{Im}\{K_\mathrm{s}/k_0\}$ for $a = 1.047 \cdot 10^{-2}\,\mu\mathrm{m}$, $m_\mathrm{r} = 1.789$ and $m = 1.0$. The results are computed with the $\boldsymbol{T}$-matrix method, quasicrystalline approximation (QCA) and quasicrystalline approximation with coherent potential (QCA-CP)

concentration is $c = 0.2$ and the relative refractive index of the particles is $m_\mathrm{r} = 1.789$. The significant feature in Fig. 3.82 is the occurrence of a maximum in $\mathrm{Re}\{K_\mathrm{s}\}$ at $x = 1.6$ for spherical particles. In the low-frequency regime up to $x = 0.5$, the $\mathrm{Im}\{K_\mathrm{s}\}$ curves increase rapidly with x and then show a smooth

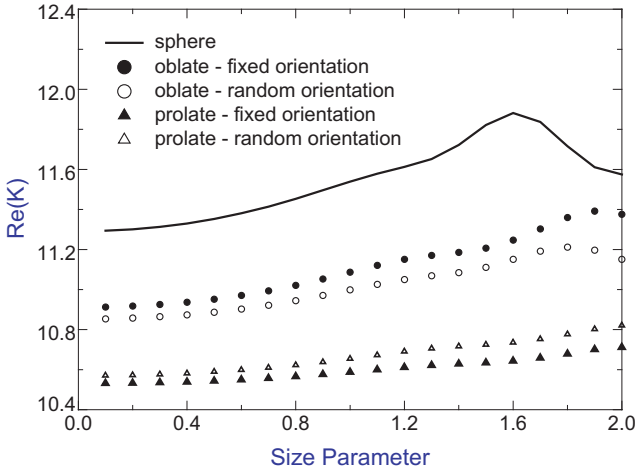

Fig. 3.82. $\mathrm{Re}\{K_\mathrm{s}\}$ versus the size parameter $x = k_\mathrm{s}\max\{a, b\}$ for oblate and prolate spheroids with $a/b = 0.66$ and $a/b = 1.5$, respectively. The calculations are performed for $c = 0.2$, $m_\mathrm{r} = 1.789$ and $m = 1.0$

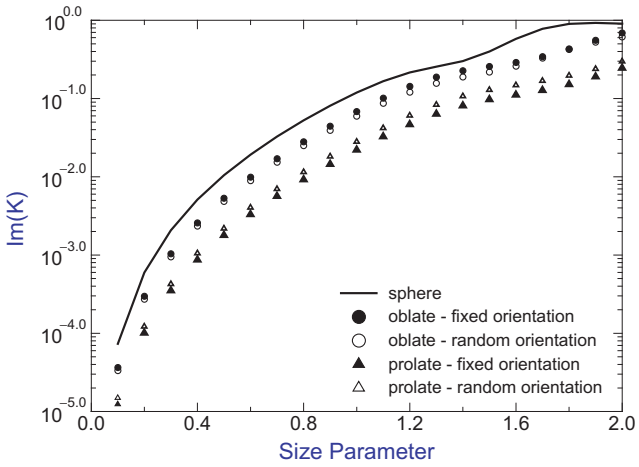

Fig. 3.83. $\mathrm{Im}\{K_\mathrm{s}\}$ versus the size parameter $x = k_\mathrm{s}\max\{a, b\}$ for oblate and prolate spheroids. The parameters of calculation are as in Fig. 3.82

increase with x. Note that for a given size parameter x, the radius of a spherical particle is larger than the equal-volume-sphere radii of an oblate and a prolate spheroid, and this feature is reflected in the variations of $\mathrm{Re}\{K_\mathrm{s}\}$ and $\mathrm{Im}\{K_\mathrm{s}\}$.

A

Spherical Functions

In this appendix we recall the basic properties of the solutions to the Bessel and Legendre differential equations and discuss some computational aspects. Properties of spherical Bessel and Hankel functions and (associated) Legendre functions can be found in [1, 40, 215, 238].

In a source-free isotropic medium the electric and magnetic fields satisfy the equations

$$\begin{aligned} \nabla \times \nabla \times \boldsymbol{X} - k^2 \boldsymbol{X} &= 0, \\ \nabla \cdot \boldsymbol{X} &= 0, \end{aligned}$$

where $\boldsymbol{X}$ stands for $\boldsymbol{E}$ or $\boldsymbol{H}$. Since

$$\nabla \times \nabla \times \boldsymbol{X} = -\Delta \boldsymbol{X} + \nabla \left(\nabla \cdot \boldsymbol{X} \right),$$

we see that $\boldsymbol{X}$ satisfies the vector wave equation

$$\Delta \boldsymbol{X} + k^2 \boldsymbol{X} = 0$$

and we deduce that each component of $\boldsymbol{X}$ satisfies the scalar wave equation or the Helmholtz equation

$$\Delta u + k^2 u = 0.$$

The Helmholtz equation written in spherical coordinates as

$$\frac{1}{r^2} \frac{\partial}{\partial r} \left(r^2 \frac{\partial u}{\partial r} \right) + \frac{1}{r^2 \sin \theta} \frac{\partial}{\partial \theta} \left(\sin \theta \frac{\partial u}{\partial \theta} \right) + \frac{1}{r^2 \sin^2 \theta} \frac{\partial^2 u}{\partial \varphi^2} + k^2 u = 0$$

is separable, so that upon replacing

$$u(\boldsymbol{r}) = f_1(r) Y(\theta, \varphi),$$

where (r, θ, φ) are the spherical coordinates of the position vector $\boldsymbol{r}$, we obtain

$$r^2 f_1'' + 2r f_1' + \left[k^2 r^2 - n(n+1)\right] f_1 = 0, \tag{A.1}$$

$$\frac{1}{\sin\theta}\frac{\partial}{\partial\theta}\left(\sin\theta\frac{\partial Y}{\partial\theta}\right) + \frac{1}{\sin^2\theta}\frac{\partial^2 Y}{\partial\varphi^2} + n(n+1)Y = 0. \tag{A.2}$$

The above equations are known as the Bessel differential equation and the differential equation for the spherical harmonics. Further, setting

$$Y(\theta, \varphi) = f_2(\theta) f_3(\varphi),$$

we find that

$$\frac{1}{\sin\theta}\frac{\mathrm{d}}{\mathrm{d}\theta}\left(\sin\theta\frac{\mathrm{d}f_2}{\mathrm{d}\theta}\right) + \left[n(n+1) - \frac{m^2}{\sin^2\theta}\right] f_2 = 0, \tag{A.3}$$

$$f_3'' + m^2 f_3 = 0. \tag{A.4}$$

The differential equation (A.3) is known as the associated Legendre equation, while the solution to the differential equation (A.4) is $f_3(\varphi) = \exp(\mathrm{j}\, m\varphi)$.

A.1 Spherical Bessel Functions

With the substitution $x = kr$, the spherical Bessel differential equation can be written in the standard form

$$x^2 f''(x) + 2x f'(x) + \left[x^2 - n(n+1)\right] f(x) = 0.$$

For $n = 0, 1, \ldots$, the functions

$$j_n(x) = \sum_{p=0}^{\infty} \frac{(-1)^p x^{n+2p}}{2^p p!(2n+2p+1)!!}$$

and

$$y_n(x) = -\frac{(2n)!}{2^n n!}\sum_{p=0}^{\infty} \frac{(-1)^p x^{2p-n-1}}{2^p p!\,(-2n+1)\,(-2n+3)\cdots(-2n+2p-1)}, \tag{A.5}$$

where $1 \cdot 3 \cdots (2n+2p+1) = (2n+2p+1)!!$, are solutions to the spherical Bessel differential equation (the first coefficient in the series (A.5) has to be set equal to one). The functions j_n and y_n are called the spherical Bessel and Neumann functions of order n, respectively, and the linear combinations

$$h_n^{(1,2)} = j_n \pm \mathrm{j} y_n$$

are known as the spherical Hankel functions of the first and second kind. From the series representations we see that

$$\frac{2n+1}{x} z_n(x) = z_{n-1}(x) + z_{n+1}(x), \tag{A.6}$$

$$(2n+1)\, z_n'(x) = n z_{n-1}(x) - (n+1) z_{n+1}(x), \tag{A.7}$$

and

$$\frac{\mathrm{d}}{\mathrm{d}x}\left[x z_n(x)\right] = x z_{n-1}(x) - n z_n(x), \tag{A.8}$$

where z_n stands for any spherical function. The Wronskian relation for the spherical Bessel and Neumann functions is

$$j_n(x) y_n'(x) - j_n'(x) y_n(x) = \frac{1}{x^2}$$

and for small values of the argument we have

$$j_n(x) = \frac{x^n}{(2n+1)!!}\left\{1 + \mathrm{O}\left(x^2\right)\right\},$$

$$y_n(x) = -\frac{(2n-1)!!}{x^{n+1}}\left\{1 + \mathrm{O}\left(x^2\right)\right\}$$

as $x \to 0$, while for large value of the argument,

$$j_n(x) = \frac{1}{x}\cos\left[x - \frac{(n+1)\pi}{2}\right]\left\{1 + \mathrm{O}\left(\frac{1}{x}\right)\right\},$$

$$y_n(x) = \frac{1}{x}\sin\left[x - \frac{(n+1)\pi}{2}\right]\left\{1 + \mathrm{O}\left(\frac{1}{x}\right)\right\},$$

$$h_n^{(1)}(x) = \frac{\mathrm{e}^{\mathrm{j}[x-(n+1)\pi/2]}}{x}\left\{1 + \mathrm{O}\left(\frac{1}{x}\right)\right\},$$

$$h_n^{(2)}(x) = \frac{\mathrm{e}^{-\mathrm{j}[x-(n+1)\pi/2]}}{x}\left\{1 + O\left(\frac{1}{x}\right)\right\}$$

as $x \to \infty$.

Spherical Bessel functions can be expressed in terms of trigonometric functions, and the first few spherical functions have the explicit forms

$$j_0(x) = \frac{\sin x}{x}, \tag{A.9}$$

$$y_0(x) = -\frac{\cos x}{x}, \tag{A.10}$$

$$j_1(x) = \frac{\sin x}{x^2} - \frac{\cos x}{x}, \tag{A.11}$$

$$y_1(x) = -\frac{\cos x}{x^2} - \frac{\sin x}{x}, \tag{A.12}$$

and

$$h_0^{(1)}(x) = \frac{\mathrm{e}^{\mathrm{j}x}}{\mathrm{j}x}\,,$$
$$h_0^{(2)}(x) = -\frac{\mathrm{e}^{-\mathrm{j}x}}{\mathrm{j}x}\,.$$

The spherical Bessel functions are computed by downward recursion. This recursion begins with two successive functions of small values and produces functions proportional to the Bessel functions rather than the actual Bessel functions. The constant of proportionality between the two sets of functions is obtained from the function of order zero j_0. Alternatively, the spherical Bessel functions can be computed with an algorithm involving the auxiliary function χ_n [169]

$$\chi_n(x) = \frac{j_n(x)}{j_{n-1}(x)}.$$

In this case, the functions χ_n are calculated with the downward recurrence relation

$$\chi_n(x) = \frac{1}{\frac{2n+1}{x} - \chi_{n+1}(x)},$$

the constant of proportionality is obtained from the function of order one, $\chi_1(x) = 1/x - \cot x$, and the spherical Bessel functions are computed with the upward recursion

$$j_n(x) = \chi_n(x) j_{n-1}(x)$$

starting at j_1. The spherical Neumann functions are calculated by upward recursion starting with the functions of order zero and one, y_0 and y_1, respectively.

A.2 Legendre Functions

With the substitution $x = \cos\theta$, the associated Legendre equation transforms to

$$\left(1 - x^2\right) f''(x) - 2x f'(x) + \left[n(n+1) - \frac{m^2}{1-x^2}\right] f(x) = 0. \tag{A.13}$$

This equation is characterized by regular singularities at the points $x = \pm 1$ and at infinity. For $m = 0$, there are two linearly independent solutions to the Legendre differential equation and these solutions can be expressed as power series about the origin $x = 0$. In general, these series do not converge for

$x = \pm 1$, but if n is a positive integer, one of the series breaks off after a finite number of terms and has a finite value at the poles. These polynomial solutions are called Legendre polynomials and are denoted by $\widetilde{P}_n(x)$. For $m \neq 0$, the solutions to (A.13) which are finite at the poles $x = \pm 1$ are the associated Legendre functions. If m and n are integers, the associated Legendre functions are defined as

$$\widetilde{P}_n^m(x) = \left(1 - x^2\right)^{m/2} \frac{\mathrm{d}^m \widetilde{P}_n(x)}{\mathrm{d}x^m}\,.$$

Useful recurrence relations satisfied by $\widetilde{P}_n^m$ are

$$(2n+1)\, x \widetilde{P}_n^m(x) = (n-m+1)\, \widetilde{P}_{n+1}^m(x) + (n+m)\, \widetilde{P}_{n-1}^m(x), \tag{A.14}$$

$$\begin{aligned}(2n+1)\, \sqrt{1-x^2}\, \widetilde{P}_n^m(x) &= (n+m-1)\,(n+m)\, \widetilde{P}_{n-1}^{m-1}(x) \\ &\quad - (n-m+1)\,(n-m+2)\, \widetilde{P}_{n+1}^{m-1}(x),\end{aligned} \tag{A.15}$$

$$(2n+1)\, \sqrt{1-x^2}\, \widetilde{P}_n^{m-1}(x) = \widetilde{P}_{n+1}^m(x) - \widetilde{P}_{n-1}^m(\cos\theta)\,, \tag{A.16}$$

$$\begin{aligned}(2n+1)\left(1-x^2\right) \frac{\mathrm{d}}{\mathrm{d}x} \widetilde{P}_n^m(x) &= (n+1)\,(n+m)\, \widetilde{P}_{n-1}^m(x) \\ &\quad - n\,(n-m+1)\, \widetilde{P}_{n+1}^m(x),\end{aligned} \tag{A.17}$$

$$\left(1-x^2\right) \frac{\mathrm{d}}{\mathrm{d}x} \widetilde{P}_n^m(x) = (n+m) \widetilde{P}_{n-1}^m(x) - n x \widetilde{P}_n^m(x). \tag{A.18}$$

The angular functions $\widetilde{\pi}_n^m$ and $\widetilde{\tau}_n^m$ are related to the associated Legendre functions by the relations

$$\widetilde{\pi}_n^m(\theta) = \frac{\widetilde{P}_n^m(\cos\theta)}{\sin\theta}, \tag{A.19}$$

$$\widetilde{\tau}_n^m(\theta) = \frac{\mathrm{d}}{\mathrm{d}\theta} \widetilde{P}_n^m(\cos\theta). \tag{A.20}$$

For positive values of m and for $\theta \to 0$ or $\theta \to \pi$,

$$\widetilde{P}_n^m(\cos\theta) \to \frac{(n+m)!}{(n-m)!} \left(\frac{2}{2n+1}\right)^m J_m\left(\frac{2n+1}{2}\theta\right)$$

and

$$m\widetilde{\pi}_n^m(\theta) \to \frac{1}{2} \frac{(n+m)!}{(n-m)!(m-1)!} \left(\frac{\theta}{2}\right)^{m-1},$$

$$\widetilde{\tau}_n^m(\theta) \to \frac{1}{2} \frac{(n+m)!}{(n-m)!(m-1)!} \left(\frac{\theta}{2}\right)^{m-1},$$

while for $n \gg 1$ and away from $\theta = 0$ and $\theta = \pi$, we have

$$\widetilde{P}_n^m(\cos\theta) \to \left(\frac{2}{\pi}\right)^{\frac{1}{2}} (\sin\theta)^{-\frac{1}{2}}\, n^{m-\frac{1}{2}} \cos\left(\frac{2n+1}{2}\theta + \frac{m\pi}{2} - \frac{\pi}{4}\right)$$

and

$$\widetilde{\pi}_n^m(\theta) \to \left(\frac{2}{\pi}\right)^{\frac{1}{2}} (\sin\theta)^{-\frac{3}{2}}\, n^{m-\frac{1}{2}} \cos\left(\frac{2n+1}{2}\theta + \frac{m\pi}{2} - \frac{\pi}{4}\right),$$

$$\widetilde{\tau}_n^m(\theta) \to \left(\frac{2}{\pi}\right)^{\frac{1}{2}} (\sin\theta)^{-\frac{1}{2}}\, n^{m+\frac{1}{2}} \sin\left(\frac{2n+1}{2}\theta + \frac{m\pi}{2} - \frac{\pi}{4}\right).$$

In our analysis we use the associated Legendre functions with positive values of the index m. For $m \geq 0$, the normalized associated Legendre functions are given by

$$P_n^m(\cos\theta) = c_{mn}\widetilde{P}_n^m(\cos\theta), \tag{A.21}$$

where c_{mn} is a normalization constant and

$$c_{mn} = \sqrt{\frac{2n+1}{2} \cdot \frac{(n-m)!}{(n+m)!}}.$$

Similarly, the normalized angular functions π_n^m and τ_n^m are related to the angular functions $\widetilde{\pi}_n^m$ and $\widetilde{\tau}_n^m$ by the relations

$$\pi_n^m(\theta) = c_{mn}\widetilde{\pi}_n^m(\theta), \tag{A.22}$$

$$\tau_n^m(\theta) = c_{mn}\widetilde{\tau}_n^m(\theta)\,. \tag{A.23}$$

An algorithm for computing the normalized associated Legendre functions P_n^m involves the following steps.

(1) For $m = 0$, compute P_{n+1} by using the recurrence relation

$$P_{n+1}(\cos\theta) = \frac{1}{n+1}\sqrt{(2n+1)(2n+3)}\cos\theta P_n(\cos\theta) - \frac{n}{n+1}\sqrt{\frac{2n+3}{2n-1}}P_{n-1}(\cos\theta)\,, \quad n \geq 1$$

with the starting values

$$P_0(\cos\theta) = \frac{\sqrt{2}}{2},$$

$$P_1(\cos\theta) = \sqrt{\frac{3}{2}}\cos\theta.$$

(2) For $m \geq 1$, compute P_{n+1}^m by using the recurrence relation

$$P_{n+1}^m(\cos\theta) = \sqrt{\frac{(2n+1)(2n+3)}{(n+1-m)(n+1+m)}}\cos\theta P_n^m(\cos\theta)$$
$$-\sqrt{\frac{(2n+3)(n-m)(n+m)}{(2n-1)(n+1-m)(n+1+m)}}P_{n-1}^m(\cos\theta), \quad n \geq m$$

with the initial values

$$P_m^{m-1}(\cos\theta) = 0,$$
$$P_m^m(\cos\theta) = \sqrt{\frac{2m+1}{2\,(2m)!}}(2m-1)!!\sin^m\theta.$$

Considering the angular functions π_n^m, we see that π_n^0 diverges at $\theta = 0$ and $\theta = \pi$. Because in our applications, the product $m\pi_n^m$ appears explicitly, we set $\pi_n^0 = 0$ for $n \geq 0$. For $m \geq 1$, the angular functions π_n^m are computed by using (A.19), (A.21) and (A.22), and the recurrence relations for the normalized associated Legendre functions.

The angular functions τ_n^m can be calculated with the following algorithm.

(1) For $m = 0$, compute

$$\frac{\mathrm{d}}{\mathrm{d}\cos\theta}P_n\left(\cos\theta\right) = P_n'\left(\cos\theta\right)$$

by using the recurrence relation

$$P_n'(\cos\theta) = n\sqrt{\frac{2n+1}{2n-1}}P_{n-1}(\cos\theta) + \sqrt{\frac{2n+1}{2n-1}}\cos\theta P_{n-1}'(\cos\theta)$$

with the starting value

$$P_0'\left(\cos\theta\right) = 0,$$

and set [144]

$$\tau_n^0(\theta) = -\sin\theta P_n'\left(\cos\theta\right), \quad n \geq 0\,.$$

(2) For $m \geq 1$, compute τ_n^m with the recurrence relation

$$\tau_n^m(\theta) = n\cos\theta\pi_n^m\left(\theta\right) - (n+m)\sqrt{\frac{(2n+1)(n-m)}{(2n-1)(n+m)}}\pi_{n-1}^m(\theta), \quad n \geq m.$$

The following orthogonality relations are important for solving scattering problems:

$$\int_0^\pi P_n^m(\cos\theta)P_{n'}^m(\cos\theta)\sin\theta\,\mathrm{d}\theta = \delta_{nn'},$$

$$\int_0^\pi \left[\tau_n^m(\theta)\tau_{n'}^m(\theta) + m^2\pi_n^m(\theta)\pi_{n'}^m(\theta)\right]\sin\theta\,\mathrm{d}\theta = n(n+1)\delta_{nn'},$$

$$\int_0^\pi \left[\pi_n^m(\theta)\tau_{n'}^m(\theta) + \tau_n^m(\theta)\pi_{n'}^m(\theta)\right]\sin\theta\,\mathrm{d}\theta = 0.$$

For negative arguments we have the symmetry relation

$$P_n^m(-\cos\theta) = (-1)^{n-m}P_n^m(\cos\theta)$$

and consequently,

$$\pi_n^m(\pi-\theta) = (-1)^{n-m}\pi_n^m(\theta), \tag{A.24}$$

$$\tau_n^m(\pi-\theta) = (-1)^{n-m+1}\tau_n^m(\theta). \tag{A.25}$$

B

Wave Functions

In this appendix, we summarize the basic properties of the characteristic solutions to the scalar and vector wave equations. We recall the integral and orthogonality relations, and the addition theorems under coordinate rotations and translations.

B.1 Scalar Wave Functions

The spherical wave functions form a set of characteristic solutions to the Helmholtz equation and are given by [215]

$$u_{mn}^{1,3}(k\boldsymbol{r}) = z_n^{1,3}(kr)\, P_n^{|m|}(\cos\theta)\, e^{\mathrm{j}m\varphi},$$

where $n = 0, 1, \ldots,$, $m = -n, \ldots, n$, (r, θ, φ) are the spherical coordinates of the position vector $\boldsymbol{r}$, z_n^1 designates the spherical Bessel functions j_n, z_n^3 stands for the spherical Hankel functions of the first-order $h_n^{(1)}$, and $P_n^{|m|}$ denotes the normalized associated Legendre functions. u_{mn}^1 is an entire solution to the Helmholtz equation (solution which are defined in all of $\boldsymbol{R}^3$) and u_{mn}^3 is a radiating solution to the Helmholtz equation in $\boldsymbol{R}^3 - \{0\}$.

The Green function or the fundamental solution is defined as

$$g(k, \boldsymbol{r}, \boldsymbol{r}') = \frac{\mathrm{e}^{\mathrm{j}k|\boldsymbol{r}-\boldsymbol{r}'|}}{4\pi\,|\boldsymbol{r}-\boldsymbol{r}'|}, \quad \boldsymbol{r} \neq \boldsymbol{r}'$$

and straightforward differentiation shows that for fixed $\boldsymbol{r}' \in \boldsymbol{R}^3$, the fundamental solution satisfies the Helmholtz equation in $\boldsymbol{R}^3 - \{\boldsymbol{r}'\}$. The expansion of the Green function in terms of spherical wave functions is given by

$$g(k, \boldsymbol{r}, \boldsymbol{r}') = \frac{\mathrm{j}k}{2\pi} \sum_{n=0}^{\infty} \sum_{m=-n}^{n} \begin{cases} u_{-mn}^3(k\boldsymbol{r}')\, u_{mn}^1(k\boldsymbol{r}), & r < r' \\ u_{-mn}^1(k\boldsymbol{r}')\, u_{mn}^3(k\boldsymbol{r}), & r > r'. \end{cases}$$

The spherical harmonics are defined as

$$Y_{mn}(\theta,\varphi) = P_n^{|m|}(\cos\theta)\,\mathrm{e}^{\mathrm{j}m\varphi}$$

and they satisfy the orthogonality relation

$$\int_0^{2\pi}\int_0^{\pi} Y_{mn}(\theta,\varphi)\,Y_{m'n'}(\theta,\varphi)\sin\theta\,\mathrm{d}\theta\,\mathrm{d}\varphi = 2\pi\delta_{m,-m'}\delta_{nn'}.$$

The spherical wave functions can be expressed as integrals over plane waves [26, 70, 215]

$$u_{mn}^1(k\boldsymbol{r}) = \frac{1}{4\pi\mathrm{j}^n}\int_0^{2\pi}\int_0^{\pi} Y_{mn}(\beta,\alpha)\,\mathrm{e}^{\mathrm{j}\boldsymbol{k}(\beta,\alpha)\cdot\boldsymbol{r}}\sin\beta\,\mathrm{d}\beta\,\mathrm{d}\alpha \tag{B.1}$$

and

$$u_{mn}^3(k\boldsymbol{r}) = \frac{1}{2\pi\mathrm{j}^n}\int_0^{2\pi}\int_0^{\frac{\pi}{2}-\mathrm{j}\infty} Y_{mn}(\beta,\alpha)\,\mathrm{e}^{\mathrm{j}\boldsymbol{k}(\beta,\alpha)\cdot\boldsymbol{r}}\sin\beta\,\mathrm{d}\beta\,\mathrm{d}\alpha, \tag{B.2}$$

where (k,β,α) are the spherical coordinates of the wave vector $\boldsymbol{k}$. We note that (B.2) is valid for $z>0$ since only then the integral converges.

The spherical wave expansion of the plane wave $\exp(\mathrm{j}\boldsymbol{k}\cdot\boldsymbol{r})$ is of significant importance in electromagnetic scattering and is given by [215]

$$P(k,\beta,\alpha,\boldsymbol{r}) = \mathrm{e}^{\mathrm{j}\boldsymbol{k}(\beta,\alpha)\cdot\boldsymbol{r}} = \sum_{n=0}^{\infty}\sum_{m=-n}^{n} 2\mathrm{j}^n Y_{-mn}(\beta,\alpha)\,u_{mn}^1(k\boldsymbol{r}). \tag{B.3}$$

The quasi-plane waves have been introduced by Devaney [46], and for $z>0$, they are defined as

$$Q(k,\beta,\alpha,\boldsymbol{r}) = \int_0^{2\pi}\int_0^{\frac{\pi}{2}-\mathrm{j}\infty} \Delta(\beta,\alpha,\beta',\alpha')\mathrm{e}^{\mathrm{j}\boldsymbol{k}'(\beta',\alpha')\cdot\boldsymbol{r}}\sin\beta'\,\mathrm{d}\beta'\,\mathrm{d}\alpha',$$

where

$$\Delta(\beta,\alpha,\beta',\alpha') = \frac{1}{2\pi}\sum_{n=0}^{\infty}\sum_{m=-n}^{n} Y_{-mn}(\beta,\alpha)\,Y_{mn}(\beta',\alpha').$$

If β and β' belong to $[0,\pi]$, the expression of Δ simplifies to

$$\Delta(\beta,\alpha,\beta',\alpha') = \delta(\cos\beta'-\cos\beta)\delta(\alpha'-\alpha).$$

As in (B.3), the expansion of quasi-plane waves in terms of radiating spherical wave functions is given by

$$Q(k,\beta,\alpha,\boldsymbol{r}) = \sum_{n=0}^{\infty}\sum_{m=-n}^{n} \mathrm{j}^n Y_{-mn}(\beta,\alpha)\,u_{mn}^3(k\boldsymbol{r}). \tag{B.4}$$

The function Δ allows to formally analytically continue a function $f(\beta,\alpha)$, defined for real β, onto the complex values of β. In particular we see that

$$f(\beta,\alpha)=\int_0^{2\pi}\int_0^{\pi} f\left(\beta',\alpha'\right)\Delta(\beta,\alpha,\beta',\alpha')\sin\beta'\,\mathrm{d}\beta'\,\mathrm{d}\alpha',$$

where β can assume all values lying on the contour $[0,\frac{\pi}{2}-\mathrm{j}\infty)$, and therefore

$$\begin{aligned}\int_0^{2\pi}\int_0^{\frac{\pi}{2}-\mathrm{j}\infty} & f(\beta,\alpha)\mathrm{e}^{\mathrm{j}\boldsymbol{k}(\beta,\alpha)\cdot\boldsymbol{r}}\sin\beta\,\mathrm{d}\beta\,\mathrm{d}\alpha\\ &=\int_0^{2\pi}\int_0^{\pi} f(\beta,\alpha)Q(k,\beta,\alpha,\boldsymbol{r})\sin\beta\,\mathrm{d}\beta\,\mathrm{d}\alpha,\end{aligned}\tag{B.5}$$

where we have used the definition of Q. In view of (B.2) and (B.5), we deduce that the integral representation for the radiating spherical wave functions is given by

$$u^3_{mn}(k\boldsymbol{r})=\frac{1}{2\pi\mathrm{j}^n}\int_0^{2\pi}\int_0^{\pi} Y_{mn}\left(\beta,\alpha\right)Q(k,\beta,\alpha,\boldsymbol{r})\sin\beta\,\mathrm{d}\beta\,\mathrm{d}\alpha.\tag{B.6}$$

In the far-field region, a plane wave can be expressed as a superposition of incoming and outgoing spherical waves. To derive this expression, we start with the series representation (B.3) written as

$$P(k,\beta,\alpha,\boldsymbol{r})=\mathrm{e}^{\mathrm{j}\boldsymbol{k}(\beta,\alpha)\cdot\boldsymbol{r}}=\sum_{n=0}^{\infty}\sum_{m=-n}^{n}2\mathrm{j}^n j_n(kr)Y_{-mn}\left(\beta,\alpha\right)Y_{mn}(\theta,\varphi),$$

use the asymptotic behavior of the spherical Bessel functions for large values of the argument

$$\begin{aligned}j_n\left(kr\right)&=\frac{1}{kr}\sin\left(kr-\frac{n\pi}{2}\right)\\ &=\frac{1}{2\mathrm{j}kr}\left[\mathrm{e}^{\mathrm{j}\left(kr-\frac{n\pi}{2}\right)}-\mathrm{e}^{-\mathrm{j}\left(kr-\frac{n\pi}{2}\right)}\right],\quad kr\to\infty\end{aligned}$$

take into account the completeness relations for spherical harmonics,

$$\begin{aligned}\delta\left(\boldsymbol{e}_r-\boldsymbol{e}_k\right)&=\delta(\varphi-\alpha)\delta(\cos\theta-\cos\beta)\\ &=\frac{1}{2\pi}\sum_{n=0}^{\infty}\sum_{m=-n}^{n}Y_{-mn}\left(\beta,\alpha\right)Y_{mn}\left(\theta,\varphi\right),\\ \delta\left(\boldsymbol{e}_r+\boldsymbol{e}_k\right)&=\delta\left[(\pi+\varphi)-\alpha\right]\delta\left[\cos\left(\pi-\theta\right)-\cos\beta\right]\\ &=\frac{1}{2\pi}\sum_{n=0}^{\infty}\sum_{m=-n}^{n}(-1)^n Y_{-mn}\left(\beta,\alpha\right)Y_{mn}\left(\theta,\varphi\right),\end{aligned}$$

where $\boldsymbol{e}_r$ and $\boldsymbol{e}_k$ are the unit vectors in the directions of $\boldsymbol{r}$ and $\boldsymbol{k}$, respectively, and obtain

$$\mathrm{e}^{\mathrm{j}\boldsymbol{k}\cdot\boldsymbol{r}} = \frac{2\pi}{\mathrm{j}kr}\left[\delta\left(\boldsymbol{e}_r - \boldsymbol{e}_k\right)\mathrm{e}^{\mathrm{j}kr} - \delta\left(\boldsymbol{e}_r + \boldsymbol{e}_k\right)\mathrm{e}^{-\mathrm{j}kr}\right], \quad kr \to \infty. \tag{B.7}$$

The vector spherical harmonics are defined as [175, 228, 229]

$$\boldsymbol{m}_{mn}(\theta,\varphi) = \frac{1}{\sqrt{2n(n+1)}}\left[\mathrm{j}m\pi_n^{|m|}(\theta)\boldsymbol{e}_\theta - \tau_n^{|m|}(\theta)\boldsymbol{e}_\varphi\right]\mathrm{e}^{\mathrm{j}m\varphi}, \tag{B.8}$$

$$\boldsymbol{n}_{mn}(\theta,\varphi) = \frac{1}{\sqrt{2n(n+1)}}\left[\tau_n^{|m|}(\theta)\boldsymbol{e}_\theta + \mathrm{j}m\pi_n^{|m|}\boldsymbol{e}_\varphi\right]\mathrm{e}^{\mathrm{j}m\varphi}, \tag{B.9}$$

where $(\boldsymbol{e}_r, \boldsymbol{e}_\theta, \boldsymbol{e}_\varphi)$ are the spherical unit vectors of the position vector $\boldsymbol{r}$, and we have $\boldsymbol{e}_r \times \boldsymbol{m}_{mn} = \boldsymbol{n}_{mn}$ and $\boldsymbol{e}_r \times \boldsymbol{n}_{mn} = -\boldsymbol{m}_{mn}$. We omit the third vector spherical harmonics

$$\boldsymbol{p}_{mn}(\theta,\varphi) = \frac{1}{\sqrt{2n(n+1)}}Y_{mn}(\theta,\varphi)\boldsymbol{e}_r$$

since it will be not encountered in our analysis. The orthogonality relations for vector spherical harmonics are

$$\begin{aligned}&\int_0^{2\pi}\int_0^{\pi}\boldsymbol{m}_{mn}(\theta,\varphi)\cdot\boldsymbol{m}_{m'n'}(\theta,\varphi)\sin\theta\,\mathrm{d}\theta\,\mathrm{d}\varphi\\ &= \int_0^{2\pi}\int_0^{\pi}\boldsymbol{n}_{mn}(\theta,\varphi)\cdot\boldsymbol{n}_{m'n'}(\theta,\varphi)\sin\theta\,\mathrm{d}\theta\,\mathrm{d}\varphi = \pi\delta_{m,-m'}\delta_{nn'},\end{aligned} \tag{B.10}$$

and

$$\int_0^{2\pi}\int_0^{\pi}\boldsymbol{m}_{mn}(\theta,\varphi)\cdot\boldsymbol{n}_{m'n'}(\theta,\varphi)\sin\theta\mathrm{d}\theta\,\mathrm{d}\varphi = 0\,. \tag{B.11}$$

The system of vector spherical harmonics is orthogonal and complete in $L^2_{\tan}(\Omega)$ (the space of square integrable tangential fields defined on the unit sphere Ω) and in terms of the scalar product in $L^2_{\tan}(\Omega)$ we have

$$\begin{aligned}&\int_0^{2\pi}\int_0^{\pi}\boldsymbol{m}_{mn}(\theta,\varphi)\cdot\boldsymbol{m}^*_{m'n'}(\theta,\varphi)\sin\theta\,\mathrm{d}\theta\,\mathrm{d}\varphi\\ &= \int_0^{2\pi}\int_0^{\pi}\boldsymbol{n}_{mn}(\theta,\varphi)\cdot\boldsymbol{n}^*_{m'n'}(\theta,\varphi)\sin\theta\,\mathrm{d}\theta\,\mathrm{d}\varphi = \pi\delta_{mm'}\delta_{nn'}\end{aligned} \tag{B.12}$$

and

$$\int_0^{2\pi}\int_0^{\pi}\boldsymbol{m}_{mn}(\theta,\varphi)\cdot\boldsymbol{n}^*_{m'n'}(\theta,\varphi)\sin\theta\,\mathrm{d}\theta\,\mathrm{d}\varphi = 0. \tag{B.13}$$

We define the vector spherical harmonics of left- and right-handed type as

$$\begin{aligned}\boldsymbol{l}_{mn}(\theta,\varphi) &= \frac{1}{\sqrt{2}}\left[\boldsymbol{m}_{mn}(\theta,\varphi) + \mathrm{j}\boldsymbol{n}_{mn}(\theta,\varphi)\right] \\ &= \frac{\mathrm{j}}{2\sqrt{n(n+1)}}\left[m\pi_n^{|m|}(\theta) + \tau_n^{|m|}(\theta)\right](\boldsymbol{e}_\theta + \mathrm{j}\boldsymbol{e}_\varphi)\mathrm{e}^{\mathrm{j}m\varphi}\end{aligned} \tag{B.14}$$

and

$$\begin{aligned}\boldsymbol{r}_{mn}(\theta,\varphi) &= \frac{1}{\sqrt{2}}\left[\boldsymbol{m}_{mn}(\theta,\varphi) - \mathrm{j}\boldsymbol{n}_{mn}(\theta,\varphi)\right] \\ &= \frac{\mathrm{j}}{2\sqrt{n(n+1)}}\left[m\pi_n^{|m|}(\theta) - \tau_n^{|m|}(\theta)\right](\boldsymbol{e}_\theta - \mathrm{j}\boldsymbol{e}_\varphi)\mathrm{e}^{\mathrm{j}m\varphi},\end{aligned} \tag{B.15}$$

respectively, and it is straightforward to verify the orthogonality relations

$$\begin{aligned}&\int_0^{2\pi}\int_0^{\pi} \boldsymbol{l}_{mn}(\theta,\varphi)\cdot\boldsymbol{l}^*_{m'n'}(\theta,\varphi)\sin\theta\,\mathrm{d}\theta\,\mathrm{d}\varphi \\ &= \int_0^{2\pi}\int_0^{\pi} \boldsymbol{r}_{mn}(\theta,\varphi)\cdot\boldsymbol{r}^*_{m'n'}(\theta,\varphi)\sin\theta\,\mathrm{d}\theta\,\mathrm{d}\varphi = \pi\delta_{mm'}\delta_{nn'}\end{aligned} \tag{B.16}$$

and

$$\int_0^{2\pi}\int_0^{\pi} \boldsymbol{l}_{mn}(\theta,\varphi)\cdot\boldsymbol{r}^*_{m'n'}(\theta,\varphi)\sin\theta\,\mathrm{d}\theta\,\mathrm{d}\varphi = 0. \tag{B.17}$$

Since $\boldsymbol{l}_{mn}$ and $\boldsymbol{r}_{mn}$ are linear combinations of $\boldsymbol{m}_{mn}$ and $\boldsymbol{n}_{mn}$, we deduce that the system of vector spherical harmonics of left- and right-handed type is also orthogonal and complete in $L^2_{\tan}(\Omega)$.

B.2 Vector Wave Functions

The independent solutions to the vector wave equations can be constructed as [215]

$$\begin{aligned}\boldsymbol{M}^{1,3}_{mn}(k\boldsymbol{r}) &= \frac{1}{\sqrt{2n(n+1)}}\nabla u^{1,3}_{mn}(k\boldsymbol{r})\times\boldsymbol{r}, \\ \boldsymbol{N}^{1,3}_{mn}(k\boldsymbol{r}) &= \frac{1}{k}\nabla\times\boldsymbol{M}^{1,3}_{mn}(k\boldsymbol{r}),\end{aligned}$$

where $n = 1, 2, ...,$ and $m = -n, ..., n$. The explicit expressions of the vector spherical wave functions are given by

$$\boldsymbol{M}_{mn}^{1,3}(k\boldsymbol{r}) = \frac{1}{\sqrt{2n(n+1)}} z_n^{1,3}(kr)\left[\mathrm{j}m\pi_n^{|m|}(\theta)\,\boldsymbol{e}_\theta - \tau_n^{|m|}(\theta)\,\boldsymbol{e}_\varphi\right]\mathrm{e}^{\mathrm{j}m\varphi},$$

$$\boldsymbol{N}_{mn}^{1,3}(k\boldsymbol{r}) = \frac{1}{\sqrt{2n(n+1)}}\left\{n(n+1)\frac{z_n^{1,3}(kr)}{kr}P_n^{|m|}(\cos\theta)\boldsymbol{e}_r + \frac{\left[krz_n^{1,3}(kr)\right]'}{kr}\left[\tau_n^{|m|}(\theta)\boldsymbol{e}_\theta + \mathrm{j}m\pi_n^{|m|}(\theta)\boldsymbol{e}_\varphi\right]\right\}\mathrm{e}^{\mathrm{j}m\varphi},$$

where

$$\left[krz_n^{1,3}(kr)\right]' = \frac{\mathrm{d}}{\mathrm{d}\,(kr)}\left[krz_n^{1,3}(kr)\right].$$

The superscript '1' stands for the regular vector spherical wave functions while the superscript '3' stands for the radiating vector spherical wave functions. It is useful to note that for $n = m = 0$, we have $\boldsymbol{M}_{00}^{1,3} = \boldsymbol{N}_{00}^{1,3} = 0$. $\boldsymbol{M}_{mn}^{1}$, $\boldsymbol{N}_{mn}^{1}$ is an entire solution to the Maxwell equations and $\boldsymbol{M}_{mn}^{3}$, $\boldsymbol{N}_{mn}^{3}$ is a radiating solution to the Maxwell equations in $\boldsymbol{R}^3 - \{0\}$.

The vector spherical wave functions can be expressed in terms of vector spherical harmonics as follows:

$$\boldsymbol{M}_{mn}^{1,3}(k\boldsymbol{r}) = z_n^{1,3}(kr)\boldsymbol{m}_{mn}(\theta,\varphi),$$

$$\boldsymbol{N}_{mn}^{1,3}(k\boldsymbol{r}) = \sqrt{\frac{n(n+1)}{2}}\frac{z_n^{1,3}(kr)}{kr}Y_{mn}(\theta,\varphi)\,\boldsymbol{e}_r + \frac{\left[krz_n^{1,3}(kr)\right]'}{kr}\boldsymbol{n}_{mn}(\theta,\varphi),$$

In the far-field region, the asymptotic behavior of the spherical Hankel functions for large value of the argument yields the following representations for the radiating vector spherical wave functions [40]:

$$\boldsymbol{M}_{mn}^{3}(k\boldsymbol{r}) = \frac{\mathrm{e}^{\mathrm{j}kr}}{kr}\left\{(-\mathrm{j})^{n+1}\,\boldsymbol{m}_{mn}(\theta,\varphi) + O\left(\frac{1}{r}\right)\right\}, \quad r\to\infty,$$

$$\boldsymbol{N}_{mn}^{3}(k\boldsymbol{r}) = \frac{\mathrm{e}^{\mathrm{j}kr}}{kr}\left\{\mathrm{j}\,(-\mathrm{j})^{n+1}\,\boldsymbol{n}_{mn}(\theta,\varphi) + O\left(\frac{1}{r}\right)\right\}, \quad r\to\infty.$$

The orthogonality relations on a sphere S_c, of radius R, are

$$\int_{S_\mathrm{c}}[\boldsymbol{e}_r\times\boldsymbol{M}_{mn}(k\boldsymbol{r})]\cdot[\boldsymbol{e}_r\times\boldsymbol{M}_{m'n'}(k\boldsymbol{r})]\,\mathrm{d}S(\boldsymbol{r}) = \pi R^2 z_n^2(kR)\delta_{m,-m'}\delta_{nn'},$$

$$\int_{S_\mathrm{c}}[\boldsymbol{e}_r\times\boldsymbol{N}_{mn}(k\boldsymbol{r})]\cdot[\boldsymbol{e}_r\times\boldsymbol{N}_{m'n'}(k\boldsymbol{r})]\,\mathrm{d}S(\boldsymbol{r}) = \pi R^2\left\{\frac{[kRz_n(kR)]'}{kR}\right\}^2 \times\delta_{m,-m'}\delta_{nn'},$$

and

$$\int_{S_c} [\boldsymbol{e}_r \times \boldsymbol{M}_{mn}(k\boldsymbol{r})] \cdot [\boldsymbol{e}_r \times \boldsymbol{N}_{m'n'}(k\boldsymbol{r})] \, \mathrm{d}S(\boldsymbol{r}) = 0,$$

and we also have

$$\begin{aligned} &\int_{S_c} [\boldsymbol{e}_r \times \boldsymbol{M}_{mn}(k\boldsymbol{r})] \cdot \boldsymbol{N}_{m'n'}(k\boldsymbol{r}) \mathrm{d}S(\boldsymbol{r}) \\ &= -\int_{S_c} [\boldsymbol{e}_r \times \boldsymbol{N}_{mn}(k\boldsymbol{r})] \cdot \boldsymbol{M}_{m'n'}(k\boldsymbol{r}) \mathrm{d}S(\boldsymbol{r}) \\ &= \pi R^2 z_n(kR) \frac{[kRz_n(kR)]'}{kR} \delta_{m,-m'} \delta_{nn'} \end{aligned} \tag{B.18}$$

and

$$\begin{aligned} &\int_{S_c} [\boldsymbol{e}_r \times \boldsymbol{M}_{mn}(k\boldsymbol{r})] \cdot \boldsymbol{M}_{m'n'}(k\boldsymbol{r}) \mathrm{d}S(\boldsymbol{r}) \\ &= \int_{S_c} [\boldsymbol{e}_r \times \boldsymbol{N}_{mn}(k\boldsymbol{r})] \cdot \boldsymbol{N}_{m'n'}(k\boldsymbol{r}) \mathrm{d}S(\boldsymbol{r}) = 0. \end{aligned} \tag{B.19}$$

The spherical vector wave expansion of the dyad $g\overline{\boldsymbol{I}}$ is of basic importance in our analysis and is given by [175, 228, 229]

$$\begin{aligned} &g(k, \boldsymbol{r}, \boldsymbol{r}')\overline{\boldsymbol{I}} \\ &= \frac{\mathrm{j}k}{\pi} \sum_{n=1}^{\infty} \sum_{m=-n}^{n} \begin{cases} \left[\boldsymbol{M}^3_{-mn}(k\boldsymbol{r}')\boldsymbol{M}^1_{mn}(k\boldsymbol{r}) + \boldsymbol{N}^3_{-mn}(k\boldsymbol{r}')\boldsymbol{N}^1_{mn}(k\boldsymbol{r})\right] \\ \quad +\text{Irrotational terms}, \quad r < r' \\ \left[\boldsymbol{M}^1_{-mn}(k\boldsymbol{r}')\boldsymbol{M}^3_{mn}(k\boldsymbol{r}) + \boldsymbol{N}^1_{-mn}(k\boldsymbol{r}')\boldsymbol{N}^3_{mn}(k\boldsymbol{r})\right] \\ \quad +\text{Irrotational terms}, \quad r > r' \end{cases} \end{aligned} \tag{B.20}$$

Using the calculation rules for dyadic functions and the identity $\boldsymbol{a}g = \boldsymbol{a} \cdot g\overline{\boldsymbol{I}}$, we find the following simple but useful expansions

$$\begin{aligned} &\nabla \times [\boldsymbol{a}(\boldsymbol{r}')g(k, \boldsymbol{r}, \boldsymbol{r}')] \\ &= \frac{\mathrm{j}k^2}{\pi} \sum_{n=1}^{\infty} \sum_{m=-n}^{n} \begin{cases} \left\{\left[\boldsymbol{a}(\boldsymbol{r}') \cdot \boldsymbol{M}^3_{-mn}(k\boldsymbol{r}')\right] \boldsymbol{N}^1_{mn}(k\boldsymbol{r}) \right. \\ \quad \left. + \left[\boldsymbol{a}(\boldsymbol{r}') \cdot \boldsymbol{N}^3_{-mn}(k\boldsymbol{r}')\right] \boldsymbol{M}^1_{mn}(k\boldsymbol{r})\right\}, \quad r < r' \\ \left\{\left[\boldsymbol{a}(\boldsymbol{r}') \cdot \boldsymbol{M}^1_{-mn}(k\boldsymbol{r}')\right] \boldsymbol{N}^3_{mn}(k\boldsymbol{r}) \right. \\ \quad \left. + \left[\boldsymbol{a}(\boldsymbol{r}') \cdot \boldsymbol{N}^1_{-mn}(k\boldsymbol{r}')\right] \boldsymbol{M}^3_{mn}(k\boldsymbol{r})\right\}, \quad r > r' \end{cases} \end{aligned} \tag{B.21}$$

and

$$\begin{aligned}
&\nabla\times\nabla\times[\boldsymbol{a}(\boldsymbol{r}')g(k,\boldsymbol{r},\boldsymbol{r}')]\\
&=\frac{\mathrm{j}k^3}{\pi}\sum_{n=1}^{\infty}\sum_{m=-n}^{n}\begin{cases}\left\{\left[\boldsymbol{a}(\boldsymbol{r}')\cdot\boldsymbol{M}^3_{-mn}(k\boldsymbol{r}')\right]\boldsymbol{M}^1_{mn}(k\boldsymbol{r})\right.\\\quad\left.+\left[\boldsymbol{a}(\boldsymbol{r}')\cdot\boldsymbol{N}^3_{-mn}(k\boldsymbol{r}')\right]\boldsymbol{N}^1_{mn}(k\boldsymbol{r})\right\}, & r<r'\\
\left\{\left[\boldsymbol{a}(\boldsymbol{r}')\cdot\boldsymbol{M}^1_{-mn}(k\boldsymbol{r}')\right]\boldsymbol{M}^3_{mn}(k\boldsymbol{r})\right.\\\quad\left.+\left[\boldsymbol{a}(\boldsymbol{r}')\cdot\boldsymbol{N}^1_{-mn}(k\boldsymbol{r}')\right]\boldsymbol{N}^3_{mn}(k\boldsymbol{r})\right\}, & r>r'\end{cases}
\end{aligned}\tag{B.22}$$

Relying on these expansions and using the Stratton–Chu representation theorem, orthogonality relations of vector spherical wave functions on arbitrarily closed surfaces can be derived. Let D_i be a bounded domain with boundary S and exterior D_s, and let $\boldsymbol{n}$ be the unit normal vector to S directed into D_s. The wave number in the domain D_s is denoted by k_s, while the wave number in the domain D_i is denoted by k_i. For $\boldsymbol{r}\in D_\mathrm{i}$, application of Stratton–Chu representation theorem to the vector fields $\boldsymbol{E}_\mathrm{s}(\boldsymbol{r})=\boldsymbol{M}^3_{mn}(k_\mathrm{s}\boldsymbol{r})$ and $\boldsymbol{H}_\mathrm{s}(\boldsymbol{r})=-\mathrm{j}\sqrt{\varepsilon_\mathrm{s}/\mu_\mathrm{s}}\boldsymbol{N}^3_{mn}(k_\mathrm{s}\boldsymbol{r})$ gives

$$\int_S\left[(\boldsymbol{n}\times\boldsymbol{M}^3_{mn})\cdot\begin{pmatrix}\boldsymbol{M}^3_{-m'n'}\\\boldsymbol{N}^3_{-m'n'}\end{pmatrix}+(\boldsymbol{n}\times\boldsymbol{N}^3_{mn})\cdot\begin{pmatrix}\boldsymbol{N}^3_{-m'n'}\\\boldsymbol{M}^3_{-m'n'}\end{pmatrix}\right]\mathrm{d}S=0,\tag{B.23}$$

while for $\boldsymbol{r}\in D_\mathrm{s}$, yields

$$\begin{aligned}
&\frac{\mathrm{j}k_\mathrm{s}^2}{\pi}\int_S\left[(\boldsymbol{n}\times\boldsymbol{M}^3_{mn})\cdot\begin{pmatrix}\boldsymbol{M}^1_{-m'n'}\\\boldsymbol{N}^1_{-m'n'}\end{pmatrix}+(\boldsymbol{n}\times\boldsymbol{N}^3_{mn})\cdot\begin{pmatrix}\boldsymbol{N}^1_{-m'n'}\\\boldsymbol{M}^1_{-m'n'}\end{pmatrix}\right]\mathrm{d}S\\
&=\begin{pmatrix}0\\\delta_{mm'}\delta_{nn'}\end{pmatrix}.
\end{aligned}\tag{B.24}$$

Similarly, for $\boldsymbol{r}\in D_\mathrm{s}$, the Stratton–Chu representation theorem applied to the vector fields $\boldsymbol{E}_\mathrm{i}(\boldsymbol{r})=\boldsymbol{M}^1_{mn}(k_\mathrm{i}\boldsymbol{r})$ and $\boldsymbol{H}_\mathrm{i}(\boldsymbol{r})=-\mathrm{j}\sqrt{\varepsilon_\mathrm{i}/\mu_\mathrm{i}}\boldsymbol{N}^1_{mn}(k_\mathrm{i}\boldsymbol{r})$ leads to

$$\int_S\left[(\boldsymbol{n}\times\boldsymbol{M}^1_{mn})\cdot\begin{pmatrix}\boldsymbol{M}^1_{-m'n'}\\\boldsymbol{N}^1_{-m'n'}\end{pmatrix}+(\boldsymbol{n}\times\boldsymbol{N}^1_{mn})\cdot\begin{pmatrix}\boldsymbol{N}^1_{-m'n'}\\\boldsymbol{M}^1_{-m'n'}\end{pmatrix}\right]\mathrm{d}S=0.\tag{B.25}$$

The regular and radiating spherical vector wave functions can be expressed as integrals over vector spherical harmonics [26]

$$\boldsymbol{M}^1_{mn}(k\boldsymbol{r})=-\frac{1}{4\pi\mathrm{j}^{n+1}}\int_0^{2\pi}\int_0^{\pi}(-\mathrm{j})\,\boldsymbol{m}_{mn}(\beta,\alpha)\,\mathrm{e}^{\mathrm{j}\boldsymbol{k}(\beta,\alpha)\cdot\boldsymbol{r}}\sin\beta\,\mathrm{d}\beta\,\mathrm{d}\alpha,\tag{B.26}$$

$$\boldsymbol{N}^1_{mn}(k\boldsymbol{r})=-\frac{1}{4\pi\mathrm{j}^{n+1}}\int_0^{2\pi}\int_0^{\pi}\boldsymbol{n}_{mn}(\beta,\alpha)\,\mathrm{e}^{\mathrm{j}\boldsymbol{k}(\beta,\alpha)\cdot\boldsymbol{r}}\sin\beta\,\mathrm{d}\beta\,\mathrm{d}\alpha,\tag{B.27}$$

and

$$\boldsymbol{M}^3_{mn}(k\boldsymbol{r}) = -\frac{1}{2\pi \mathrm{j}^{n+1}} \int_0^{2\pi} \int_0^{\frac{\pi}{2}-\mathrm{j}\infty} (-\mathrm{j})\, \boldsymbol{m}_{mn}(\beta,\alpha)\, \mathrm{e}^{\mathrm{j}\boldsymbol{k}(\beta,\alpha)\cdot\boldsymbol{r}} \sin\beta \,\mathrm{d}\beta \,\mathrm{d}\alpha, \tag{B.28}$$

$$\boldsymbol{N}^3_{mn}(k\boldsymbol{r}) = -\frac{1}{2\pi \mathrm{j}^{n+1}} \int_0^{2\pi} \int_0^{\frac{\pi}{2}-\mathrm{j}\infty} \boldsymbol{n}_{mn}(\beta,\alpha)\, \mathrm{e}^{\mathrm{j}\boldsymbol{k}(\beta,\alpha)\cdot\boldsymbol{r}} \sin\beta \,\mathrm{d}\beta \,\mathrm{d}\alpha \tag{B.29}$$

for $z > 0$, respectively.

The above system of vector functions is also known as the system of localized vector spherical wave functions. Another system of vector functions which is suitable for analyzing axisymmetric particles with extreme geometries is the system of distributed vector spherical wave functions [49]. For an axisymmetric particle with the axis of rotation along the z-axis, the distributed vector spherical wave functions are defined as

$$\begin{aligned} \mathcal{M}^{1,3}_{mn}(k\boldsymbol{r}) &= \boldsymbol{M}^{1,3}_{m,|m|+l}\left[k(\boldsymbol{r} - z_n\boldsymbol{e}_z)\right], \\ \mathcal{N}^{1,3}_{mn}(k\boldsymbol{r}) &= \boldsymbol{N}^{1,3}_{m,|m|+l}\left[k(\boldsymbol{r} - z_n\boldsymbol{e}_z)\right], \end{aligned} \tag{B.30}$$

where $\{z_n\}_{n=1}^{\infty}$ is a dense set of points on the z-axis (Fig. B.1), $\boldsymbol{e}_z$ is the unit vector in the direction of the z-axis, $n = 1, 2, ..., m \in \boldsymbol{Z}$, and $l = 1$ if $m = 0$ and $l = 0$, if $m \neq 0$. $\mathcal{M}^1_{mn}$, $\mathcal{N}^1_{mn}$ is an entire solution to the Maxwell equations and $\mathcal{M}^3_{mn}$, $\mathcal{N}^3_{mn}$ is a radiating solution to the Maxwell equations in $\boldsymbol{R}^3 - \{z_n\boldsymbol{e}_z\}$. In the case of prolate scatterers, the distribution of the poles on the axis of rotation adequately describes the particle geometry. In contrast, it is clear from physical considerations that this arrangement is not suitable for oblate scatterers. In this case, the procedure of analytic continuation of the vector fields onto the complex plane along the source coordinate z_n can be used

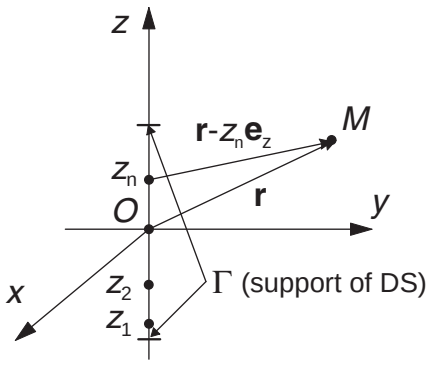

Fig. B.1. Sources distributed on the z-axis

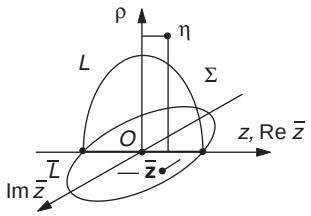

Fig. B.2. Illustration of the complex plane. L is the generatrix of the surface and $\overline{L}$ is the image of L in the complex plane

(Fig. B.2). The complex plane $\widehat{\Sigma} = \{\widehat{\boldsymbol{z}} = (\mathrm{Re}\,\widehat{\boldsymbol{z}}, \mathrm{Im}\,\widehat{\boldsymbol{z}})/\mathrm{Re}\,\widehat{\boldsymbol{z}}, \mathrm{Im}\,\widehat{\boldsymbol{z}} \in \boldsymbol{R}\}$ is the dual of the azimuthal plane $\varphi = \text{const.}$, $\Sigma = \{\boldsymbol{\eta} = (\rho, z)/\rho \geq 0, z \in \boldsymbol{R}\}$, and is defined by taking the real axis $\mathrm{Re}\,\widehat{\boldsymbol{z}}$ along the z-axis. The vector spherical wave functions can be expressed in terms of the coordinates of the source point $\widehat{\boldsymbol{z}} \in \widehat{\Sigma}$ and the field point $\boldsymbol{\eta} \in \Sigma$ as

$$\begin{aligned}\boldsymbol{M}_{mn}^{1,3}(k\boldsymbol{r}) = \frac{1}{\sqrt{2n(n+1)}} z_n^{1,3}(kR) \Big\{ \mathrm{j}m\pi_n^{|m|}\left(\widehat{\theta}\right)\Big[\sin(\theta-\widehat{\theta})\boldsymbol{e}_r \\ + \cos(\theta-\widehat{\theta})\boldsymbol{e}_\theta\Big] - \tau_n^{|m|}\left(\widehat{\theta}\right)\boldsymbol{e}_\varphi\Big\}\,\mathrm{e}^{\mathrm{j}m\varphi}\end{aligned} \tag{B.31}$$

and

$$\begin{aligned}\boldsymbol{N}_{mn}^{1,3}(k\boldsymbol{r}) = \frac{1}{\sqrt{2n(n+1)}} \Bigg\{ n(n+1)\frac{z_n^{1,3}(kR)}{kR} P_n^{|m|}(\cos\widehat{\theta}) \\ \times \Big[\cos(\theta-\widehat{\theta})\boldsymbol{e}_r - \sin(\theta-\widehat{\theta})\boldsymbol{e}_\theta\Big] + \frac{\left[kRz_n^{1,3}(kR)\right]'}{kR} \\ \times \Big\{\tau_n^{|m|}\left(\widehat{\theta}\right)\Big[\sin(\theta-\widehat{\theta})\boldsymbol{e}_r + \cos(\theta-\widehat{\theta})\boldsymbol{e}_\theta\Big] \\ + \mathrm{j}m\pi_n^{|m|}\left(\widehat{\theta}\right)\boldsymbol{e}_\varphi\Big\}\Bigg\}\,\mathrm{e}^{\mathrm{j}m\varphi},\end{aligned} \tag{B.32}$$

where

$$R^2 = \rho^2 + (z-\widehat{\boldsymbol{z}})^2, \quad \sin\widehat{\theta} = \frac{\rho}{R} \quad \text{and} \quad \cos\widehat{\theta} = \frac{z-\widehat{\boldsymbol{z}}}{R}.$$

B.3 Rotations

We consider two coordinate systems $Oxyz$ and $Ox_1y_1z_1$ having the same origin. The coordinate system $Ox_1y_1z_1$ is obtained by rotating the coordinate

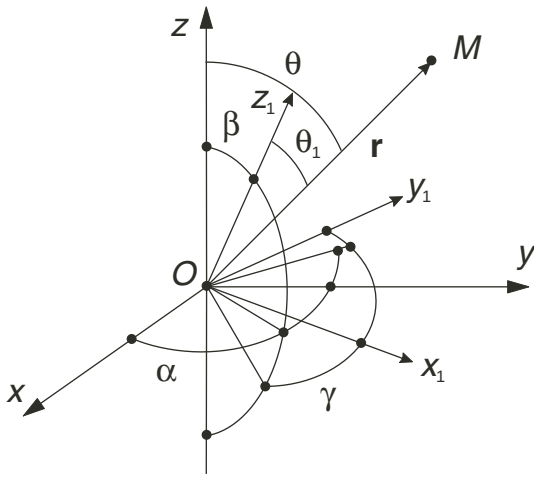

Fig. B.3. Coordinate rotations

system $Oxyz$ thought the Euler angles (α, β, γ) as shown in Fig. B.3. With (θ, φ) and (θ_1, φ_1) being the spherical angles of the same position vector $\boldsymbol{r}$ in the coordinate systems $Oxyz$ and $Ox_1y_1z_1$, the addition theorem for spherical wave functions under coordinate rotations is [58, 213, 239]

$$u^{1,3}_{mn}(kr, \theta, \varphi) = \sum_{m'=-n}^{n} D^n_{mm'}(\alpha, \beta, \gamma) u^{1,3}_{m'n}(kr, \theta_1, \varphi_1), \tag{B.33}$$

where the Wigner D-functions are defined as [262]

$$D^n_{mm'}(\alpha, \beta, \gamma) = (-1)^{m+m'} \mathrm{e}^{\mathrm{j}m\alpha} \widetilde{d}^n_{mm'}(\beta) e^{\mathrm{j}m'\gamma}\,. \tag{B.34}$$

The functions $\widetilde{d}$ are given by

$$\widetilde{d}^n_{mm'}(\beta) = \Delta_{mm'} d^n_{mm'}(\beta), \tag{B.35}$$

where $d^n_{mm'}$ are the Wigner d-functions and

$$\Delta_{mm'} = \begin{cases} 1, & m \geq 0\,, \quad m' \geq 0 \\ (-1)^{m'}, & m \geq 0\,, \quad m' < 0 \\ (-1)^{m}\,, & m < 0\,, \quad m' \geq 0 \\ (-1)^{m+m'}\,, & m < 0\,, \quad m' < 0, \end{cases} \tag{B.36}$$

with the property $\Delta_{mm'} = \Delta_{m'm}$. The expression of Wigner d-functions for positive and negative values of the indices m and m' is given by

$$d^n_{mm'}(\beta) = \sqrt{\frac{(n+m')!(n-m')!}{(n+m)!(n-m)!}} \sum_{\sigma} (-1)^{n-m'-\sigma} C^{n-m'-\sigma}_{n+m} C^{\sigma}_{n-m}$$
$$\times \left(\cos\frac{\beta}{2}\right)^{m+m'+2\sigma} \left(\sin\frac{\beta}{2}\right)^{2n-m-m'-2\sigma}$$

and note that the above equation is valid for $\beta < 0$, if

$$\cos\left(\frac{\beta}{2}\right) = \sqrt{\frac{1+\cos\beta}{2}}\,, \quad \sin\left(\frac{\beta}{2}\right) = -\sqrt{\frac{1-\cos\beta}{2}}$$

and for $\beta > \pi$, if

$$\cos\left(\frac{\beta}{2}\right) = -\sqrt{\frac{1+\cos\beta}{2}}\,, \quad \sin\left(\frac{\beta}{2}\right) = \sqrt{\frac{1-\cos\beta}{2}}.$$

The Wigner d-functions are real and have the following symmetry properties [58]:

$$d^n_{m-m'}(\beta) = (-1)^{n+m'} d^n_{mm'}(\beta+\pi), \tag{B.37}$$

$$d^n_{-mm'}(\beta) = (-1)^{n+m} d^n_{mm'}(\beta+\pi), \tag{B.38}$$

$$d^n_{-m-m'}(\beta) = (-1)^{m+m'} d^n_{mm'}(\beta), \tag{B.39}$$

$$d^n_{mm'}(\beta) = (-1)^{m+m'} d^n_{m'm}(\beta), \tag{B.40}$$

and

$$d^n_{mm'}(-\beta) = (-1)^{m+m'} d^n_{mm'}(\beta) = d^n_{m'm}(\beta). \tag{B.41}$$

Taking into account the above symmetry relations, we can express the $\widetilde{d}$-functions in terms of the d-functions with positive values of the indices m and m'

$$\widetilde{d}^n_{mm'}(\beta) = \begin{cases} d^n_{mm'}(\beta)\,, & m \geq 0\,, \quad m' \geq 0, \\ (-1)^n d^n_{m-m'}(\beta+\pi)\,, & m \geq 0\,, \quad m' < 0, \\ (-1)^n d^n_{-mm'}(\beta+\pi)\,, & m < 0\,, \quad m' \geq 0, \\ d^n_{-m-m'}(\beta), & m < 0\,, \quad m' < 0. \end{cases} \tag{B.42}$$

The orthogonality property of the Wigner d-functions is similar to that of the associated Legendre functions and is given by

$$\int_0^\pi d^n_{mm'}(\beta) d^{n'}_{mm'}(\beta) \sin\beta \mathrm{d}\beta = \frac{2}{2n+1}\delta_{nn'}. \tag{B.43}$$

The Wigner d-functions are related to the generalized spherical functions $P^n_{mm'}$ by the relation [78]

$$d^n_{mm'}(\beta) = \mathrm{j}^{m'-m} P^n_{mm'}(\cos\beta)\,. \tag{B.44}$$

The generalized spherical functions are complex and have the following symmetry properties:

$$
\begin{aligned}
P^n_{m-m'}(x) &= (-1)^n P^n_{mm'}(-x),\\
P^n_{-mm'}(x) &= (-1)^n P^n_{mm'}(-x),\\
P^n_{-m-m'}(x) &= P^n_{mm'}(x),\\
P^n_{mm'}(x) &= P^n_{m'm}(x),
\end{aligned}
$$

where $x = \cos\beta$. The orthogonality relation for the generalized spherical functions follows from the orthogonality relation for the Wigner d-function:

$$
\int_0^\pi P^n_{mm'}(\cos\beta)\, P^{n'}_{mm'}(\cos\beta)\sin\beta \mathrm{d}\beta = \frac{(-1)^{m+m'}}{2n+1}\delta_{nn'}\,.
$$

In practice, the generalized spherical functions can be found from the recurrence relation [162]

$$
\begin{aligned}
&n\sqrt{(n+1)^2-m^2}\sqrt{(n+1)^2-m'^2}P^{n+1}_{mm'}(x)\\
&= (2n+1)\left[n(n+1)x - mm'\right]P^n_{mm'}(x)\\
&\quad -(n+1)\sqrt{n^2-m^2}\sqrt{n^2-m'^2}P^{n-1}_{mm'}(x)
\end{aligned}
$$

with the initial values

$$
\begin{aligned}
P^{n_0-1}_{mm'}(x) &= 0,\\
P^{n_0}_{mm'}(x) &= \frac{(-\mathrm{j})^{|m-m'|}}{2^{n_0}}\sqrt{\frac{(2n_0)!}{(|m-m'|)!\,(|m+m'|)!}}\\
&\quad \times (1-x)^{\frac{|m-m'|}{2}}(1+x)^{\frac{|m+m'|}{2}}\,,
\end{aligned}
$$

and $n_0 = \max(|m|,|m'|)$. From (B.42) and (B.44) we see that it is sufficient to compute the generalized spherical functions for positive values of the indices m and m'.

If the Euler angles $(\alpha_1,\beta_1,\gamma_1)$ and $(\alpha_2,\beta_2,\gamma_2)$ describe two consecutive rotations of a coordinate system and the Euler angles (α,β,γ) describes the resulting rotation, the addition theorem for the D-functions is [169, 239]

$$
D^n_{mm'}(\alpha,\beta,\gamma) = \sum_{m''=-n}^{n} D^n_{mm''}(\alpha_1,\beta_1,\gamma_1)D^n_{m''m'}(\alpha_2,\beta_2,\gamma_2) \tag{B.45}
$$

and the unitarity condition read as

$$
\sum_{m''=-n}^{n} D^n_{mm''}(\alpha_1,\beta_1,\gamma_1)D^n_{m''m'}(-\gamma_1,-\beta_1,-\alpha_1) = D^n_{mm'}(0,0,0) = \delta_{mm'}. \tag{B.46}
$$

If in (B.45) we set $\alpha_1 = \alpha_2 = 0$ and $\gamma_1 = \gamma_2 = 0$, then $\beta = \beta_1 + \beta_2$, and we obtain the addition theorem for the d-functions

$$d^n_{mm'}(\beta) = \sum_{m''=-n}^{n} d^n_{mm''}(\beta_1) d^n_{m''m'}(\beta_2).$$

In particular, when $\beta_2 = -\beta_1$ we derive the unitarity condition

$$\begin{aligned}\sum_{m''=-n}^{n} d^n_{mm''}(\beta_1) d^n_{m''m'}(-\beta_1) &= \sum_{m''=-n}^{n} (-1)^{m'+m''} d^n_{mm''}(\beta_1) d^n_{m''m'}(\beta_1) \\ &= \sum_{m''=-n}^{n} d^n_{mm''}(\beta_1) d^n_{m'm''}(\beta_1) = d^n_{mm'}(0) = \delta_{mm'}.\end{aligned}$$

The product of two d-functions can be expanded in terms of the Clebsch–Gordan coefficients $C^{m+m_1 u}_{mn,m_1 n_1}$

$$d^n_{mm'}(\beta) d^{n_1}_{m_1 m'_1}(\beta) = \sum_{u=|n-n_1|}^{n+n_1} C^{m+m_1 u}_{mn,m_1 n_1} d^u_{m+m_1 m'+m'_1}(\beta)\, C^{m'+m'_1 u}_{m'n,m'_1 n_1}, \quad \text{(B.47)}$$

and note that the Clebsch–Gordan coefficients are nonzero only when $|n - n_1| \le u \le n + n_1$. The following symmetry properties of the Clebsch–Gordan coefficients are used in our analysis [169, 239]:

$$C^{m+m_1 u}_{mn,m_1 n_1} = (-1)^{n+n_1+u} C^{-m-m_1 u}_{-mn,-m_1 n_1}, \quad \text{(B.48)}$$

$$C^{m+m_1 u}_{mn,m_1 n_1} = (-1)^{n+n_1+u} C^{m+m_1 u}_{m_1 n_1,mn}, \quad \text{(B.49)}$$

$$C^{m+m_1 u}_{mn,m_1 n_1} = (-1)^{m+n} \sqrt{\frac{2u+1}{2n_1+1}} C^{-m_1 n_1}_{mn,-m-m_1 u}, \quad \text{(B.50)}$$

$$C^{m+m_1 u}_{mn,m_1 n_1} = (-1)^{m_1+n+u} \sqrt{\frac{2u+1}{2n+1}} C^{mn}_{m+m_1 u,-m_1 n_1}. \quad \text{(B.51)}$$

To compute the Clebsch–Gordan coefficients we first define the coefficients $S^u_{mn,m_1 n_1}$ by the relation [77]

$$C^{m+m_1 u}_{mn,m_1 n_1} = g^u_{mn,m_1 n_1} S^u_{mn,m_1 n_1},$$

where

$$\begin{aligned}g^u_{mn,m_1 n_1} = \sqrt{2u+1} &\sqrt{\frac{(u+m+m_1)!(u-m-m_1)!}{(n-m)!(n+m)!}} \\ &\times \sqrt{\frac{(n+n_1-u)!\,(u+n-n_1)!\,(u-n+n_1)!}{(n_1-m_1)!(n_1+m_1)!\,(n+n_1+u+1)!}}\end{aligned}$$

The S-coefficients obey the three-term downward recurrence relation

$$S^{u-1}_{mn,m_1n_1} = p_u S^{u}_{mn,m_1n_1} + q_u S^{u+1}_{mn,m_1n_1}$$

for $u = n + n_1, n + n_1 - 1, \ldots, \max(|m + m_1|, |n - n_1|)$ with

$$p_u = \frac{(2u+1)\left\{(m-m_1)u(u+1) - (m+m_1)\left[n\left(n+1\right) - n_1\left(n_1+1\right)\right]\right\}}{\left(u+1\right)\left(n+n_1-u+1\right)\left(n+n_1+u+1\right)},$$

$$q_u = -\frac{u(u+n-n_1+1)\left(u-n+n_1+1\right)}{\left(u+1\right)\left(n+n_1-u+1\right)} \times \frac{\left(u+m+m_1+1\right)\left(u-m-m_1+1\right)}{n+n_1+u+1}$$

and the starting values

$$S^{n+n_1+1}_{mn,m_1n_1} = 0,$$
$$S^{n+n_1}_{mn,m_1n_1} = 1.$$

The rotation addition theorem for vector spherical wave functions is [213]

$$\boldsymbol{M}^{1,3}_{mn}\left(kr,\theta,\varphi\right) = \sum_{m'=-n}^{n} D^{n}_{mm'}(\alpha,\beta,\gamma)\boldsymbol{M}^{1,3}_{m'n}(kr,\theta_1,\varphi_1), \tag{B.52}$$

$$\boldsymbol{N}^{1,3}_{mn}\left(kr,\theta,\varphi\right) = \sum_{m'=-n}^{n} D^{n}_{mm'}(\alpha,\beta,\gamma)\boldsymbol{N}^{1,3}_{m'n}(kr,\theta_1,\varphi_1)\,, \tag{B.53}$$

and in matrix form we have

$$\begin{bmatrix} \boldsymbol{M}^{1,3}_{mn}\left(kr,\theta,\varphi\right) \\ \boldsymbol{N}^{1,3}_{mn}\left(kr,\theta,\varphi\right) \end{bmatrix} = \mathcal{R}\left(\alpha,\beta,\gamma\right) \begin{bmatrix} \boldsymbol{M}^{1,3}_{m'n'}(kr,\theta_1,\varphi_1) \\ \boldsymbol{N}^{1,3}_{m'n'}(kr,\theta_1,\varphi_1) \end{bmatrix},$$

where $\mathcal{R}$ is the rotation matrix. The rotation matrix has a block-diagonal structure and is given by

$$\mathcal{R}\left(\alpha,\beta,\gamma\right) = \begin{bmatrix} R_{mn,m'n'}\left(\alpha,\beta,\gamma\right) & 0 \\ 0 & R_{mn,m'n'}\left(\alpha,\beta,\gamma\right) \end{bmatrix},$$

where

$$R_{mn,m'n'}\left(\alpha,\beta,\gamma\right) = D^{n}_{mm'}(\alpha,\beta,\gamma)\delta_{nn'}.$$

The unitarity condition for the D-functions yields

$$\mathcal{R}\left(-\gamma,-\beta,-\alpha\right) = \mathcal{R}^{-1}\left(\alpha,\beta,\gamma\right) \tag{B.54}$$

and since

$$D^{n}_{m'm}\left(-\gamma,-\beta,-\alpha\right)=D^{n*}_{mm'}(\alpha,\beta,\gamma),$$

we also have

$$\mathcal{R}\left(-\gamma,-\beta,-\alpha\right)=\mathcal{R}^{\dagger}\left(\alpha,\beta,\gamma\right), \tag{B.55}$$

where $X^{\dagger}$ stands for the complex conjugate transpose of the matrix X.

Properties of Wigner functions and generalized spherical functions (which have been introduced in the quantum theory of angular momentum) are also discussed in [27, 160].

B.4 Translations

We consider two coordinate systems $Oxyz$ and $Ox_1y_1z_1$ having identical spatial orientations but different origins (Fig. B.4). The vectors $\boldsymbol{r}$ and $\boldsymbol{r}_1$ are the position vectors of the same field point in the coordinate systems $Oxyz$ and $Ox_1y_1z_1$, respectively, while the vector $\boldsymbol{r}_0$ connects the origins of both coordinate systems and is given by $\boldsymbol{r}_0=\boldsymbol{r}-\boldsymbol{r}_1$.

In general, the addition theorem for spherical wave functions can be written as [27, 70]

$$u_{mn}\left(k\boldsymbol{r}\right)=\sum_{n'=0}^{\infty}\sum_{m'=-n'}^{n'}C_{mn,m'n'}\left(k\boldsymbol{r}_0\right)u_{m'n'}\left(k\boldsymbol{r}_1\right).$$

Integral and series representations for the translation coefficients $C_{mn,m'n'}$ can be obtained by using the integral representations for the spherical wave

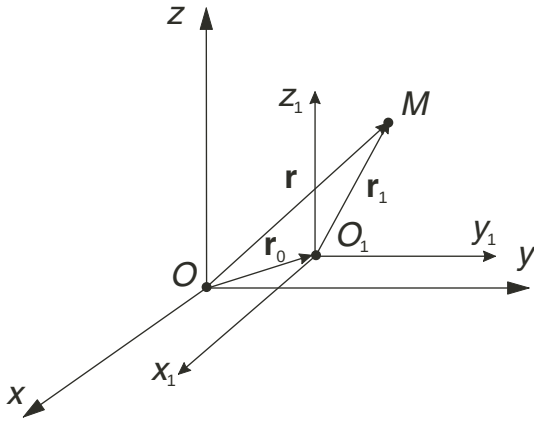

Fig. B.4. Coordinate translation

functions. For regular spherical wave functions, we use the integral representation (B.1), the relation $\boldsymbol{r} = \boldsymbol{r}_0 + \boldsymbol{r}_1$, and the spherical wave expansion of the plane wave $\exp(\mathrm{j}\boldsymbol{k}\cdot\boldsymbol{r}_1)$ to obtain

$$u^1_{mn}(k\boldsymbol{r}) = \sum_{n'=0}^{\infty}\sum_{m'=-n'}^{n'} C^1_{mn,m'n'}(k\boldsymbol{r}_0)\, u^1_{m'n'}(k\boldsymbol{r}_1) \tag{B.56}$$

with

$$C^1_{mn,m'n'}(k\boldsymbol{r}_0) = \frac{\mathrm{j}^{n'-n}}{2\pi}\int_0^{2\pi}\int_0^{\pi} Y_{mn}(\beta,\alpha)\, Y_{-m'n'}(\beta,\alpha)\, e^{\mathrm{j}\boldsymbol{k}(\beta,\alpha)\cdot\boldsymbol{r}_0}\sin\beta\,\mathrm{d}\beta\,\mathrm{d}\alpha\,. \tag{B.57}$$

Taking into account the spherical wave expansion of the plane wave $\exp(\mathrm{j}\boldsymbol{k}\cdot\boldsymbol{r}_0)$ and integrating over α, we find the series representation

$$C^1_{mn,m'n'}(k\boldsymbol{r}_0) = 2\mathrm{j}^{n'-n}\sum_{n''}\mathrm{j}^{n''}\, a(m,m'\mid n'',n,n')\, u^1_{m-m'n''}(k\boldsymbol{r}_0) \tag{B.58}$$

with the expansion coefficients

$$a(m,m'\mid n'',n,n') = \int_0^{\pi} P_n^{|m|}(\cos\beta)\, P_{n'}^{|m'|}(\cos\beta)\, P_{n''}^{|m-m'|}(\cos\beta)\sin\beta\mathrm{d}\beta.$$

We note that the expansion coefficients $a(\cdot)$ are defined by the spherical harmonic expansion theorem [70]

$$P_n^{|m|}(\cos\beta)\, P_{n'}^{|m'|}(\cos\beta) = \sum_{n''} a(m,-m'\mid n'',n,n')\, P_{n''}^{|m+m'|}(\cos\beta)\,,$$

where the summation over n'' is finite covering the range $|n-n'|, |n-n'|+2, ..., n+n'$. These coefficients can be identified with a product of two Wigner $3j$ symbols, which are associated with the coupling of two angular momentum eigenvectors. The azimuthal integration in (B.57) can be analytically performed by using the identity

$$\boldsymbol{k}\cdot\boldsymbol{r}_0 = k\rho_0\sin\beta\cos(\alpha-\varphi_0) + kz_0\cos\beta$$

and the standard integral

$$\int_0^{2\pi} \mathrm{e}^{\mathrm{j}x\cos(\alpha-\varphi_0)} e^{\mathrm{j}(m-m')\alpha}\,\mathrm{d}\alpha = 2\pi\mathrm{j}^{m'-m} J_{m'-m}(x) e^{-\mathrm{j}(m'-m)\varphi_0}\,,$$

where (ρ_0,φ_0,z_0) are the cylindrical coordinates of $\boldsymbol{r}_0$, and the result is

$$C^1_{mn,m'n'}(k\boldsymbol{r}_0) = \mathrm{j}^{n'+m'-n-m}\mathrm{e}^{-\mathrm{j}(m'-m)\varphi_0}\int_0^{\pi} J_{m'-m}(k\rho_0\sin\beta) \times P_n^{|m|}(\cos\beta)\, P_{n'}^{|m'|}(\cos\beta)\,\mathrm{e}^{\mathrm{j}kz_0\cos\beta}\sin\beta\,\mathrm{d}\beta\,. \tag{B.59}$$

If the translation is along the z-axis, the addition theorem involves a single summation

$$u^1_{mn}\left(k\boldsymbol{r}\right) = \sum_{n'=0}^{\infty} C^1_{mn,mn'}\left(kz_0\right) u^1_{mn'}\left(k\boldsymbol{r}_1\right)$$

and the translation coefficients simplify to

$$C^1_{mn,mn'}\left(kz_0\right) = \mathrm{j}^{n'-n} \int_0^{\pi} P_n^{|m|}\left(\cos\beta\right) P_{n'}^{|m|}\left(\cos\beta\right) \mathrm{e}^{\mathrm{j}kz_0\cos\beta} \sin\beta\,\mathrm{d}\beta. \quad \text{(B.60)}$$

For radiating spherical wave functions we consider the integral representation (B.2) and the relation $\boldsymbol{r} = \boldsymbol{r}_0 + \boldsymbol{r}_1$. For $r_1 > r_0$, we express u^3_{mn} as (cf. (B.5))

$$u^3_{mn}(k\boldsymbol{r}) = \frac{1}{2\pi\mathrm{j}^n} \int_0^{2\pi} \int_0^{\pi} Y_{mn}\left(\beta,\alpha\right) Q(k,\beta,\alpha,\boldsymbol{r}_1) \mathrm{e}^{\mathrm{j}\boldsymbol{k}(\beta,\alpha)\cdot\boldsymbol{r}_0} \sin\beta \mathrm{d}\beta\mathrm{d}\alpha$$

and use the spherical wave expansion of the quasi-plane wave $Q(k,\beta,\alpha,\boldsymbol{r}_1)$ to derive

$$u^3_{mn}\left(k\boldsymbol{r}\right) = \sum_{n'=0}^{\infty} \sum_{m'=-n'}^{n'} C^1_{mn,m'n'}\left(k\boldsymbol{r}_0\right) u^3_{m'n'}\left(k\boldsymbol{r}_1\right).$$

For $r_1 < r_0$, we represent the radiating spherical wave functions as

$$u^3_{mn}(k\boldsymbol{r}) = \frac{1}{2\pi\mathrm{j}^n} \int_0^{2\pi} \int_0^{\pi} Y_{mn}\left(\beta,\alpha\right) Q(k,\beta,\alpha,\boldsymbol{r}_0) \mathrm{e}^{\mathrm{j}\boldsymbol{k}(\beta,\alpha)\cdot\boldsymbol{r}_1} \sin\beta \mathrm{d}\beta\mathrm{d}\alpha$$

and use the spherical wave expansion of the plane wave $\exp(\mathrm{j}\boldsymbol{k}\cdot\boldsymbol{r}_1)$ to obtain

$$u^3_{mn}\left(k\boldsymbol{r}\right) = \sum_{n'=0}^{\infty} \sum_{m'=-n'}^{n'} C^3_{mn,m'n'}\left(k\boldsymbol{r}_0\right) u^1_{m'n'}\left(k\boldsymbol{r}_1\right)$$

with

$$\begin{aligned} &C^3_{mn,m'n'}\left(k\boldsymbol{r}_0\right) \\ &= \frac{\mathrm{j}^{n'-n}}{\pi} \int_0^{2\pi} \int_0^{\pi} Y_{mn}\left(\beta,\alpha\right) Y_{-m'n'}\left(\beta,\alpha\right) Q(k,\beta,\alpha,\boldsymbol{r}_0) \sin\beta\,\mathrm{d}\beta\,\mathrm{d}\alpha\,. \end{aligned} \quad \text{(B.61)}$$

Inserting the spherical wave expansion of the quasi-plane wave $Q(k,\beta,\alpha,\boldsymbol{r}_0)$ into (B.61) yields

$$C^3_{mn,m'n'}\left(k\boldsymbol{r}_0\right) = 2\mathrm{j}^{n'-n} \sum_{n''} \mathrm{j}^{n''} a\left(m,m' \mid n'',n,n'\right) u^3_{m-m'n''}\left(k\boldsymbol{r}_0\right). \quad \text{(B.62)}$$

Finally, we note the integral representation for the translation coefficients $C^3_{mn,m'n'}$ in the specific case of axial translation:

$$C^3_{mn,mn'}(kz_0) = 2\mathrm{j}^{n'-n}\int_0^{\frac{\pi}{2}-\mathrm{j}\infty} P_n^{|m|}(\cos\beta)\, P_{n'}^{|m|}(\cos\beta)\, \mathrm{e}^{\mathrm{j}kz_0\cos\beta}\sin\beta \mathrm{d}\beta\,. \tag{B.63}$$

Recurrence relations have been derived for the $C_{mn,mn'}$ coefficients [150]. The derivation is simple for the case of axial translation and positive m. Using the integral representation (B.60) (or (B.63)) and the recurrence relations for the normalized associated Legendre functions (A.15) and (A.16), give

$$\begin{aligned}
&\sqrt{\frac{(n-m-1)(n-m+1)}{(2n-1)(2n+1)}}C_{mn-1,mn'}(kz_0)\\
&\quad+\sqrt{\frac{(n+m)(n+m+1)}{(2n+1)(2n+3)}}C_{mn+1,mn'}(kz_0)\\
&=\sqrt{\frac{(n'+m-1)(n'+m)}{(2n'-1)(2n'+1)}}C_{m-1n,m-1n'-1}(kz_0)\\
&\quad+\sqrt{\frac{(n'-m+1)(n'-m+2)}{(2n'+1)(2n'+3)}}C_{m-1n,m-1n'+1}(kz_0)\,,
\end{aligned} \tag{B.64}$$

while the recurrence relation (A.14), yields

$$\begin{aligned}
&\sqrt{\frac{(n-m+1)(n+m+1)}{(2n+1)(2n+3)}}C_{mn+1,mn'}(kz_0)\\
&\quad-\sqrt{\frac{(n-m)(n+m)}{(2n-1)(2n+1)}}C_{mn-1,mn'}(kz_0)\\
&=\sqrt{\frac{(n'-m)(n'+m)}{(2n'-1)(2n'+1)}}C_{mn,mn'-1}(kz_0)\\
&\quad-\sqrt{\frac{(n'-m+1)(n'+m+1)}{(2n'+1)(2n'+3)}}C_{mn,mn'+1}(kz_0)\,.
\end{aligned} \tag{B.65}$$

We note that the convention $C_{mn,mn'} = 0$ for $m > n$ or $m > n'$, is assumed in the above equations. For the recurrence relationships to be of practical use, initial values are needed. This is accomplished by using the integral representations

$$\begin{aligned}
j_n(kz_0) &= \frac{1}{\mathrm{j}^n\sqrt{2(2n+1)}}\int_0^{\pi} P_n(\cos\beta)\,\mathrm{e}^{\mathrm{j}kz_0\cos\beta}\sin\beta\,\mathrm{d}\beta,\\
h_n^{(1)}(kz_0) &= \frac{1}{\mathrm{j}^n}\sqrt{\frac{2}{2n+1}}\int_0^{\frac{\pi}{2}-\mathrm{j}\infty} P_n(\cos\beta)\,\mathrm{e}^{\mathrm{j}kz_0\cos\beta}\sin\beta\,\mathrm{d}\beta\,,
\end{aligned}$$

which yields

$$C^1_{00,0n'}\left(kz_0\right) = (-1)^{n'}\sqrt{2n'+1}j_{n'}\left(kz_0\right),$$

$$C^3_{00,0n'}\left(kz_0\right) = (-1)^{n'}\sqrt{2n'+1}h^{(1)}_{n'}\left(kz_0\right).$$

Using these starting values, the $C_{mm,mn'}$ coefficients can be computed from the recurrence relation (B.64) with $m = n+1$,

$$C_{mm,mn'}(kz_0) = \sqrt{\frac{2m+1}{2m}}\left[\sqrt{\frac{(n'+m-1)\,(n'+m)}{(2n'-1)\,(2n'+1)}}C_{m-1m-1,m-1n'-1}(kz_0)\right.$$
$$\left. + \sqrt{\frac{(n'-m+1)\,(n'-m+2)}{(2n'+1)\,(2n'+3)}}C_{m-1m-1,m-1n'+1}\left(kz_0\right)\right],$$

where $C_{mm,mn'}$ can be obtained from $C_{00,0n'}$ for all values of $m \geq 1$ and $n' \geq m$, while (B.65) can then be used to compute $C_{mn,mn'}$ for $n \geq m+1$.

In general, the translation addition theorem for vector spherical wave functions can be written as [43, 213]

$$\boldsymbol{M}_{mn}\left(k\boldsymbol{r}\right) = \sum_{n'=1}^{\infty}\sum_{m'=-n'}^{n'} A_{mn,m'n'}(k\boldsymbol{r}_0)\boldsymbol{M}_{m'n'}(k\boldsymbol{r}_1)$$
$$+B_{mn,m'n'}(k\boldsymbol{r}_0)\boldsymbol{N}_{m'n'}(k\boldsymbol{r}_1),$$
$$\boldsymbol{N}_{mn}\left(k\boldsymbol{r}\right) = \sum_{n'=1}^{\infty}\sum_{m'=-n'}^{n'} B_{mn,m'n'}(k\boldsymbol{r}_0)\boldsymbol{M}_{m'n'}(k\boldsymbol{r}_1)$$
$$+A_{mn,m'n'}(k\boldsymbol{r}_0)\boldsymbol{N}_{m'n'}(k\boldsymbol{r}_1).$$

As in the scalar case, integral and series representations for the translation coefficients can be obtained by using the integral representations for the vector spherical wave functions. First we consider the case of regular vector spherical wave functions. Using the integral representation (B.26), the relation $\boldsymbol{r} = \boldsymbol{r}_0 + \boldsymbol{r}_1$, and the vector spherical wave expansion

$$(-\mathrm{j})\,\boldsymbol{m}_{mn}\left(\beta,\alpha\right)\mathrm{e}^{\mathrm{j}\boldsymbol{k}(\beta,\alpha)\cdot\boldsymbol{r}_1} = \sum_{n'=1}^{\infty}\sum_{m'=-n'}^{n'} a^1_{mn,m'n'}\boldsymbol{M}^1_{m'n'}\left(k\boldsymbol{r}_1\right)$$
$$+b^1_{mn,m'n'}\boldsymbol{N}^1_{m'n'}\left(k\boldsymbol{r}_1\right)$$

with

$$a^1_{mn,m'n'} = -\frac{4\mathrm{j}^{n'+1}}{\sqrt{2n'\,(n'+1)}}\left[mm'\pi_n^{|m|}(\beta)\pi_{n'}^{|m'|}(\beta) + \tau_n^{|m|}(\beta)\tau_{n'}^{|m'|}(\beta)\right]\mathrm{e}^{-\mathrm{j}m'\alpha},$$

$$b^1_{mn,m'n'} = -\frac{4\mathrm{j}^{n'+1}}{\sqrt{2n'\,(n'+1)}}\left[m\pi_n^{|m|}(\beta)\tau_{n'}^{|m'|}\,(\beta) + m'\tau_n^{|m|}(\beta)\pi_{n'}^{|m'|}(\beta)\right]\mathrm{e}^{-\mathrm{j}m'\alpha},$$

we obtain

$$\boldsymbol{M}^1_{mn}\,(k\boldsymbol{r}) = \sum_{n'=1}^{\infty}\sum_{m'=-n'}^{n'} A^1_{mn,m'n'}(k\boldsymbol{r}_0)\boldsymbol{M}^1_{m'n'}(k\boldsymbol{r}_1) + B^1_{mn,m'n'}(k\boldsymbol{r}_0)\boldsymbol{N}^1_{m'n'}(k\boldsymbol{r}_1), \tag{B.66}$$

$$\boldsymbol{N}^1_{mn}\,(k\boldsymbol{r}) = \sum_{n'=1}^{\infty}\sum_{m'=-n'}^{n'} B^1_{mn,m'n'}(k\boldsymbol{r}_0)\boldsymbol{M}^1_{m'n'}(k\boldsymbol{r}_1) + A^1_{mn,m'n'}(k\boldsymbol{r}_0)\boldsymbol{N}^1_{m'n'}(k\boldsymbol{r}_1), \tag{B.67}$$

where

$$A^1_{mn,m'n'}(k\boldsymbol{r}_0) = \frac{\mathrm{j}^{n'-n}}{2\pi\sqrt{nn'(n+1)\,(n'+1)}}\int_0^{2\pi}\int_0^{\pi}\left[mm'\pi_n^{|m|}(\beta)\pi_{n'}^{|m'|}(\beta) + \tau_n^{|m|}(\beta)\tau_{n'}^{|m'|}(\beta)\right]\mathrm{e}^{\mathrm{j}(m-m')\alpha}\mathrm{e}^{\mathrm{j}\boldsymbol{k}(\beta,\alpha)\cdot\boldsymbol{r}_0}\sin\beta\,\mathrm{d}\beta\mathrm{d}\alpha,$$

$$B^1_{mn,m'n'}(k\boldsymbol{r}_0) = \frac{\mathrm{j}^{n'-n}}{2\pi\sqrt{nn'(n+1)\,(n'+1)}}\int_0^{2\pi}\int_0^{\pi}\left[m\pi_n^{|m|}(\beta)\tau_{n'}^{|m'|}(\beta) + m'\tau_n^{|m|}(\beta)\pi_{n'}^{|m'|}(\beta)\right]\mathrm{e}^{\mathrm{j}(m-m')\alpha}\mathrm{e}^{\mathrm{j}\boldsymbol{k}(\beta,\alpha)\cdot\boldsymbol{r}_0}\sin\beta\mathrm{d}\beta\,\mathrm{d}\alpha.$$

Inserting the spherical wave expansion of the plane wave $\exp(\mathrm{j}\boldsymbol{k}\cdot\boldsymbol{r}_0)$ and integrating over α, we derive the following series representation for the translation coefficients:

$$A^1_{mn,m'n'}(k\boldsymbol{r}_0) = \frac{2\mathrm{j}^{n'-n}}{\sqrt{nn'(n+1)\,(n'+1)}} \sum_{n''} \mathrm{j}^{n''} \times a_1\left(m,m' \mid n'',n,n'\right) u^1_{m-m'n''}\left(k\boldsymbol{r}_0\right),$$

$$B^1_{mn,m'n'}(k\boldsymbol{r}_0) = \frac{2\mathrm{j}^{n'-n}}{\sqrt{nn'(n+1)\,(n'+1)}} \sum_{n''} \mathrm{j}^{n''} \times b_1\left(m,m' \mid n'',n,n'\right) u^1_{m-m'n''}\left(k\boldsymbol{r}_0\right),$$

where

$$a_1\left(m,m' \mid n'',n,n'\right) = \int_0^\pi \left[mm'\pi_n^{|m|}(\beta)\pi_{n'}^{|m'|}(\beta) + \tau_n^{|m|}(\beta)\tau_{n'}^{|m'|}(\beta)\right] \times P_{n''}^{|m-m'|}(\cos\beta)\sin\beta\,\mathrm{d}\beta, \tag{B.68}$$

$$b_1\left(m,m' \mid n'',n,n'\right) = \int_0^\pi \left[m\pi_n^{|m|}(\beta)\,\tau_{n'}^{|m'|}(\beta) + m'\tau_n^{|m|}(\beta)\pi_{n'}^{|m'|}(\beta)\right] \times P_{n''}^{|m-m'|}(\cos\beta)\sin\beta\,\mathrm{d}\beta. \tag{B.69}$$

We note that the coefficients $a_1(\cdot)$ and $b_1(\cdot)$ can be expressed in terms of the coefficients $a(\cdot)$ by making use of the recurrence relations for the associated Legendre functions. As in the scalar case, the integration with respect to the azimuthal angle α gives

$$A^1_{mn,m'n'}(k\boldsymbol{r}_0) = \frac{\mathrm{j}^{n'+m'-n-m}}{\sqrt{nn'(n+1)\,(n'+1)}}\mathrm{e}^{-j(m'-m)\varphi_0} \times \int_0^\pi J_{m'-m}(k\rho_0\sin\beta)\left[mm'\pi_n^{|m|}(\beta)\pi_{n'}^{|m'|}(\beta) + \tau_n^{|m|}(\beta)\tau_{n'}^{|m'|}(\beta)\right]\mathrm{e}^{\mathrm{j}kz_0\cos\beta}\sin\beta\,\mathrm{d}\beta$$

and

$$B^1_{mn,m'n'}(k\boldsymbol{r}_0) = \frac{\mathrm{j}^{n'+m'-n-m}}{\sqrt{nn'(n+1)\,(n'+1)}}\mathrm{e}^{-j(m'-m)\varphi_0} \times \int_0^\pi J_{m'-m}(k\rho_0 \sin\beta)\left[m\pi_n^{|m|}(\beta)\tau_{n'}^{|m'|}(\beta) + m'\tau_n^{|m|}(\beta)\pi_{n'}^{|m'|}(\beta)\right]\mathrm{e}^{\mathrm{j}kz_0\cos\beta}\sin\beta\mathrm{d}\beta.$$

If the translation is along the z-axis the double summation in (B.66) and (B.67) reduces to a single summation over the index n', and we have

$$A^1_{mn,mn'}(kz_0) = \frac{\mathrm{j}^{n'-n}}{\sqrt{nn'(n+1)\,(n'+1)}}\int_0^\pi \left[m^2\pi_n^{|m|}(\beta)\pi_{n'}^{|m|}(\beta) + \tau_n^{|m|}(\beta)\tau_{n'}^{|m|}(\beta)\right]\mathrm{e}^{\mathrm{j}kz_0\cos\beta}\sin\beta\,\mathrm{d}\beta$$

and

$$B^1_{mn,mn'}(kz_0) = \frac{m\mathrm{j}^{n'-n}}{\sqrt{nn'(n+1)\,(n'+1)}}\int_0^\pi \left[\pi_n^{|m|}(\beta)\tau_{n'}^{|m|}(\beta) + \tau_n^{|m|}(\beta)\pi_{n'}^{|m|}(\beta)\right]\mathrm{e}^{\mathrm{j}kz_0\cos\beta}\sin\beta\,\mathrm{d}\beta.$$

Passing to the radiating vector spherical wave functions we consider the integral representation (B.28) and the relation $\boldsymbol{r} = \boldsymbol{r}_0 + \boldsymbol{r}_1$. For $r_1 > r_0$, this representation can written as

$$\boldsymbol{M}^3_{mn}(k\boldsymbol{r}) = -\frac{1}{2\pi\mathrm{j}^{n+1}}\int_0^{2\pi}\int_0^\pi (-\mathrm{j})\,\boldsymbol{m}_{mn}(\beta,\alpha)\,Q(k,\beta,\alpha,\boldsymbol{r}_1)\mathrm{e}^{\mathrm{j}\boldsymbol{k}(\beta,\alpha)\cdot\boldsymbol{r}_0} \times \sin\beta\,\mathrm{d}\beta\,\mathrm{d}\alpha,$$

whence, using the vector spherical wave expansion

$$(-\mathrm{j})\,\boldsymbol{m}_{mn}(\beta,\alpha)\,Q(k,\beta,\alpha,\boldsymbol{r}_1) = \sum_{n'=1}^{\infty}\sum_{m'=-n'}^{n'} a^3_{mn,m'n'}\boldsymbol{M}^3_{m'n'}(k\boldsymbol{r}_1) + b^3_{mn,m'n'}\boldsymbol{N}^1_{m'n'}(k\boldsymbol{r}_1),$$

with

$$a^3_{mn,m'n'} = \frac{1}{2}a^1_{mn,m'n'}, \quad b^3_{mn,m'n'} = \frac{1}{2}b^1_{mn,m'n'},$$

yields

$$\begin{aligned}\boldsymbol{M}^3_{mn}(k\boldsymbol{r}) &= \sum_{n'=1}^{\infty}\sum_{m'=-n'}^{n'} A^1_{mn,m'n'}(k\boldsymbol{r}_0)\boldsymbol{M}^3_{m'n'}(k\boldsymbol{r}_1)\\ &\quad + B^1_{mn,m'n'}(k\boldsymbol{r}_0)\boldsymbol{N}^3_{m'n'}(k\boldsymbol{r}_1),\\ \boldsymbol{N}^3_{mn}(k\boldsymbol{r}) &= \sum_{n'=1}^{\infty}\sum_{m'=-n'}^{n'} B^1_{mn,m'n'}(k\boldsymbol{r}_0)\boldsymbol{M}^3_{m'n'}(k\boldsymbol{r}_1)\\ &\quad + A^1_{mn,m'n'}(k\boldsymbol{r}_0)\boldsymbol{N}^3_{m'n'}(k\boldsymbol{r}_1).\end{aligned}$$

For $r_1 < r_0$, we represent the radiating vector spherical wave functions as

$$\begin{aligned}\boldsymbol{M}^3_{mn}(k\boldsymbol{r}) = -\frac{1}{2\pi \mathrm{j}^{n+1}}\int_0^{2\pi}\int_0^{\pi}(-\mathrm{j})\,\boldsymbol{m}_{mn}(\beta,\alpha)\,Q(k,\beta,\alpha,\boldsymbol{r}_0)\mathrm{e}^{\mathrm{j}\boldsymbol{k}(\beta,\alpha)\cdot\boldsymbol{r}_1}\\ \times \sin\beta\,\mathrm{d}\beta\,\mathrm{d}\alpha,\end{aligned}$$

proceed as in the case of regular vector spherical wave functions, and obtain

$$\begin{aligned}\boldsymbol{M}^3_{mn}(k\boldsymbol{r}) &= \sum_{n'=1}^{\infty}\sum_{m'=-n'}^{n'} A^3_{mn,m'n'}(k\boldsymbol{r}_0)\boldsymbol{M}^3_{m'n'}(k\boldsymbol{r}_1)\\ &\quad + B^3_{mn,m'n'}(k\boldsymbol{r}_0)\boldsymbol{N}^3_{m'n'}(k\boldsymbol{r}_1),\end{aligned}$$

$$\begin{aligned}\boldsymbol{N}^3_{mn}(k\boldsymbol{r}) &= \sum_{n'=1}^{\infty}\sum_{m'=-n'}^{n'} B^3_{mn,m'n'}(k\boldsymbol{r}_0)\boldsymbol{M}^3_{m'n'}(k\boldsymbol{r}_1)\\ &\quad + A^3_{mn,m'n'}(k\boldsymbol{r}_0)\boldsymbol{N}^3_{m'n'}(k\boldsymbol{r}_1),\end{aligned}$$

where

$$\begin{aligned}A^3_{mn,m'n'}(k\boldsymbol{r}_0) &= \frac{\mathrm{j}^{n'-n}}{\pi\sqrt{nn'(n+1)\,(n'+1)}}\int_0^{2\pi}\int_0^{\pi}\Big[mm'\pi_n^{|m|}(\beta)\pi_{n'}^{|m'|}(\beta)\\ &\quad + \tau_n^{|m|}(\beta)\tau_{n'}^{|m'|}(\beta)\Big]\mathrm{e}^{\mathrm{j}(m-m')\alpha}Q(k,\beta,\alpha,\boldsymbol{r}_0)\sin\beta\mathrm{d}\beta\mathrm{d}\alpha,\end{aligned} \tag{B.70}$$

$$\begin{aligned}B^3_{mn,m'n'}(k\boldsymbol{r}_0) &= \frac{\mathrm{j}^{n'-n}}{\pi\sqrt{nn'(n+1)\,(n'+1)}}\int_0^{2\pi}\int_0^{\pi}\Big[m\pi_n^{|m|}(\beta)\tau_{n'}^{|m'|}(\beta)\\ &\quad + m'\tau_n^{|m|}(\beta)\pi_{n'}^{|m'|}(\beta)\Big]\mathrm{e}^{\mathrm{j}(m-m')\alpha}Q(k,\beta,\alpha,\boldsymbol{r}_0)\sin\beta\,\mathrm{d}\beta\,\mathrm{d}\alpha\,.\end{aligned} \tag{B.71}$$

Making use of the spherical wave expansion of the quasi-plane wave $Q(k,\beta,\alpha,\boldsymbol{r}_0)$, we derive the series representations

$$A^3_{mn,m'n'}(k\boldsymbol{r}_0) = \frac{2\mathrm{j}^{n'-n}}{\sqrt{nn'(n+1)\,(n'+1)}} \sum_{n''} \mathrm{j}^{n''} \times a_1\,(m,m' \mid n'',n,n')\,u^3_{m-m'n''}\,(k\boldsymbol{r}_0)\,, \tag{B.72}$$

$$B^3_{mn,m'n'}(k\boldsymbol{r}_0) = \frac{2\mathrm{j}^{n'-n}}{\sqrt{nn'(n+1)\,(n'+1)}} \sum_{n''} \mathrm{j}^{n''} \times b_1\,(m,m' \mid n'',n,n')\,u^3_{m-m'n''}\,(k\boldsymbol{r}_0)\,. \tag{B.73}$$

In (B.70) and (B.71) the integration with respect to the azimuthal angle α can be analytically performed and in the case of axial translation, the integral representations for the translation coefficients $A^3_{mn,m'n'}$ and $B^3_{mn,m'n'}$ read as

$$A^3_{mn,mn'}(kz_0) = \frac{2\mathrm{j}^{n'-n}}{\sqrt{nn'(n+1)\,(n'+1)}} \int_0^{\frac{\pi}{2}-\mathrm{j}\infty} \Big[m^2\pi_n^{|m|}(\beta)\pi_{n'}^{|m|}(\beta) + \tau_n^{|m|}(\beta)\tau_{n'}^{|m|}(\beta)\Big]\,\mathrm{e}^{\mathrm{j}kz_0\cos\beta}\sin\beta\,\mathrm{d}\beta,$$

and

$$B^3_{mn,mn'}(kz_0) = \frac{2m\mathrm{j}^{n'-n}}{\sqrt{nn'(n+1)\,(n'+1)}} \int_0^{\frac{\pi}{2}-\mathrm{j}\infty} \Big[\pi_n^{|m|}(\beta)\tau_{n'}^{|m|}(\beta) + \tau_n^{|m|}(\beta)\pi_{n'}^{|m|}(\beta)\Big]\,\mathrm{e}^{\mathrm{j}kz_0\cos\beta}\sin\beta\,\mathrm{d}\beta.$$

The vector addition coefficients $A_{mn,m'n'}$ and $B_{mn,m'n'}$ can be related to the scalar addition coefficients $C_{mn,m'n'}$. For axial translations and positive values of m, these relations can be obtained by partial integration and by using the integral representations for the addition coefficients, the associated Legendre equation (A.13) and the recurrence relation (A.17). We obtain [150]

$$A_{mn,mn'}(kz_0) = \sqrt{\frac{n'(n'+1)}{n(n+1)}}\,[C_{mn,mn'}\,(kz_0) + \frac{kz_0}{n'+1}\sqrt{\frac{(n'-m+1)(n'+m+1)}{(2n'+1)(2n'+3)}}C_{mn,mn'+1}\,(kz_0) + \frac{kz_0}{n'}\sqrt{\frac{(n'-m)(n'+m)}{(2n'+1)(2n'-1)}}C_{mn,mn'-1}\,(kz_0)\Big]$$

and

$$B_{mn,mn'}(kz_0) = \mathrm{j}kz_0\frac{m}{\sqrt{nn'(n+1)\,(n'+1)}}C_{mn,mn'}\,(kz_0)\,.$$

For negative values of the index m, the following symmetry relations can be used for practical calculations

$$A_{-mn,-mn'}(kz_0) = A_{mn,mn'}(kz_0),$$
$$B_{-mn,-mn'}(kz_0) = -B_{mn,mn'}(kz_0).$$

The translation coefficients for axial translation can be obtained from the above recurrence relations. In general, through rotation of coordinates, the numerical advantages to a common axis can be exploited and a transformation from $Oxyz$ to $Ox_1y_1z_1$ can be accomplished through three steps [150]:

1. The coordinate system $Oxyz$ is rotated with the Euler angles $\alpha = \varphi_0$, $\beta = \theta_0$ and $\gamma = 0$, where $(r_0, \theta_0, \varphi_0)$ are the spherical coordinates of the position vector $\boldsymbol{r}_0$.
2. The rotated coordinate system is axially translated with r_0.
3. The translated coordinate system is rotated back to the original orientation with the Euler angles $\alpha = 0$, $\beta = -\theta_0$ and $\gamma = -\varphi_0$.

The rotation-axial translation-rotation scheme gives

$$X_{mn,m'n'}(k\boldsymbol{r}_0) = \sum_{m''=-n}^{n} D^n_{mm''}(\varphi_0, \theta_0, 0) X_{m''n,m''n'}(kr_0) \times D^{n'}_{m''m'}(0, -\theta_0, -\varphi_0),$$

where X stands for A or B. The translation addition theorem can be written in matrix form as

$$\begin{bmatrix} \boldsymbol{M}^p_{mn}(k\boldsymbol{r}) \\ \boldsymbol{N}^p_{mn}(k\boldsymbol{r}) \end{bmatrix} = \mathcal{T}^{pq}(k\boldsymbol{r}_0) \begin{bmatrix} \boldsymbol{M}^q_{m'n'}(k\boldsymbol{r}_1) \\ \boldsymbol{N}^q_{m'n'}(k\boldsymbol{r}_1) \end{bmatrix},$$

where the pair (p, q) takes the values $(1,1)$, $(3,3)$, and $(3,1)$, and

$$\mathcal{T}^{11}(k\boldsymbol{r}_0) = \mathcal{T}^{33}(k\boldsymbol{r}_0) = \begin{bmatrix} A^1_{mn,m'n'}(k\boldsymbol{r}_0) & B^1_{mn,m'n'}(k\boldsymbol{r}_0) \\ B^1_{mn,m'n'}(k\boldsymbol{r}_0) & A^1_{mn,m'n'}(k\boldsymbol{r}_0) \end{bmatrix}$$

and

$$\mathcal{T}^{31}(k\boldsymbol{r}_0) = \begin{bmatrix} A^3_{mn,m'n'}(k\boldsymbol{r}_0) & B^3_{mn,m'n'}(k\boldsymbol{r}_0) \\ B^3_{mn,m'n'}(k\boldsymbol{r}_0) & A^3_{mn,m'n'}(k\boldsymbol{r}_0) \end{bmatrix}.$$

We conclude this section by noticing some symmetry properties of the translation coefficients for the inverse transformation:

$$\begin{bmatrix} \boldsymbol{M}^p_{mn}(k\boldsymbol{r}_1) \\ \boldsymbol{N}^p_{mn}(k\boldsymbol{r}_1) \end{bmatrix} = \mathcal{T}^{pq}(-k\boldsymbol{r}_0) \begin{bmatrix} \boldsymbol{M}^q_{m'n'}(k\boldsymbol{r}) \\ \boldsymbol{N}^q_{m'n'}(k\boldsymbol{r}) \end{bmatrix}.$$

Using the integral representation for the translation coefficients, making the transformation $\varphi_0 \to \varphi_0 + \pi$, changing the variable of integration from β to $\pi - \beta$ and using the identities (A.24) and (A.25), yields

$$A_{mn,m'n'}(-k\boldsymbol{r}_0) = (-1)^{n+n'} A_{mn,m'n'}(k\boldsymbol{r}_0),$$
$$B_{mn,m'n'}(-k\boldsymbol{r}_0) = (-1)^{n+n'+1} B_{mn,m'n'}(k\boldsymbol{r}_0).$$

Further, since

$$A_{mn,m'n'}(k\boldsymbol{r}_0) = (-1)^{n+n'} A_{-m'n',-mn}(k\boldsymbol{r}_0),$$
$$B_{mn,m'n'}(k\boldsymbol{r}_0) = (-1)^{n+n'+1} B_{-m'n',-mn}(k\boldsymbol{r}_0),$$

we obtain

$$A_{mn,m'n'}(-k\boldsymbol{r}_0) = A_{-m'n',-mn}(k\boldsymbol{r}_0), \tag{B.74}$$
$$B_{mn,m'n'}(-k\boldsymbol{r}_0) = B_{-m'n',-mn}(k\boldsymbol{r}_0). \tag{B.75}$$

Recurrence relations for the scalar and vector addition theorem has also been given by Chew [32,33], Chew and Wang [35] and Kim [117]. The relationship between the coefficients of the vector addition theorem and those of the scalar addition theorem has been discussed by Bruning and Lo [29], and Chew [32].

C

Computational Aspects in Effective Medium Theory

In this appendix we compute the basic integrals appearing in the analysis of electromagnetic scattering from a half-space of randomly distributed particles. Our derivation follows the procedures described by Varadan et al. [236], Tsang and Kong [223, 226], and Tsang et al. [228].

C.1 Computation of the Integral $\boldsymbol{I^1_{mm'n''}}$

The integral $\mathcal{I}^1_{mm'n''}$ is

$$\mathcal{I}^1_{mm'n''} = \int_{D_p} \mathrm{e}^{\mathrm{j}\boldsymbol{K}_\mathrm{e}\cdot\boldsymbol{r}_{0p}} u^3_{m'-mn''}\left(k_\mathrm{s}\boldsymbol{r}_{lp}\right)\,\mathrm{d}V\left(\boldsymbol{r}_{0p}\right),$$

where $\boldsymbol{K}_\mathrm{e} = K_\mathrm{s}\boldsymbol{e}_z$, and the integration domain D_p is the half-space $z_{0p} \geq 0$, excluding a spherical volume of radius $2R$ centered at $\boldsymbol{r}_{0l}$. The volume integral can be transformed into a surface integral by making use of the following result. Let u and v be two scalar fields satisfying the Helmholtz equation in the bounded domain D, with the wave numbers K_s and k_s, i.e.,

$$\begin{aligned}\Delta u + K_\mathrm{s}^2 u = 0,\\ \Delta v + k_\mathrm{s}^2 v = 0.\end{aligned}$$

Then, from Green's theorem we have

$$\begin{aligned}\int_D uv\mathrm{d}V &= \frac{1}{k_\mathrm{s}^2 - K_\mathrm{s}^2}\int_D \left(v\Delta u - u\Delta v\right)\mathrm{d}V\\ &= \frac{1}{k_\mathrm{s}^2 - K_\mathrm{s}^2}\int_S \left(v\frac{\partial u}{\partial \boldsymbol{n}} - u\frac{\partial v}{\partial \boldsymbol{n}}\right)\mathrm{d}S,\end{aligned}$$

where S is the boundary surface of the domain D, and $\boldsymbol{n}$ is the outward unit normal vector to S. Using this result we transform the integral $\mathcal{I}^1_{mm'n''}$ as follows:

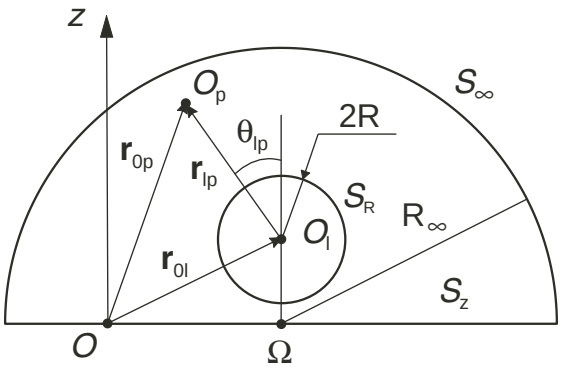

Fig. C.1. Integration surfaces S_R, S_∞ and S_z

$$\mathcal{I}^1_{mm'n''} = \frac{1}{k_\mathrm{s}^2 - K_\mathrm{s}^2} \int_{S_R \cup S_\infty \cup S_z} \left[u^3_{m'-mn''}\left(k_\mathrm{s}\boldsymbol{r}_{lp}\right) \frac{\partial}{\partial \boldsymbol{n}} \left(\mathrm{e}^{\mathrm{j}\boldsymbol{K}_\mathrm{e}\cdot\boldsymbol{r}_{0p}}\right) \right.$$
$$\left. - \mathrm{e}^{\mathrm{j}\boldsymbol{K}_\mathrm{e}\cdot\boldsymbol{r}_{0p}} \frac{\partial u^3_{m'-mn''}}{\partial \boldsymbol{n}} \left(k_\mathrm{s}\boldsymbol{r}_{lp}\right) \right] \mathrm{d}S\left(\boldsymbol{r}_{0p}\right).$$

The integral can be decomposed into three integrals

$$\mathcal{I}^1_{mm'n''} = \mathcal{I}^{1,R}_{mm'n''} + \mathcal{I}^{1,\infty}_{mm'n''} + \mathcal{I}^{1,z}_{mm'n''},$$

where $\mathcal{I}^{1,R}_{mm'n''}$ is the integral over the spherical surface S_R of radius $2R$ centered at $\boldsymbol{r}_{0l}$, $\mathcal{I}^{1,\infty}_{mm'n''}$ is the integral over the surface of a half-sphere S_∞ with radius R_∞ in the limit $R_\infty \to \infty$, and $\mathcal{I}^{1,z}_{mm'n''}$ is the integral over the xy-plane S_z (the plane $z = 0$). The choice of the integration surfaces is shown in Fig. C.1.

Using the identity $\boldsymbol{r}_{0p} = \boldsymbol{r}_{0l} + \boldsymbol{r}_{lp}$ and replacing, for convenience, the variables r_{lp}, θ_{lp} and φ_{lp} by r, θ and φ, respectively, we obtain

$$\mathcal{I}^{1,R}_{mm'n''} = -\frac{1}{k_\mathrm{s}^2 - K_\mathrm{s}^2} \mathrm{e}^{\mathrm{j}K_\mathrm{s} z_{0l}}$$
$$\times \int_{S_R} \left\{ h^{(1)}_{n''}\left(k_\mathrm{s} r\right) P^{|m'-m|}_{n''}\left(\cos\theta\right) \mathrm{e}^{\mathrm{j}\left(m'-m\right)\varphi} \frac{\partial}{\partial r} \left(\mathrm{e}^{\mathrm{j}\boldsymbol{K}_\mathrm{e}\cdot\boldsymbol{r}}\right) \right.$$
$$\left. - \mathrm{e}^{\mathrm{j}\boldsymbol{K}_\mathrm{e}\cdot\boldsymbol{r}} \frac{\partial}{\partial r} \left[h^{(1)}_{n''}\left(k_\mathrm{s} r\right) P^{|m'-m|}_{n''}\left(\cos\theta\right) \mathrm{e}^{\mathrm{j}\left(m'-m\right)\varphi} \right] \right\} \mathrm{d}S(\boldsymbol{r}),$$

whence, taking into account the series representation

$$\mathrm{e}^{\mathrm{j}\boldsymbol{K}_\mathrm{e}\cdot\boldsymbol{r}} = \sum_{n'=0}^{\infty} 2\mathrm{j}^{n'} \sqrt{\frac{2n'+1}{2}} j_{n'}\left(K_\mathrm{s} r\right) P_{n'}\left(\cos\theta\right) \qquad \text{(C.1)}$$

for $\boldsymbol{K}_\mathrm{e} \cdot \boldsymbol{r} = K_\mathrm{s} r \cos\theta$, the orthogonality of the associated Legendre functions and the relation $\boldsymbol{K}_\mathrm{e} \cdot \boldsymbol{r}_{0l} = K_\mathrm{s} z_{0l}$, we end up with

$$\mathcal{I}^{1,R}_{mm'n''} = \frac{16\pi R^3}{(k_\mathrm{s}R)^2 - (K_\mathrm{s}R)^2} \mathrm{j}^{n''} \sqrt{\frac{2n''+1}{2}} \mathrm{e}^{\mathrm{j}K_\mathrm{s} z_{0l}} \delta_{mm'} F_{n''}\left(K_\mathrm{s}, k_\mathrm{s}, R\right),$$

where

$$F_{n''}\left(K_\mathrm{s}, k_\mathrm{s}, R\right) = (k_\mathrm{s}R)\left(h^{(1)}_{n''}\left(2k_\mathrm{s}R\right)\right)' j_{n''}\left(2K_\mathrm{s}R\right) - (K_\mathrm{s}R)\, h^{(1)}_{n''}\left(2k_\mathrm{s}R\right)\left(j_{n''}\left(2K_\mathrm{s}R\right)\right)'.$$

To compute $\mathcal{I}^{1,\infty}_{mm'n''}$ we use the stationary point method. Using the inequality $\mathrm{Im}\{K_\mathrm{s}\} > 0$ and the asymptotic expressions of the spherical Hankel functions of the first kind

$$h^{(1)}_{n''}\left(k_\mathrm{s}r\right) = \frac{(-\mathrm{j})^{n''+1}\mathrm{e}^{\mathrm{j}k_\mathrm{s}r}}{k_\mathrm{s}r},$$

and

$$\frac{\mathrm{d}}{\mathrm{d}r}\left[h^{(1)}_{n''}\left(k_\mathrm{s}r\right)\right] = \frac{\mathrm{j}(-\mathrm{j})^{n''+1}\mathrm{e}^{\mathrm{j}k_\mathrm{s}r}}{r},$$

we see that $\mathcal{I}^{1,\infty}_{mm'n''}$ vanishes as $R_\infty \to \infty$.

To evaluate $\mathcal{I}^{1,z}_{mm'n''}$ we pass to cylindrical coordinates, integrate over φ, and obtain

$$\mathcal{I}^{1,z}_{mm'n''} = -\frac{2\pi}{k_\mathrm{s}^2 - K_\mathrm{s}^2}\delta_{mm'} \int_0^\infty \Big\{ \mathrm{j}K_\mathrm{s} h^{(1)}_{n''}\left(k_\mathrm{s}r\right) P_{n''}\left(\cos\theta\right) - \frac{\partial}{\partial z}\left[h^{(1)}_{n''}\left(k_\mathrm{s}r\right) P_{n''}\left(\cos\theta\right)\right] \Big\}_{z=-z_{0l}} \rho\,\mathrm{d}\rho.$$

Further, using Kasterin's representation [228, 258]

$$h^{(1)}_{n''}\left(k_\mathrm{s}r\right) P_{n''}\left(\cos\theta\right) = (-\mathrm{j})^{n''} P_{n''}\left(\frac{1}{\mathrm{j}k_\mathrm{s}}\frac{\partial}{\partial z}\right) h^{(1)}_0\left(k_\mathrm{s}r\right)$$

with

$$h^{(1)}_0\left(k_\mathrm{s}r\right) = \frac{\mathrm{e}^{\mathrm{j}k_\mathrm{s}r}}{\mathrm{j}k_\mathrm{s}r},$$

we find that

$$\mathcal{I}^{1,z}_{mm'n''} = -\frac{2\pi}{k_\mathrm{s}^2 - K_\mathrm{s}^2}(-\mathrm{j})^{n''}\delta_{mm'} \times \int_0^\infty \left[\left(\mathrm{j}K_\mathrm{s} - \frac{\partial}{\partial z}\right) P_{n''}\left(\frac{1}{\mathrm{j}k_\mathrm{s}}\frac{\partial}{\partial z}\right) \frac{\mathrm{e}^{\mathrm{j}k_\mathrm{s}\sqrt{\rho^2+z^2}}}{\mathrm{j}k_\mathrm{s}\sqrt{\rho^2+z^2}}\right]_{z=-z_{0l}} \rho\,\mathrm{d}\rho.$$

Performing the integration and using the relation

$$P_{n''}\left(\frac{1}{\mathrm{j}k_\mathrm{s}}\frac{\partial}{\partial z}\right)\left(\frac{\mathrm{e}^{-\mathrm{j}k_\mathrm{s}z}}{k_\mathrm{s}^2}\right)=(-1)^{n''}\frac{1}{k_\mathrm{s}^2}\sqrt{\frac{2n''+1}{2}}\mathrm{e}^{-\mathrm{j}k_\mathrm{s}z},$$

we obtain

$$\mathcal{I}^{1,z}_{mm'n''}=\frac{2\pi}{k_\mathrm{s}^2\left(K_\mathrm{s}-k_\mathrm{s}\right)}\mathrm{j}^{n''+1}\sqrt{\frac{2n''+1}{2}}\mathrm{e}^{\mathrm{j}k_\mathrm{s}z_{0l}}\delta_{mm'}.$$

The final result is

$$\begin{aligned}\mathcal{I}^{1}_{mm'n''}&=\mathcal{I}^{1,R}_{mm'n''}+\mathcal{I}^{1,z}_{mm'n''}\\&=\frac{16\pi R^3}{\left(k_\mathrm{s}R\right)^2-\left(K_\mathrm{s}R\right)^2}\mathrm{j}^{n''}\sqrt{\frac{2n''+1}{2}}\mathrm{e}^{\mathrm{j}K_\mathrm{s}z_{0l}}\delta_{mm'}F_{n''}\left(K_\mathrm{s},k_\mathrm{s},R\right)\\&\quad+\frac{2\pi}{k_\mathrm{s}^2\left(K_\mathrm{s}-k_\mathrm{s}\right)}\mathrm{j}^{n''+1}\sqrt{\frac{2n''+1}{2}}\mathrm{e}^{\mathrm{j}k_\mathrm{s}z_{0l}}\delta_{mm'}\,.\end{aligned}\tag{C.2}$$

C.2 Computation of the Integral $I^2_{mm'n''}$

The integral $\mathcal{I}^2_{mm'n''}$ is

$$\mathcal{I}^2_{mm'n''}=\int_{D_p}\left[g\left(\boldsymbol{r}_{lp}\right)-1\right]\mathrm{e}^{\mathrm{j}\boldsymbol{K}_\mathrm{e}\cdot\boldsymbol{r}_{0p}}u^3_{m'-mn''}\left(k_\mathrm{s}\boldsymbol{r}_{lp}\right)\mathrm{d}V\left(\boldsymbol{r}_{0p}\right),$$

where $\boldsymbol{K}_\mathrm{e}=K_\mathrm{s}\boldsymbol{e}_z$, and the domain of integration contains the half-space $z_{0p}\geq 0$ less a sphere of radius $2R$ centered at $\boldsymbol{r}_{0l}$. For a spherical symmetric pair distribution function, $g(\boldsymbol{r}_{lp})=g(r_{lp})$, the function $g(r_{lp})-1$ tends to zero for a few $2R$-values. Therefore, if the point $\boldsymbol{r}_{0l}$ is at least several diameters deep in the scattering medium, the volume of integration can be extended to infinity (Fig. C.2). Taking into account that $\boldsymbol{r}_{0p}=\boldsymbol{r}_{0l}+\boldsymbol{r}_{lp}$, and replacing the variables r_{lp}, θ_{lp} and φ_{lp} by r, θ and φ, respectively, we obtain

$$\begin{aligned}\mathcal{I}^2_{mm'n''}=\mathrm{e}^{\mathrm{j}\boldsymbol{K}_\mathrm{e}\cdot\boldsymbol{r}_{0l}}&\int_0^{2\pi}\int_0^{\pi}\int_{2R}^{\infty}\left[g(r)-1\right]\mathrm{e}^{\mathrm{j}\boldsymbol{K}_\mathrm{e}\cdot\boldsymbol{r}}h^{(1)}_{n''}\left(k_\mathrm{s}r\right)P^{|m'-m|}_{n''}\left(\cos\theta\right)\\&\times\mathrm{e}^{\mathrm{j}\left(m'-m\right)\varphi}r^2\sin\theta\,\mathrm{d}r\,\mathrm{d}\theta\,\mathrm{d}\varphi\,.\end{aligned}$$

Using the plane wave expansion (C.1), the orthogonality relations of the associated Legendre functions and the equation $\boldsymbol{K}_\mathrm{e}\cdot\boldsymbol{r}_{0l}=K_\mathrm{s}z_{0l}$, we derive

$$\mathcal{I}^2_{mm'n''}=4\pi\mathrm{j}^{n''}\sqrt{\frac{2n''+1}{2}}\mathrm{e}^{\mathrm{j}K_\mathrm{s}z_{0l}}\delta_{mm'}\int_{2R}^{\infty}\left[g(r)-1\right]j_{n''}\left(K_\mathrm{s}r\right)h^{(1)}_{n''}\left(k_\mathrm{s}r\right)r^2\mathrm{d}r.$$

Changing the variables from r to $x=r/(2R)$, we find that

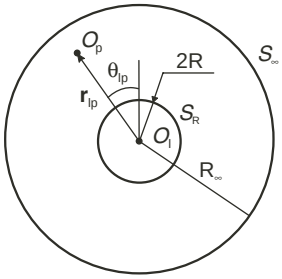

Fig. C.2. Illustration of the domain of integration bounded by the spherical surface S_R and a sphere situated in the far-field region

$$\mathcal{I}^2_{mm'n''} = 32\pi R^3 \mathrm{j}^{n''} \sqrt{\frac{2n''+1}{2}} \mathrm{e}^{\mathrm{j}K_\mathrm{s} z_{0l}} \delta_{mm'} G_{n''}\left(K_\mathrm{s}, k_\mathrm{s}, R\right), \tag{C.3}$$

where

$$G_{n''}\left(K_\mathrm{s}, k_\mathrm{s}, R\right) = \int_1^\infty \left[g\left(2Rx\right) - 1\right] h^{(1)}_{n''}\left(2k_\mathrm{s}Rx\right) j_{n''}\left(2K_\mathrm{s}Rx\right) x^2 \mathrm{d}x.$$

C.3 Computation of the Terms $S^1_{1nn'}$ and $S^2_{1nn'}$

The terms $\mathcal{S}^1_{1nn'}$ and $\mathcal{S}^2_{1nn'}$ are given by

$$\mathcal{S}^1_{1nn'} = \sum_{n''=0}^{\infty} (-1)^{n''} \sqrt{\frac{2n''+1}{2}} I^1_{1nn'n''},$$
$$\mathcal{S}^2_{1nn'} = \sum_{n''=0}^{\infty} (-1)^{n''} \sqrt{\frac{2n''+1}{2}} I^2_{1nn'n''},$$

where

$$I^1_{1nn'n''} = \int_0^\pi \left[\pi^1_n(\beta)\pi^1_{n'}(\beta) + \tau^1_n(\beta)\tau^1_{n'}(\beta)\right] P_{n''}\left(\cos\beta\right) \sin\beta \,\mathrm{d}\beta,$$
$$I^2_{1nn'n''} = \int_0^\pi \left[\pi^1_n(\beta)\tau^1_{n'}(\beta) + \tau^1_n(\beta)\pi^1_{n'}(\beta)\right] P_{n''}\left(\cos\beta\right) \sin\beta \,\mathrm{d}\beta.$$

To compute $\mathcal{S}^1_{1nn'}$, we consider the function

$$f_{nn'}(\beta) = \pi^1_n(\beta)\pi^1_{n'}(\beta) + \tau^1_n(\beta)\tau^1_{n'}(\beta) \tag{C.4}$$

for fixed values of the indices n and n'. This function can be expanded in terms of Legendre polynomials

$$f_{nn'}(\beta) = \sum_{n''=0}^{\infty} a_{nn',n''} P_{n''}(\cos\beta), \tag{C.5}$$

where the expansion coefficients are given by

$$a_{nn',n''} = \int_0^{\pi} f_{nn'}(\beta) P_{n''}(\cos\beta) \sin\beta \, \mathrm{d}\beta = I^1_{1nn'n''}.$$

Using the special value of the Legendre polynomial at $\beta = \pi$,

$$P_{n''}(\cos\pi) = (-1)^{n''} \sqrt{\frac{2n''+1}{2}},$$

we see that (C.5) leads to

$$f_{nn'}(\pi) = \sum_{n''=0}^{\infty} (-1)^{n''} \sqrt{\frac{2n''+1}{2}} I^1_{1nn'n''} = \mathcal{S}^1_{1nn'}.$$

On the other hand, since

$$\pi^1_n(\pi) = \frac{(-1)^{n-1}}{2\sqrt{2}} \sqrt{n(n+1)(2n+1)},$$
$$\tau^1_n(\pi) = \frac{(-1)^{n}}{2\sqrt{2}} \sqrt{n(n+1)(2n+1)}.$$

(C.4) implies that

$$f_{nn'}(\pi) = s_{nn'} = \frac{(-1)^{n+n'}}{4} \sqrt{n(n+1)(2n+1)} \sqrt{n'(n'+1)(2n'+1)} \tag{C.6}$$

and therefore,

$$\mathcal{S}^1_{1nn'} = s_{nn'}.$$

Analogously, we find that

$$\mathcal{S}^2_{1nn'} = -s_{nn'}.$$

D

Completeness of Vector Spherical Wave Functions

The completeness and linear independence of the systems of radiating and regular vector spherical wave functions on closed surfaces have been established by Doicu et al. [49]. In this appendix we prove the completeness and linear independence of the regular and radiating vector spherical wave functions on two enclosing surfaces. A similar result has been given by Aydin and Hizal [5] for both the regular and radiating vector spherical wave functions with nonzero divergence, i.e., the solutions to the vector Helmholtz equation.

Before formulating the boundary-value problem for the Maxwell equations we introduce some normed spaces which are relevant in electromagnetic scattering theory. With S being the boundary of a domain $D_{\rm i}$ we denote by [39, 40]

$$\mathcal{C}_{\tan}(S) = \{\boldsymbol{a}/\boldsymbol{a} \in C(S), \boldsymbol{n}\cdot\boldsymbol{a} = 0\}$$

the space of all continuous tangential fields and by

$$\mathcal{C}^{0,\alpha}_{\tan}(S) = \left\{\boldsymbol{a}/\boldsymbol{a} \in C^{0,\alpha}(S), \boldsymbol{n}\cdot\boldsymbol{a} = 0\right\}, \quad 0 < \alpha \leq 1\,,$$

the space of all uniformly Hölder continuous tangential fields equipped with the supremum norm and the Hölder norm, respectively. The space of uniformly Hölder continuous tangential fields with uniformly Hölder continuous surface divergence ($\nabla_{\rm s}$) is defined as

$$\mathcal{C}^{0,\alpha}_{\tan,{\rm d}}(S) = \left\{\boldsymbol{a}/\boldsymbol{a} \in \mathcal{C}^{0,\alpha}_{\tan}(S), \nabla_{\rm s}\cdot\boldsymbol{a} \in C^{0,\alpha}(S)\right\}, \quad 0 < \alpha \leq 1\,,$$

while the space of square integrable tangential fields is introduced as

$$\mathcal{L}^2_{\tan}(S) = \left\{\boldsymbol{a}/\boldsymbol{a} \in L^2(S), \boldsymbol{n}\cdot\boldsymbol{a} = 0\right\}.$$

Now, let S_1 and S_2 be two closed surfaces of class C^2, with S_1 enclosing S_2 (Fig. D.1). Let the doubly connected domain between S_1 and S_2 be denoted by $D_{\rm i,1}$, the domain interior to S_2 by $D_{\rm i,2}$, the domain interior to S_1 by $D_{\rm i}$,

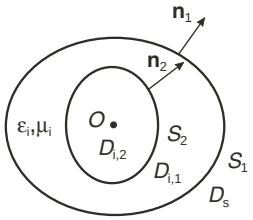

Fig. D.1. The closed surfaces S_1 and S_2

and the domain exterior to S_1 by D_s. We assume that the origin is in $D_{\mathrm{i},2}$, and denote by $\boldsymbol{n}_1$ and $\boldsymbol{n}_2$ the outward normal unit vectors to S_1 and S_2, respectively. The wave number in the domain $D_{\mathrm{i},1}$ is $k_\mathrm{i} = k_0\sqrt{\varepsilon_\mathrm{i}\mu_\mathrm{i}}$, where k_0 is the wave number in free space, and ε_i and μ_i are the relative permittivity and permeability of the domain $D_{\mathrm{i},1}$. We introduce the product spaces

$$\begin{aligned}
\mathfrak{C}_\mathrm{tan}(S_{1,2}) &= \mathcal{C}_\mathrm{tan}(S_1) \times \mathcal{C}_\mathrm{tan}(S_2),\\
\mathfrak{C}^{0,\alpha}_\mathrm{tan}(S_{1,2}) &= \mathcal{C}^{0,\alpha}_\mathrm{tan}(S_1) \times \mathcal{C}^{0,\alpha}_\mathrm{tan}(S_2)\,,\\
\mathfrak{C}^{0,\alpha}_{\mathrm{tan},d}(S_{1,2}) &= \mathcal{C}^{0,\alpha}_{\mathrm{tan},d}(S_1) \times \mathcal{C}^{0,\alpha}_{\mathrm{tan},d}(S_2)\,,\\
\mathfrak{L}^2_\mathrm{tan}(S_{1,2}) &= \mathcal{L}^2_\mathrm{tan}(S_1) \times \mathcal{L}^2_\mathrm{tan}(S_2),
\end{aligned}$$

and define the scalar product in $\mathfrak{L}^2_\mathrm{tan}(S_{1,2})$ by

$$\left\langle \begin{pmatrix} \boldsymbol{x}_1 \\ \boldsymbol{x}_2 \end{pmatrix}, \quad \begin{pmatrix} \boldsymbol{y}_1 \\ \boldsymbol{y}_2 \end{pmatrix} \right\rangle_{2,S_{1,2}} = \langle \boldsymbol{x}_1, \boldsymbol{y}_1 \rangle_{2,S_1} + \langle \boldsymbol{x}_2, \boldsymbol{y}_2 \rangle_{2,S_2}\,.$$

The Maxwell boundary-value problem for the doubly connected domain $D_{\mathrm{i},1}$ has the following formulation.

Find a solution $\boldsymbol{E}_\mathrm{i}, \boldsymbol{H}_\mathrm{i} \in C^1(D_{\mathrm{i},1}) \cap C(\overline{D}_{\mathrm{i},1})$ *to the Maxwell equations in* $D_{\mathrm{i},1}$

$$\nabla \times \boldsymbol{E}_\mathrm{i} = \mathrm{j}k_0\mu_\mathrm{i}\boldsymbol{H}_\mathrm{i}\,, \quad \nabla \times \boldsymbol{H}_\mathrm{i} = -\mathrm{j}k_0\varepsilon_\mathrm{i}\boldsymbol{E}_\mathrm{i},$$

satisfying the boundary conditions

$$\begin{aligned}
\boldsymbol{n}_1 \times \boldsymbol{E}_\mathrm{i} &= \boldsymbol{f}_1 \quad \textit{on} \quad S_1\,,\\
\boldsymbol{n}_2 \times \boldsymbol{E}_\mathrm{i} &= \boldsymbol{f}_2 \quad \textit{on} \quad S_2\,,
\end{aligned}$$

where $\boldsymbol{f}_1$ *and* $\boldsymbol{f}_2$ *are given tangential vector fields.*

Denoting by $\sigma(D_{\mathrm{i},1})$ the spectrum of eigenvalues of the Maxwell boundary-value problem, we assume that for $\boldsymbol{f}_1 \in \mathcal{C}^{0,\alpha}_{\mathrm{tan,d}}(S_1)$ and $\boldsymbol{f}_2 \in \mathcal{C}^{0,\alpha}_{\mathrm{tan,d}}(S_2)$, both

$\boldsymbol{E}_{\mathrm{i}}$ and $\boldsymbol{H}_{\mathrm{i}}$ belong to $C^{0,\alpha}(\overline{D}_{\mathrm{i},1})$, and for $k_{\mathrm{i}} \notin \sigma(D_{\mathrm{i},1})$, the Maxwell boundary-value problem possesses an unique solution.

Theorem 1. *Consider $D_{\mathrm{i},1}$ a bounded domain of class C^2 with boundaries S_1 and S_2. Define the vector potentials*

$$\boldsymbol{A}_1(\boldsymbol{r}) = \int_{S_1} \boldsymbol{a}_1(\boldsymbol{r}')g(k_{\mathrm{i}}, \boldsymbol{r}, \boldsymbol{r}')\mathrm{d}S(\boldsymbol{r}')\,,$$
$$\boldsymbol{A}_2(\boldsymbol{r}) = \int_{S_2} \boldsymbol{a}_2(\boldsymbol{r}')g(k_{\mathrm{i}}, \boldsymbol{r}, \boldsymbol{r}')\mathrm{d}S(\boldsymbol{r}')$$

for $\boldsymbol{a}_1 \in \mathcal{L}^2_{\tan}(S_1)$ and $\boldsymbol{a}_2 \in \mathcal{L}^2_{\tan}(S_2)$, assume $k_{\mathrm{i}} \notin \sigma(D_{\mathrm{i},1})$ and

$$\nabla \times \nabla \times \boldsymbol{A}_1 + \nabla \times \nabla \times \boldsymbol{A}_2 = 0$$

in D_{s} and $D_{\mathrm{i},2}$. Then $\boldsymbol{a}_1 \sim 0$ on S_1 ($\boldsymbol{a}_1$ vanishes almost everywhere on S_1), and $\boldsymbol{a}_2 \sim 0$ on S_2.

Proof. Defining the electromagnetic fields

$$\mathcal{E} = \frac{\mathrm{j}}{k_0\varepsilon_{\mathrm{i}}}\left(\nabla \times \nabla \times \boldsymbol{A}_1 + \nabla \times \nabla \times \boldsymbol{A}_2\right),$$
$$\mathcal{H} = -\frac{\mathrm{j}}{k_0\mu_{\mathrm{i}}}\nabla \times \mathcal{E} = \nabla \times \boldsymbol{A}_1 + \nabla \times \boldsymbol{A}_2,$$

passing to the boundary along a normal direction and using the jump relations for the *curl* of a vector potential with square integrable density [49], we find that

$$\begin{aligned} 0 = \lim_{h\to 0_+} \Big\| & \boldsymbol{n}_1 \times \mathcal{H}\left(\cdot + h\boldsymbol{n}_1\left(\cdot\right)\right) \\ & - \left\{\boldsymbol{n}_1 \times \left[\nabla \times \int_{S_1} \boldsymbol{a}_1(\boldsymbol{r}')g(k_{\mathrm{i}}, \cdot, \boldsymbol{r}')\mathrm{d}S(\boldsymbol{r}')\right] + \frac{1}{2}\boldsymbol{a}_1\right\} \\ & - \boldsymbol{n}_1 \times \left[\nabla \times \int_{S_2} \boldsymbol{a}_2(\boldsymbol{r}')g(k_{\mathrm{i}}, \cdot, \boldsymbol{r}')\mathrm{d}S(\boldsymbol{r}')\right]\Big\|_{2,S_1} \end{aligned}$$

and

$$\begin{aligned} 0 = \lim_{h\to 0_+} \Big\| & \boldsymbol{n}_2 \times \mathcal{H}\left(\cdot - h\boldsymbol{n}_2\left(\cdot\right)\right) \\ & - \left\{\boldsymbol{n}_2 \times \left[\nabla \times \int_{S_2} \boldsymbol{a}_2(\boldsymbol{r}')g(k_{\mathrm{i}}, \cdot, \boldsymbol{r}')\mathrm{d}S(\boldsymbol{r}')\right] - \frac{1}{2}\boldsymbol{a}_2\right\} \\ & - \boldsymbol{n}_2 \times \left[\nabla \times \int_{S_1} \boldsymbol{a}_1(\boldsymbol{r}')g(k_{\mathrm{i}}, \cdot, \boldsymbol{r}')\mathrm{d}S(\boldsymbol{r}')\right]\Big\|_{2,S_2}. \end{aligned}$$

Defining the operators

$$(\mathcal{M}_{11}\boldsymbol{a})(\boldsymbol{r}) = \boldsymbol{n}_1(\boldsymbol{r}) \times \left[\nabla \times \int_{S_1} \boldsymbol{a}(\boldsymbol{r}')g(k_i, \boldsymbol{r}, \boldsymbol{r}')\mathrm{d}S(\boldsymbol{r}')\right], \quad \boldsymbol{r} \in S_1,$$

$$(\mathcal{M}_{12}\boldsymbol{a})(\boldsymbol{r}) = \boldsymbol{n}_1(\boldsymbol{r}) \times \left[\nabla \times \int_{S_2} \boldsymbol{a}(\boldsymbol{r}')g(k_i, \boldsymbol{r}, \boldsymbol{r}')\mathrm{d}S(\boldsymbol{r}')\right], \quad \boldsymbol{r} \in S_1\,,$$

and

$$(\mathcal{M}_{21}\boldsymbol{a})(\boldsymbol{r}) = \boldsymbol{n}_2(\boldsymbol{r}) \times \left[\nabla \times \int_{S_1} \boldsymbol{a}(\boldsymbol{r}')g(k_\mathrm{i}, \boldsymbol{r}, \boldsymbol{r}')\mathrm{d}S(\boldsymbol{r}')\right], \quad \boldsymbol{r} \in S_2\,,$$

$$(\mathcal{M}_{22}\boldsymbol{a})(\boldsymbol{r}) = \boldsymbol{n}_2(\boldsymbol{r}) \times \left[\nabla \times \int_{S_2} \boldsymbol{a}(\boldsymbol{r}')g(k_\mathrm{i}, \boldsymbol{r}, \boldsymbol{r}')\mathrm{d}S(\boldsymbol{r}')\right], \quad \boldsymbol{r} \in S_2\,,$$

we obtain

$$\left(\frac{1}{2}I + \mathcal{M}_{11}\right)\boldsymbol{a}_1 + \mathcal{M}_{12}\boldsymbol{a}_2 = 0,$$

almost everywhere on S_1, and

$$-\mathcal{M}_{21}\boldsymbol{a}_1 + \left(\frac{1}{2}I - \mathcal{M}_{22}\right)\boldsymbol{a}_2 = 0,$$

almost everywhere on S_2. Note that $\mathcal{M}_{11}$ and $\mathcal{M}_{22}$ are the singular magnetic operators on the surfaces S_1 and S_2, respectively, while $\mathcal{M}_{12}$ and $\mathcal{M}_{21}$ are nonsingular operators. In compact operator form, we have

$$\boldsymbol{a} + \mathcal{K}\boldsymbol{a} = 0,$$

where

$$\boldsymbol{a} = \begin{pmatrix} \boldsymbol{a}_1 \\ \boldsymbol{a}_2 \end{pmatrix} \quad \text{and} \quad \mathcal{K} = \begin{bmatrix} 2\mathcal{M}_{11} & 2\mathcal{M}_{12} \\ -2\mathcal{M}_{21} & -2\mathcal{M}_{22} \end{bmatrix}.$$

The above integral equation is a Fredholm integral equation of the second kind, and according to Mikhlin [161] we find that $\boldsymbol{a} \sim \boldsymbol{a}_0 \in \mathfrak{C}_{\tan}(S_{1,2})$. Noticing that the operator $\mathcal{K}$ map $\mathfrak{C}_{\tan}(S_{1,2})$ into $\mathfrak{C}^{0,\alpha}_{\tan}(S_{1,2})$ and $\mathfrak{C}^{0,\alpha}_{\tan}(S_{1,2})$ into $\mathfrak{C}^{0,\alpha}_{\tan,\mathrm{d}}(S_{1,2})$, we see that $\boldsymbol{a} \sim \boldsymbol{a}_0 \in \mathfrak{C}^{0,\alpha}_{\tan,\mathrm{d}}(S_{1,2})$, where $\boldsymbol{a}_0 = \begin{pmatrix} \boldsymbol{a}_{10} \\ \boldsymbol{a}_{20} \end{pmatrix}$. The properties of the vector potentials with uniformly Hölder continuous densities, then yields $\mathcal{E}$, $\mathcal{H} \in C^{0,\alpha}(\overline{D}_{\mathrm{i},1})$. The jump relations for the double *curl* of the vector potentials $\boldsymbol{A}_1$ and $\boldsymbol{A}_2$ [49], give $\boldsymbol{n}_1 \times \mathcal{E}_- = 0$ on S_1, and $\boldsymbol{n}_2 \times \mathcal{E}_+ = 0$ on S_2. Therefore, $\mathcal{E}$ and $\mathcal{H}$ solve the homogeneous Maxwell boundary-value problem, and since $k_\mathrm{i} \notin \sigma(D_{\mathrm{i},1})$, it follows that $\mathcal{E} = \mathcal{H} = 0$ in $D_{\mathrm{i},1}$. Finally, from the jump relations (for continuous densities)

$$\boldsymbol{n}_1 \times \mathcal{H}_+ - \boldsymbol{n}_1 \times \mathcal{H}_- = \boldsymbol{a}_{10} = 0,$$

and

$$\boldsymbol{n}_2 \times \mathcal{H}_+ - \boldsymbol{n}_2 \times \mathcal{H}_- = \boldsymbol{a}_{20} = 0,$$

we obtain $\boldsymbol{a}_1 \sim 0$ on S_1, and $\boldsymbol{a}_2 \sim 0$ on S_2. □

The following theorems state the completeness and linear independence of the system of regular and radiating spherical vector wave functions on two enclosing surfaces.

Theorem 2. *Let S_1 and S_2 be two closed surfaces of class C^2, with S_1 enclosing S_2, and let $\boldsymbol{n}_1$ and $\boldsymbol{n}_2$ be the outward normal unit vectors to S_1 and S_2, respectively. The system of vector functions*

$$\left\{ \begin{pmatrix} \boldsymbol{n}_1 \times \boldsymbol{M}^3_{mn} \\ \boldsymbol{n}_2 \times \boldsymbol{M}^3_{mn} \end{pmatrix}, \begin{pmatrix} \boldsymbol{n}_1 \times \boldsymbol{N}^3_{mn} \\ \boldsymbol{n}_2 \times \boldsymbol{N}^3_{mn} \end{pmatrix}, \begin{pmatrix} \boldsymbol{n}_1 \times \boldsymbol{M}^1_{mn} \\ \boldsymbol{n}_2 \times \boldsymbol{M}^1_{mn} \end{pmatrix}, \begin{pmatrix} \boldsymbol{n}_1 \times \boldsymbol{N}^1_{mn} \\ \boldsymbol{n}_2 \times \boldsymbol{N}^1_{mn} \end{pmatrix}, \right.$$

$$\left. n = 1, 2, \ldots,\ m = -n, \ldots,\ n/k_i \notin \sigma\left(D_{i,1}\right) \right\}$$

is complete in $\mathfrak{L}^2_{\tan}(S_{1,2})$.

Proof. It is sufficient to show that for $\boldsymbol{a} = \begin{pmatrix} \boldsymbol{a}_1 \\ \boldsymbol{a}_2 \end{pmatrix} \in \mathfrak{L}^2_{\tan}(S_{1,2})$, the set of closure relations

$$\int_{S_1} \boldsymbol{a}_1^* \cdot \left(\boldsymbol{n}_1 \times \boldsymbol{M}^3_{mn}\right) \mathrm{d}S + \int_{S_2} \boldsymbol{a}_2^* \cdot \left(\boldsymbol{n}_2 \times \boldsymbol{M}^3_{mn}\right) \mathrm{d}S = 0,$$

$$\int_{S_1} \boldsymbol{a}_1^* \cdot \left(\boldsymbol{n}_1 \times \boldsymbol{N}^3_{mn}\right) \mathrm{d}S + \int_{S_2} \boldsymbol{a}_2^* \cdot \left(\boldsymbol{n}_2 \times \boldsymbol{N}^3_{mn}\right) \mathrm{d}S = 0,$$

and

$$\int_{S_1} \boldsymbol{a}_1^* \cdot \left(\boldsymbol{n}_1 \times \boldsymbol{M}^1_{mn}\right) \mathrm{d}S + \int_{S_2} \boldsymbol{a}_2^* \cdot \left(\boldsymbol{n}_2 \times \boldsymbol{M}^1_{mn}\right) \mathrm{d}S = 0,$$

$$\int_{S_1} \boldsymbol{a}_1^* \cdot \left(\boldsymbol{n}_1 \times \boldsymbol{N}^1_{mn}\right) \mathrm{d}S + \int_{S_2} \boldsymbol{a}_2^* \cdot \left(\boldsymbol{n}_2 \times \boldsymbol{N}^1_{mn}\right) \mathrm{d}S = 0$$

for $n = 1, 2, \ldots$, and $m = -n, \ldots, n$, yields $\boldsymbol{a}_1 \sim 0$ on S_1, and $\boldsymbol{a}_2 \sim 0$ on S_2. As in the proof of Theorem 1, we consider the vector potentials $\boldsymbol{A}_1$ and $\boldsymbol{A}_2$ with densities $\boldsymbol{a}_1' = \boldsymbol{n}_1 \times \boldsymbol{a}_1^*$, and $\boldsymbol{a}_2' = \boldsymbol{n}_2 \times \boldsymbol{a}_2^*$, respectively, and define the vector field

$$\mathcal{E} = \frac{\mathrm{j}}{k_0 \varepsilon_\mathrm{i}} (\nabla \times \nabla \times \boldsymbol{A}_1 + \nabla \times \nabla \times \boldsymbol{A}_2).$$

Restricting $\boldsymbol{r}$ to lies inside a sphere enclosed in S_2 and using the vector spherical wave expansion of the dyad $g\overline{\boldsymbol{I}}$, we see that the first set of closure relations gives $\mathcal{E} = 0$ in $D_{\mathrm{i},2}$. Analogously, but restricting $\boldsymbol{r}$ to lies outside a sphere enclosing S_1, we deduce that the second set of closure relations yields $\mathcal{E} = 0$ in D_s. Theorem 1 can now be used to conclude. □

Theorem 3. *Under the same assumptions as in Theorem 2, the system of vector functions*

$$\left\{ \begin{pmatrix} \boldsymbol{n}_1 \times \boldsymbol{M}^3_{mn} \\ \boldsymbol{n}_2 \times \boldsymbol{M}^3_{mn} \end{pmatrix}, \begin{pmatrix} \boldsymbol{n}_1 \times \boldsymbol{N}^3_{mn} \\ \boldsymbol{n}_2 \times \boldsymbol{N}^3_{mn} \end{pmatrix}, \begin{pmatrix} \boldsymbol{n}_1 \times \boldsymbol{M}^1_{mn} \\ \boldsymbol{n}_2 \times \boldsymbol{M}^1_{mn} \end{pmatrix}, \begin{pmatrix} \boldsymbol{n}_1 \times \boldsymbol{N}^1_{mn} \\ \boldsymbol{n}_2 \times \boldsymbol{N}^1_{mn} \end{pmatrix}, \right.$$
$$\left. n = 1, 2, \ldots,\ m = -n, \ldots, n/k_i \notin \sigma\left(D_{\mathrm{i},1}\right) \right\}$$

is linearly independent in $\mathfrak{L}^2_{\tan}(S_{1,2})$.

Proof. We need to show that for any N_{rank}, the relations

$$\sum_{n=1}^{N_{\mathrm{rank}}} \sum_{m=-n}^{n} \alpha_{mn} \begin{pmatrix} \boldsymbol{n}_1 \times \boldsymbol{M}^3_{mn} \\ \boldsymbol{n}_2 \times \boldsymbol{M}^3_{mn} \end{pmatrix} + \beta_{mn} \begin{pmatrix} \boldsymbol{n}_1 \times \boldsymbol{N}^3_{mn} \\ \boldsymbol{n}_2 \times \boldsymbol{N}^3_{mn} \end{pmatrix}$$
$$+\gamma_{mn} \begin{pmatrix} \boldsymbol{n}_1 \times \boldsymbol{M}^1_{mn} \\ \boldsymbol{n}_2 \times \boldsymbol{M}^1_{mn} \end{pmatrix} + \delta_{mn} \begin{pmatrix} \boldsymbol{n}_1 \times \boldsymbol{N}^1_{mn} \\ \boldsymbol{n}_2 \times \boldsymbol{N}^1_{mn} \end{pmatrix} = 0\,, \quad \begin{pmatrix} \text{on} & S_1 \\ \text{on} & S_2 \end{pmatrix}$$

give $\alpha_{mn} = \beta_{mn} = \gamma_{mn} = \delta_{mn} = 0$, for $n = 1, 2, \ldots, N_{\mathrm{rank}}$ and $m = -n, \ldots, n$. Defining the electromagnetic field

$$\mathcal{E} = \sum_{n=1}^{N_{\mathrm{rank}}} \sum_{m=-n}^{n} \alpha_{mn} \boldsymbol{M}^3_{mn} + \beta_{mn} \boldsymbol{N}^3_{mn} + \gamma_{mn} \boldsymbol{M}^1_{mn} + \delta_{mn} \boldsymbol{N}^1_{mn},$$

we see that $\boldsymbol{n}_1 \times \mathcal{E} = 0$ on S_1 and $\boldsymbol{n}_2 \times \mathcal{E} = 0$ on S_2. The uniqueness of the Maxwell boundary-value problem then gives $\mathcal{E} = 0$ in $D_{\mathrm{i},1}$, and since $\mathcal{E}$ is an analytic function we deduce that $\mathcal{E} = 0$ in $D_{\mathrm{i}} - \{0\}$. Using the representations for the vector spherical wave functions $\boldsymbol{M}^{1,3}_{mn}$ and $\boldsymbol{N}^{1,3}_{mn}$ in terms of vector spherical harmonincs $\boldsymbol{m}_{mn}$ and $\boldsymbol{n}_{mn}$, and the fact that the system of vector spherical harmonics is orthogonal on the unit sphere, we obtain

$$\alpha_{mn} h^{(1)}_n\left(k_{\mathrm{i}} r\right) + \gamma_{mn} j_n\left(k_{\mathrm{i}} r\right) = 0,$$
$$\beta_{mn} \left[k_{\mathrm{i}} r h^{(1)}_n\left(k_{\mathrm{i}} r\right)\right]' + \delta_{mn} \left[k_{\mathrm{i}} r j_n\left(k_{\mathrm{i}} r\right)\right]' = 0,$$

for $r > 0$. Taking into account the expressions of the spherical Bessel and Hankel functions for small value of the argument

$$j_n(x) = \frac{x^n}{(2n+1)!!} \left\{1 + \mathrm{O}\left(x^2\right)\right\}$$

and

$$h^{(1)}_n(x) = -\mathrm{j} \frac{(2n-1)!!}{x^{n+1}} \left\{1 + \mathrm{O}\left(x^2\right)\right\},$$

we multiply the first equation by $(k_{\mathrm{i}}r)^{n+1}$ and let $k_{\mathrm{i}}r \to 0$. We obtain $\alpha_{mn} = 0$ and further $\gamma_{mn} = 0$. Employing the same arguments for the second equation, we deduce that $\beta_{mn} = 0$ and $\delta_{mn} = 0$. $\square$

In the same manner we can prove the completeness and linear independence of the system of distributed vector spherical wave functions $\mathcal{M}_{mn}^{1,3}$ and $\mathcal{N}_{mn}^{1,3}$.

References

1. M. Abramowitz, I.A. Stegun, *Handbook of Mathematical Functions with Formulas, Graphs and Mathematical Tables* (National Bureau of Standards, Washington, DC, 1964)
2. A.L. Aden, Electromagnetic scattering from spheres with sizes comparable to the wavelength, J. Appl. Phys. **22**, 601 (1951)
3. S. Amari, J. Bornemann, Efficient numerical computation of singular integrals with application to electromagnetics, IEEE Trans. Antennas Propagat. **43**, 1343 (1995)
4. J.C. Auger, B. Stout, A recursive centered T-matrix algorithm to solve the multiple scattering equations: Numerical validation, J. Quant. Spectrosc. Radiat. Transfer **79–80**, 533 (2003)
5. K.A. Aydin, A. Hizal, On the completeness of the spherical vector wave functions, J. Math. Anal. Appl. **117**, 428 (1986)
6. A.J. Baran, P. Yang, S. Havemann, Calculation of the single-scattering properties of randomly oriented hexagonal ice columns: A comparison of the T-matrix and the finite-difference time-domain methods, Appl. Opt. **40**, 4376 (2001)
7. P.W. Barber, Differential scattering of electromagnetic waves by homogeneous isotropic dielectric bodies. Ph.D. Thesis, University of California, Los Angeles (1973)
8. P.W. Barber, S.C. Hill, *Light Scattering by Particles: Computational Methods* (World Scientific, Singapore 1990)
9. J.P. Barton, D.R. Alexander, Fifth-order corrected electromagnetic field component for a fundamental Gaussian beam, J. Appl. Phys. **66**, 2800 (1989)
10. R.H.T. Bates, Modal expansions for electromagnetic scattering from perfectly conducting cylinders of arbitrary cross-sections, Proc. IEE **115**, 1443 (1968)
11. R.H.T. Bates, Analytic constraints on electromagnetic field computations, IEEE Trans. Microwave Theory Tech. **23**, 605 (1975)
12. R.H.T. Bates, D.J.N. Wall, Null field approach to scalar diffraction: I. General method; II. Approximate methods; III. Inverse methods, Philos. Trans. R. Soc. London **287**, 45 (1977)
13. R. Bhandri, Scattering coefficients for a multilayered sphere: Analytic expressions and algorithms, Appl. Opt. **24**, 1960 (1985)

14. G.C. Bishop, J. Smith, Scattering from an elastic shell and a rough fluid-elestic interface: Theory, J. Acoust. Soc. Am. **101**, 767 (1997)
15. P.A. Bobbert, J. Vlieger, Light scattering by a sphere on a substrate, Physica **137**, 209 (1986)
16. C.F. Bohren, Light scattering by an optically active sphere, Chem. Phys. Lett. **29**, 458 (1974)
17. C.F. Bohren, D.R. Huffman, *Absorption and Scattering of Light by Small Particles* (Wiley, New York, 1983)
18. L. Bomholt, MMP-3D-A Computer Code for Electromagnetic Scattering Based on GMT, Ph.D. Thesis, Swiss Polytechnical Institute of Technology, Zürich (1990)
19. M. Born, E. Wolf, *Principles of Optics* (Cambridge University Press, Cambridge, 1999)
20. F. Borghese, P. Denti, R. Saija, Optical properties of spheres containing several spherical inclusions, Appl. Opt. **33**, 484 (1994)
21. F. Borghese, P. Denti, G. Toscano, O.I. Sindoni, Electromagnetic scattering by a cluster of spheres, Appl. Opt. **18**, 116 (1979)
22. F. Borghese, P. Denti, R. Saija, O.I. Sindoni, Optical properties of spheres containing a spherical eccentric inclusion, J. Opt. Soc. Am. A **9**, 1327 (1992)
23. F. Borghese, P. Denti, R. Saija, et al., Optical properties of a dispersion of anisotropic particles with non-randomly distributed orientations. The case of atmospheric ice crystals, J. Quant. Spectrosc. Radiat. Transfer **70**, 237 (2001)
24. F. Borghese, P. Dentl, R. Saija, *Scattering from Model Nonspherical Particles. Theory and Applications to Environmental Physics* (Springer, Berlin Heidelberg New York, 2003)
25. A. Boström, Scattering of acoustic waves by a layered elastic obstacle immersed in a fluid: An improved null field approach, J. Acoust. Soc. Am. **76**, 588 (1984)
26. A. Boström, G. Kristensson, S. Ström, Transformation properties of plane, spherical and cylindrical scalar and vector wave functions, in *Field Representations and Introduction to Scattering*, ed. by V.V. Varadan, A. Lakhtakia, V.K. Varadan (North Holland, Amsterdam, 1991) pp. 165–210
27. D.M. Brink, G.R. Satchler, *Angular Momentum* (Oxford University Press, London, 1979)
28. V.N. Bringi, V.V. Varadan, V.K. Varadan, The effects on pair correlation function of coherent wave attenuation in discrete random media, IEEE Trans. Antennas Propagat. **30**, 805 (1982)
29. J.H. Bruning, Y.T. Lo, Multiple scattering of EM waves by spheres. Part I and II, IEEE Trans. Antennas Propagat. **19**, 378 (1971)
30. A. Campion, P. Kambhampati, Surface-enhanced Raman scattering, Chem. Soc. Rev. **27**, 241 (1998)
31. P.C. Chaumet, A. Rahmani, F. Fornel, J.-P. Dufour, Evanescent light scattering: The validity of the dipole approximation, Phys. Rev. **58**, 2310 (1998)
32. W.C. Chew, A derivation of the vector addition theorem, Microwave Opt. Technol. Lett. **3**, 256 (1990)
33. W.C. Chew, Recurrence relations for three-dimensional scalar addition theorem, J. Electromag. Waves Appl. **6**, 133 (1992)
34. W.C. Chew, *Waves and Fields in Inhomogeneous Media* (IEEE, New York, 1995)

35. W.C. Chew, Y.M. Wang, Efficient way to compute the vector addition theorem, J. Electromag. Waves Appl. **7**, 651 (1993)
36. P. Chylek, G. Videen, Effective medium approximations for heterogeneous particles, in *Light Scattering by Nonspherical Particles: Theory, Measurements and Applications*, ed. by M.I. Mishchenko, J.W. Hovenier, L.D. Travis (Academic, San Diego, 2000) pp. 273–308
37. A. Clebsch, Über die Reflexion an einer Kugelfläche. J. Math. **61**, 195 (1863)
38. M. Clemens, T. Weiland, Discrete electromagnetism with the finite integration technique. PIER **32**, 65 (2001)
39. D. Colton, R. Kress, *Integral Equation Methods in Scattering Theory* (Wiley, New York, 1983)
40. D. Colton, R. Kress, *Inverse Acoustic and Electromagnetic Scattering Theory* (Springer, Berlin Heidelberg New York, 1992)
41. M.F.R. Cooray, I.R. Ciric, Scattering of electromagnetic waves by a coated dielectric spheroid, J. Electromag. Waves Appl. **6**, 1491 (1992)
42. C.W. Crowley, P.P. Silvester, H. Hurwitz, Jr., Covariant projection elements for 3D vector field problems. IEEE Trans. Magn. **24**, 397 (1988)
43. O.R. Cruzan, Translational addition theorems for spherical vector wave functions, Quart. Appl. Math. **20**, 33 (1962)
44. A.G. Dallas, On the convergence and numerical stability of the second Waterman scheme for approximation of the acoustic field scattered by a hard object. Technical Report, Dept. of Mathematical Sciences, University of Delaware, No. 2000-7:1-35 (2000)
45. L.W. Davis, Theory of electromagnetic beams, Phys. Rev. **19**, 1177 (1979)
46. A.J. Devaney, Quasi-plane waves and their use in radiation and scattering problems, Opt. Commun. **35**, 1 (1980)
47. K.H. Ding, C.E. Mandt, L. Tsang, J.A. Kong, Monte Carlo simulations of pair distribution functions of dense discrete random media with multipole sizes of particles, J. Electromag. Waves Appl. **6**, 1015 (1992)
48. A. Doicu, T. Wriedt, Plane wave spectrum of electromagnetic beams, Opt. Commun. **136**, 114 (1997)
49. A. Doicu, Y. Eremin, T. Wriedt, *Acoustic and Electromagnetic Scattering Analysis Using Discrete Sources* (Academic, London 2000)
50. A. Doicu, T. Wriedt, Null-field method with discrete sources to electromagnetic scattering from layered scatterers, Comput. Phys. Commun. **138**, 136 (2001)
51. A. Doicu, T. Wriedt, Null-field method with discrete sources to electromagnetic scattering from composite objects, Comput. Phys. Commun. **190**, 13 (2001)
52. W.T. Doyle, Optical properties of a suspension of metal spheres, Phys. Rev. **39**, 9852 (1989)
53. B.T. Draine, The discrete-dipole approximation and its applications to interstellar graphite grains, Astrophys. J. **333**, 848 (1988)
54. B.T. Draine, P.J. Flatau, Discrete-dipole approximation for scattering calculations, J. Opt. Soc. Am. A **11**, 1491 (1994)
55. B.T. Draine, P.J. Flatau, User guide for the discrete dipole approximation code DDSCAT 6.0., http://arxiv.org/abs/astro-ph/0309069 (2003)
56. B.T. Draine, J.J. Goodman, Beyond Clausius-Mossotti: Wave propagation on a polarizable point lattice and the discrete dipole approximation, Astrophys. J. **405**, 685 (1993)

57. C.E. Dungey, C.F. Bohren, Light scattering by nonspherical particles: A refinement to the coupled-dipole method, J. Opt. Soc. Am. A **8**, 81 (1991)
58. A.R. Edmonds, *Angular Momentum in Quantum Mechanics* (Princeton University Press, Princeton, 1974)
59. Y.A. Eremin, N.V. Orlov, Simulation of light scattering from a particle upon a wafer surface, Appl. Opt. **35**, 6599 (1996)
60. Y.A. Eremin, N.V. Orlov, Analysis of light scattering by microparticles on the surface of a silicon wafer, Opt. Spectrosc. **82**, 434 (1997)
61. Y.A. Eremin, N.V. Orlov, Modeling of light scattering by nonspherical particles based on discrete sources method, J. Quant. Spectrosc. Radiat. Transfer **60**, 451 (1998)
62. Y.A. Eremin, A.G. Sveshnikov, *The Discrete Sources Method in Electromagnetic Diffraction Problems* (Moscow State University Press, Moscow 1992), in Russian
63. G. Fairweather, A. Karageorghis, P.A. Martin, The method of fundamental solutions for scattering and radiation problems, Eng. Anal. Bound. Elem. **27**, 759 (2003)
64. J.G. Fikioris, N.K. Uzunoglu, Scattering from an eccentrically stratified dielectric sphere, J. Opt. Soc. Am. A **69**, 1359 (1979)
65. J.G. Fikioris, P.C. Waterman, Multiple scattering of waves, II, Hole corrections in the scalar case, J. Math. Phys. **5**, 1413 (1964)
66. A.V. Filippov, M. Zurita, D.E. Rosner, Fractal-like aggregates: Relation between morphology and physical properties, J. Colloid. Interface Sci. **229**, 261 (2000)
67. P.J. Flatau, SCATTERLIB: Light Scattering Codes Library. http://atol.ucsd.edu/~pflatau/scatlib/ (1998)
68. P.J. Flatau, G.L. Stephens, B.T. Draine, Light scattering by rectangular solids in the discrete-dipole approximation: A new algorithm exploiting the Block-Töplitz structure, J. Opt. Soc. Am. A **7**, 593 (1990)
69. L.L. Foldy, The multiple scattering of waves, Phys. Rev. **67**, 107 (1945)
70. B. Friedman, J. Russek, Addition theorems for spherical waves, Quart. Appl. Math. **12**, 13 (1954)
71. E. Fucile, F. Borghese, P. Denti, R. Saija, Theoretical description of dynamic light scattering from an assembly of large axially symmetric particles, J. Opt. Soc. Am. A **10**, 2611 (1993)
72. K.A. Fuller, Optical resonances and two-sphere systems, Appl. Opt. **33**, 4716 (1991)
73. K.A. Fuller, Scattering of light by coated spheres, Opt. Lett. **18**, 257 (1993)
74. K.A. Fuller, Scattering and absorption cross sections of compounded spheres. I. Theory for external aggregation, J. Opt. Soc. Am. A **11**, 3251 (1994)
75. K.A. Fuller, Scattering and absorption cross sections of compounded spheres. II. Calculations of external aggregation, J. Opt. Soc. Am. A **12**, 881 (1995)
76. K.A. Fuller, Scattering and absorption cross-sections of compounded spheres. III. Spheres containing arbitrarily located spherical inhomogeneities, J. Opt. Soc. Am. A **12**, 893 (1995)
77. K.A. Fuller, D.W. Mackowski, Electromagnetic scattering by compounded spherical particles, in *Light Scattering by Nonspherical Particles: Theory, Measurements, and Applications*, ed. by M.I. Mishchenko, J.W. Hovenier, L.D. Travis (Academic, San Diego 2000), pp. 225–272

78. I.M. Gelfand, R.A. Minlos, Z.Y. Shapiro, *Representations of the Rotation and Lorentz Groups and their Applications* (Pergamon, New York, 1963)
79. K. Georg, J. Tausch, Some error estimates for the numerical approximation of surface integrals, Math. Comput. **62**, 755 (1994)
80. J.J. Goodman, B.T. Draine, P.J. Flatau, Application of FFT techniques to the discrete dipole approximation, Opt. Lett. **16**, 1198 (1991)
81. G. Gouesbet, G. Grehan, Sur la generalisation de la theorie de Lorenz–Mie, J. Opt. (Paris) **13**, 97 (1982)
82. G. Gouesbet, J.A. Lock, Rigorous justification of the localized approximation to the beam shape coefficients in generalized Lorenz-Mie theory. II. Off-axis beams, J. Opt. Soc. Am. A **11**, 2516 (1994)
83. G. Gouesbet, G. Grehan, B. Maheau: Scattering of a Gaussian beam by a Mie scatterer centre using a Bromwich formalism, J. Opt. (Paris) **16**, 89 (1985)
84. G. Gouesbet, G. Grehan, B. Maheau, A localized interpretation to compute all the coefficients in the generalized Lorenz–Mie theory, J. Opt. Soc. Am. A **7**, 998 (1990)
85. G. Gouesbet, B. Maheau, G. Grehan, Light scattering from a sphere arbitrarily located in a Gaussian beam, using a Bromwich formulation, J. Opt. Soc. Am. A **5**, 1427 (1989)
86. R. Graglia, D.R. Wilton, A.F. Peterson, Higher order interpolatory vectors bases for computational electromagnetics, IEEE Trans. Antennas Propagat. **45**, 329 (1997)
87. G. Grehan, B. Maheau, G. Gouesbet, Scattering of laser beams by Mie scatterer centers: Numerical results using a localized approximation, Appl. Opt. **25**, 3539 (1986)
88. L. Gürel, W.C. Chew, A recursive T-matrix algorithm for strips and patches, Radio Sci. **27**, 387 (1992)
89. R.H. Hackman, The transition matrix for acoustic and elastic wave scattering in prolate spheroidal coordinates, J. Acoust. Soc. Am. **75**, 35 (1984)
90. R.H. Hackman, G.S. Sammelmann, Acoustic scattering in an homogeneous waveguide: Theory, J. Acoust. Soc. Am. **80**, 1447 (1986)
91. C. Hafner, *The Generalized Multipole Technique for Computational Electromagnetics* (Artech House, Boston London, 1990)
92. C. Hafner, *Max 1 A Visual Electromagnetics Platform for PCs* (Wiley, Chichester, 1998)
93. C. Hafner, *Post-modern Electromagnetics using Intelligent Maxwell Solvers* (Wiley, Chichester, 1999)
94. C. Hafner, L. Bomholt, *The 3D Electrodynamic Wave Simulator* (Wiley, Chichester 1993)
95. A.-K. Hamid, I.R. Ciric, M. Hamid, Iterative solution of the scattering by an arbitrary configuration of conducting or dielectric spheres, IEE Proc. **138**, 565 (1991)
96. R.F. Harrington, *Field Computation by Moment Methods* (McGraw-Hill, New York 1968)
97. R.F. Harrington, Boundary integral formulations for homogeneous material bodies. J. Electromag. Waves Appl. **3**, 1 (1989)
98. S. Havemann, A.J. Baran, Extension of T-matrix to scattering of electromagnetic plane waves by non-axisymmetric dielectric particles: Application to hexagonal ice cylinders, J. Quant. Spectrosc. Radiat. Transfer **70**, 139 (2001)

99. J. Hellmers, T. Wriedt, Influence of particle shape models on T-matrix light scattering simulations, J. Quant. Spectrosc. Radiat. Transfer **89**, 97 (2004)
100. J.W. Hovenier, Structure of a general pure Müller matrix. Appl. Opt. **33**, 8318 (1994)
101. J.W. Hovenier, C.V.M. van der Mee, Fundamental relationships relevant to the transfer of polarized light in a scattering atmosphere. Astron. Astrophys. **128**, 1 (1983)
102. J.W. Hovenier, C.V.M. van der Mee, Testing scattering matrices: A compendium of recipes. J. Quant. Spectroscop. Radiat. Transfer **55**, 649 (1996)
103. J.W. Hovenier, C.V.M. van der Mee, Basic relationships for matrices describing scattering by small particles, in *Light Scattering by Nonspherical Particles: Theory, Measurements and Applications,* ed. by M.I. Mishchenko, J.W. Hovenier, L.D. Travis (Academic, San Diego 2000) pp. 61–85
104. J.W. Hovenier, H.C. van de Hulst, C.V.M. van der Mee, Conditions for the elements of the scattering matrix. Astron. Astrophys. **157**, 301 (1986)
105. H.C. van de Hulst, *Light Scattering by Small Particles* (Wiley, New York, 1957)
106. HyperFun Project, Language and Software for F-rep Modeling, http://www.hyperfun.org
107. M.P. Ioannidou, D.P. Chrissoulidis, Electromagnetic-wave scattering by a sphere with multiple spherical inclusions, J. Opt. Soc. Am. A **19**, 505 (2002)
108. M.F. Iskander, A. Lakhtakia, Extension of the iterative EBCM to calculate scattering by low-loss or loss-less elongated dielectric objects. Appl. Opt. **23**, 948 (1984)
109. M.F. Iskander, A. Lakhtakia, C.H. Durney, A new procedure for improving the solution stability and extending the frequency range of the EBCM. IEEE Trans. Antennas Propagat. **31**, 317 (1983)
110. J.D. Jackson, *Classical Electrodynamics* (Wiley, New York 1998)
111. F.M. Kahnert, J.J. Stamnes, K. Stamnes, Application of the extended boundary condition method to homogeneous particles with point-group symmetries, Appl. Opt. **40**, 3110 (2001)
112. F.M. Kahnert, J.J. Stamnes, K. Stamnes, Application of the extended boundary condition method to particles with sharp edges: A comparison of two surface integration approaches, Appl. Opt. **40**, 3101 (2001)
113. M. Kawano, H. Ikuno, M. Nishimoto, Numerical analysis of 3-D scattering problems using the Yasuura method, Trans. IEICE Jpn. **79**, 1358 (1996)
114. S. Kawata, M. Ohtsu, M. Irie, *Near-Field Optics and Surface Plasmon Polaritons* (Springer, Berlin Heidelberg New York 2001)
115. M. Kerker, *The Scattering of Light and Other Electromagnetic Radiation* (Academic, San Diego 1969)
116. E.E.M. Khaled, S.C. Hill, P.W. Barber, Scattered an internal intensity of a sphere illuminated with a Gaussian beam. IEEE Trans. Antennas Propagat. **41**, 295 (1993)
117. K.T. Kim, The translation formula for vector multipole fields and the recurrence relations of the translation coefficients of scalar and vector multipole fields, IEEE Trans. Antennas Propagat. **44**, 1482 (1996)
118. K.H. King, L. Tsang, Effective propagation constants in media with densely distributed dielectric particles of multiple sizes and permittivities, PIER **12**, 45 (1989)

119. A.D. Kiselev, V.Yu. Reshetnyak, T.J. Sluckin, Light scattering by optically scatterers: T-matrix theory for radial and uniform anisotropies, Phys. Rev. **65**, 056609 (2002)
120. N.G. Khlebtsov, Orientational averaging of light-scattering observables in the T-matrix approach, Appl. Opt. **31**, 5359 (1992)
121. N. Kojekine, I. Hagiwara, V. Savchenko, Software Tools Using CSRBFs for Processing Scattered Data. Comput. Graph. **27**, 309 (2003)
122. J.A. Kong, *Electromagnetic Wave Theory* (Wiley, New York, 1990)
123. B. Krietenstein, P. Thoma, R. Schuhmann, T. Weiland, The perfect boundary approximation technique facing the big challenge of high precision computation, in *Proceedings of the 19th LINAC Conference* (Chicago 1998)
124. G. Kristensson, Electromagnetic scattering from buried inhomogeneities – a general three-dimensional formalism, J. Appl. Phys. **51**, 3486 (1980)
125. G. Kristensson, S. Ström, Scattering from buried inhomogeneities – a general three-dimensional formalism, J. Acoust. Soc. Am. **64**, 917 (1978)
126. G. Kristensson, A.G. Ramm, S. Ström, Convergence of the T-matrix approach to scattering theory II, J. Math. Phys. **24**, 2619 (1983)
127. H. Laitinen, K. Lumme, T-Matrix method for general starshaped particles: First results, J. Quant. Spectrosc. Radiat. Transfer **60**, 325 (1998)
128. A. Lakhtakia, The extended boundary condition method for scattering by a chiral scatterer in a chiral medium: Formulation and analysis. Optik **86**, 155 (1991)
129. A. Lakhtakia, Size-dependent Maxwell–Garnett formula from an integral equation formalism. Optik **91**, 134 (1992)
130. A. Lakhtakia, General theory of the Purcell-pennypacker scattering approach and its extension to bianisotropic scatterers. Astrophys. J. **394**, 494 (1992)
131. A. Lakhtakia, G.W. Mulholland, On two numerical techniques for light scattering by dielectric agglomerated structures. J. Res. Natl. Inst. Stand. Technol. **98**, 699 (1993)
132. A. Lakhtakia, M.F. Iskander, C.H. Durney, An iterative EBCM for solving the absorbtion characteristics of lossy dielectric objects of large aspect ratios. IEEE Trans. Microwave Theory Tech. **31**, 640 (1983)
133. A. Lakhtakia, V.K. Varadan, V.V. Varadan, Scattering by highly aspherical targets: EBCM coupled with reinforced orthogonalization. Appl. Opt. **23**, 3502 (1984)
134. A. Lakhtakia, V.K. Varadan, V.V. Varadan, Scattering of ultrasonic waves by oblate spheroidal voids of high aspect ration. J. Appl. Phys. **58**, 4525 (1985)
135. A. Lakhtakia, V.V. Varadan, V.K. Varadan, Scattering and absorption characteristics of lossy dielectric, chiral, nonspherical objects. Appl. Opt. **24**, 4146 (1985)
136. A. Lakhtakia, V.V. Varadan, V.K. Varadan, Field equations, Huygens's principle, integral equations, and theorems for radiation and scattering of electromagnetic waves in isotropic chiral media. J. Opt. Soc. Am. A **5**, 175 (1988)
137. L.D. Landau, E.M. Lifshitz, *Electrodynamics of Continuous Media* (Pergamon, Oxford 1960)
138. M. Lax, Multiple scattering of waves, II, The effective field in dense systems. Phys. Rev. **85**, 261 (1952)
139. J.F. Lee, D.K. Sun, Z.J. Cendes, Tangential vector finite elements for electromagnetic field computations, IEEE Trans. Magn. **27**, 4032 (1991)

140. Y. Leviatan, Z. Baharav, E. Heyman, Analysis of electromagnetic scattering using arrays of fictitious sources, IEEE Trans. Antennas Propagat. **43**, 1091 (1995)
141. L.-W. Li, X.-K. Kang, M.-S. Leong, *Spheroidal Wave Functions in Electromagnetic Theory* (Wiley, New York 2002)
142. C. Liu, T. Kaiser, S. Lange, G. Schweiger, Structural resonances in a dielectric sphere illuminated by an evanescent wave. Opt. Commun. **117**, 521 (1995)
143. S. Liu, W. Li, M.S. Leong, T.S. Yeo, Scattering by an arbitrarily shaped rotationally uniaxial anisotropic object: Electromagnetic fields and dyadic Green's functions, PIER **29**, 87 (2000)
144. J.A. Lock, Contribution of high-order rainbows to the scattering of a Gaussian beam by a spherical particle. J. Opt. Soc. Am. A **10**, 693 (1993)
145. J.A. Lock, G. Gouesbet, Rigorous justification of the localized approximation to the beam shape coefficients in generalized Lorenz-Mie theory. I. On-axis beams, J. Opt. Soc. Am. A **11**, 2503 (1994)
146. L. Lorenz, Lysbevaegelsen i og uden for en af plane Lysbolger belyst Kugle. Vidensk. Selk. Skr. **6**, 1 (1890)
147. A.C. Ludwig, A new technique for numerical electromagnetics, IEEE Antennas Propagat. Newsletter **3**, 40 (1989)
148. A.C. Ludwig, The generalized multipole technique, Comput. Phys. Commun. **68**, 306 (1991)
149. B. Luk'yanchuk, *Laser cleaning* (World Scientific, River Edge NJ, 2002)
150. D.W. Mackowski, Analysis of radiative scattering from multiple sphere configurations, Proc. R. Soc. London **433**, 599 (1991)
151. D.W. Mackowski, Discrete dipole moment method for calculation of the T matrix for nonspherical particles, J. Opt. Soc. Am. A **19**, 881 (2002)
152. D.W. Mackowski, P.D. Jones, Theoretical investigation of particles having directionally dependent absorption cross sections, J. Thermophys. Heat Transfer **9**, 193 (1995)
153. D.W. Mackowski, M.I. Mishchenko, Calculation of the T matrix and the scattering matrix for ensemble of spheres, J. Opt. Soc. Am. A **13**, 2266 (1996)
154. D.W. Mackowski, R.A. Altenkirch, M.P. Menguc, Internal absorption cross sections in a stratified sphere, Appl. Opt. **29**, 1551 (1990)
155. P.A. Martin, P. Ola, Boundary integral equations for the scattering of electromagnetic waves by a homogeneous dielectric obstacle, Proc. Roy. Soc. Edinburgh **123**, 185 (1993)
156. E. Marx, Single integral equation for wave scattering, J. Math. Phys. **23**, 1057 (1982)
157. J.R. Mautz, A stable integral equation for electromagnetic scattering from homogeneous dielectric bodies, IEEE Trans. Antennas Propagat. **37**, 1070 (1989)
158. D. Maystre, M. Saillard, G. Tayeb, Special methods of wave diffraction, in Pike, Sabatier ed. (2001) Chap. 1.5.6.
159. G. Mie, Beiträge zur Optik trüber Medien, speziell kolloidaler Metallösungen, Ann. Phys. **25**, 377 (1908)
160. A. Messiah, *Quantum Mechanics* (North Holland, Amsterdam 1958)
161. S.G. Mikhlin, *Mathematical Physics. An Advanced Course* (North Holland, Amsterdam 1970)
162. M.I. Mishchenko, Light scattering by randomly oriented axially symmetric particles, J. Opt. Soc. Am. A **8**, 871 (1991)

163. M.I. Mishchenko, Extinction and polarization of transmitted light by partially aligned nonspherical grains, Astrophys. J. **37**, 561 (1991)
164. M.I. Mishchenko, Light scattering by size-shape distributions of randomly oriented axially symmetric particles of a size comparable to a wavelength, Appl. Opt. **32**, 4652 (1993)
165. M.I. Mishchenko, D.W. Mackowski, Light scattering by randomly oriented bispheres, Opt. Lett. **19**, 1604 (1994)
166. M.I. Mishchenko, L.D. Travis, T-matrix computations of light scattering by large spheroidal particles, Opt. Commun. **109**, 16 (1994)
167. M.I. Mishchenko, L.D. Travis, Capabilities and limitations of a current FORTRAN implementation of the T-matrix method for randomly oriented, rotationally symmetric scatterers, J. Quant. Spectrosc. Radiat. Transfer **60**, 309 (1998)
168. M.I. Mishchenko, J.W. Hovenier, L.D. Travis, *Light Scattering by Nonspherical Particles: Theory, Measurements, and Applications* (Academic, San Diego 2000)
169. M.I. Mishchenko, L.D. Travis, A.A. Lacis, *Scattering, Absorption, and Emission of Light by Small Particles* (Cambridge University Press, Cambridge 2002)
170. M.I. Mishchenko, L.D. Travis, A. Macke, Scattering of light by polydisperse, randomly oriented, finite circular cylinders, Appl. Opt. **35**, 4927 (1996)
171. M.I. Mishchenko, L.D. Travis, Maxwell's equations, electromagnetic waves, and Stokes parameters, In *Photopolarimetry in Remote Sensing,* ed. by G. Videen, Ya. Yatskiv, M. Mishchenko (Kluwer, Dordrecht, 2004) pp. 1–44
172. M.I. Mishchenko, G. Videen, V.A. Babenko, N.G. Khlebtsov, T. Wriedt, T-matrix theory of electromagnetic scattering by particles and its applications: A comprehensive reference database, J. Quant. Spectrosc. Radiat. Transfer **88**, 357 (2004)
173. F. Moreno, F. Gonzalez, *Light Scattering from Microstructures* (Springer, Berlin Heidelberg New York, 2000)
174. A. Moroz, Improvement of Mishchenko's T-matrix code for absorbing particles, Appl. Opt. **44**, 3604 (2005)
175. P.M. Morse, H. Feshbach, *Methods of Theoretical Physics* (McGraw-Hill, New York 1953)
176. G. Mur, A.T. de Hoop, A finite element method for computing three-dimensional electromagnetic fields in inhomogeneous media, IEEE Trans. Magn. **21**, 2188 (1985)
177. C. Müller, *Foundations of the Mathematical Theory of Electromagnetic Waves* (Springer, Berlin Heidelberg New York 1969)
178. B.M. Nebeker, G.W. Starr, E.D. Hirleman, Light scattering from patterned surfaces and particles on surfaces, In *Optical Characterization Techniques for high Performance Microelectronic Device Manufacturing II,* ed. by J.K. Lowell, R.T. Chen, J.P. Mathur (Proc. SPIE **2638**, 1995) pp. 274–284
179. C.P. Neo, V.K. Varadan, V.V. Varadan, Comparison of long-wavelength T-matrix multiple-scattering theory and size-dependent Maxwell–Garnett formula, Microwave Opt. Technol. Lett. **23**, 1 (1999)
180. D. Ngo, G. Videen, P. Chylek, A Fortran code for the scattering of EM waves by a sphere with a nonconcentric spherical inclusion, Comput. Phys. Commun. **99**, 94 (1996)

181. T.A. Nieminen, H. Rubinsztein-Dunlop, N.R. Heckenberg, Calculation of the T-matrix: General considerations and application of the point-matching method, J. Quant. Spectrosc. Radiat. Transfer **79–80**, 1019 (2003)
182. L.E. Paramonov, T-matrix approach and the angular momentum theory in light scattering problems by ensembles of arbitrarily shaped particles, J. Opt. Soc. Am. A **12**, 2698 (1995)
183. A. Pasko, Function representation and HyperFun project, in *Proceedings of the 17th Spring Conference on Computer Graphics* (Budmerice, Slovakia 2001)
184. A. Pasko, V. Adzhiev, A. Sourin, V. Savchenko, Function representation in geometric modeling: Concepts, implementation and applications, Vis. Comput. **11**, 429 (1995)
185. J.I. Peltoniemi, Variational volume integral equation method for electromagnetic scattering by irregular grains, J. Quant. Spectrosc. Radiat. Transfer **55**, 637 (1996)
186. J.K. Percus, G.J. Yevick, Analysis of classical statistical mechanics by means of collective coordinates, Phys. Rev. **110**, 1 (1958)
187. B. Peterson, S. Ström, T-matrix for electromagnetic scattering from an arbitrary number of scatterers and representations of E(3), Phys. Rev. **8**, 3661 (1973)
188. B. Peterson, S. Ström, Matrix formulation of acoustic scattering from an arbitrary number of scatterers, J. Acoust. Soc. Am. **56**, 771 (1974)
189. B. Peterson, S. Ström, T-matrix formulation of electromagnetic scattering from multilayered scatterers, Phys. Rev. **10**, 2670 (1974)
190. B. Peterson, S. Ström, Matrix formulation of acoustic scattering from multilayered scatterers, J. Acoust. Soc. Am. **57**, 2 (1975)
191. E.R. Pike, P.C. Sabatier, *Scattering – Scattering and Inverse Scattering in Pure and Applied Science* (Academic, London 2001)
192. N.B. Piller, Coupled-dipole approximation for high permittivity materials, Opt. Commun. **160**, 10 (1999)
193. N.B. Piller, O.J.F. Martin, Extension of the generalized multipole technique to three-dimensional anisotropic scatterers, Opt. Lett. **23**, 579 (1998)
194. N.B. Piller, O.J.F. Martin, Increasing the performance of the coupled-dipole approximation: A spectral approach, IEEE Trans. Antennas Propagat. **46**, 1126 (1998)
195. D.C. Prieve, Measurement of colloidal forces with TIRM, Adv. Colloid Interface Sci. **82**, 93 (1999)
196. S. Pulbere, T. Wriedt, Light Scattering by Cylindrical Fibers with High Aspect Ratio Using the Null-Field Method with Discrete Sources, Part. Part. Syst. Charact. **21**, 213 (2004)
197. E.M. Purcell, C.R. Pennypacker, Scattering and absorption of light by nonspherical dielectric grains, Astrophysical J. **186**, 705 (1973)
198. M. Quinten, U. Kreibig, Absorption and elastic scattering of light by particle aggregates, Appl. Opt. **32**, 6173 (1993)
199. M. Quinten, A. Pack, R. Wannemacher, Scattering and extinction of evanescent waves by small particles, Appl. Phys. **68**, 87 (1999)
200. A.G. Ramm, Convergence of the T-matrix approach to scattering theory, J. Math. Phys. **23**, 1123 (1982)
201. A.G. Ramm, *Scattering by Obstacles* (D. Reidel, Dordrecht, 1986)
202. R.C. Reddick, R.J. Warmack, T.L. Ferrell, New form of scanning optical microscopy, Phys. Rev. **39**, 767 (1989)

203. R.C. Reddick, R.J. Warmack, D.W. Chilcott, S.L. Sharp, T.L. Ferrell, Photon scanning tunneling microscopy, Rev. Sci. Instrum. **61**, 3669 (1990)
204. N. Riefler, S. di Stasio, T. Wriedt, Structural Analysis of Clusters using Configurational and Orientational Averaging in Light Scattering Analysis, J. Quant. Spectrosc. Radiat. Transfer **89**, 323 (2004)
205. T. Rother, M. Kahnert, A. Doicu, J. Wauer, Surface Green's function of the Helmholtz equation in spherical coordinates, PIER **38**, 47 (2002)
206. R. Schmehl, The coupled-dipole method for light scattering from particles on plane surfaces, Diplomarbeit, Universität Karlsruhe (TH), Karlsruhe (1994)
207. J.B. Schneider, I.C. Peden, Differential cross section of a dielectric ellipsoid by the T-matrix extended boundary condition method, IEEE Trans. Antennas Propagat. **36**, 1317 (1988)
208. F.M. Schulz, K. Stamnes, J.J. Stamnes, Scattering of electromagnetic waves by spheroidal particles: A novel approach exploiting the T-matrix computed in spheroidal coordinates, Appl. Opt. **37**, 7875 (1998)
209. K. Sertel and J.L. Volakis, Method of moments solution of volume integral equations using parametric geometry modeling, Radio Sci. **37**, 1 (2002)
210. A. Sihvola, *Electromagnetic Mixing Formulas and Applications* (Institution of Electrical Engineers, London 1999)
211. A. Sihvola, R. Sharma, Scattering corrections for Maxwell–Garnett mixing rule, Microwave Opt. Technol. Lett. **22**, 229 (1999)
212. N.C. Skaropoulos, H.W.J. Russchenberg, Light scattering by arbitrarily oriented rotationally symmetric particles, J. Opt. Soc. Am. A **19**, 1583 (2002)
213. S. Stein, Addition theorems for spherical wave functions, Quart. Appl. Math. **19**, 15 (1961)
214. J.C. Stover, *Optical Scattering: Measurement and Analysis*, *2nd Edn.* (SPIE, Bellingham, WA, 1995)
215. J.A. Stratton, *Electromagnetic Theory* (McGraw-Hill, New York, 1941)
216. J.A. Stratton, L.J. Chu, Diffraction theory of electromagnetic waves, Phys. Rev. **56**, 99 (1939)
217. S. Ström, The scattered field, in *Field Representations and Introduction to Scattering*, ed. by V.V. Varadan, A. Lakhtakia, V.K. Varadan (North Holland, Amsterdam, 1991) pp. 143–164
218. S. Ström, W. Zheng, Basic features of the null field method for dielectric scatterers, Radio Sci. **22**, 1273 (1987)
219. S. Ström, W. Zheng, The null field approach to electromagnetic scattering from composite objects, IEEE Trans. Antennas Propagat. **36**, 376 (1988)
220. C.T. Tai, *Dyadic Green Functions in Electromagnetic Theory* (Institute of Electrical and Electronics Engineers, New York, 1993)
221. M.A. Taubenblatt, T.K. Tran, Calculation of light scattering from particles and structures on a surface by the coupled-dipole method, J. Opt. Soc. Am. A **10**, 912 (1993)
222. O.B. Toon, T.P. Ackerman, Algorithms for the calculation of scattering by stratified spheres, Appl. Opt. **20**, 3657 (1981)
223. L. Tsang, J.A. Kong, Multiple scattering of electromagnetic waves by random distributions of discrete scatterers with coherent potential and quantum mechanics formalisms, J. Appl. Phys. **51**, 3465 (1980)
224. L. Tsang, J.A. Kong, Effective propagation constants for coherent electromagnetics waves in media embedded with dielectric scatterers, J. Apply. Phys. **53**, 7162 (1982)

225. L. Tsang, J.A. Kong, Scattering of electromagnetic waves from a half space of densely distributed dielectric scatterrers, Radio Sci. **18**, 1260 (1983)
226. L. Tsang, J.A. Kong, Scattering of electromagnetic waves from a dense medium consisting of correlated Mie scatterrers with size distributions and applications to dry snow, J. Electromag. Waves Appl. **6**, 265 (1992)
227. L. Tsang, J.A. Kong, T. Habashy, Multiple scattering of acoustic waves by random distributions of discrete spherical scatterrers with the quasicrystalline and Percus Yevick approximations, J. Acoust. Soc. Am. **71**, 552 (1982)
228. L. Tsang, J.A. Kong, R.T. Shin, *Theory of Microwave Remote Sensing* (Wiley, New York, 1985)
229. L. Tsang, J.A. Kong, K.H. Ding, *Scattering of electromagnetic waves, Theory and Applicatios* (Wiley, New York, 2000)
230. V. Twerski, On scattering of waves by random distributions, I. Free space scatterer formulation, J. Math. Phys. **3**, 700 (1962)
231. V. Twerski, Coherent electromagnetic waves in pair-correlated random distributions of aligned scatterers, J. Math. Phys. **19**, 215 (1978)
232. N.K. Uzunoglu, P.G. Cottis, J.G. Fikioris, Excitation of electromagnetic waves in a pyroelectric cylinder, IEEE Trans. Antennas Propagat. **33**, 90 (1995)
233. V.K. Varadan, Multiple scattering of acoustic, electromagnetic and elastic waves, in *Acoustic, Electromagnetic and Elatic Wave Scattering-Focus on the T-Matrix Approach*, ed. by V.K. Varadan, V.V. Varadan (Pergamon, New York 1980) pp. 103–134
234. V.V. Varadan, V.K. Varadan, *Acoustic, Electromagnetic and Elastic Waves Scattering-Focus on the T-matrix Approach* (Pergamon, New York, 1980)
235. V.K. Varadan, V.V. Varadan, Multiple scattering of electromagnetic waves by randomly distributed and oriented dielectric scatterrers, Phys. Rev. **21**, 388 (1980)
236. V.K. Varadan, V.N. Bringi, V.V. Varadan, Coherent electromagnetic waves propagation through randomly distributed dielectric scatterrers, Phys. Rev. **19**, 2480 (1979)
237. V.V. Varadan, A. Lakhtakia, V.K. Varadan, Scattering by three-dimensional anisotropic scatterers, IEEE Trans. Antennas Propagat. **37**, 800 (1989)
238. V.V. Varadan, A. Lakhtakia, V.K. Varadan, *Field representation and Introduction to Scattering* (Elsevier Science, Amsterdam, 1991)
239. D.A. Varshalovich, A.N. Moskalev, V.K. Khersonskii, *Quantum Theory of Angular Momentum* (World Scientific, Singapore, 1988)
240. G. Videen, Light scattering from a sphere on or near a surface, J. Opt. Soc. Am. A **8**, 483 (1991)
241. G. Videen, Light scattering from a sphere behind a surface, J. Opt. Soc. Am. A **10**, 110 (1993)
242. G. Videen, Scattering from a small sphere near a surface, J. Opt. Soc. Am. A **10**, 118 (1993)
243. G. Videen, D. Ngo, P. Chylek, R.G. Pinnick, Light scattering from a sphere with an irregular inclusion, J. Opt. Soc. Am. A **12**, 922 (1995)
244. G. Videen, R.G. Pinnick, D. Ngo et al., Asymmetry parameters and aggregate particles, Appl. Opt. **37**, 1104 (1998)
245. J.L. Volakis, Alternative field representations and integral equations for modeling inhomogeneous dielectrics, IEEE Trans. Microwave Theory Tech. **40**, 604 (1992)

246. J.L. Volakis, K. Sertel, E. Jorgensen, R.W. Kindt, Hybride finite element and volume integral methods for scattering using parametric geometry, CMES **1**, 11 (2000)
247. D. Wall, Methods of overcoming numerical instabilities associated with the T-matrix method. In *Acoustic, Electromagnetic and Elastic Waves Scattering-Focus on the T-matrix Approach*, ed. by V.V. Varadan, V.K. Varadan (Pergamon, New York 1980) pp. 269–286
248. D.S. Wang, P.W. Barber, Scattering by inhomogeneous nonspherical objects, Appl. Opt. **18**, 1190 (1979)
249. J.S. Wang, N. Ida, Curvilinear and higher order edge finite elements in electromagnetic field computation, IEEE Trans. Magn. **29**, 1491 (1993)
250. Y.M. Wang, W.C. Chew, An efficient algorithm for solution of a scattering problem, Micro. Opt. Tech. Lett. **3**, 102 (1990)
251. Y.M. Wang, W.C. Chew, A recursive T-matrix approach for the solution of electromagnetic scattering by many spheres, IEEE Trans. Antennas Propagat. **41**, 1633 (1993)
252. R. Wannemacher, A. Pack, M. Quinten, Resonant absorption and scattering in evanescent fields, Appl. Phys. **68**, 225 (1999)
253. P.C. Waterman, Matrix formulation of electromagnetic scattering, Proc. IEEE **53**, 805 (1965)
254. P.C. Waterman, Scattering by dielectric obstacles. Alta Freq. **38**, 348 (1969)
255. P.C. Waterman, New formulation of acoustic scattering, J. Acoust. Soc. Am. **45**, 1417 (1969)
256. P.C. Waterman, Symmetry, unitarity and geometry in electromagnetic scattering, Phys. Rev. **3**, 825 (1971)
257. P.C. Waterman, Numerical solution of electromagnetic scattering problems, in *Computer Techniques for Electromagnetics*, ed. by R. Mittra (Pergamon, Oxford 1973)
258. P.C. Waterman, R. Truell, Multiple scattering of waves, J. Math. Phys. **2**, 512 (1961)
259. J.P. Webb, B. Forghani, Hierarchical scalar and vector tetrahedra, IEEE Trans. Magn. **29**, 1495 (1993)
260. T. Weiland, A discretization method for the solution of Maxwell's equations for six-component fields, Electronics and Communications AEÜ **31**, 116 (1977)
261. D.J. Wielaard, M.I. Mishchenko, A. Macke, B.E. Carlson, Improved T-matrix computations for large, nonabsorbing and weakly absorbing nonspherical particles and comparison with geometrical-optics approximation, Appl. Opt. **36**, 4305 (1997)
262. E.P. Wigner, *Group Theory and its Application to the Quantum Mechanics of Atomic Spectra* (Academic, New York 1959)
263. W.J. Wiscombe, A. Mugnai, Single scattering from nonspherical Chebyshev particles: A compendium of calculations, NASA Ref. Publ. NASA RP-1157 (1986)
264. W.J. Wiscombe, A. Mugnai, Scattering from nonspherical Chebyshev particles. 2: Means of angular scattering patterns, Appl. Opt. **27**, 2405 (1988)
265. K.L. Wong, H.T. Chen, Electromagnetic scattering by a uniaxially anisotropic sphere, Proc. IEEE **139**, 314 (1992)
266. T. Wriedt, Electromagnetic Scattering Programs, http://www.t-matrix.de (2006)

267. T. Wriedt, *Generalized Multipole Techniques for Electromagnetic and Light Scattering* (Elsevier, Amsterdam, 1999)
268. T. Wriedt, Using T-matrix method for light scattering computations by non-axisymmetric particles: Superellipsoids and realistically shaped particles, Part. Part. Syst. Charact **19**, 256 (2002)
269. T. Wriedt, U. Comberg, Comparison of computational scattering methods, J. Quant. Spectrosc. Radiat. Transfer **60**, 411 (1998)
270. T. Wriedt, A. Doicu, Light scattering from a particle on or a near a surface, Opt. Commun **152**, 376 (1998)
271. Y.-L. Xu, Electromagnetic scattering by an aggregate of spheres, Appl. Opt. **34**, 4573 (1995)
272. Y.-L. Xu, B.A.S. Gustafson, A generalized multiparticle Mie-solution: Further experimental verification, J. Quant. Spectrosc. Radiat. Transfer **70**, 395 (2001)
273. Y.-L. Xu, B.A.S. Gustafson, Experimental and theoretical results of light scattering by aggregates of spheres, Appl. Opt. **36**, 8026 (1997)
274. Y.-L. Xu, Scattering Mueller matrix of an ensemble of variously shaped small particles, J. Opt. Soc. Am. A **20**, 11, 2093 (2003)
275. R. Zaridze, *The Method of Auxiliary Sources* (Institute of Radio-Engineering of Academy of Sciences, Moscow, 1984)
276. W. Zheng, The null field approach to electromagnetic scattering from composite objects: The case with three or more constituents, IEEE Trans. Antennas Propagat. **36**, 1396 (1988)
277. W. Zheng, Computation of complex resonance frequencies of isolated composite objects, IEEE Trans. Microwave Theory Tech. **37**, 953 (1989)
278. W. Zheng, H. Shao, Electromagnetic resonant scattering by multiple objects, Radio Sci. **26**, 191 (1991)
279. W. Zheng, S. Ström, The null field approach to electromagnetic scattering from composite objects: The case of concavo-convex constituents, IEEE Trans. Antennas Propagat. **37**, 373 (1989)

Index

Springer Series in

OPTICAL SCIENCES

Volume 1

1 **Solid-State Laser Engineering**
By W. Koechner, 5th revised and updated ed. 1999, 472 figs., 55 tabs., XII, 746 pages

Published titles since volume 90

90/1 **Raman Amplifiers for Telecommunications 1**
Physical Principles
By M.N. Islam (Ed.), 2004, 488 figs., XXVIII, 328 pages

90/2 **Raman Amplifiers for Telecommunications 2**
Sub-Systems and Systems
By M.N. Islam (Ed.), 2004, 278 figs., XXVIII, 420 pages

91 **Optical Super Resolution**
By Z. Zalevsky, D. Mendlovic, 2004, 164 figs., XVIII, 232 pages

92 **UV-Visible Reflection Spectroscopy of Liquids**
By J.A. Räty, K.-E. Peiponen, T. Asakura, 2004, 131 figs., XII, 219 pages

93 **Fundamentals of Semiconductor Lasers**
By T. Numai, 2004, 166 figs., XII, 264 pages

94 **Photonic Crystals**
Physics, Fabrication and Applications
By K. Inoue, K. Ohtaka (Eds.), 2004, 209 figs., XV, 320 pages

95 **Ultrafast Optics IV**
Selected Contributions to the 4th International Conference
on Ultrafast Optics, Vienna, Austria
By F. Krausz, G. Korn, P. Corkum, I.A. Walmsley (Eds.), 2004, 281 figs., XIV, 506 pages

96 **Progress in Nano-Electro Optics III**
Industrial Applications and Dynamics of the Nano-Optical System
By M. Ohtsu (Ed.), 2004, 186 figs., 8 tabs., XIV, 224 pages

97 **Microoptics**
From Technology to Applications
By J. Jahns, K.-H. Brenner, 2004, 303 figs., XI, 335 pages

98 **X-Ray Optics**
High-Energy-Resolution Applications
By Y. Shvyd'ko, 2004, 181 figs., XIV, 404 pages

99 **Mono-Cycle Photonics and Optical Scanning Tunneling Microscopy**
Route to Femtosecond Ångstrom Technology
By M. Yamashita, H. Shigekawa, R. Morita (Eds.) 2005, 241 figs., XX, 393 pages

100 **Quantum Interference and Coherence**
Theory and Experiments
By Z. Ficek and S. Swain, 2005, 178 figs., XV, 418 pages

101 **Polarization Optics in Telecommunications**
By J. Damask, 2005, 110 figs., XVI, 528 pages

102 **Lidar**
Range-Resolved Optical Remote Sensing of the Atmosphere
By C. Weitkamp (Ed.), 161 figs., XX, 416 pages

103 **Optical Fiber Fusion Splicing**
By A.D. Yablon, 2005, 137 figs., XIII, 306 pages

104 **Optoelectronics of Molecules and Polymers**
By A. Moliton, 2005, 229 figs., 592 pages

105 **Solid-State Random Lasers**
By M. Noginov, 2005, 131 figs., XII, 238 pages

Springer Series in

OPTICAL SCIENCES

106 **Coherent Sources of XUV Radiation**
Soft X-Ray Lasers and High-Order Harmonic Generation
By P. Jaeglé, 2006, 332 figs., XIII, 416 pages

107 **Optical Frequency-Modulated Continuous-Wave (FMCW) Interferometry**
By J. Zheng, 2005, 137 figs., XVIII, 254 pages

108 **Laser Resonators and Beam Propagation**
Fundamentals, Advanced Concepts and Applications
By N. Hodgson and H. Weber, 2005, 587 figs., XXVI, 794 pages

109 **Progress in Nano-Electro Optics IV**
Characterization of Nano-Optical Materials and Optical Near-Field Interactions
By M. Ohtsu (Ed.), 2005, 123 figs., XIV, 206 pages

110 **Kramers–Kronig Relations in Optical Materials Research**
By V. Lucarini, J.J. Saarinen, K.-E. Peiponen, E.M. Vartiainen, 2005,
37 figs., X, 162 pages

111 **Semiconductor Lasers**
Stability, Instability and Chaos
By J. Ohtsubo, 2005, 169 figs., XII, 438 pages

112 **Photovoltaic Solar Energy Generation**
By A. Goetzberger and V.U. Hoffmann, 2005, 139 figs., XII, 234 pages

113 **Photorefractive Materials and Their Applications 1**
Basic Effects
By P. Günter and J.P. Huignard, 2006, 169 figs., XIV, 421 pages

114 **Photorefractive Materials and Their Applications 2**
Materials
By P. Günter and J.P. Huignard, 2005, 100 figs., approx. XII, 300 pages

115 **Photorefractive Materials and Their Applications 3**
Applications
By P. Günter and J.P. Huignard, 2005, 100 figs., approx. XII, 300 pages

116 **Spatial Filtering Velocimetry**
Fundamentals and Applications
By Y. Aizu and T. Asakura, 2006, 112 figs., XII, 212 pages

117 **Progress in Nano-Electro-Optics V**
Nanophotonic Fabrications, Devices, Systems, and Their Theoretical Bases
By M. Ohtsu (Ed.), 2006, 122 figs., XIV, 188 pages

118 **Mid-infrared Semiconductor Optoelectronics**
By A. Krier (Ed.), 2006, 443 figs., XVIII, 751 pages

119 **Optical Interconnects**
The Silicon Approach
By L. Pavesi and G. Guillot (Eds.), 2006, 265 figs., XXII, 389 pages

120 **Relativistic Nonlinear Electrodynamics**
Interaction of Charged Particles with Strong and Super Strong Laser Fields
By H.K. Avetissian, 2006, 23 figs., XIII, 333 pages

121 **Thermal Processes Using Attosecond Laser Pulses**
When Time Matters
By M. Kozlowski and J. Marciak-Kozlowska, 2006, approx. 46 figs., XII, 232 pages

122 **Modeling and Analysis of Transient Processes in Open Resonant Structures**
New Methods and Techniques
By Y.K. Sirenko, N.P. Yashina, and S. Ström, 2007, approx. 110 figs., XIV, 346 pages

123 **Wavelength Filters in Fibre Optics**
By H. Venghaus (Ed.), 2007, approx. 210 figs., XXIV, 451 pages

124 **Light Scattering by Systems of Particles**
Null-Field Method with Discrete Sources: Theory and Programs
By A. Doicu, T. Wriedt, and Y.A. Eremin, 2006, 123 figs., XIII, 324 pages